SOT
SAN DIEGO, CA
65th Annual Meeting
& ToxExpo
MARCH 22-25, 2026

The Toxicologist: Late-Breaking Supplement

www.toxicology.org

Publication Date: March 11, 2026

Preface

This issue is devoted to the late-breaking abstracts of the 65th Annual Meeting of the Society of Toxicology at the San Diego Convention Center, San Diego, California, March 22–25, 2026.

The abstracts are reproduced as accepted by the Scientific Program Committee of the Society of Toxicology and appear in numerical sequence. If a number is missing in the numerical sequence, the abstract assigned to the missing number was withdrawn by the author(s). Author names that are italicized in the author block indicate that the author is a member of the Society of Toxicology. For example, *J. Smith*. SOT members may sponsor abstracts that do not include an author with SOT membership. Authors who are members of designated organizations could serve as the sponsor of the abstract if an SOT member was not a co-author; these types of sponsorships are displayed with an organization name after the sponsor name (e.g., Sponsor: A. Smith, EUROTOX).

Access *The Toxicologist* Online

The SOT website features *The Toxicologist* and *The Toxicologist: Late-Breaking Supplement*. The publications can be accessed any time from the "Publications and Historical Documents" web page. All the abstracts in this edition of *The Toxicologist* also are available in the 2026 SOT Event App and SOT Online Planner.

To cite a 2026 SOT Annual Meeting Late-Breaking Abstract, please format as follows: *The Toxicologist: Late-Breaking Supplement*, a Supplement to *Toxicological Sciences* Volume 210, Issue S2, Abstract #__ , 2026, Title, First Author.

Society of Toxicology
11190 Sunrise Valley Drive, Suite 300, Reston, VA 20191

www.toxicology.org

LATE-BREAKING POSTER SESSION MAP
Wednesday, March 25, 2026—1:45 PM to 4:15 PM—Exhibit Hall B
Poster Setup—7:30 AM to 9:00 AM
Late-Breaking Poster #s: 5000–5267

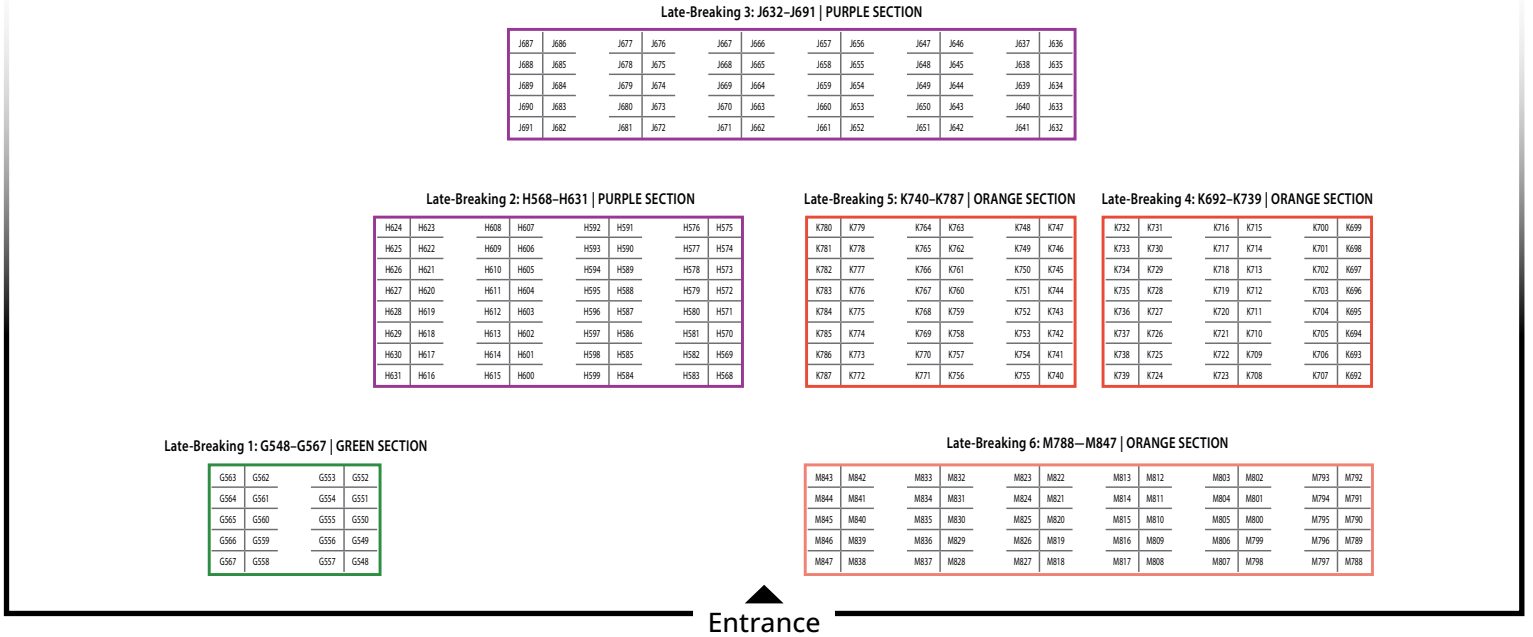

Wednesday, March 25: Poster Session by Location

SESSION TITLE	ABSTRACT #s	POSTER BOARD #s
Late-Breaking 1: Immunotoxicity; Clinical and Translational Toxicology; Liver	5000–5018	G548–G566
Late-Breaking 2: Developmental and Reproductive Toxicology; Neurotoxicity; Metals; Food Safety; Natural Products	5019–5079	H568–H629
Late-Breaking 3: Molecular Toxicology; Ecotoxicology; Air Pollution; PFAS; Respiratory Toxicology; Epidemiology and Public Health	5080–5137	J632–J690
Late-Breaking 4: Regulation/Policy; Animal Models; ADME; AI; Computational Toxicology; Cardiovascular Toxicology; Genotoxicity	5138–5184a	K692–K739
Late-Breaking 5: Safety Assessment (Non-pharmaceutical and Pharmaceutical); Dermal Toxicology; Carcinogenesis; Tobacco and ENDS	5185–5223	K749–K787
Late-Breaking 6: New Approach Methods; Risk Assessment; Human Exposure Assessment/Biomonitoring	5224–5267	M798–M846

Photography or electronic capture of posters is prohibited without the consent of the poster presenter(s)/ author(s). Please respect your colleagues' right to privacy.

Wednesday, March 25: Poster Session by Topic

TOPIC	ABSTRACT #s	BOARD #s	SESSION TITLE
ADME/Toxicokinetics	5155–5157	K709–K711	Late-Breaking 4
AI and Machine Learning	5158–5167	K712–K721	Late-Breaking 4
Air Pollution Toxicology	5099–5102	J651–J654	Late-Breaking 3
Air Pollution: Particulate Matter	5103–5107	J655–J659	Late-Breaking 3
Animal Models	5149–5154	K703–K708	Late-Breaking 4
Autoimmunity/Hypersensitivity	5168	K722	Late-Breaking 4
Biomarkers	5144–5146	K698–K700	Late-Breaking 4
Carcinogenesis	5204–5206	K768–K770	Late-Breaking 5
Cardiovascular Toxicology/Hemodynamics	5176–5177	K730–K731	Late-Breaking 4
Chemical Threats and Bioterrorism	5085–5087	J637–J639	Late-Breaking 3
Clinical and Translational Toxicology	5006–5009	G554–G557	Late-Breaking 1
Computational Toxicology and Data Integration	5169–5175	K723–K729	Late-Breaking 4

TOPIC	ABSTRACT #s	BOARD #s	SESSION TITLE
Dermal Toxicology	5193–5200	K757–K764	Late-Breaking 5
Developmental and Juvenile Toxicology	5019–5026	H568–H575	Late-Breaking 2
Ecotoxicology	5092–5098	J644–J650	Late-Breaking 3
Endocrine Toxicology	5035–5036	H584–H585	Late-Breaking 2
Engineered Nanomaterials	5147–5148	K701–K702	Late-Breaking 4
Epidemiology and Public Health	5132–5137	J685–J690	Late-Breaking 3
Epigenetics	5178–5179	K732–K733	Late-Breaking 4
Ethical, Legal, Social, Historical Issues	5180	K734	Late-Breaking 4
Food Safety/Nutrition	5066–5072	H616–H622	Late-Breaking 2
Genotoxicity/DNA Repair	5181–5184	K735–K738	Late-Breaking 4
Human Exposure Assessment/ Biomonitoring	5265–5267	M844–M846	Late-Breaking 6
Immunotoxicity	5000–5003	G548–G551	Late-Breaking 1
Inflammation	5004–5005	G552–G553	Late-Breaking 1

TOPIC	ABSTRACT #s	BOARD #s	SESSION TITLE
Liver: *In Vitro*	5010–5013	G558–G561	Late-Breaking 1
Liver: *In Vivo*	5014–5018	G562–G566	Late-Breaking 1
Medical Devices	5078–5079	H628–H629	Late-Breaking 2
Metals	5061–5065	H611–H615	Late-Breaking 2
Micro- and Nanoplastics	5088–5091	J640–J643	Late-Breaking 3
Molecular Toxicology	5080–5084	J632–J636	Late-Breaking 3
Natural Products	5073–5077	H623–H627	Late-Breaking 2
Neurotoxicity: Developmental	5037–5042	H586–H591	Late-Breaking 2
Neurotoxicity: General	5043–5049	H593–H599	Late-Breaking 2
Neurotoxicity: Metals	5050	H600	Late-Breaking 2
Neurotoxicity: Neurodegeneration	5051–5056	H601–H606	Late-Breaking 2
Neurotoxicity: Pesticides	5057–5058	H607–H608	Late-Breaking 2
New Approach Methods: Computational	5248–5251	M822–M825	Late-Breaking 6

TOPIC	ABSTRACT #s	BOARD #s	SESSION TITLE
New Approach Methods: General	5224–5226	M798–M800	Late-Breaking 6
New Approach Methods: *In Vitro*	5227–5247	M801–M821	Late-Breaking 6
Ocular Toxicology	5192	K756	Late-Breaking 5
Perfluorinated Alkyl Substances (PFAS)	5108–5117	J660–J669	Late-Breaking 3
Persistent Organic Pollutants (POPs)	5118–5120	J670–J672	Late-Breaking 3
Pesticides	5059–5060	H609–H610	Late-Breaking 2
Regulation/Policy	5138–5143	K692–K697	Late-Breaking 4
Reproductive Toxicology	5027–5034	H576–H583	Late-Breaking 2
Respiratory Toxicology	5121–5131	J673–J683	Late-Breaking 3
Risk Assessment	5252–5264	M831–M843	Late-Breaking 6
Safety Assessment: Non-pharmaceutical	5185–5186	K749–K750	Late-Breaking 5
Safety Assessment: Pharmaceutical —Drug Development	5184a; 5188–5191	K739; K752–K755	Late-Breaking 5

TOPIC	ABSTRACT #s	BOARD #s	SESSION TITLE
Safety Assessment: Pharmaceutical —Drug Discovery	5187	K751	Late-Breaking 5
Stem Cell Biology and Toxicology	5201–5203	K765–K767	Late-Breaking 5
Tobacco, ENDS, and Smoking-Related Toxicology	5207–5223	K771–K787	Late-Breaking 5

ABSTRACT NUMBER: 5000 **Poster Board Number:** G548

TITLE: A High-Throughput Imaging-Based Assay for Quantifying Phagocytosis in Neutrophil- and Macrophage-Like Cell Lines

AUTHORS (FIRST INITIAL, LAST NAME) AND INSTITUTIONS: N. R. Barbo[1,2], *D. W. Phelps*[1,2], S. N. Caty[1,2], S. N. Martos[2], and K. Slentz-Kesler[2]. [1]Oak Ridge Institute for Science and Education, Oak Ridge, TN; and [2]United States Environmental Protection Agency, Durham, NC.

KEYWORDS: Immunotoxicology; *In Vitro* and Alternatives; Macrophage

ABSTRACT: Background and Purpose: Exposure to immunosuppressive chemicals may inhibit innate immune functions, such as phagocytosis, potentially increasing susceptibility to pathogens. Existing phagocytosis assays are typically low-throughput, impeding rapid chemical safety testing for this endpoint. To efficiently quantify the immunosuppressive potential of many chemicals, we developed a high-throughput imaging-based assay that assesses the phagocytic function of neutrophils and macrophages. This assay employs pH-sensitive pHrodo™ BioParticles™ *E. coli* conjugates (Invitrogen), which are presented to neutrophil-like HL-60 (nHL-60) cells or macrophage-like THP-1 cells. The phagocytosed pHrodo particles fluoresce only in the acidic environment of the phagosome. This fluorescence is measured on a per-cell level to quantify phagocytosis. Here, we optimized a high-content imaging-based phagocytosis assay to quantify changes in phagocytic ability following chemical exposure of nHL-60 cells and macrophage-like THP-1 cells. **Methods:** To select a neutrophil differentiation method, we compared HL-60 cells that were differentiated using dimethyl sulfoxide (DMSO) for 5 days, with or without an additional day where DMSO was removed (i.e. 5 or 6 days of differentiation). For macrophages, we assessed the phagocytic ability of THP-1 cells differentiated into three different cell types: (1) naïve macrophages, differentiated with phorbol 12-myristate 13-acetate (PMA), (2) pro-inflammatory macrophages, differentiated with PMA, lipopolysaccharide, and interferon γ, or (3) anti-inflammatory macrophages, differentiated with PMA, IL-4, and IL-13. To find the optimal cell-to-pHrodo bioparticle ratio and measurement timepoint, nHL-60 cells were plated at a density of either 25,000, 50,000, or 100,000 cells/well. pHrodo bioparticles were added to each of these cell densities at either 5, 10, or 15 µL/well and phagocytosis was quantified after 1, 3, 6, 9, 12, 15, 18, 21, and 24 hours. This same experiment was also performed with naïve and anti-inflammatory macrophage-like cells. Finally, nHL-60 or macrophage-like cells were imaged with either immunoglobulin G-opsonized or non-opsonized pHrodo bioparticles to determine whether opsonization would stimulate higher phagocytosis levels. **Results:** Six-day differentiated nHL-60 cells showed 18.7% more phagocytosis than 5-day differentiated cells. Among the macrophages, naïve macrophages demonstrated the greatest phagocytic ability. Naïve macrophages showed 23.9% more phagocytosis than anti-inflammatory macrophages and 67.5% more phagocytosis than pro-inflammatory macrophages. Given these results and the fact that phagocytosis is a major function of anti-inflammatory macrophages, subsequent assays included only naïve and anti-inflammatory macrophages. The optimal cell-to-pHrodo bioparticle ratio was 50,000 cells with 15 µL of pHrodo bioparticles for the nHL-60 assay and 25,000 cells with 15 µL of pHrodo bioparticles for the naïve and anti-inflammatory macrophage assays. These conditions showed the best robust Z factor (rZ') and coefficient of variance (CV) (nHL-60 rZ' = 0.47, CV = 0.002%; naïve macrophage rZ' = 0.73, CV = 6.73%; anti-inflammatory macrophage rZ' = 0.70, CV = 7.78%). The timepoint with the greatest dynamic range across all cell types was the 3-hour timepoint. Opsonizing the pHrodo bioparticles increased their cellular uptake across all cell types, especially among nHL-60 cells, where opsonization resulted in 89% more fluorescence compared to non-opsonized pHrodo bioparticles. In naïve and anti-inflammatory

macrophages, there were 36% and 33% increases, respectively, in opsonized pHrodo bioparticle fluorescence compared to non-opsonized fluorescence. **Conclusions:** The development and optimization of this *in vitro*, high-throughput assay will allow for rapid screening of chemicals for immunosuppressive potential via phagocytosis inhibition. Further efforts will employ known reference chemicals to further assess this assay's ability to detect changes in phagocytic function among nHL-60 cells and macrophage-like THP-1 cells following chemical exposure. *This abstract does not reflect the official policy of the US EPA.*

ABSTRACT NUMBER: 5001 **Poster Board Number:** G549
TITLE: Investigating AhR signaling in Th17 and Treg $CD4^+$ T cells in NOD mice

AUTHORS (FIRST INITIAL, LAST NAME) AND INSTITUTIONS: C. Martinez, K. Malany, M. Goodson, and *A. Ehrlich*. University of California, Davis, Davis, CA.
KEYWORDS: Immunotoxicology; T Cell; Dioxin

ABSTRACT: Background and Purpose: One link between the environment and autoimmune disease is the aryl hydrocarbon receptor (AhR), a ligand activated transcription factor that can bind a diverse repertoire of ligands. In a variety of autoimmune disease mouse models, AhR activation has been linked to the induction of both proinflammatory T-helper 17 cells (Th17) and regulatory T cells (Tregs). However, the environmental factors that influence Th17 versus Treg differentiation are not fully clear. Using the non-obese diabetic (NOD) model for type 1 diabetes (T1D), studies in our laboratory have previously shown that AhR activation by indole-3-carbinol (I3C), a diet-derived ligand, led to AhR signaling in the intestine, an increase in proinflammatory Th17 cells, changes to the microbiome, and an exacerbation of insulitis. In contrast, AhR activation by 2,3,7,8-tetrachlorodibenzo-p-dioxin (TCDD), led to systemic AhR activation, increases in immunosuppressive Tregs, decreases in Th17 cells and prevented the development of T1D. These data suggest that the tissue location and extent of AhR activation influence the subsequent immune outcomes. In the current study, we assessed whether these differential outcomes following exposure to I3C and TCDD were both dependent on AhR signaling directly within $CD4^+$ T cells. **Methods:** Using the BDC2.5 transgenic T cell receptor model for TID, donor $AhR^{+/+}$ or $AhR^{-/-}$ $CD4^+CD62L^+TCRV\beta4^+$ cells from NOD BDC2.5 mice were injected into NOD SCID recipients, followed by treatment with either diet-supplemented I3C or TCDD by oral gavage. **Results:** We found that TCDD treatment of NOD SCID mice that received wildtype transgenic $CD4^+$ T cells had a significant delay in the onset of T1D. This protection from T1D required AhR signaling in $CD4^+$ T cells, as TCDD treatment in the NOD SCID recipients which received $AhR^{-/-}$ $CD4^+$ T cells had no impact on the course of disease. Using flow cytometry, we found that TCDD decreased the percentage of antigen-specific $CD4^+$ cells in $AhR^{+/+}$ $CD4^+$ T cell recipients, but not in $AhR^{-/-}$ $CD4^+$ T cell recipients. Unlike TCDD, treatment with I3C did not alter the development of hyperglycemia induced by transgenic $CD4^+$ T cells. **Conclusions:** These findings suggest the mechanism of action for immunomodulation in NOD mice by TCDD, but not I3C, is through AhR signaling directly within $CD4^+$ T cells.

ABSTRACT NUMBER: 5002 **Poster Board Number:** G550

TITLE: Application of high-content imaging to detect chemically mediated changes in neutrophil counts in transgenic zebrafish larvae

AUTHORS (FIRST INITIAL, LAST NAME) AND INSTITUTIONS: S. N. Caty[1,2], N. Barbo[1,2], *D. W. Phelps*[1,2], and K. Slentz-Kesler[1]. [1]US EPA, Durham, NC; and [2]Oak Ridge Institute for Science and Education, Oak Ridge, TN.

KEYWORDS: Immunotoxicology; Transgenic Models; High Content Imaging

ABSTRACT: Background and Purpose: The development of high-throughput new approach methods (NAMs) for assessing chemically induced immunotoxicity facilitates rapid identification of potential immunotoxicants in the environment. Zebrafish (*Danio rerio*) are a common model for toxicity studies due to their rapid development and ability to metabolize chemicals. They are also useful for immunotoxicity studies because they possess the same major immune cell lineages as humans. Here, we sought to apply a high-content imaging strategy to characterize the effects of chemicals on neutrophil development, a key cell type of the innate immune system. **Methods:** To count neutrophils, we used a transgenic zebrafish line with fluorescently labeled neutrophils (Tg(lyz:TagRFP)) (Lam 2012, PMID: 22946052). Neutrophils develop rapidly in the larval zebrafish and can be detected at approximately 48 hours post fertilization. We tested the effect of dibutyl phthalate, a plasticizer previously shown to decrease neutrophil counts (Efromson 2023, PMID 38060605), along with DB1976, an inhibitor of the hematopoiesis transcription factor *pu.1* (Antony-Debré 2017 PMID 29083320) for their ability to impact neutrophil counts. Zebrafish were raised in 10% Hanks buffered salt solution and exposed to a vehicle control (0.4% DMSO), or various concentrations of chemical beginning at 8 hours post fertilization. Zebrafish were reared at either 26°C or 28°C for three to five days post fertilization (dpf) and then fixed with 4% paraformaldehyde for imaging. Chemical treatment was maintained until fixation, with or without daily refreshment, depending on the experiment. Fixed zebrafish were positioned in agar molds in 96-well plates and imaged with the Opera Phenix Plus high-content imaging platform at 10x magnification in confocal mode. After imaging, fluorescent neutrophils were identified and counted using spot detection in the Harmony software application. **Results:** High-content imaging facilitated rapid data acquisition and quantification of neutrophils in transgenic zebrafish, enabling detection of both chemically mediated increases and decreases in neutrophil numbers. The number of neutrophils decreased significantly with exposure to repeated or single dosing of 2 µM dibutyl phthalate when assessed at 3 dpf, but not when observed at 5 dpf. The *pu.1* inhibitor DB1976 altered neutrophil counts at 5 dpf in a time-dependent manner, such that when fish received a single 3 µM dose of the chemical at either 0, 1, 2, or 3 dpf, neutrophil counts increased, but no differences were observed between control and treated fish when dosed at 4 dpf. **Conclusions:** A high-content imaging strategy is a promising method to increase throughput for immunotoxicity assays in zebrafish. Future work will seek to standardize assay parameters, including the timing for assessing neutrophil numbers (3 days vs 5 days), temperature for rearing, and single vs. repeated dosing, with a goal of facilitating ease of experimentation while still capturing biological signals. Subsequently, we will test additional environmental chemicals of concern for potential immunotoxicity. *The views expressed here are those of the author(s) and do not necessarily represent the views or policies of the U.S. EPA.*

ABSTRACT NUMBER: 5003 **Poster Board Number:** G551

TITLE: The effects of BPA on human IL-17A regulation in naïve CD4$^+$ T cells *in vitro*

AUTHORS (FIRST INITIAL, LAST NAME) AND INSTITUTIONS: *L. K. Blevins*[1,2], R. B. Crawford[1,2], and *N. E. Kaminski*[1,3,2]. [1]Michigan State University, East Lansing, MI; [2]Institute for Integrative Toxicology, East Lansing, MI; and [3]Department of Pharmacology and Toxicology, East Lansing, MI.

KEYWORDS: Immunotoxicity; T Cell; Cytokines; Bisphenol A

ABSTRACT: Background and Purpose: The objective of this study was to investigate whether direct addition of BPA to cultured naïve CD4$^+$ T cells isolated from human peripheral blood mononuclear cells (PBMC) promoted the production of the proinflammatory cytokine IL-17A, IL-22, another Th17 associated cytokine, and Th17 cell differentiation. **Methods:** Naïve CD4$^+$ T cells were purified from single cell suspensions of PBMC isolated from human donors by magnetic assisted cell sorting. Naïve CD4$^+$ T cells were then activated with plate bound anti-CD3 and soluble anti-CD28 antibodies under both normal and Th17 polarizing culture conditions for 7 days to establish the kinetics of IL-17A secretion (ELISA) and production (flow cytometry). In addition, IL-22 secretion and intracellular RORγt, a transcription factor associated with IL-17A production, were also quantified. At the time of activation, cells were treated with either 10nM TCDD (AhR agonist), increasing concentrations of FICZ (AhR agonist), and 10µM AHR antagonist, CH223191, as negative and positive controls of IL-17A induction. For studies examining BPA (0.05, 5, 500, 5000, and 50000nM), naïve CD4$^+$ T cells were isolated and activated as above in normal and Th17 polarizing conditions with 50nM FICZ and 10µM CH223191 as positive and negative controls for 4 days. On days 5 and 6 post activation, IL-17A and IL-22 secretion were quantified by ELISA and the frequencies of IL-17A$^+$, IL-22$^+$, and RORγt$^+$ cells were quantified by flow cytometry. **Results:** The initial studies to establish the kinetics of IL-17A secretion showed that IL-17A concentrations peaked by day 6 post activation in both Th17 polarizing and non-polarizing conditions. Moreover, on day 5, AHR antagonism by 10µM CH223191 promoted significant IL-17A production while IL-22 secretion was reduced compared to vehicle treated controls. By contrast, FICZ decreased IL-17A secretion while increasing IL-22 secretion, suggesting that CH223191 is an appropriate positive control for IL-17A induction while FICZ is an appropriate positive control for IL-22 induction. Treatment of CD4$^+$ T cells with BPA did not produce a significant increase in cells positive for IL-17A or result in increased secretion of IL-17A, while CH223191 induced significant increases in IL-17A under non-polarizing and/or polarizing conditions. It is noteworthy that the highest concentration of BPA (50000nM) utilized resulted in altered cellular morphology and decreased cytokine secretion, characteristics of reduced T cell activation. None of the aforementioned changes in IL-17A$^+$ cells or IL-17A secretion corresponded to changes in RORγt positivity in any treatment group. **Conclusions:** These studies suggest that treatment of mature, naïve CD4$^+$ T cells with BPA does not induce IL-17A or IL-22 secretion while AHR antagonist CH223191 promotes IL-17A and FICZ promotes IL-22. Interestingly, induction of IL-17A and IL-22 was not due to CH223191 or FICZ effects on the frequency of cells expressing RORγt. Given these results, BPA does not affect the production of IL-17A, IL-22, or Th17 differentiation by human CD4$^+$ T cells. In addition, CH223191 induced IL-17A but not IL-22.

ABSTRACT NUMBER: 5004 **Poster Board Number:** G552

TITLE: 30-day glyphosate exposure triggers inflammation and a blood-detectable biomarker of neuronal injury in control mice, while exacerbating neuropathology in a mouse model of alzheimer's disease

AUTHORS (FIRST INITIAL, LAST NAME) AND INSTITUTIONS: W. H. Gendron[1], W. Winslow[1], S. K. Bartholomew[1], P. Pirrotte[2], and *R. Velazquez*[1]. [1]Arizona State University, Tempe, AZ; and [2]Translational Genomics Research Institute, Phoenix, AZ.

KEYWORDS: Neurotoxicity; Pesticides; Cytokine, Signalling; Transgenic Models; Alzheimer's Disease; Glyphosate

ABSTRACT: Background and Purpose: Glyphosate (GLY) is a broad-spectrum herbicide whose use has increased with the adoption of GLY-tolerant crops. Despite widespread human exposure, as evidenced by its detection in consumer products and human biofluids, the neurobiological effects of GLY remain poorly understood. The Velazquez lab was among the first to demonstrate that GLY penetrates the brain and increases inflammatory cytokines in 4-month-old C57BL/6J mice exposed for 14 days using the No Observed Adverse Effect Level (NOAEL) and lower doses (500, 250, or 125mg/kg). While GLY is proposed to be excreted primarily through urine and feces, a recent report found that a 13-week exposure (500 or 50mg/kg) followed by a 6-month cessation period resulted in detection of the GLY major metabolite, aminomethylphosphonic acid (AMPA), in the brain, in addition to a dose-dependent increase in AD-like neuropathology and elevations in neuroinflammatory cytokines. Notably, 3xTg-AD mice displayed dose-dependent increases in blood plasma neurofilament light chain (NfL), indicating heightened neuroaxonal damage, which is consistent with recent emerging human data linking urinary GLY to circulating NfL. It remains unknown whether the U.S. Environmental Protection Agency's (EPA) chronic reference dose (cRfD; 1.75 mg/kg/day) induces similar neuropathological outcomes following short-term exposure. In the present study, 3xTg-AD and NonTg mice underwent 30 days of daily GLY exposure at the cRfD to assess blood NfL, inflammatory cytokine levels in both blood and brain, and AD-like pathology. It was hypothesized that GLY exposure would increase blood NfL and pro-inflammatory cytokines in both blood and brain in both control and AD genotypes, while exacerbating pathological markers of amyloid and tau in GLY-exposed 3xTg-AD mice. **Methods:** A cohort of 4-5-month-old NonTg and 3xTg-AD mice, balanced for sex, received daily oral gavage of GLY for 30 days, followed by collection of blood and hippocampal (Hp) brain tissue. The Hp was prioritized due to its selective vulnerability in neurodegenerative disorders, including AD. The GLY dose (21.52 mg/kg) was selected to reflect the human tolerable daily intake (1.75 mg/kg), adjusted for species-specific metabolic differences using FDA-recommended guidelines. Vehicle (Veh) served as the control exposure, yielding the following groups: NonTg Veh (n = 7), NonTg GLY (n = 7), 3xTg-AD Veh (n = 13), and 3xTg-AD GLY (n = 16). Enzyme-linked immunosorbent assays quantified circulating plasma NfL and Hp AD-related pathology, including soluble and insoluble Aβ40 and Aβ42 and phosphorylated tau (pT181). Inflammatory responses in plasma and Hp tissue were assessed using multiplex cytokine assays. **Results:** Exposure to GLY at 21.52 mg/kg significantly increased circulating plasma NfL levels in both NonTg and 3xTg-AD mice, with higher levels observed in 3xTg-AD mice. GLY exposure also significantly elevated multiple pro-inflammatory cytokines associated with neurodegenerative processes in both plasma and Hp tissue, including TNF-α, IFN-γ, and IL-1β, in NonTg and 3xTg-AD mice. In the Hp, insoluble Aβ40, soluble and insoluble Aβ42 and pTau T181 were significantly increased in GLY-exposed 3xTg-AD mice compared with Veh controls. Notably, plasma NfL levels were positively correlated with Hp insoluble Aβ40, soluble and insoluble Aβ42 and pTau T181. **Conclusions:** These findings show that just 30 days of GLY exposure at the mouse-equivalent cRfD

induces neuroinflammatory and neurodegenerative changes that are detectable in blood using the neuronal injury biomarker NfL and correlate with underlying neuropathology. These effects were amplified in the vulnerable 3xTg-AD mouse. Together, these results raise significant concerns regarding widespread GLY exposure and support the combined use of NfL with GLY and AMPA measurements to monitor GLY-associated neurotoxicity in at-risk populations.

ABSTRACT NUMBER: 5005 **Poster Board Number:** G553
TITLE: Kinetics of Mucoinflammatory Responses Following a Single Allergen Exposure

AUTHORS (FIRST INITIAL, LAST NAME) AND INSTITUTIONS: *D. Singamsetty*[1], S. Ramamoorthy[1], *S. Patial*[2], and *Y. Saini*[1]. [1]North Carolina State University, Raleigh, NC; and [2]National Institute of Environmental Health Sciences, Durham, NC.
KEYWORDS: Lung; Pulmonary or Respiratory System; Inhalation Toxicology; Inflammation; Asthma

ABSTRACT: Background and Purpose: Asthma is a chronic mucoinflammatory lung disease affecting millions worldwide, leading to significant morbidity and healthcare burden. A pathological hallmark of asthma is mucous cell metaplasia (MCM), a process in which airway epithelial cells transdifferentiate into goblet cells that secrete excessive mucins (primarily MUC5AC and MUC5B). This abnormal accumulation of mucus causes airway obstruction, impaired mucociliary clearance, increased susceptibility to microbial infections, and persistent inflammation that contributes to disease exacerbations. MCM is tightly regulated by epithelial-immune crosstalk and driven by multiple signaling pathways including IL-13/STAT6, EGFR, and Notch. Th2 cytokines (IL-4, IL-5, IL-13) secreted by type-2 helper T cells and type-2 innate lymphoid cells (ILC2s) are key inducers of MCM, promoting goblet cell differentiation through transcriptional activation of SPDEF (SAM Pointed Domain Containing ETS Transcription Factor) and FOXA3. Additionally, EGFR ligands (such as amphiregulin and TGF-α) released by inflammatory and epithelial cells can independently or synergistically enhance mucin gene expression and epithelial remodeling. Despite extensive knowledge of these pathways, the temporal dynamics and early initiating events that govern the onset and resolution of MCM during allergic inflammation remain poorly characterized. This study aimed to establish a single mixed allergen (MA) exposure model in mice to characterize the temporal progression of inflammatory responses and epithelial remodeling leading to MCM. Understanding this sequence of events will provide insight into early therapeutic intervention points to prevent irreversible airway remodeling. **Methods:** Adult C57BL/6J mice received a single intranasal challenge with mixed allergen (MA; 0.8 μg/μL) cocktail consisting of ovalbumin, house dust mite, *Alternaria alternata*, and *Aspergillus fumigatus* extracts. Animals were euthanized at 12, 24, 48, or 96 hours post-challenge to capture the evolving immune and epithelial responses. Control mice received saline and were necropsied at 96 hours. Bronchoalveolar lavage fluid (BALF) and lung tissues were analyzed for immune cell infiltration, levels of inflammatory biomarkers, and histopathological assessment of MCM using Alcian blue-periodic acid-Schiff (AB-PAS) staining and immunolabeling for MUC5B and MUC5AC. **Results:** MA-challenge induced a biphasic inflammatory response. MA-challenged mice exhibited increased immune cell infiltration compared to the saline-challenged mice, peaking at 24 hours and declining thereafter. Neutrophils predominated at 24 hours before declining, while eosinophils emerged at 24 hours and progressively increased till 96 hour time point. A single MA dose was sufficient to induce MCM, which steadily increased in a time-dependent manner, peaking at 96 hours. Cytokine responses followed a temporal arc: early innate activation peaking at 12 hours, followed by regulatory and transitional signals peaking between 24-48 hours. **Conclusions:** These findings

establish a robust acute allergic asthma model for investigating the progression of asthma-induced MCM. This model provides a foundation for elucidating the mechanisms driving mucous cell metaplasia in inflammatory airway diseases, with implications for therapeutic advances in toxicology and respiratory health.

ABSTRACT NUMBER: 5006 **Poster Board Number:** G554
TITLE: Transparent machine learning unlocks hidden toxicological signals in routine blood tests for improving acetaminophen overdose care

AUTHORS (FIRST INITIAL, LAST NAME) AND INSTITUTIONS: C. Humphries, and *J. W. Dear*. University of Edinburgh, Edinburgh, United Kingdom.
KEYWORDS: Clinical Toxicology; Clinical Trials/Human Studies

ABSTRACT: Background and Purpose: Acetaminophen overdose remains the leading cause of acute liver failure (ALF) in high-income countries. Acetylcysteine is an effective antidote, but does not prevent all cases of liver injury. To address this, novel therapies for paracetamol overdose are emerging, but we lack accurate methods for prospectively identifying who will benefit. Current tools, such as the 'ALT×APAP' product do not account for dynamic injury evolution and result in 'indeterminate' risk classifications for 1 in 3 patients. We hypothesised that a stratified, transparent machine learning approach could not only improve predictive accuracy using routine biomarkers but also deconvolute the changing pathophysiological drivers of liver injury to enable precision targeting of novel therapies. **Methods:** A retrospective cohort study of 4,705 unique patient admissions to three UK hospitals (2008-2024), with 119 cases of subsequent hepatotoxicity (peak ALT >1000 U/L). To address the evolving biology of toxicity, we developed Elastic Net logistic regression models stratified by presentation ALT: 'Pre-Injury' (ALT ≤50 U/L) and 'Established Injury' (ALT 51-1000 U/L). This machine learning architecture handles multicollinearity among 17 routinely collected biomarkers (including renal and liver function, coagulation, and differential white cell counts) to reveal complex multi-system signals. Performance was assessed on a strictly held-out 25% test set using discrimination (AUROC), calibration (with Platt scaling), clinical utility (Decision Curve Analysis), and reclassification (Integrated Discrimination Improvement, IDI; Net Reclassification Index, NRI; McNemar's test). Robustness was also evaluated in the pediatric subgroup and across treatment protocols (traditional 21-hour regimen vs. 12-hour SNAP).Ethical approval: Edinburgh Medical School REC (25-EMREC-070), data extraction and transfer approval: NHS Lothian Caldicott Guardian (ref. 24167). **Results:** The Stratified Model significantly outperformed the ALT×APAP standard (AUROC 0.933 vs 0.830; IDI 0.154, $p<0.001$). Crucially, it resolved diagnostic uncertainty, successfully reclassifying all 'indeterminate' patients into definitive risk groups (NRI 0.675, $p<0.001$), by making significantly different decisions (McNemar's $p<0.001$). Feature importance analysis revealed a pathophysiological shift. In the Pre-Injury phase, risk was dominated by toxicological load (acetaminophen concentration) and electrolyte disturbance (hyponatraemia, hypokalaemia), favouring sparse models. Conversely, the Established Injury phase retained all predictors, integrating multi-system dysfunction: alongside liver function markers, lymphocytopenia and raised basophils emerged as important, independent predictors. At a sensitivity threshold of 75.9%, the model achieved 96.4% specificity and a Negative Predictive Value of 99.4%, reducing the number of patients flagged for escalated care by 74.7% compared to ALT×APAP. Safety was demonstrated in the pediatric subgroup (specificity 98.2%), and performance remained robust across different two different acetylcysteine dosing protocols, confirming the model is regimen-agnostic. **Conclusions:** Routine toxicology data

contains rich prognostic signals masked by complex interactions. Transparent machine learning decodes these patterns, revealing a verifiable biological transition: risk effectively shifts from a dose-dependent toxicological model to a multi-system inflammatory response as injury becomes established. The strong predictive value of lymphocyte and basophil dynamics in established injury offers new targets for laboratory investigation. The resulting decision rule, with explicit coefficients for all predictors, is immediately deployable clinically, without requiring novel biomarkers or proprietary technology. This approach provides a clear basis for both targeting novel therapies to improve patient outcomes, and delivering efficient clinical trials.

ABSTRACT NUMBER: 5007 **Poster Board Number:** G555
TITLE: Influence of Maternal BMI on Associations of Early Pregnancy Exposome Profiles with Pregnancy Outcomes

AUTHORS (FIRST INITIAL, LAST NAME) AND INSTITUTIONS: *N. Saadat*[1], *S. Thangaraj*[1], J. Chovatiya[2], R. Jagani[2], S. Andra[2], and *V. Padmanabhan*[1]. [1]University of Michigan, Ann Arbor, MI; and [2]Institute for Exposomic Research, Icahn School of Medicine at Mount Sinai, New York, NY.
KEYWORDS: Exposure, Environmental; Clinical Toxicology; Epidemiology

ABSTRACT: Background and Purpose: Maternal exposures to environmental chemicals (ECs) are linked to adverse pregnancy outcomes. Exposure burden during pregnancy results from chronic, concurrent exposure to multitude of ECs. A compromised maternal metabolic and physiological state associated with higher body mass index (BMI) may further complicate exposure burden and influence the body's response to ECs. Several chemical classes are prone to bioaccumulation, and higher maternal adiposity increases the risk of sustained exposure for both the mother and the developing baby. **Methods:** To investigate the influence of maternal BMI on the impact of environmental chemicals on gestational age at birth (GA) and birth weight, we profiled urinary exposome burden in first-trimester urine samples of 119 women (BMI ≥ 25 = 55, and BMI <25 =64) that were part of the Michigan Mother-Infant Pair cohort. A targeted, automated, low-volume, and high-sensitivity multi-class assay was used to measure ninety-six environmental chemicals that included personal care and consumer product chemicals (PCPs), polycyclic aromatic hydrocarbons (PAHs), organophosphate flame retardants (OPFRs), pesticides, volatile organic compounds (VOCs), phthalate and phthalate alternative metabolites (PHTH), tobacco and smoke metabolites, and phytoestrogens. **Results:** Maternal BMI showed no association with GA but a positive association with birth weight (r = 0.195 and unadjusted p =0.037). Antimicrobials showed positive associations with GA in both low (r = 0.255, unadjusted p = 0.046) and high (r= 0.317, unadjusted p = 0.021) BMI groups, with slightly higher magnitude in the high BMI group. The patterns of associations of other exposure classes with GA and birth weight differed between lower and higher BMI groups. While most of the associations of exposure classes with GA and birth weight were positive in the low BMI group and negative in the high BMI group, they failed to reach significance. At the individual analyte level, in the high BMI group, phthalates and phthalate alternatives, mono-2-ethyl-5-oxohexylterephthalate (MEOHTP), mono-2-ethyl-5-hydroxyhexyl terephthalate (MEHHTP), mono-2-ethyl-5- carboxypentyl terephthalate (MECPTP) and polycyclic aromatic hydrocarbon- PYR1 showed negative associations($p<0.05$) with GA. In contrast, phthalate- mono-(2-ethylhexyl) terephthalate (MEHTP) and antimicrobial compound- Triclosan(TCS) showed positive associations ($p<0.05$) with GA in high BMI group. The associations with GA did not reach significance in the low BMI group, except for a trend of negative associations with tobacco smoke metabolite Norcotinine (NCOTT) and bisphenol-4,4'-

Cyclo-hexylidenebisphenol (BPZ), and a positive trend ($p<0.1$) of neonicotinoid insecticide N-Desmethyl-acetamiprid (NDMA) with GA. Several analytes, Polycyclic Aromatic Hydrocarbon- 3-Hydroxyfluorene (FLUO3) and pesticides- Dimethyldithiophosphate (DMDP), Dimethylthiophosphate (DMTP), and Dimethylphosphate (DMP) showed positive association, while two of the tobacco smoke metabolites NCOTT) and 4-Hydroxy-4-(3-pyridyl)- butanoic acid (HYPYBUT) showed a negative association with birth weight in the low BMI group ($p<0.05$). In the high BMI group, VOC (HPMA2), phthalate MEHHTP, Pesticides/fungicides- Cis-1,2,3,6- Tetrahydrophthalimide (THPI) showed negative associations ($p<0.05$) with birth weight. **Conclusions:** Our findings highlight the differential impact of environmental exposures on birth outcomes according to maternal BMI. The negative associations of phthalates and phthalate metabolites with GA and birth weight in women with higher BMI are suggestive of higher susceptibility of these women to the adverse impact of phthalates. Phthalates, which are lipophilic, may bioaccumulate in adipose tissue and are also considered obesogens. These findings also suggest tobacco smoke metabolites have increased impact on pregnancy outcomes in women with lower BMI. Maternal BMI should be incorporated into the evaluation of exposure burden and its effects on pregnant women and in establishing guidelines to mitigate the negative impact, not merely as a covariate but as a factor that may actively shape biological responses.

ABSTRACT NUMBER: 5008 **Poster Board Number:** G556

TITLE: Exploring the Impact of Medical Marijuana on Pain Control and Quality of Life in Patients with Sickle Cell Disease Attending Palliative Care Clinic

AUTHORS (FIRST INITIAL, LAST NAME) AND INSTITUTIONS: S. J. Allen[1], M. Mitchell[2], and I. Musa Yola[3]. [1]Southern University A&M College, Baton Rouge, LA; [2]Lousiana State University, Baton Rouge, LA; and [3]Louisiana State University, Baton Rouge, LA. Sponsor: *J. Luyendyk*

KEYWORDS: Clinical Toxicology; Clinical Trials/Human Studies; Pharmaceuticals

ABSTRACT: Background and Purpose: Sickle cell disease is a chronic hematologic disorder marked by recurrent pain crises that significantly limit daily functioning and quality of life. Standard opioid based therapies often provide incomplete relief and are associated with risks such as dependence, tolerance, and adverse side effects. These limitations emphasize the need for alternative pain management strategies. This study examined the impact of medical marijuana on pain control and quality of life in adult patients with sickle cell disease receiving care in a palliative care clinic. **Methods:** A prospective observational cohort design was used. Eligible participants were adults eighteen years of age or older with a confirmed diagnosis of sickle cell disease and documented pre and post treatment pain assessments. Patients with recreational marijuana use or incomplete medical records were excluded. Pain scores and relevant clinical data were obtained from electronic health records. Descriptive statistics were used to summarize patient characteristics. Paired sample t tests evaluated within group changes in pain scores, and independent t tests compared outcomes between patients receiving medical marijuana and those managed with alternative pain treatments. **Results:** Patients prescribed medical marijuana showed a reduction in post treatment pain scores compared with baseline values. Although this decrease did not reach statistical significance, the results demonstrated a consistent downward trend that suggests potential clinical benefit. Variability in patient responses and the limited sample size, influenced by the exclusion of individuals using recreational marijuana, likely contributed to the lack of statistical significance. **Conclusions:** Medical marijuana shows potential as an adjunctive therapy for pain management in patients with sickle cell disease receiving palliative care. While the findings are

preliminary and not statistically conclusive, they indicate possible improvements in pain control and quality of life. Larger controlled studies are needed to confirm efficacy, establish standardized dosing protocols, and evaluate long-term safety. This study supports continued investigation into integrative approaches for managing chronic pain in sickle cell disease populations.

ABSTRACT NUMBER: 5009 **Poster Board Number:** G557
TITLE: Leveraging rare genetic syndromes to understand genetic influence on metabolic dysregulation

AUTHORS (FIRST INITIAL, LAST NAME) AND INSTITUTIONS: *S. Karim*[1], and E. Davis[1,2]. [1]Stanley Manne Children's Research Institute, Ann & Robert H Lurie Children's Hosp. of Chicago, Chicago, IL; and [2]Departments of Pediatrics and Cell and Developmental Biology, Feinberg School of Medicine, Northwestern University, Chicago, IL.
KEYWORDS: Clinical Toxicology; Metabolism; Mutation

ABSTRACT: Background and Purpose: Bardet-Biedl syndrome (BBS) is a rare autosomal recessive ciliopathy characterized by early-onset obesity and metabolic dysregulation. Obesity in BBS has been linked to impaired hypothalamic melanocortin-4 receptor (MC4R) signaling, which regulates appetite and energy balance. BBS is caused by pathogenic variants in at least 26 genes, however, the role of the encoded BBS proteins in coordinating central and peripheral metabolic pathways remains poorly understood. The only FDA-approved medication for obesity in BBS is Setmelanotide, a selective MC4R agonist. However, clinical responses are variable, and effects beyond appetite regulation remain limited. Alternative treatments for obesity in BBS are being used off-label, and include Tirzepatide, a dual Glucagon-like peptide-1/ Glucose-dependent insulinotropic polypeptide (GLP-1/GIP) receptor agonist that promotes weight loss by suppressing appetite and improving insulin sensitivity. However, its efficacy and mechanistic relevance in ciliopathy-driven obesity are not yet established. This study aimed to use a zebrafish model to: (1) define how loss of BBS4 function affects appetite regulation and glucose homeostasis using a zebrafish model of BBS and (2) test Tirzepatide to determine whether incretin-based therapy can rescue metabolic defects in *bbs4* mutants. **Methods:** We utilized a genetically stable *bbs4* mutant zebrafish line harboring a 5-base-pair deletion resulting in loss of gene function. Feeding behavior, lipid accumulation, and body mass index (BMI) were quantified using established behavioral and physiological assays. Expression of appetite-regulating and glucose homeostasis genes was measured under fasting and feeding conditions using qRT-PCR in biological triplicate pools of larvae with three technical replicates per condition. Comparisons between *bbs4* homozygous mutants and wild-type (WT) controls were analyzed using Dunnett's multiple comparison test, with $p < 0.05$ considered statistically significant. **Results:** Behavioral analyses revealed no significant differences in feeding activity, lipid accumulation, or BMI between *bbs4* mutants and WT controls. In contrast, transcriptional profiling uncovered marked metabolic alterations. During fasting, *bbs4* mutants exhibited significantly reduced ***mc4r*** and ***leptin (lepa/lepb)*** expression, accompanied by a ~8-fold increase in ***insulin (insa)*** expression and elevated activation of glucagon and gluconeogenic genes, indicative of fasting-associated hyperinsulinism. Under feeding conditions, satiety-associated gene expression failed to activate in *bbs4* mutants, consistent with impaired leptin responsiveness. **Conclusions:** These findings demonstrate that *bbs4* mutant zebrafish maintain baseline feeding behavior but exhibit molecular defects in leptin-MC4R signaling and glucose regulation, including inappropriate insulin activation during fasting. These data highlight a critical role for BBS4 in coordinating metabolic signaling across tissues. The zebrafish *bbs4*

model provides a valuable preclinical and translational platform for dissecting ciliopathy-driven metabolic disease mechanisms and for evaluating therapeutic strategies targeting obesity in BBS.

ABSTRACT NUMBER: 5010 **Poster Board Number:** G558
TITLE: Pfas mediated pathway analysis in high insulin high glucose condition as compared to normoglycemic conditions in human primary cell liver spheroids

AUTHORS (FIRST INITIAL, LAST NAME) AND INSTITUTIONS: *E. Atlas*, M. J. Meier, and L. Bradford. Health Canada, Ottawa, ON, Canada.
KEYWORDS: Chemical of Concern; Methods/Mechanism; Liver; PFAS

ABSTRACT: Background and Purpose: Per- and polyfluoroalkyl substances (PFAS) are persistent and ubiquitous environmental contaminants. Epidemiological studies have associated PFAS exposure with hypercholesterolemia, diminished immune responses to vaccination, and increased cancer risk; however, their underlying modes of action remain poorly understood. The purpose of this study was to evaluate the response of liver cells spheroids to PFAS in different glycemic conditions. **Methods:** Liver cell spheroids were exposed for ten days, followed by transcriptomic analysis using the TempO-seq platform. Differentially expressed genes were subsequently analyzed using Ingenuity Pathway Analysis (IPA). **Results:** Our results revealed condition-dependent differences in susceptibility to specific PFAS, as well as distinct patterns of pathway modulation and upstream regulator activation or inhibition depending on the metabolic environment. **Conclusions:** Overall, this transcriptomic analysis provides insight into potential interactions between metabolic disease states, such as diabetes, and PFAS exposure, and suggests that underlying health conditions may influence susceptibility to chemical-induced effects.

ABSTRACT NUMBER: 5013 **Poster Board Number:** G561
TITLE: Mechanistic study of the cytotoxicity of cannabidiol and its metabolites in HepG2 cells

AUTHORS (FIRST INITIAL, LAST NAME) AND INSTITUTIONS: *S. Chen*[1], *Y. Li*[1], M. Puig[2], *F. Moulin*[2], S. Choudhuri[3], J. Gingrich[3], and *L. Guo*[1]. [1]National Center for Toxicological Research, U.S. FDA, Jefferson, AR; [2]Center for Drug Evaluation and Research, U.S. FDA, Silver Spring, MD; and [3]Human Foods Program, U.S. FDA, College Park, MD.
KEYWORDS: Cytotoxicity; Hepatocytes; Mechanisms

ABSTRACT: Background and Purpose: The cannabidiol (CBD)-based drug Epidiolex is approved by the U.S. Food and Drug Administration (FDA) for treating seizures in specific childhood-onset epileptic disorders. However, CBD-associated liver toxicity is a serious adverse effect noted on the drug label. Our previous studies demonstrated that CBD, 7-hydroxy-CBD, and 7-carboxy-CBD induce cytotoxicity in primary human hepatocytes and HepG2 cells, involving cell cycle disturbances, endoplasmic reticulum (ER) stress, and apoptosis. The purpose of this study was to comprehensively characterize the signaling pathways associated with CBD-induced cytotoxicity in HepG2 cells and to determine whether 7-hydroxy-CBD and 7-carboxy-CBD act through similar mechanisms. **Methods:** We employed a transcriptomic approach using mRNA-sequencing to identify signaling pathways altered by CBD exposure. The concentration-dependence of these pathway changes was then validated using a series of biochemical and morphological assays, including mitochondrial complex activity assays, JC-1 assay, glucose-galactose assay, Western blotting, assessment of autophagosome formation, and autophagic flux analysis.

Results: Downregulation of oxidative phosphorylation genes and upregulation of genes associated with mitochondrial dysfunction, autophagy, and ER stress were among the top 10 canonical pathways consistently affected across CBD concentrations. Direct measurement of mitochondrial respiratory complex activities demonstrated that CBD strongly inhibited Complexes IV and V and moderately inhibited Complexes II and III. CBD-induced mitochondrial dysfunction was further supported by a classic glucose-galactose assay, and loss of mitochondrial membrane potential was confirmed using the JC-1 assay. Additionally, CBD induced autophagy, as evidenced by autophagosome formation and increased autophagic flux. Similar to CBD, 7-hydroxy-CBD strongly inhibited Complexes IV and V, induced mitochondrial dysfunction, and promoted autophagy. In contrast, 7-carboxy-CBD induced autophagy but caused only marginal inhibition of the respiratory complexes and did not produce detectable mitochondrial dysfunction. **Conclusions:** Autophagy appears to be a shared mechanism underlying cytotoxicity induced by CBD, 7-hydroxy-CBD, and 7-carboxy-CBD. Inhibition of mitochondrial respiratory complexes and mitochondrial dysfunction were evident with CBD and 7-hydroxy-CBD but not with 7-carboxy-CBD.

ABSTRACT NUMBER: 5016 **Poster Board Number:** G564
TITLE: Impact of tissue transglutaminase 2 (TG2) on fibrin(ogen) crosslinking and clot formation

AUTHORS (FIRST INITIAL, LAST NAME) AND INSTITUTIONS: *N. K. Kwabi Boateng*, and *J. P. Luyendyk*. Michigan State University, East Lansing, MI.
KEYWORDS: Mechanisms; Liver; Protein Structure; Acetaminophen

ABSTRACT: Background and Purpose: Activation of the blood coagulation cascade and deposition of fibrinogen are defining features of acute hepatic injury induced by acetaminophen (APAP) overdose. Fibrinogen is a heterohexameric protein composed of two sets of Aα, Bβ, and γ chains. The coagulation protease thrombin cleaves fibrinopeptides from soluble fibrinogen to generate fibrin. Fibrin polymers are crosslinked by the plasma transglutaminase coagulation factor XIII (FXIII). In acute tissue injury, these events occur alongside crosslinking of fibrin(ogen) by the ubiquitously expressed transglutaminase, tissue transglutaminase 2 (TG2). As an initial step to define how TG2 may impact functions of fibrin(ogen) in the APAP-injured liver, we sought to determine the impact of TG2 on thrombin-induced fibrin clot formation *in vitro*. **Methods:** Purified human fibrinogen (2 mg/ml) was incubated with various concentrations of recombinant human TG2 (0-8.3 µg/ml) in the presence or absence of human α-thrombin (1U/ml). Fibrin(ogen) crosslinking was analyzed by immunoblotting of reactions using fibrinogen chain-selective polyclonal antibodies and monoclonal anti-fibrin β-chain antibody that specifically detects thrombin-cleaved fibrin β-chain. (59D8). TG2's impact on fibrin polymerization kinetics was assessed by turbidity at 405nm. **Results:** TG2 induced a concentration- and time-dependent increase in fibrin α-γ crosslinks and catalyzed the formation of high molecular weight β-chain species, consistent with TG2-mediated β-chain crosslinking. Thrombin-induced fibrin polymerization was evidenced by increased turbidity. Notably, the addition of TG2 caused a significant and concentration-dependent reduction in peak turbidity, although TG2 did not alter thrombin-mediated cleavage of fibrinopeptides A and B. **Conclusions:** These results demonstrate that TG2 crosslinks fibrin(ogen) and that these crosslinks substantially alter fundamental fibrin clot properties. Further studies are required to determine how specific covalent crosslinks imposed by TG2 impact fibrin function in injured tissue.

ABSTRACT NUMBER: 5017 **Poster Board Number:** G565

TITLE: Environmental Pollution Exposures Indirectly Contribute to the Severity of Human Alcohol-Associated Steatohepatitis

AUTHORS (FIRST INITIAL, LAST NAME) AND INSTITUTIONS: *M. C. Cave*[1,2], X. Li[3], *M. R. Smith*[4,5], J. Luo[1], W. Zhang[1], *Y. Go*[4], *D. P. Jones*[4], *C. J. McClain*[1], M. Kong[1], and H. Jiang[3]. [1]University of Louisville, Louisville, KY; [2]VA Healthcare System, Louisville, KY; [3]Northwestern University, Evanston, IL; [4]Emory University, Atlanta, GA; and [5]VA Healthcare System, Atlanta, GA.

KEYWORDS: Clinical Trials/Human Studies; Hepatic; Environmental Toxicology; Exposome

ABSTRACT: Background and Purpose: Alcohol-associated liver disease (ALD) is a leading cause of liver-related death and liver transplantation. Alcohol-associated steatohepatitis (ASH) is a form of ALD that can be fatal. However, patients with ASH may present with broad range of clinical disease severities. We hypothesize that environmental pollution exposures are disease modifying factors contributing to ASH severity. To test this hypothesis, we performed an untargeted integrated multi-omics analysis to determine the direct effects and indirect effects (via metabolomic mediators) of pollution in ASH severity. **Methods:** Previously collected and de-identified materials from 114 participants in the Defeat Alcoholic Steatohepatitis clinical trial with moderate to severe ASH were utilized in this cross-sectional analysis. Untargeted plasma exposomics (GC-MS^2) and metabolomics (LC-MS^2) were performed by the HERCULES Exposome Research Center to identify the exposure and mediator biomarkers respectively. Only those exposures previously validated by authentic standards were included. The ASH disease severity outcome biomarker was the Model for End-Stage Liver Disease (MELD) score. Lasso and Elastic Net were used as screening tools to reduce the dimensionality of candidate exposures and mediators prior to downstream analysis. Mediation analysis was performed using a novel method based on sparse canonical correlation analysis (SCCA), designed specifically for settings where both exposures and mediators are high-dimensional. Metabolome-wide association studies followed by pathway analyses were performed using MetaboAnalyst 6.0. All analyses were confounder-adjusted with statistical significance set at either $p<0.05$ or FDR<0.05. **Results:** The mean age was 45.5±10.8; the mean MELD was 21.9 and 60.5% were male. 685 exposures and 9,894 metabolites were detected in this study. The selection procedures retained 79 exposures and 87 metabolites for mediation analysis. For the individual pollutant exposures, no significant direct effects on MELD were observed at the selected FDR threshold. However, 6 pollutants were indirectly associated with ASH severity. Tris(chloropropyl)phosphate (TCPP) and 4-naphthoquinone had positive indirect associations consistent with increased disease severity which were mediated by four and one intermediary metabolites, respectively. Cypermethrin, ethyl heptanoate, chloro-2-nitrotoluene, and n-tridecane had inverse indirect associations with MELD mediated by a total of nine unique intermediary metabolites. A single phosphatidylcholine mediator, dinervonoyllecithin, was common to all four inversely associated exposures. When considering only the significant exposure (n=6) and mediator biomarkers (n=14), the R^2 was 0.25, indicating that these variables explained 25% of the observed variability in MELD score. Dinervonoyllecithin was associated with enrichment in pathways related linoleate, nitrogen/redox, and carbon metabolism. Such pathways have previously been implicated in ASH pathogenesis. **Conclusions:** This was the first untargeted exposomics research study in ASH, and it utilized novel biostatistical approaches. Pollution exposures were common in ASH. Specific exposures partially explained the observed variability in liver disease severity when the metabolomic mediators were considered. The potential harmful effects of TCPP and 4-naphthoquinone exposures as well as the potential beneficial

effects of the dinervonoyllecithin mediator warrant future investigation in ASH. Reverse causality cannot be excluded owing to the cross-sectional study design.

ABSTRACT NUMBER: 5018 **Poster Board Number:** G566
TITLE: Functional role of GPR119 agonist in hepatic stellate cells

AUTHORS (FIRST INITIAL, LAST NAME) AND INSTITUTIONS: K. Kang, J. Park, and J. Yang. College of Pharmacy and Research Institute of Pharmaceutical Sciences, Seoul National University, Seoul, Korea, Republic of. Sponsor: *D. Kim*
KEYWORDS:

ABSTRACT: Background and Purpose: Liver fibrosis arises from chronic hepatic injury and remains a major clinical challenge due to the lack of effective therapies. Although G-protein-coupled receptor 119 (GPR119) has been explored as a metabolic target in type 2 diabetes, its role in liver fibrogenesis is not well understood. **Methods:** In this study, GPR119 expression was evaluated in mouse primary hepatic stellate cells (HSCs) using immunostaining and RT-PCR. The anti-fibrotic activity of GPR119 agonists was assessed in primary HSCs, LX-2 cells, and a carbon tetrachloride (CCl_4)-induced mouse model of liver fibrosis. **Results:** Treatment with the GPR119 agonists MBX-2982 and GSK1292263 inhibited HSC activation, suppressed transforming growth factor-β1 (TGF-β1)-induced Smad2/3 phosphorylation, and reduced the expression of fibrogenic genes. *In vivo*, oral administration of MBX-2982 attenuated collagen accumulation and decreased hepatic α-smooth muscle actin and TGF-β expression in CCl_4-treated mice. Mechanistically, MBX-2982 activated AMP-activated protein kinase (AMPK), and pharmacological inhibition of AMPK reversed its anti-fibrogenic effects. MBX-2982 further reduced Smad3 acetylation by disrupting Smad3-p300 interactions and promoting AMPK-dependent proteasomal degradation of p300. **Conclusions:** These results identify GPR119 as a regulator of HSC activation and highlight GPR119 agonists as promising therapeutic candidates for liver fibrosis.

ABSTRACT NUMBER: 5019 **Poster Board Number:** H568
TITLE: Advancing Synaptic Quantification and Physiological Readouts for Developmental Neurotoxicity Assessment in Human Brain Microphysiological Systems

AUTHORS (FIRST INITIAL, LAST NAME) AND INSTITUTIONS: *B. Kincaid*, *J. Zhang*, *D. Alam-El Din*, *L. Smirnova*, and *T. Hartung*. Johns Hopkins Bloomberg School of Public Health, Baltimore, MD.
KEYWORDS: Developmental Toxicity; Prenatal; Neurotoxicity; Developmental; Computational Toxicology; Inorganic

ABSTRACT: Background and Purpose: Traditional staining and transcriptomic endpoints often fail to detect the subtle functional disturbances that characterize developmental neurotoxicity (DNT). To address this gap, we combined novel high-content image analysis of synapse geometry with sensitive electrophysiological and calcium transience assays in a human brain microphysiological system (bMPS) exposed to environmentally relevant concentrations of arsenic (As), cadmium (Cd), chromium (Cr), Lead (Pb) and a mixture of all compounds during weeks 8 to 12 post-differentiation. **Methods:** We developed Pynapse, a Python-based reimplementation and enhancement of the SynapseJ ImageJ plugin, enabling rapid, memory-efficient quantification of four-marker synaptic colocalization and geometric parameters in densely labeled confocal images. Pynapse interfaces directly with the ImageJ API, incorporates optimized memory management and parallel processing, and exports unique pre-, post-, and complete

synapse IDs with associated geometric parameters. To bolster structural observations, we integrated Pynapse analyses with calcium transience imaging and microelectrode array (MEA) recordings tracking network activity and connectivity throughout continued development over the course of 5 weeks post-exposure. **Results:** Application of Pynapse to human bMPS exposed to low-dose inorganic contaminants revealed subtle but distinct morphological alterations undetected by prior analyses. Cadmium exposure decreased synapse union perimeter and minimum feret diameter, indicating synaptic compaction, while arsenic selectively increased the feret diameter of the pre/post overlap region, suggesting elongation of the synaptic contact zone. Chromium exposure increased the density of postsynaptic and complete synapses. Complementary functional assays demonstrated reduced numbers of actively firing neurons and altered electrophysiological activity, including decreased burst firing, number of peaks, and spikes per burst per electrode for Cr and increased burst duration and interspike intervals for Cd and Cr. Interestingly, these changes were not reflected in mixture exposed bMPS. **Conclusions:** Integrating longitudinal functional assays with high-resolution synaptic geometry exposes nuanced developmental neurotoxic effects of low-dose metals, demonstrating a powerful framework for mechanistic DNT evaluation in human-relevant brain MPS models. Together, these findings demonstrate how improved image-analysis methodology can uncover previously inaccessible geometric features of human synapses, providing mechanistic insights into the developmental neurotoxicity of environmentally relevant metal exposures and advancing the application of MPS as predictive developmental neurotoxicity models.

ABSTRACT NUMBER: 5020 **Poster Board Number:** H569

TITLE: Early-life exposure to bisphenols and naphthalene metabolites in human milk and infant formula: implications for skeletal muscle metabolic programming

AUTHORS (FIRST INITIAL, LAST NAME) AND INSTITUTIONS: *J. M. dos Santos*, B. Leggat, M. L. Glasser, and J. R. Demirci. University of Pittsburgh, School of Nursing, Pittsburg, PA.

KEYWORDS: Developmental Toxicity; Post-Natal; Endocrine Disruptors; Nutritional Toxicity; Human Milk; Diabetes Programing

ABSTRACT: Background and Purpose: Exposure to endocrine-disrupting chemicals (EDCs) through food and air—such as bisphenol A and S (BPA and BPS) and naphthalene, a byproduct of fossil fuel and wood combustion—has been associated with an increased risk of type 2 diabetes (T2D). Human exposure to these xenoestrogens can begin early in life, as BPA and BPS have been detected in breast milk and may contribute to metabolic programming. This study aimed to quantify BPA, BPS, and 2-naphthol (a naphthalene metabolite) in human milk and commercially available infant formulas and to evaluate their effects on insulin resistance-related pathways and mitochondrial integrity during skeletal muscle development *in vitro*. **Methods:** Human milk samples (n = 38) were collected from 20 lactating mothers at 12-20 weeks postpartum from an existing cohort (R01HD098186). Eight infant formula products—including animal-based (powdered and ready-to-feed) and plant-based formulations—were prepared according to manufacturer instructions. Lipoprotein fractions were extracted from all samples, and BPA, BPS, and 2-naphthol concentrations were quantified using ELISA assays (Detroit R&D, Inc.). The impact of these chemicals on mitochondria dysfunction, insulin signaling pathway and GLUT4 expression in human skeletal muscle cells (HSkMC) under differentiation phase (myoblast to myotubule) was also evaluated. MtDNA copy number and GLUT4 were assessed by real-time rtPCR. **Results:** BPA levels in human milk (13.2 ± 10.7 ng/mL) and infant formula (23.4 ± 33.1 ng/mL) showed wide inter-sample variability (up to 30-fold), with no statistically significant difference between the two. Among baby

formulas, BPA and BPS levels were higher in plant-based and ready-made formulas when compared to animal-based ones. BPS and 2-Naphthol concentrations were significantly higher in human milk (4.3 ± 10.7 and 6.8± 6,7 ng/mL, respectively) than in infant formulas (2.1 ± 1.0 and 2.51± 3.8 ng/ml, p = 0.004 and p=0.015, respectively). Exposure to BPA decreased levels of GLUT4 mRNA expression by over 50% in HSkMC, while exposure to BPS decreased mtDNA copy number by over 35%. **Conclusions:** These findings demonstrate that BPA and BPS disrupt distinct metabolic pathways in skeletal muscle cells, potentially contributing to early-life programming of T2D risk. The detection of BPA, BPS, and 2-naphthol in both human milk and infant formulas highlights multiple routes of early exposure. However, the low concentration observed in some samples suggest that exposure can be reduced. Continued monitoring and regulation of EDCs in infant nutrition sources are warranted to mitigate long-term metabolic health risks.

ABSTRACT NUMBER: 5021 **Poster Board Number:** H570

TITLE: Developmental and Transcriptomic Responses to EHDPHP and Its Metabolites in Zebrafish Embryos

AUTHORS (FIRST INITIAL, LAST NAME) AND INSTITUTIONS: J. Lee[1], Y. Kawai[1], A. Covaci[2], and *A. Kubota*[1].
[1]Obihiro University of Agriculture and Veterinary Medicine, Obihiro, Japan; and [2]University of Antwerp, Antwerp, Belgium.

KEYWORDS:

ABSTRACT: Background and Purpose: Following the regulatory restrictions and phase-out of polybrominated diphenyl ethers, particularly PentaBDE, the global flame-retardant market has shifted toward alternative compounds, including organophosphate flame retardants (OPFRs). Among these, 2-ethylhexyl diphenyl phosphate (EHDPHP) is widely used and frequently detected in food, indoor environments, and biological samples, raising concerns regarding aquatic exposure and developmental toxicity. EHDPHP is readily metabolized *in vivo*, and its major metabolites, 2-ethyl-5-hydroxyhexyl diphenyl phosphate (5-HO-EHDPHP) and 2-ethylhexyl phenyl phosphate (EHPHP), are consistently detected in biomonitoring studies. Despite increasing evidence that OPFR metabolites can contribute substantially to biological effects, most developmental toxicity studies have focused primarily on the parent compound. Therefore, this study aimed to systematically compare the developmental toxicity and transcriptomic responses induced by EHDPHP and its major metabolites in zebrafish (Danio rerio) embryos. **Methods:** Zebrafish embryos were exposed from 72 to 96 hours post-fertilization to EHDPHP, 5-HO-EHDPHP, or EHPHP at multiple concentrations. Developmental toxicity was evaluated by assessing circulatory-related endpoints, including pericardial edema and reduced blood flow, using a semi-quantitative scoring system. To investigate early molecular responses in the absence of overt toxicity, embryos were also exposed to sub-toxic concentrations and subjected to exploratory RNA sequencing (RNA-Seq). Putative differential gene expression (PDEGs) was identified using a stringent fold-change-based criterion, and transcriptomic profiles were compared across compounds. **Results:** EHDPHP induced pronounced circulatory failure, characterized by pericardial edema and reduced blood flow, at 10 and 30 µM. The hydroxylated metabolite 5-HO-EHDPHP elicited similar circulatory abnormalities only at the highest concentration tested, whereas EHPHP did not induce overt morphological abnormalities within the examined concentration range. An exploratory RNA-seq revealed robust transcriptional responses at sub-toxic exposure levels for all three compounds. Each compound induced more than 100 PDEGs, even in the absence of visible developmental defects. Comparative analysis revealed substantial

overlap in affected biological processes among EHDPHP and its metabolites, with common transcriptional signatures involving G-protein-coupled receptor signaling, vascular regulation, immune-related pathways, and oxidative stress responses. Several genes exhibited consistent directionality of expression changes across the parent compound and its metabolites, indicating shared molecular response pathways in embryos without overt morphological abnormalities. **Conclusions:** These findings indicate that EHDPHP-related compounds engage common early molecular response pathways during embryonic development and support the utility of transcriptomic profiling for contextualizing developmental toxicity and generating hypotheses regarding adverse outcome pathways associated with organophosphate flame retardant exposure.

ABSTRACT NUMBER: 5022 **Poster Board Number:** H571
TITLE: Early Life Cadmium Exposure and Mechanisms of Hepatocellular Carcinoma

AUTHORS (FIRST INITIAL, LAST NAME) AND INSTITUTIONS: *V. Shang*, S. Riegl, D. Jima, and *M. Cowley*. North Carolina State University, Raleigh, NC.
KEYWORDS: Developmental Toxicity; Post-Natal; Liver; Carcinogenesis; Cadmium

ABSTRACT: Background and Purpose: Hepatocellular carcinoma (HCC) is the most common form of primary liver malignancy, the sixth most commonly diagnosed cancer and the third leading cause of cancer death. Of concern, HCC accounts for 20-33% of all pediatric liver cancers worldwide. Pediatric HCC is most commonly diagnosed in adolescents (aged 10-14 years) although it has been described in children 5 years and younger. HCC presents earlier at advanced stages in children than in adults. The etiology of pediatric HCC and the reasons for rapid disease progression are poorly understood. We focused our attention on the contribution of the early life environment to pediatric HCC, previously shown to be a key factor that predisposes children to disease outcomes later in life. We demonstrated using mice that early life exposure to the toxic metal cadmium (Cd) is sufficient to induce liver disease. Cd is among the top ten toxicants of major public health concern. We observed increased inflammation, cellular hyperplasia, fibrosis, and collagen deposition, indicative of metabolic dysfunction-associated steatotic liver disease (MASLD). These inflammatory responses could become prolonged or chronic and increase the risk of HCC. Currently, little is known about the role of Cd in tumor initiation, promotion and progression in the developing liver. We hypothesized a causative link between early life Cd exposure and pediatric HCC. **Methods:** To test this hypothesis, a mouse model was generated whereby dams were exposed to 50 ppm cadmium chloride ($CdCl_2$) for 5 weeks prior to mating with unexposed male mice. Dams were continually exposed to Cd until postnatal day (PND) 10; pups were then sacrificed at PND21. Livers of pups were harvested and evaluated for MASLD and cancer hallmarks using biochemical, histological and molecular methods. **Results:** Although histological analysis did not identify tumors, we demonstrated that livers from Cd-exposed mice exhibited enlarged nuclear size, dysplasia and increased binucleation of hepatocytes and neutrophil accumulation, all of which are morphological changes observed in pre-cancerous and cancerous environments. RNA-seq showed activation of many hallmarks of HCC. We validated RNA-seq data by performing qRT-PCR. Analysis of gene expression showed increased transcript abundance of oncogenic genes, metabolic reprogramming genes, cirrhotic genes and pro-inflammatory genes, and decreased levels of tumor suppressor genes. Among the elevated genes were Inhibitor of Differentiation 1 (*Id1*), *Myc* proto-oncogene, Matrix Metalloproteinases (*Mmp8, Mmp9, Mmp25*), Transforming growth factor beta1 (*Tgfb1*), glycolytic genes (*Hk2, Eno2*), and stemness marker genes (*Cd133, Cd44, Cd29a*). Western blot showed downregulation of p53, a cell cycle arrest

protein. Additionally, increased protein levels of phospho-STAT3, a pro-inflammatory marker and indicator of the proliferative state of the injured livers, was observed. **Conclusions:** Our findings demonstrate that early life exposure to Cd is sufficient to induce molecular and pathological signatures of HCC in young mice. Our data suggest that early life Cd exposure may be a contributory factor to pediatric HCC in humans. Ongoing work using mouse and cell culture models is focused on determining the causative mechanisms that link early life Cd exposure to HCC with a view to identifying therapeutic targets to mitigate the impacts of exposure.

ABSTRACT NUMBER: 5023 **Poster Board Number:** H572

TITLE: The Role of Imprinted *H19* in Programming Perinatal Cadmium-Induced Metabolic Dysfunction-Associated Steatotic Liver Disease

AUTHORS (FIRST INITIAL, LAST NAME) AND INSTITUTIONS: *L. Dameris*[1,2], J. Hartsell[2], *J. R. Chappel*[1], *R. Lichtler*[2], C. M. Gebert[3], K. Pfeifer[3], X. Liu[2], *J. E. Rager*[1], and *M. Cowley*[2]. [1]The University of North Carolina at Chapel Hill, Chapel Hill, NC; [2]North Carolina State University, Raleigh, NC; and [3]Eunice Kennedy Shriver National Institute of Child Health and Human Development (NICHD), Bethesda, MD.

KEYWORDS: Juvenile Toxicity; Metals; Liver; Cadmium

ABSTRACT: Background and Purpose: The most prevalent pediatric liver disease in the U.S. is metabolic dysfunction-associated steatotic liver disease (MASLD). While the pathogenesis of MASLD is well-understood, its etiologies in children are not clear. We have shown that perinatal exposure to the heavy metal cadmium (Cd) is sufficient to program MASLD and fibrosis in juvenile mice. The manifestation of these outcomes is associated with the activation of a network of coordinately-expressed imprinted genes, the imprinted gene network (IGN). One of the most significantly upregulated imprinted genes in our mouse model of perinatal Cd exposure, *H19*, has previously been implicated in MASLD pathogenesis. We hypothesize that H19 is required to program the onset of perinatal Cd-induced MASLD in juvenile mice. **Methods:** To test our hypothesis, we leveraged a novel systemic *H19* knockout (KO) mouse model to determine if *H19* ablation could protect against MASLD in male and female juvenile mice after perinatal exposure to 0 or 30 ppm $CdCl_2$. Elementally, trunk blood was used to quantify the concentrations of essential trace metals. Histologically, we stained sectioned livers to qualitatively examine the liver for morphological changes and the deposition of collagen fibers. Biochemically, we quantified hepatic hydroxyproline, a major component of collagen fibers. We also performed liver lipidomic analyses to identify differentially abundant lipids. Finally, molecularly, we isolated total RNA from the liver to assess expression changes of pertinent genes related to MASLD and the IGN via qRT-PCR. We also performed liver transcriptomics to identify gene pathways associated with MASLD pathogenesis and liver homeostasis. **Results:** In this study, Cd-exposed offspring did not present with overt MASLD phenotypes, as evidenced by unaltered hepatic histomorphology. Biochemically, however, Cd induced MASLD-related outcomes including significantly increased fasting blood glucose levels in males and significantly perturbed lipid abundances in the livers of males and females. Among those lipids altered, we found a significant enrichment of triacylglycerides (TAGs) and of polyunsaturated fatty acids (PUFAs) in both sexes. The expression of hepatic MASLD-related genes was perturbed by Cd such as *Fabp4*, *Dgat2*, *Hmgb1*, and *Col6a1*; RNA-seq analyses found significant alterations in canonical pathways related to MASLD progression and metabolic homeostasis. Further, Cd exposure significantly affected essential metal homeostasis in blood and affected the expression of imprinted genes in the liver. The deletion of *H19*, however, did not appear to modulate the onset of MASLD. Notably, the

expression of *Igf2* dramatically increased in the livers of Cd-exposed *H19* KO mice. Given Igf2's similar metabolic function to H19 in liver disease pathology, it is possible that *Igf2* was able to inhibit the protective effects of *H19* ablation. **Conclusions:** The results of our study showed perinatal exposure to Cd was sufficient to program biochemical and molecular signatures of MASLD, perturb the expression of IGN genes in the liver, and modulate essential metal homeostasis in the blood at PND 21; however, the ablation of *H19* did not reduce the manifestation of these outcomes. Future studies will explore the role of Igf2 and other imprinted genes in driving MASLD in children.

ABSTRACT NUMBER: 5024 **Poster Board Number:** H573

TITLE: Human iPSC-mesendoderm differentiation model reveals possible novel off-targets of cereblon-based molecular glues related to developmental toxicity outcomes

AUTHORS (FIRST INITIAL, LAST NAME) AND INSTITUTIONS: *A. Rengarajan*[1], A. Vogt[2], Y. Feng[1], K. M. Pearson[1], *R. J. Gonzalez*[1], H. Planatscher[2], O. Poetz[2], A. Stermer[1], and *A. G. Aslamkhan*[1]. [1]Merck & Co Inc, West Point, PA; and [2]SIGNATOPE GmbH, Reutlingen, Germany.

KEYWORDS: Developmental/Teratology; Induced Pluripotent Stem Cells; *In Vitro* and Alternatives; Thalidomide; Molecular Glue

ABSTRACT: Background and Purpose: Cereblon-based molecular glues (CRBN-MGs) are therapeutic molecules that work by degrading a protein of interest. A major concern with CRBN-MGs is the potential for causing teratogenicity and developmental toxicity in humans. Thalidomide is a CRBN-MG with documented evidence of babies born with fetal malformations and developmental defects. SALL4 is a key developmental protein that is degraded by CRBN-MGs, and there is evidence that SALL4 degradation may be associated with teratogenicity effects of CRBN-MGs. However, other developmental proteins are also reported to be degraded by CRBN-MGs in the literature, including PLZF and TP63. Targets of CRBN-MGs share a G-loop structure which facilitates the interaction of target, CRBN, and molecular glue. We hypothesize that not all developmental related proteins that are degraded by CRBN-MGs have been identified and are attempting to identify additional proteins in a developmentally relevant model. We leverage an iPSC-mesendoderm developmental model to identify such proteins. **Methods:** Induced pluripotent stem cells (iPSC) were differentiated into a mesendoderm stage in the presence of APEL2 media supplemented with GSK inhibitor (CHIR99021) over 2 days. Cells were treated with DMSO (control), thalidomide, lenalidomide, or pomalidomide over the final 24 hours. Cell lysate was collected and proteolyzed. Peptides were enriched using 20 motif-based TXP antibodies which were selected to enrich peptides from proteins containing G-loop associated sequences. Immunoprecipitated peptides were analyzed with LC-MS/MS and changes with CRBN-MG treatment were identified using Fisher exact test and differential expression analysis. **Results:** SALL4A was reduced in samples treated with thalidomide, lenalidomide, and pomalidomide as expected. Our proteomics results identified ZFP91 and ZBTB39 from iPSC-mesendoderm lysate, two proteins previously shown to be degraded by CRBN-MGs in embryonic stem cells. In total, we identified 16 hits through Fisher analysis and 29 hits through Limma results. Based on phenotypic outcomes observed in mouse knockout models (from publicly available IMPC database), 25 proteins from the combined hits are of potential interest for developmental toxicity. **Conclusions:** We leverage an iPSC-mesendoderm model to identify off-targets of CRBN-MGs related to developmental toxicity and have identified a putative list of 25 proteins. These proteins will be studied further through targeted proteomics assays. It is possible that some of these proteins may explain the differences in malformation effects of CRBN-MGs among preclinical species including mice, rats, rabbits,

and chicken compared to humans. These proteins can potentially be added to panels for use with screening CRBN-MGs in future.

ABSTRACT NUMBER: 5025 **Poster Board Number:** H574
TITLE: Early Developmental Exposure to Liquid Crystal Display Extracts Impacts Zebrafish Locomotive Behavior, Cellular Respiration, and Adiposity

AUTHORS (FIRST INITIAL, LAST NAME) AND INSTITUTIONS: *S. Heldman*[1], *R. Bérubé*[2], *B. Murray*[1], S. Korzeniewski[1], *K. Siegel*[1], and *C. Kassotis*[1]. [1]Wayne State University Integrative Biosciences Center, Detroit, MI; and [2]McGill University School of Biomedical Sciences, Montreal, QC, Canada.
KEYWORDS: Aquatic Toxicology; Reproductive and Developmental Toxicology; Persistent Organic Chemicals; LCM; metabolism disrupting chemical; zebrafish;

ABSTRACT: Background and Purpose: Liquid crystal monomers (LCMs) are ubiquitous environmental contaminants found in food, human breast milk, and serum that are released from the liquid crystal display (LCD) panels of various electronic devices. Such exposures may negatively impact human metabolic health as our lab has previously shown a small subset of commonly detected LCMs, individually and in mixtures, can significantly disrupt the transcriptional activity of nuclear receptors involved in key metabolic pathways as well as induce adipogenesis *in vitro*. Furthermore, early developmental exposure to these adipogenic LCM mixtures was found to increase fat accumulation in larval zebrafish. Building on these findings, we set out to explore whether exposure to LCD panel extracted LCM mixtures would similarly induce metabolic disruption in zebrafish, offering insight into the toxicological effects of exposure to commercially utilized mixtures. **Methods:** LCD panels were isolated from four cellphones, two monitors, and one television collected from local electronic waste collection sites. The iridescent LCM layer was rinsed into a collection vial with a 1:1 hexane:acetone mixture and centrifuged to remove particulate. The resulting supernatant was collected, dried, weighed, and reconstituted in 100% DMSO to a stock concentration of ~2500 µg LCM/mL. To make the cellphone and monitor dosing stocks, equal volumes from each extract of the same device type were pooled. Zebrafish embryos were exposed via spiked embryo media (0.1% DMSO) from 24 hours post fertilization (hpf) to 6 days post fertilization (dpf) to 2.5, 25, 250, or 2500 ng/mL of either the cellphone, monitor, or television extracts. Embryos reared in chemical free embryo media; media spiked with DMSO; and media spiked with either 0.01, 0.1, or 1 nM of tributyltin chloride (TBT); served as negative, vehicle, and positive controls respectively. To explore the acute metabolic impacts of exposure to the LCM mixtures, larval cellular respiration and locomotor behavior were evaluated immediately following exposure, at 6 dpf, using an alamar blue energy expenditure assay and locomotor response test with alternating light/dark periods (LMR-L/D), respectively. At ~30 dpf, larval adiposity (quantified using fluorescence microscopy), wet weight, and standard length were measured to characterize the persistent metabolic health impacts of exposure. **Results:** At 6 dpf, significant 0.73- to 0.84-fold reductions in cellular respiration were observed in larvae exposed to the 25 ng/mL cellphone extract, 2.5 and 2500 ng/mL monitor extracts, and the 250 and 2500 ng/mL television extract relative to vehicle controls. Furthermore, all doses of the cellphone, monitor, and television extracts were found to increase larval locomotor activity by 11-35% in at least one photoperiod relative to vehicle controls. By ~30 dpf, larvae exposed to the 250 ng/mL cellphone extract during early development exhibited significant ($p<0.05$) reductions in weight and length (7% and 31% respectively), as well as a near significant ($p<0.1$) reduction in adipose tissue area (42%). No other doses were found to have any effect on weight, length, or

adiposity. Interestingly, these trends were not observed when weighted quartile regression analysis was used to explore changes in body adiposity adjusted for changes in body size. Instead, significant associations were observed between increased adipose area and early developmental exposure to the 250 and 2500 ng/mL doses of the monitor extract as well as the 2.5 and 2500 ng/mL doses of the television extract. Exposure to these doses produced 93%, 81%, 59%, and 55% increases in adipose area relative to vehicles controls, respectively, which was comparable to or higher than the 46% increase in adipose area observed in larvae exposed to 1 nM of TBT, the positive control obesogen. **Conclusions:** It has yet to be determined whether the unique effects of these extracts are driven by differences in LCM composition or the influence of other confounding contaminants potentially released from the LCD panels. However, similar to the pure LCM mixtures previously evaluated, these results are indicative of exposure-induced disruptions of metabolic homeostasis at environmentally relevant doses, highlighting the clear and urgent need to further evaluate and characterize impacts of cumulative LCM exposure on human health.

ABSTRACT NUMBER: 5026 **Poster Board Number:** H575

TITLE: Lineage Specific Transcriptional Effects of ZYN Extracts Exposure on Human Embryonic Stem Cell Differentiation

AUTHORS (FIRST INITIAL, LAST NAME) AND INSTITUTIONS: *L. B. Bertotto*, *N. Iwobi*, *K. Khanal*, *R. Meletz*, *M. Vera-Colón*, and *N. R. Sparks*. University of California, Irvine, Irvine, CA.

KEYWORDS: Embryonic Stem Cells; Developmental/Teratology; Gene Expression/Regulation

ABSTRACT: Background and Purpose: ZYN is the most widely used nicotine pouch product globally and is marketed as a reduced-harm alternative to conventional tobacco products. Due to its novelty, the potential developmental toxicity of ZYN products remains poorly characterized. Nicotine is a known teratogen and has documented adverse effects on bone development and formation. Here, we used human embryonic stem cells (hESCs; H9 line) to understand the effects of ZYN lineage-specific transcriptional responses during osteoblast differentiation, the bone-forming cell. **Methods:** Human ESCs were differentiated into osteoblasts using 10 mM β-glycerophosphate (βGP), 120 µM ascorbic acid (AA), and 1.2x10-7 M 1,25(OH)2 vitamin D3 (VD3) and concomitantly exposed to extracts from four commercially available ZYN flavors (Original, Smooth, Chill, and Wintergreen) at two different nicotine strengths (3 and 6 mg nicotine). Dose-response analyses identified IC50 concentrations that reduced alkaline phosphatase (ALP) activity and perturbed osteoblast differentiation. Single-cell RNA sequencing was performed to assess transcriptional changes across differentiation-associated cell populations. **Results:** ZYN extract exposure led to 2-9 times more differentially expressed genes (DEGs) in mesodermal/mesenchymal stem cell-associated clusters than in neural crest-associated clusters. Furthermore, in accordance with previous results, Wintergreen 6 mg nicotine exposure resulted in greater transcriptional disruption than all flavors and nicotine strengths tested. **Conclusions:** These findings indicate that Zyn extracts can cause lineage-specific transcriptional alterations during early skeletal differentiation, which may lead to developmental and skeletal harm, raising concerns regarding the presumed safety of nicotine pouch products.

ABSTRACT NUMBER: 5027 **Poster Board Number:** H576

TITLE: Cannabidiol-induced transcriptomic responses in mouse leydig and sertoli cells: mechanistic comparison to human cells

AUTHORS (FIRST INITIAL, LAST NAME) AND INSTITUTIONS: *Y. Li*[1], *X. Li*[1], P. Cournoyer[2], S. Choudhuri[3], *L. Guo*[1], and *S. Chen*[1]. [1]National Center for Toxicological Research, Jefferson, AR; [2]U.S. Food and Drug Administration, Silver Spring, MD; and [3]U.S. Food and Drug Administration, College Park, MD.

KEYWORDS: *In Vitro* and Alternatives; Reproductive System; Testis; Cannabidiol

ABSTRACT: Background and Purpose: Cannabidiol (CBD), a major cannabinoid from *Cannabis sativa L.*, is used clinically to treat seizures associated with Lennox-Gastaut syndrome, Dravet syndrome, and tuberous sclerosis complex in pediatric patients. Male reproductive toxicity of CBD has been reported in several animal models. However, the underlying mechanisms and the relevance of these findings to humans are not well understood. This study aimed to characterize the cytotoxic effects of CBD in mouse testicular cells and compare them with primary human testicular cell responses. **Methods:** Mouse TM3 Leydig cells were exposed to CBD or its major metabolites, 7-hydroxy-CBD and 7-carboxy-CBD, for analysis of cell viability, apoptosis, and the cell cycle. Transcriptomic profiling was performed in TM3 Leydig cells and primary human Leydig cells to identify conserved and divergent molecular responses. Additional transcriptomic analyses were conducted in mouse TM4 Sertoli cells and compared with primary human Sertoli cells to evaluate cell-type specific responses. **Results:** In TM3 Leydig cells, CBD reduced cell viability, induced G1 cell cycle arrest, and inhibited DNA synthesis at concentrations below 30 µM, whereas higher or prolonged exposure led to apoptosis. Similar cytotoxic effects were observed with CBD's major metabolites, 7-hydroxy-CBD and 7-carboxy-CBD. Comparative transcriptomics revealed conserved responses between mouse and human Leydig cells, including mitochondrial and lysosomal dysfunction, oxidative stress, and autophagy activation. In contrast, mouse Sertoli TM4 cells responded differently from primary human Sertoli cells. While human Sertoli cells developed cellular senescence due to inhibited DNA replication, cell cycle progression, and DNA repair, TM4 cells predominantly underwent apoptosis, with activation of immune and cellular stress pathways. **Conclusions:** CBD shows cell-type-specific and species-specific cytotoxicity in testicular cells *in vitro*. Leydig cell responses are largely conserved between mice and humans, whereas Sertoli cells show divergent transcriptomic profiles. These findings highlight key considerations for extrapolating reproductive toxicity data across species and provide mechanistic insight into the potential male reproductive risks associated with CBD exposure.

ABSTRACT NUMBER: 5028 **Poster Board Number:** H577
TITLE: Quantitative Evaluation and Risk Assessment of Heavy Metal Leachate and Absorption from Menstrual Tampon Use

AUTHORS (FIRST INITIAL, LAST NAME) AND INSTITUTIONS: *A. Shakya*, S. Berlinski, and *D. Paustenbach*. TRC Strategic Health Sciences, Jackson, WY.
KEYWORDS: Cutaneous or Skin Toxicity; Exposure Assessment; Metals

ABSTRACT: Background and Purpose: Although menstrual tampons are used by millions worldwide and regulated for decades as Class II medical devices, little empirical work has addressed the potential for systemic exposure to heavy metals via the vaginal route. Recent media reports and litigation have raised concerns that trace metals in tampons, originating from paper or fabrics, could reach systemic circulation and pose health risks. However, most published studies report only bulk metal content and lack data on leaching, mucosal absorption, or health-based dose reconstruction. This study addresses these gaps by providing leachate and absorption data for six heavy metals [lead (Pb), cadmium (Cd), arsenic (As), mercury (Hg), chromium (Cr), and cobalt (Co)] and translating these findings into a quantitative risk assessment under conditions approximating real-world use. Results were compared to established toxicological reference values to assess the adequacy of current regulatory guidance. **Methods:** Six commercial tampons were incubated in 12 mL artificial menstrual fluid at 37 °C for 12 hours. Leachates and acid-digested tampon matrices were analyzed by ICP-MS using validated methods from Charles River Laboratories (SOPs 32006813A/B). Reconstructed human vaginal epithelium (EpiVaginal™ FT) in Franz diffusion cells apparatus was dosed with undiluted leachate and 1,000× and 10,000× fortified solutions conservative upper-bound conditions. Tissues (n=6/group) were maintained for 12 hours, with TEER measured pre- and post-dose to confirm barrier integrity. Receptor fluids, rinsates, and tissue digests were analyzed by ICP-MS. Absorption data were incorporated into Average Daily Dose (ADD) and Hazard Quotient (HQ) calculations following U.S. EPA dermal risk guidance (RAGS Part E). Exposure assumptions reflect typical use scenarios (six tampons per day, 5 days per cycle, 12 cycles per year, 40-year duration, 60 kg body weight). **Results:** Trace levels of all six metals were detected in whole tampon digests, with geometric mean concentrations (ng/g) of 5.2 As, 3.7 Cd, 13.0 Co, 168 Cr, 88.7 Pb, and 13.7 Hg. Leachate concentrations (ng/mL) were all below quantification limits (As 0.37, Cd 0.35, Co 1.78, Cr 2.10, Pb 2.69, Hg 0.22). Following exposure of EpiVaginal™ tissues to leachates, no metals were quantifiable in receptor fluids indicating negligible trans-epithelial metal penetration. Under fortified exposures, metal levels in receptor fluid remained near detection limits and were not dose-responsive. Mass-balance analysis showed most metal content was recovered in apical rinse (50-90%), with limited quantities present in the tissues (≤10-40%), and minimal receptor fluid recovery (≤0-5%). TEER values declined post-dose but remained within the high-resistance range, indicating no compromise of epithelial barrier integrity. Modeled ADDs were orders of magnitude below U.S. EPA reference doses, with HQs well under 1 across all scenarios. **Conclusions:** The data show that metals in tampons are present only at trace levels, exhibit virtually no measurable leaching into artificial menstrual fluid, and do not permeate the vaginal epithelium under simulated-use conditions. The estimated absorption of metals was far below toxicological thresholds established by the U.S. EPA and WHO, indicating that tampon use is not a meaningful contributor to overall heavy-metal exposure. When comparing relative source contributions of metal intake, our findings indicate that tampon use contributes far less than <0.1% of daily metal intake relative to food and drinking water on days of use, with an even smaller contribution to chronic intake based on typical frequency of use. These findings

support the adequacy of current regulatory standards governing tampon manufacture and labeling and reaffirm that the presence of trace elements does not equate to toxicological risk for the user. In short, claims made in related litigation had no apparent scientific foundation. Clear and accurate communication of these types of data is essential for maintaining consumer confidence and for producing evidence-based public health decision making.

ABSTRACT NUMBER: 5030 **Poster Board Number:** H579
TITLE: Human Placental Trophoblasts as a Target of PFOA Toxicity: Oxidative Stress, Apoptosis, and Hormonal Dysregulation

AUTHORS (FIRST INITIAL, LAST NAME) AND INSTITUTIONS: *P. Kini*, *A. Ofosu*, B. Gibson, D. Liles, *A. Ishaque*, and A. Elnabawi. University of Maryland Eastern Shore, Princess Anne, MD.
KEYWORDS:

ABSTRACT: Background and Purpose: Per- and polyfluoroalkyl substances (PFAS) are persistent environmental contaminants widely detected in human serum, placenta, amniotic fluid, and umbilical cord blood. Perfluorooctanoic acid (PFOA), one of the most used PFAS in the United States, is linked to reproductive toxicity in males and females, affecting hormone levels, fertility, and offspring development. The placenta serves as the primary interface regulating nutrient transport, hormone production, immune tolerance, and oxidative balance throughout pregnancy. Disruption of placental structure or function can compromise pregnancy maintenance, fetal development and long-term health effects. Oxidative stress is of relevance to placental toxicity, as excessive reactive oxygen species (ROS) production can overwhelm antioxidant defenses, leading to trophoblast apoptosis, impaired hormone synthesis, and placental insufficiency. Apoptosis is a tightly regulated process required for normal placental development; however, excessive activation of apoptotic pathways has been associated with pathological pregnancies. Human chorionic gonadotropin (hCG) is a critical placental hormone essential for implantation, trophoblast differentiation, and maintenance of early pregnancy. Altered hCG secretion is a sensitive indicator of trophoblast dysfunction and has been associated with adverse pregnancy outcomes. Despite growing evidence implicating PFAS in reproductive toxicity, the cellular mechanisms by which PFOA disrupts placental endocrine function and trophoblast survival remain incompletely understood. This study aimed to examine the effects of PFOA on cell viability, oxidative stress, the release of hCG, and apoptosis in the human placental trophoblast (BeWo) cells. **Methods:** BeWo cells were treated with various concentrations of PFOA for different time intervals. Hydrogen peroxide (H_2O_2) served as a positive control. Cell viability and death were assessed alongside intracellular ROS production, caspase-3 activity, hCG release, and apoptotic responses. Mechanistic involvement of oxidative stress and caspase-3 activation was evaluated using N-acetyl-L-cysteine (NAC) and the caspase-3 inhibitor Ac-DEVD-CHO. **Results:** PFOA significantly reduced cell viability in a concentration-dependent manner after 24 hours. Low concentrations of PFOA (0.00001-1 μM) significantly increased ROS generation in a time-dependent manner; this effect was attenuated by NAC. PFOA exposure significantly increased caspase-3 activity and apoptosis in a time- and concentration-dependent manner, both of which were significantly reduced by NAC or Ac-DEVD-CHO, indicating oxidative stress-mediated, caspase-3-dependent apoptosis. Exposure of BeWo cells to PFOA significantly decreased hCG levels, indicating impaired trophoblast function. **Conclusions:** These findings indicate that PFOA could disrupt placental function, which in turn, could lead to adverse effects on pregnancy outcome, fetal development, and possibly long-term effect in adult life. Supported by Title III

ABSTRACT NUMBER: 5031 **Poster Board Number:** H580

TITLE: Transcriptomic Impacts of Lead Exposure on the Murine Uterus during Pregnancy

AUTHORS (FIRST INITIAL, LAST NAME) AND INSTITUTIONS: M. R. Rea[1], S. Varma[1], C. Thach[1], A. Tapaswi[1], *D. C. Dolinoy*[1], *J. A. Colacino*[1], *B. P. Perera*[1,2], and *S. M. Harris*[1]. [1]University of Michigan, Ann Arbor, MI; and [2]University of California, Berkeley, Berkeley, CA.

KEYWORDS: Reproductive and Developmental Toxicology; Toxicogenomics; Metals; Lead

ABSTRACT: Background and Purpose: Lead is a widespread environmental pollutant. Exposure occurs through paint dust, industrial processes, and drinking water contaminated by lead pipes. Detrimental effects to many organ systems have been identified, including neurological, reproductive, and immunological systems. Lead exposure is also associated with adverse pregnancy outcomes (APOs) like preeclampsia, preterm birth, and miscarriage. However, the mechanisms and organ-specific effects underlying these associations are poorly understood, including impacts on the uterine environment during pregnancy and how they may connect to APOs. This study seeks to explore these effects on the uterine environment during pregnancy, including on the uterine immune system, which is critical for many processes of healthy pregnancies. **Methods:** Adult female C57BL/6J mice (6-8 weeks old) were exposed to either control or lead acetate drinking water at 32 ppm beginning two weeks before mating and continuing through gestational days 10-12. Dams were euthanized at gestational days 13-15 and uterine tissue proximal to embryos was collected and flash frozen. RNA was extracted, and bulk RNA sequencing was performed (n=18 controls, n= 19 lead treated). Raw sequencing data was mapped to the mouse genome before downstream analyses were performed. Differential gene expression analysis was conducted using the "edgeR" package followed by gene set enrichment analysis using "msigdbr" and "fgsea" to identify highly annotated biological pathways. Transcription factor (TF) enrichment analysis of all differentially expressed genes (DEGs) with FDR < 0.05 was conducted via Enrichr. Immune system genes were referenced from the Mouse Genome Informatics database, using the GO:0002376 gene set. **Results:** 12,070 genes were identified in bulk RNA sequencing. Between control and lead treated groups, 206 DEGs were identified (logFC > or < 0, FDR < 0.05). Highly downregulated genes include *Slc13a1*, *Slc34A2*, and *Dcdc2a* (logFC < -1.56). Highly upregulated genes include *Thrsp*, *Upk1a*, and *Scd1* (logFC > 3.24). GSEA revealed these DEGs were enriched for pathways including sulfur compound metabolism, phosphate metabolism and transport, embryonic development, lipid metabolism, and immune system regulation ($p < 0.05$), processes which are all important for uterine development and function throughout pregnancy. Highly enriched TFs include Rbl2, Brca1, and E2f4 (odds ratio > 24, p-value < 0.05). Each of these TFs plays a role in cell cycle regulation and cell proliferation, which are critical for uterine development and pregnancy maintenance. As lead has known immunotoxic effects and the uterine immune system plays a significant role in the establishment and maintenance of pregnancy, differential gene expression analysis was conducted on a subset of 1,886 immune system genes identified in the RNA sequencing. 26 genes (12.62% of all DEGs) were differentially expressed between lead and control groups (logFC > or < 0, FDR < 0.05). Highly downregulated genes include *Ch25h*, *Gbp3*, and *Racgap1* (logFC < -0.75), and are involved in processes including lipid metabolism, cell proliferation and cancer growth, and inflammasome regulation and antiviral activities. Highly upregulated genes include *Ighα*, *Igκc*, and *Jchain* (logFC > 2.61), which are involved in antibody production, immune cell differentiation, and immunoglobulin complexes. **Conclusions:** This research identifies lead-induced alterations in biological pathways in the pregnant uterus that may contribute to APOs. For example, downregulation of *Slc13a1*, a gene important for sulfate distribution, may contribute to reduced fetal

growth through reduced maternally circulating sulfate. Upregulation of *Up1ka*, a gene involved in stabilization of the urothelial lining, has been associated with very early spontaneous preterm birth. Similarly, dysregulation of the immune system and inflammation at the maternal-fetal interface, including the uterine environment, can contribute to APOs. The functional outcomes of the transcriptomic changes observed in this study have all been associated with these APOs: decreased inflammasome and anti-pathogenic activities as well as increased antibody production and immune cell differentiation have been associated with preterm birth, preeclampsia, and miscarriage.

ABSTRACT NUMBER: 5032 **Poster Board Number:** H581

TITLE: The effects of a 15month chronic exposure to diisononyl phthalate (DiNP) on the uteri in female mice

AUTHORS (FIRST INITIAL, LAST NAME) AND INSTITUTIONS: C. N. Sexton, *L. Y. Parra Forero*, D. N. Juarez, *S. Ibrahim*, A. R. Andrus, *M. J. Laws*, *J. A. Flaws*, and *R. A. Nowak*. University of Illinois Urbana-Champaign, Champaign, IL.

KEYWORDS: Phthalates; Endocrine Disruptors; Reproductive Tract; Female

ABSTRACT: Background and Purpose: Phthalates are a class of chemicals known for their endocrine-disrupting properties, including mimicking or antagonizing hormones and interfering with biological processes. Phthalates are commonly found in plastics, where they are used to improve flexibility and durability. Humans are subject to daily exposure to phthalates through ingestion, dermal contact, and inhalation in a variety of everyday products. The aim of this study was to determine how long term, chronic exposure to Diisononyl Phthalate (DiNP) would affect uterine morphology, cell proliferation, inflammation and fibrosis-related gene expression. **Methods:** Over a fifteen-month period, 40-45-day old CD-1 mice were fed chow containing 0.15 ppm DiNP, 1.5 ppm DiNP, 1500 ppm of DiNP, or a vehicle control, daily. After the dosing period, the mice were euthanized in diestrus, and the uteri were collected for histology and RNA isolation. Quantitative PCR was carried out to quantify changes in expression of genes associated with inflammasome-associated signaling (*Il18*, *Il1b*, *Nlrp3*), inflammation (*Il6* and *Il10*), fibrosis (*Tgfb1*, *Tgfb3*, *Col1a1*, *Col3a1*, *Col4a1*, *Itgb1*/Integrin beta-1, *Bgn*/Biglycan), and oxidative stress (*Sod1*, *Cat*, *Gpx1*, and *Prdx2*). **Results:** Consistent upregulation of expression of *Gpx1*, *Prdx2*, *Il18*, and *Itgb1* was observed across all DiNP exposure groups. In contrast, expression of *Il6* was markedly reduced across all treatment groups. Exposure to 1.5 ppm DiNP also showed upregulation of *Cat*, *Sod1*, *Col4a1* and *Bgn*, while the highest DiNP exposure treatment of 1500 ppm was associated with significantly increased expression of *Sod1*, *Col4a1* and *Tgfb3*. **Conclusions:** These results demonstrate that long term chronic exposure to DiNP leads to increased oxidative stress responses, altered inflammatory gene expression and upregulation of genes associated with extracellular matrix remodeling and fibrosis in the uterus, likely in response to the increased oxidative stress and inflammatory signaling. Immunohistochemistry is currently underway to assess the effects of chronic exposure to DiNP on cell proliferation and macrophage infiltration in the uterus. (Funded by NIH ES034112 to RAN and JAF, NIH T32 ES007326 to ARA, and a Toxicology Scholarship to SI).

ABSTRACT NUMBER: 5033 **Poster Board Number:** H582

TITLE: Chronic Exposure to Di(2-ethylhexyl) Phthalate Leads to Increased Inflammation in the Uterus of Mice

AUTHORS (FIRST INITIAL, LAST NAME) AND INSTITUTIONS: A. R. Andrus[1], L. Y. Parra-Forero[1], C. N. Sexton[1], *S. Ibrahim*[1], K. C. Liu[1], S. M. Rush[1], *M. J. Laws*[2], *J. A. Flaws*[2], and *R. A. Nowak*[1]. [1]University of Illinois Urbana-Champaign, Department of Animal Sciences, Urbana, IL; and [2]College of Veterinary Medicine at the University of Illinois Urbana-Champaign, Department of Comparative Biosciences, Urbana, IL.

KEYWORDS: Endocrine Disruptors; Phthalates; Reproductive Tract; Female; DEHP and DiNP

ABSTRACT: Background and Purpose: Phthalates are a class of synthetic compounds known as endocrine-disrupting chemicals (EDCs), meaning they are exogenous substances that alter the functions of the endocrine system. They are frequently used in consumer products such as personal care items, medical equipment, and food products. One of the most common phthalates is di(2-ethylhexyl) phthalate (DEHP), a plasticizer used to improve the flexibility and durability of numerous plastics. DEHP exposure has been shown to have negative effects on female reproductive health, likely due to its EDC properties. The goal of this study was to investigate the impacts of chronic DEHP exposure on the female reproductive tract of mice with a focus on inflammation and oxidative stress responses. **Methods:** Over a 9-month period, adult female CD-1 mice were dosed with DEHP (0, 0.15 ppm, 1.5 ppm, or 1500 ppm) incorporated into the rodent chow. After 9 months exposure, the mice were euthanized when they were in diestrus, and the uteri were collected for histology and RNA analysis. Fixed tissue sections were stained with hematoxylin and eosin to measure morphological changes. Immunohistochemistry was performed for the proliferation marker Ki67, for the smooth muscle cell and pericyte marker α-smooth muscle actin, and the macrophage marker CD68. Quantitative PCR (qPCR) was used to investigate changes in the levels of expression of genes associated with the inflammasome (*IL-18*, *IL-1β, Nlrp3*), with inflammation (*IL-6 and IL-10*), and with regulation of responses to oxidative stress (*Sod1*, *Cat, Gpx1, and Prdx2).* Data were normalized to the housekeeping genes *GAPDH* and *Rplp0* (n=6/treatment group). **Results:** No change in expression was seen for inflammasome or oxidative stress-related genes. However, the highest dose of DEHP (1500 ppm) resulted in a downregulation of *IL-10* expression, while the 1.5 ppm dose resulted in upregulation of *IL-6* expression. Histological analysis for α-smooth muscle actin showed that chronic exposure to DEHP did not alter the thickness of the inner or outer myometrium. Immunostaining for Ki67 revealed that the 1.5 ppm and 1500 ppm doses increased cell proliferation in the luminal epithelial cells. Analysis of CD68 staining showed a significant increase in macrophage infiltration in the 1.5 ppm exposure group. **Conclusions:** These results indicate that chronic exposure to DEHP leads to increased inflammation in the uteri of mice. (Funded by NIH ES034112 to RAN and JAF, NIH T32 ES007326 to ARA, and a Toxicology Scholarship to SI).

ABSTRACT NUMBER: 5034 **Poster Board Number:** H583
TITLE: Chronic Exposure to Di(2-ethylhexyl) Phthalate Promotes Progressive Uterine Fibrosis in Mice

AUTHORS (FIRST INITIAL, LAST NAME) AND INSTITUTIONS: *S. Ibrahim*, *L. Y. Parra Forero*, E. Sizemore, C. N. Sexton, A. R. Andrus, *M. J. Laws*, *J. A. Flaws*, and R. A. Nowak. University of Illinois Urbana Champaign, Urbana, IL.
KEYWORDS: Phthalates; Endocrine Disruptors; Reproductive System

ABSTRACT: Background and Purpose: Di-(2-ethylhexyl) phthalate (DEHP) is a widely used plasticizer and endocrine-disrupting chemical with known reproductive toxicity, for which ingestion is the most common route of exposure. While acute developmental effects of DEHP have been studied, the consequences of chronic, long-term exposure on uterine fibrotic remodeling, particularly with aging, remain poorly understood. This study investigated whether prolonged oral exposure to DEHP induces fibrosis associated molecular and structural changes in the uterus. **Methods:** Adult CD-1 female mice (n=6/group) were orally dosed with vehicle (corn oil), 0.15 ppm, 1.5 ppm, or 1500 ppm DEHP in the chow for 9 or 15 months. Mice were euthanized during diestrus. Uterine tissues were collected for gene expression and histological analyses. Quantitative PCR (qPCR) was performed to assess genes associated with profibrotic signaling and fibroblast activation (*Tgfb3* and *Tgfb1*), extracellular matrix (ECM) production and deposition (*Col1a1, Col3a1, Col4a1*), and cell matrix adhesion and tissue remodeling (*Itgb1*, *Biglycan*). Histological assessment was conducted using Masson's trichrome staining, which was quantitatively analyzed using Image J to measure collagen deposition, and picrosirius red staining was used to qualitatively evaluate collagen type I and type III organization. Slides were scanned using Hamamatsu NanoZoomer 2.0 HT and Axioscan Z1 systems, and statistical analyses were performed using GraphPad Prism 9.4.0 with significance set at $p<0.05$. **Results:** Chronic DEHP exposure resulted in duration dependent alterations in fibrosis associated gene expression. At 9 months, *Tgfb3* was significantly upregulated at 1500 ppm DEHP, while *Col4a1* expression was significantly increased at all DEHP doses, with no significant changes observed in *Col1a1* or *Col3a1* compared to controls. *Itgb1* expression was significantly downregulated at all DEHP doses, whereas *Biglycan* was significantly upregulated at 1500 ppm DEHP compared to controls. Following 15 months of exposure, fibrotic responses were more pronounced, with significant upregulation of *Itgb1* at 1.5 and 1500 ppm DEHP and increased *Col1a1* expression at 1500 ppm, while *Col3a1* and *Col4a1* were not significantly altered compared to controls. Masson's trichrome staining revealed no significant differences, but a borderline increase at 1500 ppm DEHP ($p= 0.06$) at 9 months and picrosirius red staining revealed subtle alterations in collagen I and III organization at 9 months compared to controls. **Conclusions:** Collectively, these findings demonstrate that chronic DEHP exposure induces progressive, time dependent molecular signatures of uterine fibrotic remodeling, potentially mediated in part through TGF-β associated and inflammatory signaling pathways, highlighting the importance of considering long term environmental chemical exposure in the context of uterine aging and reproductive health. (Funded by NIH ES034112 to RAN and JAF, NIH T32 ES007326 to ARA, and a Toxicology Scholarship to SI)

ABSTRACT NUMBER: 5035 **Poster Board Number:** H584

TITLE: Experiences with a Desk Based Programme to Determine Endocrine Disruption potential according to the CLP regulation

AUTHORS (FIRST INITIAL, LAST NAME) AND INSTITUTIONS: *B. L. Ross*[1], M. Matzke[1], J. Marshall[1], J. Miller[1], K. B. Paul[1], P. Remuzat[2], S. Watters[1], and D. S. Carson[1]. [1]Blue Frog Scientific Limited, Edinburgh, United Kingdom; and [2]Blue Frog Scientific SAS, Lyon, France.

KEYWORDS: Endocrine Disruptors; Chemical Hazard Assessment; Regulatory Science/Regulatory Toxicology; Endocrine Disruption Assessment

ABSTRACT: Background and Purpose: With implementation of new endocrine disruption (ED) hazard classes in the CLP regulation (Regulation (EC) No 1272/2008) and the increasing regulatory scrutiny under REACH (EU & UK), the Biocidal Products Regulation (BPR) and the Plant Protection Products Regulation (PPPR), ED Assessment of substances/actives must be proactively addressed to ensure compliance and market access. **Methods:** Using expert judgement based on extensive collective technical and regulatory knowledge and experience, alongside key regulatory guidance documents, we developed a pragmatic, stepwise approach to assessment of ED properties based on available or alternative information. This tiered approach, from initial screening (Phase I) to full ED assessment (Phase II), aids in the fulfilment of the requirements under the new CLP hazard classes, avoids additional animal testing, and aligns with state of the art of scientific regulatory science. **Results:** In brief, Phase I includes a search & rapid review to identify potentially relevant data from the open literature, evaluation of selected literature to retrieve relevant and reliable information, database searches and a bespoke programme of *in silico* profiling. From the assembled information, lines of evidence are collated in a structured format, which allows for integration and interpretation of all available information according to Conceptual Framework (CF) Level and modality, in accordance with the ECHA/EFSA Guidance (2018). The next step is then to screen for adverse effects to human health and environmental species that may be plausibly linked to an endocrine mode of action and thus considered as contributory evidence for classification as an endocrine disruptor. Phase I is concluded with a screening report summarising the available data, its interpretation, any conclusions and an options analysis if relevant. At this point, if sufficient evidence to support a conclusion is identified the process stops. Alternatively, a Phase II full ED assessment commences if justified. **Conclusions:** Using examples based on real-life experience, we demonstrate how this structured flow of activities allows us to support pragmatic assessment of complex datasets. Through this, we are able to generate robust, coherent conclusions on ED which are in compliance with the new CLP requirements for hazard communication on endocrine disruption, and support longevity of registration for applicants.

ABSTRACT NUMBER: 5036 **Poster Board Number:** H585

TITLE: Structural Signatures of Endocrine Disrupting Chemicals: Linking Chemical Architecture to Thyroid and Reproductive Health

AUTHORS (FIRST INITIAL, LAST NAME) AND INSTITUTIONS: *I. A. Sheikh*[1], I. H. Bhat[2], T. A. Zughaibi[1], *A. Abdelmoneim*[3], M. Beg[1], *M. A. Ghorab*[4], S. A. Alharthy[1], and *A. M. Kadry*[5]. [1]King Abdulaziz University, Jeddah, Saudi Arabia; [2]University of Bahrain, Zallaq, Bahrain; [3]Louisiana State University, Baton Rouge, LA; [4]University of California, Davis, CA; and [5]University of Maryland, College Park, MD.

KEYWORDS: Endocrine Disruptors; Environmental Toxicology; Mechanisms

ABSTRACT: Background and Purpose: Endocrine-disrupting chemicals (EDCs) represent a chemically diverse group of environmental agents capable of disrupting endocrine hormone signaling, with some specifically targeting thyroid and reproductive pathways. Within major classes such as polybrominated diphenyl ethers (PBDEs), bisphenols, phthalates, alternative plasticizers, and pyrethroids, individual compounds display marked differences in molecular architecture that can substantially influence biological activity. Understanding how these structural variations govern interactions with hormone-regulating proteins is essential for elucidating mechanisms of endocrine disruption and for distinguishing compounds with genuine biological relevance from structurally similar but functionally inactive analogues. **Methods:** Protein and ligand structures were retrieved from the Protein Data Bank and PubChem and prepared using the Schrödinger 2019 suite. Protein preparation involved addition of hydrogens and charges, removal of water molecules, optimization of hydrogen-bonding networks, and energy minimization, while ligands were prepared using LigPrep to generate energetically favorable conformations. Protein-ligand interactions were examined using the Induced Fit Docking workflow, which allows flexibility of both the ligand and the binding site through grid generation, constrained protein minimization, Glide docking, side-chain refinement, and redocking. Binding free energy was estimated using the MM-GBSA method implemented in the Prime module. The resulting complexes were further analyzed to characterize hydrogen-bonding, hydrophobic and electrostatic interactions, ligand orientation, and complex stability, enabling mechanistic assessment of structure-function relationships for representative endocrine-disrupting chemicals interacting with hormone-regulating proteins. **Results:** The analyses revealed distinct and class-specific molecular interaction patterns, showing that even subtle variations in molecular geometry, substituent positioning, and functional group orientation can markedly influence binding affinity and receptor selectivity. Differences in molecular flexibility and conformational adaptability further affected ligand accommodation, binding stability, and complex dynamics. Collectively, these features defined characteristic structural signatures that govern target recognition and provide mechanistic insight into the differential modulation of thyroid and reproductive hormone signaling pathways. **Conclusions:** These findings establish a clear relationship between chemical architecture and endocrine-disrupting potential, highlighting specific molecular features that may contribute to dysregulation of thyroid and reproductive systems. By integrating structure-based binding characterization with mechanistic interpretation, this work offers a predictive framework for prioritizing emerging EDCs for toxicological evaluation and supports the development of safer chemical alternatives. More broadly, the study underscores the value of structure-guided approaches in advancing mechanistic toxicology and informing risk-relevant chemical screening strategies. *** Correspondence**: Ishfaq Ahmad Sheikh, King Fahd Medical Research Center, King Abdulaziz University, P.O. Box 80216, Jeddah-21589, Saudi Arabia. E-mail: iasheikh@kau.edu.sa

ABSTRACT NUMBER: 5037 **Poster Board Number:** H586

TITLE: Perinatal exposure to organophosphate flame-retardants and chronic variable mild stress on cognition and anxiety-like behavior in male and female mice

AUTHORS (FIRST INITIAL, LAST NAME) AND INSTITUTIONS: *K. Wiersielis*, and S. Newman. The Pennsylvania State University, University Park, PA.

KEYWORDS: Endocrine Disruptors; Behavior; Developmental Toxicity; Prenatal; Developmental Toxicity; Post-Natal; Organophosphate Flame Retardants

ABSTRACT: Background and Purpose: Endocrine disrupting compounds are environmental chemicals that interfere with typical endocrine function. Among these, flame retardants are of particular concern due to their interactions with steroid and nuclear receptors. Humans are routinely exposed to flame retardants through everyday items such as furniture, clothing, toys, and electronics. A widely used class of flame retardants, organophosphate flame retardants (OPFRs), have been shown to alter adult behavior in rodents following developmental exposure. Previously, we observed that male mice perinatally exposed to OPFRs exhibited a trending reduction in locomotor activity, whereas females showed a significant increase in the open field test. Additionally, males perinatally exposed to OPFRs displayed anxiolytic-like behavior in the elevated plus maze. Despite these findings, the interaction between perinatal OPFR exposure and stress remains poorly understood. The purpose of this study was to evaluate the combined effects of perinatal OPFR exposure and adult chronic variable mild stress on cognition and anxiety-like behavior in male and female mice. **Methods:** Male and female adult offspring were perinatally exposed to a mixture of OPFRs (tris(1,3-dichloro-2-propyl)phosphate, triphenyl phosphate, tricresyl phosphate) or vehicle (1mg/kg/day) from gestational day 7 to postnatal day (PND)14. To investigate the combined effects of developmental chemical exposure and stress, a 6-week chronic variable mild stress (CVMS) paradigm was implemented from PND 49 to PND 91 on offspring. Starting at PND 92, offspring were assessed on anxiety-like behavior using the open field test, while cognition was evaluated using the Y-maze, spatial object recognition (SOR), novel object recognition (NOR), and short- and long-term memory Barnes maze. **Results:** Behavioral results revealed that OPFR and CVMS treated females spent less time in the center of the open field, less percentage of time in the unknown arm of the Y-maze, and showed reduced time exploring the displaced object in the SOR. This suggests a sex-, stress-, and OPFR-induced increase in anxiety-like behavior as well as impaired spatial navigation and spatial object orientation. OPFR and CVMS treated males displayed reduced time and bouts with the displaced object in the SOR, and a reduction in time spent with the novel object in the NOR. In males, this indicates deficits in spatial object orientation as well as hippocampal-independent object orientation memory. We did not detect any differences in the short- or long-term memory Barnes maze. **Conclusions:** Perinatal OPFR exposure produces long-lasting, sex-specific effects on cognition and anxiety-like behavior, which are further modulated by chronic variable mild stress in adulthood. These findings suggest that developmental chemical exposure can interact with later-life stress to influence behavioral outcomes, highlighting the importance of considering both early-life environmental insults and adult stressors in studies of neurodevelopmental toxicity. Future studies will examine underlying structural changes through dendritic spine density analysis in the hippocampus and prefrontal cortex.

ABSTRACT NUMBER: 5038 **Poster Board Number:** H587
TITLE: Bayesian Network Modeling for Developmental Neurotoxicity *in vitro* data

AUTHORS (FIRST INITIAL, LAST NAME) AND INSTITUTIONS: K. T. Truong, *M. Feshuk*, and *K. Carstens*. US EPA, Durham, NC.
KEYWORDS: Neurotoxicity; Developmental

ABSTRACT: Background and Purpose: A battery of *in vitro* assays was developed to measure developmental neurotoxicity (DNT) potential for critical neurodevelopmental processes, including proliferation, differentiation, migration, apoptosis, neurite outgrowth (NOG), synaptogenesis, and neural network formation. Due to the complexity of these processes, these assays use different cell models (e.g., human/ rodent) and detection platforms, resulting in a highly complex set of endpoints. Presently, only a subset of chemicals has been tested across the full battery of assays, and even fewer with *in vivo* DNT-relevant evidence for benchmarking, which makes building and validating DNT predictive models difficult. In this work, the DNT *in vitro* battery (IVB) data landscape was leveraged to build a DNT predictive model using a Bayesian network (BN) approach. BN models can encode conditional dependencies between variables within a directed acyclic graph, allowing for probabilistic inference and offering advantages when working with small, uncertain, or missing datasets. **Methods:** The DNT IVB in ToxCast (invitrodb v4.3) is comprised of 18 distinct assays (66 endpoints) that map to 7 neurodevelopmental processes, with a total of 510 chemicals tested in at least one assay. The data was evaluated to inform data pre-processing, e.g., concordance between assays measuring the same neurodevelopmental process. For the BN model, a network structure was constructed based on expert knowledge in which the nodes represented each DNT neurodevelopmental process, with an additional node capturing 'DNT potential' based on reference chemicals. The directed edges encoded the biological relationships and probabilistic dependencies between the nodes. The network structure was trained on ToxCast bioactivity data and a set of 120 expert-curated reference chemicals with evidence (or lack) of *in vivo* DNT (89 positives/ 31 negatives). BN models were trained on either bioactivity hitcalls (discrete) or an efficacy metric (Gaussian). The posterior probabilities of the 'DNT potential' node were queried to inform the classification as a putative DNT 'positive' or 'negative'. The sensitivity (sens), specificity (spec), and balanced accuracy (BA) were calculated to evaluate the performance of the models. The results of the BN models were compared to a rudimentary approach ('1 hit') that has been previously used to classify a DNT chemical: a chemical was considered 'positive' if it was active in at least one (out of 66) DNT IVB endpoint. Lastly, a random forest (RF) model was explored to understand the most important feature for classifying DNT chemicals. **Results:** Of the 510 chemicals tested in at least one DNT IVB assay, 200 chemicals were tested across all DNT IVB neurodevelopmental processes. Chemical-endpoint hitcalls across cell models measuring the same neurodevelopmental process revealed concordance ranging from 64% to 98%. Based on this result, a chemical was defined as active in the neurodevelopmental process if active in any assay to improve the sensitivity of the model. Comparing the two BN models, the discrete model performed with a BA of 71% (sens: 72%, spec: 71%) and the Gaussian model performed with a BA of 79% (sens: 65%, spec: 94%), noting a higher specificity but lower sensitivity in the Gaussian model. For the '1 hit' approach, a BA of 65% (sens: 81%, spec: 48%) was achieved, suggesting that the '1 hit' approach was more sensitive compared to the BN models, at the loss of specificity. Neural network formation was found to be the most informative process for DNT classification based on RF feature importance ranking. **Conclusions:** This work demonstrates that the implementation of BN modeling with the DNT IVB data supports the classification of putative *in vivo* DNT

reference chemicals compared to a '1 hit' rule. Optimal model selection may depend on whether the user prioritizes sensitivity versus specificity. BN modeling offers advantages for regulatory assessment, providing transparent, interpretable results that quantify uncertainty and integrate expert judgement with limited data. Moreover, BN models can be updated as new data becomes available. Overall, this work contributes to an effort to build confidence in the DNT IVB data for regulatory decision-making. Disclaimer: The views expressed in this abstract are those of the authors and do not necessarily represent the views or policies of US EPA.

ABSTRACT NUMBER: 5039 **Poster Board Number:** H588
TITLE: Postnatal Bisphenol A Exposure Alters Myelination Trajectories: A High-Field MRI Study

AUTHORS (FIRST INITIAL, LAST NAME) AND INSTITUTIONS: *A. D. Edmondson*[1,2], J. Levoy[1], E. Fugate[1], and D. Lindquist[1]. [1]Cincinnati Children's Hospital Medical Center, Cincinnati, OH; and [2]University of Cincinnati College of Medicine, Cincinnati, OH.
KEYWORDS: Endocrine Disruptors; Neurotoxicity; Developmental; MRI; Bisphenol A

ABSTRACT: Background and Purpose: Epidemiological research suggests a link between childhood anxiety and early-life exposure to endocrine-disrupting chemicals (EDCs), specifically bisphenol-A (BPA). However, co-exposure to multiple EDCs in human cohorts makes it difficult to isolate BPA's specific neurodevelopmental effects. Because BPA influences oligodendrocyte differentiation and maturation, we established a translational rat model using high-resolution neuroimaging to investigate how postnatal BPA exposure affects myelination and anxiety-like behavior. **Methods:** Sprague-Dawley rats (n=115; 53% female) were dosed via oral gavage with BPA (control, 2.5, 25, or 250 µg/kg-bw) starting on postnatal day 1 (PND 1). High-resolution 2D T2-weighted (T2w) MRI and diffusion tensor imaging (DTI; 6 directions) were acquired at PND 30, PND 60, and PND 90 using a 7T Bruker scanner. Images were registered to the SIGMA atlas for precise anatomical segmentation. For each dose × sex × timepoint group, ROI-to-ROI correlation matrices were generated to evaluate whole-brain myelination patterns. Developmental trajectories were compared across groups using Spearman correlation coefficients. **Results:** Preliminary analyses show high intra-group similarity across all BPA-dosed cohorts, which collectively diverge from control trajectories. Strikingly, PND 30 BPA-exposed brains exhibit myelination profiles that more closely resemble PND 90 controls than age-matched animals, suggesting dysregulated white matter maturation. These trends persist across both sexes and all doses, indicating a possible dose-independent shift in the developmental "myelination clock." **Conclusions:** Early findings indicate that postnatal BPA exposure may shift the temporal trajectory of white-matter development, potentially predisposing animals to anxiety-related phenotypes. This analytical pipeline provides a translational approach for linking rodent neuroimaging biomarkers to human clinical outcomes in toxicology research.

ABSTRACT NUMBER: 5040 **Poster Board Number:** H589

TITLE: Developmental Exposure to 3,3'-Dichlorophenyl (PCB 11) Differentially Modulates Astrocytic Reactivity in C57BL/6J vs. *Cyp2abfgs*-null Juvenile Mice

AUTHORS (FIRST INITIAL, LAST NAME) AND INSTITUTIONS: *R. Mendieta*[1], *R. J. Wilson*[1], *Y. Tsai*[1], *A. Venezuela*[1], *X. Ding*[2], *H. Lehmler*[3], and *P. J. Lein*[1]. [1]University of California, Davis, CA; [2]University of Arizona, Tucson, AZ; and [3]University of Iowa, Iowa City, IA.

KEYWORDS: Polychlorinated Biphenyls; Neurotoxicity; Developmental; Persistent Organic Chemicals; Polychlorinated Biphenyls (PCBs)

ABSTRACT: Background and Purpose: PCB 11, a widespread environmental contaminant of increasing public health concern, was identified as the second-most abundant PCB congener in the serum of pregnant women at increased risk of having a child with a neurodevelopmental disorder (NDD). Our preliminary investigations suggest that juvenile mice exposed to PCB 11 in the maternal diet during gestation and lactation exhibit aberrant behavior and neuronal morphogenesis that are translationally relevant to NDDs (see poster #3140). Astrocytes play a critical role in neurodevelopment by regulating neural circuits and maintaining homeostasis in the central nervous system, but whether developmental exposure to PCB 11 modulates astrocytic reactivity remains unexamined. Here, we tested the hypotheses that (1) astrocytic reactivity is altered in the brain of juvenile mice developmentally exposed to PCB 11 in a sex- and/or dose- dependent manner; and (2) cytochrome P450 (CYP) mediated metabolism modulates PCB 11 effects on astrocytic reactivity. **Methods:** To test this hypothesis, we exposed 8-10 week old female wildtype (C57BL/6J) and *Cyp2a,2b,2f2,2g1*, and *2s1* gene knockout (*Cyp2abfgs*-null or CYP-null) mice to PCB 11 at 0.1, 1, or 6 mg/kg/d or vehicle (peanut oil) throughout gestation and lactation. Astrocytic reactivity was quantified in male and female offspring at weaning on postnatal day 21. Frozen brain sections were immunostained with antibodies specific for glial fibrillary acidic protein (GFAP) and C3, and then counterstained with DAPI to identify cell nuclei. Astrocytes were imaged using a Leica Spinning Disc Confocal Microscope at 20x magnification. Images were analyzed using ImageJ software to quantify the number and morphology of reactive astrocytes in the amygdala, hippocampus (CA1, CA2, CA3, and dentate gyrus), somatosensory cortex, entorhinal cortex, and piriform cortex. **Results:** Developmental exposure to PCB 11 produced significant dose-, sex-, and genotype-dependent effects on reactive astrocyte morphology, which varied across brain regions. In the amygdala, hippocampus, entorhinal cortex, and piriform cortex of wildtype mice, exposure to 0.1 and 1 mg/kg/d PCB 11 led to notable morphological changes in astrocytes, while the 6 mg/kg/day dose resulted in less pronounced changes. Variations in the number of reactive astrocytes, as well as astrocyte branch number, branch length, and area, were dependent on dose, brain region, and/or sex. Notably, the CA3 and entorhinal cortex exhibited the greatest number of morphological changes, suggesting that astrocyte sensitivity to PCB may be region-dependent. In contrast, astrocytes in the brains of CYP-null weanlings displayed minimal morphological changes following developmental PCB 11 exposure, indicating that PCB 11 effects on astrocytes are likely primarily mediated by its metabolites. Interestingly, there were negligible changes in the number of reactive astrocytes quantified across all groups in the regions of interest. **Conclusions:** These findings identify astrocytes as cellular targets of developmental PCB 11 exposures and suggest that astrocytes may contribute to PCB 11 effects on neuronal connectivity and behavior. These findings also build on preliminary evidence indicating that PCB 11 metabolites are key mediators of developmental neurotoxicity. Collectively, these findings support our hypotheses and add to the growing body of evidence that lower-chlorinated PCBs pose a

risk to the developing brain. This work was supported by the NIEHS (R01 ES014901 to XD, HJL, and PJL; T32 ES007059 to RM), the UC Davis Emmy Werner and Stanley Jacobsen Fellowship (to RJW), and the UC Davis Professors for the Future Fellowship Program (to RJW).

ABSTRACT NUMBER: 5041 **Poster Board Number:** H590
TITLE: Prenatal Cannabidiol Exposure Alters Offspring Behavior

AUTHORS (FIRST INITIAL, LAST NAME) AND INSTITUTIONS: M. Rusnak, I. Fleischer, and J. D. Thomas. San Diego State University, San Diego, CA. Sponsor: *M. Trimble*
KEYWORDS: Behavior; Developmental Toxicity; Prenatal; Neurotoxicity; Developmental; Cannabidiol

ABSTRACT: Background and Purpose: Cannabis is the most commonly used illicit drug among pregnant women. Increasing evidence suggests that prenatal exposure to tetrahydrocannabinol (THC), the psychoactive component of cannabis, alters fetal development. However, less is known of the consequences of prenatal exposure to cannabidiol (CBD), the primary non-psychoactive constituent of cannabis, despite growing rates of CBD use. In fact, recent estimates suggest that 20% of pregnant women in the U.S. and Canada use CBD (Bhatia et al., 2024). This popularity is due, in part, to the perception that CBD can reduce pregnancy-related symptoms such as pain and nausea. Further, its reputation as a natural substance has led to the perception that it is safe to use during pregnancy. To identify the consequences of prenatal CBD, we developed a rodent model of oral CBD exposure to mimic the administrative route commonly used by pregnant individuals. Recently, we found adverse behavioral effects in offspring exposed to a high dose of prenatal CBD (50 mg/kg). Thus, the purpose of this study was to examine the effects of prenatal exposure to a range of prenatal CBD doses on cognition and early motor development of offspring. **Methods:** Pregnant rats were given 5, 10, or 25 mg/kg of CBD daily during gestational days 5-20 via a honey and cookie dough vehicle. On postnatal days (PD) 2-12, early motor reflexes (including righting, grasping, and geotaxis reflexes) were tested in the neonatal offspring, with success and latency (time) recorded. On postnatal days (PD) 55-60, adult offspring were tested on the working memory version of the Morris Water Maze. During the working memory task, subjects were placed in a tank of water and required to find a hidden escape platform using visuospatial cues around the room. Each session included a dyad of trials: a training trial during which the location of the platform was moved to a new location, and a test trial to test for memory of the new location. Subjects were tested for 2 sessions/day with intertrial intervals (ITI) of 0 sec or 60 sec. **Results:** Neonates exposed to 25 mg/kg/day CBD prenatally demonstrated advancements in geotaxis reflex performance and hindlimb grasping, whereas subjects exposed to the lower doses of prenatal CBD exhibited delays in forelimb grasping. On the working memory test, prenatal CBD exposure produced a dose-dependent effect on latency and path length to find the platform during the training trial among female offspring. Females exposed to 25 mg/kg/day CBD took longer to find the escape platform, whereas females exposed to the 5 mg/kg/day found the escape platform faster. Given that these effects were seen during the training trial but not testing trials, these effects were not due to impacts on memory, but other performance variables (i.e., search strategy, stress). Indeed, females exposed to the highest dose of prenatal CBD spent significantly more time in thigmotaxis in later trials than all other groups, suggesting a heightened stress response. **Conclusions:** The findings suggest that prenatal CBD exposure can modify development in a dose- and sex-dependent manner. Alterations in the trajectory of motor development could reflect disruptions in the delicate balance of developmental processes associated with motor function and could lead to long-lasting changes in motor ability. Further, prenatal CBD exposure altered behavior on

the water maze task, likely by influencing stress regulation. Our findings suggest that prenatal CBD may lead to long-lasting emotional dysregulation in female adult rodents. Thus, exposure to even low doses of CBD during pregnancy may pose risks to the developing fetus. These findings have important implications for our understanding of how cannabinoids affect development and for public policies related to the use of CBD. Supported by CMCR P64-07-001.

ABSTRACT NUMBER: 5042 **Poster Board Number:** H591

TITLE: Human iPSC-derived Neural Progenitor and TriCNS Platform for assessing toxicity of environmental and industrial compounds on progenitor cells, neuronal activity, and glial morphology

AUTHORS (FIRST INITIAL, LAST NAME) AND INSTITUTIONS: K. L. Gordon, C. Rines, S. Gilmore, L. Harrison, L. Oja, A. Smith, R. Ingermanson, B. Tekwani, J. Price, and P. McDonough. Vala Sciences, Inc., San Diego, CA. Sponsor: *M. Hancock*

KEYWORDS: Neurotoxicity; Developmental; Induced Pluripotent Stem Cells; *In Vitro* and Alternatives

ABSTRACT: Background and Purpose: Neurodevelopmental disorders (NDs), which affect nearly 15% of children in the US, display altered growth and function of the developing brain, and can manifest as impairments to learning, speech, memory, social interactions, and motor skills. Certain environmental toxicants and industrial chemicals have been linked to NDs, with chemicals generally being linked after adverse human effects have emerged. We are developing *in-vitro* human-relevant platforms using both Neural Progenitor Cells (NPCs) and neuron-astrocyte-microglia TriCNS system for screening toxic effects of chemicals on neurodevelopmental processes so that harmful effects can be detected before adverse human effects occur. **Methods:** To assess NPC proliferation and viability, we plated iPSC-derived NPCs (StemCell Technologies) in 384-well dishes and exposed them to various compounds for 72 hours. Cells were labeled for proliferative capacity (Ki67) and pluripotency (Sox2) and a nuclear marker (Hoechst). Cells were imaged using Vala's IC200 HTS instrument, and NPC viability, proliferative capacity, and pluripotency were assessed using Vala's CyteSeer® software. The TriCNS model features isogenic cultures of neurons, astrocytes, and microglia (BrainXell) plated in 384-well dishes and matured for 3-4 weeks. After 48-96 hours of compound treatment, effects on neuronal function were assessed using a multiplexed assay for calcium activity (Cal520 AM) and mitochondrial health (TMRM) on the IC200 KIC®. After the live imaging, the cultures were fixed to evaluate morphological changes to neurons (B3TUBB), astrocytes (GFAP), and microglia (IBA1) elicited by the compounds. The functional and morphological changes were assessed using CyteSeer® analysis software. Compounds of various classes were chosen from the NIEHS Developmental Neurotoxicity Screening Assay Chemical Lists and tested in NPC and TriCNS models to assess toxicity. Compounds were tested in 6pt dose response (0.3 uM, 1 uM, 3 uM, 10 uM, 30 uM, and 100 uM). **Results:** Sixteen compounds of different classes, including positive and negative controls, were screened on the NPC platform to evaluate toxicity. The negative controls, Acetaminophen and L-ascorbic acid, show little effects on cell viability, Sox2+ count and Ki67+ count. The two positive controls, Rotenone and Vorinistat had significant effects on cell viability, with a dose dependent decrease observed. Cytarabine demonstrated a 40% decrease in cell viability at the lowest dose tested (0.3 uM), and unexpected cell loss was observed with the compound Cerulenin. All four of these compounds showed decreases in the percent of Sox2+ cells, although the percentage of Ki67 cells increases as cell death increases. This may suggest the less proliferative cells are more sensitive to toxicity. Dolutegravir, Azoxystrobin, and Cannabidiol showed mild toxicity at the highest does tested, in terms of cell death and decreased percent of Sox2+ cells. Five compounds were screened on the TriCNS

platform. Azoxystrobin had the strongest effect, causing neuron and microglial death, mitochondrial depolarization, a decrease in active cells and spikes per cells, and altered microglial and astrocyte morphology. Dolutegravir, chlorpyrifos, and bisphenol-A reduced astrocyte branching with mild effects on calcium activity. **Conclusions:** We have built iPSC-derived platforms of NPCs and TriCNS for detecting developmental neurotoxicity caused by medications, herbicide/fungicide/pesticides, and industrial chemicals. Using these platforms, we can assess toxicity to CNS cells at different levels of cell maturity that may point to toxicity at different moments in fetal development or lead to different neurodevelopmental disorder phenotypes. The high-throughput platforms can allow discovery of chemicals that will have developmentally neurotoxic outcomes before the long-term effects of human exposure come to light. We will be expanding our screen to test the larger panel of compounds of interest on the TriCNS model which will allow us to compare the toxicity between the differentiated and undifferentiated CNS cells.

ABSTRACT NUMBER: 5043 **Poster Board Number:** H593
TITLE: A Potential Pharmacological Treatment for Intoxication by Tetrodotoxin

AUTHORS (FIRST INITIAL, LAST NAME) AND INSTITUTIONS: H. G. Steier, M. F. Stone, A. Chen, A. Wang, C. R. Schultz, L. A. Lumley, and M. Adler. United States Army Medical Research Institute of Chemical Defense, Gunpowder, MD. Sponsor: *L. Wright*
KEYWORDS: Neurotoxicology; Muscle Toxicity; Dose-Response; Tetrodotoxin

ABSTRACT: Background and Purpose: Tetrodotoxin (TTX) is a potent marine neurotoxin that acts by inhibiting voltage-gated Na+ channels (at site 1), leading to inhibition of action potential generation in nerve and muscle cells. Intoxication usually develops 30 min to 4 h after oral exposure, with characteristic signs consisting of paresthesias (especially around the mouth), limb weakness and ascending paralysis. High doses generally culminate in respiratory failure, cardiovascular collapse and death. The most common vector for human intoxication is the puffer fish, which avoids intoxication by sequestering TTX in internal organs and by expressing variants of voltage-gated Na+ channels that are resistant to TTX. Therapy for TTX intoxication consists of gastric lavage to remove the toxin from the GI system and artificial ventilation along with other symptomatic and supportive treatments. To identify a specific treatment for TTX intoxication, we examined the ability of the cholinesterase inhibitor neostigmine (Neo) to reverse the paralytic actions of TTX in *ex vivo* mouse phrenic nerve-hemidiaphragm preparations. The diaphragm muscle was selected since TTX-induced failure of this muscle is the proximal cause of death. Neo is an FDA approved drug that has been used off-label to treat sporadic cases of TTX intoxication in humans; its efficacy, however, has not been established due to the absence of animal studies or controlled human clinical trials. **Methods:** Supramaximal isometric twitch tensions of isolated mouse hemidiaphragm muscles were recorded following stimulation of the phrenic nerve. Dose-response relationships were first established in the presence of TTX or Neo alone and then the ability of Neo to reverse TTX-mediated inhibition was tested. **Results:** In our study, hemidiaphragm muscles were first intoxicated with TTX to produce a ~50% inhibition of twitch tension. Addition of 1 µM Neo to TTX-intoxicated muscles restored tensions to control levels within 5 min, and tensions remained potentiated at nearly 80% of control even two hours after addition of Neo. **Conclusions:** This concentration of Neo is in the range found in human plasma in patients receiving Neo to reverse the actions of neuromuscular blockers following surgery. These results are encouraging since they indicate

that a non-toxic concentration of an FDA-approved drug can rapidly reverse TTX-induced muscle paralysis.

ABSTRACT NUMBER: 5044 **Poster Board Number:** H594
TITLE: Region-specific neuroimmune and glial modulation in adult rat brains by pharmaceuticals associated with psychiatric and psychological adverse events

AUTHORS (FIRST INITIAL, LAST NAME) AND INSTITUTIONS: *F. Carvalho*[1,2], S. I. Marques[1,2], V. Stevanović[3], J. Aranđelović[3], M. Savić[3], H. Carmo[1,2], S. I. Sá[4,5], and *J. P. Silva*[1,2]. [1]UCIBIO, Laboratory of Toxicology, Faculty of Pharmacy, University of Porto, Portugal, Porto, Portugal; [2]i4HB, Faculty of Pharmacy, University of Porto, Porto, Portugal; [3]Faculty of Pharmacy, University of Belgrade, Serbia, Belgrade, Serbia; [4]Unit of Anatomy, Faculty of Medicine, University of Porto, Porto, Portugal; and [5]CINTESIS@RISE, Faculty of Medicine, University of Porto, Porto, Portugal.
KEYWORDS: Biomarkers; Astrocytes; Neurotoxicology

ABSTRACT: Background and Purpose: Neuroimmune dysregulation has been increasingly associated with drug-induced psychiatric and psychological adverse events (PPAEs), with glial cells and inflammatory signaling pathways being recognized as sensitive indicators of central neurotoxicity. Still, predicting PPAEs during early drug R&D remains a major challenge. This study thus aimed to identify brain region-specific neuroimmune signatures induced by clinically relevant doses of three drugs associated with neuropsychiatric liability: dimethyl fumarate (DMF), paroxetine, and varenicline. **Methods:** Adult male Sprague-Dawley rats received daily oral administration of varenicline (0.3 and 3 mg/kg), paroxetine (1.5 and 15 mg/kg), or DMF (10 and 50 mg/kg) for 28 days. The expression of astrocytic, microglial, and cytokine receptor markers, namely glial fibrillary acidic protein (GFAP), CD11b, and interleukin-17 receptor (IL-17R), was quantified by immunohistochemistry (IHC) and immunofluorescence (IF) in the prefrontal cortex (PFC), nucleus accumbens (NAcc), and hippocampal subregions (dentate gyrus, hilus, CA1, CA3). Quantitative image analysis was conducted using standardized image-analysis workflows. **Results:** DMF reduced astrocyte density in PFC and NAcc at both doses (by 40 and 44%, respectively). At 50 mg/kg, DMF markedly increased CD11b expression across NAcc and hippocampal regions (ranging from 66 to 136%). The lower DMF dose (10 mg/kg) also reduced IL-17R expression in NAcc and hippocampus (by 22 to 42%), but increased this marker's levels at 50 mg/kg across all regions analyzed (ranging between 25 and 68%). Paroxetine increased GFAP-positive cell density in the NAcc (39%) and CA1 (60%) at the lower dose tested (1.5 mg/kg), and in the PFC (13%) and hippocampal regions (around 56%) at the higher dose (15 mg/kg). This drug also increased CD11b immunoreactivity in PFC, hilus, and CA3 at both doses (ranging from 22 to 58%), with additional increases in the NAcc (by 33%) at the higher dose. Moreover, paroxetine increased IL-17R expression in PFC and NAcc (35 to 37%, respectively) but decreased this marker's levels in hilus (23%) and CA1 (15%). Varenicline only increased astrocyte density in CA3 (56%) and for the lower dose tested (0.3 mg/kg). Nonetheless, it significantly reduced CD11b expression in the NAcc (by 20% at 0.3 mg/kg), CA3 (by 34% at 3 mg/kg), and dentate gyrus and CA1 (by 31 and 40% at both doses). This drug further decreased IL-17R levels in PFC and NAcc (by 15 and 30%, respectively). **Conclusions:** Distinct drug-specific and region-dependent neuroimmune signatures were identified. Varenicline showed an overall suppressive inflammatory profile, paroxetine induced broad glial activation with differential IL-17R modulation, and DMF displayed a dose-dependent biphasic immune response. These findings support the combined use of GFAP, CD11b, and IL-17R as sensitive translational biomarkers for early detection of neuroimmune

liability in CNS safety and toxicology pipelines. **Acknowledgments:** This work was funded by the Innovative Medicines Initiative 2 Joint Undertaking, supported by EU's H2020 Research Framework and EFPIA, under the grant agreement No 821528 (NeuroDeRisk); and by the Portuguese Foundation for Science and Technology (FCT) by projects UIDP/04378/2020 and UIDB/04378/2020 (UCIBIO), and LA/P/0140/2020 (i4HB). S.I.M. and JPS also acknowledge FCT for PhD grant 2020.09080.BD and research contract (under Scientific Employment Stimulus) 2021.01789.CEECIND/CP1662/CT0014, respectively.

ABSTRACT NUMBER: 5045 **Poster Board Number:** H595

TITLE: Peripheral Myeloid HMGB1 Selectively Regulates Neuroimmune Signaling in a Mouse Model of Gulf War Illness

AUTHORS (FIRST INITIAL, LAST NAME) AND INSTITUTIONS: *J. A. Johnson Jr.*, A. Tsoggerel, *L. Miller*, and A. Oblak. Indiana University School of Medicine, Stark Neuroscience Center, Indianapolis, IN.

KEYWORDS: Neurotoxicology; Inflammation; Immunotoxicity; Gulf War Illness

ABSTRACT: Background and Purpose: Gulf War Illness (GWI) is a chronic, multisymptom disorder characterized by persistent central nervous system (CNS) and peripheral immune dysregulation long after wartime toxicant exposure and immune challenge. Circulating high-mobility group box 1 (HMGB1), a damage-associated molecular pattern and immune signaling factor, is elevated in veterans with GWI and drives persistent microglial activation in murine models. However, the contribution of peripheral myeloid-derived HMGB1 to sustained neuroimmune signaling and its compartment-specific actions remain unclear. **Methods:** Conditional HMGB1$^{fl/fl}$ LysMcre^{+} mice with selective deletion of HMGB1 in peripheral myeloid cells, without alterations in microglia or brain HMGB1, and littermate controls received a single intraperitoneal injection of lipopolysaccharide (LPS; 5 mg/kg) or saline. Tissues were analyzed at 3 h (initiation phase) and 7 days (persistent phase) post-injection. Serum HMGB1 and cytokines were measured by ELISA. Gene expression in the midbrain and peripheral immune organs was assessed using NanoString nCounter panels. Immune cell accumulation at the choroid plexus was evaluated by immunofluorescence, and cognitive performance was assessed using the Y-maze. **Results:** LPS induced sustained elevations of circulating HMGB1, IL-1β, and TNFα in both genotypes, indicating that peripheral myeloid cells are not the primary source of extracellular HMGB1. Despite this, myeloid HMGB1 deletion produced time-dependent, genotype-specific changes in midbrain neuroinflammatory gene expression. Acute (3 h) LPS exposure increased Il1b, *Tnf*, and *Iba1* expression, with the greatest Iba1 induction observed in knockdown mice. In contrast, persistent (7-day) expression of proinflammatory genes (*Tnf, Gzma*, *Cd69*, *Cxcl10*) was significantly attenuated in HMGB1-deficient mice. Iba1 expression was not elevated at 7 days, and no genotype differences were observed, suggesting that sustained neuroimmune activation does not involve myeloid cell translocation into the brain parenchyma. Instead, cervical lymph nodes exhibited a distinct persistent transcriptional signature at 7 days, including altered complement, antigen presentation, and inflammasome pathways, identifying peripheral immune compartments as modulators of chronic CNS inflammation. Transcriptional responses in spleen, liver, and bone marrow were minimal. CD45^{+} cell accumulation at the choroid plexus and behavioral performance were unchanged. **Conclusions:** Peripheral myeloid-derived HMGB1 regulates persistent neuroimmune signaling through spatially and temporally restricted mechanisms that act independently of circulating cytokines or direct immune cell infiltration into the brain. These findings implicate extra-parenchymal immune compartments, including the cervical lymph nodes and

potentially glymphatic-associated pathways, as critical mediators linking peripheral inflammation to chronic CNS immune dysregulation in GWI-like pathology.

ABSTRACT NUMBER: 5046 **Poster Board Number:** H596
TITLE: The advantages of CNS-3D Organoids for functional neuromodulation studies

AUTHORS (FIRST INITIAL, LAST NAME) AND INSTITUTIONS: V. K. Alstat, N. S. Coungeris, J. Perkins, E. Johns, and A. S. LaCroix. 28bio Inc., Maple Grove, MN. Sponsor: *L. Smirnova*
KEYWORDS: Neurotoxicology; Stem Cells; Biological Modeling

ABSTRACT: Background and Purpose: A recent surge in support for microphysiological systems (MPS) in drug development has increased emphasis on human induced pluripotent stem cell (hiPSC)-derived technologies to improve clinical translation. One of the most attractive aspects of hiPSC-derived models is their scale and compatibility with high-throughput screening (HTS), though this requires high organoid-to-organoid reproducibility to be effective. Traditional neural spheroid models typically combine terminally differentiated neuronal subtypes and glia, enabling precise control of cellular ratios and regional specification of brain identity[1]. Alternatively, neural organoids utilize hiPSCs as starting material thereby permitting differentiation into a variety of neuronal subtypes, though this is often at the cost of high variability in size and cell composition between organoids. To this end, CNS-3D Functional Organoids (CNS-3D) were developed. This hiPSC-derived cortical organoid technology uses a scalable batch production process which yields a co-differentiated mixture of key neural cell populations aligned with human neurodevelopment[2]. While both spheroid- and organoid-based approaches are well-established, a direct comparison of their functional advantages has yet to be described. **Methods:** To generate CNS-3D, neural progenitor cells (NPCs) were expanded and seeded into ultra-low attachment plates, wherein they self-organized into 3D organoids, one organoid per well. Over the course of 5 weeks, NPCs co-differentiated into neurons and astrocytes. Spontaneous oscillatory functional activity and response to a panel of excitatory and inhibitory insults was measured using calcium imaging (FLIPR) at the end of week 5. Spheroids were generated using healthy differentiated iPSC-derived neurons and astrocytes which were thawed and seeded into ultra-low attachment plates in a 50:50 ratio. Plates were maintained for 3 weeks prior to being assayed for spontaneous activity and drug response using FLIPR [2]. Brightfield images of both organoids and spheroids were captured on a weekly basis, as well as immediately prior to assaying, to capture size and growth trends. Following FLIPR, samples were collected for bulk RNAseq analysis. **Results:** CNS-3D's functional phenotype proved stable and reproducible over a four-week window, establishing that this technology is amenable to sub-chronic dosing paradigms. In contrast, neural spheroids showed lower signal-to-noise ratio, and protocol limitations constrained chronic dosing. CNS-3D also displayed balanced neuronal and astrocytic populations and multiple neuronal subtypes absent from the spheroid model, as measured by single nuclei RNAseq. Transcriptomic analysis showed CNS-3D gene expression closely correlated with both fetal and adult human brain tissue ($R^2 > 0.9$ for key receptor systems). In comparison, the gene expression profile of the spheroid model was markedly different, reflecting its simpler biological composition. While spheroids allow flexible control of cellular composition, this appears to come at the cost of increased lot-to-lot variability compared to CNS-3D. **Conclusions:** When benchmarked against traditional spheroid generation protocols, it was found that CNS-3D Functional Organoids exhibited a more reproducible spontaneous functional phenotype, lower signal to noise ratio, and lower CVs for diameter within and between plates. Collectively, these data demonstrate that CNS-3D Functional

Organoids provide superior functional robustness, biological complexity, and reproducibility compared with traditional neural spheroids, supporting their use in neurological drug development.References:[1] Strong, C.E., Zhang, J., Carrasco, M. et al. Functional brain region-specific neural spheroids for modeling neurological diseases and therapeutics screening. Commun Biol 6, 1211 (2023). https://doi.org/10.1038/s42003-023-05582-8[2] Wang Q, Cohen JD, Yukawa T, Estrella H, Leonard C, Nunes J, Choi C, Lewis L, Baker KS, Kuga K, Dragan YP, Wagoner MP, Mishra N. Assessment of a 3D neural spheroid model to detect pharmaceutical-induced neurotoxicity. ALTEX. 2022;39(4):560-582. doi: 10.14573/altex.2112221. Epub 2022 Apr 19. PMID: 35502629.

ABSTRACT NUMBER: 5047 **Poster Board Number:** H597
TITLE: Bisphenol S Induces Mitochondria-Dependent Neurotoxicity in Human Dopaminergic Cells

AUTHORS (FIRST INITIAL, LAST NAME) AND INSTITUTIONS: B. H. Gibson, *A. Ofosu*, *P. Kini*, *A. Ishaque*, and *A. Elnabawi*. University of Maryland Eastern Shore, Princess Anne, MD.
KEYWORDS: Cell Culture; Oxidative Injury; Neurotoxicology; Bisphenol S

ABSTRACT: Background and Purpose: Bisphenol S (BPS) is a synthetic compound increasingly used as a substitute for bisphenol A (BPA) in the production of polycarbonate plastics, epoxy resins, and thermal paper. Although BPS has been introduced as a safer alternative due to regulatory restrictions on BPA, growing evidence indicates that BPS is not biologically inert and may pose comparable or greater health risks. The nervous system appears particularly susceptible to BPS exposure, as BPS can cross the blood-brain barrier and disrupt neurodevelopmental, neurophysiological, and neurodegenerative processes. Mitochondria play a pivotal role in neuronal survival by regulating energy production, calcium homeostasis, redox balance, and apoptotic signaling. Given the high energetic demands and limited regenerative capacity of neurons, mitochondrial dysfunction has emerged as a central mechanism in neurodegeneration. This study aimed to investigate the neurotoxic effects of BPS and its potential involvement in mitochondrial dysfunction using human dopaminergic neuronal (SH-SY5Y) cells. **Methods:** Human neuroblastoma SH-SY5Y cells were exposed to various concentrations of BPS for different time intervals. Cell viability and death, intracellular reactive oxygen species (ROS) generation, mitochondrial membrane potential, cytochrome c release, intracellular ATP levels, and activation of apoptotic pathways were assessed. **Results:** BPS exposure significantly reduced cell viability in a concentration-dependent manner in SH-SY5Y cells. Low concentrations of BPS (0.001-100 µM) markedly increased ROS production at 3 and 6 hours, an effect that was attenuated by the antioxidant N-acetyl-L-cysteine (NAC). BPS also induced time- and concentration-dependent increases in caspase-3 activity and apoptosis, both of which were significantly inhibited by NAC or the caspase-3 inhibitor Ac-DEVD-CHO, indicating oxidative stress-mediated, caspase-3-dependent apoptosis. Furthermore, BPS caused a significant loss of mitochondrial membrane potential comparable to that induced by the mitochondrial uncoupler carbonyl cyanide m-chlorophenyl hydrazone (CCCP) and significantly reduced intracellular ATP levels following 24 hours of exposure. **Conclusions:** These findings demonstrate that BPS induces neurotoxicity through mechanisms involving oxidative stress, mitochondrial dysfunction, ATP depletion, and apoptotic cell death. Mitochondrial impairment appears to be a key mechanistic link between BPS exposure and nervous system toxicity, suggesting that BPS may represent a potential risk factor for neurodegenerative diseases. Supported by Title III.

ABSTRACT NUMBER: 5048 **Poster Board Number:** H598

TITLE: Cns-3d functional organoids predict clinical neurotoxicity outcomes for small molecules and anti-sense oligonucleotides

AUTHORS (FIRST INITIAL, LAST NAME) AND INSTITUTIONS: V. K. Alstat[1], D. Gallegos[2], N. S. Coungeris[1], P. Botta[3], M. Muhammad[4], J. Perkins[1], E. Johns[1], and A. S. LaCroix[1]. [1]28bio Inc., Maple Grove, MN; [2]Takeda Pharmaceuticals, Cambridge, MA; [3]Lundbeck Pharmaceuticals, Copenhagen, Denmark; and [4]Anthropic, San Francisco, CA. Sponsor: *L. Smirnova*

KEYWORDS: Neurotoxicology; Neurotoxicity; Developmental; Alternatives to Animal Testing

ABSTRACT: Background and Purpose: Unanticipated central nervous system (CNS) neurotoxicity remains a leading cause of late-stage clinical attrition, particularly for compounds that advance through traditional animal-based safety testing without revealing human-relevant liabilities. This challenge is compounded for emerging therapeutic modalities, such as anti-sense oligonucleotides (ASOs), where CNS adverse events including seizures are difficult to predict from sequence or target biology alone. Complex *in vitro* models (CIVMs) derived from human induced pluripotent stem cells (hiPSCs) offer an opportunity to model human-relevant neurobiology and functional network behavior *in vitro*. We have previously reported a high-throughput compatible, hiPSC-derived cortical organoid platform (CNS-3D) capable of predicting clinical neurotoxicity outcomes for small molecules with high specificity (>90%) and moderate sensitivity (>50%)[1]. The purpose of the present work was to improve predictive sensitivity, expand coverage across clinically relevant neurotoxic adverse events, and evaluate the model's applicability to ASO therapeutics. **Methods:** Human iPSC-derived cortical organoids were differentiated and matured to establish stable, spontaneous network-level electrophysiological activity incorporating both excitatory and inhibitory circuitry. Organoid activity was recorded using calcium imaging-based functional assays following acute compound exposure (0 - 4 hours). Waveform features describing the number, size, and shape of each network burst were extracted using AnalytiX, a proprietary waveform processing pipeline. Machine learning models were trained using a curated reference dataset of small molecules with known clinical neurotoxicity outcomes. The original logistic regression-based classifier was replaced with a gradient-boosted decision tree algorithm (XGBoost) to better capture nonlinear relationships between electrophysiological features and clinical outcomes and allow for the model to interpret and learn from both dose- and time-dependent data. The dataset was expanded from 84 to >150 small molecules with well-established neurotoxicity profiles, enabling stratified analyses by adverse event class (e.g., seizure, neurodegeneration, movement disorders). In parallel, a panel of ASOs administered clinically via intrathecal delivery was evaluated, and model performance was assessed against reported CNS seizure liabilities. **Results:** Transitioning to the XGBoost-based machine learning framework increased overall sensitivity for predicting clinical neurotoxicity to >75% while maintaining high specificity. Expansion of the small molecule reference dataset enabled improved discrimination of distinct neurotoxic phenotypes, with differential electrophysiological signatures observed for seizure-associated versus neurodegenerative or motor-related adverse events. Application of the CNS-3D platform to ASOs revealed that acute changes in network peak frequency alone were highly predictive of clinical seizure liability. These findings suggest that ASO-associated CNS seizures may arise from nonspecific functional perturbations of neural networks following intrathecal administration rather than sequence-dependent mechanisms. **Conclusions:** These results demonstrate that iterative improvements in machine learning methodology, dataset breadth, and modality coverage substantially enhance the translational performance of a

human CNS-3D organoid platform for neurotoxicity risk assessment. The ability to sensitively and specifically predict seizure liability for both small molecules and ASOs highlights the value of functional, human-relevant neurophysiological endpoints in preclinical safety testing. Collectively, this work supports the integration of CNS MPS technologies into neurotoxicology workflows to better de-risk clinical development and reduce late-stage CNS safety failures. References[1] Q Wang, et al., (2022). ALTEX 39(4):560-582. doi: 10.14573/altex.2112221

ABSTRACT NUMBER: 5049 **Poster Board Number:** H599
TITLE: An *In Vitro* Pipeline for Rapid Assessment of Neurotoxicity Screening

AUTHORS (FIRST INITIAL, LAST NAME) AND INSTITUTIONS: M. E. Huddleston[1,2], S. Kambarova[1,2], K. A. Jones[1,2], and *M. W. Grogg*[2]. [1]AV Inc., Dayton, OH; and [2]Air Force Research Laboratory, Wright-Patterson Air Force Base, OH.
KEYWORDS: Chemical Hazard Assessment; Risk Assessment

ABSTRACT: Background and Purpose: Neurotoxicity is an ongoing concern for the Warfighter as exposures, including organophosphates (e.g., chlorpyrifos; CPF, diisopropyl fluorophosphate; DFP) and carbamates (e.g., carbaryl; CAR), can impair cognitive function and readiness. Traditional *in vivo* toxicity testing is resource-intensive and often too slow for rapid operational decisions to be made. A lot of work has been done on high doses of chemical exposures but there is evidence to suggest that repeated exposures to lower doses may also negatively impact cognitive, behavioral, and physiological responses. This data will be extrapolated in conjunction with side-by-side *in vivo and ex vivo* data to examine the ability of *in vitro* models to assess predictive capacity of non-animal models. This study aims to develop a high-throughput *in vitro* pipeline using human induced pluripotent stem cell (iPSEC)-derived neurons and the power of microelectrode arrays to rapidly screen chemical compounds that can impact cognitive function. **Methods:** Human brain models were composed of a co-culture of iPSC-derived DopaNeurons and Astrocytes. Cells were exposed to 0.16, 0.8, 4, 20, and 100 µM chlorpyrifos (CPF), chlorpyrifos-oxon (CPF-O), diisopropyl fluorophosphate (DFP), or carbaryl (CAR) for up to 24 h. High-density microelectrode array (MEA) methods were developed to monitor neuronal activity (spiking and bursting). Additionally, mitochondrial respiration was quantified by extracellular oxygen flux, and cellular apoptosis was assessed using flow cytometry. **Results:** A significant decrease in features of network activity, spiking, and bursting were observed within minutes to exposure of the compounds at 100 µM compared to no treatment that persisted for 24 h. Neuronal activity was able to recover for most of the compounds post-exposure, with the amount of recovery observed showing compound-specific responses. Extracellular flux data showed that after 24 h of exposure to any concentration of compound, diminished neuronal basal and maximal respiration as well as ATP production were observed. Additionally, mitochondrial activity was affected after 4 h of exposure, but only at 100 µM. Furthermore, compound-specific differences were seen at similar concentrations. **Conclusions:** These findings demonstrate that the proposed *in vitro* pipeline effectively captures rapid neurotoxicological signatures relevant to cognitive function. Future work will incorporate a more complex 3D microphysiological system with a vascular endothelial layer to simulate blood-brain barrier penetration and further refine neurotoxicological predictability.

ABSTRACT NUMBER: 5050 **Poster Board Number:** H600
TITLE: Legacy effects of cadmium on vision and behavior

AUTHORS (FIRST INITIAL, LAST NAME) AND INSTITUTIONS: G. J. Pérez González, C. Va, R. Popp, J. M. Cunill-Flores, A. M. Oehlert, and *D. S. Shelton*. University of Miami, Coral Gables, FL.
KEYWORDS: Epigenetics; Metals; Ocular Toxicity; Cadmium

ABSTRACT: Background and Purpose: Cadmium (Cd) is a toxic metal primarily acquired through diet that accumulates in human eyes and other organs, where it can persist with a half-life of 10-30 years. To understand the long-term impact of Cd on vision, we must determine whether Cd accumulates in ocular, neural and reproductive tissues, leading to tissue injury transgenerationally. **Methods:** We exposed zebrafish (*Danio rerio*) to a control diet (0 µg/g Cd), a human dietary-relevant cadmium concentration (30 µg/g), and a high-exposure condition (600 µg/g) slightly exceeding the highest cadmium intake reported for individuals who consume shellfish beginning at 14 days post-fertilization until adulthood (or 67 days). After a 7-month depuration, directly exposed fish (F0) were spawned to generate germline (F1) and epigenetically (F2) exposed generations. For all generations, we assessed the optomotor response and other visually guided behavior, fecundity, organ toxicity, and cadmium body burden. **Results:** While we detected Cd accumulation only in the F0, our behavioral and fecundity assays suggest Cd induces visual alterations inter-generationally and reproductive deficits transgenerationally. We anticipate Cd accumulation in F0 neural and reproductive tissues with gonadal accumulation potentially driving tissue damage in the F1 and F2 generations. **Conclusions:** These results will provide insights into the role of organ-specific damage on the generational legacy of Cd.

ABSTRACT NUMBER: 5051 **Poster Board Number:** H601
TITLE: Chronic Toxicity Evaluation of iPSC-Derived Neural Microtissues with Dopaminergic Neurons in RNU Nude Rats: Advancing Cell Therapy for Parkinson's Disease

AUTHORS (FIRST INITIAL, LAST NAME) AND INSTITUTIONS: G. Quesseveur[1], G. Dabee[2], P. Vignand[1], F. Thomas[1], F. Pontet[1], A. Perrot[1], N. Prudon[2], A. Machado-Hitau[2], E. Faggiani[2], and B. Tamarit[2]. [1]Charles River Laboratories, Saint-Germain-Nuelles, France; and [2]Treefrog Therapeutics, Pessac, France. Sponsor: G. Quesseveur, EUROTOX
KEYWORDS: Induced Pluripotent Stem Cells; Toxicity; Chronic; Nervous System; Parkinson's disease, cell and gene therapy

ABSTRACT: Background and Purpose: Parkinson's Disease (PD) is a prevalent neurodegenerative disorder and currently represents the fastest-growing neurological condition worldwide. Epidemiological projections indicate that the global number of individuals affected by PD will approximately double, reaching an estimated 20 million cases by the year 2050. The pathological hallmark of PD is the progressive degeneration of dopaminergic (DA) neurons within the substantia nigra pars compacta. This neuronal loss leads to a significant reduction in dopaminergic terminals in the putamen, which is a critical component of the basal ganglia circuitry responsible for motor control. Consequently, one of the primary functional impairments observed in PD patients is the inability to initiate and sustain voluntary, effortful movements. Emerging neuroimaging and morphometric studies have further demonstrated that putamen atrophy may serve as a robust clinical biomarker, correlating strongly with motor dysfunction and the severity of neurological symptoms in PD. Preclinical investigations, complemented by ongoing clinical trials, have provided compelling evidence supporting the therapeutic potential of

pluripotent stem cell-derived dopaminergic neuron replacement strategies for ameliorating motor symptoms in PD. **Methods:** In alignment with this rationale, we have developed an advanced platform technology, C-Stem™, which enables the exponential amplification of induced pluripotent stem cells (iPSCs) followed by their directed differentiation into dopaminergic neurons within a fully closed and controlled bioprocessing system. This proprietary approach facilitates the generation of three-dimensional (3D) neural microtissues composed of mature DA neurons and DA progenitors. These microtissues exhibit enhanced structural integrity, reduced susceptibility to mechanical stress, and improved resilience during stereotactic injection procedures. Recent *in vivo* studies have demonstrated that administration of these 3D neural microtissues (designated TFG-001) into hemiparkinsonian rodent models results in robust innervation of the lesioned striatum by tyrosine hydroxylase-positive (TH+) dopaminergic projections. This reinnervation is associated with significant restoration of motor function, thereby validating the therapeutic concept. Building upon this proof-of-concept, we have undertaken a comprehensive regulatory chronic toxicity study to evaluate the safety profile and biodistribution of TFG-001 as part of a formal submission to support subsequent clinical development. The study involved bilateral intra-putamen administration of TFG-001 in RNU Nude rats, a well-established immunodeficient transplantation model, followed by an extensive toxicological assessment encompassing histopathology, systemic toxicity, and biodistribution analyses. **Results:** Bilateral intra-putamen administrations of TFG-001 in the RNU Nude rat were successfully completed and were not associated with any clinical sign or premature death. Preliminary *in vivo* results demonstrated the absence of any adverse impact of TFG-001 on the clinical status of the animals up to 9 months post-injection. There was no TFG-001-related effect on clinical pathology parameters at the time of the interim sacrifice (Day 8). Immunohistochemistry and qPCR evaluations will confirm the biodistribution of TGF-001 in the brain and in the other peripheral organs, respectively. **Conclusions:** Collectively, these results underscore the safety and translational potential of this innovative cell therapy approach for Parkinson's Disease.

ABSTRACT NUMBER: 5052 **Poster Board Number:** H602

TITLE: Standardization and Harmonization of Neuropathological Data from the NIH NeuroBioBank: Enabling Research in Substance Abuse Disorders

AUTHORS (FIRST INITIAL, LAST NAME) AND INSTITUTIONS: O. Stroganov, A. Pathak, L. Ivanov, S. Karcher, A. Lafontaine, K. Armah, L. Mabe, O. Tyurina, and E. Moler. Rancho BioSciences, Rancho Santa Fe, CA. Sponsor: *C. Grondin*

KEYWORDS: Neurotoxicology; Histopathology; Nervous System; Brain bank; Data portal

ABSTRACT: Background and Purpose: The NIH NeuroBioBank (NBB), established in 2013, serves as a critical national resource providing researchers with human post-mortem brain tissue and biospecimens for investigating neurological conditions. Despite the wealth of data encompassing medical records, neuropathological reports, and whole genome sequencing data, a significant barrier exists: results from gross and microscopic brain examinations remain trapped in unstructured PDF pathology reports with inconsistent formats across collection sites. This lack of standardization severely limits researchers' ability to correlate neuropathological findings with clinical and genomic data, particularly for understudied populations such as individuals with substance abuse disorders. **Methods:** We developed a systematic approach for extracting, cleaning, and harmonizing neuropathological data from over 6,000 de-identified reports representing seven NeuroBioBank collection sites. The pipeline transforms

unstructured pathology reports through OCR processing, format conversion, LLM-based data extraction with controlled output generation, merging, interactive harmonization with user feedback loops, and validation. A graphical interface was developed for data exploration, featuring donor filtering, brain visualization mapped from the Allen Human Brain Atlas, and report review capabilities. A focused analysis was conducted on donors with substance abuse disorders. **Results:** The harmonization effort successfully converted unstructured pathology reports into standardized, machine-readable formats enabling systematic queries across the NBB collection. The Brain Data Portal now supports investigations into substance abuse-related neuropathology, facilitating correlations between drug exposure history, clinical presentation, and post-mortem brain findings. To demonstrate the value of the dataset, preliminary analysis of microscopic and macroscopic findings for brains of donors with substance abuse disorders was conducted. **Conclusions:** The standardization and harmonization of NBB neuropathological data addresses a critical gap in data accessibility that previously hindered research into disease mechanisms and therapeutic development. The application of this framework to substance abuse disorders demonstrates its potential for enabling research in populations where neuropathological correlates remain poorly characterized.

ABSTRACT NUMBER: 5053 **Poster Board Number:** H603
TITLE: Systemic inflammation induces tau hyperphosphorylation in Late Onset Alzheimer's Disease (LOAD3ε4) mice

AUTHORS (FIRST INITIAL, LAST NAME) AND INSTITUTIONS: J. Kotulski, Z. Villaseñor, *S. Phatak*, *M. Campen*, and K. Bhaskar. University of New Mexico, Albuquerque, NM.
KEYWORDS: Aging; Exposure, Environmental; Transgenic Models; Dementia; lipopolysaccharide

ABSTRACT: Background and Purpose: Alzheimer's disease (AD) is a progressive neurodegenerative disorder marked by cognitive decline and memory loss. Its neuropathological hallmarks include the accumulation of amyloid-β (Aβ) plaques and neurofibrillary tangles composed of hyperphosphorylated tau (pTau). These pathological aggregates disrupt neuronal communication and contribute to synaptic dysfunction, ultimately impairing executive function and memory. Increasing evidence suggests that AD pathology is not solely driven by Aβ and pTau; neuroinflammation has emerged as a critical third component of disease initiation and progression. Activated microglia- resident immune cells of the central nervous system (CNS)- are increasingly recognized as key mediators of inflammatory signaling that may exacerbate tau pathology and neuronal injury. In parallel, environmental exposures ("exposomes") are now recognized as key modulators of CNS inflammation. For instance, inhalation of wildfire smoke, a growing concern in the Western United States, can trigger systemic inflammation via the lung-brain axis and elevate circulating proinflammatory mediators such as tumor necrosis factor alpha (TNFα) and protein tyrosine phosphatase receptor type C (CD45). Our group previously demonstrated that systemic inflammation induced by bacterial endotoxin, specifically lipopolysaccharide (LPS), promotes tau hyperphosphorylation in mouse models- indicating that peripheral immune activation can influence neurodegeneration in the brain. Here, we investigated whether inflammatory environmental insults can accelerate tau pathology in a genetically relevant model of late-onset AD. **Methods:** To further explore the contribution of environmental and inflammatory exposomes to AD risk, we employed the LOAD3ε4 mouse model developed by the MODEL-AD consortium. This model expresses humanized Aβ and tau along with the apolipoprotein E4/E4 genotype, the strongest genetic risk factor for late-onset, sporadic AD. We administered a single

intraperitoneal injection of LPS (5 mg/kg) to two age cohorts of LOAD3ε4 mice (3.0 months and 5.3 months old), mimicking an acute systemic inflammatory challenge. Twenty-four hours post-injection, hippocampal tissue was collected for analysis of tau phosphorylation at specific epitopes corresponding to early and intermediate stages of tau pathology. Phosphorylation was quantified using site-specific antibodies AT180 (threonine 231) and AT8 (serine 202) relative to total tau (Tau12). **Results:** We observed increased tau phosphorylation in the hippocampus of LPS injected LOAD3ε4 mice. Upon quantification, the AT180/total tau ratio was modestly increased, but the AT8/total tau ratio was significantly increased in LPS-injected LOAD3ε4 mice compared to vehicle treated controls, indicating site-selective enhancement of pathological phosphorylation in response to acute systemic inflammation. **Conclusions:** This ongoing study provides preliminary evidence linking systemic inflammation to late-onset AD-related tau pathology in the LOAD3ε4 model. These data underscore the sensitivity of the aging brain to immune challenges and highlight inflammation as a modifiable risk factor for neurodegeneration. Our forthcoming work will expand upon these findings by examining the cumulative effects of multiple environmental insults—including wildfire smoke, metal contaminants, micro-/nano-plastics, and Western diet—on neuroinflammation, tau pathology, and dementia risk in the LOAD3ε4 model. Understanding these gene-environment interactions will be essential for developing preventive strategies against environmentally influenced forms of dementia.

ABSTRACT NUMBER: 5054 **Poster Board Number:** H604
TITLE: Sex and Type of Mold Inhaled Affects the Lung-Brain Axis Response in C57BL/6J Mice

AUTHORS (FIRST INITIAL, LAST NAME) AND INSTITUTIONS: M. M. Miller, K. L. Weaver, *J. A. Johnson Jr.*, and A. L. Oblak. Indiana University School of Medicine, Indianapolis, IN.
KEYWORDS: Lung; Pulmonary or Respiratory System; Nervous System; Exposure, Environmental; Alzheimer's disease; Mold

ABSTRACT: Background and Purpose: *Aspergillus versicolor (Av)* and *Stachybotrys chartarum (Sc)* are common fungi found in damp indoor environments, where human exposure is linked to cognitive complaints, allergy, and asthma. Recent studies have associated these allergic diseases with an increased risk for Alzheimer's Disease (AD). Moreover, a dysregulated microglial phenotype and maladaptive immune cell trafficking are observed in these specific types of fungal inhalations and in AD. What remains poorly understood are how these environmental exposures are culpable in the disruption of peripheral immune responses regulating the brain; thereby, contributing to or exacerbating this devastating form of dementia. According to the lung-brain-axis hypothesis, the pulmonary response to environmental exposures dysregulates microglia through changes in peripheral immune cells and circulating factors that regulate central nervous system (CNS) in health and disease. But it is unclear how sex differences and according to type of mold inhaled can affect these regulatory processes. **Methods:** Male and female C57BL/6J mice were exposed to HEPA-filtered air, *Av* (3×10^5) or *Sc* (1×10^4) spores in nose-only chambers twice weekly for 10-weeks to explore sex and exposure differences in the midbrain, hippocampus, lung-immune and spleen-immune transcriptome, along with microglial morphology and serum cytokines. **Results:** *Sc*-inhalation moderately affected the hippocampal transcriptome in both sexes, but *Av* failed to elicit a response in this brain region. In midbrain, a highly significant exposure by sex difference was observed in *Av*-females and *Sc*-males, indicating type of exposure according to sex, significantly affected the transcriptomic response. Other significant CNS effects were in microglial morphology changes observed in the hippocampus and midbrain of exposed mice compared to air only

controls. In the periphery, lung immune transcriptome demonstrated significant differences with sex, and *Av* or *Sc* mold inhalation with exposed males having the most robust response. While in serum, significant exposure effects and/or significant interaction by exposure with sex effects was observed in just a few circulating cytokines; however, only *Av*-males mounted a significant splenic immune response. **Conclusions:** Taken together, these findings support sex and type of mold inhaled effect the response of the lung-brain axis. Our findings suggest a dysregulated microglial response, with the midbrain as the main CNS target. The primary and significant immune response are from the lungs corresponding to sex and type of spore inhaled which also affects the circulating immune cells. Further studies are needed to explore how these differences translate to amyloid and tau pathology to substantiate AD contribution to these types of environmental exposures in a sex dependent manner.

ABSTRACT NUMBER: 5055 **Poster Board Number:** H605
TITLE: Bisphenol A Potentiates Alpha-Synuclein Aggregation and Neurotoxicity in Human Neuronal Cells

AUTHORS (FIRST INITIAL, LAST NAME) AND INSTITUTIONS: *A. A. Ofosu*, *B. Bediako*, *P. Kini*, B. Gibson, *A. Ishaque*, and A. Elnabawi. University of Maryland Eastern Shore, Princess Anne, MD.
KEYWORDS:; Bishpenol A (BPA)

ABSTRACT: Background and Purpose: Bisphenol A (BPA) is a widely used industrial chemical and is recognized as a major public health concern due to its pervasive environmental presence and widespread human exposure. Even low-dose BPA exposure has been associated with a range of adverse pathological, cellular, and molecular effects, raising concerns about its potential role in chronic disease development. Increasing evidence suggests that BPA may exert neurotoxic effects that contribute to the onset and progression of neurodegenerative disorders. Synucleinopathies represent a group of neurodegenerative diseases characterized by the abnormal accumulation and aggregation of α-synuclein in both the central and peripheral nervous systems. Misfolding of α-synuclein leads to the formation of toxic oligomeric species, which are believed to play a critical role in neuronal dysfunction and cell death, particularly in Parkinson's disease. Emerging studies indicate that environmental toxicants may influence α-synuclein aggregation and exacerbate neurodegenerative processes. Mitochondrial dysfunction has been increasingly implicated in neurodegeneration, as neurons rely heavily on mitochondrial oxidative phosphorylation to meet their high energy demands. Impairment of the mitochondrial electron transport chain can lead to reduced adenosine triphosphate (ATP) production, oxidative stress, and activation of apoptotic pathways. Notably, direct interactions between α-synuclein and mitochondria have been consistently observed in cellular models and in various brain regions of transgenic mouse models, suggesting a mechanistic link between protein aggregation and mitochondrial impairment. The present study aimed to investigate the cellular and molecular mechanisms underlying BPA-induced neurodegeneration, with a particular focus on α-synuclein-related pathways. **Methods:** Neuronal cells were treated with alpha-synuclein or BPA at various concentrations alone or in combination for different time intervals. Cell viability and cell death, ROS production, apoptosis and ATP level were evaluated. **Results:** Exposure to α-synuclein oligomers significantly reduced cell viability in a concentration-dependent manner after 24 hours. Co-treatment of SH-SY5Y cells with α-synuclein oligomers and graded concentrations of BPA (0.001-80 μM) for 24 hours markedly enhanced α-synuclein-induced cytotoxicity. BPA significantly increased α-synuclein-induced intracellular ROS production, an effect that was attenuated by the antioxidant N-acetyl-L-cysteine (NAC). Pretreatment with α-synuclein oligomers followed by BPA exposure resulted in a concentration-

dependent increase in caspase-3 activation and apoptotic cell death, both of which were significantly reduced by NAC or the caspase-3 inhibitor Ac-DEVD-CHO, indicating oxidative stress-mediated, caspase-3-dependent apoptosis. In addition, intracellular ATP levels were significantly reduced following combined exposure to BPA and α-synuclein oligomers. BPA-treated cells also exhibited increased α-synuclein aggregation, suggesting that BPA promotes protein aggregation and exacerbates neurodegenerative processes. **Conclusions:** These findings indicate that BPA enhances α-synuclein aggregation and potentiates α-synuclein-induced neurotoxicity through mechanisms involving oxidative stress, mitochondrial dysfunction, ATP depletion, and apoptosis. Collectively, the results suggest that BPA exposure may contribute to neurodegeneration by aggravating synucleinopathy-related pathogenic pathways. Supported by Title III.

ABSTRACT NUMBER: 5056 **Poster Board Number:** H606
TITLE: Neuropathology and Neuroinflammatory Hallmarks in Aging Felines with Cognitive Dysfunction

AUTHORS (FIRST INITIAL, LAST NAME) AND INSTITUTIONS: *A. W. Flanagan*, *A. Alsulami*, *C. Dobkins*, and *J. A. Moreno*. Colorado State University, Fort Collins, CO.
KEYWORDS: Neurotoxicology; Histopathology; Undergraduate Student

ABSTRACT: Background and Purpose: Neurodegenerative disorders like Alzheimer's Disease (AD) and other Alzheimer's Disease Related Dementias (ADRDs) affect over 55 million people worldwide. Current animal research models rely on genetically engineered rodents that only mimic AD symptoms. What these models fail to account for are differences in environmental exposures, genetics, and natural aging pathology, all main contributors to AD.Natural aging pathology presents with aggregation of amyloid beta (Aβ) plaques primarily accumulating in the neocortex, which spread inward eventually reaching the cerebellum. Aging also exhibits hyperphosphorylation of the tau protein, accumulating as neurofibrillary tangles (NFTs) in the trans-entorhinal cortex and spreading to limbic areas and the neocortex. These plaque buildups are associated with oxidative stress and neuroinflammation seen through activation of glial support cells throughout the CNS. Specifically, microglia and astrocytes are important for upholding homeostasis, decreasing plaque buildup, and supporting the blood-brain barrier. Because of the comparability of natural aging pathology, genetic diversity, and environmental exposures, the use of companion felines is thought to be a natural and accurate model for AD research. We hypothesize that at different age stages, and with increasing plaques and tangles, felines will show heightened levels of neuroinflammation. **Methods:** Immunohistochemistry (IHC) staining was performed on coronal sections of feline brains, with histopathology used to identify brain regions. Donated feline brains were trimmed and embedded using paraffin. Cortical and hippocampal regions were stained for Aβ using antibody 6E10, P-tau, microglial marker Iba1, and astrocyte markers S100β and GFAP. Animals were not grouped based on sex or breed. Exclusion criteria included brain and nervous system comorbidities such as cancer and sclerosis. Hemispheres were treated the same. Samples were processed in batches over 18 months. This was an observational trend study with no controls. Cells were counted using software trained to differentiate cells in IHC, including QuPath and ImageJ. Glial morphology was identified using 40 variables including radius, circularity, branching, and number of branches. These were grouped into four categories based on the main glial conformations. **Results:** A higher percentage of tissue coverage with amyloid beta plaques was observed in aged felines compared to young felines, and this difference was significant. Mature adult felines did not show significant plaque coverage. Patterns were similar between antibodies. P-tau was analyzed in neurons as well as all cells to show progression of aging.

While significance was observed, variability within age groups was extreme. Despite this variability, group averages showed significance. Some aged animals did not show many symptoms, paralleling certain humans who do not show clear signs of brain aging. Proinflammatory glial cells showed no measurable association with plaques or tangles. While greater correlations in glial activation between age groups were expected, percent tissue coverage of amyloid beta was consistent with expectations. **Conclusions:** The lack of correlation observed was largely due to not a large enough sample size and small inaccuracies associated with software analysis. Grouping strategies may need to be adjusted. These findings do not support felines as a consistent model for Alzheimer's Disease. Cognitive dysfunction appears sporadic while also being age dependent, making differentiation difficult. A more controlled study would be beneficial, and the use of different pathological markers may further improve interpretation.

ABSTRACT NUMBER: 5057 **Poster Board Number:** H607
TITLE: Chlorpyrifos and Chlorpyrifos-Oxon Induce Astrocytic Activation

AUTHORS (FIRST INITIAL, LAST NAME) AND INSTITUTIONS: J. Bekos, *S. Sakar*, *A. Anchan*, and *P. Reina-Gonzalez*. University of Rochester, Rochester, NY.
KEYWORDS: Neurotoxicity; Pesticides; Undergraduate Student; Organophosphates; Astroytes

ABSTRACT: Background and Purpose: Parkinson's Disease (PD) is one of the most common motor neurodegenerative disorders, characterized by the loss of tyrosine hydroxylase (TH)- positive neurons in the midbrain and the formation of α-synuclein-rich aggregates, known as Lewy Bodies. Although mutations in various genes have been implicated in PD, only approximately 10-15% of cases can be attributed to genetics alone. Numerous epidemiological studies have identified a link between exposure to the organophosphate pesticide chlorpyrifos (CP) and increased risk for PD. In the human body, CP is metabolized into its more potent form, chlorpyrifos-oxon (CPO). While it has been established for its function as a potent AChE inhibitor and ability to cause neurological disease, the precise mechanisms by which both forms of CP drive neurodegenerative diseases are unknown. Astrocytes are the most abundant cell type in the brain and play an important role in maintaining neuronal health and function. Astrocytic activation and dysfunction have been shown to drive various neurodegenerative diseases such as PD. The effects of CP and CPO on astrocytic activation have yet to be established; therefore, this project aims to demonstrate and define these effects. **Methods:** To investigate the effects of chlorpyrifos (CP) and chlorpyrifos-oxon (CPO) on astrocytes, a dose-response study was performed using the MTS assay to demonstrate the effects of CP and CPO on astrocytes. From here, we determined the dosages that significantly reduced metabolic activity; 150 µM for CP and 50 µM for CPO. Based on these results, astrocytes were treated at these concentrations and were further analyzed using a Seahorse Mitostress Test to evaluate alterations in mitochondrial metabolic dynamics following CP and CPO exposure. To assess astrocytic activation and inflammatory responses, immunocytochemistry (ICC) and quantitative polymerase chain reaction (qPCR) were performed on treated astrocytes, focusing on the expression of the pro-inflammatory cytokine interleukin-6 (IL-6). **Results:** Exposure to chlorpyrifos (CP) and its metabolite chlorpyrifos-oxon (CPO) led to significant, dose-dependent reductions in astrocytic metabolic activity as measured by the MTS assay and the Seahorse MitoStress test. CPO produced a greater decrease in metabolic activity at lower concentrations compared to CP. Consequently, 150 µM CP and 50 µM CPO were selected for subsequent analyses. Notably, CPO exposure caused a more pronounced reduction in astrocytic metabolic activity than CP at comparable concentrations.

Assessment of astrocytic activation using ICC and qPCR showed increased inflammatory signaling with both compounds, as indicated by elevated expression of the pro-inflammatory cytokine IL-6. CPO treatment resulted in higher IL-6 expression compared to CP treatment, suggesting astrocytes are more sensitive to CPO and exhibit stronger activation in response to it. **Conclusions:** The study demonstrates that both chlorpyrifos and its bioactive metabolite chlorpyrifos-oxon induce astrocytic dysfunction characterized by reduced metabolic activity, mitochondrial impairment, and increased inflammatory signaling. CPO consistently elicited a more severe astrocytic activation than CP, highlighting the neurotoxic potential of the oxon metabolite. These findings suggest that astrocytes may play a role in non-cell autonomous neurodegeneration in the context of pesticide neurotoxicity and could potentially be a target for drug intervention.

ABSTRACT NUMBER: 5058 **Poster Board Number:** H608
TITLE: Ziram-induced apoptotic cytotoxicity is caspase-independent in human dopaminergic neurons

AUTHORS (FIRST INITIAL, LAST NAME) AND INSTITUTIONS: *Z. B. Tong*, L. H. EI Touny, L. Mitchell, and *D. L. Gerhold*. NIH/NCATS, Rockville, MD.
KEYWORDS: Apoptosis; Neurotoxicity; Pesticides; Neurotoxicology

ABSTRACT: Background and Purpose: Ziram is a broad-spectrum fungicide and pesticide. Structurally, it contains a zinc atom between two sulfur atoms and is a bidentate metal chelator. Because of its wide applications in agriculture and food industry, and its potential toxicity to animals and humans, ziram is considered a significant environmental toxicant. Its neurotoxic effects in humans are suspected to cause degeneration of dopaminergic neurons and Parkinson's disease (PD). Previously, we found the activation of metallothionein genes (*MT1G, MT1E, MT2A*) in human dopaminergic neurons treated with several Parkinsonian toxicants such as ziram, rotenone, 6-hydroxydopamine, MPP+ and methylmercury (*Tong et al, Neurotox Res 2020, 35:967-978*) and engineered a reporter dopaminergic neuronal cell line expressing MT1G-HiBiT fusion protein to facilitate compound screening for *MT1G* activation (*Tong et al, SLAS Discovery 2025 June 21:35:100244*) . Interestingly, chelators were the most identified hits from these screens, and most of them also caused cell death. We are interested in defining the molecular mechanisms underlying *MT1G* activation by chelators and its relationship to cell death in neurons. Ziram appears to be one of the most potent chemicals to result in *MT1G* activation and cell death. We are using ziram as an example to determine the mechanisms underlying its toxicity in human dopaminergic neurons, define the relationship between *MT1G* activation and cell death, and hopefully provide insights into the PD etiology due to the environmental impacts on human health. **Methods:** We differentiated LUHMES cells to dopaminergic neurons in either 96- or 384-well plates and treated them with chemicals at various concentrations to induce cytotoxicity and cellular responses (*Tong et al, J. Appl Toxicol. 2017. 37(2):167-180. SLAS Discovery 2024, 29:1001*). Treated LUHMES cells were assayed for (1) cell viability and caspase 3/7 activity using CellTiterGlo and Caspase3/7 luminescent kits (Promega), respectively. (2) Apoptosis /necrosis using the FITC Annexin V Apoptosis Kit with 7-AAD (Biolegend) and flow cytometry. (3) Single cell viability and lipid peroxidation using LIVE/DEAD Viability/Cytotoxicity and Image-iT Peroxidation Kits (Thermo Fisher), respectively. Images were captured using an Opera Phenix and analyzed using Signals Image Artist. **Results:** We evaluated ziram-induced cytotoxicity and caspase 3/7 activity in LUHMES-derived dopaminergic neurons in comparison to known toxicants with distinct mechanisms. Staurosporine treatment, a known apoptotic inducer, resulted in significant reduction in viability at 18hrs with an EC_{50} of ~ 80 nM, concomitant with increased caspase 3/7 activity. Ziram also

resulted in neuronal cell death at an EC_{50} of ~3 µM but did not increase caspase 3/7 activity after treatment (up to 50 µM) for 16-18 hours. We further confirmed that ziram does not increase caspase activity up to 24 hours of treatment with a dose range of 0.3-20 µM. Using Annexin V staining, we observed that ziram induced apoptosis in ~70-80% of cells treated with 5 and 10 µM for 4 and 8hrs, similarly to staurosporine. Ziram was also more efficient and faster than staurosporine at inducing apoptosis in LHUMES neurons. Furthermore, the caspase inhibitor Z-VAD-FMK did not prevent apoptotic death resulting from treatment with either compound, suggesting that ziram and staurosporine-induced apoptosis is caspase 3/7- independent in LUHMES neurons. In comparison, Z-VAD-FMK reduced terfenadine-induced apoptosis and increased neuronal viability.Ziram also increased lipid peroxidation at 5 µM as seen with RSL3 treatment. Ferrostatin-1 inhibited ziram and RSL3-induced lipid peroxidation, but only rescued RSL3 and not ziram-induced neuronal cell death, suggesting that ziram does not ind uce ferroptosis in LUHMES neurons. **Conclusions:** We performed toxicity studies in human dopaminergic neurons using several chemicals known to cause cell death through apoptosis or ferroptosis. Taken together, ziram induces apoptotic cell death with no caspase 3/7 activation, while staurosporine induces a caspase 3/7 independent apoptotic cell death despite caspase activation. Ziram also increases lipid peroxidation without causing ferroptosis. This suggests that ziram-neurotoxicity in LUHMES neurons is not dependent on canonical apoptotic pathways. This research was supported in part by the Intramural research program of the NCATS, NIH.

ABSTRACT NUMBER: 5059 **Poster Board Number:** H609

TITLE: Dual ESI/APCI StayClean™ Ion Source QSight LC-MS/MS for Analysis of Near 400 Polar and Non-polar Pesticide Residues in Tea

AUTHORS (FIRST INITIAL, LAST NAME) AND INSTITUTIONS: S. Cai[1], and J. Jalali[2]. [1]PerkinElmer US LLC, Shelton, CA; and [2]PerkinElmer US LLC, Shelton, CT. Sponsor: S. Cai, Society of Environmental Toxicology and Chemistry

KEYWORDS: Food Safety; Pesticides; StayClean LC-MS/MS

ABSTRACT: Background and Purpose: Detecting pesticides in the environment and products we consume is becoming crucial. Pesticides are widely used in agriculture which could result in consumer exposure and negative health effects. Pesticides residues are commonly found in teas, and demand for analytical detection is increasing as global tea consumption increases. We developed a robust analytical method that enables almost 400 both polar and non-polar pesticides to be analyzed under ESI and APCI utilizing a dual source LC-MS/MS. This method eliminates the need for GC-MS/MS analysis by analyzing a list of 50 pesticides using APCI. **Methods:** Experiments were carried out using a QSight 420 UHPLC-MS/MS via a divert valve. For sample extraction, 15 mL centrifuge tubes, a high-capacity vortex mixer, and a refrigerated centrifuge were used. A solvent extraction sample prep procedure with internal standard dilution was employed. Matrix effects were evaluated using black tea. Absolute matrix effects determined in the additional tea matrices of chamomile, herbal blend, and catnip were determined by comparing peak areas between a post-extract spike and solvent-only standards at 10 ng/mL and 100 ng/mL. In total, 690 MRM transitions were monitored for 345 compounds in the ESI method, and 100 MRM transitions were monitored for 50 compounds in the APCI method. For both LC methods, a single C18 column was used. **Results:** By analyzing black tea, chamomile tea, herbal blend tea, and catnip samples, we demonstrate how a practical simple solvent extraction can be utilized to achieve the analysis of a large multi-residue panel of pesticides, with low limits of detection (with 319 of 395

analytes displaying LOQs of 5 ng/g or below), minimal matrix effects (94% of compounds with negligible %SSE in black tea), and excellent method performance (93% of compounds with accuracies within 70 - 120% and RSD < 20%). **Conclusions:** StayClean™ Technology allows for simple sample preparation with significantly reduced instrument downtime. It allows injection of thousands of dirty sample extracts with virtually no instrument cleaning and maintenance. Dual Source hardware design enables APCI analysis on traditionally GC-only compounds to be included in this LC pesticide panel, reducing instrument workload and potentially eliminating the need for complementary GC-MS protocol for multi-residue pesticide quantification. It allows automatic LC method and MS probe switching without manual intervention. Simple sample preparation and reliable instrumentation allow for a robust analytical solution with the potential to analyze hundreds of pesticides in many different matrices.

ABSTRACT NUMBER: 5060 **Poster Board Number:** H610
TITLE: Disposition and Metabolic Behavior of the Pyrethroid Insecticide, Cypermethrin in Laying Hen using Radiotracer Technology

AUTHORS (FIRST INITIAL, LAST NAME) AND INSTITUTIONS: K. Ahn, and B. Osterman. Eurofins Agroscience Services, Hercules, CA. Sponsor: *J. Luyendyk*
KEYWORDS:

ABSTRACT: Background and Purpose: Cypermethrin is a Type II synthetic pyrethroid insecticide used for the control of ectoparasites in caged laying hens. To characterize cypermethrin-derived residues, [cyclopropane (CY)-^{14}C]- and [phenoxy (PH)-^{14}C]-labeled cypermethrin (cis/trans isomers=40/60) were orally administered to laying hens once daily for eight consecutive days. **Methods:** Excreta and eggs were collected throughout dosing, and liver, fat and muscles tissues were collected at sacrifice. **Results:** Total radiolabel recovery in collected samples exceeded 82% of the administered dose. The majority of the administered radioactivity was recovered in excreta (77.1-79.4%) and gastrointestinal tract contents (3.2-4.2%), with minimal distribution to eggs (0.1-0.2%) and fat and muscle tissues (<0.1%). Residues were highest in liver and fat tissues, with fat concentrations exceeding those in muscle, consistent with the lipophilicity of cypermethrin. **Conclusions:** Parent cypermethrin was the major residue in fat tissues (~38-44% of total radioactive residues) and was present at low levels in eggs. Cypemethirn was present in egg yolk but not in egg white. Tissue samples showed a slight increase in cis isomers relative to the administered material, suggesting that trans isomers experience greater degradation. Cypermethrin was extensively metabolized via ester cleavage and oxidation of the phenoxybenzyl moiety, forming DCVC acid, 3-phenoxybenzoic acid, and conjugated metabolites, which were efficiently eliminated in excreta.

ABSTRACT NUMBER: 5061 **Poster Board Number:** H611
TITLE: Absorption and Toxicity of Tampon-Leached Metals in 2D and 3D Human Vaginal Cell Models

AUTHORS (FIRST INITIAL, LAST NAME) AND INSTITUTIONS: G. Katz, H. Hannoush, S. Kaneshiro, *D. Re*, and K. Schilling. Columbia University, New York, NY.
KEYWORDS: Metals; Reproductive Tract; Female; Cell Culture; Organotypic model; Toxic metals

ABSTRACT: Background and Purpose: Tampon use is common with around 100 million people using tampons daily globally, and the cumulative exposure over a lifetime is extensive (16-24 hours per day, 4-7 days monthly, over an average of 456 menses). Various chemicals, including endocrine disruptors, carcinogens, and reproductive toxicants, have been found in menstrual products including tampons. Our group was the first to characterize the metal content in tampons, including toxic metals lead (Pb), cadmium (Cd), and arsenic (As), as well as zinc (Zn) which was found at particularly high levels, as Zn nanoparticles are often added for antimicrobial purposes. More recently, our group demonstrated that metals leach from tampons under simulated vaginal and menstrual fluid conditions. Tampons are used internally and are designed to expand to make direct contact with the vaginal epithelium. The vagina is a permeable mucous membrane distinct from the dermal barrier with 10-80 times higher absorption compared to the dermis. However, there are no data on whether the leachable metals from menstrual products can be absorbed by vaginal cells, cross the epithelium, and cause local and/or distal harm. This study aims to understand the health implications of metal exposure in the vagina, including absorption potential, cytotoxic effect, and downstream impacts, and to highlight an understudied source of toxicants. **Methods:** To estimate real-world exposure doses, we quantified leachable metals from several different tampon types (e.g. absorbency levels, brands) under physiologically relevant conditions. Tampons were incubated with simulated menstrual fluid (pH 7.4) and vaginal fluid (pH 4.5) for 8 hours (maximum recommended use duration) and leachable metal levels were measured using inductively coupled plasma mass spectrometry (ICP-MS). These leachable metal concentrations informed absorption experiments using both a 2D model composed of human primary vaginal epithelial cells (Lifeline Cell Technology) and a 3D full-thickness human vaginal multilayer model (Mattek). Both models were treated with the average leachable levels of Pb, Cd, and As (as a mixture), and Zn (alone or combined with the other metals). Exposure durations were 2, 4, and 8 hours for the 2D model and 8, 24, and 48 hours for the 3D model. We quantified cellular metal uptake and measured metal penetration through the different mucosal layers in the 3D model using ICP-MS. Cell viability and cytotoxicity (XTT; immunostaining) were assessed over the same periods. Statistical analyses were performed using one-way ANOVA and t-tests (R; GraphPad Prism). **Results:** It was found that vaginal epithelial cells efficiently uptake all the tested metals, that these metals effectively cross the different layers of the vaginal mucosa in a time-dependent manner in a 3D model, and that Zn nanoparticles potentiate the absorption of Cd and Pb, likely due to the high sorption capacity of Zn oxide nanoparticles for divalent cations. Indeed, there was a statistically significant increase in the uptake of Cd (8.07-fold, p=4.065e-07) and Pb (4.23-fold p=3.339e-09) when in the presence of Zn nanoparticles at the average concentrations leached from tampons. Remarkably, in this real-world exposure dose experiment, it is shown that Zn nanoparticles are highly toxic to vaginal cells and drive the toxicity of the metal mixture. **Conclusions:** Our findings demonstrate a measurable risk of local vaginal toxicity from metals leached from tampons and illuminate an important exposure route, as toxicants entering through the vaginal route would bypass the liver and enter circulation. Our results on the penetration of metals through the multiple layers of the vaginal mucosa strongly suggest that this route of absorption can contribute to chronic

systemic metal exposure and associated adverse health effects. In addition, our results raise concern about the use of antimicrobial additives such as Zn nanoparticles in menstrual products and the need for expanding product safety standards to protect sexual and reproductive health.

ABSTRACT NUMBER: 5062 **Poster Board Number:** H612
TITLE: Metals in Toenails are Associated with Increased Likelihood of Poor Mental Health in Nova Scotian Adults

AUTHORS (FIRST INITIAL, LAST NAME) AND INSTITUTIONS: *A. Del Favero-Campbell*[1], E. Briand[2], D. E. Fleming[2], E. Sweeney[1], and *K. C. Fong*[3]. [1]Dalhousie University, Halifax, NS, Canada; [2]Mount Allison University, Sackville, NB, Canada; and [3]George Washington University, Washington, DC. Sponsor: A. Del Favero-Campbell, American Academy of Clinical Toxicology
KEYWORDS: Metals; Neurotoxicity; Metals; Environmental Toxicology

ABSTRACT: Background and Purpose: Nova Scotia contains geogenic sources of metals in its soils and private drinking water systems, resulting in chronic low-level exposure in some communities. Chronic metal exposures have been linked to adverse neurobehavioral outcomes. However, the combined effects of metal mixtures on mental health remain poorly understood, particularly in the Canadian Maritimes. Toenail biomarkers reflect longer-term metal exposure and provide insight into cumulative toxicological burden. The purpose of this study was to evaluate associations between a mixture of metals and trace elements measured in toenails and indicators of poor mental health in middle-aged and older adults (ages 45-80) residing in Nova Scotia, Canada. **Methods:** Data were obtained from 400 participants in the Atlantic Partnership for Tomorrow's Health (PATH) cohort who provided toenail samples and completed baseline health questionnaires. Poor mental health was defined as meeting at least one of the following criteria: Patient Health Questionnaire (PHQ-9) score ≥10, Generalized Anxiety Disorder Questionnaire (GAD-7) score ≥8, or self-reported physician diagnosis of depression. A matched case-control design was employed, with cases matched to controls based on age (±3 years) and gender. Toenail levels of 17 metals and trace elements were measured using portable X-ray fluorescence, with elemental values expressed as thickness-adjusted ratios derived from Compton peak normalization to account for nail thickness and density variability. Bayesian Kernel Machine Regression (BKMR) was used to estimate overall mixture effects, evaluate non-linear exposure-response relationships, assess potential metal-metal interactions, and identify metals contributing most strongly to the mixture association using posterior inclusion probabilities. Models were adjusted for socioeconomic status, cigarette smoking, alcohol use, and marijuana use. **Results:** Higher combined metal levels in toenails were associated with increased odds of poor mental health across mixture quantiles. When comparing moderate-to-upper versus median mixture exposure levels, odds ratios (OR) for poor mental health were approximately 1.8 to 2.1, with greater uncertainty at the highest exposure quantiles. Posterior inclusion probability analyses consistently identified arsenic, iron, zinc, and cobalt as primary contributors to the mixture effect. In conditional single-metal contrasts derived from the BKMR framework, holding other metals at median levels, higher arsenic was associated with increased odds of poor mental health (OR = 4.62; 95% CI: 1.36-15.68), while higher zinc suggested an inverse association (OR = 0.96; 95% CI: 0.92-1.01). Evidence of non-linear exposure-response relationships and potential metal-metal interactions was observed. **Conclusions:** These findings suggest that combined levels of multiple metals, as reflected by toenails as a biomarker, may be associated with indicators of poor mental health in middle-aged and older adults in Nova Scotia. Identification of specific metals

contributing to mixture effects underscores the importance of evaluating complex exposure profiles rather than single-metal metrics in environmental toxicology. This work supports the application of mixture-based analytical approaches for assessing potential neurobehavioral risks associated with chronic low-dose metal exposure in human populations.

ABSTRACT NUMBER: 5063 **Poster Board Number:** H613
TITLE: Environmentally Sourced Uranium Alters Gut Microbial Function and Host Metabolism

AUTHORS (FIRST INITIAL, LAST NAME) AND INSTITUTIONS: F. T. Lauer[1], S. S. Goitom[1], B. B. Maes[1], A. S. Romero[1], J. A. Rivas[1], H. Park[2], A. Uhlemann[2], *C. Shuey*[1], *J. M. Cerrato*[3], and *E. F. Castillo*[1]. [1]UNM HSC, Albuquerque, NM; [2]Columbia University Irving Medical Center, New York, NY; and [3]UNM, Albuquerque, NM.
KEYWORDS: Microbiome; Metals; Metabolism

ABSTRACT: Background and Purpose: Incomplete remediation of legacy uranium mining sites contribute to the contamination of uranium and other heavy metals in the environment, which can lead to possible exposures in humans and animals. While uranium toxicity has been extensively studied using purified uranyl salts, the biological consequences of environmentally sourced uranium exposures and their interactions with the gut microbiome remain poorly understood. **Methods:** Therefore, C57BL/6J (B6) mice were provided drinking water collected upstream (RPW-C, [^{238}U: <0.5 ppb]) or downstream (RPW-M, [^{238}U: 581.5 ppb]) of the Jackpile mine (Village of Paguate, NM) for 42 days. Waters were filtered and analyzed for metals prior to exposure and revealed RPW-M contained markedly elevated uranium, while other metals were present at low ppb concentrations. Intestinal and metabolic endpoints were assessed, and fecal microbiota were analyzed by shotgun metagenomics. To evaluate microbiota-mediated effects, fecal microbiota from RPW-C or RPW-M exposed mice were transplanted into antibiotic-treated B6 recipient mice maintained on either a normal diet or a high-fat/high-cholesterol diet (HFD). **Results:** Direct exposure to RPW-M water did not induce overt intestinal inflammation, as measured by fecal lipocalin-2, nor did it alter body weight. However, RPW-M-exposed mice exhibited significantly reduced circulating leptin and increased colonic Muc2 staining, consistent with altered metabolic signaling and mucus dynamics. Metagenomic analysis yielded 146 high-quality metagenome-assembled genomes (MAGs). Although broad taxonomic shifts were limited, uranium exposure significantly altered microbial α- and β-diversity at six weeks and enriched specific taxa, including *Pseudomonas* sp. and *Salmonella enterica*. Functional profiling revealed a three-fold enrichment of metal-stress and oxidative defense pathways in MAGs from uranium-exposed mice (Fisher's exact p = 0.0024). Following fecal microbiota transfer, recipients of RPW-M microbiota developed hepatic alterations, which were more pronounced under HFD conditions, consistent with diet-dependent amplification of microbiota-driven effects. **Conclusions:** Overall, our data suggest chronic ingestion of environmentally sourced uranium-contaminated drinking water reshapes gut microbial functional capacity without causing overt intestinal inflammation. Reduced circulating leptin, together with transmissible, diet-sensitive hepatic effects, supports a model in which uranium-associated microbiota alterations contribute to early metabolic dysregulation. Importantly, these effects were observed using real-world uranium exposure matrices, emphasizing that environmentally relevant uranium sources may elicit microbiome-mediated metabolic effects not captured by traditional uranyl salt models and are consistent with a second-hit paradigm in which dietary stress unmasks latent toxicity.

ABSTRACT NUMBER: 5064 **Poster Board Number:** H614

TITLE: Essential and Toxic Metals in Urine and Their Association with the Incidence of Preeclampsia - A Case-Control Study in Botucatu, Brazil

AUTHORS (FIRST INITIAL, LAST NAME) AND INSTITUTIONS: B. C. Jorge[1,2], S. T. Santos[1], J. P. Silva[1], T. M. Silva[3], F. Barbosa[4], V. C. Sandrim[1], and A. C. Arena[1]. [1]São Paulo State University, Botucatu, Brazil; [2]University of Mississippi Medical Center, Jackson, MS; [3]University of São Paulo - Ribeirão Preto Campus, Ribeirão Preto, Brazil; and [4]University of São Paulo (USP) Ribeirão Preto Campus, Ribeirão Preto, Brazil.
Sponsor: *W. Scarano*
KEYWORDS: Exposure Assessment; Environmental Toxicology; Metals

ABSTRACT: Background and Purpose: Preeclampsia (PE) is a hypertensive disorder of pregnancy associated with significant maternal and neonatal morbidity and mortality. Although abnormal placentation and maternal endothelial dysfunction are central to its pathophysiology, environmental contributors remain insufficiently explored. Numerous essential and non-essential metals function as endocrine-disrupting agents, interfering with hormonal signaling, oxidative balance, and placental vascular regulation, mechanistic pathways that are intrinsically linked to PE. This study quantified urinary levels of these metals in pregnant women and investigated their association with the occurrence of PE at the Botucatu Maternity Hospital in São Paulo, Brazil. **Methods:** A total of 185 pregnant women were included, comprising 155 with PE and 30 healthy controls. Clinical and obstetric data were collected from medical records at HCFMB after informed consent. Urine samples were analyzed for Li, Mn, Co, Cu, Se, Sr, Cd, Cs, Ba, Hg, Tl, and Pb using inductively coupled plasma mass spectrometry (ICP-MS). Statistical analyses included t tests or Kruskal-Wallis tests and nonlinear regression. **Results:** The mean maternal age was 28 years, with a median parity of two children. Prepregnancy BMI was higher in the PE group (25 [23-28] vs. 29 [26-35] kg/m²; $p = 0.0034$). Women with PE had higher systolic (120 [119-130] vs. 145 [131-160] mmHg; $p < 0.0001$) and diastolic blood pressure (80 [78-85] vs. 91 [85-100] mmHg; $p < 0.0001$). Gestational age at delivery was lower in the PE group (40 [39-40] vs. 37 [36-38] weeks; $p < 0.0001$). Fetal weight was slightly reduced in the PE group (3.19 [2.92-3.48] vs. 3.00 [2.52-3.38] grams; $p = 0.0131$). Five metals showed similar urinary concentrations between groups: Li, Sr, Cd, Cs, and Hg. In contrast, significant increases were observed for Mn (1.23 [0.79-1.71] vs. 3.35 [2.04-4.69]; $p < 0.0001$), Co (0.05 [0.01-0.97] vs. 1.60 [0.75-2.58]; $p < 0.0001$), Cu (13.49 [9.74-21.85] vs. 28.79 [18.38-44.86]; $p < 0.0001$), Se (18.95 [11.47-29.17] vs. 25.91 [16.64-36.61]; $p = 0.0141$), and Ba (1.12 [0.52-2.02] vs. 3.13 [1.16-8.47]; $p = 0.0003$). Reduced levels of Tl (0.27 [0.15-0.39] vs. 0.17 [0.10-0.28]; $p = 0.0165$) and Pb (0.84 [0.35-1.31] vs. 0.50 [0.22-0.90]; $p = 0.0354$) were observed in PE. Mn (OR = 1.001; 95% CI: 1.000-1.001; $p < 0.0001$), Co, Cu, Ba, and Se showed strong associations with PE incidence. **Conclusions:** This study demonstrates that pregnant women with PE exhibit a distinct urinary metal profile characterized by elevations in Mn, Co, Cu, Se, and Ba, alongside reductions in Tl and Pb. Given the endocrine-disrupting properties of several of these metals, such alterations may contribute to impaired placental signaling, vascular dysfunction, and the systemic imbalance characteristic of PE. These findings highlight the relevance of environmental metal biomarkers in understanding PE pathogenesis and underscore the need for longitudinal studies to clarify causal mechanisms and metabolic disruptions underlying these associations.

ABSTRACT NUMBER: 5065 **Poster Board Number:** H615

TITLE: Region-specific metal accumulation in cetacean brains: implications for neurological vulnerability

AUTHORS (FIRST INITIAL, LAST NAME) AND INSTITUTIONS: S. Salcedo[1], J. Crespo[2], and E. Martínez-López[1]. [1]University of Murcia, Murcia, Spain; and [2]Fundación Oceanogràfic, Valencia, Spain. Sponsor: *J. Wise*

KEYWORDS: Metals; Ecotoxicology; Neurotoxicity; Metals; Marine mammals

ABSTRACT: Background and Purpose: Cetaceans accumulate some of the highest levels of metals on Earth, yet little is known about their concentrations in the brain or their potential neurological effects. Given the structural and functional complexity of the brain, sensitivity to contaminants varies among regions and cell types, and whole-brain analyses may obscure localized patterns of accumulation and toxicity. Evidence from multiple species indicates that metals accumulate unevenly across brain regions, potentially causing region-specific pathological alterations. The aim of this study was to quantify metal concentrations in cetacean brains, examine regional differences in accumulation, and assess how contaminant exposure may differentially affect brain regions and associated neurological functions in marine mammals. **Methods:** We determined concentrations of Cd, Pb, As, Cr, Zn, Cu, Hg, Se, and the molar Se:Hg ratio in multiple brain regions of 51 cetaceans stranded along the Western Mediterranean coast between 2019 and 2025. Analyzed regions included the cerebral cortex, metencephalon, diencephalon, and hippocampus, as well as more detailed subregions: the four cortical lobes, hypothalamus, thalamus, brainstem, cerebellar hemispheres, and vermis. Samples were digested using a microwave digestion system and analyzed by inductively coupled plasma mass spectrometry (ICP-MS). Studied species included striped dolphin (*Stenella coeruleoalba*, n = 31), bottlenose dolphin (*Tursiops truncatus*, n = 10), common dolphin (*Delphinus delphis*, n = 2), long-finned pilot whale (*Globicephala melas*, n = 2), Risso's dolphin (*Grampus griseus*, n = 1), and Cuvier's beaked whale (*Ziphius cavirostris*, n = 1). **Results:** Overall, the highest concentrations were observed for Zn, followed by Cu, Hg, Se, As, Cr, Pb, and Cd. Regional distribution patterns showed the highest concentrations for most metals in the diencephalon, with the exception of Zn, which predominated in the cerebral cortex (median: 14.32 mg/kg). Median concentrations in the diencephalon were: Cu (3.40 mg/kg), Hg (1.50 mg/kg), Se (1.14 mg/kg), As (0.29 mg/kg), Cr (0.05 mg/kg), Pb (0.07 mg/kg), and Cd (0.01 mg/kg). Comparisons between striped dolphins and bottlenose dolphins revealed significant differences in Se ($Z = -3.43$, $p < 0.001$), Zn ($F = 0.131$, $p = 0.004$), and Pb ($F = 7.97$, $p = 0.035$). Sex-related differences were observed for most metals, with higher concentrations in females for Hg, Se, Cr, and Pb, and higher levels in males for As. Age-related differences were detected for Zn, As, Se, Cd, and Hg, with distinct accumulation patterns across developmental stages. In most cases, Se:Hg molar ratios exceeded 1, indicating a molar excess of Se, which may itself be toxic at elevated concentrations. **Conclusions:** Our results demonstrate that metal accumulation in cetacean brains is highly region-specific and influenced by species, sex, and age. The preferential accumulation of multiple metals in the diencephalon highlights this region as potentially vulnerable to contaminant-related neurotoxicity. These findings underscore the limitations of whole-brain approaches and emphasize the need for region-specific analyses to better understand the neurological risks posed by metal exposure in marine mammals.

ABSTRACT NUMBER: 5066 **Poster Board Number:** H616

TITLE: Advancing Risk-Based Food Safety Governance: An Assessment of the United Arab Emirates National Food Control System and Implications for Human Health Protection

AUTHORS (FIRST INITIAL, LAST NAME) AND INSTITUTIONS: M. S. Alhammadi[1], A. S. Jannan[1], S. Mansour[2], M. Cardo[2], M. Badr[2], E. Elhassan[2], A. A. Al Mannae[1], M. A. Abualush[1], A. H. Bin Harib[1], E. A. Nassar[3], and *A. M. Kadry*[1]. [1]Ministry of Climate Change and Environment (MOCCAE), Dubai, United Arab Emirates; [2]Food and Agriculture Organization of the United Nations (FAO), Rome, Italy; and [3]Abu Dhabi Agriculture and Food Safety Authority (ADAFSA), Abu Dhabi, United Arab Emirates.

KEYWORDS: Food Safety; Risk Assessment; Regulatory Science/Regulatory Toxicology; FAO/WHO Evaluation Tool

ABSTRACT: Background and Purpose: Risk-based approaches are a foundational element of contemporary food safety governance, enabling competent authorities to prioritize hazards of greatest public health relevance while allocating regulatory resources efficiently and transparently. Over the past decade, the United Arab Emirates (UAE) has undertaken sustained reforms to strengthen its national food control system, with particular emphasis on science-based risk analysis, enhancement of laboratory capacity, and improved cross-sectoral coordination. This abstract presents the findings of a collaborative, multi-institutional initiative led by the Ministry of Climate Change and Environment, in partnership with the Food and Agriculture Organization of the United Nations (FAO), to evaluate the structure, performance, and public health relevance of the UAE national food control system using the FAO/WHO National Food Control System Evaluation Tool. Specific attention was given to the development and operationalization of risk profiling, risk categorization, and evidence-informed decision-making processes that underpin regulatory prioritization and human health protection. **Methods:** A comprehensive system-level evaluation was conducted by FAO/WHO experts in accordance with established FAO/WHO guidance and internationally recognized criteria for food control system performance. Evidence was reviewed across federal and emirate-level Competent Authorities, encompassing legislative and regulatory frameworks, risk-based inspection and compliance systems, laboratory accreditation and proficiency testing programs, national and subnational food monitoring activities, surveillance platforms, and documented risk profiles. Qualitative and semi-quantitative analytical approaches were applied to assess how risk analysis principles are implemented in practice, how data are generated and integrated into regulatory decision-making, and how institutional governance arrangements support food safety and toxicological risk management. **Results:** The evaluation identified a well-developed and increasingly integrated national food control system supported by strong scientific, technical, and institutional foundations. Risk-based inspection frameworks and food business categorization schemes are widely implemented across Emirates and are routinely applied to both domestic controls and import oversight. Official control laboratories demonstrated consistently high analytical performance, supported by accreditation and satisfactory proficiency testing outcomes, enabling reliable detection of chemical and microbiological hazards relevant to human exposure. A diverse portfolio of risk profiles addressing priority hazards including pesticide residues, veterinary drug residues, food additives, micro- and nano-plastics, and zoonotic agents illustrates the progressive integration of risk-informed approaches into regulatory practice. National coordination mechanisms, notably the National Food Safety Committee and its Risk Assessment Team, provide an effective platform for harmonization, data integration, and the continued strengthening of national risk assessment capacity. Strategic collaboration with international partners

further enhances technical capability and alignment with global best practices. **Conclusions:** Overall, the UAE national food control system reflects a mature, science-driven approach that is closely aligned with internationally accepted principles of risk-based food safety management. Continued efforts to harmonize risk categorization methodologies, consolidate monitoring and surveillance data at the national level, and transition from qualitative risk profiling toward more formal quantitative risk assessments will further strengthen public health protection. The UAE experience offers a valuable case study demonstrating how sustained investment in risk analysis infrastructure, laboratory excellence, and intersectoral governance can support effective, resilient, and evidence-based food safety systems in complex and rapidly evolving food environments.

ABSTRACT NUMBER: 5067 **Poster Board Number:** H617
TITLE: Safety evaluation of dietary supplements under the US FDA's Human Foods Program

AUTHORS (FIRST INITIAL, LAST NAME) AND INSTITUTIONS: *P. Iyer*, A. Abdel-Rahman, E. Evaristus, *L. T. Steen*, and *R. P. Yeager*. US FDA, College Park, MD.
KEYWORDS: Safety Evaluation; Food Toxicity; Regulatory Science/Regulatory Toxicology; Dietary Supplements; Botanicals

ABSTRACT: Background and Purpose: We present here elements of the safety review process, and the methodologies reviewers employ to assess a new dietary ingredient (NDI) within the context of FDA's regulation of dietary supplements (DS) and challenges that may arise. FDA's authority to regulate dietary supplements is established in the Federal Food, Drug, and Cosmetic Act (FDCA). DS are a category of food and defined as supplementary to the diet. **Methods:** Unlike other FDA regulated products, FDCA does not require pre-market approval for dietary supplements, but does require manufacturers and distributors of certain NDIs, i.e., dietary ingredients not marketed in the U.S. before 1994, to submit a safety notification at least 75 days before introducing the ingredient to market. NDI notifications require a description of the ingredient, the proposed conditions of use and a history of use (HOU) or other evidence of safety (OES) demonstrating a reasonable expectation of safety for the NDI under the proposed conditions of use. FDA substantively reviews the information submitted to support the identity of an NDI, and the safety data in an NDI, including HOU and OES. The safety review for the NDI is focused primarily on safety rather than efficacy, defining a risk-only paradigm. HOU includes any reference that supports historical or current use of the NDI as/in food or DS, while OES typically includes genetic toxicity, preclinical animal studies, clinical studies, or case reports. **Results:** The amount, quality and type of safety data varies significantly by notification, but the FDA safety review focuses on prioritizing, evaluating, and integrating data to identify signals of harm. Characterization of the risk from the proposed exposure to the NDI is used to determine if there is a reasonable expectation of safety. Challenges to our safety review include inadequate identification, missing quantitative and qualitative details of historical use, and considerations for vulnerable subpopulations. Following our review, a response letter is sent acknowledging the notification without objection or with objection based on our safety conclusion. Review of post-market dietary supplements uses a similar paradigm. However, the quality of toxicity signals from different sources varies and can be difficult to attribute to an ingredient because other factors confound the data, such as multi-ingredient dietary supplements, , concomitant use of drugs and dietary supplements, as well as incomplete patient history. **Conclusions:** The increasing use of DS as evidenced by the growth of the dietary supplement industry justifies continued safety assessment of these products to protect public health.

ABSTRACT NUMBER: 5068 **Poster Board Number:** H618

TITLE: Antimicrobial activity of *Alternaria* mycotoxins and gut microbiota-dependent modulation of mycotoxin immunotoxicity

AUTHORS (FIRST INITIAL, LAST NAME) AND INSTITUTIONS: F. Crudo[1], P. Petri[1], C. Dall'Asta[2], N. Birse[3], D. Berry[1], and D. Marko[1]. [1]University of Vienna, Vienna, Austria; [2]University of Parma, Parma, Italy; and [3]Queen's University Belfast, Belfast, United Kingdom. Sponsor: *J. Vondrácek*

KEYWORDS: Microbiome; Immunotoxicity; Alternaria mycotoxins

ABSTRACT: Background and Purpose: The human gut microbiota represents a key barrier against dietary contaminants and pathogens and plays essential roles in digestion, immune regulation, and host homeostasis. *Alternaria* mycotoxins are frequently detected in fruits, cereals, infant foods, and human breast milk, and several have been reported to exert immunosuppressive effects *in vitro*. If, on the one hand, this class of emerging contaminants might target the gut microbiota leading to potential adverse health outcomes, on the other hand, the gut microbiota might modify the toxicodynamics of these mycotoxins. Based on this, the present study evaluated the immunosuppressive properties of the understudied mycotoxin alterperylenol (ALTP), characterized the antimicrobial activity of four *Alternaria* mycotoxins, and assessed the capacity of human gut bacteria to modulate their immunotoxic effects. **Methods:** Immunosuppressive activity of ALTP was evaluated in a co-culture model of Caco-2 and HT29-MTX-E12 cells separated from THP-1 Lucia monocytes by a semipermeable membrane, using an NF-κB reporter gene assay. Antimicrobial activity of ALTP, alternariol (AOH), alternariol monomethyl ether (AME), and altersetin (AST) was assessed in a panel of gut bacterial strains representative of adult and infant microbiota (*Bacteroides vulgatus, Bacteroides thetaiotaomicron, Escherichia coli, Bifidobacterium adolescentis, Clostridium perfringens, Enterococcus faecalis, Klebsiella michiganensis, and Lactiplantibacillus plantarum*). Bacterial growth was monitored over 24 hours under anaerobic conditions via repeated OD_{600} measurements across increasing mycotoxin concentrations. Microbiota-dependent modulation of immunotoxicity was examined by exposing THP-1 Lucia monocytes to bacterial culture supernatants. High-resolution LC-MS analysis was performed to investigate microbial metabolism of selected mycotoxins following incubation with viable and non-viable bacteria. **Results:** In the co-culture model, ALTP significantly suppressed immune activation, decreasing lipopolysaccharide-induced NF-κB signaling by approximately 40% at 5 µM, thereby demonstrating its ability to cross the intestinal barrier and directly affect THP-1 monocytes. Among the mycotoxins tested, AST showed the strongest antimicrobial activity, reducing bacterial growth already at nanomolar to low-micromolar concentrations and completely inhibiting most strains at 10 µM. In contrast, AOH required substantially higher concentrations, with initial growth-reducing effects appearing around 1 µM, while complete inhibition was generally observed only at 50 µM. AME and ALTP induced only minor growth inhibition across the tested concentration range. NF-κB reporter assays revealed that specific gut bacteria markedly altered the immunosuppressive activity of individual mycotoxins. Notably, the immunosuppressive effect of ALTP was completely abolished after incubation with viable *E. coli*, while no changes occurred with non-viable bacteria. LC-MS analysis identified, for the first time, the bacterial conversion of ALTP into altertoxin-I, a structurally related *Alternaria* mycotoxin lacking a double bond. **Conclusions:** This study demonstrates a complex bidirectional interplay between *Alternaria* mycotoxins

and the gut microbiota: while certain mycotoxins exhibit antimicrobial activity, gut bacteria can potentially metabolize these compounds and substantially modulate their immunotoxic potential. Such microbiota-dependent effects should be considered in future risk assessments addressing chronic dietary exposure to *Alternaria* mycotoxins. **Acknowledgments:** This research was funded by the Austrian Science Fund (FWF) [grant DOI: 10.55776/PAT4370324; *MycoGut* project] and by the European Union's Horizon Europe research and innovation programme under the Marie Skłodowska-Curie Actions [grant agreement No. 101131125; *Mycobeans* project].

ABSTRACT NUMBER: 5069 **Poster Board Number:** H619

TITLE: Development of a computational dashboard for predicting potential for biopersistence of chemicals

AUTHORS (FIRST INITIAL, LAST NAME) AND INSTITUTIONS: *J. A. Camacho*[1], M. Ferguson[1], *C. Sauders*[1], M. F. Santillo[2], *P. Rice*[1], and *S. V. Kabadi*[1]. [1]FDA, College Park, MD; and [2]FDA, Laurel, MD.

KEYWORDS: Food Safety; Risk Assessment; Computational Toxicology; Biopersistence, QSAR model

ABSTRACT: Background and Purpose: The biopersistence potential of a chemical may contribute to its toxicity, and safety assessments using default safety factors may not be applicable to biopersistent chemicals. There are very few guidance documents available that discuss general considerations for assessing potential for biopersistence, and no regulatory guidelines for assessing safety of potentially biopersistent food chemicals. Additionally, there are no computational platforms available to predict the potential for biopersistence of chemicals in the body. Furthermore, the multiple factors that could contribute to the biopersistence potential have not been examined from the perspective of proposing a safety assessment approach to potentially biopersistent chemicals. We created an internal database of relevant structural, physicochemical, toxicokinetic (TK) and toxicity parameters for over 300 functionally diverse chemicals, including food substances, environmental chemicals and drugs, by searching published literature and databases, as well as data in Agency files. We retrieved additional physicochemical parameters from publicly available Application Programming Interfaces (API) to fill in data gaps in the curated datasets. All these data were used to develop an internal computational dashboard to predict oral bioavailability (F), elimination half-lives ($t_{1/2}$) and chronic No Observed Adverse Effect Levels (cNOAEL) of test chemicals. This internal dashboard will serve as an important resource for assessing hazard related to potential for biopersistence of chemicals with sparse toxicological data. **Methods:** A training dataset of over 300 chemicals was compiled and data on structural, physicochemical, TK and toxicity characteristics were curated to develop an internal database. Additional descriptors/features (e.g.; Topological polar surface area (TPSA), ring count, etc.) were retrieved using the R webchem package from the PubChem and CACTUS open chemistry databases at the National Institutes of Health. The biopersistence indicators were then translated to ordinal indicators. $t_{1/2}$ was categorized as follows: < 12 hours, 12 - 24 hours, 1 week and > 1 week. F was tiered into low (<50%), moderate (50-85%) and high (>85%) categories. cNOAEL was categorized as < 1 mg/kg bw/day, 1- 10 mg/kg bw/day, 10 - 100 mg/kg bw/day and > 100 mg/kg bw/day. A QSAR model was developed using a gradient-boosted random forest in the xgboost R package, to predict biopersistence from the chemical properties. Finally, a user-friendly and accessible dashboard was built in R Shiny to implement these methods. **Results:** Utilizing a curated internal database of over 300 chemicals and including descriptors of structural, physicochemical, and toxicity retrieved from public APIs, we were able to predict the biopersistence indicators of F, $t_{1/2}$ and cNOAEL. Prediction accuracy for a random

subsample of the training data was, on average, at least 95% for all three biopersistence indicators. In one example, our internal dashboard accurately predicted a long half-life, low bioavailability, and low cNOAEL for perfluorooctyl iodide. **Conclusions:** Our internal computational dashboard is useful for predicting potential for biopersistence based on the totality of F, $t_{1/2}$ and cNOAEL, with the assistance of machine learning. We will continue to further develop and ultimately validate our dashboard with external test set of chemicals as we expand and maintain our internal database and add more features to improve user experience. The ultimate goal of this project is to identify a suitable approach to evaluate safety of potentially biopersistent chemicals based on the predicted indicators.

ABSTRACT NUMBER: 5070 **Poster Board Number:** H620
TITLE: Valorization of Seaweeds from Andaman and Nicobar Islands as Safe and Sustainable Blue Foods: Nutritional, Bioactive, and Food Safety Perspectives

AUTHORS (FIRST INITIAL, LAST NAME) AND INSTITUTIONS: T. Jindal. Amity University Uttar Pradesh, Noida, India. Sponsor: T. Jindal, Society of Environmental Toxicology and Chemistry
KEYWORDS: Food Safety; Natural Products; Nutrition

ABSTRACT: Background and Purpose: Seaweeds are increasingly recognized as sustainable “blue foods” with significant potential to enhance food and nutrition security. However, their capacity to accumulate harmful compounds and potentially toxic elements poses challenges to food safety. Despite the rich seaweed biodiversity of the Andaman and Nicobar (A & N) Islands, comprehensive evaluations integrating nutritional value, bioactive potential, and chemical safety remain limited. This study aims to valorize selected seaweeds from the A & N Islands by systematically assessing their nutritional composition, bioactive properties, and food safety to support their safe utilization as sustainable blue foods. **Methods:** Coastal seaweeds from the A & N Islands were mapped and taxonomically documented to assess distribution and yield potential. Representative green, red, and brown seaweeds (*Ulva, Enteromorpha, Gracilaria, Kappaphycus,* and *Sargassum*) were analyzed for proximate composition, dietary fiber, essential minerals, vitamins, and nutraceutical constituents. Potentially toxic elements, including arsenic, cadmium, lead, mercury, and excess iodine, were quantified using validated analytical techniques such as ICP-MS, GC-MS, FTIR, and NMR. Bioactive compounds were extracted using green technologies and evaluated for antioxidant, anti-inflammatory, enzyme inhibitory, and antimicrobial activities through *in vitro* assays. Toxicological screening was conducted to support safety characterization. Additionally, seaweed-derived biopolymers were assessed for edible thin-film food packaging applications, with emphasis on contaminant migration and consumer exposure. **Results:** The studied seaweeds demonstrated high nutritional value, characterized by substantial dietary fiber, essential minerals, and bioactive nutraceuticals. Bioactive extracts exhibited significant antioxidant, antimicrobial, and enzyme inhibitory activities. While most samples showed contaminant levels within permissible limits, species-specific variations in potentially toxic elements highlighted the need for risk-based selection and processing. Seaweed-derived biopolymers displayed promising functional properties for edible packaging, with minimal risk of contaminant transfer under controlled conditions. **Conclusions:** This integrated nutritional, bioactivity, and food safety evaluation establishes a scientific basis for the safe utilization of seaweeds from the Andaman and Nicobar Islands as functional blue foods. The findings support evidence-based risk-benefit assessment, promote sustainable seaweed valorization, and contribute to blue economy initiatives while ensuring public health protection for island and coastal communities.

ABSTRACT NUMBER: 5071 **Poster Board Number:** H621

TITLE: Predicting Impurity Stability in Food Contact Substances: A NAMs-based Case Study

AUTHORS (FIRST INITIAL, LAST NAME) AND INSTITUTIONS: *L. C. Markley*[1], P. Turowski[1], and M. Santillo[2]. [1]US FDA/ Human Foods Program, College Park, MD; and [2]US FDA/ Human Foods Program, Laurel, MD.

KEYWORDS: Food Safety; Risk Assessment; New Approach Methodologies; Triethylborane

ABSTRACT: Background and Purpose: The safety assessment of a novel biodegradable polymer for food-contact use presents a unique challenge due to its potential manufacturing impurity, triethylborane (TEB). We considered whether TEB would hydrolyze to boric acid during manufacturing of the food contact substance (FCS) or upon ingestion, which would eliminate the need for dietary exposure assessment. To inform whether dietary exposure to TEB would be anticipated, we evaluated its chemical stability and the potential for metabolic transformation under FCS manufacturing and physiological conditions. No relevant toxicological data were available that would support the estimated dietary exposure per FDA's Toxicology Guidance for the safety evaluation of food contact substances. **Methods:** In the absence of relevant toxicological data, we used new approach methodologies (NAMs) to evaluate TEB degradation potential under chemical and physiological conditions. To evaluate TEB's stability and potential metabolism, a multi-pronged approach was used: (1) assessment of TEB's chemical stability in water and acid; (2) *in silico* metabolism modeling using the EPA Chemical Transformation Simulator and Meteor Nexus to predict potential metabolites; and (3) re-analysis of historical acute toxicity studies to assess toxicokinetic differences between exposure routes to evaluate its absorption upon oral exposure. This multi-pronged strategy allowed us to assess the likelihood of chemical degradation or metabolic transformation in the absence of conventional toxicology studies. **Results:** The predictions of our analyses indicated that TEB is stable in a polymer matrix, is immiscible in water, and is unlikely to hydrolyze under acidic conditions. *In silico* models predicted no TEB metabolites upon oral exposure with moderate to high confidence. A critical review of historical data based on acute toxicity studies found a substantial difference between the oral LD50 (235 mg/kg) and the intraperitoneal LD50 (22.7 mg/kg) in rats. This implied that slow gastrointestinal absorption, rather than metabolism, dictated its acute oral toxicity. Updated literature searches did not identify any subchronic or chronic toxicity studies to further evaluate the absorption profile of TEB in longer-term exposure scenarios. These results collectively indicate that TEB is stable in a polymer matrix, does not hydrolyze, is not metabolized under physiological conditions, and does exhibit oral toxicity driven by limited absorption rather than biotransformation. **Conclusions:** Chemical and *in silico* modeling confirmed TEB stability under food-contact and physiological conditions, indicating no degradation during manufacturing of the FCS or ingestion. Therefore, dietary exposure to TEB as a potential impurity in an FCS would be expected. Furthermore, available acute toxicity data indicate that slow gastrointestinal absorption, and not metabolism, could impact its toxicity profile upon oral exposure. Considering that relevant toxicological data are not available per FDA’s Toxicology Guidance, the safety evaluation of the impurity TEB in the FCS remains a data gap. This case study illustrates how NAMs can provide important insights into chemical fate and support exposure assessment approaches for regulatory decision-making.

ABSTRACT NUMBER: 5072 **Poster Board Number:** H622
TITLE: From Past to Plate: Toxicological Considerations for Novel Mycelia-Based Food Ingredients

AUTHORS (FIRST INITIAL, LAST NAME) AND INSTITUTIONS: *S. VanEtten*, and *L. Markley*. FDA Human Foods Program, College Park, MD.
KEYWORDS: Food Safety; Food Toxicity; Food Allergy; Mycelia

ABSTRACT: Background and Purpose: Mycelia-based food ingredients represent an emerging category of novel protein-carbohydrate mixtures with applications in meat and dairy alternatives. Unlike traditional mushroom fruiting bodies, mycelia are vegetative fungal structures with distinct metabolite profiles and gene expression patterns. This analysis characterizes the existing toxicological data landscape and identifies data patterns in mycelia safety research methodologies. **Methods:** We conducted a comprehensive literature review of publicly available toxicological data for mushroom mycelia and fruiting bodies. Studies were evaluated for the type and extent of toxicological information, including acute toxicity, repeated-dose testing, genetic toxicity, and human tolerance data. Approaches used in the literature to support comparison between developmental stages or related species were examined using scientific considerations for biological similarity and toxicological relevance. **Results:** The review identified that toxicological information specific to mycelia is limited compared with the more extensive data available for mushroom fruiting bodies. Many assessments relied on extrapolations from fruiting body data or from related fungal species. Mycelia-specific toxicological studies were more commonly associated with low-dose therapeutic research rather than food-relevant exposure ranges. Metabolomic comparisons were used in some studies to characterize similarities or differences between mycelia and fruiting bodies or to inform cross-species extrapolations. **Conclusions:** Publicly available information indicates that toxicological characterization of mycelia-based ingredients may be constrained by the limited availability of mycelia-specific toxicological data and the frequent use of developmental stage or species comparison approaches. Additional toxicological studies tailored to the relevant fungal species and biological stage could enhance the scientific foundation available to inform scientific evaluations of these emerging ingredients. This analysis underscores scientific considerations that may be important when characterizing novel mycelia-based food components.

ABSTRACT NUMBER: 5073 **Poster Board Number:** H623
TITLE: Pre-clinical dose dependent safety evaluation of *Piper methysticum (*Kava) extract

AUTHORS (FIRST INITIAL, LAST NAME) AND INSTITUTIONS: *S. S. Panchal*[1], R. Niddel[2], S. Saini[1], A. Kalra[1], P. Gandhi[1], K. Patel[1], and A. Srivastava[2]. [1]Institute of Pharmacy, Nirma University, Ahmedabad, India; and [2]Diversified Botonics, Draper, UT.
KEYWORDS: Safety Evaluation; Kava

ABSTRACT: Background and Purpose: *Piper methysticum*, commonly known as Kava, is a traditional South Pacific plant which is traditionally used for preparation of beverages known for their calming and mood enhancing effects. It is popular for anxiolytic and muscle relaxant effect and many a time consumed as an alternative to other anxiolytic agents. The present study aimed to investigate the dose dependent pre-clinical *in-vivo* safety profile of Kava extract. **Methods:** Healthy Adult Wistar rats were administered Kava extract for 30 days orally at three dose levels (28.4, 141.2 and 282.4 mg/kg), corresponding to human equivalent and upto tenfold higher doses. As a positive control groups, alcohol at two different dose levels (5% and 20% in drinking water) was given upto 30 days. The study protocol

was approved by Institutional Anima Ethics Committee as per Committee for Control and Supervision of Experiments on Animals (CCSEA) guidelines as per Government of India. Hematological and biochemical (serum glucose level, hepatic and renal) parameters were evaluated. Histopathological examination was performed for all five vital organs. **Results:** Hematological parameters were found within normal range for all the animals. Total and direct bilirubin, total protein, albumin, SGPT, SGOT, ALP, BUN, creatinine and electrolytes were found unaltered in all the treated groups when compared with normal control animals after 30 days treatment. Histopathology study indicated significate morphological changes in liver in 20% alcohol treated group compared to normal control and kava treated groups. In liver, lung and kidney significant morphological changes were observed with 20% alcohol treatment compared to all other groups. **Conclusions:** In conclusion, kava extract was well tolerated in rats at the human-equivalent dose and at doses up to ten-fold higher where no signs of systemic or liver and renal toxicity when compared with the selected alcohol dose levels.

ABSTRACT NUMBER: 5074 **Poster Board Number:** H624

TITLE: Phytochemical composition of Valerian root extract: A strategy for lot selection for toxicity testing using targeted and non-targeted chemical analysis

AUTHORS (FIRST INITIAL, LAST NAME) AND INSTITUTIONS: J. T. Sloop[1], T. Cristy[2], J. Pierfelice[2], and *S. Waidyanatha*[1]. [1]NIEHS, Durham, NC; and [2]Battelle, Columbus, OH.

KEYWORDS: Botanicals; Chemical Characterization

ABSTRACT: Background and Purpose: Botanical dietary supplements are widely used around the world for their purported therapeutic properties. Data for safe use of these products are limited and assessing their safety presents a unique challenge due to natural complexity and variability of consumer products. Valeriana is a genus of flowering plants with about 200 species in Europe, Asia, and North America. *Valeriana officinalis* is one of these species, and *V. officinalis* root has been traditionally used for sedative and antispasmodic purposes. Due to limited data available to assess safe use of valerian root extract, we are conducting toxicology studies using rodent models. Using an appropriate, quality botanical product representative of what consumers use is key to generate robust safety data that can be compared widely across studies and used to evaluate risk. The purpose of this work was to investigate multiple commercially available Valerian products to (a) select a lot as the test article for these studies, and (b) perform market comparison over the course of 10 years to determine what products reflect authentic *V. officinalis* material and which appear to be adulterated/inconsistent with true botanical identity. **Methods:** During the initial lot selection (approx. 10 years ago), multiple vendors were identified for procuring bulk quantities of eight lots of unfinished (i.e., bulk extract used as source material for a finished material) Valerian root extract. A suite of analyses was performed on these, including valerenic acids (marker constituents of valerian), water content, elemental composition, saccharides, methanol/hexane extractables, total carbohydrate, and starch content. A comprehensive characterization was performed on the lot selected for testing in rodents (i.e., test article lot), including analyses previously mentioned, as well as quantitation of sterols/tocopherols, screening for volatiles, and storage stability using valerian marker constituents. During the market comparison, we procured and analyzed commercially available unfinished and finished materials of *V. officinalis*. During this, a Valerian extract reference material was commercially available and was included in the analyses. All samples, including the previously procured material, were analyzed using a non-targeted analysis/suspect screening approach. Principal components analysis (PCA), hierarchical clustering

analysis (HCA), and K-means clustering were performed to better visualize the differences between the chemical composition of the samples. **Results:** Across the initial screening, water content and inorganic constituents varied minimally. The lots were largely composed of carbohydrates and contained variable amounts of simple sugars. Valerenic acids were generally scarce, with only one lot containing >0.1% total valerenic acids. Based on minimizing metals and saccharides while maximizing valerenic acids and reducing non-Valerian chemicals, a comprehensive characterization was performed on a separate lot from the same vendor to serve as the test article for ongoing toxicology studies. The test article was found to have similar levels of water, inorganics, carbohydrates, and methanol/hexane extractables as the initial lots, but contained 0.668% total valerenic acids, similar to reference material. During the market comparison, multivariate statistical analyses (PCA, HCA, K-means) of all Valerian samples showed that only a few of the unfinished and finished materials (including the test article lot) were similar to the reference material, with most being very dissimilar from the reference. **Conclusions:** By evaluating an array of physicochemical attributes, we distinguished authentic *V. officinalis* extracts from materials exhibiting substantial deviations/evidence of adulteration. Identifying a single lot with chemical features consistent with genuine Valerian enabled the selection of a reliable test article for toxicology studies, and demonstrated the value of applying systematic, multi-parameter screening approaches to botanical materials. The market comparison revealed that many commercially available products advertised as Valerian had little chemical resemblance to well-characterized reference material, highlighting significant variability and potential quality concerns in the marketplace.

ABSTRACT NUMBER: 5075 **Poster Board Number:** H625

TITLE: The bioactive S3F6 fraction of *Rhus trilobata* suppresses the expression of inflammatory mediators in lipopolysaccharide-stimulated J77A.4 macrophages without cytotoxicity

AUTHORS (FIRST INITIAL, LAST NAME) AND INSTITUTIONS: *B. Sánchez-Ramírez*, D. Rodríguez-Guerrero, R. Infante-Ramírez, T. S. Siqueiros-Cendón, C. González-Horta, E. Burrola-Barraza, and J. Mendoza-Chacón. Facultad de Ciencias Químicas, Universidad Autónoma de Chihuahua, Chihuahua, Mexico.
KEYWORDS: Inflammation; Cell Culture; Macrophage; Rhus trilobata

ABSTRACT: Background and Purpose: Chronic non-communicable diseases (CNCD) such as cancer, diabetes, and cardiovascular disease are caused by poor control of the inflammatory process and represent a major cause of death worldwide. Finding compounds with anti-inflammatory activity and low toxicity is a challenge for current therapeutics of CNCD. Recently, we reported that the F6 fraction of the aqueous extract of *Rhus trilobata* stems possesses anti-inflammatory activity *in vivo* and *in vitro* in a lipopolysaccharide-induced J774A.1 macrophage model. However, the F6 chemical composition is complex; thus, this work aimed to identify a subfraction of F6 capable of decreasing the expression of COX-2, TNF-α, and IL-1β mRNAs in this model. **Methods:** Subfractions (S1F6 to S4F6) were obtained using methanol-water ratios, and their cytotoxicity was assessed using the resazurin method at a single concentration of 15 µg/mL, with incubation for 24 h. COX-2, TNF-α, and IL-1β mRNA gene expression was analyzed by end-point RT-PCR. Unstimulated, LPS-stimulated, and dexamethasone-treated (10 µM) cultures were used as controls. **Results:** Subfraction S3F6 showed the highest yield (54.22%) and did not present significant cytotoxicity. All subfractions decreased the expression of the analyzed genes; however, S3F6 achieved a significant reduction of all three, suggesting a higher concentration of active or synergistic compounds. **Conclusions:** These results demonstrate that the S3F6 subfraction contains

compounds with significant anti-inflammatory activity and low cytotoxicity. Studies are currently underway to obtain the chemical characterization of this fraction.

ABSTRACT NUMBER: 5076 **Poster Board Number:** H626

TITLE: Modulation of Cypermethrin-Induced Toxicity by Essential Oil Combinations in an *In Vitro* Human Keratinocyte Model

AUTHORS (FIRST INITIAL, LAST NAME) AND INSTITUTIONS: S. Yazar[1], M. Caglayan[2], H. Fidan[3], *S. Yilmaz*[2], A. Stoyanova[3], B. Goktas[2], and S. Stankov[3]. [1]Yeniyuzyil University, İstanbul, Turkey; [2]Ankara University, Ankara, Turkey; and [3]Food Technology University of Plovdiv, Plovdiv, Bulgaria.

KEYWORDS: Cytotoxicity; Natural Products

ABSTRACT: Background and Purpose: Human keratinocytes constitute the primary cellular barrier against dermal exposure to pesticides and bioactive natural compounds. Cypermethrin is commonly encountered through skin contact, while essential oils such as Lavandula angustifolia, Origanum heracleoticum, and Matricaria recutita are widely used in topical and cosmetic formulations. Despite their frequent co-exposure potential, limited data exist regarding their combined effects on keratinocyte viability. This study aimed to investigate the cytotoxic effects of cypermethrin and these three essential oils, both individually and in combination, in HaCaT human keratinocyte cells, with a particular focus on possible interaction- or modulation-related effects. **Methods:** HaCaT human keratinocyte cells were treated with increasing concentrations of Lavandula angustifolia (Oil 1), Origanum heracleoticum (Oil 2), and Matricaria recutita (Oil 3) essential oils, as well as cypermethrin, for up to 24 h. Cell viability was determined using the MTT assay, and IC_{50} values were calculated for each treatment. Combination experiments were conducted by applying cypermethrin together with each essential oil at a 1:5 ratio, mirroring the experimental design used in the fibroblast model to enable cross-cell-line comparison. **Results:** After 24 h exposure, oils 2 and 3 exhibited pronounced cytotoxic activity in HaCaT cells, with IC_{50} values of 1.10 µg/mL and 0.76 µg/mL, respectively, which were significantly lower than that of oil 1 (IC_{50} = 4.53 µg/mL). Cytotoxicity increased with prolonged exposure time. Cypermethrin alone did not induce detectable toxicity within the tested concentration range (IC_{50} > 50 µg/mL). In contrast to single treatments, all oil-cypermethrin combinations resulted in a marked reduction in cytotoxicity, reflected by increased IC_{50} values. Notably, cypermethrin attenuated the cytotoxic effects of all tested oils, with the strongest protective effect observed in the oil 1 + cypermethrin combination. Even oils with high intrinsic cytotoxicity (oils 2 and 3) showed significantly reduced adverse effects on cell viability when combined with cypermethrin. **Conclusions:** The results indicate that essential oils exhibit strong, oil-specific cytotoxic effects in human keratinocytes, whereas cypermethrin alone is not cytotoxic under the tested conditions. Interestingly, cypermethrin significantly mitigated essential oil-induced cytotoxicity in HaCaT cells, suggesting a cell-type-specific interaction between cypermethrin and essential oils. These findings provide important insights into dermal toxicology and the complex biological interactions of pesticides and natural compounds in skin-related exposure scenarios.

ABSTRACT NUMBER: 5077 **Poster Board Number:** H627

TITLE: Effects of Cypermethrin and Essential Oil Treatments on Cell Viability in an L929 Mouse Fibroblast Mode

AUTHORS (FIRST INITIAL, LAST NAME) AND INSTITUTIONS: M. Caglayan[1], S. Yazar[2], H. Fidan[3], A. Stoyanova[3], S. Stankov[3], A. Ucar[4], S. Donmez[5], and *S. Yilmaz*[4]. [1]Biruni University, İstanbul, Turkey; [2]Yeniyuzyil University, İstanbul, Turkey; [3]Food Technology University of Plovdiv, Plovdiv, Bulgaria; [4]Ankara University, Ankara, Turkey; and [5]Gebze Teknik University, Kocaeli, Turkey.

KEYWORDS: Natural Products; Cytotoxicity; Carcinogenesis

ABSTRACT: Background and Purpose: Cypermethrin is a widely used synthetic pyrethroid insecticide, and exposure through environmental or occupational routes may result in cytotoxic effects on connective tissue cells. Essential oils such as Lavandula angustifolia, Origanum heracleoticum, and Matricaria recutita are frequently investigated for their biological activities, including antioxidant, cytotoxic, and cytoprotective properties. However, their interaction with pesticide-induced toxicity remains insufficiently characterized. This study aimed to evaluate the cytotoxic effects of cypermethrin and these three essential oils, applied individually and in combination, in the L929 mouse fibroblast cell line, and to assess their potential modulatory roles in cypermethrin-induced cytotoxicity. **Methods:** L929 mouse fibroblast cells were cultured under standard conditions and exposed to increasing concentrations of Lavandula angustifolia (Oil 1), Origanum heracleoticum (Oil 2), and Matricaria recutita (Oil 3) essential oils, as well as cypermethrin, for 1 h and 24 h. Cell viability was assessed using the MTT assay, and IC_{50} values were calculated to determine cytotoxic potency. Combination treatments were performed by co-administering cypermethrin with each essential oil at a fixed 1:5 ratio, with maximum concentrations of 25 µg/mL cypermethrin and 5 µg/mL essential oil. **Results:** After 1 h exposure, all tested essential oils exhibited low cytotoxicity. Oils 2 and 3 caused a slight reduction in cell viability, with IC_{50} values of 200.04 ± 5.9 µg/mL and 235 ± 4 µg/mL, respectively, while oil 1 showed no significant toxicity (IC_{50} > 1000 µg/mL). Cypermethrin alone did not induce cytotoxicity at this time point (IC_{50} > 50 µg/mL). After 24 h, cytotoxicity increased for all oils, with oil 3 demonstrating the highest toxic potential. Cypermethrin remained non-toxic even at the highest tested concentration. In combination treatments, oils 1 and 2 did not enhance cypermethrin toxicity and maintained cell viability, whereas the oil 3 + cypermethrin combination resulted in increased toxicity and a reduced IC_{50} value. **Conclusions:** These findings demonstrate that essential oils exert time-dependent cytotoxic effects in L929 fibroblast cells. Importantly, oils 1 and 2 exhibited a protective effect against cypermethrin-induced toxicity, while oil 3 failed to provide protection and increased cytotoxicity when combined with cypermethrin. This study highlights the differential modulatory roles of essential oils in pesticide-related cytotoxicity and supports their selective evaluation for toxicological risk mitigation.

ABSTRACT NUMBER: 5078 **Poster Board Number:** H628

TITLE: Combined *In Vitro* Neurocytotoxicity and Toxicological Risk Assessment Framework to Address Local and Systemic Neurotoxicity per ISO 10993-1:2025

AUTHORS (FIRST INITIAL, LAST NAME) AND INSTITUTIONS: L. Hou[1], X. Sun[1], C. Liu[1], and *X. Dai*[2]. [1]China NMPA Jinan Medical Device Product Quality Supervision and Inspection Center, Jinan, China; and [2]Abbott Laboratories, St. Paul, MN.

KEYWORDS: Medical Device; Neurotoxicology; Risk Assessment

ABSTRACT: Background and Purpose: ISO 10993 1:2025 introduces explicit requirements for assessing neurotoxicity when identifying neurotoxicants in medical devices, particularly emphasis on evaluating both local and systemic neurotoxicity. Current neurotoxicity evaluation for medical devices relies predominantly on *in vivo* implantation studies in animals. These approaches, lack specificity for detecting neural tissues related toxicological effects, do not align with the principles of the 3Rs, and provide limited mechanistic insight into neural tissue specific toxicity. There is a growing need for more mechanistically informative methods to support neurotoxicity evaluation under the updated ISO 10993-1 framework. To address these gaps, this work integrates an *in vitro* neurocytotoxicity approach and a systematic TRA to provide a framework for assessing potential neurotoxic risks of medical device. **Methods:** Local neurocytotoxicity of two neurotoxins, acrylamide 0.01 to 10 mM and vincristine 0.001 to 1 uM, were evaluated using SH SY5Y cells, a human neural cell line. L929 cells were used as the control cells. HDPE, an ISO 10993-5 recommended negative control material, was extracted using cell culture medium. Serial concentrations of neurotoxins were added to the extract and applied to cells under two conditions: 24 hr exposure to assess cell viability using CCK 8 assay for differentiated SH SY5Y cells or MTT assay for L929 cells, and 72 hr exposure during SH SY5Y cell differentiation to evaluate neurite outgrowth and synapse formation using β III tubulin biomarker imaging. Parallel L929 cytotoxicity and imaging were conducted to compare conventional cytotoxicity with neurocytotoxicity. Systemic neurotoxicity was assessed through a TRA following ISO 10993 17. A comprehensive literature review was conducted to assess the neurotoxicity, focusing on the applicability and quality of publicly available data, including route of exposure, neural tissue specificity, mechanistic evidence, and dose responses. These data were used to establish TI values specific to neurotoxicity and then compared with NOAEL established in neurocytotoxicity. **Results:** Acrylamide and vincristine both demonstrated neurocytotoxicity in differentiated SH SY5Y cells. Morphological changes related cytotoxicity exhibited at ≥1 mM acrylamide and ≥0.1 µM vincristine. In contrast, cytotoxicity results in L929 cells showed acrylamide induced cytotoxicity only at conc. ≥10 mM, whereas vincristine caused no detectable cytotoxicity even at ≥1 µM. These findings indicate that differentiated SH SY5Y cells were about 10 fold more sensitive to acrylamide and 100 fold more to vincristine compared with L929 cells. Both neurotoxins also disrupted neurite outgrowth and synapse formation in SH SY5Y cells at conc. similar to those causing morphological neurocytotoxicity: ≥1 mM acrylamide and ≥0.1 µM vincristine. For systemic neurotoxicity, the literature review of repeated dose toxicity studies identified a lowest NOAEL of 1 mg/kg bw/day for acrylamide based on developmental neurotoxicity endpoint. Applying appropriate uncertainty factors resulted a TI of 10 µg/kg bw/d. For vincristine, a TI of 40 µg/kg bw/d was derived from clinical dosing information, based on the i.v. dose of 1.4 mg/m² induced neuropathy with an average 1.7 m² body surface area in adults. The comparison between *in vitro* neurocytotoxicity NOAELs from the human neural cell lines and *in vivo* TI values for humans revealed a contrast between two neurotoxins. *In vitro*, acrylamide exhibited a NOAEL at least 10,000 fold higher than vincristine in SH

SY5Y cells, indicating far lower potency toward neuronal cells in this assay system. In contrast, the *in vivo* systemic TI for acrylamide is 25% of the TI derived for vincristine, reflecting acrylamide's well studied systemic neurotoxicity risk due to systemic exposure. **Conclusions:** This study demonstrates that *in vitro* neurocytotoxicity potency does not necessarily correlate with *in vivo* systemic neurotoxicity potency, highlighting the importance of integrating cell based assays for local neurotoxicity with TRA for systemic neurotoxicity, rather than relying on either approach alone. This integrated strategy, combining *in vitro* neurocytotoxicity NOAEL derivation, systemic TI based toxicological risk assessment, and direct comparison, is able to provide a framework for evaluating both local neurocytotoxicity and systemic neurotoxicological risk, supporting compliance with ISO 10993-1:2025.

ABSTRACT NUMBER: 5079 **Poster Board Number:** H629

TITLE: Integrating experimental data and mechanistic modeling to assess potential lead exposure from tampon use

AUTHORS (FIRST INITIAL, LAST NAME) AND INSTITUTIONS: *K. E. Woeller*, P. Doyle, C. Haven, D. McClenathan, C. Obringer, and *C. Ellison*. The Procter & Gamble Company, Cincinnati, OH.

KEYWORDS: Bioavailability; Metals; Exposure Assessment; Mechanistic modeling; Lead

ABSTRACT: Background and Purpose: Trace levels of lead (Pb) have been reported in tampons, prompting concerns regarding potential exposure during menstrual product use. In response, the U.S. Food and Drug Administration (FDA) conducted an independent systematic literature review and reaffirmed the historical safety of tampons. Several of the studies in the literature review highlight the presence of trace contaminants in menstrual products following harsh, non-physiological extraction conditions and conservative assumptions (e.g., complete absorption), without evaluating product release or biological relevance. Importantly, the presence of a chemical in a product does not necessarily translate to meaningful exposure. Accurate exposure assessment requires consideration of chemical release under physiological conditions, binding, and bioaccessibility within menstrual fluid, and potential absorption across the vaginal epithelium. Menstrual fluid is a complex biological matrix that may strongly bind contaminants and limit bioavailability. The purpose of this work was to characterize the distribution and binding of Pb, as a model chemical, in menstrual fluid and to integrate these data into a deterministic, compartmental mass-balance model to evaluate the potential release and fate of Pb that may be present as an inadvertent trace impurity in tampons. **Methods:** Menstrual fluid was collected noninvasively from adult donors using menstrual cups over designated days of the menstrual cycle. Endogenous Pb concentrations were measured in whole menstrual fluid and in isolated plasma and red blood cell (RBC) fractions. To assess exogenous Pb distribution, menstrual fluid samples were spiked with 1, 10, or 25 ng Pb/mL. Plasma protein binding of Pb was determined using rapid equilibrium dialysis in menstrual fluid-derived plasma and systemic plasma. Pb concentrations were quantified by ICP-MS. Partition coefficients were calculated from experimentally measured Pb concentrations in whole menstrual fluid and corresponding isolated fractions. A deterministic, compartmental mass-balance model was developed and implemented in Berkeley Madonna to describe potential Pb release from a tampon, partitioning within menstrual fluid, re-absorption into the tampon with fluid uptake, and potential permeation across vaginal tissue. **Results:** Pb preferentially partitioned to the RBC fraction of menstrual fluid, with the remaining Pb distributed in the plasma fraction, where the majority was protein-bound. These characteristics were broadly comparable to those reported for systemic blood. Model simulations for a four-hour tampon wear scenario predicted that the majority of theoretically

released Pb is reabsorbed into the tampon, with only a very small fraction (<1 ng; <0.3%) available for potential absorption into vaginal tissue. **Conclusions:** Binding within menstrual fluid and re-absorption into the tampon substantially limit Pb bioavailability, resulting in negligible tissue uptake under realistic use conditions. Integration of experimental measurements with mechanistic modeling provides critical context for interpreting analytical findings and supports science-based evaluation of tampon safety.

ABSTRACT NUMBER: 5080 **Poster Board Number:** J632
TITLE: The antimicrobial compounds C10- and C12- benzalkonium chloride are likely potent inhibitors of phospholipase B that induce phospholipidosis

AUTHORS (FIRST INITIAL, LAST NAME) AND INSTITUTIONS: N. Yiv, *A. Ettayapuram Ramaprasad*, *C. M. McHale*, J. Wang, and *M. T. Smith*. UC Berkeley, Berkeley, CA.
KEYWORDS:; Quaternary ammonium cations

ABSTRACT: Background and Purpose: Quaternary ammonium cations (QACs) are commonly used chemicals in disinfectants, antiseptics, preservatives, and fabric softeners. QACs have been suggested to have negative health impacts on people, with exposure being associated with dermal, respiratory, and immune issues. QACs also share structural similarities with cationic amphipathic drugs that are known to induce phospholipidosis, raising concern about them producing adverse outcomes through similar toxicity mechanisms. **Methods:** A list of 64 QACs was obtained from the California OEHHA (Office of Environmental Health Hazard Assessment). Each QAC was evaluated for phospholipidosis potential including its predicted pKa and cLogP values. The QACs that met the physicochemical requirements were analyzed using A MAchine Learning platform for predicting drug-induced PHosphoIpidosis (AMALPHI) server and similarity ensemble SEA search server. The two QACs that had the highest predicted likelihood to induce phospholipidosis were tested *in vitro* using human lung (A549) cells. **Results:** AMALPHI and SEA analysis identified 7 QACs that were predicted to induce phospholipidosis through interactions with phospholipase, suggesting a possible mechanism. *In vitro* studies show that the two highest-risk QACs, namely C10- and C12 benzalkonium chloride induce phospholipidosis in A549 cells at low concentrations comparable to known inducers such as amiodarone. **Conclusions:** QAC exposure can induce phospholipidosis and impair cellular function through targeting phospholipases, which can impair cellular function and contribute to adverse effects, including asthma. These findings underscore the need to further characterize the health impact of QACs such as C10- and C12-benzalkonium chloride on adverse outcomes caused by phospholipidosis and to understand their broader effect on human health.

ABSTRACT NUMBER: 5081 **Poster Board Number:** J633
TITLE: Disruption of Melanin Synthesis and Cellular Stress Pathways in Melanocytes Following PFAS Exposure

AUTHORS (FIRST INITIAL, LAST NAME) AND INSTITUTIONS: *S. Sharma*, *M. Meister*, *H. Young*, and *C. Wright*. UL Research Institutes, Marietta, GA.
KEYWORDS:

ABSTRACT: Background and Purpose: While PFAS are recognized for their systemic toxicity, their effects on melanocyte function and pigmentation biology remain poorly understood. Emerging epidemiological evidence linking PFAS exposure to melanoma risk underscores the urgent need to elucidate how these

compounds disrupt melanocyte regulatory and redox pathways. Recent observations associating PFAS exposure with altered skin physiology and increased melanoma incidence further emphasize this knowledge gap. This study investigates whether PFAS modifies melanin synthesis and induces cytotoxic or genotoxic responses in melanocytes derived from racially diverse populations, with the goal of identifying potential population-level differences in PFAS susceptibility. **Methods:** Primary human melanocytes from different racial backgrounds were exposed for 24 hours to individual PFAS compounds (PFPeA, PFHxA, PFHpA, PFOA, PFNA, PFDA) or a PFAS mixture at 10 nM or 10 μM. Proliferation, ROS generation, melanin content, S100β expression, and transcription of key melanocyte regulatory genes were quantified. **Results:** PFAS exposure elicited distinct ancestry-dependent effects on melanocyte function. Caucasian melanocytes exhibited dose-dependent increases in both proliferation and ROS generation. Asian melanocytes showed moderate responses characterized by reduced proliferation and lower ROS levels, while Black melanocytes demonstrated minimal changes. These differential responses corresponded with divergent baseline transcriptional profiles: Caucasian cells expressed the highest levels of MITF and SLC7A11, Asian cells exhibited the highest TYRP1 but lowest MITF expression, and Black cells showed elevated ASIP alongside markedly reduced SLC7A11. PFAS exposure further modulated these ancestry-specific programs, inducing suppression of MITF and TYRP1 at high doses across groups, downregulation of SLC7A11 coupled with ASIP induction in Asian cells, and chain-length-dependent upregulation of TYRP1 and SLC7A11 in Black cells. Notably, S100β was consistently upregulated across all melanocyte populations, revealing a conserved oncogenic signal that persists despite divergent cellular stress responses. **Conclusions:** PFAS responses in melanocytes are strongly influenced by ancestry-linked cellular programs rather than melanin content alone. Caucasian and Asian melanocytes showed greater sensitivity to PFAS-induced genotoxicity, while Black melanocytes displayed more resilient profiles. Distinct transcriptional shifts highlight how intrinsic pigmentation pathways shape PFAS vulnerability. Despite varied responses, all groups exhibited increased melanoma-associated markers, underscoring a common oncogenic pressure. These results emphasize the need to incorporate cellular diversity into environmental health assessments.

ABSTRACT NUMBER: 5082 **Poster Board Number:** J634

TITLE: Mitochondria-targeted non-apoptotic cell death inducers overcome chemoresistance in triple-negative breast cancer

AUTHORS (FIRST INITIAL, LAST NAME) AND INSTITUTIONS: *A. K. Tiwari*. University of Arkansas for Medical Sciences, Little Rock, AR.

KEYWORDS: Agents; Apoptosis; Cell Proliferation; Necroptosis; thieno-pyrimidin-4-yl-hydrazinylidene derivatives

ABSTRACT: Background and Purpose: Over 90% of advanced triple-negative breast cancer (TNBC) patients develop multidrug resistance (MDR) to taxanes and anthracyclines due to efflux transporter overexpression, metastasis, and apoptotic resistance, leading to early relapse and poor survival. Current therapies predominantly induce apoptosis, which is frequently evaded in resistant TNBC. Mitochondria regulate multiple non-apoptotic cell death (NACD) pathways. We hypothesized that caspase-independent NACD inducers could bypass resistance. We identified thieno-pyrimidin-4-yl-hydrazinylidene (TPH) derivatives that selectively trigger NACD by targeting Drp1, a mitochondrial fission protein linked to TNBC aggressiveness and resistance. Objectives: define SAR for NACD induction, identify the most potent drug-like Drp1 inhibitor, and elucidate how Drp1 targeting suppresses MDR

TNBC phenotypes. **Methods:** A focused library of 34 TPH analogs was designed, synthesized, and fully characterized. Structure-activity relationships (SAR) were established through cytotoxicity screening in TNBC cell lines (BT-20, MDA-MB-231, MDA-MB-468). Drug-likeness parameters were evaluated using the ACD/Percepta suite. The lead compound, TPH104m, was assessed for potency and selectivity using MTT, SRB, live-cell imaging, and CellTiter-Blue assays in TNBC cells and non-malignant mammary epithelial cells (MCF-10A, HMEC). Cell death modality was characterized via Annexin V/propidium iodide staining, Hoechst 33342 nuclear morphology assessment, caspase-3/7 activity measurement, and pan-caspase inhibition with Z-VAD-FMK. TPH104m-Drp1 interaction was investigated, and mitochondrial effects were examined through TMRE-based mitochondrial membrane potential (MMP) analysis, cytochrome c immunofluorescence, Western blotting of mitochondrial dynamics proteins (Drp1, p-Drp1[S616], MFF, FIS1, MFN1/2, OPA1), multi-omics profiling (genomics and proteomics), and functional validation in CRISPR/Cas9-mediated Drp1-knockout models. Bioenergetic alterations were quantified using Seahorse XF Mito Stress Test and ATP Real-Time Rate assays to measure oxygen consumption rate (OCR), extracellular acidification rate (ECAR), ATP production, mitochondrial reactive oxygen species (ROS), mtDNA copy number, and bioenergetic health index (BHI). **Results:** TPH104m was identified as the most efficacious, drug-like lead, exhibiting potent, selective cytotoxicity against TNBC cells (IC_{50} 0.18-0.47 μM) with negligible effects on normal mammary epithelial cells. SAR analysis delineated critical structural features conferring activity. TPH104m-treated TNBC cells displayed hallmark NACD morphology, including cellular swelling and rupture, without nuclear fragmentation. Absence of caspase-3/7 activation, lack of PARP cleavage, and failure of Z-VAD-FMK to rescue viability confirmed caspase-independent death. TPH104m induced profound MMP depolarization in the absence of cytochrome c release or overt ROS accumulation. Immunoblotting and immunofluorescence demonstrated marked downregulation of total and phosphorylated Drp1 (Ser616). CRISPR/Cas9-mediated Drp1 ablation significantly attenuated TPH104m sensitivity, establishing Drp1 as the primary mediator of cytotoxicity. TPH104m selectively impaired mitochondrial fission in TNBC cells without perturbing mitochondrial homeostasis in non-malignant counterparts. Seahorse profiling revealed reduced OCR, diminished ATP synthesis, elevated mitochondrial ROS, mtDNA depletion, loss of oxidative phosphorylation capacity, and a marked decline in BHI, resulting in metabolic reprogramming toward compromised bioenergetics, ATP crisis, and NACD. **Conclusions:** TPH104m represents a lead mitochondria-targeted, Drp1-specific inducer of caspase-independent NACD with robust activity against chemoresistant TNBC. By suppressing Drp1 expression and mitochondrial fission, TPH104m elicits mitochondrial dysfunction characterized by MMP dissipation, ATP depletion, and collapse of bioenergetic reserve. This dual impairment of prosurvival signaling and metabolic plasticity circumvents apoptotic resistance, positioning Drp1-targeted, mitochondria-directed therapies as a promising next-generation strategy for apoptosis-refractory malignancies such as TNBC.

ABSTRACT NUMBER: 5083 **Poster Board Number:** J635

TITLE: Evaluating induced high oxidative stress environments and protein methylation inhibitors, for combinatorial treatments against chemo-resistant colorectal cancer cell lines

AUTHORS (FIRST INITIAL, LAST NAME) AND INSTITUTIONS: *J. de Oliveira Mallia*, K. Fenech, R. Gatt, and B. Baron. University of Malta, Msida, Malta.

KEYWORDS:

ABSTRACT: Background and Purpose: Colorectal cancer (CRC), especially in its advanced stages, frequently shows abnormal regulation of protein methyltransferases (PMTs), which promote cell survival pathways that are associated with poor clinical outcomes. The use of PMT inhibitors can counteract these adaptive processes, limiting the ability of cancer cells to evade cell death. Plasma-activated medium (PAM), which contains abundant reactive oxygen species, induces oxidative stress that selectively targets rapidly dividing cancer cells. Although PAM is known to induce apoptosis, emerging evidence suggests that cancer cells may exploit PMT-mediated epigenetic and post-translational modifications that mitigate oxidative damage. However, little is understood about the role of protein methylation in modulating PAM-induced cell death, or how enhanced PMT activity may enable cancer cells to evade it. This study, therefore, examined the combined therapeutic potential of PAM and specific PMT inhibitors targeting EZH2 (Tazemetostat), SETD7 (PFI-2), EHMT2 (A-366), and PRMT5 (EPZ015666) to improve PAM's anticancer efficacy against CRC. **Methods:** A non-thermal Argon plasma jet reactor was used to activate cell media. The pH, conductivity, and oxidation-reduction potential were measured after treatment using an electrochemical meter equipped with the appropriate probes. A ferrous oxidation xylenol orange (FOX) assay was used to assess the PAM's oxidative capacity. A CRC cell panel consisting of HCT116, DLD1, and LoVo, as well as the normal colon fibroblast cell line CCD 841 CoN were cultured in DMEM:F12 and incubated at 37°C and 5% CO_2. Cells resistant to 5-fluorouracil (5-FU) were generated from the three cancer cell lines. Cell viability assays were used to identify a PAM dose close to the IC50 and determine the combinatorial effect of treating both the parental and the 5-FU-resistant CRC cell lines with PAM alone or in combination with one of the four selected PMT inhibitors (Tazemetostat, PFI-2, A-366, and EPZ015666). Spheroids from the CRC cell panel were generated using micro-patterned plates with a specific geometry and non-stick coating over a period of 48 hours after which they were first pre-treated with the selected PMT inhibitors and subsequently with PAM. Western blotting was done to examine specific cell death signalling pathways of apoptosis (Casp3), extrinsic apoptosis (Casp8), DNA damage-induced apoptosis (Parp1), and ferroptosis (GPX4) It was also used to observe changes in the different degrees of lysine (mono, di, tri) and arginine (mono, di-symmetrical, di-asymmetrical) methylation. **Results:** After 3 hours of non-thermal plasma treatment, the DMEM:F12 PAM had an average pH of 7.42±0.01, conductivity of 13678±2 S/cm and an oxidation-reduction potential of 147.9±0.7 mV. It was also determined using the FOX assay that the DMEM:F12 PAM had an average equivalent H_2O_2 concentration of 188.5±24.6 ppm. Cell viability assays showed that CCD 841 CoN are the most sensitive to peroxide stress, whereas DLD1 are the least affected. Similarly, the IC_{50} of PAM increases from CCD 841 CoN to DLD1, with HCT116 and LoVo showing intermediate sensitivity. A significant difference in PAM efficacy was observed between the parental cell lines and the generated 5-FU-resistant cells in 2D, with the latter being more sensitive to PAM. In 3D cultures, no significant improvement in efficacy was observed for the combinatorial treatments. Western blots did not reveal differences in cell death mechanisms between the parental cell lines and the 5-FU-resistant cells generated. There were few observable differences in the banding

patterns of lysine methylation vs. arginine methylation before vs. after PAM treatment. **Conclusions:** Exposure of CRC cells to PAM-induced stress was associated with alterations in methylation patterns, implying that PMT activity may contribute to the regulation of cell death mechanisms. However, the combination of PAM with PMT inhibitors did not result in a substantial increase in cytotoxicity compared to PAM treatment alone. These results provide a valuable foundation for further investigation into the role of protein methylation in PAM-mediated cell death pathways and its potential relevance to combination cancer therapies. Project MIAPAM-CaT (REP-2024-028) was financed by the Malta Council for Science & Technology, for and on behalf of the Foundation for Science and Technology, through the FUSION: R&I Research Excellence Programme.

ABSTRACT NUMBER: 5084 **Poster Board Number:** J636

TITLE: Spatial RNAseq Reveals that Retene Exposure Induces Xenobiotic Response and Crystallin Gene Expression in Heart, Notochord, and Eyes of Developing Zebrafish

AUTHORS (FIRST INITIAL, LAST NAME) AND INSTITUTIONS: *C. Rude*, *S. Stinson*, and *R. Tanguay*. Oregon State University, Corvallis, OR.

KEYWORDS: Polycyclic Aromatic Hydrocarbons; Developmental/Teratology; Spatial RNAseq

ABSTRACT: Background and Purpose: Retene (1-methyl-7-isopropyl phenanthrene) is a toxic polycyclic aromatic hydrocarbon (PAH) derived from both petrogenic and pyrogenic sources. It is frequently the most abundant PAH measured in wildfire smoke and is toxic in mammalian cellular models and teleost fish. Exposure to retene activates the human aryl hydrocarbon receptor (AHR) and its zebrafish homolog, Ahr2, to mobilize transcription of genes involved in xenobiotic metabolism and other AHR related processes. In developing teleost fish, cardiac malformation mediated by ahr2 is considered the most sensitive toxic endpoint to retene; however, information regarding toxicity to other organs is lacking. Zebrafish are an excellent model for investigating retene developmental toxicity because of their rapid transparent development, well-annotated genome, and conservation of developmental processes with other vertebrates. This study utilizes spatial RNA sequencing (Spatial RNAseq) with static exposures in embryonic zebrafish to probe retene-induced developmental toxicity over multiple organs and tissue regions. **Methods:** Enzymatically dechorionated zebrafish embryos were statically exposed to vehicle control or 28.5 µM retene in 1% DMSO beginning at 8 hpf. Embryos were reared to 48 hpf, visually inspected for malformation, and flash frozen in optimal cutting temperature medium. Cryosections, 10 µm in thickness, each containing approximately 20 larvae, were fixed to a 10X Visium slide with two replicates per treatment condition. Spatial RNAseq libraries were prepped from cryosections according to manufacturer specifications and sequenced with an Illumina Novaseq 6000. Reads were mapped to the zebrafish reference genome (GRCz11) using Space Ranger and manually aggregated across sections. Spatial capture locations were filtered to detect at least 400 unique genes and 4,000 total reads. Read counts were normalized using SCRAN and spatially clustered with BayesSpace. Spatial clusters were manually annotated with tissues or organs using histological images and gene expression profiles. Differential expression analysis was conducted on spatial clusters between treatment groups using Wilcoxon rank-sum tests or pseudobulk aggregation and testing in DESeq2. **Results:** After filtering, spatial RNAseq analysis yielded 1,875 and 2,205 spatial RNAseq capture locations for control and retene exposed larvae respectively. They averaged 17,600 reads and 2,540 unique genes per capture location. Spatially resolved clusters included ocular, brain, notochord, heart, pancrease, liver, gut, and muscle gene expression signatures. Characteristic AHR responsive genes such as cyp1a,

cyp1c1, sult6b1, foxq1a, and ugt1b5 had widespread increased expression, with the largest increases corresponding cardiac, gill, and otic regions. Genes encoding crystallin family proteins made up 31 of the top 66 differentially expressed genes. Most crystallins were of the β - and γ - crystallin families. They exhibited the largest relative increases in heart and notochord tissues and largest absolute expression changes in notochord and eye adjacent tissues. **Conclusions:** Widespread induction of ahr2-responsive genes indicates retene's effect on developing zebrafish involves multiple organs including the skin, notochord, pancreas, developing ear, and heart. Strong differential expression in the heart supports the notion that cardiac toxicity is the most sensitive endpoint to retene in developing teleost fish. Marked increases in crystallin gene expression, particularly in the notochord and heart where they were otherwise undetected, was unexpected. β - and γ - crystallins are structural proteins that support the formation of the lens, but also play roles in stabilizing protein complexes and ameliorating damage in cell types such as neurons and astrocytes. A previous study reported induction of crystallin genes in developing zebrafish exposed to complex mixtures of PAHs and other hydrophobic contaminants from the Portland Harbor Superfund Site; however, there do not appear to be other examples resulting from retene or other PAH exposures. Future studies should clarify the timing, dose response, extent of translation to protein, and mechanism by which retene augments the abundance of crystallin genes during development. This research was supported by the NIEHS of the National Institutes of Health under Award Number P42 ES016465, P30 ES030287, and T32 ES007060.

ABSTRACT NUMBER: 5085 **Poster Board Number:** J637
TITLE: Metformin reduces vesicant-induced skin injury in a human perfused skin model

AUTHORS (FIRST INITIAL, LAST NAME) AND INSTITUTIONS: A. Ejaz. University of Pittsburgh, Pittsburgh, PA. Sponsor: A. Ejaz , American Association for Cancer Research
KEYWORDS: Alkylating Agents; Alternatives to Animal Testing; Chemical and Biological Weapons

ABSTRACT: Background and Purpose: This study aimed to define how nitrogen mustard, a vesicant and alkylating agent, produces progressive injury in human skin and to determine whether metformin can mitigate this damage. **Methods:** Full-thickness human skin flaps were maintained in a perfused *ex vivo* system and exposed to nitrogen mustard at 10, 30, or 60 mg/cm². After exposure, one set of samples remained untreated, while a separate set received topical metformin to assess treatment effects. Biopsies from both metformin-treated and untreated tissues were collected at 0, 2, 6, 24, 125, and 200 hours to evaluate structural injury, inflammation, and apoptosis using standard histologic staining and TUNEL assay. **Results:** Nitrogen mustard produced a concentration-dependent pattern of epidermal thinning, dermal,-epidermal separation, and increased inflammatory infiltration. Higher concentrations caused prominent nuclear vacuolization and ballooning degeneration of epidermal cells. Metformin treatment reduced these structural abnormalities and limited inflammatory cell accumulation across time points. Early after exposure, all nitrogen mustard groups demonstrated acute inflammation, but metformin-treated tissues showed reduced dermal cellularity. By 24 hours, inflammatory infiltration intensified in higher nitrogen mustard doses, whereas metformin markedly blunted this response. Apoptotic cell burden increased significantly after nitrogen mustard exposure and was consistently lower in metformin-treated samples. At later intervals, metformin-treated tissues demonstrated improved preservation of epidermal architecture and greater overall recovery. **Conclusions:** These findings indicate that nitrogen mustard induces progressive inflammatory and apoptotic injury in human skin and that metformin can substantially mitigate these effects. This perfused human skin model

provides a valuable platform for studying vesicant-induced injury and for evaluating potential therapeutic interventions.

ABSTRACT NUMBER: 5086 **Poster Board Number:** J638

TITLE: Fentanyl-induced cortical and cardiopulmonary damage linked to immune response functions and apoptosis-necrosis networks in a multi-omics mouse model

AUTHORS (FIRST INITIAL, LAST NAME) AND INSTITUTIONS: N. Chakraborty[1], S. Kannan[1], M. Patel[1], G. Dimitrov[1], A. Gautam[1], M. Newman[2], *J. Boyd*[3], and R. Hammamieh[1]. [1]WRAIR, Silver Spring, MD; [2]Virginia Commonwealth University School of Medicine, Richmond, VA; and [3]University of Colorado School of Medicine, Aurora, Aurora, CO.

KEYWORDS: Systems Biology; Agents; Genomics; Fentanyl

ABSTRACT: Background and Purpose: The opioid epidemic and high lethality of fentanyl, and other ultrapotent synthetic opioids is largely driven by illicit misuse since the opioid prescribing practices have declined secondary to the public health crisis. Fentanyl-related overdoses have now surpassed those of all other opioids combined, becoming the leading cause of worldwide opioid-related deaths. The significant challenge to counter fentanyl is its capability to rapidly overpower brain and cardiopulmonary functions by taking advantage of its high pharmacokinetics, which warrants a systems-level investigation to elucidate the early host response profile. **Methods:** Meeting this objective, we developed a SKH-1 mouse model to integrate the *ex vivo* images with multi-omics data to comprehend the time- and tissue-level dynamics of fentanyl exposure. Our previous study published in Pharmaceuticals 2024, screened the phenotypes of this mouse model to customize the dose-gradient and determine timepoints linked to major clinical manifestations caused by the lethal dose. Expanding upon these observations, murine cortex, heart and lungs were collected post-mortem at 40m, 6h, 24h, and 7d after the administrations of one of three fentanyl doses, namely the highest non-lethal dose (HNLD), LD10 and LD50. *Ex vivo* imaging data in addition to multiple clinical interrogation, such as blood glucose measurement, body weight etc., were supported by multi-tissue multi-omics analysis to screen mRNA, miRNA and proteomics landscape. **Results:** Differentially expressed miRNAs were screened using ML-tools to find those, which are sequentially conserved and functionally similar between mouse and human. Systems Biology based multi-domain data integration identified the immune response networks and apoptosis-necrosis functions as the primary targets of fentanyl. Cortical and pulmonary immune responses showed dose-dependent latencies, but remained activated 7d post-exposure, while the cardiac immune response was suppressed over time. In parallel, a rapid activation of pulmonary apoptosis-necrosis was contrasted by its delayed dose-dependent activation in the heart; and its cortical trajectory took a monophasic longitudinal pattern with delayed activation past 24h followed by regression. Together, tissue-specific time windows were suggested for early intervention. Subsequent machine learning analysis identified phylogenetically conserved miRNAs, such as miR-146-5p and miR-877-3p that showed consistent time- and dose-independent regulations in lungs and cortex, respectively. Functional association of these miRNAs to tissue specific lesions underlined their potential therapeutic values. By integrating the gene transcriptomic and miRNA data across multiple organs, current study reported longitudinal, tissue-specific trajectories of molecular response to fentanyl overdose. **Conclusions:** The deliverables included the molecular targets, such as the phylogenetically conserved miRNA-mRNA, which would be instrumental in designing next generation therapeutic interventions. Furthermore, this result identified the variable response profile of different organs to a dose-gradient, and this knowledge can aid in

designing precision drug delivery to achieve rapid mitigation of the fentanyl's toxicity. Further interrogation of miRNA-mRNA data and their downstream target analysis can lead to developing precision countermeasures of fentanyl.

ABSTRACT NUMBER: 5087 **Poster Board Number:** J639
TITLE: Evaluating VX metabolism by human cytochrome P450s and carboxylesterase

AUTHORS (FIRST INITIAL, LAST NAME) AND INSTITUTIONS: *T. R. Lane*[1], D. Koebel[2], E. A. Lucas[2], S. Cleary[2], R. Moyer[2], and S. Ekins[1]. [1]Collaborations Pharmaceuticals, Inc., Raleigh, NC; and [2]Battelle Memorial Institute, Columbus, OH.
KEYWORDS: Agents; Chemical and Biological Weapons; Cytochrome P450; carboxylesterase; VX

ABSTRACT: Background and Purpose: VX is a well-known organophosphate acetylcholinesterase (AChE) inhibitor and likely one of the most toxic AChE inhibitors known. However, the metabolism of VX in humans is not well characterized, with only a single poisoning event enabling the identification of several metabolites. VX has also been suggested to be metabolized *in vitro* by paraoxonase-1 and phosphotriesterase, although their binding constants were higher than the $LD_{50,}$ which may limit physiological relevance. We have recently characterized the metabolism of VX *in vitro* (Lane et al PMID: 38594080) and identified multiple metabolites in human liver microsomes (HLM). We also identified a biphasic decay with two distinct rates of metabolism. The formation of VX metabolites was shown to be shifted with HLMs, suggesting a pathway enhancement over simple hydrolysis. We found that an FDA-approved drug (EDTA) enhances the metabolic rate. Microsomes contain a wide variety of xenobiotic-metabolizing proteins in addition to cytochrome P450s, with over 300 hydrolases identified in HLMs. The most abundant hydrolase found in HLMs is carboxylesterase (CES) 1. We now describe a preliminary evaluation of the role of human P450 and CES1 in the metabolism of VX in HLMs and recombinant cytochrome P450 enzymes (CYPs). **Methods:** A series of experiments with HLMs were designed to probe for the enzymes responsible for the metabolism of VX. Final concentrations of VX and HLMs were at 200 ng/ml (~740 nM) and 0.5 mg/ml, respectively. We performed experiments with and without the following reagents in TRIS buffer: 1. Pefabloc®, which is a generalized hydrolase inhibitor (irreversible serine protease inhibitor). 2. Oleanolic acid (OA), which is a specific CES1 inhibitor with no CYP inhibition at 10µM. 3. Atipamezole, which is a pan-CYP inhibitor at 100µM. 4. NADPH, which is cofactor that is known to be critical for activity of CYPs as well as other enzymes such as flavin-containing monooxygenases (FMO), glutathione reductase (GST), Fatty Acid Synthase, etc. VX (~740 nM) experiments were also performed with the recombinant CYPs 1A2, 2B6, 2C8, 2C9, 2C19, 2D6, and 3A4 to generate half-life data with and without EDTA. **Results:** In HLMs and non-HLM control, Pefabloc drastically increased the rate of hydrolysis in TRIS buffer over the control, making interpretation challenging. Similarly to what we had previously observed, inhibition of CYPs in HLMs using the pan-CYP inhibitor atipamezole reduced the rate of VX metabolism, which was still significantly faster than the buffer control. Experiments characterizing the effects of NADPH and or a pan-CYP inhibitor on VX metabolism showed complex results but suggest a partial NADPH dependence on the metabolism of VX. All HLM-containing conditions had an early, rapid disappearance of VX for the first 8-10 hrs regardless of NADPH. Less remaining VX was seen at 48 hr with NADPH than without. Pan-CYP inhibition with no NADPH completely stabilized at approximately 20 hrs. The addition of pan-CYP inhibitor without EDTA has a similar effect on VX metabolism as with EDTA. Atipamezole by itself without HLMs had no effect on VX stability in buffer controls, suggesting that its effect in HLMs is enzymatic and/or affecting

competitive protein binding. The lack of an effect from addition of oleanolic acid (OA) suggests that there is no apparent enzymatic role of CES1 on VX metabolism in HLMs. The VX half-life with individual recombinant CYPs varied from 76-110 hrs, which is similar to the background hydrolysis of VX without HLMs or CYPs present (~75hr). All of the CYPs tested were shown to be active for the metabolism of fluorogenic (non-OP) substrates. This suggests that these particular CYPs which represent the major human hepatic drug metabolizing enzymes, play little or no role in VX metabolism. **Conclusions:** While much is known about AChE inhibition by VX, its human metabolism is poorly characterized and limited to partial reports. This study now updates our knowledge on human metabolism of VX. Our results suggest that other enzymes in HLMs besides CYPs and CES1 are likely responsible for the metabolism of VX. Future studies are currently ongoing in human plasma to further characterize the metabolism of VX and other CWAs.

ABSTRACT NUMBER: 5088 **Poster Board Number:** J640
TITLE: Assessing the Potential Risks for Nanoplastics in South Korea Based on Real-World Plastic Emission Rates

AUTHORS (FIRST INITIAL, LAST NAME) AND INSTITUTIONS: *H. Moon*. Korea Institute of Toxicology, Jinju, Korea, Republic of.
KEYWORDS: Risk Assessment; Nanoparticles; Environmental Toxicology

ABSTRACT: Background and Purpose: South Korea is one of the world's major producers and consumers of plastic, which raises growing concerns about the generation and environmental dispersion of micro- and nanoplastics (MNPs). Nanoplastics (NPs), typically defined as plastic particles smaller than 1 μm, exhibit distinct physicochemical behavior and potential toxicity compared with larger microplastics, yet their environmental occurrence and health risks remain poorly understood in Korea. This study proposes a national-scale risk screening framework for NPs that links real-world plastic emission rates with environmental release, transformation, and exposure pathways relevant to the Korean context. Using recent statistics on plastic production and waste management in South Korea, combined with literature-based emission factors and fragmentation rates, we estimate NP loads to air, surface water, coastal environments, and soils under multiple scenarios. These exposure estimates are integrated with a modular risk assessment framework originally developed for micro- and nanoplastics, emphasizing inhalation and oral uptake as key routes of human exposure and incorporating poorly soluble low-toxicity particle concepts, fibre pathogenicity paradigms, and new approach methodologies. The results highlight that, under conservative assumptions, NP exposure levels in densely populated urban and coastal regions may approach or exceed current effect thresholds derived from *in vitro* and *in vivo* studies on particle uptake, oxidative stress, and inflammation, whereas risks for remote regions appear comparatively lower. Although substantial uncertainties remain in NP quantification, dose-response relationships, and mixture effects with co-contaminants, the proposed framework provides a transparent basis for prioritizing high-risk scenarios, guiding monitoring strategies, and informing regulatory discussions on nano-scale plastic management in South Korea. **Methods:** The study builds on recently proposed modular risk assessment frameworks for micro- and nanoplastics that integrate physicochemical characterization, exposure assessment, and toxicological evaluation through an integrated approaches to testing and assessment (IATA) scheme. The framework applied here consists of four main modules: (i) source and emission characterization based on national plastic production and waste-management data; (ii) NP generation and environmental release modeling using literature-

derived fragmentation and loss factors; (iii) exposure assessment for environmental receptors and humans, with emphasis on inhalation and oral intake; and (iv) risk characterization using a combination of effect thresholds, benchmark dose information, and particle toxicology concepts such as poorly soluble low-toxicity particles. For the Korean context, the general framework was adapted to incorporate local plastic-flow data, environmental monitoring results, and region-specific exposure scenarios, particularly for densely populated urban centers and microplastic-impacted coastal zones. The resulting approach is intended as a screening-level tool that prioritizes transparency and reproducibility over detailed mechanistic modeling, acknowledging current limitations in NP detection and dose-response data. **Results:** The results indicate that, even under conservative assumptions, nanoplastic exposures in certain Korean urban and coastal environments may approach levels of potential concern for both human health and ecosystems. These findings support integrating NPs into ongoing national discussions on microplastic management and chemical safety, including consideration of restriction measures for intentionally added microplastics and sector-specific emission controls. **Conclusions:** For policy makers, the proposed framework demonstrates how existing plastic-flow data and emerging NP risk-assessment concepts can be combined to inform prioritization of monitoring and mitigation efforts in the absence of comprehensive NP measurements. In the Korean context, reducing plastic production and single-use plastics, improving waste-management systems, and targeting high-emission sectors such as transport, textiles, and fisheries are likely to yield co-benefits for climate mitigation and NP risk reduction.

ABSTRACT NUMBER: 5089 **Poster Board Number:** J641
TITLE: Genetic Expression Changes Induced by Atmospheric Nanoplastics in Human Lung Epithelia Reduced at Environmentally Relevant Concentrations

AUTHORS (FIRST INITIAL, LAST NAME) AND INSTITUTIONS: E. F. Wooliever, E. J. Hale, R. P. Carney, and *S. C. Nicklisch*. University of California, Davis, Davis, CA.
KEYWORDS: RT-PCR; Cell Culture; Respiratory Toxicology; Nanoplastics

ABSTRACT: Background and Purpose: Lung epithelia experience direct exposure to the environment, making them a critical barrier for environmental toxicity and xenobiotic defense. As a highly vascularized organ, the lung also presents a substantial route of xenobiotic absorption and associated systemic effects. Fine particulate matter, including PM2.5, and gas phase pollutants can settle in bronchioles and alveolar sacs in addition to larger airways, resulting in a high surface area of potentially impacted epithelium. Following inhalation, PM2.5 and pollutants can disrupt the functioning of bronchial and alveolar epithelia on impact and during prolonged contact, resulting in increased risk of lung disease as well as absorption into the bloodstream. Recent studies have detected atmospheric microplastics (MPs) and nanoplastics (NPs) in air samples and lung tissue, implicating the lung as a substantial pathway for local and systemic plastic absorption. However, NP mechanisms of toxic action on lung epithelia are still poorly understood, especially at environmentally relevant concentrations. Additionally, because atmospheric NPs are likely to only be a component of air pollutant exposures, the role that NPs play on the toxicity of other compounds needs to be better understood to fully assess aerosolized NP-associated health burdens. **Methods:** Human bronchial epithelial cells (HBECs) and human alveolar basal adenocarcinoma cells (A549s) were each exposed to pristine 220nm diameter polystyrene (PS) NPs at environmentally relevant concentrations (0.1-25 ng/mL). Additional exposures were performed with the same PS-NPs at elevated concentrations (35-3500 ng/mL), the organophosphate pesticide diazinon

(DZN; 3.5-350 ng/mL), or co-exposures of PS-NPs and DZN at the same respective concentrations. Negative controls (no treatment) were run in addition to three positive controls: lipopolysaccharide (LPS), H_2O_2, and a literature relevant PS-NP concentration (100 µg/mL). All exposures lasted 12 hours and were repeated three times. Within each exposure, treatments were performed in triplicate (totaling n = 9). Following exposure, cells were lysed in-well with TRIzol and flash frozen to preserve RNA, which was then isolated and converted into cDNA. Primers for key markers in pathways of interest (oxidative stress, inflammation, proliferation) and housekeeping genes were designed and validated for SYBR Green qPCR analysis, run in triplicate for each sample with ROX normalization dye and melt curve quality screening. Resulting cycle threshold (Ct) values were then normalized to housekeeping genes (ACTB and GAPDH) before calculating fold change relative to the negative control. For each gene within a cell line, normal distribution was assessed with a Shapiro test and statistical analysis was performed using either a one-way ANOVA with Tukey post hoc test or a Kruskal-Wallis with a Dunn post hoc test. **Results:** None of the genes of interest showed significant differential expression compared to the negative control ($p > 0.05$) following 12-hour exposures to PS-NPs, DZN, or PS-DZN in either cell line. This included markers for inflammation (IL6, TNFα), proliferation (VEGFα, EGFR), and oxidative stress (HMOX1). **Conclusions:** The results of this present study suggest that PS-NPs at environmentally relevant concentrations do not induce major changes in gene expression for key inflammatory, proliferative, and oxidative stress markers in pulmonary epithelial cells. However, biochemical assays may reveal non-transcriptional responses in future studies. Additionally, chronic effects or transient transcriptional responses may be captured with extended exposure or time course studies. The results of our current study underline the importance of environmentally relevant exposure levels when assessing atmospheric NP toxicity.

ABSTRACT NUMBER: 5090 **Poster Board Number:** J642

TITLE: Study Quality Evaluation of *In Vitro* Genotoxicity and Cytotoxicity Testing for Polyolefin Nano- and Microplastics with Artificial Intelligence (AI)-Assistance

AUTHORS (FIRST INITIAL, LAST NAME) AND INSTITUTIONS: *A. Yeh*, C. Heil, *M. LeBaron*, *A. Scott*, and *R. Ellis-Hutchings*. Dow, Midland, MI.

KEYWORDS: Risk Assessment; Genotoxicity; Cytotoxicity; Nano- and microplastics

ABSTRACT: Background and Purpose: Plastic nano- and microparticles (plastic NMP) have been evaluated for potential cytotoxicity and genotoxicity. There are no validated genotoxicity test guidelines (TG) specific for plastic NMP (although OECD Guidance Document (GD) 359 modifies the *in vitro* micronucleus assay [OECD TG 487] to evaluate insoluble nanoparticles), and few publications have evaluated the quality and reliability of peer-reviewed literature for use in the context of risk assessment. Large language models (LLMs) show promise for assisting with data quality evaluations in the nascent field of plastic NMP research. Here, we evaluated the quality of *in vitro* genotoxicity studies of plastic NMP in mammalian cells, focusing on polyolefins (e.g., polyethylene [PE], polypropylene [PP]) due to their common use in consumer products. **Methods: Literature search** - The SciFinder and Scopus databases each identified 560 documents published before November 2025 using the search string: “microplastic* OR nanoplastic* AND genotox* OR muta*”. Title and abstract screening determined 47 studies were in scope for evaluation, i.e., measured apical (mutagenicity) or indicator genotoxicity endpoints in mammalian cells. Thirteen additional studies were identified from review of a subset of review articles yielded from the initial search. Thus, 60 studies were evaluated in total. **Study quality evaluation approach** - Study quality was evaluated by a published toxicity study assessment tool with 25

criteria (16 mandatory, nine non-mandatory) in three categories: particle characterization, experimental design, and risk assessment applicability (Gouin et al., 2022). For each category, total scores were classified as Low, Medium, High, or Unacceptable (if any mandatory criteria scored 0). **AI-assisted data quality evaluations** - We used a random subset of 12 of the 60 studies to develop an AI workflow (leveraging frontier LLMs, e.g., Open AI's GPT-5) to score study quality. After validating the workflow, AI scored the remaining 48 studies by the evaluation framework, with a subset validated by a human evaluator. **Results: AI-assisted quality evaluations** - AI and human scores were closely matched for particle characterization and experimental design; more mismatches occurred in risk assessment applicability. Prompt refinement improved the alignment of AI to human scores. **Study quality evaluation** - No study received total scores classified as "High" in any category. Common limitations included poor characterization of test materials (e.g., surface chemistry), background contamination, particle stability, and exposure homogeneity, inability to assess dose-response, and unclear environmental relevance of test materials and concentrations. **Polyolefin genotoxicity studies** - Of the 60 studies, only eight evaluated polyolefins (eight PE; two also PP); four reported increased micronucleus formation, and one reported DNA fragmentation. However, no studies evaluated mutagenicity, so whether these effects would be sufficient to cause permanent DNA changes or would be repaired by normal physiological adaptive responses is unclear. Overall, no studies followed validated test guidelines (specific to plastic NMP or otherwise, e.g., OECD GD 359, OECD TG 487) and the studies shared many quality limitations described above, warranting caution in interpreting results. One study employed an inverted cell culture system to address buoyancy of certain polyolefin NMP and reported no genotoxicity of PE (particle size 200-9,900 nm) via DNA fragmentation. **Conclusions:** Most *in vitro* genotoxicity studies of plastic NMP, including polyolefins, are insufficiently reliable for risk assessment. Evidence is inadequate to demonstrate association between polyolefins and genotoxicity in mammalian cells. Recommendations to improve *in vitro* genotoxicity testing of plastic NMP include increased analytical characterization of test materials and dosimetry in cell cultures, and use of OECD GD 359 for micronucleus studies or modifying other OECD test guidelines for plastic NMP (e.g., inverted culture systems for buoyant polyolefin materials). AI tools can help extract study data and evaluate the reliability and quality of plastic NMP study data, but struggle with criteria requiring toxicological expertise (e.g., evidence of dose-response).

ABSTRACT NUMBER: 5091 **Poster Board Number:** J643

TITLE: Pulmonary effects of aerosolized polyamide-6 nanoplastics: comparing transcriptomic alterations in alveolar epithelial air-liquid interface cell cultures

AUTHORS (FIRST INITIAL, LAST NAME) AND INSTITUTIONS: *A. H. Remels*[1], I. Gosselink[1], E. Tha[2], F. Gruenschlaeger[2], P. Leonhardt[1], L. Ma-Hock[2], *F. van Schooten*[1], I. Kooter[1], M. Eichenlaub[2], and R. Landsiedel[2]. [1]Maastricht University, Maastricht, Netherlands; and [2]BASF SE, Ludwigshafen, Germany.

KEYWORDS: Inhalation Toxicology; Nanoparticles; Lung; Pulmonary or Respiratory System; Nanoplastics; Polyamide

ABSTRACT: Background and Purpose: Current knowledge on the toxicological effects of airborne, environmentally relevant nanoplastics remains limited. In this study, we compared the acute (24 h) cellular responses to polyamide-6 (PA-6) nanoplastics in both an alveolar epithelial cell line (A549) and a primary alveolar tissue model (AlveolAir™; single donor), each cultured at the air-liquid interface (ALI). **Methods:** ALI cultures were exposed to three concentrations of aerosolized PA-6 nanoplastics (30-200

nm). Deposited doses, assessed with a quartz crystal microbalance, ranged from 2.3 to 34.3 μg/cm^2. Endpoints included cytotoxicity, interleukin-8 secretion and gene expression analysis. **Results:** In both cultures, PA-6 nanoplastics did not induce substantial cell death. Transcriptomic analysis revealed a strong enrichment of inflammatory pathways in response to PA-6 in both cultures. This response was primary driven by pro-inflammatory genes encoding chemoattractants (*CXCL8, CCL20, CXCL5)* and interleukins (*IL32*). Consistent with these findings, PA-6 exposure induced interleukin-8 secretion up to 8-fold and 2-fold in A549 and primary cultures, respectively. Notably, only ~5% of the differentially expressed genes overlapped between the two models. High doses of PA-6 induced distinct transcriptomic changes in each model: pathways unique to A549 were associated with ER stress responses, while those unique to primary cultures were related to cellular metabolism, particularly lipid and sterol metabolism. **Conclusions:** PA-6 nanoplastics elicited a pro-inflammatory response in both *in vitro* models of the alveolar epithelium, with minimum cytotoxicity. Nonetheless, substantial differences in the gene expression profile between the alveolar cultures underscore the limitations of relying on a cell line model to predict responses in primary alveolar tissue.

ABSTRACT NUMBER: 5092 **Poster Board Number:** J644

TITLE: School Gardens as Experiential Learning Environments for Medicinal Plant Education: A Hermeneutic Mixed-Methods Approach

AUTHORS (FIRST INITIAL, LAST NAME) AND INSTITUTIONS: A. Botero Alvarez[1], G. Montes Hernandez[1], I. Portillo Barrios[1], M. Montiel Otero[1], and *B. Arroyo Salgado*[2,3]. [1]Liceo Campestre Jean Piaget, Chinu, Colombia; [2]Universidad de Cartagena Biomedical, Toxicological and Environmental Sciences Research Group, Cartagena, Colombia; and [3]SEMIDET, Universidad de Cartagena, Faculty of Medicine, Cartagena, Colombia.

KEYWORDS: Alternatives Assessment; Environmental Toxicology; Biotech Products; Young researchers; Bioactive compounds

ABSTRACT: Background and Purpose: Medicinal plants are widely used in traditional and contemporary health practices; however, limited toxicological literacy can contribute to inappropriate or unsafe use of bioactive compounds. This study examined the educational impact of a school garden as an experiential learning environment for medicinal plant education. The purpose was to assess how students develop criteria-based scientific literacy and evidence-based reasoning to identify, locate, and critically evaluate plant bioactive compounds within a non-laboratory educational context. **Methods:** The study employed a hermeneutic mixed-methods approach within a non-experimental educational framework. Students participated in regular visits to the school garden every Monday and Tuesday during school hours, where the garden functioned as a living pedagogical and observational space. Qualitative data were collected through systematic observations, student reflections, and guided discussions, while quantitative data were obtained from structured learning tasks and concept-recognition assessments aligned with Natural Sciences competencies. Instruction focused on plant morphology, localization of bioactive compounds, and criteria for informed and responsible medicinal use. **Results:** Students studied a diverse group of medicinal species, including *Mentha spicata* (spearmint), *Mentha piperita* (peppermint), *Melissa officinalis* (lemon balm), *Ocimum basilicum* (basil), *Tilia* spp. (linden), *Origanum vulgare* (oregano), *Aloe barbadensis* Mill. (aloe), *Thymus vulgaris* (thyme), *Ruta graveolens* (rue), and *Zingiber officinale* (ginger). Findings indicate that learners progressed from descriptive knowledge to analytical evaluation by identifying the presence and distribution of bioactive compounds within specific

plant structures (e.g., leaves, roots, stems, flowers, or gels). Students demonstrated criteria-based scientific literacy by questioning traditional claims, comparing species, and justifying medicinal uses based on observable morphological and phytochemical characteristics. This process strengthened critical thinking, inquiry skills, and early toxicological reasoning related to plant-part specificity and potential misuse. Increased engagement, responsibility, and sustained commitment to scientific inquiry were consistently observed. **Conclusions:** The integration of biotechnology concepts, environmental education, and ancestral knowledge within a regularly visited school garden supports the development of foundational toxicological literacy and evidence-based decision-making. For educators and outreach professionals, these findings highlight school gardens as effective platforms for introducing concepts related to bioactive compounds, risk awareness, and responsible use of medicinal plants. At an institutional level, the study supports experiential and interdisciplinary strategies that foster early scientific vocations, environmental ethics, and informed evaluation of natural products relevant to toxicology education and public health.

ABSTRACT NUMBER: 5093 **Poster Board Number:** J645

TITLE: Mercury exposure in fish from the San Juan River impacted by gold mining in the Colombian Pacific

AUTHORS (FIRST INITIAL, LAST NAME) AND INSTITUTIONS: Y. Palacios-Torres, D. Perea-Ruíz, K. Martínez-Copete, F. Ortiz-Mosquera, A. Romaña-Palacios, E. Moreno-Mosquera, and N. Nagles-Vergara. Technological University of Choco-DLC, QUIBDO, Colombia. Sponsor: *J. Olivero Verbel*

KEYWORDS: Metals; Ecotoxicology; Aquatic Toxicology; Pacific; Mercury

ABSTRACT: Background and Purpose: Mercury (Hg) is a persistent contaminant widely used in artisanal and small-scale gold mining. It bioaccumulates in aquatic organisms and increases with trophic level. **Methods:** We quantified Hg concentrations in fish tissue samples (n=167) using a Lumex RA-915M Differential Atomic Absorption Spectrometer. **Results:** A total of 15 species, 15 genera, 10 families, and 4 orders were recorded, with Siluriformes (46%) and Characiformes (40%) being the most representative. Characidae (n=18) and Heptapteridae (n=17) were the best-represented families. Hoplias malabaricus and Rhamdia guatemalensis (13% each) were the most dominant species. The greatest mean lengths were recorded for Rhamdia guatemalensis (27.05 ± 4.86 cm), Eigenmannia humboldtii (25.0 ± 9.25 cm), Spatuloricaria sp. (24.36 ± 2.92 cm), and Hoplias malabaricus (23.64 ± 4.39 cm). Mean mercury concentrations decreased in the following order: Paimado (117.6 ± 17.54 µg/kg) > Condoto (63.0 ± 6.45 µg/kg) > Río Iro (59.0 ± 9.05 µg/kg) > Andagoya (52.0 ± 5.84 µg/kg). Significant differences were found between the average mercury concentrations of trophic guilds (ANOVA, $P < 0.0001$) and sites (Kruskal-Wallis test, $P < 0.0001$). Hg concentrations ranged from 14.9 to 555.7 µg/kg, with an overall average of 78.33 ± 5.05 µg/kg. Hoplias malabaricus and Sternopygus aequilabiatus showed values close to 200 µg/kg. **Conclusions:** Implement actions under the Minamata Convention to reduce the risk associated with mercury exposure.

ABSTRACT NUMBER: 5094 **Poster Board Number:** J646
TITLE: Dose-dependent Transcriptomic Signatures of PFBA-induced Hormesis in *Spodoptera frugiperda*

AUTHORS (FIRST INITIAL, LAST NAME) AND INSTITUTIONS: *W. Omagamre*, and J. Pitula. University of Maryland Eastern Shore, Princess Anne, MD.
KEYWORDS: Perfluoronated Agents; Non-Mammalian Species; Ecotoxicology; Hormesis; Perfluorobutanoic Acid

ABSTRACT: Background and Purpose: Low-dose, non-monotonic responses challenge conventional toxicological assumptions but remain poorly resolved for short-chain per- and polyfluoroalkyl substances (PFAS). Perfluorobutanoic acid (PFBA), an increasingly prevalent short-chain PFAS in agricultural and environmental matrices, is often considered less biologically active than long-chain analogs, despite limited evaluation of its biological effects at environmentally relevant concentrations. Here, we integrate phenotypic endpoints with time-resolved transcriptomic profiling to investigate dose-dependent PFBA toxicity and hormetic responses in larvae of the fall armyworm (*Spodoptera frugiperda*), a tractable *in vivo* model for developmental toxicology. **Methods:** An initial 24-hour phenotypic screening assay was conducted across a broad PFBA concentration range (0.0001-50,000 µg/g diet) in two noctuid species, *S. frugiperda* and *Spodoptera exigua*, to identify conserved stimulatory and inhibitory response thresholds. Both species exhibited a non-monotonic, biphasic growth response, indicating a conserved early phenotypic sensitivity to PFBA. Based on these results, *S. frugiperda* was selected for mechanistic analysis due to the availability of a well-annotated reference genome. Larvae were exposed for seven days to control diet, a low-dose stimulatory concentration (1 µg/g), or a high-dose inhibitory concentration (20 mg/g). Growth, feeding behavior, and developmental progression were monitored, and larvae were sampled at days 1 and 5 for transcriptomic analysis. **Results:** An initial 24-hour phenotypic screening assay was conducted across a broad PFBA concentration range (0.0001-50,000 µg/g diet) in two noctuid species, *S. frugiperda* and *Spodoptera exigua*, to identify conserved stimulatory and inhibitory response thresholds. Both species exhibited a non-monotonic, biphasic growth response, indicating a conserved early phenotypic sensitivity to PFBA. Based on these results, *S. frugiperda* was selected for mechanistic analysis due to the availability of a well-annotated reference genome. Larvae were exposed for seven days to control diet, a low-dose stimulatory concentration (1 µg/g), or a high-dose inhibitory concentration (20 mg/g). Growth, feeding behavior, and developmental progression were monitored, and larvae were sampled at days 1 and 5 for transcriptomic analysis.Low-dose PFBA exposure produced approximately 40% enhancement of larval growth and transient increases in feeding, whereas high-dose exposure markedly inhibited growth without inducing acute mortality. RNA sequencing revealed dose- and time-specific transcriptomic signatures underlying these divergent phenotypes. Low-dose exposure selectively activated gene networks associated with structural remodeling, nutrient metabolism, and endocrine regulation, consistent with accelerated developmental progression. By contrast, high-dose exposure induced a stress-dominated transcriptional state characterized by activation of detoxification, oxidative stress, protein quality control, and neuronal calcium-signaling pathways, alongside suppression of juvenile hormone, ecdysone-associated, and metabolic regulators. By day 5, transcriptional signatures indicated that low-dose PFBA exposure aligned with early pre-pupal reorganization, whereas high-dose exposure disrupted pathways required for coordinated developmental transitions. **Conclusions:** Collectively, these findings demonstrate that PFBA elicits hormetic responses through dose-specific engagement of developmental versus stress-response pathways. These results highlight the importance of incorporating bidirectional dose effects and

molecular mode-of-action data into toxicological evaluation and risk assessment of short-chain PFAS, particularly for frameworks that rely on linear or monotonic dose-response assumptions.

ABSTRACT NUMBER: 5095 **Poster Board Number:** J647
TITLE: Improving Method Performance of *Artemia salina* Acute Toxicity Assays Through Standardized Procedures

AUTHORS (FIRST INITIAL, LAST NAME) AND INSTITUTIONS: M. Cavieres, C. Veragua, D. Vasquez, and F. Carvajal. University of Valparaíso, Valparaíso, Chile. Sponsor: *J. Manautou*
KEYWORDS: Aquatic Toxicology; Toxicity; Acute; Reproducibility and Method Performance

ABSTRACT: Background and Purpose: Acute toxicity assays using Artemia salina are widely applied as rapid screening tools in ecotoxicology and environmental hazard assessment, particularly as alternatives to vertebrate testing. However, variability in experimental procedures within and across laboratories can limit confidence in the reproducibility and reliability of derived toxicity endpoints. This study aimed to evaluate the effect of methodological standardization on method performance in Artemia salina acute toxicity assays, focusing on intralaboratory reproducibility, precision, and dispersion of LC50 estimates using a reference toxicant. **Methods:** Independent acute toxicity assays were conducted with Artemia salina nauplii exposed to potassium dichromate ($K_2Cr_2O_7$) under controlled laboratory conditions. Toxicity was initially evaluated at 24 and 48 h. LC50 values were estimated using Probit dose-response modeling exclusively for assay runs that met predefined acceptance criteria, including ≤10% control mortality and adequate model fit. Multiple operators and two exposure media (synthetic seawater, Instant Ocean, and natural seawater) were included to evaluate sources of intralaboratory variability. Method performance was assessed using LC50 dispersion, confidence interval overlap, and coefficients of variation. **Results:** At 48 h exposure, complete mortality occurred at all tested concentrations, preventing concentration-response modeling; therefore, quantitative analyses were restricted to 24 h. From 24 independent assays conducted at 24 h, 13 met all acceptance criteria and were included in the final analysis. LC50 values clustered within a defined range (34-111 mg/L), with a median of approximately 45 mg/L and substantial overlap of 95% confidence intervals across accepted runs. The overall coefficient of variation for LC50 estimates was 37.2%, indicating moderate intralaboratory variability. Stratification by exposure medium revealed lower dispersion when synthetic seawater was used (CV = 13.0%) compared with natural seawater (CV = 50.1%). Exposure to 200 mg/L potassium dichromate consistently resulted in complete mortality, supporting its use as a reproducible positive control. **Conclusions:** These results demonstrate that methodological standardization is a critical determinant of method performance in Artemia salina acute toxicity assays. When standardized procedures and objective acceptance criteria are applied, reproducible LC50 estimates can be obtained within a single laboratory, while variability is largely attributable to operational and matrix-related factors. The findings support the use of Artemia salina as a robust alternative screening tool for acute toxicity assessment and highlight the importance of standardized procedures to improve data quality and comparability in bioassay-based decision-making.

ABSTRACT NUMBER: 5096 **Poster Board Number:** J648

TITLE: A comparison of plastic additive effects on*Daphnia magna*development, reproduction, and epigenetic expression

AUTHORS (FIRST INITIAL, LAST NAME) AND INSTITUTIONS: *C. Mazariegos*, and *J. Cañas-Carrell*. Texas Tech University, Lubbock, TX.

KEYWORDS: Aquatic Toxicology; Behavior; Ecotoxicology; Phthalate; DEHP, DEHA

ABSTRACT: Background and Purpose: *Daphnia magna* is a well-established model organism for evaluating the toxicity of environmental contaminants due to its advantageous biological traits, including high pollutant sensitivity, ease of laboratory cultivation, parthenogenetic reproduction, short generation time, large brood size, and the capacity to assess diverse toxicological endpoints. Phthalates, such as di(2-ethylhexyl) phthalate (DEHP), have demonstrated adverse effects across both vertebrate and invertebrate species, such as generational collapse in invertebrates and endocrine disruption in vertebrates. In response to these concerns, non-phthalate alternatives like di(2-ethylhexyl) phthalate (DEHA) have been introduced in plastic manufacturing. DEHP and DEHA are structurally similar plasticizers but differ in chemical composition, environmental behavior, and toxicity. Structurally, DEHA features an aliphatic structure, which makes it more biodegradable. However, despite its chemical advantages, DEHA's safety profile remains insufficiently characterized. This study examines the comparative effects of DEHP and DEHA on D. magna, with a focus on developmental outcomes, reproductive performance, and epigenetic expression patterns. **Methods:** Following EPA 850 guidelines, DEHP and DEHA concentrations will be established to determine the no-observed-effect concentration (NOEC) and median lethal concentration (LC_{50}) values. Then, *D. magna* juveniles will be exposed for 24 h and adults for 48 h to assess developmental and reproductive parameters. In parallel, juveniles and adults will be exposed under identical conditions to evaluate global DNA methylation levels and the expression of key epigenetic regulators, including dnmt1a, dnmt3a.1, and dnmt3a.2. To further validate any observed changes in development and reproduction, mRNA abundance of vtg2, hsp70, and EcR will be quantified using RT-qPCR. **Results:** Daphnia juveniles were exposed to five DEHP and DEHA concentrations (100, 250, 500, 750, and 1000 µg/L). Mortality in Daphnia magna juveniles and adults was higher at concentrations of 750 and 1000 ug/L. Specifically, higher concentrations of DEHP (1000 µm) caused juveniles of Daphnia to collapse up to 50% of the population. Preliminary results showed that Daphnia exposure to DEHP and DEHA at a concentration of 1000 µm/L resulted in modulation of dnmt1A, hps70, vtg2, and EcR. There was an increase in gene dysregulation observed in the DEHP exposure group. **Conclusions:** This study showed that plastic additives (DEHP and DEHA) can modulate growth, reproductive, and epigenetic genes, specially exposed groups to DEHP. To further analyze the effects of these plasticizers on Daphnia magna and subsequent offspring, the phototactic behavior test, reproductive success through the number of offspring (EPA 850 guidelines), developmental endpoints (hps70 and EcR), and epigenetic biomarkers (dnmt1a, dnmt3a.1, and dnmt3a.2) will be analyzed via RT-qPCR. This project is currently in progress.

ABSTRACT NUMBER: 5097 **Poster Board Number:** J649
TITLE: Plastic Additive Fingerprints across Contrasting Aquatic Ecosystems: Cross-System Indicators of Polymer Degradation and Input Pressure

AUTHORS (FIRST INITIAL, LAST NAME) AND INSTITUTIONS: *A. O. Adeogun*[1], *A. V. Chukwuka*[2], *O. R. Ibor*[3], *E. D. Omogbemi*[1], and *A. Arukwe*[4]. [1]University of Ibadan, Ibadan, Nigeria; [2]National Environmental Standards and Regulations Enforcement Agency, Abuja, Nigeria; [3]University of Calabar, Calabar, Nigeria; and [4]Norwegian University of Science and Technology, Trondheim, Norway.
KEYWORDS: Phthalates; Aquatic Toxicology; Plastic Additives, Urban contamination, Polymer

ABSTRACT: Background and Purpose: Plastic additive residues offer crucial chemical evidence of polymer degradation and environmental loading. **Methods:** Eleven phthalate esters and Bisphenol A (BPA) in fish species from an industrial estuary (Lagos Lagoon), peri-urban estuary (Epe Lagoon), and urban freshwater lake (Eleyele Lake) were quantified in this study using GC-MS. **Results:** Total phthalate ester concentrations (ΣPEs) ranged from 1.28 to 4.62 μg g^{-1} ww, while BPA varied between 0.15 and 0.84 μg g^{-1} ww across sites. Lagos Lagoon fish exhibited the highest additive burden (mean ≈ 4.1 μg g^{-1}), followed by Epe (2.6 μg g^{-1}) and Eleyele (1.7 μg g^{-1}). Dibutyl phthalate (DBP) and benzyl butyl phthalate (BBP) dominated, accounting for 46-61% of ΣPEs, consistent with emissions from flexible PVC and packaging films. BPA was detected in every fish sample (0.15-0.84 μg g^{-1}), confirming its environmental persistence and value as a reliable indicator of consumer-plastic degradation across all three aquatic systems. The consistent additive congener profiles shared by these hydrologically distinct environments further point to widespread urban polymer inputs rather than contributions from isolated industrial point sources. Trophic trends revealed highest additive loads in demersal (*Chrysichthys nigrodigitatus*: 4.62 μg g^{-1}), intermediate levels in benthopelagic (*Polydactylus quadrifilis*: 3.05 μg g^{-1}), and lowest in pelagic (*Sardinella maderensis*: 1.28 μg g^{-1}) fish species. **Conclusions:** These chemical fingerprints demonstrate the widespread influence of urban plastic inputs across both estuarine and inland freshwater environments. Overall, the results highlight the diagnostic value of additive profiling for reconstructing polymer degradation and plastic-waste pathways across connected aquatic ecosystems.

ABSTRACT NUMBER: 5098 **Poster Board Number:** J650
TITLE: Light Absorption in Nitroaromatic Brown Carbon Chromophores: Microdroplet Insights

AUTHORS (FIRST INITIAL, LAST NAME) AND INSTITUTIONS: P. M. De Allende. University of California Riverside, Riverside, CA. Sponsor: Y. Lin, Society of Environmental Toxicology and Chemistry
KEYWORDS:

ABSTRACT: Background and Purpose: Aerosol particles play a central role in Earth's atmospheric system by scattering and absorbing radiation, serving as cloud condensation nuclei, and driving multiphase chemical reactions. Their optical properties are described by the complex refractive index (RI), (m=n+ik), which is the sum of the real part (scattering) and imaginary part (absorbing). Among these particles brown carbon (BrC), an abundant constituent, exhibits wavelength dependent light absorption in the visible region of the solar spectrum. BrC are a significant but poorly constrained contributor to radiative forcing. According to recent studies, global estimates vary by a factor of ~15 (0.04-0.57 W m^{-2}) due to variability in optical properties and chemical transformations. Single particle studies allow for precise refractive index (RI) retrieval that can decrease variability in radiative forcing calculations. This work presents an *in-situ* broadband light scattering (BLS) approach to characterize the absorption spectra of

BrC chromophores in levitated particles. We demonstrate effective retrieval of the wavelength-dependent imaginary refractive index (k) in metastable, supersaturated BrC aqueous particles. In addition, we show how optical properties may be tracked over time in response to physical and chemical changes common in the environment. **Methods:** Particles containing 4-nitrocatechol (4NC), a model aqueous BrC aerosol, were levitated in an electrodynamic balance under low, neutral and high pH conditions in a range of relative humidities (RH). Each absorbing particle was trapped alongside a non-absorbing reference particle and both were interrogated by BLS spectroscopy. The non-absorbing particle served as an *in-situ* reference for the LED, accounting for intensity variation across the measured wavelength range (420-540 nm). Normalization of the sample spectrum against the reference eliminated artefacts introduced from the LED and optical setup, enabling characterization of the absorption spectrum and retrieval of k(λ) in aqueous particles. For analyzing a 4NC spectra, the size and real part of the refractive index were first determined from scattering data in a non-absorbing region of the spectrum. The absorption features were constrained using Gaussian peaks derived from bulk UV/vis measurements. From these data a simulated spectrum was generated and compared with the experiment to find the optimal k(λ). **Results:** This technique observed sensitivity to k in the range of 0.0001-0.01 with an uncertainty of ±10%. 4NC exhibits pH dependent light absorption due to its labile protons. Its forms include neutral 4NC, 4NC-1, and 4NC-2. Each form has its own light absorption spectrum and corresponding k(λ). Exact pH could not be directly determined, however spectral changes across different pH regions were resolvable in these measurements. This was evident in the red shift of the absorption features with increasing pH, following the trends observed in UV/vis data. Gaussian peak amplitudes were compared to quantify the relative contributions of each species to absorption in the particle. Across all species, k increased as the RH decreased, consistent with the weight fraction of the chromophore increasing while the water content of the particles decreased. **Conclusions:** This particle-based method allows for the determination of k at atmospherically relevant supersaturated chromophore concentrations not accessible to bulk measurement methods. Chromophore concentrations achievable in levitated particles are orders of magnitude higher than those detectable by solution based spectroscopy. Particle based methods provide a closer analogue to real atmospheric aerosol components allowing for more accurate radiative forcing calculations and improving our understanding of the link between aerosol composition, and environmental impact.

ABSTRACT NUMBER: 5099 **Poster Board Number:** J651

TITLE: Impact of Post-Combustion Ammonia and Ash-Forming Lubricating Oil on Secondary Aerosol Formation and Toxicity of Marine Engine Emissions

AUTHORS (FIRST INITIAL, LAST NAME) AND INSTITUTIONS: T. Zavodna[1], T. Cervena[1], K. Honkova[1], M. Vojtisek-Lom[1], P. Marjanen[2], K. Kylämäki[2], L. Barreira[3], M. Aurela[3], H. Kuutt[4], T. Hangasmaa[4], M. Jäppi[2], R. Asgher[2], S. Farhoudian[2], A. Kumar[2], H. Timonen[3], P. Aakko-Saksa[4], T. Rönkkö[2], and *J. Topinka*[1].
[1]Institute of Experimental Medicine of the Czech Academy of Sciences, Prague, Czech Republic; [2]Tampere University, Tampere, Finland; [3]Finnish Meteorological Institute, Helsinki, Finland; and [4]VTT Technical Research Centre of Finland Ltd, Espoo, Finland.

KEYWORDS: Toxicity; Acute; Toxicogenomics; *In Vitro* and Alternatives; Distillate Marine grade B fuel; Ammonia

ABSTRACT: Background and Purpose: Maritime transport is a major global source of air pollution. While sulfur regulations have driven changes in marine fuel composition, toxicological implications of emerging fuel additives are largely unexplored. Ammonia is promoted as a low-carbon solution for maritime decarbonization, and lubricants remain unavoidable contributors to marine exhaust particles. Both can substantially alter aerosol chemistry and aging processes. Secondary aerosols formed through atmospheric oxidation may differ strongly from fresh emissions, yet are rarely included in toxicity assessments due to the experimental complexity. Thus, the impact of emerging marine fuel additives on emission aging processes is almost completely unknown. Here, we present the first integrated *in vitro* study combining controlled marine emissions, simulated atmospheric aging, and on-site air-liquid interface (ALI) toxicology, investigating how ammonia and lubricating oil influence secondary aerosol formation in marine fuels and associated biological responses. **Methods:** Distillate Marine grade B fuel (DMB) was used alone, combined with post-combustion ammonia injection (DMB+NH_3), or enriched prior to combustion with high-ash marine lubricating oil to introduce ash-forming constituents and mimic exhausts typical of high-sulfur ash-containing marine engine fuels (DMB+LO). These fuels were combusted in a single-cylinder diesel engine under controlled laboratory conditions. Secondary aerosols were generated using a Potential Aerosol Mass Oxidation Flow Reactor simulating ~2.4 days of atmospheric aging. Aerosols were characterized for total particle number, PM_1 mass, and chemical composition. Human BEAS-2B bronchial epithelial cells were exposed to diluted (~100 x) fresh or aged emissions for 90 mins, while a 3D human airway epithelium MucilAir™ was exposed for 120 mins to diluted fresh emissions only, using a portable ALI exposure system. Cytotoxicity (LDH release), cell layer integrity (transepithelial electrical resistance), DNA damage (Comet assay), oxidative stress (oxidative DNA damage by Comet assays with FPG and 15-F_{2t}-isopostane as a marker of lipid peroxidation), and whole genome expression changes were assessed after 24h recovery. **Results:** Post-combustion ammonia and ash-forming lubricating oil addition resulted in distinct changes in emission composition, particle size distribution, aerosol aging, and biological responses. Lubricating oil increased nucleation-mode particles and reduced black carbon. Post-combustion ammonia injection led to a 14-fold increase in PM_1 mass, driven mainly by formation of secondary inorganic aerosol dominated by ammonium nitrate. No cytotoxicity, genotoxicity, or oxidative stress were detected in any of the exposure scenarios. Transcriptomic responses in BEAS-2B cells were weak (1-2 differentially expressed genes (DEGs)) for both fresh and aged DMB and DMB+LO. DMB+NH_3 exposure resulted in 28 DEGs linked to oxidative stress and inflammatory signaling, mitochondrial and ribosomal stress, and chromatin remodeling. Ammonia-derived secondary aerosols elicited the strongest response with 699 DEGs associated with

nucleolar and ribosomal stress, RNA splicing, protein-RNA and protein-DNA complex assembly, and nucleosome organization pathways. These changes indicate a coordinated cellular adaptation involving translational control, RNA processing, and chromatin remodeling in response to pollutant-induced stress, consistent with the high inorganic aerosol load and altered redox environment generated during ammonia-driven aging. In MucilAir™, fresh DMB+NH_3 exposure caused a marked and predominantly suppressive transcriptional response (488 DEGs). **Conclusions:** Our study demonstrates that fuel additives can profoundly influence secondary aerosol formation and cellular stress responses. Post-combustion ammonia injection strongly enhanced secondary inorganic aerosol formation and triggered pronounced transcriptional changes in airway epithelial cells, whereas ash-forming lubricating oil exerts minimal effects on the exhaust aging and toxicity. The integration of realistic marine emissions, atmospheric aging, and ALI-based *in vitro* toxicology provides critical insight into health-relevant impacts of emerging marine decarbonization strategies, and supports informed regulatory and technological decisions to avoid unintended consequences of low-carbon fuels in maritime transport.

ABSTRACT NUMBER: 5100 **Poster Board Number:** J652

TITLE: Microglia involvement in particle matter induced neuroinflammation

AUTHORS (FIRST INITIAL, LAST NAME) AND INSTITUTIONS: *D. L. Menendez Escalera*[1], K. M. Casillas-Pagan[2], and *L. B. Mendez*[2]. [1]National Institutes of Health, Bethesda, MD; and [2]Universidad Ana G. Mendez, Carolina, PR.

KEYWORDS: Inflammation; Particulates; Neurotoxicology; Microglia

ABSTRACT: Background and Purpose: Epidemiological studies have associated exposure to ambient particulate matter (PM) with neuroinflammation and negative cognitive outcomes. Children, particularly, are susceptible to the effects of PM since their CNS is still in development until late adolescence. Previous behavioral testing showed that exposure to diesel exhaust particles (DEP) induced a hyperactive phenotype with executive dysfunction in juvenile mice. In addition, significant increases in the levels of proinflammatory cytokines and chemokines in the CNS were observed. Astrocytes and microglia are major sources of pro-inflammatory cytokines and chemokines in the brain and have been implicated in air pollution-induced CNS effects. It has been shown that lesions in the prefrontal cortex (PFC) of rodents can lead to hyperactivity and other negative cognitive outcomes. Since neuroinflammation is the most prominent effect observed in mice exposed to different types of PM, we hypothesize that the PFC is a target for DEP-induced neurotoxicity. **Methods:** To test this hypothesis, male and female C57BL/6J mice were exposed to either saline or increasing doses of DEP during postnatal days (PND) 25 to 33 by intranasal instillation. Cognitive and behavioral assessment was conducted during PND 36-38. On PND 39, mice were transcardially perfused with 0.1M PBS. Brains were dissected and the right hemispheres were post-fixed in 4% PFA and sent to HistoWiz for processing, immunohistochemistry and imaging. Sagittal sections of 4 µm were stained against microglia activation marker IBA-1 (Wako, 019-19741 - 1:1200, DAB) and counterstained with Hematoxylin. Whole slide images were processed in QuPath 6.0, where the prefrontal cortex was selected for cell detection, counting and classification of activated microglia. **Results:** Preliminary results (n=4/group) showed a non-significant increase of IBA-1 immunoreactivity in exposed mice when compared to controls. However, there were no changes in microglia cell counts among the groups. In contrast, six days after the last exposure, significant dose-dependent increases were observed in IL-1, IL-6, IL-12, IL-17, and MIP-1α. In addition, exposure to DEP induced significant increases in IL-9 and IFN-γ at the lowest dose

and IL-17a at the highest dose compared to controls. **Conclusions:** Overall, the results demonstrated persistent neuroinflammatory responses in mice exposed to DEP. However, no significant differences were observed in microglial levels within the PFC. Future studies will focus on a detailed morphological analysis of microglia to assess their activation phenotype, as well as the evaluation of other brain regions. This approach will help shed light on the contribution of region-specific microglial alterations to DEP-induced neuroinflammation and associated neuropathological outcomes.

ABSTRACT NUMBER: 5101 **Poster Board Number:** J653
TITLE: Neurological consequences of chronic wildfire smoke exposure in mice

AUTHORS (FIRST INITIAL, LAST NAME) AND INSTITUTIONS: *A. Lessard*, *J. Smoot*, M. Johnson, A. Wood, *J. A. Moreno*, R. McCosh, and *L. Montrose*. Colorado State University, Fort Collins, CO.
KEYWORDS: Neurotoxicology; Inhalants; Inflammation

ABSTRACT: Background and Purpose: Wildfire activity is increasingly more intense and frequent in conjunction with hotter and drier conditions, particularly in the Western US. Epidemiologic studies link higher dementia incidence with long-term exposure to wildfire-sourced $PM_{2.5}$. Yet, the mechanisms by which wildfire-sourced $PM_{2.5}$ contributes to neurodegeneration have not been fully elucidated. This project uses a whole-body exposure model to investigate how a chronic and hazardous exposure to wildfire smoke may impact neurological health. We hypothesize that chronic exposure to hazardous levels of wildfire-sourced $PM_{2.5}$ will alter behavior, modify neuronal abundance, and lead to changes in accumulation and distribution of inflammatory factors within the brain. **Methods:** To assess the neurological consequences of chronic wildfire smoke, fourteen male mice were exposed 2 hours/day to either filtered air or 40mg/m3 of wildfire smoke by burning Douglas fir needles at a smoldering temperature of 460C in an exposure chamber for 55 days over a 3-month period. Weekly behavioral assays were conducted to measure locomotor activity, anxiety-like behavior, recognition memory, and exploration. To assess pre-mortem neurological health, post-mortem analysis was conducted using immunohistochemistry. This analysis identifies levels of neuronal density and inflammation in the brain and examines how this inflammation is distributed across brain regions. **Results:** The behavior analysis demonstrated a modest trend toward anxiety-like behavior in the wildfire smoke exposed mice. Although the data is largely mixed and levels of significance were rarely below p=0.05, we see suggestive evidence of regionally distinct glial activation and a reduction of mature neurons. **Conclusions:** These findings lay a foundation for work that will expand the field's understanding of how wildfire smoke interferes with neurological health and supports future efforts to develop strategies to protect neurological health in the face of increasing wildfire smoke exposure.

ABSTRACT NUMBER: 5102 **Poster Board Number:** J654

TITLE: Evaluation of Sex-Specific Reproductive Effects in Mice Following an Acute Simulated Wildfire Smoke Particulate Exposure

AUTHORS (FIRST INITIAL, LAST NAME) AND INSTITUTIONS: *J. Smoot*, *L. Montrose*, E. Kaplan, D. Krapf, E. Morales-Arguello, P. Blei, and R. McCosh. Colorado State University, Fort Collins, CO.

KEYWORDS:

ABSTRACT: Background and Purpose: Wildfires are increasing year over year as hotter and drier conditions become more common across the United States. Wildfire smoke (WFS) contains a complex mixture of chemicals known to affect the cardiopulmonary system, yet a growing body of evidence suggests WFS can also negatively impact the brain and reproductive system. Interestingly, both direct and indirect mechanisms have been proposed for reproductive system impacts where the indirect mechanism involves the brain. To better understand this phenomenon, we leveraged WFS extracted from filters produced during laboratory combustion of Douglas-fir needles to represent the Rocky Mountain region and a mixture of eucalyptus and manzanita to represent California wildfires. **Methods:** Adult C57BL/6 mice were exposed to simulated WFS to assess impacts on the male and female reproductive fitness and fertility. Animals received 50 µL per day of lung surfactant mimic as a vehicle, Douglas-fir smoke extract, or eucalyptus/manzanita smoke extract (1 mg/mL) via intranasal installations (n = 6-12 per group). Males were sacrificed 24 hours post-exposure and females were followed for 5 additional days to monitor estrus cyclicity. **Results:** QPCR analysis of HPG axis-related genes in the gonads and pituitary largely did not change following the simulated WFS exposure treatment. Sperm concentration and estrus cyclicity was similarly unchanged. Sperm motility from eucalyptus/manzanita and Douglas fir exposed males displayed significant reductions in curvilinear velocity, average-path velocity, straight-line velocity, linearity, and mean amplitude of lateral head displacement versus controls following assessment via Computer Aided Sperm Analysis (CASA). Additionally, overall rates of defects in sperm morphology increased in both WFS treatments. **Conclusions:** Collectively, these data indicate that while acute WFS exposure does not interrupt estrus cyclicity in female mice, it is linked to significant decreases in some metrics of caudal sperm motility, possibly through direct exposure on the stored sperm population by WFS or secondary inflammatory mediators. These findings further motivate a study with a longer exposure duration that is more likely to engage the HPG axis and a more physiologically relevant exposure route (e.g., whole body rather than intranasal) that more closely reflects how humans are exposed to WFS.

ABSTRACT NUMBER: 5103 **Poster Board Number:** J655

TITLE: Macrophage Handling of Particulate-laden Cell Corpses Drives Retention and Inflammation

AUTHORS (FIRST INITIAL, LAST NAME) AND INSTITUTIONS: *S. Bersie*[1], S. Hott[2], and A. McCubbrey[2].
[1]University of Colorado Anschutz Medical Campus; National Jewish Health, Denver, CO; and [2]National Jewish Health, Denver, CO.

KEYWORDS: Macrophage; Particulates; Inflammation; Cell death

ABSTRACT: Background and Purpose: The human lungs are constantly exposed to inhaled particulate matter (PM), and bioaccumulation of non-degradable PM in the lungs can drive inflammation and disease. Approximately 15% of inhaled PM reaches the lower respiratory tract where it is engulfed by alveolar macrophages (AM). AM are crucial to maintaining homeostasis by clearing inhaled pathogens, foreign PM, and cell corpses from the local environment. Knowledge gaps remain regarding the mechanisms of PM persistence. This study explores the fate of PM contained within macrophages following cell death, examining the hypothesis that 1) non-degradable PM remains within apoptotic and necrotic cells and is transferred to new, living macrophages during cell corpse clearance, and 2) macrophage engulfment of PM-laden cell corpses alters immunometabolic programming, and the nature of cell death (i.e apoptosis, necrosis) will modify the degree of impact to the engulfing phagocyte. This work provides insight into novel mechanisms promoting PM retention in macrophage populations and explores how this drives inflammation and disease. **Methods:** PM retention and transfer were modeled *in vitro* and *in vivo*. *In vitro,* THP-1 macrophages were cultured with 1µm polystyrene beads, amorphous silica, or urban PM. Apoptosis or necrosis was induced to generate PM-loaded corpses, then cells were assessed visually or co-cultured with live bone marrow-derived macrophages (BMDM). BMDM were analyzed for THP-1 corpse and PM content (microscopy, flow cytometry) or changes in gene expression (RT-PCR). *In vivo*, C57BL/6 mice were exposed to fluorescent PM alongside a PKH26 membrane dye via intratracheal instillation. This generated dye-labeled, PM-loaded resident AM. Clodronate treatment at day 7 induced resident AM apoptosis and called monocyte-derived recruited AM to the lungs. Bronchoalveolar lavage was collected 4 days later, and PM or resident AM material transfer to recruited AM were assessed by flow cytometry. **Results:** *In vitro,* intracellular PM remained within apoptotic and necrotic cells after death. Microscopy further revealed that BMDM co-cultured with PM-laden corpses obtained PM via whole corpse engulfment or modes unique to the type of cell death. Unique to apoptotic cells, BMDM engulfed PM contained within apoptotic blebs and bodies. Unique to necrotic cells, BMDM attached and engulfed intracellular PM in the absence of corpse-derived plasma membrane. Following engulfment of PM-laden versus naïve cell corpses, BMDM upregulated proinflammatory and metal response genes. Treatment with a metal chelator significantly decreased *Tnfα* expression, indicating inflammatory processes linked to PM-derived metals. BMDM pre-exposed to PM prior to co-culture further displayed decreased engulfment of dead cells. This indicates an impairment to phagocytic capacity when undegraded intracellular PM is present. *In vivo* findings support *in vitro* observations for PM transfer. *In vivo,* PM/PKH26 instillation led to durably labeled PM-laden resident AM. Clodronate instillation caused resident AM death, and recruited AM infiltrates were present in day 4 lavage fluid. Flow cytometry revealed that both PM and PKH26 were contained within the recruited AM subset. This indicates *in vivo* material transfer from apoptotic to live engulfing macrophages. **Conclusions:** Understanding the fate of non-degradable PM will advance understanding of how environmental exposures drive inflammation and the development of pulmonary disease. This work describes the unique nature of PM retention and transfer from dead to

living macrophages, which drives a “re-exposure” and PM persistence within the phagocytic cell pool. This process perturbs normal transcriptional programming and phagocytic function of the engulfing macrophage. This work will be expanded upon in future *in vitro* and *in vivo* -omics studies to investigate the widespread impacts to immunometabolism.

ABSTRACT NUMBER: 5104 **Poster Board Number:** J656
TITLE: Hair Loss and Collagen Deposition Altered in C57Bl/6 Mice in Response to Deisel Exhaust Particulate and/or Desert Sand Dust Expo

AUTHORS (FIRST INITIAL, LAST NAME) AND INSTITUTIONS: J. Irwin, and *L. J. Schneider*. Defense Centers for Public Health - Aberdeen, APG, MD.
KEYWORDS: Inhalation Toxicology; Exposure, Environmental; Particulates

ABSTRACT: Background and Purpose: Service members are often deployed to Southwest Asia where they are exposed to airborne particulate matter (PM) concentrates that exceed that of the average population by as much as 10x - with diesel exhaust particulate (DEP) and desert sand dust (DSD) frequently being the most prevalent PM constituents. Hair loss has been reported by many service members after deployments to Southwest Asia over the past several decades and is often a symptom report by patients with Guld War Illness. These exposures have a known correlated to neurological, respiratory, and cardiovascular diseases; however, little is known regarding the effects these inhaled particulates have on skin and hair health. Therefore, we proposed to investigate the effects of inhaled DEP and DSD on hair loss. **Methods:** 2-month old male and female C57Bl/6 mice were exposed by nasal instillation to low, medium, and high doses of DEP, DSD, or DEP+DSD suspended in saline or saline alone (control) twice per week for a 60-day period. 14-16 hours after the last exposure, the animals were sacrificed by euthanasia with Euthasol (100 µL per mouse) followed by exsanguination. Total hair loss scores were assigned based on the amount of hair lost by the animal. Tissues were collected and snap frozen in liquid nitrogen or placed in formalin for histology. Tissues for histology were processed, paraffin-embedded, and sectioned at 4 µm prior to being stained for Masson’s Trichrome following the manufacturer’s protocol. Brightfield microscopy at 10x was performed and images were quantified using Fiji/ImageJ. Total hair loss scores at the time were attributed to the amount of hair lost by the animal. **Results:** Significant increased hair loss was observed in our female low DSD group and all male and female DEP+DSD exposure groups. Interestingly, the hair loss pattern differed between our male and female animals. While throat hair loss occurred in both our male and female exposure groups and further progressed to the abdomen area in some animals, facial and head hair loss was exhibited in several of the female mice also exhibited hair loss on their face and heads albeit not statistical. Therefore, we investigated collagen deposition via Masson’s Trichrome staining. Significant alterations were observed within nearly all of our exposure groups. **Conclusions:** While significant hair loss was mostly observed with the DEP+DSD exposure groups, alterations in collagen deposition were much more widespread. Limited investigation has been performed to explore the potential mechanisms associated with hair loss in response to inhaled PM. Therefore, further investigation and analysis are currently underway to analyze potential morphological changes and investigate molecular endpoints of interest.

ABSTRACT NUMBER: 5105 **Poster Board Number:** J657
TITLE: Airborne Ultrafine Particulate Matter Compromises Bone Health: Potential Consequences for Fetal Skeletal Development

AUTHORS (FIRST INITIAL, LAST NAME) AND INSTITUTIONS: K. Khanal, *M. Vera-Colon*, *N. Sparks*, *M. Kleinman*, *A. Vizcaya-Ruiz*, and *D. Herman*. University of California, Irvine, Irvine, CA.
KEYWORDS: Environmental Toxicology; Particulates; Toxicity; Chronic

ABSTRACT: Background and Purpose: Air pollution remains one of the most pressing global public health challenges, including fine and ultrafine particulate matter (PM) contributing to approximately 4.2 million premature deaths annually, primarily from cardiovascular and respiratory diseases. Ultrafine particles (PM0.15) are especially hazardous due to their ability to penetrate deep into the lungs, translocate into systemic circulation, and reach distant organs. Their high surface area and reactive chemical composition enable them to induce oxidative stress, systemic inflammation, and endothelial dysfunction. While most research on PM toxicity has focused on the cardiopulmonary system, emerging evidence links PM exposure to adverse effects on bone health. Chronic exposure to ambient PM has been associated with reduced bone mineral density and increased fracture risk in humans. However, the skeletal effects of ultrafine PM remain poorly characterized, particularly regarding its mechanistic interactions with metabolism, inflammation, and osteoclast activation, key processes in bone remodeling. **Methods:** This study focuses on elucidating the impacts of ultrafine PM on bone mineralization,bone structure, mitochondrial dysfunction, and osteoclast activity, aiming to uncover how chronic exposure disrupts bone homeostasis at both structural and cellular levels. This project investigates how chronic exposure to ambient PM0.15 affects bone integrity in genetically susceptible mouse models ($LDL^{-}/^{-}$ and $ApoE^{-}/^{-}$) under different dietary conditions. **Results:** Early results suggest that PM exposure, especially when combined with a high-fat diet, promotes bone marrow adiposity, trabecular bone loss, and inflammatory infiltration, findings that may mirror the combined effects of environmental and metabolic stressors in humans. These studies in adult mice serve as a proof of concept that PM targets bone and will provide the foundation for future mechanistic investigations into how PM exposure affects fetal bone development. **Conclusions:** We hypothesize that exposure to PM0.15 disrupts bone homeostasis through mechanisms involving oxidative stress, mitochondrial dysfunction, inflammation, and osteoclast activation, with greater effects in metabolically susceptible ($LDL^{-}/^{-}$ and $ApoE^{-}/^{-}$) models and under high-fat dietary conditions.

ABSTRACT NUMBER: 5106 **Poster Board Number:** J658
TITLE: Diesel Exhaust Particulate and/or Desert Sand Dust Promote Alterations in Lungs of Male and Female C57Bl/6 Mice

AUTHORS (FIRST INITIAL, LAST NAME) AND INSTITUTIONS: J. David-West, and *L. J. Schneider*. Defense Centers for Public Health - Aberdeen, APG, MD.
KEYWORDS: Exposure, Environmental; Inhalation Toxicology; Lung; Pulmonary or Respiratory System

ABSTRACT: Background and Purpose: Military missions often dictate deployment of service members to austere environments that result in exposures to airborne particulate matter (PM), such as diesel exhaust particulate (DEP) and/or desert sand dust (DSD), at concentrations exceeding the exposure levels of the average population. These exposures have been correlated to detrimental health outcomes such as respiratory, cardiovascular, and neurological diseases. Additionally, data supports that service

members with combat deployments are 24-30% more likely to be diagnosed with asthma than their non-deploying counterparts. Previous studies have demonstrated a significant shift within the bacterial phyla of the lung microbiome in response to DEP exposures. Recent studies have demonstrated a correlation between lung microbiome profiles and lung diseases. **Methods:** 7-8-week-old male and female C57Bl/6 mice were exposed via nasal instillation to low, medium, or high doses of DEP, DSD, or a combination of DEP+DSD suspended in saline or saline (control) twice per week for a period of 60-days. Mice were sacrificed 14-16 hours after the last exposure by euthanizing with Euthasol (100 µL per mouse) followed by exsanguination. Tissues were harvested and either immediately snap frozen in liquid nitrogen or placed in formalin for histology. Histology tissues were processed, paraffin-embedded, and sectioned at 4 µm. Histological staining was performed for Masson's Trichrome following manufacturer's protocol contained in the staining kit. Brightfield microscopy was performed at 10x and images were quantified using Fiji/ImageJ. Bronchioalveolar lavage fluid was collected, centrifuged at 6,000 xg for 30 minutes at 4°C. Samples were immediately removed from the centrifuge, supernatant was removed, and the remaining pellet was stored at -80°C for microbiome profiling. **Results:** When compared to controls or DEP only exposure groups, several of our DSD and DEP+DSD exposure groups exhibited increased lung weights within our male mice; however, no significant lung weight difference was observed between the exposure groups of our female mice. Additionally, preliminary data shows a significant increase in fibrosis with the lungs of our study animals in response to DEP and/or DSD exposure. However, interestingly, the fibrosis quantitated by histology within the lungs of our female mice appears to be significantly less than that of males within the same exposure groups. **Conclusions:** The development of fibrosis is common in the pathogenesis of chronic lung diseases. Given the lung weight differences and fibrotic changes observed with our animals, it is likely that the differences in lung weight are attributed to the increased fibrosis deposition. Further investigation is currently underway to characterize the extra cellular matrix composition, analyze morphological changes within the lungs, and perform microbiome profiling to assess potential changes attributed to DEP and/or DSD inhalation exposure.

ABSTRACT NUMBER: 5107 **Poster Board Number:** J659

TITLE: $Pm_{2.5}$ exposure induces concentration-dependent calcium signaling in human airway smooth muscle cells

AUTHORS (FIRST INITIAL, LAST NAME) AND INSTITUTIONS: *M. Cage*[1], T. Rich[1], T. Stevens[1], N. Annamdevula[1], A. Britain[1], R. Penn[2], and D. Deshpande[2]. [1]University of South Alabama Whiddon School of Medicine, Mobile, AL; and [2]Thomas Jefferson University, Philadelphia, PA.

KEYWORDS: Lung; Pulmonary or Respiratory System; Particulates; PM2.5

ABSTRACT: Background and Purpose: Fine particulate matter ($PM_{2.5}$) exposure is a major environmental health concern associated with increased respiratory morbidity and mortality. Airway smooth muscle cell dysfunction plays a critical role in $PM_{2.5}$-induced airway hyperresponsiveness and bronchoconstriction. Intracellular calcium signaling is a notable mechanism regulating smooth muscle contraction, proliferation, and inflammatory responses. Recent evidence suggests $PM_{2.5}$ may disrupt calcium homeostasis through activation of transient receptor potential (TRP) channels and calcium release pathways. However, the direct concentration-response relationship between $PM_{2.5}$ exposure and calcium signaling in human airway smooth muscle cells remains poorly understood. This studies investigated whether $PM_{2.5}$ exposure triggers intracellular calcium responses in human airway smooth

muscle cells and characterized the concentration-response relationship. **Methods:** Human ASM cells were isolated from healthy donor lung tissue and cultured in F-12 ASM growth media. Cells were grown to confluency, sub-cultured into six-well dishes, and serum-starved for 24 hours. Cells were exposed to $PM_{2.5}$ (8-110 µg/ml) for 24 hours or monitored in real-time for 30 minutes using hyperspectral imaging. Average in intracellular calcium levels relative to control quantified concentration-dependent effects. **Results:** $PM_{2.5}$ exposure induced concentration-dependent increases in intracellular calcium in HASM cells. Control cells (0 µg/ml) maintained baseline calcium levels throughout the 30-minute observation period. The calcium response exhibited sustained elevation throughout the monitoring period, indicating persistent calcium dysregulation rather than transient signaling. **Conclusions:** $PM_{2.5}$ triggers concentration-dependent calcium signaling in ASM cells, which may contribute to hypercontractility and airway hyperresponsiveness. The concentration-response relationship identified in this study supports the biological plausibility of $PM_{2.5}$-induced respiratory effects at environmentally relevant exposure levels. These findings advance our understanding of the cellular mechanisms underlying $PM_{2.5}$-induced respiratory toxicity and identify calcium signaling as a potential therapeutic target for mitigating adverse respiratory effects of particulate air pollution. Future studies should explore specific calcium channels and pathways involved. NIH R01HL169522

ABSTRACT NUMBER: 5108 **Poster Board Number:** J660
TITLE: Unrecognized Domestic PFAS Exposures: Targeted Quantification in Common Household Cleaners

AUTHORS (FIRST INITIAL, LAST NAME) AND INSTITUTIONS: J. R. Walker, I. C. Sunday, D. Chen, *A. M. Kadry*, and Y. J. Tong. Georgetown University, Washington, DC.
KEYWORDS: Perfluoronated Agents; Exposure Assessment; Exposure, Environmental

ABSTRACT: Background and Purpose: Per- and polyfluoroalkyl substances (PFAS) are a broad class of synthetic chemicals with extensive environmental contamination and extreme persistence, contributing to their reputation as “forever chemicals”. PFAS present a significant public health concern with the increasing knowledge of widespread contamination coupled with a growing understanding of the toxicological risks to human and ecological health. Cleaning products have become an important and ubiquitous exposure route in American households, particularly following increased use during the COVID-19 pandemic. Reports have documented the presence of per- and polyfluoroalkyl substances (PFAS) in certain cleaning products, but the risks associated with these exposures remain unclear due to limited hazard quantification. Researchers have demonstrated challenges with quantifying PFAS in solvent-heavy, non-aqueous cleaner matrices, including limited extraction efficiency and coelution in the liquid chromatography column. **Methods:** This study prioritized targeted PFAS quantification in abrasive, acidic, alkaline, degreaser, and detergent cleaning formulations using a workflow adapted from EPA Method 1633A: “Analysis of Per- and Polyfluoroalkyl Substances (PFAS) in Aqueous, Solid, Biosolids, and Tissue Samples by LC-MS/MS”. An Agilent 1260 Infinity II Liquid Chromatograph was operated in tandem with an Agilent Ultivo Triple Quadrupole Mass Spectrometer to measure concentrations to the part-per-trillion (ppt) level for 30 targeted PFAS compounds within five representative pilot samples: abrasive Bar Keepers Friend Cleanser Powder, detergent Dawn Platinum Dishwashing Foam Fresh Rapids, degreaser Lysol Kitchen Pro Daily Cleaner, acidic OxiClean Daily Clean Multi-Purpose Disinfectant, and alkaline Windex Crystal Rain Scent Ammonia-Free Glass Cleaner Spray. An optimized solid-phase extraction process was used for the four liquid samples prior to analysis, while the Bar Keepers Friend powder required alkaline extraction, two sonication and centrifugation cycles, and a graphitized carbon cleanup

prior to PFAS extraction with weak anionic exchange sorbent cartridges. **Results:** PFAS were detected in all five of the pilot samples. Of the 30 target PFAS compounds, 11 were quantified with 95% confidence intervals above 0 ppt in specific formulations. The Bar Keepers Friend sample contained the most PFAS with non-zero concentrations (8), followed by Lysol (6) and Dawn (5). 8:2 FTSA and PFBA were detected with non-zero concentrations across all five formulations, while the highest average concentration detected was HFPO-DA in the Dawn sample at 518.904 - 1239.091 ppt. **Conclusions:** This study found that an LC-MS/MS workflow adapted from EPA Method 1633A can be used for targeted quantification of PFAS in non-aqueous household cleaning formulations. Expanded sampling will enable PFAS profile comparison across brands, prices, geographic regions, ingredients, and labels. PFAS profiles within cleaning samples can be used to develop dermal and inhalation exposure models based on residential use scenarios.

ABSTRACT NUMBER: 5109 **Poster Board Number:** J661

TITLE: Thermal Degradation Products and Emission Profiles of Commercial Fluorine-Free Firefighting Foams (FFF)

AUTHORS (FIRST INITIAL, LAST NAME) AND INSTITUTIONS: *D. Bello*, *K. Biswas*, *S. Bhandari*, C. S. Sahabanduge, P. Liu, and A. Bello. University of Massachusetts Lowell, Lowell, MA.

KEYWORDS: Chemical Characterization; Perfluoronated Agents; Persistent Organic Chemicals; Fluorine-free foams, Thermal Decomposition Product

ABSTRACT: Background and Purpose: Per- and polyfluoroalkyl substances (PFAS) pose significant environmental and human health risks. Aqueous film-forming foams (AFFF), historically used in firefighting and a major source of PFAS contamination, are increasingly being replaced by fluorine-free firefighting foams (FFF). However, many FFF formulations have been introduced into the market with limited understanding of their chemical composition and toxicological properties, especially concerning their thermal degradation products (TDPs) and performance under fire-relevant conditions. This study aimed to characterize the chemical composition of commercially available FFFs and to evaluate their thermal degradation profiles and emission characteristics. **Methods:** The study utilized an experimental platform to analyze the thermal degradation and physicochemical behavior of FFFs under controlled conditions. Twenty-two commercially available FFF products were analyzed for PFAS (both targeted and untargeted screening) and other matrix components. Seven well-characterized FFFs were combusted from 25°C to 800°C (10°C/min) in an oxygen-rich atmosphere (21%). Emissions—including nano-aerosols, volatile organic compounds (VOCs), aldehydes, toxic gases (CO, SO_2, NO), and reactive oxygen species (ROS)—were quantified using a suite of analytical instruments. Foam formulations, freshly generated aerosols, and one-hour-aged aerosols were also evaluated and compared. **Results:** Targeted analysis detected PFAS in 5 of 22 foams (0.04-0.5 ppm), while untargeted analysis detected 3-5 PFAS in 21 FFFs, with one formulation remaining PFAS-free across all analyses. TOF concentrations exceeded 40 ppm in five FFFs, with 82% of samples ranging from 0.05 to 262 ppm. Thermal degradation produced nanoscale aerosols with median particle sizes of 13-90 nm. Ten of twelve aldehydes were consistently detected across all combusted FFFs, with formaldehyde, acetaldehyde, and acetone being most abundant. Combustion also released toxic gases, including CO, SO_2, and NO, while HF and ROS were not detected. Additionally, 14 matrix components, including surfactants, corrosion inhibitors, and antimicrobial agents, were quantified in both bulk foam and aerosol phases. **Conclusions:** While FFFs are marketed as PFAS-free, most tested products contained trace PFAS, likely due to supply chain

contamination, though intentional addition is suspected in at least five cases. Thermal degradation of FFFs generates substantial concentrations of nanoscale aerosols, aldehydes, and toxic gases. While FFFs represent a safer alternative to conventional AFFF by reducing fluorine exposure, these data suggest that "safer" does not equate to "safe," as the thermal degradation products pose their own distinct inhalation hazards.

ABSTRACT NUMBER: 5110 **Poster Board Number:** J662
TITLE: Compound-Specific Evidence of PFAS-Related Immunotoxicity: A Systematic Review

AUTHORS (FIRST INITIAL, LAST NAME) AND INSTITUTIONS: *D. Lauer*[1], *H. Lynch*[2], V. Whitman[3], *J. Kozal*[4], and M. Wilming[5]. [1]Integral, Inc., Boulder, CO; [2]Integral, Inc., Boston, MA; [3]Integral, Inc., New York, NY; [4]Integral, Inc., San Francisco, CA; and [5]Integral, Inc., Boise, ID.
KEYWORDS: Chemical Hazard Assessment; Immunotoxicity; Perfluoronated Agents

ABSTRACT: Background and Purpose: In 2024, EPA promulgated a drinking water standard value of 4 ppt for PFOA based on the co-critical effects of immune, developmental, cardiovascular, and hepatic endpoints observed in epidemiological studies. However, uncertainties remain about whether the epidemiological data addressing immune responses in children following routine vaccinations is appropriate for deriving quantitative health guidance values. Further, the available literature on immunosuppression has generally focused on the legacy PFAS compounds such that the evidence base for other PFAS compounds has not been sufficiently assessed. The primary objective of this assessment was to evaluate and integrate three key lines of evidence for individual PFAS compounds and immunosuppression. **Methods:** A comprehensive literature review was conducted to identify relevant epidemiological, toxicological, and *in vitro* evidence investigating immune related responses associated with exposure to 14 PFAS compounds. Inclusion and exclusion criteria were developed for each line of evidence based on specific study design considerations. Each study was elevated for methodological rigor and study quality based on EPA criteria. Consistent with systematic review methods, data for each line of evidence was synthesized for PFAS compounds. When adequate data was available, evidence streams were integrated to arrive at an overall weight of evidence determination for compound-specific associations and potential immunotoxicity. **Results:** In general, an adequate evidence base was identified for PFOA, PFOS, PFNA, PFDA, and PFHxS. Studies assessing the potential association between other PFAS and immune outcomes were too limited for reliable determinations. At high test doses exceeding human-relevant exposure levels and associated with systemic toxicity, rodent data shows that some PFAS (most consistently PFOA and PFOS) reduce antibody response to antigen challenges. In epidemiological studies of children with near background PFAS levels, some statistically significant associations are observed between PFAS serum levels and decreases in antigen-specific antibodies. Critically, inconsistencies are observed across antigens and time period assessed, and these subclinical changes in antibody concentrations were not associated with clear risks of infectious disease morbidity in children or adults. Mechanistic evidence is insufficient across all PFAS evaluated to confidently determine a MOA for potential immunosuppressive outcomes, although *in vitro* data is suggestive of effects that may be partly mediated by the PPAR-alpha pathway, which could explain species-specific responses for some PFAS. Limited data and mixed evidence for many short-chain PFAS and some long-chain PFAS precluded any confident determinations regarding immunotoxicity. **Conclusions:** Considering the lack of consistency across epidemiological studies and across antigens, as well as the uncertainties in

the clinical relevance of reported associations, immune endpoints – particularly from epidemiology studies – may not be sufficiently robust for quantitative toxicity assessment of PFAS.

ABSTRACT NUMBER: 5111 **Poster Board Number:** J663
TITLE: Stayclean™ Qsight lc-ms/ms for analysis of pfas in surface water/wastewater using automated spe based on epa method 1633

AUTHORS (FIRST INITIAL, LAST NAME) AND INSTITUTIONS: S. Cai, and J. Jalali. PerkinElmer US LLC, Shelton, CT. Sponsor: S. Cai, Society of Environmental Toxicology and Chemistry
KEYWORDS: Persistent Organic Chemicals; Perfluoronated Agents; PFAS; PFAS

ABSTRACT: Background and Purpose: PFAS have been classified as persistent organic pollutants and have become the current hot topics around the world due to their unique chemical properties, long-term persistence in environment, and associated risks for human health. Since surface waters are the primary sources of drinking water in many areas around the world, there have been many studies on PFAS exposure in these water resources and the PFAS concentrations were found in the range from low ng/L to µg/L levels. In this study, seven surface water samples collected in Toronto Lake shore area (Lake Ontario, Humber Bay River, Mimico Creek, and Grenadier Pond) and eight wastewater samples from Ontario, Canada were analyzed using automated SPE and QSight LC-MS/MS. **Methods:** Analysis of PFAS was performed on an QSight® 420 UHPLC-MS/MS system. Column separation was achieved by using a Brownlee™ SPP C18 column and a delay column installed between LC pump and the autosampler. The details of the column separation gradient elution program and the optimized MS source parameters will be presented. The instrument was calibrated with at least 6 levels of calibration standards by an internal calibration method. Data were acquired in MRM mode. All samples were prepared by following EPA method 1633 and an automated SPE system was used for sample cleanup and PFAS concentration. The stacked GCB/WAX cartridges were used instead of carbon cleanup, both cutting downs sample prep time and decreasing the chance of recovery losses. **Results:** In this study, a highly sensitive LC-MS/MS method for PFAS analysis was developed using QSight 420 system. Combined with an automated SPE sample preparation procedure, this method was applied for the determination of 40 PFAS in seven surface water and eight wastewater samples with good recoveries (70 to 130%), precision (RSD<20%, n=3) and sensitivity (LOQ < EPA listed values for all PFAS).The method was validated by spiking three different concentrations of PFAS in one surface water and one wastewater sample matrices, and the recoveries were within the range of 70% to 130%. The method was further validated with a proficiency testing sample and all PFAS results were within the expected ranges. **Conclusions:** All performance criteria of EPA 1633 are met for wastewater and surface water sample analysis, demonstrating equivalency of the workflow used. The method can be applied for real water sample analysis with good precision and accuracy. Moreover, StayClean patented technology allows analysis of dirty samples with almost no instrument cleaning and maintenance.

ABSTRACT NUMBER: 5112 **Poster Board Number:** J664
TITLE: Ph-driven destruction of sulfonated PFAS: mechanistic insights into PFOS and PFHxS defluorination via UV/sulfite treatment

AUTHORS (FIRST INITIAL, LAST NAME) AND INSTITUTIONS: T. Honaker, M. Everitt, R. Patel, C. Weidner, K. O'Malley, D. Chen, *A. Kadry*, and Y. J. Tong. Georgetown University, Washington, DC.
KEYWORDS: Perfluoronated Agents; Hazard Identification/Reduction; Methods/Mechanism; Non-target analysis; PFAS

ABSTRACT: Background and Purpose: Per- and polyfluoroalkyl substances (PFAS) are persistent fluorinated chemicals widely detected in water due to strong carbon-fluorine bonds. Perfluorooctanesulfonic acid (PFOS) and perfluorohexanesulfonic acid (PFHxS) are sulfonated PFAS of concern because of their environmental persistence, mobility, and associations with adverse health outcomes, including developmental, immunological, and carcinogenic effects. Conventional water treatment relies primarily on physical removal and does not destroy PFAS, motivating evaluation of treatment technologies capable of chemically transforming these compounds. **Methods:** This study aimed to identify degradation products and quantify degradation efficiency of PFOS and PFHxS after treatment in a UV/ sulfite system under alkaline conditions. Using a Rayonet Photochemical Reactor (254 nm), PFOS and PFHxS were treated across pH 10-13 with time-resolved sampling. Degradation efficiency was quantified by LC-MS/MS (triple quadrupole) and transformation products were characterized using solid phase extraction followed by non-target LC-TOF-HRMS. **Results:** This study found PFOS degraded >99% and PFHxS >90% under tested conditions, with PFOS degrading faster and showing stronger pH sensitivity in observed rate constants than PFHxS. Non-target analysis showed pH-dependent product distributions: PFOS at pH 12 exhibited broad chain-shortened products (C2-C8) and select fully defluorinated sulfonated products, whereas pH 13 favored larger fragments (dominant C7-range products) with limited progression to fully defluorinated endpoints. PFHxS at pH 12 formed products spanning C2-C6 with a dominant C2 sulfonated product ($C_2H_3F_2SO_3^-$) reflecting ~60% defluorination and accounting for ~55% of PFHxS-related product signal, but no fully defluorinated PFHxS products were detected. **Conclusions:** UV/sulfite treatment under alkaline conditions effectively destroys sulfonated PFAS, achieving >99% degradation of PFOS and >90% degradation of PFHxS. Degradation pathways were strongly pH- and structure-dependent, with PFOS exhibiting deeper defluorination than PFHxS. These findings demonstrate the potential of UV/sulfite treatment for true chemical destruction of persistent PFAS rather than physical removal.

ABSTRACT NUMBER: 5113 **Poster Board Number:** J665
TITLE: Per- and Polyfluoroalkyl Substances (PFAS) Induce Carboplatin Resistance in Human Triple-Negative Breast Cancer Cells

AUTHORS (FIRST INITIAL, LAST NAME) AND INSTITUTIONS: *S. S. Johal*, *D. S. Guzman*, and *M. A. La Merrill*. University of California, Davis, Davis, CA.
KEYWORDS:

ABSTRACT: Background and Purpose: Per- and polyfluoroalkyl substances (PFAS) are highly persistent environmental contaminants. The legacy PFAS perfluorooctanoic acid (PFOA) is classified as carcinogenic to humans (Group 1) by the International Agency for Research on Cancer (IARC) and is also associated with an increased risk of immunotoxicity and endocrine disruption. Regulatory restrictions on PFOA

have driven the introduction of replacement PFAS, including perfluoropentanoic acid (PFPA), hexafluoropropylene oxide trimer acid (HFPO-TA), and hexafluoropropylene oxide tetrameric acid (HFPO-TeA). However, the toxicity profiles of these replacement PFAS remain poorly characterized. Recent evidence suggests that PFOA exposure can interfere with chemotherapy response in gynecological cancers. Yet, whether PFOA or other PFAS influence sensitivity to carboplatin, a common platinum-based chemotherapeutic, in aggressive human triple-negative breast cancer (TNBC), remains largely unexplored. **Methods:** In this study, human TNBC cells were exposed to sub-cytotoxic, biologically active concentrations of PFOA, PFPA, HFPO-TA, or HFPO-TeA. Relative viability was assessed using the CellTiter-Glo luminescence assay, which quantifies intracellular ATP content as a surrogate for metabolically active cells. Cells were subsequently pre-exposed to low-micromolar concentrations of PFOA, PFPA, HFPO-TeA, or HFPO-TA for 48 hours and then treated with carboplatin at its IC50 for an additional 48 hours. **Results:** None of the tested PFAS significantly altered relative viability when administered alone at low-micromolar concentrations compared to PFAS-negative controls. However, low micromolar pre-exposure of HFPO-TA and HFPO-TeA to TNBC cells significantly increased relative proliferation following carboplatin treatment compared to carboplatin-only controls ($p<0.05$). In contrast, PFPA and PFOA did not significantly alter carboplatin response at any concentration tested. **Conclusions:** These findings suggest that low-micromolar exposures of HFPO-TA and HFPO-TeA induce a significant reduction in carboplatin efficacy on human TNBC cells. These concentrations fall within the low-micromolar range reported to elicit endocrine and immune-related biological activity in independent experimental studies, including human estrogen receptor-β binding by HFPO-TeA and suppression of RAG1 and RAG2 expression by HFPO-TA in human immune cells. This raises significant public health concerns as exposure to replacement PFAS continues to rise and may have implications for chemotherapy treatment in exposed populations. Ongoing transcriptomic analysis will investigate the molecular pathways potentially underlying HFPO-TA and HFPO-TeA associated modulation of carboplatin response.

ABSTRACT NUMBER: 5114 **Poster Board Number:** J666
TITLE: Matrix-specific patterns of PFAS exposure in African savanna elephants

AUTHORS (FIRST INITIAL, LAST NAME) AND INSTITUTIONS: D. E. Chusyd[1], Y. Essandoh[1], K. Kalande[2], L. Chisaka[2], I. Ngombwa[3], M. Wasserman[1], and M. Venier[1]. [1]Indiana University-Bloomington, Bloomington, IN; [2]Game Rangers International, Lusaka, Zambia; and [3]Zambia's Department of National Parks and Wildlife, Chilanga, Zambia. Sponsor: D. Chusyd, Society of Environmental Toxicology and Chemistry
KEYWORDS: Wildlife Biology

ABSTRACT: Background and Purpose: Per- and polyfluoroalkyl substances (PFAS) are persistent environmental contaminants of global concern, yet data on PFAS exposure in large terrestrial wildlife in Africa remain extremely limited. **Methods:** This study investigated PFAS occurrence, concentration, and composition in paired serum and fecal samples collected from African savanna elephants (*Loxodonta africana*) in Kafue National Park, Zambia to evaluate matrix-specific exposure patterns and elimination pathways. Twenty-four PFAS compounds were quantified in serum (n = 21) and fecal (n = 15) samples using liquid chromatography tandem mass spectrometry (LC-MS/MS). **Results:** Total median $\sum_{24}$PFAS concentrations were 0.36 ng/mL in serum and 4.96 ng/g in feces, indicating substantially higher PFAS burdens in fecal material compared to circulating blood. In serum, the most abundant compounds with detection frequencies >50% were PFOS, PFNA, PFDA, and PFHxDA, reflecting dominance of long-chain

PFAS commonly associated with bioaccumulation. In contrast, fecal samples were dominated by PFBS, PFHxDA, PFHpA, and PFNA, suggesting preferential excretion of certain short-chain and mobile PFAS. Chain-length analysis further highlighted matrix-dependent patterns. In serum, long-chain PFAS (0.23 ng/mL) slightly exceeded short-chain PFAS (0.20 ng/mL), consistent with retention of longer-chain compounds in biological tissues. Conversely, fecal samples were dominated by short-chain PFAS (3.94 ng/g), with substantially lower contributions from long-chain PFAS (0.68 ng/g), indicating fecal elimination as an important pathway for short-chain PFAS in elephants. **Conclusions:** These findings provide some of the first PFAS data for African savanna elephants and demonstrate clear differences in PFAS profiles between serum and feces. The results reflect the value of non-invasive fecal sampling for monitoring PFAS exposure in large, protected wildlife species and understanding PFAS exposure pathways in African ecosystems.

ABSTRACT NUMBER: 5115 **Poster Board Number:** J667

TITLE: Divergent Transcriptome Signatures in Human Placental and Umbilical Cord tissues associated with Maternal Exposure to Per- and Polyfluoroalkyl Substances

AUTHORS (FIRST INITIAL, LAST NAME) AND INSTITUTIONS: *S. Thangaraj*, *M. Li*, *K. Wang*, *J. Goodrich*, *K. Bakulski*, M. Sartor, and *V. Padmanabhan*. University of Michigan, Ann Arbor, MI.

KEYWORDS: Perfluoronated Agents; Reproductive and Developmental Toxicology; Gene Expression/Regulation; Placental and cord tissue

ABSTRACT: Background and Purpose: Prenatal exposure to endocrine-disrupting environmental chemicals, such as per- and polyfluoroalkyl substances (PFAS), may program adverse health outcomes in offspring. PFAS is prevalent in some cosmetics, non-stick cookware, fast-food packaging, waterproof clothing, cleaning supplies and single-use plastics. Maternal PFAS-exposure is linked to gestational diabetes, pre-eclampsia and placental lipid dysfunction, which negatively impacts fetal development. Accordingly, epidemiological studies have demonstrated associations between maternal PFAS levels and decreased birthweight, reduced birth length, shortened gestational duration, small for gestational age neonates, and early indicators of adult obesity in girls. Animal studies have demonstrated that PFAS chemicals accumulate in the placenta and fetal organs, disrupt placental function, alter lipid metabolism, and induce oxidative stress, which are all factors detrimental to fetal development. Despite the well-established adverse health effects of PFAS on maternal and child health, the underlying molecular mechanisms driving these outcomes are largely unknown. Understanding these mechanisms requires a closer look at the unique biology of gestational tissues. The placental and umbilical cord, shaped by different developmental trajectories, possess unique characteristics stemming from their separate germinal origins and cell fates. As a result, these tissues are expected to exhibit distinct transcriptomic responses to PFAS exposure; however, direct comparisons of their transcriptomic profiles in this context are not yet available. This exploratory omics study addresses a critical knowledge gap by examining transcriptomic alterations in placental and umbilical cord tissues associated with maternal PFAS exposure, with a focus on understanding their implications for neonatal health. **Methods:** RNA was extracted from matched, term placental and cord tissue samples (n=57) collected between 2010 to 2015 from the Michigan Mother-Infant Pair cohort. Transcriptomic profiling was performed using paired-end RNA sequencing of rRNA-depleted total RNA. First trimester maternal plasma samples were analyzed for nine PFAS chemicals using high-performance liquid chromatography-isotope dilution tandem mass spectrometry. Differentially expressed genes (DEG) were identified using Limma, adjusting for neonate

sex, parity, smoking status, maternal body mass index (BMI) and top three surrogate variables. For each PFAS chemical, expression models were run separately and in an additive model, with PFAS exposure dichotomized (high/low) at the median. Genes with adjusted p<0.05 and log fold change >0.5 were considered DEG. The bioconductor R package ClusterProfiler was used for pathway enrichment analysis. **Results:** The study participants had a mean age of 32.8 ± 3.83 years and a pre-pregnancy BMI of 26.1 ± 5.38. Among the participants, 30 delivered male infants, and 27 delivered female infants. Among the measured PFAS chemicals, PFOS showed the highest mean concentration (6.05 ± 2.78 ng/mL), followed by PFHxS (1.47 ± 1.05 ng/mL). Transcriptomic profiling revealed 1163 DEG between placental and cord tissues. The DEG in placental and cord tissues in response to maternal PFAS exposure differed between the two tissues. In the placenta DEGs were identified for PFHxS (n= 406), PFNA (n= 443) and PFOS (n= 2031). In cord tissue DEGs were identified for PFNA (n= 493), PFOA (n= 1325) and PFOS (847). The top enriched gene ontology terms among DEG in placenta were related to the regulation of cellular secretion, protein localization, apoptotic process and protein maturation, while the top enriched terms among cord were related to regulation of anatomical structure, molecular function, signal release and monoatomic cation homeostasis. Both placental and cord tissue DEG were enriched for terms related to vesicle mediated transport and activation of immune response. **Conclusions:** Findings from this study highlight the distinctive transcriptomic profiles of placental and cord tissues. The tissue-specific transcriptomic signature relative to different maternal PFAS exposures highlights the varied mechanisms by which PFAS may impair gestational tissue function and ultimately influence fetal development. Together, these findings stress the need for considering multiple gestational tissues to fully characterize the impact of environmental exposures on neonatal health.

ABSTRACT NUMBER: 5116 **Poster Board Number:** J668

TITLE: Perfluoroalkyl Acids and Related Compounds Induce Orphan Nuclear Receptor 4A1 (NR4A1)-Dependent Cancer Cell and Tumor Growth

AUTHORS (FIRST INITIAL, LAST NAME) AND INSTITUTIONS: A. Hailemariam, S. Upadhyay, V. Srivastava, W. T. Tsui, and *S. Safe*. Texas A&M University, College Station, TX.

KEYWORDS:; PFAS, perfluoroalkyl acids, cancer, proliferation

ABSTRACT: Background and Purpose: Polyfluoroalkyl substances (PFAS) represent a class of industrial chemicals that are ubiquitous environmental pollutants, permeating nearly all ecosystems worldwide at multiple trophic levels—from aquatic and terrestrial fauna to human populations. Humans are exposed to PFAS from aquatic contamination, municipal water treatment facilities, and defense installations across the United States, and in some locations, PFAS concentrations that exceed safety thresholds established by U.S. regulatory bodies. Epidemiological studies demonstrate a positive association between elevated PFAS levels in human biological samples and the development of numerous pathological conditions, encompassing both malignant and non-malignant disease states. The pathological mechanisms underlying some PFAS-related health consequences involve the activation or dysregulation of the orphan nuclear receptor 4A1 (NR4A1), suggesting that NR4A1 may serve as a key molecular target through which specific PFAS compounds—such as linear perfluorooctanoic acid (PFOA) and related perfluorinated carboxylic acids—exert their toxic effects on human health. **Methods:** Direct interactions between PFAS compounds and the NR4A1 receptor protein were determined using a fluorescence assay to assess the quenching of tryptophan (Trp) residue fluorescence within the ligand binding domain (LBD) of NR4A1. Cell viability was quantified through a resazurin reduction assay, which

measures the metabolic conversion of resazurin to its fluorescent product resorufin as an indicator of cellular metabolic activity. Cell migratory capacity was evaluated using scratch-wound (wound healing) assays, while cellular invasive potential was assessed through Boyden chamber (transwell) assays. Western blotting analysis of protein extracts derived from both cultured cells and tumor tissues was conducted to determine the effects of PFAS exposure on genes that are transcriptionally controlled by NR4A1. **Results:** The results show that PFOA and its structural analogues on NR4A1-responsive gene on Rh30 rhabdomyosarcoma cell bound the ligand-binding domain of NR4A1, with dissociation constants (K_D) falling within the low micromolar concentration range. Among the perfluoroalkyl acids, the K_D values for the hexa-, octa-, and nona- were 1.04, 2.41, and 2.06 µmol/L, respectively. These compounds enhanced the proliferation of Rh30 and other human cancer cell lines. In NR4A1-responsive rhabdomyosarcoma Rh30 cells, PFOA enhanced cell proliferation was NR4A1-dependent, as evidenced by significantly decreased proliferation in NR4A1-deficient Rh30 cells. Comparable NR4A1-dependent proliferative effects were similarly observed following treatment with other NR4A1-active perfluoroalkyl acids. Furthermore, PFOA upregulated the expression of multiple NR4A1-regulated gene products, including the PAX3-FOX01 fusion oncogene and the histone methyltransferase G9a in Rh30 cells, indicating activation of transcriptional programs associated with cellular transformation and epigenetic remodeling. **Conclusions:** This study demonstrates that PFOA binds NR4A1 and functions as an NR4A1 agonist, promoting tumorigenic processes by activating this receptor. The results show that interactions of PFOA and related compounds with NR4A1 enhance cancer cell growth and migration, and this correlates with human observations associating increased cancer risk with higher levels of human exposure to PFAS. Ongoing studies show that some perfluoroalkyl acid-induced toxicities are also NR4A1-dependent, suggesting that this receptor may be an important intracellular target for PFAS.

ABSTRACT NUMBER: 5117 **Poster Board Number:** J669

TITLE: Per- and polyfluoroalkyl substances (PFAS) exposure and adolescent bone mineral density: extracellular vesicles (EVs) as potential mediators

AUTHORS (FIRST INITIAL, LAST NAME) AND INSTITUTIONS: K. Malone[1], A. Spring[1], C. Seifert[1], A. Mordant[1], L. Herring[1], J. M. Braun[2], K. Yolton[3], K. Cecil[3], J. P. Buckley[1], and *J. E. Rager*[1]. [1]The University of North Carolina at Chapel Hill, Chapel Hill, NC; [2]Brown University, Providence, RI; and [3]University of Cincinnati, Cincinnati, OH.

KEYWORDS: Perfluoronated Agents; Proteomics

ABSTRACT: Background and Purpose: Bone mineral accrual during adolescence is a critical determinant of lifelong bone health. While healthy bone development is influenced by lifestyle, diet, and behavior, there is increasing evidence thatenvironmental exposures, including per- and polyfluoroalkyl substances (PFAS), may impair bone mineral accrual. Extracellular vesicles (EVs) have a role in mediating bone remodeling pathways, and previousresearch has found that *in vitro* EV expression and cargo are altered by PFAS exposure, suggesting that EVs may be a mediator between PFAS exposure and adverse bone health outcomes. The goal of this pilot study is to evaluate the role of EVs in the relationship between PFAS exposure and bone mineral density (BMD) in adolescence. **Methods:** We conducted a proteomics analysis of EV-enriched blood serum samples collected from 40 adolescents in the Health Outcomes and Measures of the Environment (HOME) Study at the 12-year follow-up. We selected 40 participants based on the highest or lowest summed serum PFAS concentrations (PFHxS, PFNA, PFOA, PFOS) at the 12-year follow-up, separately for males and females (n=10 per group). Serum concentrations of PFAS

were compared with height-adjusted, age- and sex-standardized BMD Z-scores assessed by dual energy X-ray absorptiometry at six skeletal sites. Blood serum EVs were extracted using Mag-Net EV enrichment, and EV proteomic signatures were measured using LC-MS/MS. Differential protein expression was assessed with linear models adjusting for covariates using the limma R package. **Results:** Summed PFAS concentrations ranged from 7.9 - 17.8 ng/mL in the high PFAS group and from 1.7 - 3.7 ng/mL in the low PFAS group. Covariate-adjusted BMD Z-scores at several skeletal sites differed byPFAS group; for example, ultradistal radius BMD Z-scores were significantly lower in the high PFAS group, with a mean of -0.36 (+/- 0.96), compared to 0.08 (+/- 1.02) in the low PFAS group. There were no sex differences in blood PFAS concentration or BMD Z-scores. Proteomic analysis of EV-enriched samples yielded 2,665 total measurable proteins. Of the identified proteins, 1,767 have the gene ontology cellular component term “extracellular”, indicating they may be EV-derived. Principal component analysis and hierarchical clustering both indicated that measured EV protein signatures did not clearly cluster by PFAS group or sex. However, statistical comparisons of EV protein signatures identified 100 proteins at differential levels when comparing participants with high PFAS vs low PFAS concentrations ($|\text{Log2 fold change}| \geq 0.58$, $p < 0.05$). When stratified by sex, there were 71 and 122 differentially abundant proteins in male and female samples, respectively. Of note, collagen alpha-1(I) chain (CO1A1) was less abundant in the high PFAS group compared to the low PFAS group (Log2FC = -0.62, $p < 0.001$). CO1A1 is the most prevalent protein in bone and is necessary for bone matrix formation, so differential abundance in EV-derived CO1A1 indicates a potential bone health regulatory mechanism impacted by PFAS exposure. Other extracellular matrix-related proteins had similar associations with high PFAS exposure, including fibulin-2 (FBLN2) and cartilage intermediate layer protein 1 (CLIP1). Transforming growth factor beta-2 proprotein (TGFB2), an important regulator in bone development and osteoblast differentiation, was found a higher abundance in samples in the low PFAS group compared to the high PFAS group (Log2FC = -0.64, $p < 0.05$). **Conclusions:** This study explores the relationship between PFAS exposure and adolescent BMD and the potential mediating role of EVs. We identified protein candidates that were differentially abundant between EV-enriched blood serum samples with high and low PFAS concentrations, some of which have significant implications for bone remodeling pathways. These results suggest the importance of EVs in PFAS toxicity and inform potential mechanisms of PFAS exposure impacting bone development and remodeling.

ABSTRACT NUMBER: 5118 **Poster Board Number:** J670

TITLE: Characterizing Bioavailable Organic Contaminants in the Lower Columbia River Using Passive Sampling Devices

AUTHORS (FIRST INITIAL, LAST NAME) AND INSTITUTIONS: K. M. Gurfield, L. Tidwell, and K. Anderson. Oregon State University, Corvallis, OR. Sponsor: K. Anderson, Society of Environmental Toxicology and Chemistry

KEYWORDS: Persistent Organic Chemicals; Environmental Fate; Polycyclic Aromatic Hydrocarbons

ABSTRACT: Background and Purpose: The Columbia River is an important resource for hydropower, transportation, recreation, food, and agriculture. As a watershed that spans 250,000 square miles, the health of this ecosystem has wide implications for the animals and people that rely on its resources. The river has recently become a focal point for research, given its history and proximity to heavy industrial activity. To assess the health of the river, this study utilizes passive sampling; for a continuous 365 days, passive sampling devices were deployed to characterize contaminants in the lower 200 miles of the river

to provide valuable insight into the movement of chemicals downriver throughout the course of an entire year. Specifically, this study analyzed and quantified a suite of ~1500 contaminants (PAHs, PCBs, flame retardants, dibenzofurans, pesticides, personal care products, and pharmaceuticals) and quantified their concentrations using GC-MS targeted and suspect methods. Of special interest was the effect of human-altered systems; PSDs were deployed above and below two dam systems and a highly industrialized/urbanized Superfund area located at the confluence of the Columbia and Willamette Rivers. The PSDs only sample the dissolved fraction in the water column, therefore only representing the bioavailable chemicals that pose risks to organism exposure. By identifying specific sites or times of year that show concerning levels of contaminants, the data may be used to inform cleanup efforts and aquatic and human-related toxicological decisions for ongoing restoration and preservation of the river. **Methods:** Low density polyethylene (LDPE) strips (110cm) were fortified with performance reference compounds (PRCs), then deployed at 10 different sites along the lower 200 miles of the Columbia River. One site was located on the Willamette River, a major tributary to the Columbia River. After 30 days, the LDPE water samplers were retrieved, and new PRC fortified LDPE samplers were deployed in the same locations. Retrieved LDPE was quantitatively analyzed using two methods: Targeted analysis for 64 PAHs using GC-MS/MS and suspect analysis for ~1500 compounds using a Multiple Analyte Screening and Deconvolution Software (MASV) via GC-MS. Environmental concentrations were calculated based on dissipation rates of PRCs. Throughout, various quality controls were prepared and analyzed concurrently. **Results:** Data obtained from both the MASV and 64 PAH methods show similar chemical profiles above and below the engineered systems of interest for this study; according to the MASV data, the total number of detections above and below the dams did not vary by more than 20%, indicating that the same species are present regardless of dam activity. The data from the targeted PAH method shows similar results, with the most abundant compounds being conserved across sites: naphthalene (0.574-17.7 ng/L), pyrene (0.153-8.9 ng/L), phenanthrene (0.689-3.8 ng/L), and acenaphthene (0.314-4.13 ng/L). Consistently, the Portland Harbor Superfund sampler, located at River Mile 3.5 of the Willamette River, had the largest concentrations, with concentrations at least double than those at the other sites. It is inconclusive whether the Willamette contributes to increased inputs in the Columbia River. **Conclusions:** This research is part of an ongoing project where field sampling will culminate in the summer of 2026. As such, these results are preliminary and only represent one third of the planned sampling events. While the data does not suggest the influence of dams on the bioavailable fraction of species in the river, some chemicals remained consistent across all sampling events. For example, PAHs and aPAHs, some of which are known suspected carcinogens, were detected in all samples. Further analysis will be conducted to determine the fate of contaminants across temporal and spatial gradients, thereby providing insight into the health of the river and associated ecological and human health risks.

ABSTRACT NUMBER: 5119 **Poster Board Number:** J671

TITLE: Two Decades of Spatial and Temporal Patterns of Alkylated PAHs (APAHs) in Water and Resident Crayfish from a Dynamic Urban Harbor

AUTHORS (FIRST INITIAL, LAST NAME) AND INSTITUTIONS: E. M. Luera, L. G. Tidwell, and K. A. Anderson. Oregon State University, Corvallis, OR. Sponsor: K. Anderson, Society of Environmental Toxicology and Chemistry

KEYWORDS: Polycyclic Aromatic Hydrocarbons; Food Safety; Exposure, Environmental; Alkylated PAHs

ABSTRACT: Background and Purpose: In sites impacted by petroleum contamination, most polycyclic aromatic hydrocarbons (PAHs) are alkylated PAHs (APAHs). In comparison to parent PAHs, APAHs and their isomers differ in both environmental movement and toxicity, with some alkylated derivatives being more toxic. Despite APAHs having unique toxicities and being more environmentally abundant, most toxicological studies on PAHs focus only on the parent compounds. This potentially neglects the true impact of environmentally relevant PAH mixtures. Signal crayfish are a common food source for many communities, including Eastern European and Indigenous populations, and are commonly caught by recreational fishermen. Crayfish can be used as a site-specific biomonitoring organism because of their benthic nature and their ability to accumulate PAHs in their hepatopancreas due to low levels of cytochrome P450, a PAH-metabolizing enzyme. Investigating both parent PAH and APAH accumulation in crayfish can help assess the risks posed by human consumption. Low-density polyethylene passive sampling devices (PSDs) capture the bioavailable fraction of organic contaminants in their environment, providing a time-weighted average concentration that can be used to predict exposure levels for the deployment period. The goals of this project are to assess changes in PAHs and APAHs in Portland Harbor over the last two decades and to develop a model capable of accurately predicting PAH and APAH concentrations in crayfish viscera using PSD concentrations. **Methods:** PSDs were deployed and resident crayfish were collected from several sites within and around the Portland Harbor Superfund Megasite in the years 2003, 2013, and 2023. Crayfish viscera and PSDs are analyzed for 113 APAHs and 48 unsubstituted PAHs with a novel gas chromatography-tandem mass spectrometry method. Spatial and temporal changes in the APAH profile of these sites are investigated over a twenty-year period, during which remediation efforts within the Superfund Megasite and notable urban development throughout the Portland Metro Area have both occurred. A model created in a previous phase of this study predicted crayfish viscera PAH concentrations within 2 times the measured sample; however, that model was created using only 64 PAHs. This study aims to expand on the previous model by incorporating a total of 161 PAHs, investigating a larger number of contaminants to predict exposure more accurately. **Results:** Alkylated PAHs are more abundant and more highly concentrated in crayfish viscera than unsubstituted PAHs. For example, the median C3-Phenanthrene concentration was nearly nine times higher than the parent compound. This profile, with APAHs being more abundant than parents, is typical for petrogenic sources of PAHs. As a result of remediation efforts, overall PAH concentrations of crayfish viscera within the superfund site decreased from 310ng/g in 2003 to 160ng/g in 2013. However, in 2023, visceral sum PAHs returned to nearly those in 2003. Despite similar concentrations, the most abundant PAH species are notably different between 2003 and 2023. For example, retene comprised nearly a quarter of all PAHs found in 2003, but it was not within the top ten most abundant PAHs found in 2023. **Conclusions:** APAHs were often found in concentrations several times higher than the parent PAHs in crayfish viscera, so considering only parent PAHs misrepresents the risks of exposure to real-world mixtures during consumption. The changing PAH profiles at Portland

Harbor from 2003 to 2023 suggest a change in the primary source of contamination. Since the most abundant PAHs can fluctuate over time, it is important to consider a larger suite of both PAHs and APAHs when performing risk assessments to better protect human health.

ABSTRACT NUMBER: 5120 **Poster Board Number:** J672
TITLE: Environmental PCBs and cancer prevalence in two southern municipalities of Puerto Rico: Guanica and Guayama

AUTHORS (FIRST INITIAL, LAST NAME) AND INSTITUTIONS: *B. D. Jiménez-Vélez*[1], K. Torres-Millan[2], D. Arroyo Amparo[3], and A. Ruiz-Quiles[4]. [1]University of Puerto Rico, Medical Sciences Campus, Biochemistry Department, San Juan, PR; [2]University of Puerto Rico at Humacao Campus, Biology Department, Humacao, PR; [3]University of Puerto Rico, Rio Piedras Campus, Biology Department, Rio Piedras, PR; and [4]University of Puerto Rico, Rio Piedras Campus, Physics Department, Rio Piedras, PR.
KEYWORDS: Polychlorinated Biphenyls; Carcinogenesis; Environmental Toxicology; Diabetes; PCB

ABSTRACT: Background and Purpose: Various studies have reported PCB levels in aquatic sediments and fish from two municipalities *(Guánica and Guayama)* in the southern coast of Puerto Rico. We have gathered and analyzed information on environmental PCBs and health factors from these municipalities. One study found very high PCBs levels in the aquatic sediments from Guánica Bay; these were reported as being the second highest concentration in the USA. Hence, after scheduling a sampling program in Guánica, the US Environmental Protection Agency (EPA) designated the area as one of Puerto Rico's superfund sites. The purpose of this study was to closely examine available PCB data (soil concentration, aquatic sediments, fish tissue and biota) and to predict possible health risk and further investigate health outcome at these sites. **Methods:** We examined and compared the PCB concentrations reported in Guánica and in Guayama (Master Thesis from the University of South Florida). In addition, the data reported in a recent study (2025) made by the Graduate School of Public Health from the University of Puerto Rico, Medical Sciences Campus was used to evaluate a series of chronic diseases in Guánica and Maunabo. We proceeded to use data provided by the Puerto Rico Cancer Center to calculate and compare the prevalence of three types of cancer (prostate, breast, and colorectal) in these two municipalities at various time intervals. **Results:** PCB concentrations as high as 129,283 ng/g in Guánica were >100X fold higher than the highest level reported for Guayama, 1,232 ng/g. The average range of PCBs concentration in Guánicas aquatic sediments was353 ng/g (NOAA) vs 59,215 ng/g (U-Miami) (n=20) compared to 4 ng/g (NOAA) vs 218 ng/g (USF) in Guayama (n=61). The PCB concentrations were highest at the eastern boundaries of both estuaries. In addition, elevated concentrations of PCBs were reported in two resident fish species (a pelagic snapper, *Lutjanus analis,* (1,623 ng/g) and a benthic mojarra, *Eucinostomus gula* (3,768 ng/g) from the Guánica Bay. Personal interviews with residents revealed consumption of these fish species in their diet, suggesting transfer of PCBs through the food chain. We identified the 10 most abundant PCB congeners found in these two fish species. Among these are PCB congeners 153/132, 47/48/75, 52, 49 and 180. Some of the congeners identified have been reported to be associated to various diseases such as type two diabetes (T2DM) and cancer. **Conclusions:** The Graduate School of Public Health report attributes a higher prevalence of T2DM in Guánica to be associated with PCBs when compared to the municipality of Maunabo. After evaluating data from the Puerto Rico Cancer Registry, we found that the highest prevalence of cancer in these two municipalities (Guánica) was breast cancer followed by prostate and colorectal cancer. The prevalence of breast cancer has been increasing for the last 21 years (since 2000) in both municipalities. However,

the prevalence of breast cancer has suffered a reduction in the last 5 years in Guayama while it continued to rise in Guánica, exhibiting its greatest difference in the last 5 years (2015–2020). The prevalence of prostate cancer has been consistently high throughout 21 years in Guayama except for the period of 2010-2014 where it was lower than in Guánica. Although the prevalence of colorectal cancer is much lower than the other types of cancers studied, interestingly it is a slightly similar pattern as that seen for breast cancer in Guánica. The data presented here indicates that breast and colorectal cancers are slightly more prevalent in Guánica where environmental PCB levels may be up to 100-fold higher than those found in Guayama. In addition, it is important to expand measurements of other toxic substances such as heavy metals and persistent organic pollutants to better understand and investigate the relationships of environmental health risk factors and be able to predict, remediate and/or prevent the development of acute and chronic diseases at these two municipalities and worldwide.

ABSTRACT NUMBER: 5121 **Poster Board Number:** J673

TITLE: Polyhexamethylene guanidine phosphate exacerbates asthmatic responses in ovalbumin-sensitized murine and human 3D airway models

AUTHORS (FIRST INITIAL, LAST NAME) AND INSTITUTIONS: G. Kim[1], I. Bang[2], J. Lim[1,3], Y. Han[2], and H. Kim[1,3]. [1]College of Pharmacy, Korea University, Sejong-si, Korea, Republic of; [2]Institute of Pharmaceutical Science and Translational Research, Korea University, Sejong-si, Korea, Republic of; and [3]Interdisciplinary Major Program in Innovative Pharmaceutical Sciences, Korea University, Sejong-si, Korea, Republic of.
Sponsor: *K. Lim*

KEYWORDS: Inhalation Toxicology; *In Vivo* Models; *In Vitro* and Alternatives; Asthma; Phmg-p

ABSTRACT: Background and Purpose: Polyhexamethylene guanidine phosphate (PHMG-p), a guanidine-based polymer biocide, was previously incorporated into humidifier disinfectants due to its strong antimicrobial properties. However, recent epidemiological studies reported that PHMG-p increased the risk of asthma. We investigated the effect of PHMG-p on asthmatic responses and immune activation using both murine asthma models and human airway epithelial tissues. **Methods:** In the *in vivo* model, BALB/c mice were sensitized by intraperitoneal injection of ovalbumin (OVA, 20 μg) mixed with aluminum hydroxide (1 mg), followed by intratracheal challenge with OVA (20 μg) and PHMG-p (0.1 or 0.5 μg/ml). The inflammatory cell influx into bronchoalveolar lavage (BAL) fluid, immunoglobulin (Ig) E levels, asthma-related cytokine levels and histological changes in the lung were analyzed. For *in vitro* analysis, MucilAir™ human 3D airway epithelial tissues were exposed to PHMG-p at 0.4 μg/ml or 2 μg/ml for 24 or 96 hours. Transcriptomic profiling was conducted using RNA sequencing to identify differentially expressed genes (DEGs), followed by functional enrichment using Gene Ontology (GO) and KEGG pathway analysis. **Results:** *In vivo*, PHMG-p significantly increased inflammatory cell counts in BAL fluid, Th2 cytokine levels (IL-4, IL-5, IL-13), and IgE levels in the OVA-sensitized mice. Histological changes included airway remodeling with epithelial thickening and inflammatory infiltration. Transcriptomic analysis using the human 3D airway epithelial model revealed substantial gene expression changes after PHMG-p exposure for both 24 and 96 hours. DEG analysis followed by GO and KEGG enrichment indicated that many of the altered genes were associated with Th17-related immune responses. Notably, critical mediators of the IL-17 signaling were significantly upregulated. **Conclusions:** PHMG-p exposure significantly aggravated airway inflammation in both *in vivo* and *in vitro*. Th2 responses were evident *in vivo* while Th17-type expression with IL-17 signaling was observed *in vitro*. These findings suggest that PHMG-p may contribute to airway inflammation and asthma exacerbation via both Th2 and

Th17-related pathways. Further studies are needed to investigate the mechanisms of PHMG-p on asthma exacerbation. This work was supported by Korea Environment Industry & Technology Institute (KEITI) through Technology Development Project for Safety Management of Household Chemical Products Program, funded by the Korea Ministry of Environment (MOE) (project number: 202300230430).

ABSTRACT NUMBER: 5122 **Poster Board Number:** J674
TITLE: Targeting Obesity-Related Asthma With GLP-1 Receptor Agonists

AUTHORS (FIRST INITIAL, LAST NAME) AND INSTITUTIONS: D. R. Gomez[1], L. Franzi[1], A. Linderholm[1], K. Y. Xiang[2], A. A. Zeki[1], and N. J. Kenyon[1]. [1]University of California, Davis, Davis, CA; and [2]University of California, Los Angeles, Los Angeles, CA. Sponsor: D. Gomez, American Association for the Advancement of Science
KEYWORDS: Receptor; G-Protein Coupled; Pulmonary; Glucagon-Like Peptide-1

ABSTRACT: Background and Purpose: Obesity-related asthma is a heterogeneous phenotype associated with severe disease, steroid resistance, and increased healthcare utilization in the United States. Epidemiologic studies demonstrate that individuals with asthma and type 2 diabetes mellitus (T2DM) treated with glucagon-like peptide-1 receptor agonists (GLP-1RAs) experience fewer exacerbations, reduced hospitalizations, and improved symptom control; however, the cellular mechanisms underlying these clinical benefits remain unknown. Our prior work shows that insulin exposure diminishes intracellular cyclic adenosine monophosphate (cAMP) signaling and induces heterologous desensitization of the beta-2-adrenergic receptor (β_2AR) pathway in human airway smooth muscle cells (HASMCs). We hypothesize that GLP-1RAs restore ASM relaxation by activating protein kinase A (PKA) signaling through the GLP-1 receptor via β_2AR-independent mechanisms. **Methods:** To model insulin-induced β_2AR dysfunction, mouse precision-cut lung slices (PCLS) were incubated with insulin and assessed for airway contractility and bronchodilator responsiveness. Methacholine-induced bronchoconstriction was followed by a β_2AR agonist challenge to quantify maximal β_2AR-mediated relaxation. In parallel, HASMCs were treated with GLP-1RAs and isoproterenol (ISO) to monitor real-time downstream signaling. To define signaling convergence, FRET-based cAMP biosensors quantified responses to ISO, Exendin-4, and combined stimulation, with and without pharmacologic GLP-1 receptor blockade. Additionally, methacholine-precontracted PCLS were treated *ex vivo* with Liraglutide alone or in combination with salbutamol to determine maximal bronchodilator capacity. **Results:** Insulin exposure increased airway contractility and reduced β_2AR mediated bronchodilation in mouse precision-cut lung slices, establishing insulin-induced β_2AR dysfunction. To determine whether GLP-1 signaling could bypass this impairment, we examined cAMP-PKA signaling in human airway smooth muscle cells. GLP-1RAs induced robust cAMP-PKA activation comparable to β-agonist stimulation. FRET imaging revealed that GLP-1 receptor activation generated larger cAMP responses than β-agonist activation, and combined GLP-1R and β_2AR stimulation failed to further increase cAMP, indicating convergence on a shared cAMP signaling compartment. Pharmacologic GLP-1 receptor blockade attenuated GLP-1RA-induced cAMP signaling, confirming receptor-dependent activation. Consistent with these signaling findings, GLP-1RAs produced rapid bronchodilation in lung slices independent of β_2AR activation, demonstrating that GLP-1R signaling can directly regulate airway smooth muscle tone. **Conclusions:** These findings identify a novel immunometabolic mechanism in which insulin impairs β_2AR-mediated relaxation in ASM and demonstrate that GLP-1RAs directly activate GLP-1 receptor-dependent cAMP-

PKA signaling to modulate airway tone. The convergence of GLP-1R and β_2AR signaling suggests that GLP-1RAs may bypass or dominate β_2AR dysfunction, providing a mechanistic basis for clinical improvements observed in patients with obesity-related asthma and T2DM. Given the rising global prevalence of metabolic disease and asthma, GLP-1RAs represent a promising dual-action therapeutic strategy targeting intertwined metabolic and respiratory pathophysiology.

ABSTRACT NUMBER: 5123 **Poster Board Number:** J675
TITLE: Applicability of an *In Vitro* Model for Respiratory Sensitization Testing Across Multiple Hazard Classes

AUTHORS (FIRST INITIAL, LAST NAME) AND INSTITUTIONS: S. Burla, G. Radicchio, and *A. C. Gutleb*. Invitrolize SA, Belvaux, Luxembourg.
KEYWORDS: Respiratory Sensitization; Alternatives to Animal Testing; *In Vitro* and Alternatives

ABSTRACT: Background and Purpose: Respiratory sensitization is becoming a regulatory relevant endpoint, yet it remains burdened by significant scientific uncertainties. The complex process of respiratory sensitization involves multiple biological pathways, and there is a clear need of methods for the identification of respiratory sensitizers, especially without relying on animal testing. In this context, the development and validation of non-animal alternative methods for respiratory sensitization is critical. The commercially available co-culture *in vitro* model ALIsens® is addressing two key events (KE) of the Adverse Outcome Pathway (AOP #39) for respiratory sensitization: KE2 - inflammation and KE3 - dendritic cell activation. **Methods:** The scope of this study was to assess the response of ALIsens® test system following exposure to an extended panel of test items nominated by a sponsor. The test items belong to different chemical classes and pose various human health hazards: 2,3-butanedione, 2,3-pentanedione, 2-methyl-4-isothiazolin-3-one, 5-chloro-2-methyl-4-isothiazolin-3-one, trans-2-hexen-1-al, acetic acid, cinnamaldehyde, ethyl isocyanate, methyl acrylate, N-vanillylnonanamide and vanillin. The complex tetraculture *in vitro* model used in this study is based on established human cell lines, A549 as epithelial, EA.hy926 as endothelial and THP-1 as immune cells - differentiated to macrophage-type cells (MΦ-THP-1) and used in their naïve state, undifferentiated dendritic-like cells (DC-THP-1). The model is brought at air-liquid interface (ALI) 24 h prior exposures which were carried out using the Tecan D300e Digital Dispenser for a precise, reproducible and fast delivery of the test items to the apical surface of the model. All test items were either solubilized in or mixed with one of the following vehicles: pure DMSO or water supplemented with 0.1% Brij® 35. The viability of the complete model was assessed using the resazurin assay and viability of DC-THP-1 cells was additionally measured by flow cytometry using the mitochondrial membrane potential stain tetramethyl rhodamine ethyl ester (TMRE) and cell apoptosis with Annexin V. The exposure doses resulting in 75% residual cell viability of the cells comprised in the apical compartment (A549 and MΦ-THP-1), endothelial cells and DC-THP-1 cells, and of the complete model as average of the viabilities of all cell types, were calculated by log-linear interpolation. The model was further exposed at two to three independent exposure doses corresponding to the calculated CV75 and activation of dendritic cells was evaluated by measuring the expression of TSLPr, CD54 and CD86 cell surface markers by flow cytometry. Responsiveness of the model was evaluated upon exposure to lipopolysaccharide and thymic stromal lymphopoietin mixture and the following controls were included: chloramine-T trihydrate as respiratory sensitizer, 2-mercaptobenzothiazol as skin sensitizer and lactic acid as non-sensitizer. **Results:** The dose-response data indicate that chemicals with different physico-chemical properties exert distinct effects on the

viability of the cell types within the test system. Moreover, certain test items (*i.e.*, cinnamaldehyde) showed toxicity specifically towards THP-1 cells included in the model. As a result, applying the CV75 exposure dose of the ALIsens® model reduced dendritic cell viability, thereby compromising the correct flow cytometric measurements of cell surface markers expression. The majority of evaluated low molecular weight (LMW) chemicals in this study were correctly identified as non-respiratory sensitizers, with 82% accuracy and 100% specificity, based on the expression of TSLPr cell surface marker. **Conclusions:** These data demonstrate the importance of defining the appropriate exposure dose for the evaluation of respiratory sensitization endpoints in the context of LMW compounds with high toxicity towards dendritic-like THP-1 cells. This novel approach of evaluating multiple exposure doses poses the advantage of assessing the impacts of LMW chemicals more robustly. In some cases, the obtained data was borderline or considered to have low confidence due to the impact on the cell viability of the THP-1 cells comprised in the test system.

ABSTRACT NUMBER: 5124 **Poster Board Number:** J676

TITLE: Development of a novel *in vitro* platform for the detection of profibrotic compounds based on primary human alveolar epithelium

AUTHORS (FIRST INITIAL, LAST NAME) AND INSTITUTIONS: X. Huang, E. Pira, B. Boda, S. Huang, and *S. Constant*. Epithelix, Plan les Ouates, Switzerland.

KEYWORDS: Lung; Pulmonary or Respiratory System; *In Vitro* and Alternatives; Respiratory Toxicology

ABSTRACT: Background and Purpose: Idiopathic pulmonary fibrosis (IPF) is a fatal interstitial lung disease characterized by recurrent alveolar injuries, dysregulated fibrotic and inflammatory responses, leading to progressive scarring of lung tissues and excessive extracellular matrix (ECM) deposition. Epithelial cells undergoing epithelial-to-mesenchymal transition (EMT) play a key role in disease progression. Several profibrotic agents, including DNA-damaging compounds (Bleomycin), inhaled fibers and advanced nanomaterials, identified as inducers of lung fibrosis in humans, were used to develop animal models for studying the mechanisms for IPF pathogenesis, identifying candidate therapeutic targets and evaluating the fibrotic potential of industrial compounds. The bleomycin-induced fibrosis model in rodent is the most widely used, but species differences (respirability, lung retention and metabolic responses) limit its translatability to human fibrosis. To overcome these limitations, alternative human-relevant model systems are being developed to bridge the gap to human clinical trials. This study aimed to develop a new *in vitro* platform for evaluating the impact of potential profibrotic compounds based on specific IPF biomarkers and an *in vitro* alveolus epithelium model, AlveolAir™, composed of ATI, ATII at the air-liquid interface and co-cultured with endothelial cells. **Methods:** AlveolAir™ cultures were exposed during 10 days to several bleomycin concentrations or to TGF-β /TNF-α, known to play a crucial role in the initiation of fibrosis. The toxicity response was assessed via barrier integrity and cytotoxicity measurements. Inflammation and EMT were evaluated through basal secretion of cytokines, gene expression analysis and tissue morphological changes. **Results:** Exposure to bleomycin triggered a panel of responses comparable to that induced by TGF-β and TNF-α. Tissue inflammation was evidenced through a significant, dose-dependent release of pro-inflammatory cytokines and chemokines, such as IL-6, IL-8 and MCP-1. EMT markers were upregulated, with a significant and dose-dependent increase in CDH2, AREG, COL1A1 and COL4A1 gene expression. Morphological alterations in alveolar type II cells were observed, as well as changes in vimentin expression. **Conclusions:** The successful performance of this *in vitro* model for bleomycin-induced

fibrosis supports its relevance for screening profibrotic compounds. Preliminary investigations with SiO_2 and SiC nanoparticles and crocidolite fibers suggest that this model could serve as a valuable tool for assessing the fibrogenic potential of various compounds.

ABSTRACT NUMBER: 5125 **Poster Board Number:** J677
TITLE: Transcriptomic Signature of Pulmonary Osteoclast-Like Cells in Silica-Exposed Rats

AUTHORS (FIRST INITIAL, LAST NAME) AND INSTITUTIONS: S. Gaboyan, *A. Perryman*, and L. E. Crotty Alexander. University of California San Diego, La Jolla, CA.
KEYWORDS: Respiratory Toxicology; Lung; Pulmonary or Respiratory System; Bioinformatics; Engineered Stone; Silica

ABSTRACT: Background and Purpose: Silicosis is a fatal occupational lung disease caused by inhalation of respirable crystalline silica dust. A rapid increase in exposure has been observed among engineered stone (ES) countertop fabricators over the past decade, in part due to insufficient respiratory protection and inadequate enforcement of workplace exposure standards. Despite this growing public health crisis, the pathogenic mechanisms driving and perpetuating fibrosis in silicosis remain poorly understood. Recent studies have discovered pulmonary osteoclast-like cells in the lungs of silica-exposed mice and miners with coal workers pneumoconiosis. Here we aim to utilize transcriptomics to identify key signatures involved in the pathogenesis of silicosis, with the hypothesis that silica dust exposure drives lung macrophages to differentiate into osteoclast-like cells, resulting in the perpetuation of lung injury and remodeling post-exposure through osteoclast-derived matrix degrading proteases and secretion of hydrochloric acid. **Methods:** Male rats were exposed to air or crystalline silica (15mg/m^3) for 6 hours/day for 5 days. RNA was extracted (miRNeasy Mini Kit, Qiagen) from lung tissue and sequenced (Total RNA Library, Illumina) at post-exposure time intervals of 1, 3, 6, 9, 12, and 18 months (n=5 per group). Reads were aligned from GSE150689 against the rat transcriptome (GRCr8) using Bowtie2 and quantified with RSEM. Differential gene expression analysis was performed with DESeq (R v4.5.1). **Results:** By 3 months, genes associated with osteoclast-like differentiation and maturation were significantly upregulated in rats with silica induced lung injury, including *Acp5, Clec5a, Dcstamp, Tnfrsfl1a, Csf1,* and *Spp1* (Log2FC>0.75, padj<0.05), and were persistently present throughout the following months. Furthermore, genes associated with osteoclast-derived matrix degrading proteases and secretion of hydrochloric acid were significantly upregulated as well, including *Ctsk*, *Mmp14,* and *Atp6v0d2* (Log2FC>0.75, padj<0.05). Markers of lung injury increased continuously throughout the post-exposure time interval through 18 months. **Conclusions:** These findings suggest that pulmonary osteoclast-like cells are present and active in the lung microenvironment of progressive silicosis and may contribute to perpetuating lung injury and driving remodeling in this terminal disease.

ABSTRACT NUMBER: 5126 **Poster Board Number:** J678

TITLE: Epithelial Membrane Protein 2 Deletion Protects Alveolar Epithelial Senescence and Lung Fibrosis

AUTHORS (FIRST INITIAL, LAST NAME) AND INSTITUTIONS: *W. Lopez-Perez*[1], W. Lin[1], P. Karmaus[1], F. De Moliner[2], M. Vendrell[2], L. Pang[2], and M. Fessler[1]. [1]NIEHS/NIH, Research Triangle Park, NC; and [2]University of Edinburgh, Edinburgh, United Kingdom.

KEYWORDS: Respiratory Toxicology; Inflammation

ABSTRACT: Background and Purpose: Epithelial membrane protein 2 (EMP2) is a tetraspan protein highly expressed by alveolar epithelial type 1 (AT1) cells, but its role in lung biology is poorly understood. We have previously reported that EMP2 regulates expression of adhesion molecules in AT1 cells and is required for transepithelial migration of neutrophils into the airspace after inhaled lipopolysaccharide. Here, we investigated roles for EMP2 in lung fibrosis and cellular senescence. **Methods:** Emp2-/-, Emp2Sftpc (lung epithelial-specific Emp2-deficient), and Emp2Sftpc-ER (AT2-specific Emp2-deficient) mice were exposed to intratracheal bleomycin and inflammatory and fibrotic (hydroxyproline assay, trichrome staining) responses profiled. Roles for the alveolar epithelium were further explored using inhaled silica and adenoviral-TGFβ, alternate models that induce less primary epithelial injury, and butylated hydroxytoluene (BHT), which induces severe AT1-predominant necrotic injury. **Results:** Compared to controls, Emp2-/- and Emp2Sftpc mice had reduced lung fibrosis after bleomycin, whereas there was no reduction in fibrosis in Emp2Sftpc-ER mice. No attenuation in fibrosis was observed in any of the Emp2-deficient strains after silica or adenoviral TGFβ. Consistent with attenuated early AT1 injury, BALF RAGE and Pdpn levels were reduced after bleomycin, as were weight loss; airway recruitment of monocytes and monocyte-derived macrophages; airway pro-inflammatory cytokines and TGFβ; and airway albumin. Emp2-/- and Emp2Sftpc mice exhibited reduced γH2AX (DNA double-strand break marker) and attenuated induction of p53 target genes in both AT1 and AT2 cells as early as 24 hours post-bleomycin, and reduced cellular senescence in AT1, AT2, and pre-AT1 transitional state (PATS) cells at later timepoints. Pro-fibrotic Krt8+B6+ PATS cells were reduced in number. Single cell RNA-sequencing analysis of bleomycin-challenged Emp2Sftpc mice corroborated reduced PATS cells and identified reduced p53 activation and dysregulated complement gene expression in PATS cells, together pointing to attenuation of quantitative and qualitative acquisition of the pro-fibrotic transitional cell state. Emp2Sftpc mice had attenuated weight loss and mortality after BHT, further suggesting that Emp2-null AT1 cells may be broadly protected against toxic insults. AT1-specific Emp2Ager mice and Emp2-null Sftpc-CreER-TdTomato AT2-lineage tracing mice are currently under study to confirm whether Emp2 deletion in AT1 cells is specifically protective and reduces AT2-PATS-AT1 flux. **Conclusions:** Emp2 deletion is protective against lung injury and fibrosis in the bleomycin model and from mortality in the BHT model. Our findings suggest that Emp2 deletion protects alveolar epithelial cells from early, acute DNA damage. Our finding of reduced damage in both AT1 and AT2 cells as early as 24 hours suggests that AT1 EMP2 may co-regulate AT2 damage via either AT1-AT2 contact-dependent or paracrine mechanisms.

ABSTRACT NUMBER: 5127 **Poster Board Number:** J679
TITLE: Regulation of airway epithelial gene expression by Interleukin 4 and Diacetyl

AUTHORS (FIRST INITIAL, LAST NAME) AND INSTITUTIONS: *T. Pressley*, D. Krenitsky, R. Rowe, *I. Rahman*, M. McGraw, and S. Georas. University of Rochester, Rochester, NY.
KEYWORDS: Respiratory Toxicology; Inflammation; Immunotoxicology; Diacetyl

ABSTRACT: Background and Purpose: Diacetyl (DA) is a respiratory hazard most well-known for its causal link to fibrotic lung conditions like Bronchiolitis Obliterans, which occurs in workers exposed to butter flavored microwave popcorn. DA is also found in many flavored vaping products, renewing interest in understanding the mechanisms by which DA inflicts damage in the lungs, particularly in acute, lower-dose exposures, rather than higher-dose chronic occupational exposures. Previous studies reported that pre-exposure to allergic inflammatory stimuli including the cytokine interleukin 4 (IL-4) synergistically enhanced DA-induced airway epithelial barrier dysfunction. This project investigated the effects of DA and IL-4 on epithelial gene expression using RNA sequencing (RNA Seq). **Methods:** 16HBE cells, a human bronchial epithelial cell line known to form tight junctions (TJ) and adherens junctions (AJ) *in vitro*, were used to model airway epithelial barriers for this study. Triplicate wells of 16HBE cells were exposed to medium control, DA (0.6 mM), IL-4 (50 ng/mL) or DA+IL-4 and total RNA was harvested using Qiagen-RNeasy mini-kit and analyzed using a Nova Seq X Plus Illumina Sequencer. Raw reads were demultiplexed and filtered using BCL Convert (v 4.1.7) and FastP (v 0.23.1) respectively. Processed/cleaned reads were then mapped to the GRCh38/gencode 42 reference using STAR_2.7.9a. Differential expression analysis was performed using DESeq2-1.34.0 with a P-value threshold of 0.05, and principal component analysis (PCA) plots were generated with pcaExplorer c2.14.2 within R (v 4.0.2). Gene ontology analyses were performed using the EnrichR and GSEA packages. **Results:** Exposure to DA alone induced large scale regulation of gene expression including 6583 upregulated transcripts and 6140 downregulated transcripts (adjusted p-value<0.05). In contrast, IL-4 alone caused upregulation of 454 genes and downregulation of 280 genes, and PCA plots revealed clustering of cells based largely on DA treatment (explaining >90% of variance). The 5 most upregulated genes by DA were: Heat Shock Protein Family A Member 6, Activity-regulated cytoskeleton-associated, Golgi-associated RAB2 interactor protein 4, Inhibitor of DNA binding 2, Snail, Growth Arrest and DNA-Damage-Inducible 45 Gamma (all ≥5-$\log_2$fold upregulated, adjusted p value < 10e-52). The 5 most downregulated genes by DA were: Hypoxia-Inducible Lipid Droplet-Associated, Small Nuclear Ribonucleoprotein U11/U12 Subunit 35, Long non-coding RNA: MIR193BHG, Transcriptional and Immune Response Regulator, Transmembrane Protein 177 (all ≥2.5- $\log_2$fold downregulated, adjusted p value <1.15e-51). Pathway analysis indicated that DA induced genes involved in cellular metabolism (e.g. fatty acid biosynthesis, amino acid degradation), protein synthesis (e.g. peptide synthesis, translation, and ER processing), and adhesion (e.g. ECM interaction, focal adhesion, α6β4 integrin signaling), whereas IL-4 alone induced genes involved in mitochondrial metabolism (e.g. oxidative phosphorylation, electron transport) and interferon responses. When comparing cells treated with IL-4 plus DA to those treated with DA alone, 1915 transcripts were upregulated, whereas 959 transcripts were downregulated. Genes upregulated more than 1.5 log fold change included 3β-hydroxysteroid dehydrogenase/isomerase type 1, keratin 6A, and Cytokine-inducible SH2-containing protein (all p<10e-20), whereas genes downregulated more than -0.9 log fold change included VE-cadherin, RIPOR Family Member 3, and Nuclear Pore Complex Interacting Protein Family Member B3 (all p<10e-4). Targeted analysis of several TJ and AJ proteins revealed differential regulation by IL-4 in cells exposed to DA including increased expression of Beta-

Catenin 1, Claudin 7, Jam 2 and decreased expression of Claudin 1, Plectin, and Zonula Occludens 1 (all p<0.001). **Conclusions:** DA induces broad regulation of gene expression in 16HBE cells that is modulated by pre-exposure to IL-4. Several potential AJ and TJ candidates were identified that might explain potentiation of DA-induced barrier dysfunction by IL-4. Our results add to growing evidence that pre-existing inflammation can modulate the response to inhaled xenobiotics.

ABSTRACT NUMBER: 5128 **Poster Board Number:** J680

TITLE: Respiratory Susceptibility to Aerosolized Per- and Polyfluoroalkyl Substances in Human 3D Airway Models

AUTHORS (FIRST INITIAL, LAST NAME) AND INSTITUTIONS: Y. Han. Korea University, Sejong-si, Korea, Republic of. Sponsor: *K. Lim*

KEYWORDS: Chemical of Concern; *In Vitro* and Alternatives; Respiratory Toxicology

ABSTRACT: Background and Purpose: Per- and polyfluoroalkyl substances (PFAS), including perfluorooctanoic acid (PFOA) and the replacement compound hexafluoropropylene oxide dimer acid (GenX, HFPO-DA), have emerged as chemicals of concern due to their potential associations with respiratory diseases. In this study, we conducted a systematic review to evaluate current studies of PFAS-related respiratory toxicity. We further investigated respiratory responses to PFAS by analyzing transcriptomic profiles using human 3D airway epithelial models. **Methods:** In a systematic review following a PECO framework, we investigated 101 experimental studies covering epidemiology, *in vivo* and *in vitro* PFAS respiratory toxicity, and PFAS inhalation exposure. Normal and asthmatic MucilAir were exposed to aerosolized PFAS using an air-liquid interface aerosol exposure system (Vitrocell). Differentially expressed gene (DEG) profiling was performed, followed by gene ontology (GO), KEGG pathway, and cell type enrichment analyses based on single sample gene set enrichment analysis (ssGSEA). We identified responses related to allergic phenotypes and shifts in airway epithelial subtypes. **Results:** First, limited articles were available for GenX. Meanwhile, PFOA has been extensively reported for associations with inflammation, impaired lung function, chronic obstructive pulmonary fibrosis (COPD), lung cancer, and airway allergies (wheezing and asthma) in human studies. Many *in vivo* and *in vitro* studies suggested fibrotic, tumor-associated, and asthmatic responses of PFOA. Following non-toxic aerosol exposure of PFOA and GenX to MucilAir, GO and KEGG pathway analysis revealed T helper cell-related immune pathways across multiple comparisons of normal versus asthmatic tissues and PFAS exposures in asthmatic conditions. Notably, multiple major histocompatibility complex (MHC) class II genes were consistently upregulated with aerosolized PFAS exposure particularly in the asthmatic background. Consistent with these findings, ssGSEA results showed a shift in airway epithelial subtypes characterized by downregulated basal subtypes and upregulated secretory subtypes (secretory and goblet). These alterations were modest in normal tissues but markedly amplified in asthmatic airway models exposed to PFOA or GenX. **Conclusions:** In summary, inhalation exposure to PFOA and GenX induced MHC class II phenotypes and shifts in airway epithelial subtypes. This indicates that aerosolized PFAS exposure may promote allergic epithelial states, particularly under asthmatic conditions.
Acknowledgement: This work was supported by Korea Environment Industry & Technology Institute (KEITI) through Technology Development Project for Safety Management of Household Chemical Products Program, funded by the Korea Ministry of Environment (MOE) (202300230430).

ABSTRACT NUMBER: 5129 **Poster Board Number:** J681

TITLE: Functional dissection of extracellular vesicle- and soluble factor-mediated responses to the airway epithelial secretome: an air-liquid interface platform for inhalation toxicology

AUTHORS (FIRST INITIAL, LAST NAME) AND INSTITUTIONS: *G. M. Elizondo*, and *N. M. Johnson*. Texas A&M University, College Station, TX.

KEYWORDS: Lung; Pulmonary or Respiratory System; Cell Communication; Inhalation Toxicology

ABSTRACT: Background and Purpose: Airway epithelial cells are at the front-line, serving as the primary target for inhaled toxicants. These cells maintain barrier integrity and coordinate immune responses through intercellular communication; however, the relative contribution of extracellular vesicles (EVs) versus soluble factors remains poorly defined. Studies resolving EV-mediated responses under physiologically relevant air-liquid interface (ALI) conditions are also limited. Here, an ALI-based platform was developed to functionally characterize epithelial secretome signaling using tumor necrosis factor-alpha (TNF-α) as a reference exposure. **Methods:** Human bronchial epithelial cells (16HBE) were cultured on inserts at ALI and apically exposed to TNF-α. Basolateral conditioned media (CM) was collected after 24 hours then fractionated by size-exclusion chromatography and pooled into EV-enriched (EV+) and EV-depleted soluble factor (EV−) fractions. Naïve 16HBE cultures were subsequently exposed to CM, EV+, EV−, or vehicle control (VC) for a 48-hour time course. Bioactivity was assessed via cytotoxicity (LDH activity), cytokine (IL-8 and TNF-α) production by ELISA, and expression of oxidative stress (HMOX1, NQO1), junctional (CLDN1, TJP1), and remodeling (MMP9) genes by RT-qPCR. EV-enriched fractions were characterized by nanoparticle tracking analysis for size and concentration and are currently being validated for EV-specific tetraspanin markers by western blot. **Results:** CM elicited the greatest cytokine response, with sustained IL-8 and TNF-α secretion across all time points. EV− produced intermediate responses, whereas EV+ remained near VC. LDH activity exhibited transient increases, with values converging to VC by the end of the time course. Fractionation revealed distinct and reproducible transcriptional patterns. At 24 hours, CM and EV− elicited the greatest induction of oxidative stress (HMOX1) and remodeling (MMP9) genes, whereas EV+ resulted in comparatively limited responses. **Conclusions:** Collectively, these findings demonstrate functionally distinct signaling pools of the epithelial secretome. In this reference exposure, soluble factors account for most measurable bioactivity relative to EV-enriched fractions, in the absence of overt cytotoxicity. This platform will be extended to relevant environmental exposures, including volatile organic compounds (VOCs), enabling resolution of exposure-specific EV signatures with implications for biomarker discovery, toxicological risk assessment, and targeted intervention of inhalation-driven disease. Supported by P42ES027704 and T32ES026568.

ABSTRACT NUMBER: 5130 **Poster Board Number:** J682
TITLE: Reference Chemical Database Development and Predictive Insights into Acute Inhalation Toxicity

AUTHORS (FIRST INITIAL, LAST NAME) AND INSTITUTIONS: J. Lim. Korea University, Sejong, Korea, Republic of. Sponsor: *K. Lim*
KEYWORDS: Inhalation Toxicology; Chemical Hazard Assessment; Alternatives Assessment

ABSTRACT: Background and Purpose: A reference chemical database is essential for developing and validating regulatory toxicological test methods. Acute inhalation toxicity is an area where alternative approaches are needed due to ethical and practical limitations of animal testing. The purpose of this study was to establish a reference chemical database for acute inhalation toxicity, and to evaluate correlations of *in vivo* LC_{50} values with physicochemical properties, *in vitro* IC_{50} data, and *in silico* model predictions, thereby providing insights into factors influencing acute inhalation toxicity. **Methods:** The database integrated *in vivo* toxicity data, UN GHS classification and labeling information, and physicochemical properties collected from regulatory agencies and publicly available sources. Reference chemicals were categorized according to exposure route (vapor, gas, dust, and mist). Using this database, correlations between *in vivo* LC50 values, physicochemical properties, and *in vitro* IC_{50} data were analyzed. In addition, *in silico* prediction tools, including STopTox and TOPKAT, were applied to the reference chemicals, and their predictive performance for acute inhalation toxicity was assessed by comparison with experimental LC_{50} values. **Results:** A total of 176 reference chemicals were collected in the database. Vapors and gases showed a positive correlation between LC50 values and vapor pressure below 10 kPa, but an opposite trend above this threshold. Dust exhibited a positive correlation between LC50 and water solubility, whereas mist showed a negative correlation. Strong correlations were observed between IC50 and LC50 values. *In silico* models demonstrated predictive capacity, with STopTox performing well for vapors and gases. **Conclusions:** This study established a curated reference chemical database for acute inhalation toxicity, providing comprehensive and valuable information that can support the development of alternative approaches. Acknowledgement: This work was supported by Korea Environment Industry & Technology Institute (KEITI) through Technology Development Project for Safety Management of Household Chemical Products Program, funded by the Korea Ministry of Environment (MOE) (202300230430).

ABSTRACT NUMBER: 5131 **Poster Board Number:** J683
TITLE: Diacetyl induces airway epithelial barrier dysfunction in a Protein Kinase D dependent manner

AUTHORS (FIRST INITIAL, LAST NAME) AND INSTITUTIONS: *T. Pressley*, D. Krenitsky, R. Lian, J. Veazey, *I. Rahman*, M. McGraw, M. Brewer, and S. Georas. University of Rochester, Rochester, NY.
KEYWORDS: Respiratory Toxicology; Diacetyl

ABSTRACT: Background and Purpose: Inhalation of diacetyl (DA) is well known as a hazard in the manufacturing of butter flavored popcorn, and can lead to airway epithelial injury and fibrotic conditions such as bronchiolitis obliterans. Despite its documented adverse effects, DA has been found in a large percentage of flavored vaping products. Diacetyl has been shown to activate airway epithelial cells *in vitro*, but its effects on epithelial barrier structure and function are not well defined. Protein Kinase D (PKD) is an enzyme that has previously been shown to play a role in potentiating epithelial barrier disruption in both viral and chemical toxicant exposure models. The purpose of this project is to identify the mechanism of DA-induced epithelial barrier dysfunction *in vitro*, and test the hypothesis

that inhibiting or knock-down of PKD would have a protective effect. **Methods:** 16HBE14o$^-$ cells (16HBE), a human bronchial epithelial cell line known to form tight junctions (TJ) and adherens junction (AJ) *in vitro*, were used to study the effects of DA on epithelial barrier structure and function. The cells were incubated with DA alone or in combination with the pan-PKD inhibitor CRT0066101 (CRT). Dose finding and kinetic assays varying the concentration (0, 0.07, 0.14, 0.3, 0.6, 1.2, or 6 mM) and timing (2-48 hrs) of DA exposure and varying CRT concentration (0.1, 0.5, 1, 5, or 10 µM) were completed. Cells were grown on Transwell inserts and macromolecular permeability to FITC-dextran (4 or 10 kDa) or Calcien, and measured decreases in Transepithelial Electrical Resistance (TEER), were used to quantify epithelial barrier dysfunction. To study changes in epithelial barrier structure, whole cell lysates were measured via Western blot and methanol fixed and fluorescently stained cells were imaged using a panel of antibodies directed against AJ and TJ proteins. Cellular cytotoxicity was examined using three different approaches: Lactate Dehydrogenase (LDH) cytotoxicity assay, a Water-Soluble Tetrazolium Salt (WST-8) cell viability assay, and counting cells stained with Trypan Blue. The CRISPR/Cas9 gene editing system was utilized to create knock out (KO) 16HBE cells deficient in PKD3, one of the three PKD isoforms known to be expressed in the airway. **Results:** When 16HBE cells were treated with varying DA concentrations (0-6m M) for 24hrs, the measured TEER values decreased in a dose-dependent manner from 70.9%±4.2 (mean± SD, n=3) to 7.6%±0.4 when compared to pre-treatment measurements. This dose-dependent decrease in TEER values was complemented by an increase in macromolecular permeability to 4kDA FITC-Dextran from 9.3±3.1 to 285.5±28.1 µg/mL (control vs. 6mM DA; $p<0.0001$). WST-8 cell viability assays revealed that the DA concentrations > 1.2 mM causes a significant ($p<0.05$) decrease in cell viability, so lower concentrations (≤0.6 mM) were used in subsequent experiments. By Western blot analyses, TJ or AJ protein expression did not change significantly using antibodies directed against Occludin, E-Cadherin, or Claudins 1 and 3. Pre-exposure to the pan-PKD inhibitor CRT (5 µM for 2 hrs) significantly protected 16HBE cells from DA-induced barrier disruption as measured by TEER and macromolecular permeability to 4 kDa FITC-Dextran. For example, in cells exposed to DA alone (0.6 mM, 24hrs), the measured 4kDa FITC-Dextran that crossed the cell monolayer and was collected in the transwell basal chamber was 25.7±7.8 µg/mL, which decreased significantly with CRT pre-treatment to 9.9±3.62 µg/mL ($p<0.0001$). Protective effects of CRT were also observed using 0.3 mM DA without or with CRT (10.7±5.2 vs. 5.8±2.6 µg/ml, $p=0.0098$). Similar results were observed using 10 kDa FITC-Dextran as well as Calcein. In preliminary experiments, cells in which PKD3 was genetically deleted using CRISPR/Cas 9 (PKD3 KO) responded similarly to DA when compared with wild-type controls. **Conclusions:** DA induces epithelial barrier dysfunction without affecting expression of several AJ and TJ proteins. DA induced airway epithelial barrier disruption is dependent on Protein Kinase D. Further research is needed to identify the exact PKD isoform involved.

ABSTRACT NUMBER: 5132 **Poster Board Number:** J685

TITLE: Inflammatory and oxidative stress pathways in pre-diagnosis serum metabolomics predict lethal prostate cancerin the Child Health and Development Studies

AUTHORS (FIRST INITIAL, LAST NAME) AND INSTITUTIONS: N. Y. Krigbaum[1], *X. Hu*[2], P. M. Cirillo[3], S. Teeny[4], B. Minasenko[5], *Y. Go*[2], *D. P. Jones*[6], and B. A. Cohn[3]. [1]Child Health and Development Studies, Public Health Institute, Berkeley, CA; [2]Emory University, Atlanta, GA; [3]Public Health Institute, Oakland, CA; [4]Clinical Biomarkers Laboratory, Division of Pulmonary, Allergy, Critical Care, and Sleep Medicine, Department of Medicine, Emory University, Atlanta, GA; [5]Gangarosa Department of Environmental Health, Rollins School of Public Health, Emory University, Atlanta, GA; and [6]Emory University;Emory University School of Medicine, Atlanta, GA.

KEYWORDS: Epidemiology; Biomarkers; Metabolomics

ABSTRACT: Background and Purpose: Prostate cancer is the second most common cancer and the second leading cause of cancer death among men in the United States. Black men are twice as likely to die from prostate cancer than other men. **Methods:** We conducted a prospective Metabolome-Wide Association Study (MWAS) of lethal prostate cancer in men the CHDS cohort. We identified 111 cases of lethal prostate cancer in Black men (median age of 74 at death) and 258 cases in non-Black men (median age of 77 at death) via linkage to the California Cancer Registry. Controls were matched on birthyear (220 Black controls; 515 non-Black controls). We conducted High-Resolution Metabolomics (HRM) on pre-diagnostic, archived serum samples collected a median of 34.5 years before diagnosis. Untargeted analyses were performed using Rodin, a Python package for metabolomics analysis. Metabolic feature intensities were log2 transformed and ANOVA was used to test for differential abundance of features at raw $p < 0.05$. Features with $p<0.05$ were used for pathway enrichment analysis with Mummichog, using C18 - ESI, C18 + ESI, HILIC - ESI and HILIC +ESI data. We identified all significant pathways and organized them into functional groups based on their relevance to oxidative stress and inflammation. P-values for significant pathways listed are for HILIC +ESI data. **Results:** Inflammation functional metabolic pathways were enriched in both populations, with a stronger representation in the non-Black men compared to the Black men. These functional groups include lipid peroxidation, eicosanoids & inflammatory lipid mediators, vitamins & cofactors with anti-inflammatory or redox roles. In particular, pathways in the inflammatory lipids functional group were highly enriched in metabolites predicting prostate cancer lethality in non-Black men, with consistent but weaker enrichment in Black men. These pathways included arachidonic acid metabolism, $p<.001$ in non-Black and $p<.05$ in Black men; leukotriene metabolism ,$p<.05$ non-Black and NS in Black men, prostaglandin formation from arachidonate, $p<.01$ non-Black and NS in Black men. An upregulated compound of interest, putatively annotated arachidonic acid, was upregulated both non-Black cases ($P<.05$) and Black cases ($P<.05$). In contrast, we found a prominent clustering of oxidative stress pathways associated with prostate cancer lethality only in Black men, which includes methionine and cysteine metabolism ($p<.005$), and selenoamino acid metabolism ($p<.05$). A compound of interest, putatively annotated as selenocysteine, was downregulated in Black cases ($P<.05$). **Conclusions:** Our results demonstrate distinct clustering of enriched metabolic pathways by functional group in Black and non-Black men. These metabolic signatures may serve as indicators of prognosis and risk of lethality. Our findings suggest that inflammatory pathways contribute to lethal prostate cancer in both Black and non-Black men, with a potentially greater role in non-Black men. Notably, this study identifies race-dependent differences in metabolic signatures associated with lethal prostate cancer and highlights the importance of oxidative stress pathways in Black men years before

cancer diagnosis. Our findings of downregulation of selenocysteine in Black men with lethal prostate cancer support existing mouse models that suggest possible links to selenocysteine deficiency accelerating prostate carcinogenesis. Next steps will be to confirm compounds of interest and investigate the link between environmental exposures and lethality mediated by these molecular pathways.

ABSTRACT NUMBER: 5133 **Poster Board Number:** J686

TITLE: Use of ATSDR's SHOWER model to establish public health thresholds for Trichlorethylene in Wisconsin Private Wells

AUTHORS (FIRST INITIAL, LAST NAME) AND INSTITUTIONS: A. Jeninga[1], J. Murray[2], J. Parrot[2], and *S. Yang*[2]. [1]University of Wisconsin, Green Bay, WI; and [2]Wisconsin Department of Health Services, Madison, WI.

KEYWORDS: Risk Assessment; Exposure Assessment; Regulatory/Policy; Public Health; Trichloroethylene (TCE)

ABSTRACT: Background and Purpose: In Wisconsin, private wells are a main source of drinking water for more than 1.6 million people but are not subject to the same mandatory testing and reporting requirements as public water systems. To reduce exposure to environmental contaminants, the Wisconsin Department of Health Services (DHS) uses public health thresholds (e.g., drinking water health advisory levels, public health groundwater enforcement standards) that are generally protective when oral ingestion is the primary exposure route. However, some contaminants, particularly volatile organic compounds (VOCs), can also pose risks through inhalation of vapor phase contaminants during household water use activities such as showering and bathing. Trichloroethylene (TCE) is a carcinogenic VOC has been identified in more than 2,200 sites across Wisconsin affecting over 2,600 private wells. To address non-oral exposure pathways of VOCs, DHS has historically established a whole house advisory threshold. Under a whole house advisory, water use is limited to toilet flushing to reduce non-oral VOC exposure. For carcinogenic VOCs, DHS sets this threshold based on concentrations corresponding with cancer risk levels of one in 10,000 people. However, a whole house advisory can significantly disrupt daily activities (i.e, not being able to wash hands, do dishes, bathe) and increase public health hazards (i.e., increased transmission of communicable diseases). As such, we used the Agency for Toxic Substances and Disease Registry's (ATSDR) Shower and Household Water-Use Exposure (SHOWER) model to evaluate the risk from non-oral exposure routes to TCE and to assess the influence of household parameters on TCE inhalation exposure. **Methods:** We used the SHOWER model to evaluate major non-oral consumption exposure routes to TCE; to assess which household use activities and parameters (i.e., number of bathrooms, bathing mode, exhaust fan use) affect exposure; and to identify alternative thresholds to the whole-house advisory. We ran a series of scenarios in the SHOWER model to obtain average daily exposure concentration (ADEC) for the highest exposed individual over a range of TCE concentrations. We evaluated risk using a hazard quotient approach in which we compared the ADEC to ATSDR's intermediate inhalation minimum risk level. Hazard quotients of one or greater were considered an indication of risk. We used this data to evaluate how various water uses and household parameters affect exposure. **Results:** We found that bathing mode and exhaust fan use have a substantial impact on exposure levels. Regardless of TCE concentration, the scenario with the highest exposure levels was where adults showers in the morning and children bath in the evening with one of the adults helping. Additionally, at all TCE levels evaluated, having the exhaust fan off results in higher

exposure levels than when the exhaust fan is on. We also found an indirect relationship between the number of bathrooms used for bathing and exposure levels, while we observed a direct relationship between household size and exposure level. From this information, we established a stepped approach to evaluate and address the risk of TCE exposure to private well users. This approach lays out three tiers of public health advisories based on the level of TCE in the drinking water and, in certain circumstances, site-specific exposure parameters. **Conclusions:** Modern risk assessment tools, such as the SHOWER model, can be utilized to establish appropriately protective contaminant thresholds to protect public health. For TCE specifically, using the SHOWER model, we were able to establish a series of appropriately protective public health thresholds to use in evaluating exposure risk from non-oral consumption uses of private well water.

ABSTRACT NUMBER: 5134 **Poster Board Number:** J687
TITLE: Assessing Cardiovascular Risks of Prescription Opioids through Mining Real-World Data in FAERS

AUTHORS (FIRST INITIAL, LAST NAME) AND INSTITUTIONS: L. Ma[1], J. Berryhill[2,1], B. Lyn-Cook[1], P. Rogers[1], W. Ge[1], H. Hong[1], *W. Tong*[1], and W. Zou[1]. [1]NCTR/FDA, Jefferson, AR; and [2]Arkansas State University, Jonesboro, AR.
KEYWORDS: Risk Assessment; Cardiovascular System; Safety Pharmacology; Prescription opioids

ABSTRACT: Background and Purpose: Prescription opioids are widely prescribed for pain management, but they are increasingly reported to be linked to cardiovascular adverse events. Understanding these risks is critical for informed prescribing of opioid drugs. Current investigations did not provide a thorough and systematic evaluation of cardiovascular risks related to various kinds of prescription opioids in the context of real-world clinical practice. This study was pursued to address knowledge gaps and comprehensively investigated cardiovascular-related risk profiles of various prescription opioids and their relationships. **Methods:** A list of prescription opioids was created using the FDA-approved drug list and the function of “getApproximateMatch” in the RxNorm API. The US FDA's Adverse Event Reporting System (FAERS) database (2004 Q1-2024 Q3) was used to retrieve the adverse event reports. The prescription opioid names were normalized by RxNorm using our published approach, and the Preferred Terms of MedDRA were utilized to filter cardiovascular-related adverse events. The R package “openEBGM” was applied to calculate the Empirical Bayes Geometric Mean (EBGM) scores to identify drug-adverse event pairs. **Results:** Around 18 million adverse events reports were retrieved and downloaded from FAERS, and 79,085 disproportionate drug-adverse event pairs were identified by EBGM analysis, linking 17 FDA-approved prescription opioids with 277 distinct cardiovascular adverse events. Examining the distributions of these pairs on drugs and adverse events revealed that fentanyl and oxycodone are the top two drugs with reported cardiovascular adverse events, while hypertension, hypotension, cardiac arrest, cardio-respiratory arrest, and myocardial infarction are the top five cardiovascular adverse events reported. Furthermore, the top 10 cardiovascular adverse events for each of the 17 prescription opioids were identified. Network analysis and hierarchical clustering analysis revealed a close association among fentanyl-remifentanil-sufentanyl and hydrocodone-tramadol-morphine based on their drug-adverse event pairs. In addition, the associations of the 17 prescription opioids based on their cardiovascular advert events profiles showed distinct patterns comparing to the previous published study based on all adverse events profiles. **Conclusions:** The results are expected to provide important information and knowledge to help FDA drug regulators, physicians, and patients be aware of cardiovascular toxicities associated with certain prescription opioids or combinations of opioids

with other prescription drugs, therefore, preventing or reducing risks of the prescription opioids-associated cardiovascular disease. The findings highlighted the need for targeted risk assessment and monitoring, could support more refined prescribing practices, and contribute to optimizing opioid safety labeling and regulatory decision-making.

ABSTRACT NUMBER: 5135 **Poster Board Number:** J688
TITLE: Butadiene Exposure and Leukemia Mortality in Synthetic Rubber Industry Workers

AUTHORS (FIRST INITIAL, LAST NAME) AND INSTITUTIONS: L. P. Marshall, C. R. Langton, and L. A. Wood. Valeo Sciences LLC, Ladera Ranch, CA. Sponsor: *A. Madl*
KEYWORDS: Epidemiology; Exposure-response relationship

ABSTRACT: Background and Purpose: Regulatory agencies across the US and EU utilize analyses of a cohort of workers in the styrene-butadiene rubber (SBR) industry to assess excess cancer risk and make policy decisions on occupational and environmental exposure limits for 1,3-butadiene (BD). Specifically, in 2024, the European Chemicals Agency (ECHA) Committee for Risk Assessment (RAC) used an analysis of the SBR data as the basis of their most recent Opinion on Occupational Exposure Limits for BD. While data from the SBR cohort have been analyzed periodically and have shown consistent associations between BD exposure and leukemia outcomes, expert recommendations provided in recent peer-reviewed publications have suggested specific modeling approaches to improve appropriateness of the estimates for risk assessment. Specifically, recommendations were to rely on β-coefficients that are from the latest and largest update of the cohort, derived from Cox regression models for the dose-response relationship between non-lagged and non-transformed cumulative BD exposure (ppm-years) and leukemia mortality, and are adjusted for age and peak exposure to BD-high intensity tasks. Furthermore, recent analyses reveal inconsistences pertaining to differing inclusion criteria for male and female workers. The objective of this study was to perform an analysis of the most recent SBR cohort data which follows statistical recommendations found in the literature and includes additional explorations of covariates and worker inclusion criteria to evaluate the quantitative effects on the exposure-response relationship between BD and leukemia mortality. **Methods:** Exposure and mortality information for 21,069 male and female workers in six North American SBR plants were obtained from the University of Alabama at Birmingham. Cox proportional hazards models were used to evaluate the association between BD and leukemia mortality. All Cox models used number of days from hire date to person day observation as the time scale and included cumulative BD as a time-varying exposure. Schoenfeld and Martingale residuals were plotted and inspected to test the proportionality of hazards assumption and the assumption of the linear relationship between BD exposure and leukemia mortality on the log-hazard scale, respectively. **Results:** There were 9,647 deaths in the cohort, of which 132 were due to leukemia. A majority of the cohort were exposed to BD (66.4%). The Cox proportional hazards model excluding female workers with less than 1 year of employment (n=1,801) and adjusted for age, BD high intensity tasks, and year of hire resulted in a statistically significant association between cumulative BD exposure and leukemia mortality ($\beta = 2.14 \times 10^{-4}$; 95% CI: 0.41-3.87 $\times 10^{-4}$; HR = 1.000214; 95% CI: 1.000041-1.000387). The same model including all female workers had similar results ($\beta = 2.21 \times 10^{-4}$; 95% CI: 0.49-3.93 $\times 10^{-4}$; HR = 1.000221; 95% CI: 1.000049-1.000393). Models that excluded workers with unknown vital status and continued employment beyond exposure assessment resulted in similar effect estimates. **Conclusions:** Our exploration of covariates and worker inclusion criteria to evaluate the quantitative effects on the exposure-response relationship between BD and leukemia

mortality demonstrates that the relationship has little variation despite covariates and worker groups included. Using the 95% upper bound of the β estimate from our preferred model to calculate excess risk, a BD exposure of 0.45 ppm results in an excess of 4 leukemia deaths per 100,000 workers. This conservative upper bound value is almost 10-fold greater than the ECHA estimate of 0.065 ppm for the same excess life-time cancer risk. These results suggest that the exposure-risk relationship derived by ECHA-RAC is overly conservative.

ABSTRACT NUMBER: 5136 **Poster Board Number:** J689

TITLE: Exposure to mercury and the national policy for comprehensive health care for rural, forest, and water populations. assessment of knowledge in primary health care using the likert scale and cronbach's alpha

AUTHORS (FIRST INITIAL, LAST NAME) AND INSTITUTIONS: *J. B. Freitas Júnior*. Universidade Federal do Pará, Altamira, Brazil.

KEYWORDS: Education; Ecotoxicology; Metals; public health

ABSTRACT: Background and Purpose: The objective of this study was to evaluate the socio-environmental aspects and the knowledge, attitude, and perception of Primary Health Care (PHC) technicians and managers in the Xingu region regarding mercury exposure and the National Policy for the Integral Health of the Rural, Forest, and Water Populations (PNSIPCFA). The socio-environmental aspects of two of the municipalities targeted by the research were similar (Senador José Porfírio and Porto de Moz): low HDI, unknown anthropogenic sources of mercury, and low coverage of health technicians to serve riverside UBSs. Regarding knowledge of the PNSIPCFA, most technicians admitted to being aware of the principles governing this policy, but perceived a need for technical training in the region. They recognized that the lack of human resources and materials are the main difficulties and that teamwork and joint planning for the organization of activities are factors that facilitate the work process. Regarding the technicians' knowledge of mercury exposure, the results showed limited knowledge and recognition of the need for training on the subject. As for managers' knowledge and perception of the PNSIPCFA and exposure to mercury, limited knowledge was demonstrated. In the perception of these managers, 80% disagreed that health technicians in the region are aware of the principles governing the PNSIPCFA and that the UBS/ESF meet the needs of the PNSIPCA in accordance with health policy. On the other hand, they agreed that ongoing education for technicians focused on the main health problems, including mercury exposure, is a necessity in the region. **Methods:** The study was conducted in three riverside municipalities in the Xingu region and used data from IBGE, IBAMA, and MS to analyze socio-environmental aspects and a five-point Likert scale and Crombach's alpha to analyze the knowledge, perception, and attitude of technicians and managers working in riverside UBS/ESF. **Results:** The socio-environmental aspects of two of the municipalities targeted by the research were similar (Senador José Porfírio and Porto de Moz): low HDI, unknown anthropogenic sources of mercury, and low coverage of health technicians to serve riverside UBSs. Regarding knowledge of the PNSIPCFA, most technicians admitted to being aware of the principles governing this policy, but perceived a need for technical training in the region. They recognized that the lack of human resources and materials are the main difficulties and that teamwork and joint planning for the organization of activities are factors that facilitate the work process. Regarding the technicians' knowledge of mercury exposure, the results showed limited knowledge and recognition of the need for training on the subject. As for managers' knowledge and perception of the PNSIPCFA and exposure to mercury, limited

knowledge was demonstrated. In the perception of these managers, 80% disagreed that health technicians in the region are aware of the principles governing the PNSIPCFA and that the UBS/ESF meet the needs of the PNSIPCA in accordance with health policy. On the other hand, they agreed that ongoing education for technicians focused on the main health problems, including mercury exposure, is a necessity in the region. **Conclusions:** It can concluded that the riverside municipalities in the Xingu region that have low human development indicators also have low coverage of health care technicians. Although they show signs of exposure to mercury, they have no known anthropogenic sources of Hg. The knowledge of health managers and technicians about PNSICFA and mercury exposure is limited and needs to be strengthened through continuing education for health technicians and managers, with a view to ensuring access to effective, high-quality, and humane health services to improve the living conditions of the riverside population in this region.

ABSTRACT NUMBER: 5137 **Poster Board Number:** J690
TITLE: Applications, Resources and Lessons from Other Health Science Professions

AUTHORS (FIRST INITIAL, LAST NAME) AND INSTITUTIONS: *R. Nocco*. Toxicology Consultant, Danville, CA.
KEYWORDS: Risk Assessment; Chemical Hazard Assessment; Exposure Assessment

ABSTRACT: Background and Purpose: Toxicology is a diverse and multifaceted discipline where we can apply principles from other health-related disciplines. Resources are often difficult to come by and can be expensive. This session will provide participants with information on free tools and resources and where to find them. Toxicology is a diverse and multifaceted discipline where we can apply principles from other health-related disciplines. Resources are often difficult to come by and can be expensive. This session will provide participants with information on free tools and resources and where to find them. This includes: (1) Related Apps; (2) Websites ; (3) Social Media Videos; (4) Online Courses; (5) Other resources. Areas covered include: (1) Toxicology; (2) Risk Assessment; (3) Epidemiology; (6) Exposure Assessment; (7) Radiation Protection; (8) Other. What is NOT covered in any detail is: (1) How to download; (2) How to use them. **Methods:** Methods used to transfer knowledge include: demonstration, show-and-tell, use of examples to emphasize concepts, and case studies. **Results:** Participants will develop knowledge on the application of tools and resources. It will expand the knowledge base and expand perspectives of toxicologists as well highlight the benefits of becoming fluent in other related disciplines. Understand the value and tradeoffs in becoming a specialized toxicologist verses being a broad-based health scientist. **Conclusions:** Toxicology is a diverse and multifaceted discipline where we can apply principles from other health-related disciplines. In today's economic environment, resources are often difficult to come by and can be expensive. There is value and tradeoffs in becoming a specialized toxicologist verses being a broad-based health scientist.

ABSTRACT NUMBER: 5138 **Poster Board Number:** K692

TITLE: A Regulatory Framework for Assessing the Variability & Safety of Nanoforms in the EU to Reduce Industry and Animal Burden

AUTHORS (FIRST INITIAL, LAST NAME) AND INSTITUTIONS: K. B. Paul[1], C. Shultz[2], R. Cross[2], G. Tsiliki[3], A. Zabeo[4], E. Moschini[5], *V. Stone*[5], W. Wohlleben[6], V. Rodriguez Unamuno[7], W. De Coen[7], D. Mestre[7], and C. Jacquet[7]. [1]Blue Frog Scientific Limited, Edinburgh, United Kingdom; [2]UK Centre for Ecology & Hydrology, Oxford, United Kingdom; [3]Purposeful IKE, Athens, Greece; [4]GreenDecision, Venice, Italy; [5]Heriot-Watt University, Edinburgh, United Kingdom; [6]ECETOC, Brussels, Belgium; and [7]European Chemicals Agency (ECHA), Helsinki, Finland.

KEYWORDS: Regulatory/Policy; Nanoparticles; Risk Assessment; Framework

ABSTRACT: Background and Purpose: The project purpose was to expedite the understanding of nanoform “sameness” and “similarity” assessments to advance the regulatory mechanisms for nanomaterials under Regulation (EC) No. 1907/2206 (herein: REACH).At the outset of the project the main goals were:

1. Identify cut-off criteria for nanoform characterisers to inform the registrant of boundary compositions setting:

a) These rules (e.g. cut-offs, fold-differences, thresholds) must lead to the nanoforms having the “same” profile

b) This framework is for identifying groups of nanoforms so similar they can be considred a single nanoform, or be used to develop **nano**form **S**ubstance **I**dentity **P**rofiles (nanoSIPs).

2. The development of a systematic framework and/or rules for clearer registrant requirements and evaluation criteria for sets of similar nanoforms

The poster will compare the non-nanoform regulatory compliance mechanisms with that of the nanoforms, to highlight aspects missing for nanoforms. It will then explore how the project has addressed this by developing the aformentioned framework based on current state of research and applying three case studies to explore the validity of a decision tree framework for "sameness".

Methods: The project first explored the state of the art of nanoform grouping strategies for hazard, exposure and risk conducting a literature search, expert interviews and hosting a stakeholder workshop. The data patterns as well as gaps will be presented. A decision tree framework was built to only rely upon nanoform characterisers (e.g. shape, size, surface functionlisation). The decision tree was then validated against known nanoforms using REACH dossier submitted data. ECHA provided 47,707 annonymised single data entries across a multitude of nanoforms and all regulatory scientific hazard disciplines i.e. physical chemical, environmental fate and (eco)toxicological properties. The data was curated and refined to three nanoform types and sub-groups of nanoforms were predetermined using unbias statistical methodologies such as Cohen's D effect size, and ordered weighted average (OWA) approaches. Further, the performance of these grouping statistics versus the performace of the decision tree framework were assessed, and the statistical robustness similarly elucidated.

Results: 1. Demonstrated proof of concept: The Decision Tree Framework provides a viable, science-based mechanism to assess acceptable variation among nanoforms using mandatory Annex VI data. **2. Framework parameters:** Statistical and case study evidence supported several fold-difference thresholds (e.g., two-fold variation in surface area), confirming that real-world nanoform variability can be captured within practical limits; however more detailed analysis is needed to potentially adjust fold-differences in the future when a broader and better comparable data base becomes available with time.

3. Conservative framework and identified data gaps: While functional, the framework remains cautious—sometimes overly so—and limited by incomplete data, particularly for higher-tier toxicological and environmental endpoints. **4. Confirmed need for integration, not replacement:** The framework should complement, not supersede, the "sets of similar nanoforms" concept, ensuring a coherent and flexible regulatory toolkit. **5. Advanced proportionality and the 3Rs:** By supporting shared registration of genuinely similar nanoforms, the approach contributes to reduced testing costs and animal use while maintaining protection for human health and the environment.
Conclusions: The research in this project provided a decision tree framework which serves as a solid basis to progress regulatory sound registration of NFs which overall proved to be a useful too but still needing further development. In many instances there was corroboration between the rejection or acceptance of a group of nanoforms selected to be a single nanoform, and the (un)acceptable variation expected from the Annex VII-X physical chemical, hazard and fate data, i.e. if the group was rejected the endpoints at Annex VII-X should show unacceptable variation and vice versa.

ABSTRACT NUMBER: 5139 **Poster Board Number:** K693
TITLE: Evaluating the Sensitivity of Toxicological Endpoints in the Safety Assessment of FCS Impurities

AUTHORS (FIRST INITIAL, LAST NAME) AND INSTITUTIONS: *S. Rattan*[1], A. K. Alexander[1], M. Ferguson[2], T. Cheng[1], and *S. V. Kabadi*[1]. [1]Division of Food Contact Substances, Office of Premarket Additive Safety, Office of Food Chemical Safety Dietary Supplements and Innovation, HFP/US FDA, College Park, MD; and [2]Division of Surveillance and Data Integration, Office of Surveillance, Strategy, and Risk Prioritization, HFP/US FDA, College Park, MD.
KEYWORDS: Regulatory/Policy; Food Safety; Carcinogenesis

ABSTRACT: Background and Purpose: The Federal Food Drug, and Cosmetic Act (FD&C Act) requires pre-market authorization of food contact substances (FCSs) by FDA. FDA considers whether available scientific information demonstrates that the intended use of an FCS is safe, which includes evaluating the safety of the FCS and its impurities. FDA's safety assessment of an FCS and its impurities is based on a tiered approach such that the toxicological data requirements vary with the increase in dietary exposure. In general, regardless of the dietary exposure, the potential for carcinogenicity must be addressed and if the dietary exposure is ≥ 2.5 µg/kg bw/d, systemic toxicity data are recommended to evaluate safety of FCS and impurities. Due to differences in the mechanisms of action underlying carcinogenicity and systemic toxicity, FDA's approach to assessing the risks associated with carcinogenicity differs from the approach to assessing the risks associated with systemic toxicity. In the case of carcinogenicity, toxicological data demonstrate that potential carcinogens act via a non-threshold mechanism, meaning that low levels of dietary exposure potentially increase the risk of cancer development. Systemic toxicity, however, often has a threshold effect or dose-dependent response, such that a dose level below which no toxic effects are observed. The purpose of this work was to build upon FDA's previous assessment (Rulis, 1987) and reevaluate the sensitivity of both toxicological endpoints using a potency-based comparison approach and basic toxicological risk assessment principles. **Methods:** Toxicological data available in agency files as well as published literature were used to identify 50 substances with both carcinogenicity and systemic toxicity data. These data were used to identify suitable points of departure: Unit Cancer Risk for carcinogenicity and No Observed Adverse Effect Level (NOAEL) for systemic toxicity. For carcinogenicity, a Lifetime Cancer Risk (LCR) of one in one million was performed, whereas for systemic toxicity, a comparison of Margin of Exposure (MOE) with

the acceptable Margin of Safety (MOS) were used to draw a potency-based assessment of the two toxicological endpoints for all substances. This analysis included the comparison of dietary exposure estimates that exceed FDA's safety threshold for each toxicological endpoint using statistical models based on a test of centrality and measure of variability. **Results:** By comparing the dietary exposure that exceeded FDA's safety threshold, FDA identified that carcinogenic studies resulted in a lower dietary exposure than systemic toxicity studies indicating that carcinogenicity is a more conservative toxicological endpoint compared to systemic toxicity. **Conclusions:** Our potency-based comparison, using fundamental toxicological principles and statistical analysis of 50 chemicals, demonstrates that carcinogenicity is a more sensitive and conservative toxicological endpoint than systemic toxicity. Our results are further supported by the understanding that carcinogenicity is based on a non-threshold mechanism whereas potential for systemic toxicity is generally assessed by considering dose-dependent and statistically significant effects which are concluded to be biologically relevant differences.

ABSTRACT NUMBER: 5140 **Poster Board Number:** K694

TITLE: Enhanced systematic process for the US FDA's post-market assessment of chemicals in food

AUTHORS (FIRST INITIAL, LAST NAME) AND INSTITUTIONS: D. Hlavaty, M. R. Barr, *D. E. DeGroot*, J. Downey, D. Folmer, J. Heilman, S. Murphy, J. W. Steele, K. Middleton, J. Van Doren, and K. Arvidson. U.S. Food and Drug Administration, College Park, MD.

KEYWORDS: Food Safety; Regulatory/Policy; Regulatory Science/Regulatory Toxicology

ABSTRACT: Background and Purpose: The Human Foods Program (HFP) within the U.S. Food and Drug Administration (FDA, we) is tasked with ensuring the safety of the nation's food supply. This includes the assessment of chemicals in food, including food additives, color additives, generally recognized as safe substances, food contact substances, and chemical contaminants. In August 2024, the FDA published a Discussion Paper on the development of an enhanced systematic process for the post-market assessment of chemicals in food. This paper broadly outlined a proposed approach for a systematic process for the FDA to proactively identify and target chemicals currently in the food supply for assessment. The Discussion Paper included six questions for public consideration, and we opened a docket for public comment at the time of its publication. In September 2024, the FDA held a public meeting to share details about the systematic process and hear stakeholder perspectives on the proposal. Here we present updated information on the FDA's systematic process for the post-market assessment of chemicals in food. **Methods:** We received over 70,000 comments which we carefully reviewed to inform our thinking and assist us in further developing the proposed process. All stakeholder feedback from both the public meeting and the submitted comments were evaluated. Following the evaluation of public comments for common themes and specific feedback, we updated the enhanced systematic process for post-market assessment of food chemicals. **Results:** The updated process encompasses four main steps: (1) signal identification and triage; (2) prioritization; (3) scientific assessment; and (4) risk management. First, machine learning algorithms and manual review are used to identify data or information (i.e., signals) which may impact food safety or public health. For example, these signals may identify a potential hazard or changes in the dietary exposure for a food chemical. The signals are triaged for substantiveness and relevance to food safety, including signals that indicate an immediate health risk. Signals that are appropriate for assessment are moved into step two, prioritization, and the remaining signals are addressed through other FDA processes as appropriate. During prioritization, food chemicals are ranked using a peer-reviewed prioritization tool developed in

the HFP. This tool is used to score a set of criteria evaluating candidate chemicals to assign priority for further review using a Multi-Criteria Decision Analysis (MCDA) framework. Food chemicals which score highly in the prioritization tool move to the next stage, step three. Scientific assessments are evaluations of scientific and technical knowledge and the comprehensive synthesis of that knowledge. Depending on the regulatory context, the FDA may conduct several different types of scientific assessments to address safety, risk, hazard, or other aspects. The FDA's scientific assessments incorporate data from all available sources, including agency records, peer-reviewed publications, and data provided by stakeholders either confidentially or through public requests for information. Preliminary scientific assessments will undergo peer review and/or public comment, as appropriate. Following evaluation of feedback, the FDA will finalize and publish the final scientific assessment. Finally, if action is needed to ensure the safety of the food supply, the FDA will also publish a risk management plan (step four) including, but not limited to, revoking or amending authorizations or approvals for certain uses. **Conclusions:** The HFP has developed a robust, science-driven, and transparent process for the assessment of chemicals in food. This process utilizes cutting-edge artificial intelligence and an MCDA framework to detect, characterize, and assess potential adverse health effects from food chemicals. This systematic yet flexible process ensures that regulatory decisions reflect current toxicological science and are based on the best available scientific evidence.

ABSTRACT NUMBER: 5141 **Poster Board Number:** K695

TITLE: Decision Trees to ensure animal testing as a last resort: Acute Oral Toxicity in the European Union as initial case example

AUTHORS (FIRST INITIAL, LAST NAME) AND INSTITUTIONS: *C. Willett*[1], and G. Pallocca[2]. [1]Humane World for Animals, Washington, DC; and [2]Humane World for Animals, Brussells, Belgium.

KEYWORDS: Nonanimal; Toxicity; Acute; Hazard Identification/Reduction; Decision Framework

ABSTRACT: Background and Purpose: Several global chemical regulations require animal testing only as a last resort, implying that *in vivo* testing should occur only when necessary for safety decisions and no suitable non-animal methods (NAMs) are available. Nevertheless, animal testing is often carried out for endpoints with available, suitable non-animal methods. highlighting the need for clearer guidance and stronger regulatory accountability. Building on the Animal Free Safety Assessment (AFSA) Collaboration's analysis (Macmillan et al. 2024), AFSA has initiated a project to develop guidance in the form of decision-trees (DTs) to provide a framework for transparent decision-making and communication to support, to support the regulatory use of NAMs and compliance with the last-resort. **Methods:** AFSA convened a workshop of global scientific and regulatory expert in April 2025, to develop the Decision Tree concept, outline DTs for 4 key regulatory endpoints (acute oral toxicity, skin and eye irritation, skin sensitization), create working groups to develop each DT, and chart the way to regulatory implementation. The results of this workshop have recently been published (Willett et al. 2025). Development of individual DTs is continuing by expert groups via conference calls and emails. The acute oral toxicity (AOT) DT has been drafted and submitted for publication (submitted). **Results:** The DTs integrate waiving and other principles described in regulatory guidance along with suitable NAMs to ensure the integration of state-of-the art science into risk assessment decision processes. As an initial application of the framework, an AFSA expert group is developed a specific DT for Acute Oral Toxicity within the context of EU REACH and CLP regulations. For this endpoint, the Collaborative Acute Toxicity Modeling Suite (CATMoS), recognized for its high performance and regulatory relevance, is featured as a

leading example of a ready-to-implement NAM for AOT assessment. This presentation will feature key sections of the DT. **Conclusions:** The DT framework provides thorough and detailed guidance for addressing regulatory endpoints through appropriate use of NAMs, while also providing a mechanism for transparent communication of both results and the decision process By enhancing accountability and NAM integration, this project aims to accelerate the shift to non-animal assessments, setting a precedent for broader regulatory adoption. References: Macmillan DS, Bergqvist A, Burgess-Allen E, et al. The last resort requirement under REACH: From principle to practice. *Regul Toxicol Pharmacol*. 2024;147:105557. doi:10.1016/j.yrtph.2023.105557. Willett C, Pallocca G, Carusi A, et al. The Decision Tree approach as a strategy for the global phase out of animal testing for acute and local toxicity for chemicals: recommendations from an expert workshop. *Regul Toxicol Pharmacol*. Published online October 22, 2025. doi:10.1016/j.yrtph.2025.105969

ABSTRACT NUMBER: 5142 **Poster Board Number:** K696

TITLE: Challenges for evaluating the safety of 'probiotic' ingredients added to preterm infant formula

AUTHORS (FIRST INITIAL, LAST NAME) AND INSTITUTIONS: *J. Gingrich*, K. Overbey, K. Kaneko, and R. Morissette. FDA, College Park, MD.

KEYWORDS: Developmental Toxicity; Post-Natal; Regulatory/Policy; International Harmonization; Probiotic

ABSTRACT: Background and Purpose: Preterm infants face heightened risks of infection and disease due to increased gut penetrance, which compromises their ability to regulate gastrointestinal microbial translocation. While oral consumption of live microorganisms, commonly referred to as “probiotics,” has been part of the human diet in fermented foods such as yogurt, sauerkraut, and kimchi, concerns remain regarding the safe use of live microorganisms in risk-prone populations such as preterm infants. The safety of “probiotics” intended to be added to infant formula presents a significant and complex challenge for regulators, who must ensure that the use of such food ingredients meet the U.S. FDA’s requirement for safety, defined as a reasonable certainty of no harm. This complexity stems from a combination of product variability (i.e., microbial strains and use levels), a heterogenous preterm infant population, and a safety standard that does not consider potential benefits. **Methods:** A review of the currently available literature on "probiotic" use in term and pre-term infants was used to inform this discussion. **Results:** A large body of literature exists regarding hazard identification for oral consumption of live microorganisms by infants. These data are complicated by studies intended to inform on efficacy of "probiotics" in treating complex neonatal morbidities. **Conclusions:** At this time, “probiotics” intended for use in preterm infant formula has not been shown to meet the reasonable certainty of no harm standard. Additional research and regulatory considerations are necessary before determining if “probiotic” use in preterm infant formula is safe.

ABSTRACT NUMBER: 5143 **Poster Board Number:** K697

TITLE: Cannabis Compliance Testing Data Analysis of Cannabinoids, Microbes, Mycotoxins and Terpenes in Maryland

AUTHORS (FIRST INITIAL, LAST NAME) AND INSTITUTIONS: *M. A. Cross*, *T. C. Somyk*, *R. S. Haney*, *K. D. Conrow*, K. G. Sweat, T. M. Cahill, and *M. C. Leung*. Arizona State University, Glendale, AZ.

KEYWORDS: Chemical Entity; Cannabis

ABSTRACT: Background and Purpose: As a regulatory measure to standardize cannabis and mitigate the harmful effect of cannabis contaminants, cannabis and cannabis products often require passing in compliance testing to be sold in state-legalized cannabis markets in the U.S. The testing panel includes analytes that are important to product quality (e.g. cannabinoids and terpenes) and patients safety (e.g., microbes and mycotoxins). **Methods:** We analyze the cannabis compliance testing data on cannabinoids, microbes and mycotoxins, terpenes, and other product qualities from the Maryland Cannabis Administration. The data was requested for products including raw plant material (buds and shake/trim), concentrates, and inhalable vape concentrates tested from January 9, 2017 to January 11, 2026. **Results:** There were 183,312 total samples between buds (n = 130,310), concentrates (n = 22,896), vape carts (n = 21,464), and shake/trim (n = 8,642). Total tetrahydrocannabinol (THC) content, including tetrahydrocannabinolic acid (THCA), was calculated using delta 9-THC (%) + 0.877 THCA (%) and showed the lowest average value in shake/trim (13%), followed by buds (23%), concentrates (72%) and vape carts (80%). Total cannabidiol (CBD) content, including cannabidiolic acid (CBDA), was calculated using CBD (%) + 0.877 CBDA (%) and showed the lowest average value in buds (0.15%), followed by shake/trim (0.23%), concentrates (0.73%) and vape carts (1.0%). The maximum value for total THC in each product category was 61% in shake/trim, 73% in buds, 72% in concentrates, and 94% in vape carts. The maximum value for total CBD in each product category was 36% in buds, 17% in shake/trim, 100% in concentrates, and 76% in vape carts. There were 735 samples (0.4%) that had detectable levels of aflatoxin B1, aflatoxin B2, aflatoxin G1, aflatoxin G2, and ochratoxin A. No samples had levels higher than 20 ppb of each individual aflatoxin. However, 4 samples failed the mycotoxin screen with levels higher than 20 ppb of ochratoxin A. Microbial tests on 4 different analytes (total yeast and mold count, total aerobic microbial count, *E. coli*, and *Salmonella spp*.) showed 6,306 (3.4%) different samples failing Maryland's regulatory action levels. Raw plant material samples were also tested for water activity and 906 (0.65%) failed the quality control limit set by Maryland. Fifty nine of those samples also failed at least one of the other microbial or mycotoxin limits set. Maryland tested the content of 17 terpenes in the samples. The three terpenes with the highest average concentration in all products were beta-caryophyllene, limonene, and beta-myrcene. Beta-caryophyllene concentrations averaged 0.46% in buds, 0.30% in shake/trim, 1.0% in concentrates, and 0.89% in vape carts. Limonene concentrations averaged 0.44% in buds, 0.24% in shake/trim, 0.95% in concentrates, and 1.2% in vape carts. Beta-myrcene concentrations averaged 0.43% in buds, 0.20% in shake/trim, 0.85% in concentrates, and 1.0% in vape carts. **Conclusions:** Vape concentrations had the highest percentage concentration of both CBD and THC, followed by concentrates while buds and shake/trim had relatively lower concentrations. Even in product categories with relatively low averages of cannabinoids, individual products can reach higher percentages than other more traditionally potent products highlighting the need for clear cannabinoid content labeling. Terpene content is also varied, which is important to consider as they may also play a role in deterring microbiological growth, and potentially enhancing pharmacological effects of THC.

ABSTRACT NUMBER: 5144 **Poster Board Number:** K698

TITLE: Quantification of Novel Urinary Renal Safety Biomarkers for the Detection of Glomerular Injury in Clinical Samples

AUTHORS (FIRST INITIAL, LAST NAME) AND INSTITUTIONS: A. Vogt[1], R. Kretz[1], E. Paul[2], S. Sutradhar[2], Y. Gu[2], S. L. Samodelov[3], H. Planatscher[1], L. Ramaiah[4], S. Ramaiah[5], T. S. Zabka[6], W. E. Glaab[2], N. M. King[7], H. Seeger[8], and O. Poetz[1]. [1]SIGNATOPE, Reutlingen, Germany; [2]Merck & Co., Inc., Rahway, NJ; [3]University of Zurich, Zurich, Switzerland; [4]Johnson & Johnson, Springhaouse, PA; [5]Pfizer, Cambridge, MA; [6]Genentech, San Francisco, CA; [7]Critical Path Institute, Tucson, AZ; and [8]Cantonal Hospital Baden, Baden, Switzerland. Sponsor: O. Poetz, International Society for the Study of Xenobiotics

KEYWORDS: Biomarkers; Kidney; Safety Pharmacology; Glomerular Biomarker; Proteomics

ABSTRACT: Background and Purpose: Urinary biomarkers for tubular kidney damage are often used in nonclinical safety assessments. However, there are limited biomarkers that can detect drug-induced glomerular damage, particularly subclinical damage that occurs before changes in estimated glomerular filtration rate (eGFR) or albuminuria. The Translational Safety Biomarker Pipeline (TransBioLine) initiative aims to validate and implement new biomarkers for drug-induced organ injury contexts of use and improve the mechanistic understanding of renal safety risks. **Methods:** We developed and validated multiplex immunoaffinity LC-MS/MS assays for use in human urine to detect the following proteins: Nephrin (NPHS1), podocin (NPHS2) and Podocalyxin (PODXL) from podocytes; markers of tubular damage, such as neutrophil gelatinase-associated lipocalin (NGAL) and kidney injury molecule-1 (KIM-1); and vascular-associated proteins, such as vascular cell adhesion molecule-1 (VCAM-1) and matrix metalloproteinase-3 (MMP-3). Urine samples from patients with histologically confirmed glomerular damage (n =49) and healthy subjects (n = 50) were analyzed. **Results:** Elevated urinary albumin-to-creatinine ratios were associated with increased levels of podocyte and vascular biomarkers. NGAL, PODXL, MMP3, and VCAM1 were significantly higher in cases of glomerular damage than in the control group. VCAM1 showed the strongest discriminatory power. NPHS1, NPHS2 and PODXL demonstrated moderate discrimination overall, but were significantly higher in patients with preserved or mildly impaired renal function (eGFR ≥ 60 mL/min/1.73 m²). They remained unchanged or decreased in patients with more advanced impairment. **Conclusions:** These data support the usefulness of a multi-component urine biomarker panel that encompasses glomerular, tubular, and vascular damage pathways for detecting and monitoring kidney damage in the context of safety assessment. Ongoing and future longitudinal studies in high-risk populations, including patients with pre-eclampsia and those treated with VEGF inhibitors for cancer, will further clarify how these biomarkers perform over time and what added value they offer compared to conventional clinical measurements.

ABSTRACT NUMBER: 5145 **Poster Board Number:** K699

TITLE: Validation and Early Clinical Evaluation of Mechanistic Protein Biomarkers for Drug-Induced Liver Injury

AUTHORS (FIRST INITIAL, LAST NAME) AND INSTITUTIONS: T. Meisinger[1], H. Planatscher[1], J. P. Grove[2], K. M. Pearson[3], S. Samodelov[4], S. Ramaiah[5], G. A. Kullak-Ublick[6], G. P. Aithal[2], and O. Poetz[1]. [1]SIGNATOPE, Reutlingen, Germany; [2]University of Nottingham, Nottingham, United Kingdom; [3]Merck & Co., Inc., Rahway, NJ; [4]University of Zurich, Zurich, Switzerland; [5]Pfizer, Cambridge, MA; and [6]Novartis, Zurich, Switzerland. Sponsor: O. Poetz, International Society for the Study of Xenobiotics

KEYWORDS: Biomarkers; Liver; Safety Pharmacology; Targeted Proteomics

ABSTRACT: Background and Purpose: Drug-induced liver injury (DILI) is a major cause of clinical trial failures and post-marketing drug withdrawals. The lack of specific biomarkers for accurate identification and prognostic assessment remains a significant challenge in clinical practice. The international Translational Safety Biomarker Pipeline (TransBioLine) project is investigating mechanistic protein biomarkers to improve DILI characterization, complementing established markers such as albumin and transaminases. Macrophage colony-stimulating factor 1 receptor (MCSF1R), osteopontin (OPN), high mobility group protein B1 (HMGB1), glutamate dehydrogenase (GLDH), keratin 18 (K18) and caspase-cleaved keratin 18 (ccK18) reflect apoptotic, necrotic and immunological processes implicated in DILI pathogenesis. **Methods:** A multiplexed assay combining immunoprecipitation with mass spectrometric readout was developed and validated in accordance with “FDA Guideline M10 Bioanalytical Method Validation and Study Sample Analysis common industry practices” for HMGB1, OPN, MCSF1R and GLDH. In addition, commercially available immunoassay kits were validated for K18 and ccK18. The three biomarker assays used by the TransBioLine consortium met the validation requirements specified in their respective method validation plans. **Results:** Sex-stratified reference data were generated from healthy volunteers sampled at a single time point (n = 44 males, n = 46 females), establishing reference ranges for all biomarkers except HMGB1 in females. In an independent healthy volunteer cohort (n = 48), the effects of fasting and feeding were evaluated, revealing significant fasting-related variation for two biomarkers. Using the validated assays, learning-phase data were generated from single time-point samples obtained from patients with suspected DILI (n = 100), nonalcoholic or alcoholic fatty liver disease (n = 53), psoriasis or rheumatoid arthritis (n = 29), and healthy volunteers (n = 50). Preliminary analyses indicate substantially higher median biomarker concentrations in suspected DILI cases compared with healthy and non-DILI controls across all measured markers, supporting their potential utility for DILI characterization. **Conclusions:** A multiplexed assay combining immunoprecipitation with mass spectrometric readout was developed and validated in accordance with “FDA Guideline M10 Bioanalytical Method Validation and Study Sample Analysis common industry practices” for HMGB1, OPN, MCSF1R and GLDH. In addition, commercially available immunoassay kits were validated for K18 and ccK18. The three biomarker assays used by the TransBioLine consortium met the validation requirements specified in their respective method validation plans.

ABSTRACT NUMBER: 5146 **Poster Board Number:** K700
TITLE: Comprehensive Reference Values for Clinical Pathology Parameters in Cynomolgus Monkeys (*Macaca fascicularis*)

AUTHORS (FIRST INITIAL, LAST NAME) AND INSTITUTIONS: *J. Stanley*[1], and R. Bell[2]. [1]Labcorp Early Development Laboratories Inc., Greenfield, IN; and [2]Labcorp Early Development Laboratories Inc., Madison, WI.
KEYWORDS: Biomarkers; Preclinical Assessments; Safety Evaluation

ABSTRACT: Background and Purpose: Nonhuman primates, particularly cynomolgus monkeys (*Macaca fascicularis*), are used in biomedical and toxicological research because of their close genetic, physiological, and metabolic similarities to humans. Establishing reliable baseline reference data for clinical pathology parameters is essential for interpreting treatment-related changes, monitoring animal health, and guiding appropriate clinical management. **Methods:** In this study, comprehensive reference values were established for hematological, biochemical, coagulation, and urinalysis parameters in cynomolgus monkeys, with an emphasis on evaluating sex-related differences. Historical control data collected from studies conducted at a Labcorp facility between 2014 and 2024 were analyzed, and from those data, clinical observations and body weights were evaluated to assess the health status of the animals. **Results:** Significant sexual dimorphism was observed in body weight and several clinical pathology parameters, including hematocrit, hemoglobin, red blood cell count, blood urea nitrogen, total bilirubin, alkaline phosphatase, creatine kinase, gamma-glutamyl transferase, and lactate dehydrogenase. Comparison with previously published data revealed discrepancies in several biochemical markers, which may reflect differences in age, sex distribution, geographic origin, fasting state, use of anesthetics, or analytical methods. **Conclusions:** Overall, this study provides comprehensive and updated reference data for clinical pathology parameters in cynomolgus monkeys, offering valuable benchmarks for the evaluation of data from preclinical studies and biomedical research involving nonhuman primates.

ABSTRACT NUMBER: 5147 **Poster Board Number:** K701
TITLE: Silk Fibroin Nanoparticles as Drug Carriers: Biocompatibility and Immunological Characterization

AUTHORS (FIRST INITIAL, LAST NAME) AND INSTITUTIONS: B. Rodrigues[1,2,3], A. Ramos[2], S. Silva[2,4], R. Pereira[5], A. Fonseca[3], J. Coelho[3,6], *M. Cruz*[1,2], and R. Fonseca[3,6]. [1]Center for Innovative Biomedicine and Biotechnology (CIBB) and Center for Neurosciences and Cell Biology (CNC), Coimbra, Portugal; [2]Faculty of Pharmacy, University of Coimbra, Coimbra, Portugal; [3]CEMMPRE, ARISE, Department of Chemical Engineering, Faculty of Sciences and Technology, University of Coimbra, Coimbra, Portugal; [4]Center for Innovative Biomedicine and Biotechnology (CIBB) and Coimbra Institute of Clinical and Biomedical Research (iCBR), University of Coimbra, Coimbra, Portugal; [5]Chemistry Center and Chemistry Department, University of Minho, Braga, Portugal; and [6]Instituto Pedro Nunes (IPN), Associação para a Inovação e Desenvolvimento em Ciência e Tecnologia, Coimbra, Portugal.
KEYWORDS: Biomaterial; Cytotoxicity; Inflammation; Silk Fibroin

ABSTRACT: Background and Purpose: Biomaterials should be biodegradable, non-toxic, and designed to minimize the risk of triggering inflammatory or immune responses. Silk fibroin (SF) is a natural polymer with exceptional mechanical strength and remarkable biological properties. **Methods:** This study aimed to evaluate the biological activity of silk fibroin nanoparticles (SFNPs), focusing on their potential as drug

delivery systems and their biocompatibility, while ensuring that they do not trigger inflammatory responses. SFNPs were prepared using the nanoprecipitation method and were thoroughly characterized. For the first time, the immunogenicity and inflammatory potential of SFNPs were investigated in peripheral blood mononuclear cells (PBMCs), monocytes, and T cells, isolated from the buffy coats of healthy donors. The cytotoxic effects of SFNPs were assessed in PBMCs, and T cell proliferation and activation in response to SFNPs exposure were also evaluated. In addition, monocytes were differentiated into dendritic cells (mo-DCs) to evaluate the impact of SFNPs on their maturation, which is a critical step in the initiation of adaptive immune responses. **Results:** SFNPs did not induce mo-DCs maturation, nor did they promote the proliferation or activation of $CD4^+$ and $CD8^+$ T cells, suggesting that SFNPs are not recognized as foreign by the immune system. The pro-inflammatory potential of SFNPs was further assessed in primary human macrophages. The results showed that SFNPs neither triggered nitric oxide release nor increased the expression of pro-inflammatory proteins, including inducible nitric oxide synthase, pro-interleukin-1β, and cyclooxygenase-2. **Conclusions:** Overall, the SFNPs exhibited safety and bio-inert behavior, showing no evidence of immune recognition, cellular activation, or pro-inflammatory mediators. These findings highlight the significant advantages of SF in biomedical applications, such as minimizing inflammatory reactions and immune rejection. Owing to these properties, SF emerges as a versatile biomaterial for next-generation drug delivery systems, with the potential to enhance clinical outcomes across various therapeutic areas.

ABSTRACT NUMBER: 5148 **Poster Board Number:** K702
TITLE: Leveraging Pulmonary Nanotoxicological Discoveries for the Design of Inhalable Nanotherapeutics

AUTHORS (FIRST INITIAL, LAST NAME) AND INSTITUTIONS: H. Meng. National Center for Nanoscience and Technology, Beijing, China. Sponsor: *X. Cao*
KEYWORDS: Nanoparticles; Biotransformation; Inflammation

ABSTRACT: Background and Purpose: Extensive research in pulmonary nanotoxicology has uncovered key mechanisms of nanoparticle-induced toxicity, including frustrated phagocytosis and NLRP3 inflammasome activation in lung-resident macrophages. These findings, combined with size-dependent lung deposition patterns, underscore the role of macrophages in clearing inhaled nanomaterials, particularly in occupational exposures. **Methods:** Building on these insights, we designed an inhalable lipid-based nanoparticle encapsulating a resolvin precursor, phosphatidylcholine, and polyethylene glycol to enhance lung permeability and mucosal barrier crossing. **Results:** These nanoparticles efficiently biodistributed in the lungs via inhalation, mitigating nanomaterial-induced inflammation and fibrosis triggered by graphene oxide, rare earth particles, and PM2.5. They reduced lipid peroxidation-driven NLRP3 activation, suppressed NF-κB signaling in macrophages, and modulated ROS-mediated TGF-β/Smad and S1P pathways in epithelial cells at ng/mL dosimetry. Recent scaled-up synthesis demonstrated reproducible particle production, high stability, optimal anti-fibrotic efficacy, and *in vivo* biocompatibility, validated in murine models. **Conclusions:** Overall, these findings highlight the therapeutic potential of this inhalable lipid-based platform for the prevention and treatment of particle-induced pulmonary injury.

ABSTRACT NUMBER: 5149 **Poster Board Number:** K703

TITLE: *Drosophila melanogaster* Tracheal System Morphometry: Implications for Inhaled Dosimetry Predictions

AUTHORS (FIRST INITIAL, LAST NAME) AND INSTITUTIONS: A. E. Santana-Cruz[1], *K. Y. Fuentes Torres*[1], E. Rodriguez-Borrero[2], and *L. B. Mendez*[1]. [1]Universidad Ana G. Mendez, Carolina, Puerto Rico; and [2]University of Puerto Rico, Cayey Campus, Cayey, Puerto Rico.

KEYWORDS: Respiratory Toxicology; Non-Mammalian Species; Dosimetry; Particulate matter

ABSTRACT: Background and Purpose: The fruit fly (*Drosophila melanogaster*) is a well-established model organism increasingly used as an alternative *in-vivo* model for toxicology testing. Recent studies have reported its use in assessing the toxicity of inhaled substances including volatile organic compounds (VOCs), cigarette smoke, and nanoparticles. Our goal is to develop *Drosophila* as a model for assessing particulate matter neurotoxicity. The fruit fly is a candidate model for inhalation studies since it possesses a tracheal system with a hierarchical branching structure ending in alveolar-like sacs. This system is well characterized at the morphological, cellular, and molecular level. However, there is limited quantitative data of its geometry which is essential for aerosol dosimetry analyses. Therefore, the objectives of this study were 1) to perform morphometric characterization of the *Drosophila* tracheal system, and 2) evaluate the feasibility of using the NCRP lung deposition model for predicting particle deposition efficiencies. **Methods:** To characterize the *Drosophila* tracheal system, third-instar larvae were fixed with 4% paraformaldehyde and either dissected or immersed in lactic acid/glycerol for 18 hours to visualize the tracheoles for quantitative anatomical description. Images acquired at 10x magnification were analyzed with ImageJ to measure diameters, lengths, branching angles, and inclination angles. A typical path model was developed from morphometric measurements of three larvae. Predicted particle deposition for unit density particles ranging from 0.001 to 10 μm in diameter were calculated with the NCRP lung deposition model equations. Equivalent ventilatory parameters were estimated from CO_2 production assuming continuous spiracle opening and a tracheal CO_2 fraction of 0.2-0.6%. **Results:** The larvae used for the analysis were 4.82 ± 0.20 mm long and 1.15 ± 0.08 mm wide. The *Drosophila* larva tracheal system is bilateral, with anterior and posterior spiracles (openings) connecting to paired dorsal trunks. Posterior spiracles averaged 0.105 mm in diameter and anterior spiracles 0.058 mm. Dorsal trunks measured 4.62 ± 0.46 mm in length and 0.09 ± 0.03 mm in diameter, with the largest diameter at its posterior end, where it connects to the posterior spiracle which serves as the main entry of air into the tracheal system when the larva hatches. Two anastomoses join the dorsal trunks; the anterior anastomosis was eight times longer than the posterior. Six generations were identified and designated as: spiracles (G0), dorsal trunks (G1), anastomoses (G2), transverse connectives (G3), visceral branches (G4), lateral trunks (G5), and ganglionic branches (G6). G3 and G4 diameters ranged from 0.024 to 0.035 mm and lengths from 0.36 to 0.60 mm. Measurements from lactic acid preparation were within 10% of dissected samples. Predicted deposition efficiencies tended to overestimate particle deposition, although most particles are expected to be retained in the spiracles. **Conclusions:** A preliminary typical path model was established for the *Drosophila* larva tracheal system, incorporating detailed morphometric measurements up to G4. The airway lengths are comparable to those reported for human terminal bronchioles, although the diameters were smaller approximately by an order of magnitude. While the NCRP lung model equations can be applied to estimate particle deposition in the fruit fly, more advanced computational approaches will be required for extrapolation to rodent and human systems, as insect ventilatory dynamics differ fundamentally from those of

mammals. Additionally, incorporating an inhalability factor specific to spiracle-mediated air intake will be necessary to refine particle deposition predictions. Future studies will focus on generating a complete morphometric model of the *Drosophila* tracheal system and validating the fruit fly inhalation model with empirical particle deposition data.

ABSTRACT NUMBER: 5150 **Poster Board Number:** K704
TITLE: Mealworm Treats as an Effective Vehicle for Dosing of PFAS in Mouse Exposure Models: QC and Dose Validation

AUTHORS (FIRST INITIAL, LAST NAME) AND INSTITUTIONS: S. G. Dame, M. Collard, *D. C. Dolinoy*, and K. E. Manz. University of Michigan, School of Public Health, Ann Arbor, MI.
KEYWORDS: *In Vivo* Models; Perfluoronated Agents; Exposure Assessment; Per- and polyfluoroalkyl substances (PFAS)

ABSTRACT: Background and Purpose: Per- and Polyfluoroalkyl Substances (PFAS) are synthetic chemicals that are ubiquitous in humans and the environment, and exhibit unique chemical properties. Perfluorooctanoic Acid (PFOA), a legacy PFAS, is of great toxicological interest as it is found in the serum of > 99% of the human population, and is associated with a number of adverse health outcomes. In animal exposure studies, validation of toxicant dose and background levels of ubiquitous chemicals is often not reported, and methods for dose validation are non-standardized. Mealworm treats are an emerging and promising vehicle for dosing of toxicants within mouse models, especially for chemicals with unique behaviors and properties, such as PFAS. Here, we provide a simple method for Ultra-High Performance Liquid Chromatography-High Resolution Mass Spectrometry (UHPLC-HRMS) validation of PFOA dose concentrations in mealworm treats, background screening for multiple PFAS in exposure controls, and laboratory considerations for reducing PFAS contamination in controls. **Methods:** PFAS concentration testing of stock solutions, and naive and PFOA-injected mealworm extracts, was done via a targeted UHPLC-HRMS screen of the 40 major PFAS analytes highlighted in EPA method 1633. Stock solutions were prepared in de-ionized water at high concentration, with concentrations confirmed via targeted UHPLC-HRMS analysis and dilution prior to injection into mealworms. Solutions were heated and vortexed prior to injection to ensure full dissolution and homogeneity. Mealworms were injected with 20 uL of concentrated solution, checked for leakage, and snap-frozen prior to homogenization. Both injected and naive mealworm larvae were snap-frozen on dry ice and homogenized via bead rupturing, and PFAS were extracted in acetonitrile with sonication. Care was taken to prevent thawing of mealworms and leakage of solution in the storage and extraction of PFAS. Quality control checks of laboratory materials and reagents were performed, and solvent rinsing of materials was performed to minimize PFAS contamination in the preparation and extraction processes. Mealworm treats were administered daily to mouse dams for 54 days, as part of a perinatal exposure, and dams were monitored to ensure the entire treat was consumed. Post-exposure, blood sampling and quantitative analysis of PFOA in serum was done to confirm internal dose. **Results:** Trace levels of several PFAS were detected in background samples and experimental controls of mealworm treats. Efforts to reduce background PFAS contamination of controls, including triple-rinsing of laboratory materials with methanol and use of certified PFAS-free extraction solvents, reduced levels of PFOA measured in controls to an average of < 5 ppt. For dose validation, injected PFOA concentrations within mealworms were found to be reasonably consistent and stable, with a coefficient of variation of under 10% for all dose groups. The high-dose PFOA exposure group had an intended dose of 0.125 mg/treat/day and an

average measured dose of 0.1126 mg/treat ± 0.0085 mg, and the low-dose PFOA exposure group had an intended dose of 0.0125 mg/treat/day and an average measured dose of 0.01127 mg/treat ± 0.0018 mg. Water-injected control mealworms had an average measured dose of 2.5E-07 mg/treat ± 4.4E-09 mg, likely due to residual contamination from laboratory materials and trace amounts of PFAS in water. **Conclusions:** Care must be taken to validate and ensure proper dosing of animals in toxicological exposure studies, and to the best of our ability, remove background contamination of ubiquitous chemicals such as PFAS. Mealworms are a valid alternative vehicle for accurate dosing of difficult-to-dose toxicants, as they enable stringent dose preparation, validation, and delivery. The daily nature of mealworm treat exposure allows for modeling of more chronic ingestion exposure. Future work will include similar dose validation with other PFAS chemicals and mixtures, assessment of internal dose at various time points following exposure, and assessment of PFAS distribution and accumulation in various tissues. Exposure to ubiquitous chemicals such as PFAS can be difficult to accurately control and measure, and this work highlights the need for background testing and confirmation of dose, alongside communication of background levels, to promote transparency and consistency in animal toxicological exposure models.

ABSTRACT NUMBER: 5151 **Poster Board Number:** K705
TITLE: Syndromic Antibiogram Analysis in Different Species of NHPs

AUTHORS (FIRST INITIAL, LAST NAME) AND INSTITUTIONS: J. Mota, L. Garcia, H. Chahar, T. Gaytan, and K. Gallegos. VRL, San Antonio, TX. Sponsor: *J. Luyendyk*
KEYWORDS: Biomarkers; antibiotic sensitivity

ABSTRACT: Background and Purpose: Traditional Antibiograms have been significantly important in clinical settings since the early days of Microbiology. Currently, a more detailed option is now available to differentiate the susceptibility of a bacteria to a specific antibiotic, including the analysis of other factors to assess a specific condition. For Non-Human Primates (NHPs), the main purpose of syndromic antibiograms is to improve empiric antibiotic therapy and colony maintenance. Syndromic antibiograms for different species of NHPs can also be of significant help in targeting common pathogens based on the antibiotic response specific to a particular NHP species. **Methods:** In this study, syndromic antibiograms were generated to evaluate susceptibility by NHP according to the species. We collected susceptibility data from Marmosets, Macaques, Cynomolgus, baboons, and spider monkeys in a period of 1 year. The data collected was based on the analysis of disk diffusion antibiotic sensitivity test for *Staphylococcus aureus*, Klebsiella pneumoniae, and *Escherichia coli* pathogens applying standard microbiological techniques. **Results:** Using specialized software, we created specie-specific antibiograms. The antibiograms were analyzed individually and compared with the other species to understand the antibiotic susceptibility rate and differences among NHP species, related to a specific pathogen. **Conclusions:** We will discuss the relevance of using syndromic antibiogram analysis, that could provide significant guidance to colony managers and Microbiology professionals, as well as potentially help improve antibiotic treatment schemes, and monitor changes in antibiotic resistance over time.

ABSTRACT NUMBER: 5152 **Poster Board Number:** K706

TITLE: Pharmacokinetics of Tacrolimus in Sinclair Nanopigs: Comparison of Traditional Blood Sampling and Automated vDBS Collection

AUTHORS (FIRST INITIAL, LAST NAME) AND INSTITUTIONS: N. Navratil[1], H. Beier[2], J. Doherty[3], M. Ahmed[3], S. Velschow[4], A. Braxton[5], T. DeGraw[3], D. Brocksmith[6], *G. Bouchard*[6], C. Rohde Johnson[2], S. Carballo[2], and K. Helke[5]. [1]Sterling Biomedical Resources, LLC, Ontario, NY; [2]BASi Research Products, West Lafayette, IN; [3]Inotiv, West Lafayette, IN; [4]Fluispotter ApS, Vedbæk, Denmark; [5]Medical University of South Carolina, Charleston, SC; and [6]Sinclair Bio Resources, Auxvasse, MO.

KEYWORDS: Pharmacokinetics; Methods/Mechanism; *In Vivo* Models; Minipig; Tacrolimus

ABSTRACT: Background and Purpose: The objective of this study was twofold: (1) to evaluate a novel automated blood sampling device for pharmacokinetic (PK) data collection in miniature swine, and (2) to generate PK data for tacrolimus in this model. Tacrolimus is commonly used as an immunosuppressant in swine for transplantation research, but limited PK data are available to inform appropriate dosing. Traditional PK studies in swine often require repeated handling for blood collection, which can induce stress and potentially confound results. Automated devices may improve animal welfare and data reliability by enabling restraint-free sampling. This study compared the Fluispotter—a wearable device that collects volumetric dried blood spots (vDBS) at programmed intervals—with traditional wet whole blood sampling for assessing tacrolimus PK in Sinclair Nanopigs. **Methods:** Three female Sinclair Nanopigs were surgically implanted with central venous catheters in the right and left jugular veins: one for traditional wet blood sampling and one connected to the Fluispotter device. The Fluispotter was secured on the animal's back and programmed to collect 10 µL vDBS samples on PerkinElmer bio-sample collection paper at specified time points. Pigs received a subcutaneous dose of 0.5 mg/kg tacrolimus. Wet blood samples (1 mL) were collected at eight time points post-dose. Due to prototype malfunctions, complete vDBS data were obtained from only one of the three animals. Tacrolimus concentrations were quantified using LC-MS/MS, with a qualified bioanalytical method for vDBS. Non-compartmental analysis was used to calculate PK parameters. **Results:** PK values from vDBS samples were comparable to those from wet blood in the same animal, with an AUC difference of less than 30%. Values also aligned with previously published data in minipigs and other species. **Conclusions:** This study demonstrates the feasibility of using Sinclair Nanopigs for tacrolimus pharmacokinetic studies. PK profiles obtained using the Fluispotter device were comparable to traditional sampling in one animal, supporting its potential as a low-stress, automated alternative for PK studies in miniature swine. Tacrolimus exposure and distribution in Nanopigs were consistent with published data in other laboratory species. Further studies are warranted to validate the Fluispotter for routine use and assess its performance across a larger cohort.

ABSTRACT NUMBER: 5153 **Poster Board Number:** K707

TITLE: The Sinclair Nanopig is the first miniature swine to use less test compound than Beagle in safety studies

AUTHORS (FIRST INITIAL, LAST NAME) AND INSTITUTIONS: *G. F. Bouchard*, and *D. Brocksmith*. Sinclair BioResources, Auxvasse, MO.

KEYWORDS: *In Vivo* Models; Preclinical Assessments; Safety Evaluation; Sinclair Nanopig

ABSTRACT: Background and Purpose: Nonclinical safety assessment is a critical component of drug development, particularly during the pre-IND and IND-enabling stages when test compound (TC) availability is often severely limited. At this stage, synthesis routes may be inefficient, yields low, and manufacturing costs high, restricting the amount of compound available for safety evaluation. Despite these constraints, regulatory frameworks typically require safety data from both rodent and non-rodent species. Historically, the Beagle has served as the default non-rodent species for general toxicology studies due to its manageable size, established historical database, and relative ease of handling. Non-human primates (NHPs) are used when pharmacological relevance or biological specificity necessitates their inclusion. However, dogs exhibit notable anatomical, physiological, and metabolic differences from humans, and NHP studies are costly, resource-intensive, ethically sensitive, and increasingly constrained by availability. Miniature swine are widely recognized for their close anatomical, physiological, and metabolic pathways similarity to humans. Despite these advantages, their adoption in regulatory toxicology has been limited due to larger body size at sexual maturity and the resulting increased TC requirements relative to dogs and NHPs. The Sinclair Nanopig (SNP) was developed through selective breeding and nutritional management to address this limitation. By achieving sexual maturity at a younger age and smaller body size, SNP enables earlier dosing and reduced TC requirements. The purpose of this work was to evaluate TC usage in SNP relative to Beagles and NHPs for acute and subacute general safety studies and to assess the implications for species selection in early nonclinical development. **Methods:** The SNP was developed over more than a decade using selective breeding strategies focused on reduced growth rate and stabilized adult body size while preserving normal physiology, organ development, and reproductive function. Nutritional management was optimized to support healthy maturation without promoting excessive early weight gain. The downsizing program resulted in the SNP to be 50% smaller than the original Sinclair miniature swine. Comparative analyses were performed between SNP, Beagles, and NHPs. The SNP data was harvested from growth curves and sexual maturity evaluations established at the end of the downsizing program. Growth curve and sexual maturity data were extracted from the literature for the Beagle and NHPs. Sexual maturity was defined as the histological presence of mature spermatozoa in the epididymis for the males and evidence of ovulation and formation of corpora lutea for the females. Test compound requirements were estimated based on standard regulatory toxicology dosing paradigms from the literature, including dose levels, dosing frequency, study duration, and body-weight-adjusted dosing. Finally, the growth curves were realigned relative to the onset of sexual maturity to enable direct comparison of TC usage across species. **Results:** SNPs reached sexual maturity at approximately 4.5 m of age, which is substantially earlier than Beagles (8-10 m of age) and non-human primates (4.1-6.7 y of age), enabling earlier initiation of regulatory safety studies and reduced pre-study growth. When growth curves were adjusted for sexual maturity, SNP demonstrated a significant reduction in TC requirements relative to Beagle. For acute (14- or 28-day) and subacute (90-day) safety studies, SNP required 29.1% and 11.9% less TC than Beagle, respectively. While TC requirements for SNP remained higher than for

NHPs, the gap difference in TC usage was reduced by more than 30% compared to traditional miniature swine models. **Conclusions:** SNP is the first miniature swine model to require less TC than the Beagle for both acute and subacute safety studies while retaining the translational advantages of swine models. Similarly, while the NHP remains more efficient in TC usage, the SNP is more commonly considered as an alternative to NHP during species selection protocols. The SNP resolved a longstanding limitation associated with miniature swine in nonclinical safety assessment—excessive TC requirements. As the first miniature swine shown to outperform the Beagle in compound efficiency, SNP has the potential to reshape species selection strategies, reduce reliance on dogs in research, and support more efficient and scientifically aligned early-stage drug development.

ABSTRACT NUMBER: 5154 **Poster Board Number:** K708
TITLE: Low Sero-prevalence of SARS-CoV-2 in NHPs Between the years 2022 and 2025

AUTHORS (FIRST INITIAL, LAST NAME) AND INSTITUTIONS: J. Mota, L. Tomanek, and L. Contenta. VRL, San Antonio, TX. Sponsor: *J. Luyendyk*
KEYWORDS:; SARS-CoV-2, Seroprevalence

ABSTRACT: Background and Purpose: Severe acute respiratory syndrome coronavirus 2 (SARS-CoV-2) is a highly contagious respiratory virus that causes COVID-19 disease. Between 2019 and 2023, SARS-CoV-2 became a global pandemic causing serious illness and mortality in humans. Both PCR and ELISA tests became quickly available as diagnostic tools to help the efforts in containing the virus and stop the spread. In non-human primates (NHPs) it has been demonstrated the viral replication and RNA presence in the respiratory tract; Rhesus macaques, African green monkeys, and baboons, among others have been used as animal models for COVID-19 disease, however there is limited information of seroprevalence in naturally infected NHPs. The objective of this work was to determine the prevalence of antibodies against SARS-CoV-2 in various NHPs species between 2022 and 2025. **Methods:** We used an indirect ELISA to detect the presence of SARS-CoV-2 antibodies in NHP serum samples. A total of 392 samples from African Greens, Cynomolgus Macaques, Rhesus Macaques, and Baboons, collected between 2022 and 2025 were used. For the ELISA, we used SARS-CoV-2 spike recombinant proteins as the capture antigen. The serum samples, alongside positive and negative controls, were included in each ELISA plate. Based on the negative controls, a cut-off was calculated for each plate, and the sample results were based on the cut-off for that specific plate. **Results:** We tested 102 samples for the year 2022, 101 samples from 2023, 83 samples from 2024 and 106 samples from 2025. Our results showed that out of 392 total samples tested only thirteen NHPs showed a positive reaction to the SARS-CoV-2 spike proteins. This is a positive rate of 3.3%. Of the 13 positive samples, overall, the species of NHP with most reactive samples was Rhesus Macaques. **Conclusions:** Despite the high efficiency of transmission of the SARS-CoV-2 virus in humans, our data shows that between 2022 and 2025 the SARS-CoV-2 sero-prevalence was low in the study population of NHPs. This could be due to many factors, including proper protective equipment of the animal handlers, or the transmission efficacy, among others. Additional studies and data from literature will be discussed.

ABSTRACT NUMBER: 5155 **Poster Board Number:** K709

TITLE: *In Vitro* Plasma Protein Binding of Highly Protein-Bound Compounds: Technical and Regulatory Considerations in the Context of ICH M12

AUTHORS (FIRST INITIAL, LAST NAME) AND INSTITUTIONS: T. Oh, K. Wang, Y. Liu, N. Zhao, and D. Colter. Resolian, Malvern, PA. Sponsor: *R. Klein*

KEYWORDS:

ABSTRACT: Background and Purpose: Accurate characterization of *in vitro* plasma protein binding (PPB) is essential for understanding unbound drug concentration, designing drug-drug interaction (DDI) studies, and translating systemic exposure across species. The 2024 ICH M12 guideline introduced updated expectations for PPB evaluation, emphasizing the need for robust, reproducible methods that can support regulatory decision-making. However, highly protein-bound drugs (fu < 1%) continue to present substantial analytical challenges due to minimal unbound concentrations, assay variability, and differences in plasma matrix composition across species. This work aimed to develop high-precision bioanalytical methods capable of accurately quantifying extremely low unbound fractions and to establish best practices for PPB assessment consistent with evolving regulatory expectations. **Methods:** Highly sensitive LC-MS/MS assays were developed and qualified for two representative highly protein-bound small molecules: warfarin and itraconazole. Method qualification parameters included sensitivity, linearity, selectivity, reproducibility, and recovery across multiple matrices. The assays were applied to an equilibrium dialysis PPB workflow, with plasma collected from five species (human, rat, mouse, dog, and monkey). Protein binding values were benchmarked against published literature ranges and internal historical datasets to assess biological and analytical concordance. In addition, modality-specific considerations were evaluated for emerging therapeutic modalities—oligonucleotides and antibody-drug conjugates (ADCs)—for which ICH M12 provides no explicit PPB guidance. **Results:** The optimized LC-MS/MS methods achieved sub-nanomolar lower limits of quantification and demonstrated strong precision and reproducibility, enabling accurate measurement of unbound fractions below 0.1%. Across species, obtained PPB values for both warfarin and itraconazole were consistent with literature ranges and showed low inter-assay variability, confirming the robustness of the combined analytical and equilibrium dialysis workflow. Matrix-dependent effects were successfully mitigated through optimized extraction and calibration approaches. Furthermore, analysis of emerging modalities identified distinct binding behaviors—such as sequence-dependent interactions for oligonucleotides and linker-payload-driven hydrophobic interactions for ADCs—highlighting the need for tailored assay strategies to ensure meaningful PPB interpretation. **Conclusions:** This work demonstrates that high-quality PPB assessment of highly protein-bound small molecules is feasible using modern LC-MS/MS methods coupled with carefully optimized equilibrium dialysis assays. The validated approach produced reliable binding estimates across species and is well aligned with the expectations of ICH M12 for DDI-relevant *in vitro* studies. For non-traditional modalities, the results outline critical experimental considerations that may guide future regulatory discussions in areas where M12 does not yet provide explicit recommendations. Collectively, these findings support a harmonized bioanalytical framework for PPB evaluation across therapeutic modalities and provide practical insights for enhancing the rigor, reproducibility, and regulatory utility of *in vitro* binding studies.

ABSTRACT NUMBER: 5156 **Poster Board Number:** K710

TITLE: Measuring *In Vitro* Percutaneous Absorption of a Volatile Organic Compound: 1,4-Dioxane

AUTHORS (FIRST INITIAL, LAST NAME) AND INSTITUTIONS: *Z. Wang*[1], V. S. Linda[2], L. Katz[1], J. Zang[1], H. Xie[1], J. Srinivasan[1], P. Manga[1], and *F. A. Beland*[2]. [1]FDA, College Park, MD; and [2]National Center for Toxicological Research, FDA, Jefferson, AR.

KEYWORDS: Chemical of Concern; Percutaneous Absorption; Bioavailability; 1,4-dioxane; 1,4-dioxane

ABSTRACT: Background and Purpose: Using excised human skin samples, we developed a method to assess the percutaneous absorption of 1, 4-dioxane, a representative volatile organic compound, in two different cosmetic matrices: a leave-on lotion and a rinse-off bath product. 1,4-dioxane is a potential carcinogen. It is primarily used as a solvent in many commercial and industrial applications; it is also a byproduct of manufacturing of certain consumer products. In the US, a significant percentage of the general population uses cosmetics. While 1,4-dioxane is not used as an ingredient in cosmetics, it may be present at low levels as a process-related contaminant. Although changes made to the manufacturing process, such as introduction of vacuum stripping, have resulted in a significant reduction in the levels of this contaminant in cosmetics over time, it is still detected in some products, such as lotions, conditioners, bath soaps and bubble baths, at 0.23 - 15.3 µg/g (ppm) in the final product. Thus, understanding the dermal exposure to 1,4-dioxane from the use of cosmetic products and its contribution to the body burden is warranted. While dermal penetration and absorption of 1,4-dioxane have been studied previously, they have not been characterized at exposure levels relevant to consumer usage. The volatility of 1,4-dioxane also presents significant challenges in the accurate measurement of its absorption. Using a modified *in vitro* skin permeation test method, we determined the percutaneous absorption of 1,4-dioxane using real-world use scenarios. **Methods:** Using excised human skin samples from donors, we assessed the percutaneous absorption of 1,4-dioxane in a Franz cell diffusion system using radiolabeled [3H]1,4-dioxane. We used a charcoal filter disk placed on top of the Franz cell to trap any volatile [3H]1,4-dioxane. We used two different cosmetic matrices as the vehicles namely: a skin care lotion, and a baby wash & shampoo. We incorporated [^{3}H]1,4-dioxane into the vehicles at target concentrations of 1, 10, 20 and 50 ppm, levels typically found in cosmetic products. We measured the amount of 1,4-dioxane that penetrated the skin at various time points (0.5, 1, 2, 3, 4, 8, and 24 hrs) using a liquid scintillation counter. Statistical analysis was performed to compare the absorption of 1,4-dioxane present in the two vehicles and to determine the relationship between the applied dose and the amount absorbed. **Results:** Use of the charcoal filter disk to trap evaporated 1,4-dioxane, enabled a total recovery of radiolabeled [3H]1,4-dioxane approaching 80%. An average of 70% of the applied radioactivity was found to be associated with the charcoal filter disk, confirming significant evaporation. For both vehicles, the amount of radioactivity in the receptor fluid of the Franz cell increased rapidly and reached a plateau after approximately 1 hr for all dose groups. There was a linear relationship between the applied concentration of 1,4-dioxane and the amount of 1,4-dioxane recovered in the receptor fluid for both cosmetic vehicles. The extent of absorption did not differ between the two vehicles, at the end of the exposure period, regardless of the levels tested. The absorption levels observed were 2.9% and 2.5% of the applied dose, in the skin care lotion and baby wash & shampoo respectively. Very small amounts of 1,4-dioxane were found in the stratum corneum (0.03% and 0.02%), epidermis (0.17% and 0.13%), and dermis (0.05% and 0.05%) of skin exposed to skin care lotion and baby wash & shampoo, respectively. The levels did not differ between the two vehicles. **Conclusions:** Using a modified *in vitro* method, this study determined the extent of percutaneous absorption of 1,4-dioxane to be

approximately 3% when applied to cosmetic vehicles containing 1, 4-dioxane at concentrations typically found as contaminants in cosmetic products. The results reported were within the range seen in previous studies using both *in vivo* and *in vitro* methods with various other vehicles.

ABSTRACT NUMBER: 5158 **Poster Board Number:** K712
TITLE: Application of Large Language Models for Automated Selection of Literature with Pharmacokinetic Parameters in Pregnancy

AUTHORS (FIRST INITIAL, LAST NAME) AND INSTITUTIONS: *K. Fairman*[1], M. Romanello Joaquim[1], *Y. Zhang*[1], *J. Xu*[1], B. George[2], and *M. Li*[3]. [1]FDA National Center for Toxicological Research, Jefferson, AR; [2]FDA Center for Drug Evaluation and Research, Silver Spring, MD; and [3]FDA Office of Colors and Cosmetics, College Park, MD.
KEYWORDS: Computational Toxicology; Physiologically Based Pharmacokinetics; Safety Pharmacology; Pregnancy

ABSTRACT: Background and Purpose: Pharmacokinetic (PK) data during pregnancy remains sparse and fragmented across the literature due to ethical constraints and safety concerns regarding fetal exposure. Manual curation of pregnancy PK literature is labor-intensive and time-consuming, creating bottlenecks in evidence synthesis for regulatory decision-making. This study developed and validated an automated literature screening system using large language models (LLMs) to identify and classify articles containing pregnancy pharmacokinetic data, with the objective of reducing manual review time while maintaining high sensitivity for relevant literature identification. **Methods:** A systematic approach was implemented using Python programming to interface with the PubMed API. Pregnancy and pharmacokinetic-related search terms were systematically queried to retrieve PubMed identifiers (PMIDs). Full-text articles and abstracts were extracted where available through open access repositories and converted to JSON format for computational analysis. Prompt engineering techniques were employed to develop structured queries incorporating specific inclusion criteria, article formatting requirements, and classification instructions. Two versions of a commercial LLM were evaluated using a manually curated training dataset of previously validated pregnancy PK literature. Performance metrics included precision, recall, and F1-scores calculated against expert-annotated ground truth classifications. **Results:** The LLM-based classification system demonstrated robust performance characteristics. Using full-text articles, the earlier LLM version achieved a precision of 0.50, recall of 1.00, and F1-score of 0.67. The updated LLM version showed improved performance with precision of 0.71, recall of 1.00, and F1-score of 0.83 when analyzing complete articles. Performance degraded substantially when using title-only or title-plus-abstract inputs, with both LLM versions showing reduced accuracy metrics across all performance measures. **Conclusions:** The automated LLM-based screening system provides an effective first-pass filter for identifying pregnancy pharmacokinetic literature from PubMed databases, achieving high sensitivity while substantially reducing manual review burden. This approach enables more efficient allocation of expert reviewer time toward higher-value activities including physiologically-based pharmacokinetic (PBPK) model development and evidence synthesis for regulatory assessments. The comprehensive literature identification facilitated by this system supports more complete pharmacokinetic trend analysis during pregnancy, ultimately contributing to improved drug safety evaluation and dosing guidance for pregnant populations.

ABSTRACT NUMBER: 5159 **Poster Board Number:** K713
TITLE: Efficient Summarization of FDA Drug Labeling Using ChatGPT: A Large-Scale Evaluation Against Human Experts

AUTHORS (FIRST INITIAL, LAST NAME) AND INSTITUTIONS: H. Fang, L. Ying, L. Wu, T. Ingle, and *W. Tong*. FDA/NCTR, Jefferson, AR.
KEYWORDS: Bioinformatics; Computational Toxicology; Safety Evaluation; Artificial Intelligence; Drug

ABSTRACT: Background and Purpose: FDA-approved drug labeling is essential for ensuring the safe and effective use of medications by healthcare providers and patients, but these documents are often lengthy and complex, containing 17 major sections and multiple subsections. To improve usability, the 2006 Physician Labeling Rule (PLR) in 21 CFR required a half-page "Highlights of Prescribing Information" that summarizes 9 major labeling sections to support efficient retrieval and use of key data. However, producing high-quality Highlights remains a manual, expert-dependent process that is labor-intensive, time-consuming, and variable across reviewers and over time. As a result, many non-PLR labeling documents approved before 2001 still lack Highlights. **Methods:** This study examines the potential of large language models (LLMs), such as ChatGPT, to automate the generation of Highlights and improve efficiency, scalability, and consistency in labeling summarization. Specifically, a dataset of 1,730 PLR-formatted labeling documents was compiled and human-authored Highlights of Prescribing Information across nine major sections was compared with ChatGPT-generated summaries, resulting in more than 14,000 section-level summary pairs. **Results:** Results showed that 87.99% of the pairs achieved similarity scores between 0.8 and 1.0, indicating a high level of consistency. The median similarity scores appeared to anti-correlate with the original section text length and followed the pattern: Boxed Warning (0.94) > Warnings and Precautions (0.85) > Adverse Reactions (0.83). Overall, ChatGPT demonstrated strong alignment with expert summaries, particularly for safety-related content, when using carefully designed prompts based on expertise in AI and labeling domain knowledge. **Conclusions:** Our findings show that ChatGPT reliably generated concise, expert-like summaries of complex drug labeling at scale. As LLMs continue to advance, integrating them into pharmacovigilance, labeling review, and regulatory workflows may improve efficiency, consistency, and evidence-based decision-making.

ABSTRACT NUMBER: 5160 **Poster Board Number:** K714
TITLE: Integrating *In Vitro* and *In Silico* NAMs for Enhanced Prediction of Drug-Induced Liver Injury

AUTHORS (FIRST INITIAL, LAST NAME) AND INSTITUTIONS: T. Li, S. Shrimali, Y. Qu, and *W. Tong*. National Center for Toxicological Research, Jefferson, AR.
KEYWORDS: Alternatives to Animal Testing; Computational Toxicology; Hepatic; Spheroid assay

ABSTRACT: Background and Purpose: Regulatory efforts to reduce animal testing have accelerated the adoption of New Approach Methodologies (NAMs). Here, we present an integrated strategy that combines *in silico* and *in vitro* NAMs to improve prediction of drug-induced liver injury (DILI) than each method alone. **Methods:** Specifically, we paired a deep learning model (DeepDILI) with three spheroid assays (InSphero n=35, Genentech n=37, AstraZeneca n=32) using a confidence-guided rule. **Results:** This approach consistently outperformed spheroids alone, improving accuracy from 0.66-0.81 to 0.80-0.88. Predictions were highly accurate for compounds where both methods agreed (0.86-0.92), while the largest gains occurred on discordant compounds (up to two-fold error reduction). Integrated results were also comparable to a liver chip on a smaller overlap set. **Conclusions:** This framework enhances

predictive performance while maintaining scalability and throughput, offering a practical path to reduce animal use. More broadly, it demonstrates how combining orthogonal NAMs can advance next-generation safety assessment, aligning with the FDA's 2025 roadmap and supporting the 3Rs principle.

ABSTRACT NUMBER: 5161 **Poster Board Number:** K715

TITLE: A machine learning approach for the development of a knowledgebase to identify systemic toxicity mechanistic targets and evaluate biological space coverage

AUTHORS (FIRST INITIAL, LAST NAME) AND INSTITUTIONS: *M. Shobair*[1], *D. Allen*[2], I. Ballone[3], M. Brüll[4], M. Burbank[5], *N. Choksi*[6], *S. Fitch*[7], A. Irizar[8], *K. Joshi*[9], S. Liu[10], *J. Tasaki*[10], *P. Kukic*[11], *T. Luechtefeld*[3], A. Najjar[4], *G. Ouedraogo*[5], K. Wolton[11], N. Yuko[10], and C. Mahony[12]. [1]Procter & Gamble, Mason, OH; [2]International Collaboration on Cosmetics Safety, Raleigh, NC; [3]Insilica LLC, Bethesda, MD; [4]Beiersdorf, Hamburg, Germany; [5]L'Oréal, Aulnay sous Bois, France; [6]ToxStrategies LLC, Research Triangle Park, NC; [7]ToxStrategies LLC, Houston, TX; [8]The International Fragrance Association (IFRA), Geneva, Switzerland; [9]Institute For Fragrance Materials (RIFM), Mahwah, NJ; [10]R&D, Safety Science Research, Kao Corporation, Kanagawa, Japan; [11]Unilever, Bedford, United Kingdom; and [12]Procter & Gamble Technical Centres Ltd, Reading, United Kingdom.

KEYWORDS: Computational Toxicology; Mode-of-Action; Predictive Toxicology; AOP

ABSTRACT: Background and Purpose: With increased reliance on New Approach Methods (NAMs) to support chemical risk assessment, mechanistic data modeling frameworks and knowledgebases are needed to facilitate hypothesis-based hazard evaluation. **Methods:** A data discovery and enrichment approach was developed using natural language processing (NLP) and large-language models (LLMs), to extract key mechanistic relationships from unstructured research articles to build a knowledgebase of adverse-outcome pathways (AOPs) related to systemic toxicity. The workflow employs contextual learning and hierarchical data extraction to connect molecular targets and biological processes with downstream events relevant to systemic toxicity. **Results:** Over 1000 mechanistic pathways for more than 9000 chemicals were identified using an integrated machine learning scheme that incorporates human input for model refinement, data confidence quantification, and ontology-based standardization. Expert curation, validation and interpretation with calibrated statistical confidence scoring achieved over 90% precision for chemical-target relationships and up to 100% precision for data cited in multiple studies. **Conclusions:** The knowledgebase was validated with AOPWiki annotations and expert-curated pharmacological datasets, providing insights into systemic toxicity mechanistic pathways. This can inform on the systemic toxicity biological space coverage and mapping needed to identify downstream mechanistic events that can further the understanding of the bioactivity-to-adversity relationship and continuum.

ABSTRACT NUMBER: 5162 **Poster Board Number:** K716

TITLE: Evaluating the Use of an Artificial Intelligence Tool in Predicting Steady-State Trough Plasma Concentrations of Dolutegravir

AUTHORS (FIRST INITIAL, LAST NAME) AND INSTITUTIONS: G. La, and S. Harirforoosh. Chapman University, Irvine, CA. Sponsor: S. Harirforoosh, International Society for the Study of Xenobiotics

KEYWORDS: Pharmacokinetics; Kidney; Infection; Artificial Intelligence; Dolutegravir

ABSTRACT: Background and Purpose: Dolutegravir is an antiretroviral drug used with other antiviral medications to treat human immunodeficiency virus (HIV). As artificial intelligence (AI) tools like ChatGPT are increasingly used to analyze large volumes of clinical data, their potential for pharmacokinetic analysis has been explored. The main goal of this study is to evaluate ChatGPT's effectiveness in predicting steady-state trough plasma concentrations of dolutegravir in HIV patients. **Methods:** A dataset of steady-state trough concentrations from 22 HIV patients who received a 50 mg oral dose of dolutegravir every 24 hours, along with other HIV medications, was obtained from a previous study [1]. The treatment duration varied among participants, but all reached steady-state concentrations. Additionally, various patient-specific data, such as gender, age, body mass index, weight, height, and glomerular filtration rate, were collected for all participants. Although only one participant had normal renal function, the other individuals exhibited some degree of renal impairment, including mild (n=13), moderate (n=7), or severe (n=1). To assess whether ChatGPT 4.0 could perform pharmacokinetic analysis and accurately predict steady-state trough concentrations, it was prompted to calculate steady-state trough levels using the provided parameters and dosages. An Excel file with these parameters was supplied alongside the prompt. Moreover, a reference article [2] detailing dolutegravir pharmacokinetics was attached to train the AI model. The trough concentrations generated by ChatGPT were compared to the reference data using regression analysis. This comparison was also performed for patients with mild or moderate renal impairment. Data are presented as mean ± standard deviation. **Results:** ChatGPT calculated steady-state trough concentrations of dolutegravir and provided individualized predictions for each patient by using pharmacokinetic information from the referenced model in the article and incorporating patient-specific data. While ChatGPT provided a comparison between observed (757.95±409.10 ng/mL) and predicted (843.27±104.58 ng/mL) steady-state trough concentrations, the predicted concentrations did not show a statistically significant correlation (R^2=0.0014, p=0.8736). The observed and predicted concentrations for patients with mild renal function were 792.80±388.96 and 800.85±58.32 ng/mL, respectively. For patients with moderate renal function, the observed concentrations were 763.27±511.60 ng/mL, and the predicted concentrations were 889.59±89.58 ng/mL. The data for mild and moderate renal functions were not correlated between observed and predicted concentrations (R^2=0.0736, p=0.3936) and (R^2=0.0136, p=0.8257), respectively. **Conclusions:** ChatGPT demonstrated the ability to incorporate patient-specific data and estimate steady-state trough concentrations, though its predictive accuracy was limited. This highlights the importance of using robust models when training AI tools to enhance the accuracy and reliability of pharmacokinetic predictions. **References:** [1] Murrell DE, Cluck DB, Moorman JP, Brown SD, Wang KS, Duffourc MM, et al. HIV Integrase Inhibitor Pharmacogenetics: An Exploratory Study. Clin Drug Investig. 2019 Mar;39(3):285-99. [2] Barcelo C, Aouri M, Courlet P, Guidi M, Braun DL, Gunthard HF, et al. Population pharmacokinetics of dolutegravir: influence of drug-drug interactions in a real-life setting. J Antimicrob Chemother. 2019 Sep 1;74(9):2690-7.

ABSTRACT NUMBER: 5163 **Poster Board Number:** K717

TITLE: Megatrans®- machine learning models for drug transporters corresponding to the fda guidance

AUTHORS (FIRST INITIAL, LAST NAME) AND INSTITUTIONS: P. A. Vignaux[1], M. Tojong[1], A. Kyu[1], L. J. Martinez Guerrero[2], J. S. Harris[1], *T. R. Lane*[1], S. H. Wright[2], *N. J. Cherrington*[2], and S. Ekins[1].
[1]Collaborations Pharmaceuticals, Inc., Raleigh, NC; and [2]University of Arizona, Tucson, AZ.

KEYWORDS: Xenobiotic Transporters; Computational Toxicology; Pharmaceuticals; machine learning; PROTACs

ABSTRACT: Background and Purpose: Regulatory guidances (e.g. FDA and EMA) require an understanding of the interactions of novel drugs, natural products and environmental toxicants with an array of transporters to avoid compounds with undesirable side effects. Computational approaches to predict such interactions using machine learning models trained on *in vitro* data could potentially prevent compounds that are transporter inhibitors with potential for drug-drug interactions from reaching the more costly development stages. We now describe the curation and machine learning model building for the transporters covered in the FDA guidance (OAT1, OAT3, OCT2, OATP1B1, OATP1B3, P-glycoprotein, BCRP, MATE1, and MATE2K) that enabled the creation of MegaTrans®, a web-based software product that enables users to input molecules and predict the inhibition of transporters of interest. **Methods:** IC_{50} datasets were downloaded from ChEMBL for the Pgp, BCRP, OATP1B3 and MATE2K inhibition models. The OAT1 and OAT3 datasets were comprised of IC_{50} data from ChEMBL, as well as from the literature. These six datasets were binarized on a specific IC_{50} value cutoff (1 µM for Pgp, BCRP, and OATP1B3; 30 µM for MATE2K and OAT1; 10 µM for OAT3) such that "active" compounds in the dataset were those with an IC_{50} value ≤ the cutoff value. The datasets for OAT1B1, MATE1, and OCT2 were comprised of published screening data binarized on specific inhibition cutoffs. The dataset for ENT1 consisted of a combination of IC_{50} values from ChEMBL, IC_{50} values of small molecules and PROTACS from our previous work with ENT1. Each dataset was used to generate machine learning models using ECFP6 fingerprints with 5-fold cross validation. These models were also applied to a dataset (N = 39) derived from 2024 and 2025 FDA approved drugs as well as a set (N = 19) of clinically relevant Proteolysis Targeting Chimeras (PROTACs).Molecule overlap was determined with our models using t-SNE. MegaTrans® software was developed as cloud-hosted, dockerized web-app which provides the machine learning models, enabling predictions and data visualization. **Results:** We used a majority-rules approach for a consensus prediction, with a four-four split ruled in favor of active inhibition, then compared these consensus predictions to the recorded transporter activity for each drug-transporter pair. While the accuracy over the whole set of drug-transporter predictions was 66% (159 accurate/241 total), and the accuracy per model family (transporter drug-profile) was >60% for 7 of the 9 transporters, the accuracy per drug (drug transporter-profile) varied widely. To address applicability domain issues, MegaTrans® offers the option for conformal predictions of a given compound or compound set. We chose an alpha of 0.2 for the novel-drug test set, which effectively represents an "acceptable" level of 20 % error in the predictions returned for each model. Rather than using consensus predictions for each model family, we performed individual-model conformal predictions using the random forest (RF) and support vector classification (SVC) models, as the prediction scores from these two algorithms represent meaningful probability-like scores. The RF models collectively returned predictions for 167 of the 241 (69.3%) drug-transporter pairs at this alpha, and the SVC models returned 172 predictions (71.4%). The true positive rates (TPRs) for the RF and SVC predictions were 30.8% (16/52) and 44.1% (26/59), respectively, compared to the TPR of 12.7% (9/71) for the non-

conformal consensus predictions. Inhibition of ENT1 has been recently identified as a potential issue for larger molecules like PROTACs. We used a curated list of clinically relevant PROTACs (2025) as a prediction set for the transporter models described herein as well as ENT1 and ENT2 models for potential DDI. As none of these PROTACs are approved drugs there is at the time of writing no available data on transporter inhibition for them to compare observed and predicted data. However, many of these molecules were predicted as ENT1 and OATP1B1 inhibitors with reasonably high Tanimoto similarity. **Conclusions:** Our application of literature *in vitro* data on transporters for building these machine learning models can be used for compound profiling of different molecule classes, representing an approach which could minimize the need for *in vitro*screening experiments and help to prioritize resources. Such applications of machine learning models could also be integrated at the drug design stages in artificial intelligence (AI) approaches.

ABSTRACT NUMBER: 5164 **Poster Board Number:** K718

TITLE: Integrated Multimodal Artificial Intelligence for Multi-Endpoint Drug Toxicity Prediction: Enhancing Human-Relevant Safety Assessment in Drug Discovery

AUTHORS (FIRST INITIAL, LAST NAME) AND INSTITUTIONS: F. Khodaee[1], R. Zandie[1], and R. Betancort[2]. [1]MIT, Cambrige, MA; and [2]Absentia Labs, Cambrige, MA. Sponsor: *R. Tanguay*

KEYWORDS: Predictive Toxicology; Alternatives to Animal Testing; Computational Toxicology; New Approach Methodologies

ABSTRACT: Background and Purpose: Traditional preclinical toxicity assessments rely heavily on animal models that often fail to predict human-specific adverse drug reactions. While New Approach Methodologies (NAMs) generate vast amounts of data, the integration of these heterogeneous data streams remains a challenge. The purpose of this study is to develop a multimodal Artificial Intelligence (AI) framework that integrates chemical structural descriptors with high-throughput transcriptomic data to predict organ-specific toxicity across multiple endpoints (hepatotoxicity, cardiotoxicity, and nephrotoxicity) with high human relevance. **Methods:** We developed a hybrid deep learning architecture consisting of a Graph Isomorphism Network (GIN) for processing molecular graphs and a Transformer-based encoder for processing textual and numerical readouts. The model was trained on a curated dataset of 3200 FDA-approved and failed drugs. To ensure biological interpretability, we applied feature extraction methods to identify key chemical moieties and physiochemical signatures driving the toxicity results. Model performance was evaluated using Area Under the Receiver Operating Characteristic (AUROC) and F1 score via 5-fold cross-validation. **Results:** The multimodal model significantly outperformed single-modality approaches, achieving a mean AUROC of 0.89 across all endpoints, compared to 0.62 for structure-only models. Specifically, for Drug-Induced Liver Injury (DILI), the integration of multiple modalities improved sensitivity by 21%. Same improvement was observed for Drug-Induced Cardiotoxicity and Drug-Induced Nephrotoxicity with 18% and 19%, respectively. Mechanistic analysis revealed a strong correlation between different types of toxicity endpoints that was not reported before. The model successfully identified mitochondrial and immune cell pathways as primary drivers for multi-organ drug toxicity. Furthermore, the framework correctly identified the toxicity of 85% of compounds in an external blind validation set of chemicals known to have human-specific toxicity not observed in rodents. **Conclusions:** The proposed multimodal AI framework demonstrates that integrating chemical and biological data streams along with multi-endpoint predictions provides a superior predictive tool for drug safety assessment. By aligning with the goals of

NAMs and providing mechanistic transparency, this approach facilitates more reliable human risk assessment and supports the reduction of animal use in early-stage drug development. This methodology offers a scalable, regulatory-aligned solution for the 21st-century toxicology paradigm.

ABSTRACT NUMBER: 5165 **Poster Board Number:** K719
TITLE: Machine learning-assisted evaluation of drug toxicity using 3D human intestinal organoids

AUTHORS (FIRST INITIAL, LAST NAME) AND INSTITUTIONS: O. Sirenko, and P. Macha. Molecular Devices, San Jose, CA. Sponsor: *I. Rusyn*
KEYWORDS: Predictive Toxicology; *In Vitro* and Alternatives; organoids

ABSTRACT: Background and Purpose: Damage to intestinal cells is one of the most common side effects of chemotherapy, often limiting therapeutic efficacy. Human intestinal organoids provide a three-dimensional (3D) culture model derived from pluripotent or adult stem cells that self-organize into miniaturized structures resembling native intestinal tissue. To better predict such adverse effects, it is essential to develop *in vitro* models and analytical tools that accurately reflect the physiological conditions of human tissues and enable pre-screening of drugs and drug candidates for toxicity. **Methods:** We developed automated organoid culture protocols and machine learning-assisted analysis methods to evaluate toxicity effects caused by anti-cancer drugs. Human duodenum organoids, derived from primary cells (OES-DP41N2-CXP1), were seeded into 50% Matrigel domes using automation, then treated with eight anti-cancer drugs known to induce intestinal toxicity (doxorubicin, cisplatin, taxol, others). Toxicity evaluation was conducted through morphological and viability assessments using high-content imaging. After 72 hours of compound exposure, organoids were stained for toxicity evaluation using viability, mitochondrial, and nuclear markers. Confocal imaging was performed with HCS.ai system, and image analysis was carried out using IN Carta software. Initially, conventional high-content image analysis was applied. Cells were scored as positive or negative based on nuclear (Hoechst), Calcein AM (viability), and MitoTracker (mitochondrial) staining. Cells positive for Calcein AM or MitoTracker were classified as intact (live) vs damaged. Positive and negative cells per organoid were counted, and average areas and intensities of positive cells were measured. Concentration-dependent responses were then evaluated to calculate IC_{50} values for compound toxicity. While this approach enables quantification of phenotypic changes and effective concentrations using individual readouts, it is complicated by the need to analyze multiple parameters separately to capture biological complexity. Machine learning tools offered a more unbiased approach to analysis by automatically identifying organoids and classifying them as intact or damaged. **Results:** We developed the ML-based image analysis protocol that first recognized images of organoids, then extracted a panel of 147 quantitative features per organoid. These included morphological descriptors (area, roundness, perimeter), intensity metrics across three fluorescent channels (mean, maximum, and minimum intensity), textural features (entropy, granularity, and contrast), and spatial distribution patterns (radial intensity and heterogeneity). Features were extracted from DAPI, FITC, and TRITC channels, enabling multidimensional phenotypic profiling of organoid populations. Classification was performed using a combination of unsupervised and supervised machine learning. Unsupervised clustering grouped organoids automatically into phenotypic clusters based on feature similarity, which were then further defined by user into biologically relevant categories. The final classification yielded percentage distributions for each phenotype allowing evaluation of compound effects in a concentration-dependent manner. In comparison with single-parameter readouts this approach incorporated a broader

morphological context, offering deeper insights into phenotypic changes. **Conclusions:** In summary, we demonstrated a fully automated workflow for toxicity evaluation using 3D human duodenum organoids, high-content imaging, and machine learning-based image analysis. The described approach enables AI-driven phenotypic profiling for assessing drug-induced toxicity in organoid models.

ABSTRACT NUMBER: 5166 **Poster Board Number:** K720

TITLE: Harnessing Computer-Based Modeling as a Proactive Strategy in the Toxicological Assessment of Functional Materials for Recyclable Electronics

AUTHORS (FIRST INITIAL, LAST NAME) AND INSTITUTIONS: *A. Sosnowska*[1,2], D. Kowalska[1], S. Zdybel[1,2], S. Carniello[3], E. Schwarz-Funder[3], and T. Puzyn[1,2]. [1]QSAR Lab Ltd, Gdansk, Poland; [2]University of Gdansk, Gdańsk, Poland; and [3]JOANNEUM RESEARCH Forschungsgesellschaft mbH, Graz, Austria.

KEYWORDS: Computational Toxicology; Environmental Toxicology; Safer Design/Green Chemistry

ABSTRACT: Background and Purpose: The shift toward environmentally friendly electronics requires materials that are both effective and safe. Paper-based Printed Circuit Boards (PCBs) are emerging as sustainable alternative to conventional plastic- or metal-based devices. A key toxicological challenge is ensuring that functional materials - flame retardants, inks, adhesives and encapsulants do not pose environmental hazards, especially in aquatic ecosystems. Traditional hazard assessments focus on individual chemicals, often neglecting processing-related transformations that can alter bioavailability and toxicity. There is a growing need to integrate ecotoxicological considerations early in material design. This study investigates how the ecotoxicity of chemicals used in paper-based PCBs changes from individual precursors to polymerized components and how *in silico* tools can support safer material design, which aligns with the Safe and Sustainable by Design (SSbD) concept. **Methods:** PCBs consist of paper, flame retardant, ink and adhesives for which the ecotoxic potential was evaluated. Initially, data-driven workflow was applied to assess the ecotoxicity (EC_{50}) of 29 chemical precursors of the main components necessary for the production of paper-based PCBs. Experimental data for fish (*Pimephales promelas*), invertebrates (*Daphnia magna*), and algae (*Green algae*) were compiled, and when data gaps existed, available quantitative structure-activity relationship (QSAR) models and read-across approaches implemented in the opensource tools (VEGA, OECD QSAR Toolbox, and alvaQSAR) were applied to predict the toxicity. Subsequently, all compounds were classified according to U.S. EPA environmental toxicity categories enambling standardized hazard comparison, identification of safer alternatives, and supporting risk-informed material design. **Results:** According to the EPA categories, 8 of 29 tested precursors were found moderately to very high toxic to fish. In comparison, only 4 showed toxicity toward invertabrate, whereas 10 precursors were toxic to algae. These results indicate that only individual precursors pose a potential environmental threat, while most are non-hazardous. Analyses also revealed that the metals used for ink production, such as silver or copper are the most hazardous. QSAR predictions suggest, for example, that a flame-retardant monomer precursor exhibits lower toxicity to fish (EC_{50} = 6.4 mg/L) compared to the monomer (EC_{50} = 1 mg/L). Therefore, it is important to highlight that the process of forming functional material (on the precursor and monomer level) may pose an environmental risk and need further investigation. However, it is expected that as a result of chemical reactions occurring during production, hazardous chemicals become bound within a compact polymeric structure (completed polimerisation scenario), leading to a reduction in their ecotoxicological potential. The obtained results are particularly relevant for toxicologists, as highlight the need to assess not only starting substances but also intermediate and final material forms within a SSbD framework.

Conclusions: This study provides new insight into how the ecotoxicity profile of PCB-related chemicals evolves across stages of material design - from individual chemical precursors to polymerized functional components. Moreover, we demonstrated the growing role of *in silico* toxicology in screening low-toxicity and biodegradable components in functional electronic materials. Remaining challenges include limited high-quality data, model applicability to novel chemicals, and assessment of mixtures or degradation products. Addressing these limitations is essential for integrating computational predictions into sustainable materials development and regulatory decision-making. While QSAR-based predictions is not new per se, their application to early-stage screening of printed electronic materials and polymerized PCB components constitutes a methodological and conceptual advancement in predictive environmental toxicology.

ABSTRACT NUMBER: 5167 **Poster Board Number:** K721
TITLE: Biomade: predicting torsades des pointes from molecular structures through biologically informed representations

AUTHORS (FIRST INITIAL, LAST NAME) AND INSTITUTIONS: J. Acitores Cortina, and N. P. Tatonetti. Cedars-Sinai Medical Center, Los Angeles, CA. Sponsor: N. Tatonetti, International Society for Computational Biology
KEYWORDS: Bioinformatics; AI

ABSTRACT: Background and Purpose: Drug-induced arrhythmias, particularly Torsade de Pointes (TdP), pose a significant risk to patient safety and can sometimes have life-threatening outcomes. They remain a major concern in drug development and regulation. Machine learning (ML) has become a powerful tool for analyzing complex biological and chemical datasets, enabling researchers to identify subtle patterns that differentiate safe compounds from those likely to cause dangerous cardiac effects. However, most existing *in silico* approaches do not sufficiently incorporate biological elements, relying heavily on chemical and structural properties or on computationally expensive simulations. **Methods:** Here, we introduce BioMADE, a novel ML framework that harnesses small-molecule-protein activity profiles from publicly available datasets to predict TdP risk without requiring exhaustive mechanistic annotation. Activity data from ChEMBL were used to train individual models for each gene, which predict activity values for any given compound. A curated set of arrhythmia-relevant genes was then used to construct a latent biological embedding (BioMADE embedding) for each molecule. Finally, BioMADE representations served as input to a support vector machine classifier to discriminate TdP-inducing drugs from safe compounds. **Results:** We validated the performance of BioMADE embeddings in distinguishing biological elements such as ATC3 class, showing superior classification performance compared with representations such as Molformer (lacks biological information) and MACCS (limited chemical properties) (0.85 AUROC vs 0.81 and 0.73, respectively). BioMADE achieved an AUROC of 0.91 in internal validation, indicating strong predictive performance. Against state-of-the-art models such as ADMEThyrst, BioMADE achieved an AUROC of 0.74 on ADMEThyrst's validation set (vs. 0.72 for ADMEThyrst). When we combined both approaches the AUROC reached 0.79. We further applied BioMADE to rank ~2 million compounds and selected three top candidates for experimental testing in induced pluripotent stem cell-derived cardiomyocytes via multi-electrode array recordings. All tested compounds exhibited pronounced arrhythmogenic effects. **Conclusions:** These results demonstrate that BioMADE provides a scalable, biology-informed, and generalizable approach for predicting drug-induced toxicities. By integrating protein activity profiles into toxicology modeling, our framework highlights the

critical role of human biology in adverse drug reaction prediction, an aspect often overshadowed by purely chemical or structural descriptors.

ABSTRACT NUMBER: 5168 **Poster Board Number:** K722

TITLE: Machine learning algorithm identifies mercury-induced autoimmunity as an accelerant of immunological aging

AUTHORS (FIRST INITIAL, LAST NAME) AND INSTITUTIONS: C. de Ocampo[1], H. Leung[2], A. K. Peiss[1], D. H. Kono[1], J. Mayeux[1], and *K. M. Pollard*[1]. [1]The Scripps Research Institute, La Jolla, CA; and [2]Georgia Institute of Technology, Atlanta, GA.

KEYWORDS: Autoimmune; Aging; Exposure, Environmental

ABSTRACT: Background and Purpose: Aging is linked to chronic low-grade inflammation (inflammaging) and increased spontaneous autoantibody production, such as anti-nuclear antibodies (ANA), in both humans and mice. However, the incidence of autoimmune diseases does not rise in later life, and the interplay between aging and xenobiotic-induced autoimmunity remains unexplored. Xenobiotics like mercury have been associated with autoimmunity, including mercury-induced autoimmunity (HgIA) in susceptible mouse strains, characterized by MHC class II-restricted anti-nucleolar autoantibodies (ANoA). This study investigates the effect of age on spontaneous and mercury-induced autoimmunity in B10.S mice, aiming to elucidate how immunosenescence affects responses to environmental triggers. **Methods:** Male and female B10.S mice were aged to mature (3 mo), adult (6 mo), middle-aged (12 mo), and old (24 mo) stages, equivalent to the human life phases of 19-26 years, 30-35 years, 40-48 years, and 65-75 years. Mice were subcutaneously injected with 40 µg $HgCl_2$ or PBS twice weekly for 4-5 weeks (n=17-57/group). Serum was analyzed for ANA and ANoA by indirect immunofluorescence on HEp-2 cells (dilutions 1:100 and 1:40 for low responders), anti-chromatin and anti-ENA5 by ELISA, immunoglobulins (IgG, IgG1, IgG2c) by ELISA. Splenocytes were assessed by multiparameter flow cytometry using 19 antibodies for T (CD4/CD8 subsets, germinal center), B (transitional, B1/B2, follicular, marginal zone, memory, germinal center, age-associated), and myeloid subsets. Cell frequencies from PBS mice were used to form a high-dimensional trajectory of immune aging that could be applied to $HgCl_2$-exposed mice. **Results:** Aging increased spontaneous ANA (0% mature, 34% middle-aged, 57% old) and anti-chromatin antibodies, with female bias and hypergammaglobulinemia (elevated IgG, IgG1, IgG2c). $HgCl_2$ augmented humoral responses across ages, but HgIA incidence declined in old mice (59% ANoA+ vs. 91-100% in younger groups). Retesting sera at 1:40 dilution revealed the presence of low-level ANoA in 56% of initially ANoA- old mice. ANoA negativity associated with lower IgG1, anti-chromatin, and germinal center B cells. Flow cytometry showed age-related changes in both $CD4^+$ and $CD8^+$ T cells, consisting of reduced naïve subsets and a shift toward effector functions, augmented by $HgCl_2$ in young but not old mice. Germinal center T and B cells profoundly increased with $HgCl_2$ in young mice. Age-associated B cells ($CD11c^+$T-bet^+) expanded in young $HgCl_2$-exposed mice. Myeloid cells increased with age and $HgCl_2$, suggesting a shift towards innate immunity. Spontaneous ANA in middle-aged mice mirrored HgIA changes (elevated germinal center cells). The elastic net regression model predicted the immune aging score of mercury-exposed mice to be between two and five months greater than their chronological age. HgIA produced more rapid immune aging in mature, adult, and middle-aged mice, and to a greater extent in female mice. Our model heavily weighted the frequencies of effector memory $CD4^+$ T cells, naïve and central memory $CD8^+$ T cells, and two distinct subsets of memory B cells in predicting immune age. **Conclusions:** Aging enhances spontaneous autoimmunity but impairs xenobiotic-induced

autoimmunity, with ~40% old mice failing to mount robust ANoA responses upon $HgCl_2$ exposure. Immunosenescence was associated with reduced germinal center formation and a shift to innate dominance. However, low-level ANoA in a portion of old mice indicates partial susceptibility persists. $HgCl_2$ promotes T cell-dependent humoral immunity and the expansion of inflammatory myeloid cells in young mice, accelerating immune aging. These findings highlight divergent mechanisms for spontaneous vs. xenobiotic-induced autoimmunity in aging, with implications for environmental risk assessment in elderly populations. Future studies should explore early immune events and genetic/epigenetic factors influencing variability.

ABSTRACT NUMBER: 5169 **Poster Board Number:** K723
TITLE: Variability in *in vivo* inhalation effect levels

AUTHORS (FIRST INITIAL, LAST NAME) AND INSTITUTIONS: *C. A. Weitekamp*, *S. Watford*, T. Wall, *J. Wambaugh*, N. Charest, *R. Sams*, and *K. Paul Friedman*. UL Research Institutes' Chemical Insights, Morrisville, NC.
KEYWORDS:

ABSTRACT: Background and Purpose: Traditional approaches to human health risk assessment largely rely on animal toxicity study data to inform chemical safety. Given the thousands of chemicals to which humans may be exposed that lack animal data, there is a need to incorporate additional approaches to evaluate safety. An obstacle to the adoption of New Approach Methods (NAMs) is understanding performance expectations. The accuracy of NAMs trained on or validated against animal data is limited by the uncertainty and variability in the animal data itself. Potential contributors to variability in animal effect levels include chemical identity, dose spacing, species, strain, life stage, and exposure duration, among others. There are also unexplained contributors to variability that are difficult to quantify, such as differences in handling, circadian effects, and microbiota. Previous work has quantified variability in orally dosed animal study data, reporting total variance in systemic lowest observed adverse effect levels that approached 1 $\log_{10}$ mg/kg-day, a root mean square error (RMSE) of approximately 0.5 $\log_{10}$ mg/kg-day, and a maximal explained variance that approached 70%. The maximal explained variance can be thought of as an upper limit on the reproducibility of *in vivo* studies given the controlled contributors to variability. Importantly, it is unknown whether performance expectations for other exposure routes deviate from this pattern. To advance evaluation of inhalation NAMs, here, we use a newly developed database of animal study data to evaluate variability in effect levels. **Methods:** Repeat dose inhalation toxicity data in adult animals, expressed as mg/m^3, were included from a newly developed database of *in vivo* toxicity studies compiled across multiple sources, such as the European Chemical Agency's IUCLID database and MAK Value Documentations, among others. Species included were rat, mouse, rabbit, and dog. Because there may be multiple effect levels per study, two separate datasets were developed for analysis: no observed adverse effect concentrations (NOAEC) and lowest observed adverse effect concentrations (LOAEC). Within each dataset, chemicals were filtered to those with two or more records. Dose was $\log_{10}$ transformed. Toxicological effects were categorized as portal of entry or systemic effects based on affected tissue. Study duration was categorized as short-term, subchronic, or chronic. Exposure method was categorized as whole body or nose/head exposure. Chemical phase was standardized to gas (e.g., vapor) or particle (inclusive of aerosols). When phase was not reported, it was inferred based on physicochemical properties. A linear mixed effects model was used to predict $\log_{10}$ NOAECs and LOAECs with chemical as the random effect and toxicological effect

type, duration, species, exposure method, and chemical phase as fixed effects. Model performance was assessed using total variance (overall variability or spread), RMSE (overall prediction error), marginal R^2 (variance explained by fixed effects only), and conditional R^2 (variance explained by fixed + random effects). The contribution from individual fixed effects was evaluated with type III ANOVA. **Results:** For NOAECs (1529 studies, 337 chemicals) and LOAECs (815 studies, 212 chemicals), respectively, total variance in inhalation effect levels was 2.0 and 2.4 $\log_{10}$ mg/m^3, residual variance was 0.26 and 0.4 $\log_{10}$ mg/m^3, RMSE was 0.44 and 0.54 $\log_{10}$ mg/m^3, marginal R^2 was 0.02 and 0.18, and conditional R^2 was 0.87 and 0.81. For both effect level types, the variables effect type, duration, and phase explained a significant portion of variance when adjusting for other fixed effects. Species did not explain additional variance, while exposure method explained a significant portion of variance only for LOAECs. A two-sided minimum prediction interval was estimated as 2.18 and 2.8 $\log_{10}$ mg/m^3 for NOAECs and LOAECs, respectively, suggesting that predicted effect levels could vary by about 150-fold and 630-fold between the lower and upper bounds. **Conclusions:** Compared to published work on oral effect levels, inhalation effect levels in this dataset had higher total variance and a wider prediction interval, indicating greater diversity in effective concentrations. However, a higher amount of total variance was explained when accounting for both fixed and random effects. These observations are consistent with the complexity of chemical exposure and toxicokinetics via inhalation compared to oral. This work provides an important first step to understanding performance expectations for inhalation NAMs.

ABSTRACT NUMBER: 5170 **Poster Board Number:** K724
TITLE: Introducing a Comprehensive Cloud Native NAMs Validation Workbench

AUTHORS (FIRST INITIAL, LAST NAME) AND INSTITUTIONS: S. Mukherjee, P. Chen, M. Davis, P. Fullerton, N. McMillian, J. Mester, C. Mukherjee, D. Rigsby, J. Schutter, C. Neumann, and *R. Moyer*. Battelle, Columbus, OH.
KEYWORDS: Computational Toxicology; Predictive Toxicology; Inhalation Toxicology

ABSTRACT: Background and Purpose: While there is significant momentum towards developing new approach methodologies (NAMS), clear validation standards remain an ongoing area of scientific work. Other challenges include access to data, integrated data analytical tools for extrapolation of *in-vitro* results to *in-vivo* scenario, custom visualization, and UI/UX. Several publications highlight the urgent need for a comprehensive platform where data can be stored, catalogued, harmonized, and integrated, and analytical models can be seamlessly deployed for visualization, interpretation, and validation. To meet this challenge, Battelle developed a proof-of-concept cloud based NAMs Validation Workbench using acute inhalation as a use case. The architecture of this workbench is modular and flexible and can be easily adapted for other Contexts of Use (COU). This comprehensive workbench can be used by NAMS developers, evaluators, and regulators alike for establishing confidence in and promoting use of NAMS in toxicology. **Methods:** This work required concomitant development of three major components: (1) a database, (2) a repository of *in-silico* models, and (3) a cloud-based workbench. **Database:** We built a PostgreSQL database that hosts *in-vitro* and *in vivo* data from sources including the Integrated Chemical Environment (ICE), Battelle MPS data from inhalation studies, data from SARS exposure in rhesus monkeys, ToxCast *in-vitro* data, and a subset of Chemical Effects in Biological System (CEBS) data. We also developed approaches to harmonize and integrate disparate data, allowing the workbench and workbench users to identify data relevant to their COU. **Modeling:** Third-party vetted tools, including tools for biokinetic modeling, dose-response modeling, quantitative structure activity

(QSAR) modeling were integrated into the workbench following a thorough review process where minimal submission requirements were checked, and codes were reviewed for compliance and vulnerabilities. Workflows were developed, where appropriate from scratch or by re-purposing existing tools, for data visualization, chemical diversity analysis, AOP network visualization, and *in-vitro* to *in-vivo* extrapolation (IVIVE) adhering to coding best-practices standards. **Workbench:** We built an Azure hosted user-friendly infrastructure with secure access that provides data exploration, NAMs experiment design, visualization, and validation utilities to authorized users. Standardized performant communication with PostgreSQL and inter-service data exchange is managed by a data access library. Apache Airflow serves as the workflow execution engine, running custom pipelines and models in code or containers with scheduling, retry logic, and monitoring. The Workbench API is integrated with Airflow to initiate and track jobs, surfacing status, logs, and results to provide end-to-end traceability. **Results:** We have developed a cloud-native workbench where authorized users can perform data exploration, get recommendations for experiment design, visualize COU, and validate NAMS data. **Data exploration** facilitates data retrieval, filtering using metadata toggles, review and visualization using custom scripts. Users can get recommendations for reference chemical set for a specified COU using the **experimental design functionality**. The tool curates an optimal reference chemical set using structural/functional diversity whose size can be constrained. Custom scripts enable visualization of the reference sets. By thoroughly curating and standardizing Adverse Outcome Pathway (AOP) wiki data, followed by semantic clustering, the **COU visualization** utility enables users to visualize AOP-networks for various domains like biological organization, taxonomic domain, cell and organ type etc. Importantly, users can perform head-to-head comparisons of MPS endpoints with animal endpoints using our **NAMS validation** utility. This utility deploys an *in-silico* validation workflow that sequentially executes dose-response analysis, estimates point-of-departures (POD), performs *in-vitro*-to-*in-vivo*-extrapolation (IVIVE), retrieves relevant *in-vivo* endpoint, and provides interactive visualization. Workflow progress can be tracked in real time, enhancing user experience. **Conclusions:** In summary, we have implemented a proof-of-concept NAMS validation workbench with multiple features that furthers the 3R mission. Users can use this workbench, interact with the database and utilities to visualize, analyze, and establish confidence in NAMS.

ABSTRACT NUMBER: 5171 **Poster Board Number:** K725

TITLE: Impact of Malaria-Acquired Immunity on COVID-19 Population Risk: A Deterministic-Stochastic Coinfection Model

AUTHORS (FIRST INITIAL, LAST NAME) AND INSTITUTIONS: *K. O. Idowu*, and G. Lin. Purdue University, West Lafayette, IN.

KEYWORDS: Biological Modeling; Risk Assessment; Computational Toxicology; Covid-Malaria Coinfection

ABSTRACT: Background and Purpose: Coinfection with COVID-19 and malaria may alter population susceptibility and disease burden in regions where malaria is endemic. While malaria-acquired immunity has been hypothesized to modify responses to other infections, its potential impact on COVID-19 population dynamics remains unclear. The purpose of this study is to quantify how malaria-acquired immunity influences COVID-19 transmission and population-level outcomes under uncertainty. **Methods:** We developed a deterministic - stochastic compartmental model describing the coupled dynamics of COVID-19 and malaria, incorporating mosquito-mediated transmission, drug-sensitive and drug-resistant malaria strains, hospitalization, disease-induced mortality, and coinfection. Malaria-

associated modulation of COVID-19 susceptibility is represented by a relative susceptibility parameter for malaria-immune individuals. Analytical properties of the model, including positivity, boundedness, and disease-free equilibria, are examined, and basic reproduction numbers are derived for the single-disease subsystems. Numerical simulations are conducted to evaluate the impact of malaria-acquired immunity on COVID-19 incidence, hospitalization, mortality, and coinfection burden under varying transmission and immunity scenarios. Sensitivity analyses are performed to identify key parameters influencing population-level risk, and uncertainty is quantified using stochastic simulations of the corresponding Itô stochastic differential equation system. Scenario-based analyses are used to examine the effects of intervention strategies, including vector control, treatment coverage, and hospitalization rates, on epidemic outcomes. **Results:** The proposed COVID 19 - malaria coinfection model is mathematically well defined, with all state variables remaining positive and bounded within biologically feasible limits. Basic reproduction numbers for the COVID-19 and malaria subsystems characterize baseline transmission thresholds and provide a reference framework for evaluating coinfection dynamics.Model analyses demonstrate that malaria-acquired immunity can significantly influence COVID-19 population outcomes. Reduced susceptibility among malaria-immune individuals leads to measurable changes in COVID-19 incidence, hospitalization, and mortality, with effects modulated by malaria transmission intensity and healthcare-related parameters. Sensitivity analyses identify malaria exposure, immunity-related susceptibility modification, and hospitalization rates as dominant drivers of coinfection burden and severe outcomes. Incorporation of stochastic effects reveals increased variability in epidemic trajectories, underscoring the importance of accounting for uncertainty when assessing population-level risk under interacting disease pressures. **Conclusions:** This study demonstrates that malaria-acquired immunity can meaningfully modify COVID-19 population dynamics in malaria-endemic settings. By integrating coinfection, vector transmission, and uncertainty into a unified modeling framework, the results highlight the importance of accounting for interacting biological stressors when assessing population-level risk. The proposed approach provides a robust quantitative foundation for informing integrated public health and risk management strategies.

ABSTRACT NUMBER: 5172 **Poster Board Number:** K726
TITLE: A cloud hosted tool for predicting drug distribution and safety based on protein-drug structure and affinity predictions

AUTHORS (FIRST INITIAL, LAST NAME) AND INSTITUTIONS: J. McCord, and *S. Krishna*. Physicians Committee for Responsible Medicine, Washington, DC.
KEYWORDS: Alternatives to Animal Testing; Biological Modeling; Computational Toxicology

ABSTRACT: Background and Purpose: Computational toxicology approaches that integrate physiologically based pharmacokinetic (PBPK) modeling with protein structure prediction offer the potential to improve human-relevant safety better than traditional animal tests. Recent advances in structural biology, specifically AlphaFold 3 based models, enable structure-informed prediction of molecular interactions relevant to drug metabolism and toxicity. Here, we describe the development of Toxicology Exposure-based Mechanistic Pathway mOdel (TEMPO), a cloud-hosted framework designed to integrate protein structure-informed affinity prediction with PBPK modeling to support exposure-based, mechanistic preclinical toxicological assessment. **Methods:** TEMPO is implemented as a Google Colab hosted notebook that initiates from a small-molecule SMILES user input alongside available physicochemical properties, clearance estimates, and dosing information. Small molecules are

processed using a structure-informed affinity and folding module (Boltz-2) and co-folded against key drug-metabolizing enzymes and transporter proteins. These structure-derived interaction predictions inform parameterization of a newly developed Python-based PBPK engine. The resulting multi-compartment PBPK model simulates systemic and tissue-specific drug exposure across a virtual population. TEMPO additionally integrates systematic harvesting of publicly available FDA pharmacokinetic and safety data (openFDA) and links PBPK-predicted tissue concentrations with protein affinity predictions, tissue-specific protein expression data, and adverse outcome (AOP) associated key initiating events (KIEs) to support mechanistic safety assessment. **Results:** This ongoing work has been parameterized and evaluated using a subset of publicly available FDA pharmacokinetic and safety data. The TEMPO framework successfully generates downloadable and visualizable pharmacokinetic outputs, including systemic and tissue-specific exposure profiles. In addition, a standardized pharmacokinetic database and a lightweight Qwen-2.5-based regulatory data extraction tool were developed to support automated data ingestion and model evaluation. Initial results demonstrate the feasibility of integrating structure-informed protein interaction predictions with PBPK modeling to support tissue-specific exposure and mechanistic toxicity hypotheses. **Conclusions:** TEMPO represents a modular, cloud-accessible platform that integrates protein structure prediction, PBPK modeling, and AOP-informed toxicological frameworks to support exposure-based, mechanistic safety assessment. By linking predicted tissue concentrations to molecular initiating events and adverse outcome pathways, this approach provides a foundation for future computational, protein structure-informed toxicology research and development of new approach methodologies for predictive safety assessment.

ABSTRACT NUMBER: 5173 **Poster Board Number:** K727
TITLE: Investigating the Synthesis of Copper Sulfate By Electrolysis: A Machine Learning Guided Approach

AUTHORS (FIRST INITIAL, LAST NAME) AND INSTITUTIONS: J. Reed, L. Ferguson, E. Precciely, C. London, and A. Stewart. Southern University and A&M College, Baton Rouge, LA. Sponsor: *T. Vaughn*
KEYWORDS: Environmental Toxicology; Aquatic Toxicology; Electrochemical Synthesis; Copper sulfate (CuSO4)

ABSTRACT: Background and Purpose: Copper(II) sulfate (CuSO4) is widely used as an algaecide, fungicide, and industrial reagent, making it a compound of significant environmental and toxicological relevance. Its toxicity in aquatic systems is well documented; however, less is known about how synthesis conditions influence product yield, chemical consistency, crystal morphology, and dose predictability prior to environmental exposure. Variability in electrochemical production could affect dosing reliability and complicate interpretation of toxicological studies. Electrochemical synthesis offers a controllable alternative to traditional chemical production but involves interdependent parameters, such as anode mass, applied voltage, current density, and reaction time, which are difficult to optimize simultaneously. The purpose of this study was to apply machine learning-based predictive analytics to model copper sulfate yield from electrochemical synthesis data, identify key factors governing production consistency, and provide insights that can enhance reliability for downstream toxicological evaluation. **Methods:** Copper sulfate was synthesized via electrolysis using a custom laboratory cell with a dilute sulfuric acid electrolyte prepared according to Always Add Acid safety protocols. Copper anodes and cathodes (99.99 percent purity) were cleaned prior to each experiment to minimize contamination. Electrolysis parameters varied systematically, including anode mass, applied voltage, current measured

at multiple time points (0 to 60 minutes), and total reaction duration. Following electrolysis, the CuSO4-rich solution was isolated, evaporated to remove excess water, cooled to induce crystallization, filtered, dried to constant mass, and weighed. Forty-four independent experimental runs were conducted. Data were preprocessed using normalization and outlier detection to ensure quality. Machine learning models, including linear regression, K-nearest neighbors, random forest for feature importance, and support vector regression (SVR), were implemented in Python to evaluate relationships between synthesis parameters, crystal formation characteristics, and copper sulfate yield. **Results:** Yield was strongly influenced by electrical parameters, particularly current measured during early and intermediate stages of electrolysis. Linear regression captured general trends but had limited predictive performance (MSE=3.0695). K-nearest neighbors improved prediction accuracy (MSE=1.5511), while SVR performed best (MSE=1.5104), effectively modeling nonlinear relationships between parameters and yield. Feature importance analysis consistently identified current at 15 minutes as the most influential predictor, followed by current at 30 minutes and anode mass. Correlation analysis supported these findings, revealing strong positive relationships between current density and yield, and moderate associations with reaction duration. Optimal yield was achieved with anode masses of 5.5 to 5.9 grams and electrolysis durations of 60 to 80 minutes. Visual inspection of crystallization patterns showed uniform crystal morphology under these conditions, supporting reproducible production. These results indicate that careful control of early-stage current and anode mass is critical to minimize batch-to-batch variability and ensure consistent dosing for toxicological evaluation. **Conclusions:** Machine learning-based modeling effectively predicts copper sulfate yield from electrochemical synthesis and identifies key parameters governing production consistency. Early-stage current control emerged as the most critical factor, aligning with electrochemical theory and demonstrating its relevance for achieving reproducible yields and crystal characteristics. Optimizing electrolysis parameters not only enhances production efficiency but also improves reliability of dosing and interpretation in environmental and toxicological studies of copper-based compounds. This integrative approach, combining experimental electrochemistry with predictive analytics, provides a robust framework for optimizing industrial production of copper sulfate while maintaining environmental and toxicological safety. The insights gained from feature importance analysis and predictive modeling can guide future research, inform risk assessment, and support the development of more consistent and controlled copper-based reagents for laboratory and industrial applications.

ABSTRACT NUMBER: 5174 **Poster Board Number:** K728

TITLE: Curation Workflows and Tools for Combining Regulatory and Research Hazard Data

AUTHORS (FIRST INITIAL, LAST NAME) AND INSTITUTIONS: J. T. Wall, S. Watford, A. Shapiro, and *C. A. Weitekamp*. UL Research Institutes' Chemical Insights, Morrisville, NC.

KEYWORDS: Computational Toxicology

ABSTRACT: Background and Purpose: ULRI is developing a hazard database to capture research and regulatory data for continued development and validation of new approach methods (NAMs) and to support delivery of high-quality hazard data for research and regulatory communities. This work expands existing efforts by combining research and regulatory information for easier aggregation of relevant, related data. The work is inspired by multiple projects including the U.S. Environmental Protection Agency (EPA)'s Toxicity Values Database, EPA's Toxicity Reference Data, Health Assessment Workspace Collaborative (HAWC), and International Uniform Chemical Information Database (IUCLID).

Herein, we describe a generalizable curation workflow for data extraction and quality assurance within a hazard database. To demonstrate the workflow, we describe the development of custom parsers for a key data source (IUCLID), as well as the development of a custom web application for quality assurance (QA) review. The goal of the application is to standardize curation across data sources and provide a web interface to enforce systematic and explainable methods for QA tasks. The overall goal is to provide the data in an easily searchable and consumable manner across ULRI projects and to enhance public accessibility. **Methods:** IUCLID was selected as a test case to develop custom parsers given its widespread use as a data submission and storage application in the format of OECD Harmonized Templates (OHTs). Two IUCLID datasets were selected for initial curation: 1) REACH Study Results and 2) US FDA Toxicity Data. A Python workflow was developed to parse the publicly available i6z zip files. Steps included flattening each document (i6d) file's XML into tabular format and decoding XSL dictionary field values. These tables were saved as parquet files by i6d and loaded into a relational database. All i6d files were linked to their parent i6z file, relevant OHT category, and related document type tables (e.g., endpoint study record, substance, etc.). Relationships between i6d files were stored in a "record relationship" table based on unique document identifiers present between i6d files in cross-reference fields. Finally, custom Python workflows were created to bulk query the IUCLID data by chemical identifiers, OHT, or document types. To develop the QA web application, "Data Quality, Extraction, and Stewardship Toolkit (Data QuEST)", Python Django (a web application framework) was used to develop the underlying data model and create the views and forms needed for the curation and QA workflow features. **Results:** The parsed REACH and US FDA datasets contain 27,390 i6z files, each representing a dataset for a specific chemical substance, with 261,662 linked reference substance entries. This includes data from 118 OHTs and links to 1,536,318 endpoint study records and 19,736 endpoint summaries. Data QuEST was developed to include controlled workflows, input forms with validation checks, full data record audit logs, and reporting mechanisms to track progress. Workflows include high-level "projects" which have "datasets", each with custom "project template" forms. Project managers define project templates with desired fields and set validation options (e.g., required, codependent, dropdown choices, numeric). Curators are assigned "allocations" to add "data records" through template forms. Once curation is complete, the allocation may be set to "QA", where two reviewers complete independent reviews of the data records. All changes made to records during QA are audit logged. Previously curated data records can be imported and allocated for QA. Projects and datasets can be exported from the application as XLSX files. **Conclusions:** Parsing of IUCLID data is a significant step toward increasing public accessibility across hazard data sources. The development of Data QuEST provides a centralized web application that facilitates standardized curation and QA workflows across projects. Next steps for Data QuEST are to include a document cataloging module that will allow curators to link with records and easily view documents during QA review. Additional visualizations are planned, including a burndown chart to track overall curation and QA progress. Overall, the curation workflows and tools developed herein are central to the development of a public hazard database that aims to capture research and regulatory data for continued development and NAM validation.

ABSTRACT NUMBER: 5175 **Poster Board Number:** K729

TITLE: Towards a combined research and regulatory *in vivo* toxicity data model: FAIR research for regulatory use

AUTHORS (FIRST INITIAL, LAST NAME) AND INSTITUTIONS: *S. Watford*, T. Wall, C. Weitekamp, A. Rashid, H. Gong, and A. Shapiro. UL Research Institutes Chemical Insights Research Institute, RTP, NC.

KEYWORDS: Computational Toxicology; Chemical Hazard Assessment; Alternatives to Animal Testing

ABSTRACT: Background and Purpose: Regulatory decisions for chemicals have traditionally relied on guideline *in vivo* toxicity studies, which are rigorous but costly and time-consuming. While animal toxicity research studies often generate valuable data, their use in regulatory contexts remains limited due to inconsistent formats and varying amount of reported information. The disconnect between guideline and research animal toxicity studies creates inefficiencies in chemical safety assessment, especially for substances with real-world exposures and unknown health risks.Attention to these challenges is increasing and efforts are underway to bridge the gap between reported research data and regulatory requirements. A recent OECD guidance document recommends adaptation of existing or creating new data standards for research that adhere to regulatory contexts as well as development of repositories and tools that implement the respective data standards (https://doi.org/10.1787/8d49ec1d-en). Successful implementation would facilitate the adoption and use of regulatory compliant data standards for researchers and publishers, while also communicating the data reporting needs for regulatory use. Also, with data more easily accessible and able to be aggregated, more research can be supported, especially the development of computational methods. However, major barriers persist slowing down or preventing this implementation. Research data vary widely in design and reporting, making it difficult to evaluate study quality and integrate findings into regulatory frameworks. It's also difficult for people to learn about and conform to new data standards or tools especially when so many tools exist for niche areas. The first step to address this challenge is development of a data standard that meets the needs of both research and regulatory users. Described here is a flexible *in vivo* toxicity data standard that harmonizes research needs with regulatory requirements, enabling consistent data capture and interoperability across diverse sources. **Methods:** We identified multiple sources of relevant information, including EPA Toxicity Values Database, EPA Toxicity Reference Database, IUCLID, NTP study reports, and the Health Assessment Workspace Collaborative. Key fields across these sources were standardized and combined into a unified data standard to support applications ranging from computational modeling to regulatory program support. Select field values were harmonized to bring consistency to the data as well. Python Django, a web application framework, was used to conceptually model and implement the standard. **Results:** The data standard includes domains such as data source, reference, experiment, dose, treatment, animal group, endpoint, and data extraction. These domains, fields, and relationships between them are designed to accommodate multiple use cases: aggregating chemical hazard values from collections of studies, capturing quantitative data from individual research studies, and documenting points of departure from guideline studies. When implemented, users can quickly determine which studies have required reported information for specific regulatory contexts or for researchers to quickly aggregate datasets in support of various questions like understanding the variability within types of animal studies. **Conclusions:** This data standard enables interoperability across diverse sources and supports applications from computational modeling to regulatory decision-making. A unified data standard for toxicity data is not only feasible but critical for accelerating chemical safety assessments and leveraging

research data to meet global regulatory needs including increasing the value of existing or new research studies. Next steps include complete implementation of a web application using this data standard and creating views to support research and regulatory workflows. *I attest that this content used AI to revise content that the authors generated.*

ABSTRACT NUMBER: 5176 **Poster Board Number:** K730

TITLE: Development of a Torsade de Pointes Risk Assessment Categorization (TRAC) Calculator Based on an International Multisite Study of Human-Induced Pluripotent Stem Cell-Derived Cardiomyocytes

AUTHORS (FIRST INITIAL, LAST NAME) AND INSTITUTIONS: T. K. Feaster[1], S. Ma[1], R. M. Geiger[1], B. Bhardwaj[1], J. Pierson[2], Q. Dang[1], and K. Blinova[1]. [1]US FDA, Silver Spring, MD; and [2]Health and Environmental Sciences Institute, Washington, DC. Sponsor: *B. Anson*

KEYWORDS:

ABSTRACT: Background and Purpose: New approach methodologies (NAMs) including human induced pluripotent stem cell-derived cardiomyocytes (hiPSC-CMs) coupled with high-throughput plate-based platforms and devices to measure indices of repolarization such as multielectrode array (MEA) and voltage-sensing optical (VSO) have proven useful for evaluating proarrhythmic risk. As such this cardiac NAM is routinely used in drug development to elucidate potential proarrhythmic risk and delayed ventricular repolarization. Consequently, its use is steadily increasing in cardiovascular safety pharmacology regulatory submissions for the latter. However, this does not routinely include a risk assessment score of the proarrhythmic potential of the test substance even though this was the focus of the hiPSC-CM comprehensive *in vitro* proarrhythmia assay (CiPA). The authors hypothesize this is because the hiPSC-CM predictivity model is computationally intensive, concealed within the text, and not user-friendly. **Methods:** The software for the TRAC calculator was written in JavaScript, with supporting HTML and CSS files to render the graphical user interface (GUI). A client-side approach was selected to ensure that the calculator can run entirely within any modern web browser, without requiring server dependencies or user authentication. This design makes the software directly portable and transparent, consistent with other field-driven cardiac risk calculators that prioritize accessibility for both clinicians and regulators. **Results:** We developed an open-source, web-based torsades de points (TdP) risk assessment categorization (TRAC) calculator utilizing the validated TdP model. The calculator employs the logistical regression model based on three hiPSC-CM compound-induced response predictors. **Conclusions:** By streamlining the estimation of TdP risk, this tool has the potential to significantly increase the frequency of such data in regulatory submissions and assist the translatability of nonclinical data. Moreover, this work provides an automated calculator to evaluate safety of novel compounds to ultimately reduce the dependance of animal studies and inform clinical trial design. Here, we present an easy-to-use online calculator based on the HESI CiPA myocyte validation TdP model to enable routine use with standard laboratory devices. **Disclaimer:** This abstract reflects the views of the author and should not be construed to represent FDA's views or policies.

ABSTRACT NUMBER: 5177 **Poster Board Number:** K731

TITLE: Action Potential Waveform Analysis in Human iPSC-Cardiomyocytes Enables Mechanistic Assessment of Multichannel Cardiac Effects

AUTHORS (FIRST INITIAL, LAST NAME) AND INSTITUTIONS: *C. Mathes*, C. Hill, and R. Kirby. Metrion Biosciences Ltd., Cambridge, United Kingdom.

KEYWORDS: Induced Pluripotent Stem Cells; Safety Pharmacology; Risk Assessment; NAMs

ABSTRACT: Background and Purpose: Recent regulatory changes, including the FDA Modernisation Act 2.0, have accelerated the adoption of human-relevant New Approach Methodologies (NAMs) for nonclinical safety assessment. In cardiac safety evaluation, reliance on single ion channel assays, such as hERG, may fail to capture the integrated electrophysiological effects that underlie proarrhythmic risk. Parameters derived from action potential waveform analysis, including triangulation and engagement of repolarisation reserve, are recognised as contributors to arrhythmogenic liability. Human induced pluripotent stem cell-derived cardiomyocytes (hiPSC-CMs) provide a translationally relevant system in which integrated multichannel cardiac effects can be assessed. The aim of this study was to evaluate whether optical voltage imaging of hiPSC-CM action potential waveforms can detect compound-induced electrophysiological changes beyond hERG block alone and enable mechanistic interpretation through correlation with ion channel electrophysiology data. **Methods:** Cryopreserved iCell2 human iPSC-derived cardiomyocytes (hiPSC-CMs; Fujifilm CDI) were thawed and seeded (50,000 cells/well) into fibronectin-coated (10 µg/mL) black-walled, optical-bottom 96-well plates and maintained at 37°C (5% CO_2) with media changes every 2-3 days. After 8 days, electrically coupled, synchronously beating monolayers were formed. Reference compounds were prepared as DMSO stocks (30 mM) and tested at 10 concentrations spanning 0.02 nM-30 µM. Action potentials were measured optically using the Volta fast-kinetic plate reader with the voltage-sensitive dye BeRST (500 nM). Cells were dye-loaded for 15 min at 37°C and equilibrated in recording buffer prior to acquisition. Fluorescence was acquired across the 96-well plate at 10 kHz (excitation 660 nm/emission 680 nm), with the instrument temperature set to 28°C. Baseline recordings (40 s) were obtained pre-dose, followed by a 30-min post-dose incubation and a second 40-s recording. Plates were returned to 37°C and assessed again at 24 h and 48 h following re-equilibration to 28°C. Action potential duration metrics, beat rate, and rise time were quantified using Volta analysis software. Triangulation was calculated per well as APD90 − APD50 (baseline- and vehicle-normalised); APD30-derived metrics were explored to assess early repolarisation effects. Waveform changes were compared with established in-house human ion channel electrophysiology datasets generated previously using automated patch clamp. **Results:** Optical voltage imaging of hiPSC-CM monolayers revealed compound-specific, concentration-dependent alterations in action potential waveform morphology consistent with known ion channel pharmacology. A panel of compounds spanning selective potassium and calcium channel blockade, as well as multichannel electrophysiological effects, was evaluated. Triangulation exhibited clear compound- and concentration-dependent effects. The selective hERG blocker dofetilide produced an early and pronounced increase in triangulation, evident at low nanomolar concentrations. Multichannel compounds, including quinidine, showed concentration-dependent increases in triangulation at higher exposures, consistent with multichannel modulation of inward and outward currents and reduced repolarisation reserve. In contrast, calcium channel blockers verapamil and nifedipine exhibited minimal effects on triangulation across most of the tested concentration range, with only modest increases at higher concentrations. Lower-risk hERG blockers such as moxifloxacin produced limited triangulation relative to dofetilide. Across the tested

concentration range, normalised triangulation differentiated agents with similar action potential duration changes but distinct underlying mechanisms, and waveform phenotypes were consistent with established in-house human ion channel electrophysiology data. **Conclusions:** Action potential waveform analysis in human iPSC-cardiomyocytes enables mechanistic differentiation of multichannel cardiac electrophysiological effects beyond action potential duration alone, supporting its application in human-relevant cardiac safety assessment.

ABSTRACT NUMBER: 5178 **Poster Board Number:** K732

TITLE: A Sex-Stratified piRNA Expression Atlas in Murine Lung and Mammary Tissues to Support Environmental Epigenomics Studies

AUTHORS (FIRST INITIAL, LAST NAME) AND INSTITUTIONS: M. Li[1], M. Collard[1], *K. Wang*[2], *K. E. Sala-Hamrick*[1], S. Dame[1], D. Wang[1], T. Jones[1], J. Miller[1], *B. P. Perera*[3], *J. M. Goodrich*[1], M. A. Sartor[1], and *D. C. Dolinoy*[1]. [1]University of Michigan, Ann Arbor, MI; [2]Indiana University, Bloomington, IN; and [3]University of California, Berkeley, Berkeley, CA.

KEYWORDS: Epigenetics; Gene Expression/Regulation; Bioinformatics

ABSTRACT: Background and Purpose: Piwi-interacting RNAs (piRNAs) are a class of small non-coding RNAs that associate with PIWI proteins to mediate transposon silencing and epigenetic regulation, primarily through DNA methylation. Although piRNAs are well characterized in the germline, recent studies have demonstrated the presence of somatic piRNAs and PIWI machinery in multiple tissues, suggesting broader regulatory roles in development and disease. Emerging evidence indicates that environmental exposures, including metals and metalloids, can alter piRNA expression and associated epigenomic programs. However, the lack of comprehensive, tissue- and sex-specific baseline piRNA maps in environmentally relevant target tissues, such as lung and mammary gland, has limited mechanistic investigations of exposure-induced piRNA dysregulation. Here, we aim to construct a comprehensive, sex-stratified baseline map of piRNA expression in murine lung and mammary tissues, providing a critical reference framework for ongoing and future studies of epigenomic responses to environmental exposures, including lead (Pb) and arsenic (As). **Methods:** We utilized four adult wild-type non-agouti a/a mice (2 females and 2 males) from a colony of viable yellow agouti strain (A^{vy}). From each mouse, both lung and mammary tissues were collected, yielding a total of eight tissue samples. Small RNAs were extracted from each tissue, and for each tissue sample, the RNA was split into two aliquots: one subjected to sodium periodate treatment, which selectively enriches for RNAs bearing 2'-O-methylation at the 3' end, a hallmark feature of piRNAs, and the other left as an untreated control. Both treated and untreated libraries were prepared and sequenced on an Element AVITI24 platform. Sequencing reads were aligned to the mouse reference genome. piRNA peaks were identified using the peak-calling tool *PePr* by group-wise comparisons of treated and untreated libraries within each tissue type. To ensure accurate estimation of fold change while properly accounting for multi-mapping reads, we used *featureCounts* to quantify read counts for each peak, assigning multi-mapping reads as fractional counts. *edgeR* was then used only to calculate fold changes (FCs) between treated and untreated groups based on these re-estimated counts. Peaks were defined as piRNA-like transcripts if they satisfied a *PePr* false discovery rate (FDR) < 0.01, an *edgeR*-estimated FC > 3, and a peak length between 20 and 45 bp. Genomic annotation of piRNA peaks was performed using *annotatr*. **Results:** In lung tissues, we identified 8,593 piRNA peaks in the combined-sex analyses, while sex-specific analyses identified 5,755 and 1,763 piRNA peaks in female and male lungs, respectively. In mammary tissues,

12,123 piRNA peaks were identified in combined-sex analyses, with 4,237 and 3,590 piRNA peaks detected in female and male mammary tissues, respectively. Cross-tissue comparison revealed strong tissue specificity, with only 208 overlapping piRNA peaks shared between lung and mammary tissues. Within each tissue type, overlap between female- and male-specific piRNA peaks was limited (200 in lung and 51 in mammary). Genomic annotation of piRNA peaks demonstrated non-random distributions, with enrichment in CpG islands, shores, and shelves, as well as in exons and introns, while showing depletion in intergenic regions. Mammary tissue exhibited a slightly higher proportion of intronic piRNA peaks than lung. **Conclusions:** Together, these findings establish a comprehensive tissue- and sex-specific piRNA expression framework in lung and mammary tissues, providing a critical baseline for future studies investigating piRNA regulation and epigenomic responses to environmental exposures, including Pb and As. These data will be incorporated into the piOxi database (https://pioxidb.dcmb.med.umich.edu/) to serve as a publicly accessible resource for the environmental epigenomics community.

ABSTRACT NUMBER: 5179 **Poster Board Number:** K733

TITLE: *Dlk1-dio3* Imprinted Gene Regulation in the Human Placenta Following Gestational Opioid Exposure

AUTHORS (FIRST INITIAL, LAST NAME) AND INSTITUTIONS: *D. Wang*[1], *B. P. Perera*[2], *A. Haidari*[1], *V. Padmanabhan*[3,4,5], C. D. Townsel[6], *D. C. Dolinoy*[1,7], and *J. M. Goodrich*[1]. [1]Department of Environmental Health Sciences, School of Public Health, University of Michigan, Ann Arbor, MI; [2]Division of Environmental Health Sciences, School of Public Health, University of California, Berkeley, CA; [3]Department of Pediatrics, University of Michigan, Ann Arbor, MI; [4]Department of Obstetrics and Gynecology, University of Michigan, Ann Arbor, MI; [5]Department of Molecular and Integrative Physiology, University of Michigan, Ann Arbor, MI; [6]Department of Obstetrics, Gynecology and Reproductive Sciences, University of Maryland, Baltimore, MD; and [7]Department of Nutritional Sciences, School of Public Health, University of Michigan, Ann Arbor, MI.

KEYWORDS: Developmental Toxicity; Prenatal; Epigenetics; Gene Expression/Regulation

ABSTRACT: Background and Purpose: Opioid use disorders are a growing public health concern. Reduced fecundity and pregnancy loss are associated with opioid use, along with neonatal opioid withdrawal syndrome (NOWS). The placenta plays a critical role in fetal development and is involved in opioid metabolism and fetal transfer. Epigenetic modifications to the placenta may contribute to inter-individual differences in response to opioid exposure during pregnancy. An epigenetic phenomenon, genomic imprinting, causes mono-allelic expression of genes depending on which parental allele they are inherited from. Dysregulation of genomic imprinting disrupts early life development and has been associated with long-term adverse health outcomes. The *DLK1-DIO3* imprinted domain on chromosome 14 contains maternally expressed long noncoding RNAs (*MEG3, MEG8*), which are involved in the regulation of genomic imprinting and are essential for embryonic development. Dysregulation of this domain is associated with adverse impacts on fetal growth and metabolic disorders. Whether opioid exposure during pregnancy dysregulates genomic imprinting in the placental *DLK1-DIO3* domain remains unknown. In this study, we investigated the association between: 1) exposure to medications for opioid use disorder (MOUDs) and placental expression of genes within the *DLK1-DIO3* locus and 2) the relationship between gene expression and severe NOWS. **Methods:** Placental samples were collected from MOUD exposed (n=30) and non-exposed (n=53) patients after delivery at Michigan Medicine.

MOUD exposed participants were taking either methadone (n=22) or buprenorphine (n=8). For the MOUD exposed participants, severe NOWS was assessed by the modified Finnegan scoring system and defined as three consecutive scores ≥8 or when the sum of three consecutive scores was ≥24 within 72 hours of life. Total RNA (n=83) was isolated from the placenta samples. Expression of *DLK1, DIO3, MEG3,* and *MEG8* was quantified using RT-qPCR and normalized to the housekeeping gene *β-actin*. Primers were first optimized, and primer efficiency tests were performed. All samples were run in triplicate, including internal quality controls, and triplicates were averaged. Generalized linear regression models, adjusting for maternal age, were used to assess relationships between MOUD exposure (either methadone or buprenorphine) and gene expression. Student's t-tests were used to compare placental gene expression levels among offspring with and without severe NOWS in the MOUD-exposed group. **Results:** In adjusted models, MOUD exposure was significantly associated with increased *MEG8* (β = 0.0019, p = 0.007) and *DIO3* (β = 0.00081, p = 0.0003) expression, compared to the non-exposed group. Expression of *DLK1* and *MEG3* did not differ significantly between exposure groups. 15 MOUD-exposed offspring (50%) exhibited severe NOWS after birth. There was no statistically significant difference in gene expression between offspring that went on to exhibit severe NOWS and those that did not. **Conclusions:** These findings suggest MOUD exposure during pregnancy is associated with disruption of genomic imprinting in the placenta. This study highlights that the *DLK1-DIO3* imprinted domain is sensitive to perinatal opioid exposure and has the potential to serve as an epigenetic biomarker of the negative impacts on the placenta. While gene expression was not associated with severe NOWS, future research should investigate other impacts on offspring health and development that may result from these molecular changes.

ABSTRACT NUMBER: 5180 **Poster Board Number:** K734

TITLE: Pharmacogenetic Considerations in Kratom Regulation: A Systematic Review Highlighting the Need for Personalized Risk Assessment Frameworks

AUTHORS (FIRST INITIAL, LAST NAME) AND INSTITUTIONS: E. Matischak, and *L. Burgoon*. Raptor Pharm & Tox, Apex, NC.

KEYWORDS:; Pharmacogenetics, CYP2D6, Polypharmacy; Mitragyna speciosa

ABSTRACT: Background and Purpose: Kratom (Mitragyna speciosa) has emerged as a significant public health concern, with the FDA Center for Food Safety and Applied Nutrition (CFSAN) Adverse Event Reporting System documenting 20 deaths (27%) among 75 adverse event reports in 2021. In 2025, these safety concerns prompted unprecedented regulatory action. Louisiana enacted a complete ban (Schedule I classification), while Texas, South Carolina, and Oklahoma implemented consumer protection frameworks with varying alkaloid limits. However, these regulations treat all kratom users as a homogeneous population, ignoring well-documented variability in drug metabolism. This systematic review examines the pharmacogenetic basis for kratom toxicity, with emphasis on CYP2D6 polymorphisms, and proposes a framework for personalized risk assessment to inform evidence-based regulation. **Methods:** A systematic literature review of PubMed and Web of Science databases (2013-2025) was conducted using search terms: kratom, mitragynine, 7-hydroxymitragynine, CYP450, CYP2D6, CYP3A4, and pharmacogenetics. Inclusion criteria comprised peer-reviewed studies examining kratom alkaloid metabolism, cytochrome P450 enzyme interactions, genetic polymorphisms, and toxicological outcomes. We analyzed state legislative documents from 2025 to assess regulatory approaches and identified gaps in pharmacogenetic consideration. **Results:** Mitragynine, the primary kratom alkaloid, is

metabolized predominantly by CYP2D6 and CYP3A4. Mitragynine demonstrates potent competitive inhibition of CYP2D6 with an IC50 of 2.2 uM and Ki of 1.1 uM, values within the range of expected human exposure following typical kratom use. CYP2D6 exhibits marked genetic polymorphism with significant inter-ethnic variability: 1-10% of Caucasians are poor metabolizers (PM), 1-2% of Asians are PM, while 22% of Ethiopians are ultrarapid metabolizers (UM). Analysis of FDA adverse event reporting data revealed 28-fold variability in blood mitragynine concentrations at time of adverse events (190-5400 ng/mL), suggesting differential metabolic capacity contributes to toxicity risk. Review of 2025 state legislation revealed no consideration of pharmacogenetic variability in regulatory frameworks, with alkaloid limits and age restrictions applied uniformly across populations. **Conclusions:** The potent inhibition of CYP2D6 by mitragynine at clinically relevant concentrations, combined with CYP2D6 genetic polymorphisms, creates a compounded risk profile not addressed in current kratom regulation. Poor metabolizers face elevated risk due to reduced clearance capacity and prolonged exposure to both mitragynine and co-administered CYP2D6 substrates, while chronic users experience cumulative enzyme depletion through time-dependent inhibition of CYP3A4. Current uniform regulatory policies inadequately protect high-risk populations. We propose a pharmacogenetic risk assessment framework incorporating: (1) consideration of CYP2D6 metabolizer phenotype in risk stratification, (2) recognition of time-dependent enzyme inactivation in chronic use scenarios, and (3) population-specific safety guidance based on known genetic variability in drug metabolism. This framework has direct implications for poison control centers requiring genetic risk factor guidance, clinical toxicologists developing personalized risk assessments, and regulatory agencies implementing evidence-based policies. Future prospective studies should link CYP2D6/CYP3A4 genotypes to kratom-related adverse events to validate and refine this framework.

ABSTRACT NUMBER: 5181 **Poster Board Number:** K735

TITLE: Genotoxicity Evaluation of Nitrosamines Using Miniaturized Ames Assays and *In Vitro* Micronucleus Test

AUTHORS (FIRST INITIAL, LAST NAME) AND INSTITUTIONS: C. Boglari[1], C. Koelbert[1], J. Raposo[2], and C. Cuceu Petrenci[2]. [1]Xenometrix, Allschwil, Switzerland; and [2]GenEvolutioN, Porcheville, France. Sponsor: C. Boglari, Environmental Mutagenesis and Genomics Society

KEYWORDS: Genetic Toxicology; Mutagen; Clastogen; Micronucleus; Nitrosamines

ABSTRACT: Background and Purpose: The detection of genotoxic impurities in pharmaceuticals, packaging materials, and other consumer and industrial products is essential for protecting public health, highlighting the need for robust and reliable safety assessment methods. Growing concerns surrounding nitrosamines have prompted international collaboration to improve testing strategies for this class of compounds. Regulatory authorities recommend the use of the Enhanced Ames Test (EAT) when *in vitro* mutagenicity testing is considered to determine the mutagenic potential of a nitrosamine. A negative result from a valid enhanced Ames assay may be used to justify a higher Acceptable Intake (AI) limit for a nitrosamine. **Methods:** In this study, we compared two miniaturized versions of the Ames assay: the agar-based MicroAmes6, in a 6-well plate format, and the liquid microplate fluctuation assay, the Ames MPF. The Ames tester strains were TA100, TA1535, and *E. coli* uvrA[pKM101] in compliance with the OECD TG 471 guideline. For the metabolic activation 30% hamster liver S9 was used - in line with the recommendations for the Enhanced Ames Test (EAT). Cytokinesis-block *in vitro* micronucleus assay was conducted to further investigate the Nitrosamine test samples. **Results:** A high level of

concordance was observed between the two miniaturized assay formats, demonstrating strong internal consistency. In addition, results from the miniaturized Ames assays showed a high degree of correlation with those obtained using the conventional Petri dish-based Ames test reported in the literature. The miniaturized Ames assays were able to detect positive nitrosamines at lower concentrations than the Petri dish-based method, indicating improved sensitivity. *In vitro* micronucleus data complemented the Ames test results to shed light on the mechanistic insights on the genotoxicity of Nitrosamines. **Conclusions:** This study demonstrates the potential of miniaturized Ames assays and the *in vitro* micronucleus test to address the data gaps in the available safety assessment information for Nitrosamines. The data generated in the scope of this project will facilitate the safety evaluation of Nitrosamines and other genotoxic impurities across the pharmaceutical and chemical industries, supporting improved public health protection, efficient decision-making, and promoting more sustainable laboratory practices.

ABSTRACT NUMBER: 5182 **Poster Board Number:** K736

TITLE: Evaluating mutagenicity of diverse chemicals in TK6 cells using error-corrected next-generation sequencing

AUTHORS (FIRST INITIAL, LAST NAME) AND INSTITUTIONS: *X. Li*, J. A. Miranda-Colon, J. R. Revollo, and *N. Mei*. National Center for Toxicological Research, Jefferson, AR.

KEYWORDS: Mutation; Genetic Toxicology; NGS

ABSTRACT: Background and Purpose: Error-corrected next-generation sequencing (ecNGS) provides an advanced means to identify rare, genome-wide mutations with high precision and may serve as a powerful complement to traditional mammalian cell mutation assays. **Methods:** In this study, PacBio HiFi sequencing was employed to assess the mutagenic activity of eight representative chemicals in human TK6 cells, encompassing both direct-acting agents and nitrosamines requiring metabolic activation. **Results:** PacBio HiFi sequencing reliably detected concentration-dependent increases in mutation frequency (MF) for known mutagens such as 4-nitroquinoline-1-oxide (4NQO), mitomycin C, N-nitroso-chlordiazepoxide, and N-nitrosodiethylamine (NDEA), while correctly identifying non-mutagenic responses for curcumin and the equivocal compounds hydroquinone, NMBA, and N-nitroso-phenylephrine. Mutation spectra aligned with known chemical mechanisms, notably G:C>T:A substitutions induced by 4NQO and mitomycin C and G:C>A:T transitions characteristic of nitroso compounds. The PacBio platform demonstrated strong specificity, showing no artificial MF increases under cytotoxic conditions. **Conclusions:** Collectively, these results highlight the reliability and sensitivity of PacBio HiFi sequencing for quantitative mutagenicity assessment and support its promise as a next-generation approach for regulatory and mechanistic applications in genetic toxicology.

ABSTRACT NUMBER: 5183 **Poster Board Number:** K737
TITLE: Genotoxicity and Mutagenicity Evaluation of *N*-Nitroso-Fluoxetine and *N*-Nitroso-Varenicline using 2D and 3D HepaRG Models

AUTHORS (FIRST INITIAL, LAST NAME) AND INSTITUTIONS: *J. Seo*[1], H. Xu[1], J. Revollo[1], J. Miranda-Colon[1], A. H. Atrakchi[2], T. J. McGovern[2], K. L. Davis Bruno[2], S. T. King[2], R. Dorsam[2], D. A. Keire[2], R. H. Heflich[1], and *X. Guo*[1]. [1]National Center for Toxicological Research, Jefferson, AR; and [2]Center for Drug Evaluation and Research, Silver Spring, MD.
KEYWORDS: Mutation; Alternatives to Animal Testing; Risk Assessment

ABSTRACT: Background and Purpose: Nitrosamine drug substance-related impurities (NDSRIs) continue to raise regulatory and public health concerns, yet carcinogenicity data for most NDSRIs remain limited. As current acceptable intake (AI) limits primarily rely on the Carcinogenic Potency Categorization Approach (CPCA), there is growing interest in incorporating mutagenicity data from mammalian systems as a secondary line of evidence following primary screening with the Enhanced Ames Test (EAT). **Methods:** In this study, we investigated the suitability of human HepaRG models as a platform for evaluating NDSRI-related genotoxicity and mutagenicity. HepaRG cells, cultured in both two-dimensional (2D) and three-dimensional (3D) spheroid formats, were exposed to two NDSRIs, *N*-nitroso-fluoxetine and *N*-nitroso-varenicline for 3 or 14 days. Genotoxicity was evaluated using the comet and micronucleus assays, and mutagenicity was assessed using an error-corrected sequencing (ECS) technology, PacBio High-Fidelity sequencing. **Results:** Both NDSRIs produced concentration- and time-dependent cytotoxicity and DNA damage in 2D and 3D systems, while micronucleus induction was observed only under the 14-day high-dose conditions in 3D spheroids. Each NDSRI generated distinct and reproducible mutational spectra in both 2D and 3D HepaRG models. Overall, 3D spheroid cultures showed more potent genotoxic and mutagenic responses compared to 2D monolayers, in line with their enhanced metabolic competency. In addition, extended 14-day exposures produced higher mutagenic responses at lower concentrations compared to the 3-day treatments. **Conclusions:** These results support using metabolically competent HepaRG models with ECS as a human-relevant *in vitro* new approach methodology (NAM) for mutagenicity assessment as a follow-up to the EAT.

ABSTRACT NUMBER: 5184 **Poster Board Number:** K738
TITLE: Endonuclease G inhibits toxicity to kidney tubular epithelial cells during cisplatin or ischemia-reperfusion injury

AUTHORS (FIRST INITIAL, LAST NAME) AND INSTITUTIONS: R. S. Shelton[1], O. Levurdiak[1], S. Li[2], T. Fite[2], and A. G. Basnakian[1,2]. [1]University of Arkansas for Medical Sciences, Little Rock, AR; and [2]Central Arkansas Veterans Healthcare System, Little Rock, AR. Sponsor: *A. Tiwari*
KEYWORDS: Apoptosis; Toxicity; Acute; Kidney; DNase; Cisplatin

ABSTRACT: Background and Purpose: EndoG (Endonuclease G, EG) is an apoptotic enzyme known to be universally induced by toxic injuries to kidney tubular epithelial (KTE) cells and translocated from mitochondria to the nucleus during cell death. Since EG is just one of several apoptotic DNases, it remains unknown whether EG itself causes apoptotic DNA fragmentation leading to cell death. EG is the only apoptotic endonuclease found in the nucleus during apoptosis, has RNase activity, and induces inactive truncated isoform of another endonuclease, DNase I (DI) in some models. We proposed that the role of EG in apoptosis may depend on the presence of DI in the cell. **Methods:** We used cisplatin kidney

injury *in vitro* and *in vivo* models as well as *in vivo* kidney ischemia-reperfusion (IR) to test this hypothesis. **Results:** To our surprise, although EG was often present in TUNEL-positive nuclei of KTE cells in mice treated with cisplatin or ischemia, it did not colocalize with DNA fragmentation measured by TUNEL or with endonuclease activity measured by a fluorescent probe in nuclei of cultured KTE NRK-52E cells. EG overexpression in DI-positive NRK-52E cells showed EG induced alternative splicing and inactivation of DI and was not cytotoxic, but instead protective against cisplatin injury (60 μM) as determined by flow cytometry. When the same experiment was repeated using DI-negative HCC1954 cells, EG was cytotoxic and promoted cisplatin-induced cell death. Further study showed that EG was induced but was not cytotoxic in cisplatin kidney injury *in vivo.* After injection of cisplatin, no protection in EG null mice versus wild-type (WT) mice was observed by BUN, serum creatinine, or histology. EG induction by cisplatin in WT mice was associated with the decrease of native DI expression and the appearance of inactive truncated DI. Similarly, kidney IR in mice led to induction of EG at 16-48 hours of reperfusion which caused inactivation of DI by alternative splicing. **Conclusions:** This study showed that EG acts as a proapoptotic enzyme in the absence of DI and it is anti-apoptotic in the presence of DI in KTE cells and the kidney during cisplatin or IR injury.

ABSTRACT NUMBER: 5184a **Poster Board Number:** K739
TITLE: Challenges and Countermeasures for Preclinical Safety Evaluation of Inhaled Small Nucleic Acid Drugs

AUTHORS (FIRST INITIAL, LAST NAME) AND INSTITUTIONS: X. Chen, L. Wei, H. Li, and X. Wang. Innostar, Shanghai, China. Sponsor: *X. Cao*
KEYWORDS:

ABSTRACT: Background and Purpose: Inhaled siRNA drugs represent an innovative therapeutic approach that directly silences genes associated with pulmonary diseases, achieving gene silencing, transcriptional regulation, or targeted therapy. Receptor for Advanced Glycation End Products (RAGE) is an oncogenic transmembrane receptor overexpressed in various human cancers. Inhaled delivery of siRNA allows drug deposition in the lungs, serving as a delivery system for local or systemic effects. Compared with traditional inhaled formulations, inhaled siRNA drugs present significant differences in formulation challenges, drug delivery properties, and key safety evaluation focus areas. **Methods:** Preclinical safety evaluation is critical to fully assess the human safety of inhaled siRNA drugs prior to clinical use. A total of 8 cynomolgus monkeys were used for toxicological safety assessment, randomly divided into 4 groups: control group and low-, medium-, high-dose test article groups, with 2 animals per group (1 male, 1 female). Animals received acclimation training for 3 consecutive days before dosing. Animals in the treatment groups received the test article at 1.5 mg/kg, 3.0 mg/kg, and 10 mg/kg respectively via nose-only inhalation, with a fixed exposure duration of 80 minutes. A negative control group received 0.9% sodium chloride injection via nose-only inhalation for 80 minutes. During the development of siRNA drug aerosol generation, it was necessary to ensure that the nebulizer did not cause siRNA strand breakage or dissociation of the ligand/linker moieties. Precise control was implemented for test article generation flow, dilution flow, and exhaust flow, along with real-time monitoring of aerosol concentration. During dosing, the particle size delivered by the inhalation device was determined, as it directly affects pulmonary drug deposition. The aerodynamic mass median aerodynamic diameter (MMAD) and geometric standard deviation (GSD) were determined using particle size analysis methods such as the Next Generation Impactor (NGI) and cascade impactor. No mortality

or moribund status was observed in any animal during the study. No notable abnormalities were found in general observations, body weight, food consumption, body temperature, respiratory function, hematology, coagulation, serum biochemistry, or immune function in any animal. Animals underwent gross necropsy at the end of the observation periods on Day 29 and Day 57, and major organs were collected for histopathological examination. Slight to mild interstitial mononuclear cell infiltration in the kidney was noted in the medium- and high-dose groups, which could not be excluded as test article-related. Cytokine analysis in bronchoalveolar lavage fluid (BALF) showed no obvious test article-related abnormalities in IL-2, IL-4, IL-5, IL-6, TNF, or IFN-γ in any dose group at the end of observation (Day 29/Day 57) compared with the concurrent control group. In addition, mRNA analysis of lung tissue showed that although variations existed in expression levels among different lung regions in the low-, medium-, and high-dose groups, reduced or trend-reduced expression of the RAGE gene was still observed in the overall lung tissue. **Results:** Under the conditions of this study, cynomolgus monkeys were administered a single nose-only inhalation exposure of the test article at 120 µg/L for 80 minutes, with delivered doses of 1.5 mg/kg, 3.0 mg/kg, and 10 mg/kg. All animals survived until scheduled necropsy. No notable abnormalities were observed in general clinical observations, body weight, food consumption, body temperature, respiratory function, hematology, coagulation, serum biochemistry, or immune function in any animal during the study period. At the end of observation (Day 29/Day 57), no test article-related abnormalities were detected in BALF cytokines, gross necropsy, or histopathology in any dose group. **Conclusions:** In summary, under the conditions of this study, the maximum tolerated dose (MTD) of the test article in cynomolgus monkeys following inhalation administration was at least 10 mg/kg (corresponding to a deposited dose of 2.5 mg/kg).

ABSTRACT NUMBER: 5185 **Poster Board Number:** K749

TITLE: Evaluating safety of *Areca catechu* palm leaf dinnerware based on toxicity data on its alkaloid constituents

AUTHORS (FIRST INITIAL, LAST NAME) AND INSTITUTIONS: A. K. Alexander, Ph.D., G. Patton, Ph.D., L. Cureton, Ph.D., K. McAdams, and *S. V. Kabadi, Ph.D.*. United States Food and Drug Administration (US FDA), College Park, MD.

KEYWORDS: Regulatory Science/Regulatory Toxicology; Safety Evaluation; QSAR; Palm leaf dinnerware; Alkaloids

ABSTRACT: Background and Purpose: Dinnerware made from the leaf sheath of the *Areca catechu* (*A. catechu*) palm are marketed in the U.S. as environmentally friendly, compostable, and biodegradable alternatives to single-use paper/plastic dinnerware. Plant-derived materials are generally considered safe, and FDA has historically not objected to their use as food contact substances provided they are of a purity such that they do not pose a safety concern. However, *A. catechu* palm leaf sheaths contain naturally occurring toxic alkaloids (*i.e*., arecoline, arecaidine, guvacoline, and guvacine). Recently, FDA published a paper that demonstrates migration of these alkaloids to food from palm leaf dinnerware products. **Methods:** To assess the safety of palm leaf dinnerware, we reviewed the available toxicological data on these alkaloids and evaluated 618 unique references related to the *A. catechu* palm and its alkaloid constituents. **Results:** Based on results of an oral carcinogenicity study of arecoline in Swiss mice, we determined that arecoline exhibited a potential for carcinogenicity based on increased incidences of lung, stomach, and liver tumors in male mice. From these results, we calculated a Unit Cancer Risk value of 0.0126 $(mg/kg\ bw/d)^{-1}$ for arecoline. There were no carcinogenicity data available

on the other alkaloids. Quantitative Structure Activity Relationship (QSAR) analysis showed a high degree of similarity between the structures of these four alkaloids and confirmed that toxicological data from arecoline could be applied to evaluate the safety of arecaidine, guvacoline, and guvacine. **Conclusions:** We concluded that all four alkaloids exhibited a potential for carcinogenicity based on positive results of the referenced carcinogenicity study on arecoline. As such, our assessment indicated safety concerns for the use of palm leaf dinnerware in contact with food based on potential resulting exposure to these alkaloids. Based on this concern, FDA determined that the use of *A. catechu* palm leaf in food-contact dinnerware is an unsafe food additive as defined under Section 409 of the Federal Food, Drug and Cosmetic Act.

ABSTRACT NUMBER: 5186 **Poster Board Number:** K750

TITLE: Metabolic Modulation of Methoxychlor-Induced Endocrine Activity Using Nuclear Receptor Reporter Assays in Co-Culture with Human Hepatocytes

AUTHORS (FIRST INITIAL, LAST NAME) AND INSTITUTIONS: *S. Maalouf*[1], Z. Elmasri[1], and *J. P. Vanden Heuvel*[1,2]. [1]INDIGO Biosciences, State College, PA; and [2]Department of Veterinary and Biomedical Sciences, Penn State University, University Park, PA.

KEYWORDS: Endocrine Disruptors; Metabolism; Hepatocytes; NAM, reporter assays

ABSTRACT: Background and Purpose: Methoxychlor is a known endocrine-disrupting pesticide with estrogenic and anti-androgenic activity. However, the role of hepatic metabolism in influencing its receptor-specific endocrine effects is not fully understood. **Methods:** In this study, we investigated the effect of coculture with metabolically competent and reproducible upcyte® hepatocytes on methoxychlor activity in nuclear receptor reporter assays for estrogen receptor (ER), androgen receptor (AR), and thyroid hormone receptor (TR). **Results:** In the absence of hepatocytes, methoxychlor showed limited direct activity in ER and AR reporter assays. In contrast, coculture with upcyte® hepatocytes revealed significant ER activation, consistent with metabolic bioactivation into estrogenic metabolites. Furthermore, methoxychlor demonstrated increased AR antagonism when hepatocytes were present, indicating that metabolism enhances its anti-androgenic potency. Notably, methoxychlor showed no agonist or antagonist activity toward TR, whether in the presence or absence of hepatocyte coculture, suggesting that its endocrine-disrupting effects are receptor-specific and not mediated through direct TR interaction. **Conclusions:** These findings show that including metabolically competent human hepatocytes can reveal endocrine liabilities not detected in traditional reporter assays and increase confidence that negative results are not due to the absence of metabolic activation. In conclusion, this coculture method offers a physiologically relevant *in vitro* model for studying metabolism-dependent endocrine disruption and enhances hazard identification for chemicals where hepatic bioactivation is essential.

ABSTRACT NUMBER: 5187 **Poster Board Number:** K751

TITLE: Bringing Bioenergetics to the Forefront-Validation for Early Detection of Mitochondrial Toxicity using Seahorse

AUTHORS (FIRST INITIAL, LAST NAME) AND INSTITUTIONS: S. Sahoo, J. Jose, S. Naik, V. R. Mekala, V. Madgula, and A. Mitra. Sai Life Sciences ltd, Hyderabad, India. Sponsor: V. Madgula, International Society for the Study of Xenobiotics

KEYWORDS: Safety Pharmacology; Mitochondrial toxicity

ABSTRACT: Background and Purpose: Mitochondrial toxicity remains a hidden liability in drug discovery, often surfacing late enough to derail promising programs with black-box warnings or market withdrawals. Analyses suggest that nearly one-third of compounds discontinued for safety/tox reasons show mitochondrial involvement, underscoring the urgency for better tools. Conventional cytotoxicity assays, while useful, frequently miss the functional disturbances that drive attrition. The Glucose/Galactose assay has long served as a benchmark, but its reliance on substrate switching provides only indirect insights. We set out to validate Seahorse extracellular flux technology as a more direct, sensitive, and translationally relevant approach to bioenergetic safety screening. **Methods:** Using Seahorse technology, we measured oxygen consumption and glycolytic flux in real time, capturing the dynamic balance of cellular bioenergetics. A diverse panel of compounds was profiled, spanning antibiotics, antiparasitic, CNS agents, statins, oncology drugs, antifungals, ion-channel modulators, and classical mitochondrial probes. Each compound's bioenergetic fingerprint was compared against known toxicological profiles to assess sensitivity, reproducibility, and translational relevance. **Results:** The Seahorse assay consistently separated compounds with mitochondrial liabilities from those with safer profiles. Toxic agents revealed characteristic disruptions, such as impaired oxidative phosphorylation, uncoupling of respiration, or suppressed glycolytic compensation, while non-toxic comparators maintained stable signatures. Importantly, Seahorse detected subtle changes overlooked by the Glu/Gal assay, demonstrating both robustness across compound classes and reproducibility suitable for scale-up. **Conclusions:** By directly probing cellular bioenergetics, Seahorse technology delivers functional insights that conventional assays miss. Its validated performance across diverse liabilities positions it as a practical and scalable solution for early safety screening. Integrating this assay into discovery pipelines can help identify risks sooner, conserve resources, and ultimately support safer drug development.

ABSTRACT NUMBER: 5188 **Poster Board Number:** K752

TITLE: Building trust in the concept of Virtual Control Groups to reduce the number of experimental animals in toxicology - the regulatory journey of the IHI VICT3R Project

AUTHORS (FIRST INITIAL, LAST NAME) AND INSTITUTIONS: K. Kopańska[1,2], *T. Hartung*[1,2,3], C. Rovida[2], M. Festag[4], F. Sanz[5], F. Bringezu[6], and T. Steger-Hartmann[7]. [1]Johns Hopkins University, Center for Alternatives to Animal Testing (CAAT), Baltimore, MD; [2]CAATevents, Solingen, Germany; [3]University of Konstanz, Center for Alternatives to Animal Testing (CAAT) – Europe, Konstanz, Germany; [4]Roche Pharmaceutical Research & Early Development, Pharmaceutical Sciences, Roche Innovation Center, Basel, Switzerland; [5]Universitat Pompeu Fabra, Hospital del Mar Research Institute, Barcelona, Spain; [6]Merck Healthcare KGaA, Chemical & Preclinical Safety, Darmstadt, Germany; and [7]Bayer AG, Pharmaceuticals, Berlin, Germany.

KEYWORDS: Alternatives to Animal Testing; Safety Evaluation; Preclinical Assessments; Virtual Control Groups

ABSTRACT: Background and Purpose: Toxicology is increasingly calling for innovative, ethical, and sustainable approaches, as highlighted in recent announcements from regulatory authorities across the Atlantic. At the same time, international regulations continue to mandate animal studies for human safety assessments. The Innovative Health Initiative (IHI) project VICT3R (*Developing and Implementing Virtual Control Groups to Reduce Animal Use in Toxicology,* Research-Grant agreement No: 101172693) is a global public-private initiative that enriches conventional toxicological testing with IT-driven and data-science-based alternative solutions, while still retaining the necessary animal studies for safety assessment and regulatory compliance. VICT3R aims to reduce animal use through novel approaches that replace concurrent control animals with Virtual Control Groups (VCGs). The development of VCGs is driven by the application of advanced statistical methods and AI, which leverage decades of historical control animal data from pharmaceuticals and other sectors. This approach has a direct ethical impact, reducing experimental animal use by up to 25% thus reinforcing the most underrepresented pillar of the 3Rs. Yet, these projections will only hold true if the qualification of the VCG concept yields reasonable results and if the use of VCGs becomes a regulatorily accepted method. **Methods:** To support the planning, execution, and reporting of retrospective and prospective studies that include VCGs for qualification purposes, VICT3R resides on strong collaboration with partners from pharmaceutical companies and CROs. These partners are actively involved in modelling different scenarios for the use of VCGs in drug development and chemical testing pipelines. Additionally, a Standard Operating Procedure (SOP) was developed, outlining requirements for collecting and curating data, generating VCGs, and reporting results in a clear, standardized, and reproducible manner. As part of our implementation strategy, formal regulatory interactions have been initiated with, among others, EMA through the Scientific Advice Working Party (SAWP) and OECD through the Working Party on Hazard Assessment (WPHA). VICT3R receives guidance on progressing these interactions from its Scientific Regulatory Advisory Board, which includes representatives from national European health authorities, ECHA, EURL ECVAM, as well as the US FDA and EPA. **Results:** During the first project year, the qualification focussed on retrospective analyses of repeat-dose toxicity studies in toxicologically relevant species, where concurrent controls were replaced with VCGs. This exercise adequately reproduced the original findings, demonstrating that the use of VCGs does not compromise study results or their final conclusions, and therefore does not pose a risk to patient or consumer safety. These results were consolidated and submitted to EMA SAWP in a request for Scientific Opinion, initiating an active feedback loop. While this

qualification procedure is ongoing, VICT3R is entering a prospective qualification phase in which VCGs are run together with concurrent controls in in general repeat dose toxicity studies. In parallel with the qualification activities, conversations were initiated with stakeholders from the OECD WPHA to obtain feedback on the procedures described in the SOP. Using this feedback, we submitted a project proposal for a "Feasibility Study on the use of VCGs in animal safety studies", which is currently being discussed. The long-term goal of these VICT3R-OECD interactions is to develop a Guidance Document outlining principles for the harmonised implementation of VCGs in preclinical studies. **Conclusions:** Through coordinated efforts with academic, industry, and regulatory partners, VICT3R is progressively building trust in the proposed VCG concept. While the qualificaiton efforts provide evidence supporting the suitability and safe use of VCGs in preclinical studies, the ongoing regulatory interactions are highly informative and interactive, allowing step-by-step progress toward regulatory acceptance. Lessons learned from these experiences will be published to support other communities aiming for qualification or regulatory acceptance of alternative methods.

ABSTRACT NUMBER: 5189 **Poster Board Number:** K753

TITLE: Safety Evaluation of CBT102, a Genetically Modified Bacteria for Treating Phenylketonuria

AUTHORS (FIRST INITIAL, LAST NAME) AND INSTITUTIONS: X. Liang[1], H. Chen[2], H. Lu[1], Y. Liu[1], B. Xiang[3], and *J. WANG*[1]. [1]Pharmaron (Beijing) TSP Services Limited (Pharmaron TSP), Beijing, China; [2]CommBio Therapeutics Co., Ltd. Room 603, Building 1, Lane 720 Cailun Road, Shanghai, Shanghai, China; and [3]CommBio Therapeutics Co., Ltd. Room 603, Building 1, Lane 720 Cailun Road, Shanghai 201203, China., Shanghai, China.

KEYWORDS: Toxicity; Acute; Pharmaceuticals; Genetic Toxicology; metabolic disorder; Genetically Modified Bacteria

ABSTRACT: Background and Purpose: Phenylketonuria (PKU) is an inherited metabolic disorder primarily resulting from mutations in the phenylalanine hydroxylase (PAH) gene, which encodes the enzyme responsible for the catabolism of phenylalanine. Current therapeutic approaches are inadequate to fully meet clinical needs. In recent years, genetically modified bacteria have attracted increasing attention as a promising therapeutic strategy. The purpose of this study is to identify and characterize potential toxicities of a genetically modified bacterial product CBT102, thereby supporting safety monitoring during clinical trials. **Methods:** Sprague-Dawley (SD) rats and Beagle dogs were selected for non-GLP toxicology studies. The design included single-dose maximum tolerated dose (MTD) studies and 14-day dose range finding (DRF) studies to determine the potential toxicity in each species. Parameters for toxicity evaluations included mortality, clinical observations, body weights, food consumptions, ophthalmology, clinical pathology, cytokines, organ weights, macroscopic and microscopic pathology, etc. Additionally, *in vivo* micronucleus assays and *in vivo* comet assays were also combined in the SD rat DRF study. **Results:** a. In the SD rat MTD study, up to 2.63×10^{12} live cell/kg/day was well tolerated. Abnormal findings were limited to brown staining around the anal area and a slight elevation in alkaline phosphatase. b. In the Beagle dog MTD study, up to 4.17×10^{10} live cell/kg/day was well tolerated. Yellow ocular discharge was found after administration in CBT102-dosed groups in clinical observations which test article effects cannot be ruled out. c. In the SD rat DRF study, up to 1.50×10^{12} live cell/kg/day was well tolerated. Abnormal findings included soft stool, anal staining (brown), and loose feces across dose groups of male animals. No abnormal body weights and body weight changes were noted in the whole dosing phase. Clinical chemistry revealed decreases in total

protein, globulin, IgG, and IgM in the 5.00×10^{11} live cell/kg/day group of male animals, decreases in CHO, TG, Na, Cl, IgG and IgM along with increases in BU, CRE and C_4 in 1.50×10^{12} live cell/kg/day group of male animals. Hematology results showed a decrease in ABRETIC and increases in WBC and ABLYMP in the 1.50×10^{12} live cell/kg/day group of male animals. Organ weight revealed decreases in liver and heart, and thymus in 1.50×10^{12} live cell/kg/day group of male animals. However, these organ weight changes lacked histopathological correlation and were considered secondary to reduced body weights. A specific real-time absolute quantitative PCR (qPCR) assay was developed to detect the genomic DNA (gDNA) copy number of CBT102. No gDNA was detected in blood samples at 1 h or 24 h post-dose in any groups, indicating rapid clearance or degradation. For the biodistribution, the gDNA was also analyzed in six tissues following 14 days of daily administration. The highest gDNA levels were observed 1 hour after the last dose. The proportion of the administered dose detected in the six organs was minimal in all dose levels, with the highest percentage being only 6.391‰ in a single sample. The distribution of gDNA was relatively uniform across all six organs, with no significant difference between genders and no dose dependency. d. In the Beagle dog DRF study, up to 8.35×10^{10} live cell/kg/day was well tolerated. Abnormal findings were limited to soft stools across all CBT102-dosed groups. By 1 h post-dose, the gDNA had become undetectable in all male animals blood samples. Following 14 days of dosing, gDNA was also analyzed in the same six tissues in Beagle dogs. The distribution of gDNA showed no notable differences between genders. The proportions of the administered dose detected in the six tissues were minimal, with the highest percentage being only 0.109‰ in a single sample. e. In the *in vivo* micronucleus assay of the SD rat DRF study, data suggested that CBT102 did not induce bone marrow cytotoxicity. f. In the *in vivo* comet assays of the SD rat DRF study, results of liver, stomach, and jejunum tissues showed that CBT102 did not induce DNA damages and genotoxic effects in the examined tissues. **Conclusions:** Overall, the genetically modified bacterial product CBT102 was well tolerated in these studies. As no adverse findings were identified, the no observed adverse effect level (NOAEL) was established at the high dose levels in all studies. These findings support further development of this product and underscore its potential as a promising additional option for PKU treatment.

ABSTRACT NUMBER: 5190 **Poster Board Number:** K754

TITLE: Proposed Mutagenic Safety Assessment Strategy for Oligomer Impurities in Oligonucleotide Therapeutics

AUTHORS (FIRST INITIAL, LAST NAME) AND INSTITUTIONS: F. Ishizuka, K. Hashikawa, R. Yamada, Y. Ota, T. Matsui, K. Okamoto, Y. Yamashita, Y. Numakura, H. Shibayama, T. Hanada, Y. Tonomura, and K. Asakura. Nippon Shinyaku Co., Ltd, Kyoto, Japan. Sponsor: F. Ishizuka, Japanese Society of Toxicology

KEYWORDS: Regulatory Science/Regulatory Toxicology; Mutagenesis; Safety Evaluation; Oligonucleotide

ABSTRACT: Background and Purpose: Impurities in oligonucleotide drug substances are generally categorized into oligonucleotide-related substances (oligomer impurities), small molecule organic impurities, and residual solvents. While guidelines such as ICH Q3 and ICH M7 are established for small molecules and solvents, there is currently no harmonized safety assessment guideline among Japan, the US, and Europe specifically for oligomer impurities. Consequently, risk assessments of genotoxicity are currently conducted on a case-by-case basis. A significant technical challenge is that the difficulty of the isolation and respective mutagenic evaluation of individual oligomer impurities due to similar physicochemical properties. The purpose of this study is to propose a systematic strategy for the mutagenicity risk assessment of oligomer impurities, focusing on establishing rational qualification

thresholds and testing decision trees. **Methods:** For a model morpholino nucleic acid therapeutic (approximate molecular weight 5,000) administered weekly, we developed a risk assessment strategy based on the classification of oligomer impurities into Classes I through IV (Capaldi et al., 2017). The assessment focuses primarily on Class IV (impurities that contain structural elements not found in the parent oligonucleotide or in naturally occurring nucleic acids), as this present potential mutagenicity risks distinct from the API. For Class IV impurities (e.g., residual protecting groups), we applied a quantitative structure-activity relationship ((Q)SAR) evaluation on the constituent monomers not found in the API structure, using two complementary prediction methodologies consistent with ICH M7 as *in silico* assessment. We also derived safety qualification thresholds by adapting ICH Q3A principles, adjusting for the molecular weight difference between small molecules and oligonucleotides, and applying Haber's Law principles for intermittent dosing. Furthermore, we incorporated the concept of threshold of toxicological concern (TTC) from ICH M7. **Results:** We calculated a specific safety qualification threshold. By adjusting the ICH Q3A qualification threshold (0.05%) for the tenfold molecular weight difference (500 (small molecules) vs. 5,000) and applying a conservative factor of 1.9 for weekly administration based on modified Haber's Law, we proposed a qualification threshold of 0.95%. If an impurity exceeds the proposed qualification thresholds and there is no available results from previous carcinogenicity study in different API with the same oligomer impurities, *in silico* assessment of the relevant monomer is conducted. Additionally, applying the ICH M7 TTC concept for weekly administration allows for a threshold of 10 µg/dose; impurities below this level are considered to have negligible mutagenicity risk. If the monomer is positive *in silico* analysis and content of oligomer impurities is exceeded to 10 µg/dose, an Ames test is conducted with representative oligomer impurity. Using a representative oligomer impurity is based on the assumption that the group shares identical physicochemical properties. The Ames test is conducted on the monomer itself if grouping is not feasible. **Conclusions:** We established a comprehensive strategy for evaluating the mutagenicity of oligomer impurities where direct isolation and testing are technically challenging. By defining a qualification threshold of 0.95% and a TTC-based limit of 10 µg/dose for weekly administered oligonucleotides (MW ~5,000), this approach provides a rational framework for safety assessment. This strategy establishes the regulatory gap for Class IV impurities, and robust risk assessment while accommodating the unique chemical characteristics of oligonucleotide therapeutics.

ABSTRACT NUMBER: 5191 **Poster Board Number:** K755

TITLE: Evidence-based evaluation for the reduction of animal testing: retrospective analysis of nonclinical safety data utility in predicting first-in-human clinical safety outcomes of monoclonal antibodies targeting infectious pathogens

AUTHORS (FIRST INITIAL, LAST NAME) AND INSTITUTIONS: *K. Noland*[1,2], K. Brant[2], C. Ellis[2], S. Dooling[3], K. Chan-Tack[4], and *T. Miller*[2]. [1]Oak Ridge Institute for Science and Education (ORISE), US Department of Energy (DOE), Oak Ridge, TN; [2]US FDA CDER/OND/OID Division of Pharmacology/Toxicology for Infectious Diseases, Silver Spring, MD; [3]US FDA CDER/OND/OID Division of Anti-Infectives, Silver Spring, MD; and [4]US FDA CDER/OND/OID Division of Anti-Virals, Silver Spring, MD.

KEYWORDS: Safety Evaluation; Preclinical Assessments; Alternatives to Animal Testing

ABSTRACT: Background and Purpose: The 2025 U.S. FDA Roadmap to Reducing Animal Testing in Preclinical Safety Studies promotes usage of new approach methodologies (NAMs) to reduce animal studies. Recent FDA publications identified gaps in traditional nonclinical safety study predictivity, leading to the 2025 FDA Roadmap encouraging incorporation of NAMs and reduced animal studies for monoclonal antibody (mAb) safety evaluation. The 2012 ICH S6(R1) guidance recommends streamlined testing for mAbs targeting foreign antigens, permitting single-species short-term studies with tissue cross-reactivity evaluation. This project evaluates traditional nonclinical animal studies' predictive utility for FIH safety outcomes using infectious disease mAb data. While NAM inclusion frequency is documented, NAM predictive utility is not evaluated here. Analysis using the ICH S6(R1) safety framework can identify opportunities for NAM incorporation into Weight of Evidence approaches, advancing 2025 FDA Roadmap initiatives. This supports regulatory decisions that reduce animal testing while maintaining safety assessment confidence and encouraging NAM development in regulatory submissions. **Methods:** BLA, EUA, and INDs for mAbs targeting infectious pathogens submitted post 2012 ICH S6(R1) that included healthy participant FIH clinical safety data were reviewed. Exclusions included antibody fragments, multi-specific antibodies, antibody-drug conjugates, and co-administered products. Nonclinical data included study types, species, adverse events, and frequency of NAM submission. FIH clinical data evaluated included dosing, routes, treatment-emergent events, and reviewer-identified findings. **Results:** *BLA:* Six of the seven licensed mAbs had no adverse findings in nonclinical toxicology studies. However, subsequent FIH clinical trials in healthy volunteers identified treatment-emergent events, typically related to hypersensitivity and/or systemic effects such as fatigue, myalgia, and nausea. *EUA:* Seven authorized mAbs had no adverse findings in nonclinical toxicology studies. A key limitation to our clinical safety analysis was that clinical findings in COVID-19 positive patients were difficult to distinguish from mAb associated events due to overlap with disease manifestations, preventing clear determination if any adverse events were treatment and/or mAb related. *IND:* Over 20 investigational mAbs had no adverse findings in nonclinical toxicology studies via the intended clinical route of administration. In FIH studies, most clinical safety outcomes were mild to moderate and self-limiting. Administration route influenced FIH event profiles: intravenous infusions were well-tolerated with minimal local reactions, while subcutaneous or intramuscular injections showed higher incidence of injection site reactions. Common treatment-emergent events included headache, malaise/fatigue, nausea, and transient laboratory abnormalities that were not clinically significant. **Conclusions:** Data analysis across BLAs, EUAs, and INDs detailed limitations in the ability of nonclinical safety studies to predict clinical safety outcomes for therapeutic mAb products. This analysis supports the need for developing refined testing strategies and establishing further considerations to

improve the utility of preclinical safety evaluations to predict FIH clinical safety. Systematic analysis of the predictive nature, accuracy, and consistency of submitted nonclinical safety data, provides key regulatory stakeholders with insight into areas of strength, deficiencies, and aspects that may benefit from further refinement of nonclinical safety evaluations. This informs and advances the FDA's 2025 Roadmap initiatives, allowing for the advancement of both traditional nonclinical approaches and alternative model development.

ABSTRACT NUMBER: 5192 **Poster Board Number:** K756

TITLE: An Alternative Model of Choroidal Neovascularization in Non-human Primates Results in a Higher Success Rate of CNV Induction and Inhibition of Leakage with Eylea and Lucentis

AUTHORS (FIRST INITIAL, LAST NAME) AND INSTITUTIONS: *S. Vasanth*, C. K. Jennings, L. N. Stall, and R. F. Boyd. Charles River Laboratories, Mattawan, MI.

KEYWORDS: Ocular Toxicity; *In Vivo* Models; Preclinical Assessments; choroidal neovascularization; VEGF

ABSTRACT: Background and Purpose: Laser-mediated photocoagulation has been extensively used in rodents and non-human primates (NHP) to induce choroidal neovascularization (CNV) to generate an induced efficacy model for testing anti-VEGF molecules intended for treatment of wet age-related macular degeneration (wet AMD). This model has historically been generated with a slit-lamp mounted 532 nm laser focused on the Bruch's membrane. Significant variability between animals have been observed in the success rate of inducing lesions and with the severity of fluorescein leakage thus requiring a large sample size (animal number) to conclusively assess differences in leakage. In this study, we aim to establish a fluorescein leakage model reminiscent of CNV in NHPs by performing photocoagulation with an endo-laser probe and to assess the efficacy of Eylea and Lucentis in alleviating leakage for up to six weeks. **Methods:** Twelve cynomolgus macaques were assigned to the study and divided into two groups of six animals each. Six laser spots were positioned bilaterally within the macula of each eye with a 532 nm laser using an endo-laser probe. Endotoxin-free phosphate buffered saline (PBS), Eylea, or Lucentis were administered intravitreally on Day 1 immediately following laser photocoagulation and on Day 22. All left eyes were administered PBS and all right eyes were either administered Lucentis (Group 1) or Eylea (Group 2). Ophthalmic examinations, intraocular pressure (IOP) measurements, fluorescein angiography (FA), and optical coherence tomography (OCT) were performed postdose. Animals underwent scheduled termination on Day 43. Eyes were fixed in Davidson's fixative and sectioned for hematoxylin and eosin (H&E) staining. **Results:** Ophthalmic examination revealed moderate intraocular inflammation (IOI) in 2/24 eyes (two animals) 2 to 3 days following laser photocoagulation. One animal received systemic nonsteroidal anti-inflammatory therapy and IOI resolved at Day 8. The second animal received weekly systemic corticosteroid therapy and topical difluprednate until IOI alleviated on Day 29. IOP measurements did not reveal any significant changes due to laser, PBS, Eylea, or Lucentis. Qualitative grading of fluorescein leakage in eyes treated with PBS showed moderate to severe leakage (Grades 3 and 4) in ~73% spots (52/71) at Day 14 and ~83% spots (60/72) at Day 28. In contrast, Eylea treated eyes abrogated Grade 3-4 leakage resulting in 100% spots that were Grade 1-2 at both Days 14 and 28. Lucentis showed a similar effect with ~92% spots showing Grade 1-2 leakage at both Days 14 and 28. These differences persisted until termination with a mean leakage grade of 3.14 for eyes administered PBS compared to 1.71 and 1.67 for Lucentis and Eylea respectively. The second dose of Eylea or Lucentis did not significantly change the severity of leakage

observed on Day 28 or prior to termination. OCT imaging showed focal edema and necrosis of the retina at the laser sites on Day 8 followed by progressive retinal thinning by Day 29. H&E staining recapitulated OCT findings of retinal thinning at the sites of photocoagulation. There were no differences in the thickness of retinal layers at the photocoagulation sites due to Eylea or Lucentis. **Conclusions:** This alternate method of laser photocoagulation using an endo-laser probe resulted in the successful induction of moderate to severe leakage in all eyes. In the slit-lamp based model, the success rate of inducing moderate to severe leakage is between 40-70% and varies significantly between investigators and animals. In this method, lasered spots in eyes administered PBS showed greater uniformity in leakage and area than those observed with the slit-lamp based model. In addition, efficacy of Eylea and Lucentis could be assessed as early as two weeks postdose, thus providing an efficient method and a high success rate of inducing spots with leakage that could be assessed for efficacy. The high success rate thus reduces the number of animals needed to test anti-VEGF drugs either administered as a peptide, antibody, or an AAV.

ABSTRACT NUMBER: 5193 **Poster Board Number:** K757

TITLE: Evaluation and Comparison of *In Vitro* Permeation Testing (IVPT), Barrier Function, and Lipid Composition in Alternative Skin Models and Excised Human Skin

AUTHORS (FIRST INITIAL, LAST NAME) AND INSTITUTIONS: *S. Modaresi*[1], J. Sun[1], *A. T. Salminen*[1], K. J. Davis[2], R. P. Felton[1], M. Maisha[1], F. A. Beland[1], K. Derr[3], M. Ferrer[3], *N. C. Kleinstreuer*[4], J. Leshin[5], P. Manga[6], N. Sadrieh[7], M. Xia[3], *S. C. Fitzpatrick*[8], and *L. Camacho*[1]. [1]National Center for Toxicological Research, U.S. Food and Drug Administration, Jefferson, AR; [2]Toxicologic Pathology Associates, Jefferson, AR; [3]National Center for Advancing Translational Sciences, National Institutes of Health, Rockville, MD; [4]NTP Interagency Center for the Evaluation of Alternative Toxicological Methods, National Institute of Environmental Health Sciences, Research Triangle Park, NC; [5]Center for Veterinary Medicine, U.S. Food and Drug Administration, College Park, MD; [6]Office of Cosmetics and Colors, U.S. Food and Drug Administration, College Park, MD; [7]Center for Drug Evaluation and Research, U.S. Food and Drug Administration, Silver Spring, MD; and [8]Human Foods Program, U.S. Food and Drug Administration, College Park, MD.

KEYWORDS: Percutaneous Absorption; *In Vitro* and Alternatives; Hazard Identification/Reduction; Reconstructed Skin

ABSTRACT: Background and Purpose: *In vitro* methods are available to evaluate the amount and rate of skin absorption of topical products and contribute to their safety and/or efficacy assessments. Excised human skin (EHS) is the 'gold standard' for *in vitro* permeation testing; however, due to high cost and supply shortages, there is a need to find suitable alternatives as skin barrier models. Previously, we evaluated the performance of a subset of skin models for *in vitro* permeation testing (IVPT) over 6 hours. In this study, we expanded our research by employing automated diffusion equipment with flow-through cells to perform IVPT for 24 hours using commercially available skin models, including an artificial membrane, reconstructed human epidermal and full-thickness models, excised minipig skin, and EHS. **Methods:** The reconstructed human skin models tested included ZenSkin, SkinEthic RHE, EpiDerm-200, and EPI-200-X as epidermal models and T-Skin, EpiDermFT-400, and Phenion-FT as full-thickness models. In addition, the artificial membrane Strat-M and excised minipig skin were evaluated, along with EHS. The cumulative amount (nmol/cm^2), flux (nmol/cm^2/h), and mass distribution (% of dose) of ^{14}C-labeled caffeine, salicylic acid, testosterone, and mannitol (dose: 10 µL/cm^2; 6 nmol/cm^2)

were compared between EHS and each alternative skin model using IVPT. Transepithelial water loss (TEWL) and histology were also compared across models to correlate their barrier function and structure. Furthermore, a method has been developed to isolate the stratum corneum of each biological skin model by trypsin enzymatic digestion (0.5% (w/v) trypsin in PBS at 37 °C), followed by a pilot liquid chromatography-high resolution mass spectrometry (LC/HRMS)-based untargeted lipidomic analysis to examine the stratum corneum lipidome in the alternative skin models and EHS. **Results:** The permeation of caffeine and salicylic acid was higher than that of testosterone and mannitol across all skin models. EHS exhibited the lowest average TEWL value, with the TEWL in alternative skin models increasing in the order EHS ≈ minipig ≈ Strat-M < EpiDerm-200-X < EpiDerm-200 ≈ SkinEthic RHE < ZenSkin ≈ T-Skin < EpiDermFT-400 ≈ Phenion-FT. The observed trend of TEWL was generally correlated to the permeation function of the skin models. Histological evaluation showed that each biological skin model had a stratified structure characteristic of the human skin anatomy. Additionally, the stratum corneum was isolated successfully from each biological skin model. Preliminary lipidomics data support the feasibility of using a LC/HRMS protocol to characterize the lipid composition of the stratum corneum from both excised and reconstructed skin models and evaluate the correlation with the permeation function of each skin model. **Conclusions:** Overall, the TEWL and IVPT data suggest that the reconstructed skin models have a weaker barrier than EHS and minipig skin, although the magnitude of differences varies by model and test compound. The lipidomics data, together with the IVPT, TEWL, and histology data, may help guide further optimization of reconstructed human skin to match the barrier properties of EHS. The systematic comparison of alternative skin models and EHS contributes to the evaluation of the potential use of these models as new approach methods (NAMs) to predict dermal absorption of FDA-regulated compounds.

ABSTRACT NUMBER: 5194 **Poster Board Number:** K758

TITLE: An immunocompetent *ex vivo* human skin platform with extended viability for evaluating antibody-drug conjugate-induced skin toxicity

AUTHORS (FIRST INITIAL, LAST NAME) AND INSTITUTIONS: J. S. Holsapple, B. L. Coates, P. Sharma, J. Michaud, P. Thompson, E. Anderson, J. Chiari, S. Hein, E. Galt, S. Lee, C. Hinojosa, and K. Jang. Outer Biosciences, Malden, MA. Sponsor: *M. Otieno*

KEYWORDS: Safety Evaluation; Alternatives to Animal Testing; Cutaneous or Skin Toxicity; Enfortumab vedotin, Monomethyl Auristatin E

ABSTRACT: Background and Purpose: Antibody-drug conjugates (ADCs) offer precise and potent cancer therapy through the coupling of a targeting antibody and cytotoxic payload. However, ADCs often exhibit severe cutaneous adverse events through on-target, off-tumor binding to antigens expressed in skin as well as toxicity related to free payloads. Conventional preclinical models often fail to completely de-risk these compounds, and recent FDA initiatives have encouraged adoption of human-relevant New Approach Methods (NAMs) for safety assessment. **Methods:** To address these limitations, we have employed our advanced human *ex vivo* skin platform featuring a novel 3D-printed culture system and extended model viability and immunocompetence for the evaluation of commercially available ADCs and their corresponding free payloads over a 14-day treatment period. This platform can utilize over 100 replicate samples per donor from a diverse pool of donors across demographics and body regions, allowing for simultaneous testing of a battery of compounds and concentrations. **Results:** We captured not only acute cytotoxic events from the free payload as measured through LDH release and

histopathology scoring, but importantly more chronic, targeted events related to ADC activity and especially as concentrations approached the clinical Cmax. Parameters from pathology scoring highlighted parakeratosis, dyskeratosis, subepidermal blistering, and lymphocyte infiltration. The inflammatory profile of this ADC-induced skin toxicity was detected via elevated IL-8 and S100A8/9 release. By combining imaging modalities, we validated diffusion of ADC via basal administration into the dermis and epidermis as well as colocalization of the payload and target antigen. In addition, our platform enabled detection of mitoses, a critical parameter in assessing the cell cycle-arresting effects of these payloads. **Conclusions:** This study recapitulated clinical observations, positioning our platform as a physiologically relevant, human-based tool for the refinement of ADCs to mitigate skin toxicities, ultimately improving both therapeutic efficacy and patient outcomes.

ABSTRACT NUMBER: 5195 **Poster Board Number:** K759

TITLE: Predicting NESIL using New Approach Methodologies: a case study on quantitative skin sensitization assessment of topical over-the-counter pharmaceutical candidates

AUTHORS (FIRST INITIAL, LAST NAME) AND INSTITUTIONS: *P. M. Radcliffe*[1], T. Lindberg[2], J. Andersson[2], and *T. L. Spriggs*[1]. [1]Haleon, Warren, NJ; and [2]SenzaGen AB, Lund, Switzerland.

KEYWORDS: Dose-Response; Safety Evaluation; Cell Culture; GARD

ABSTRACT: Background and Purpose: Skin sensitizers are chemicals capable of inducing allergic contact dermatitis (ACD), making their identification and characterization critical for protecting human health. Significant progress has been made in the development of New Approach Methodologies (NAMs) to replace animal testing for skin sensitization, resulting in internationally recognized OECD test guidelines and defined approaches that integrate *in vitro*, *in chemico*, and *in silico* data. While NAMs are widely implemented in the cosmetics and chemical sectors, their adoption within the pharmaceutical industry remains limited, where animal tests such as the Guinea Pig Maximization Test (GPMT) and Local Lymph Node Assay (LLNA) are still commonly used. This landscape is evolving rapidly in response to global regulatory initiatives promoting the Replacement, Reduction, and Refinement (3Rs) of animal testing, including EU legislation, the U.S. FDA Modernization Act 2.0, and the recently published UK roadmap toward reduced animal use. This case study demonstrates how NAMs, including the *in vitro* GARD® assays, can be applied to skin sensitization assessment of topical Over-the-Counter (OTC) pharmaceuticals. Beyond hazard identification, it enables quantitative assessment of sensitization potency, including prediction of the human No Expected Sensitization Induction Level (NESIL), thereby supporting quantitative risk assessment (QRA). **Methods:** GARD®skin (OECD TG 442E) is an *in vitro* assay for skin sensitization hazard identification based on transcriptional profiling of a 196-gene genomic prediction signature (GPS) in the dendritic-like SenzaCell® cell line. A machine-learning based prediction model generates Decision Values (DV), where positive mean DV indicates classification as a sensitizer. GARD®skin Dose-Response (DR) is an adaptation of the standard assay in which test substances are evaluated across an extended concentration range to establish the relationship between DV and concentration. From this relationship, a quantitative potency metric (cDV_o) is derived, defined as the lowest concentration generating a positive mean DV. The cDV_o can be used to predict LLNA EC3 values and human NESIL with high statistical significance. In this study, two topical gel-based OTC Non-Steroidal Anti-Inflammatory Drug (NSAID) candidate formulations (test items A and C) and a frequently used ingredient (test item B) were evaluated. All were complex mixtures containing different concentrations of active ingredients and excipients. The formulations were first assessed using GARD®skin for hazard

identification, and those classified as sensitizers were subsequently evaluated using GARD®skin Dose-Response (DR) to determine sensitization potency. **Results:** All three test items were classified as sensitizers in GARD®skin and were further assessed for potency in GARD®skin DR:

- Test item A: cDV_o = 72.5 µg/mL; predicted NESIL = 22,000 µg/cm²
- Test item B: cDV_o = 27.4 µg/mL; predicted NESIL = 8,320 µg/cm²
- Test item C: cDV_o = 90.5 µg/mL; predicted NESIL = 27,500 µg/cm²

Test item B exhibited the lowest cDV_o and NESIL, indicating weak sensitization potency when compared with established reference values. Test items A and C were positive only at the highest tested concentration, with decision values close to the classification threshold, indicating very weak potency. **Conclusions:** Although a potential skin sensitization hazard was identified for all test items, quantitative potency data indicated clear differences in sensitization strength. Test items A and C were considered at most very weak sensitizers with limited clinical relevance under the estimated exposure conditions, whereas test item B demonstrated weak potency and provides a basis for establishing a safe dose level through further QRA. Overall, this case study demonstrates how NAM-based approaches can move beyond binary hazard identification to support NESIL prediction and quantitative risk assessment for topical pharmaceuticals, enabling more evidence-based, human-relevant safety evaluations while reducing reliance on animal testing.

ABSTRACT NUMBER: 5196 **Poster Board Number:** K760

TITLE: Polyhexamethylene guanidine disrupts the skin barrier through tight junction disruption and induces skin sensitization

AUTHORS (FIRST INITIAL, LAST NAME) AND INSTITUTIONS: B. Lee, H. Kang, H. Kim, and H. Kim. National Institute of Environmental Research, Incheon, Korea, Republic of. Sponsor: *K. Lee*

KEYWORDS: Disinfection Byproducts; Cutaneous or Skin Toxicity; Chemical of Concern; Humidifier disinfectant; PHMG

ABSTRACT: Background and Purpose: Humidifier disinfectants (HDs) are household biocides used to prevent water scale and microbial growth in the water tank of humidifiers. HDs were the cause of an outbreak of lung disease in the Republic of Korea in 2011. Their toxicity has been studied over the last 10 years, but most studies have focused on the respiratory system, the primary route of exposure. However, non-respiratory diseases, such as allergic contact dermatitis, have also been reported among the victims. **Methods:** *In vitro* prediction of allergic responses has several limitations, because allergic diseases are systemic and involve immune responses mediated by multiple cell types. However, the OECD has suggested specific test guidelines, such as the human Cell Line Activation Test (h-CLAT, OECD TG 442E). This assay, corresponding to the third key event (KE3) of the skin sensitization adverse outcome pathway (AOP), evaluates the ability of monocytes to activate dendritic cells by measuring the surface expression of CD54 and CD86, which serve as co-stimulatory and adhesion molecules. However, h-CLAT cannot assess organ-specific responses, as it examines only direct chemical-monocyte interactions. **Results:** In this study, the expression of the tight junction protein claudin-8 was decreased in keratinocytes following exposure to polyhexamethylene guanidine (PHMG), a widely used ingredient in humidifier disinfectants (HDs). To assess tight junction disruption, transepithelial electrical resistance (TEER) was measured. As a result, the barrier function of keratinocytes showed a dose-dependent decrease. The other hands, the skin sensitization potential was evaluated using monocyte-keratinocyte co-culture system. THP-1 cells and the co-culture system consisting of THP-1 monocytes and HaCaT keratinocytes were exposed to PHMG for 24 hours. After exposure, the surface expression levels of

CD86 and CD54 in THP-1 cells were analyzed by flow cytometry. **Conclusions:** As a results, CD86 expression showed no significant changes, whereas CD54 expression increased more than two folds compared with THP-1 cells exposed to PHMG alone.

ABSTRACT NUMBER: 5197 **Poster Board Number:** K761
TITLE: Utilization of the DPRA to test sensitizers in acrylic adhesives used for wearable medical devices

AUTHORS (FIRST INITIAL, LAST NAME) AND INSTITUTIONS: A. Hsu, J. Deng, T. Kwa, G. Zhang, and S. Chattaraj. Medtronic MiniMed Inc., Northridge, CA. Sponsor: *K. Coleman*
KEYWORDS: Alternatives to Animal Testing; *In Vitro* and Alternatives

ABSTRACT: Background and Purpose: Wearable medical devices, such as continuous glucose monitors and insulin pumps, often use acrylic adhesives that can leach out and cause severe skin reactions. To mitigate these risks, regulatory agencies now require stricter biocompatibility testing and urge device manufacturers to eliminate or reduce sensitizing ingredients to levels below a safe Acceptable Exposure Level (AEL). Screening for potent sensitizers and adjusting formulations accordingly is highly beneficial for end users. Traditionally, sensitizer testing relied on *in-vivo* methods involving humans or animals. There is a growing emphasis on adopting *in-vitro* approaches for identifying sensitizers, with the Direct Peptide Reactivity Assay (DPRA) emerging as a promising alternative. The DPRA replicates the initial key event in the skin sensitization adverse outcome pathway, wherein a chemical (sensitizer) covalently binds to skin proteins, triggering an immune response. This method uses synthetic peptides that mimic human skin proteins and measures the reaction via high-performance liquid chromatography (HPLC). Although acrylates in medical devices are generally present at low concentrations, testing at higher concentrations (100 mM, as recommended by OECD guidelines for DPRA) enables worst-case scenario analysis and aids in identifying potential sensitizers. In this study, we compared the predictive accuracy of the DPRA with commonly used *in-vivo* sensitization test methods to assess known skin sensitizers. **Methods:** We tested the DPRA on acrylates commonly presented in acrylic adhesives, including methyl acrylate, ethyl acrylate, butyl acrylate, ethylene glycol dimethacrylate (EGDMA), isobornyl acrylate (IBOA), isobornyl methacrylate (IBOMA), and hexanediol diacrylate (HDDA), and compared results with human sensitization data and Local Lymph Node Assay (LLNA) values obtained from the SkinSensDB, Human Predictive Patch Test (HPPT) database, and other literature sources. DPRA testing was conducted in accordance with OECD 442C guidelines, utilizing synthetic cysteine (Ac-RFAACAA-COOH) or lysine (Ac-RFAAKAA-COOH) peptides incubated with 100 mM test chemicals for 24 hours at 22.5-30°C. Sensitization reactivity was quantified via peptide depletion, measured using HPLC with a detection wavelength of 220 nm. Skin sensitization potency was classified based on OECD-defined thresholds: highly reactive sensitizers exhibited >42.47% mean cysteine/lysine peak depletion or >98.24% cysteine peak depletion. LLNA strong sensitizers were identified by an EC3 value (the concentration producing a stimulation index of 3 in the LLNA) ≤2%, corresponding to UN GHS/CLP guidelines and we categorized chemicals with an EC3 ≤100% as a sensitizers according to ECETOC recommendations. Human sensitization data, such as dose per skin area (DSA ≤500 μg/cm²) or patch test results, served as the reference standard for human sensitization assessment. Performance of sensitization test methods was assessed using sensitivity (true positive rate), specificity (true negative rate), and accuracy (correct prediction rate) using a confusion matrix. **Results:** Of the seven acrylates assessed, the DPRA method identified all 5 human sensitizers (100% sensitivity), with 1 true negative and 1 false positive (50% specificity, 85.7% accuracy). LLNA predictions closely matched DPRA predictions. LLNA also detected all

5 of 5 human sensitizers (100% sensitivity), with 1 false positive and 0 false negative (0% specificity, 83.3% accuracy). **Conclusions:** This study highlights the potential of the DPRA protocol as a viable method for rapidly prescreening and identifying sensitizers in acrylic-based adhesives intended for wearable applications. This innovative approach offers a rapid, cost-effective, and animal-free alternative for detecting skin sensitizers in adhesive materials, enabling informed material selection to reduce the risk of adverse skin reactions. Future efforts will aim to adapt the DPRA for analyzing low-concentration compounds in exhaustive medical device extracts, expanding its utility in sensitizer screening. Additionally, research will explore whether the DPRA can determine the NESIL (No Expected Sensitization Induction Level) for acrylates through the use of scaling factors, further broadening its applicability.

ABSTRACT NUMBER: 5198 **Poster Board Number:** K762

TITLE: Applying the "2 out of 3" Defined Approach (OECD 497) to Assess Skin Sensitization Potential of UVCBs using the GARD®skin and EpiSensA assays

AUTHORS (FIRST INITIAL, LAST NAME) AND INSTITUTIONS: M. E. Solan[1], H. A. Nyambego[1], P. Alftrén[2], J. Andersson[2], and T. Lindberg[2]. [1]ExxonMobil Biomedical Sciences, Inc., Spring, TX; and [2]SenzaGen AB, Lund, Sweden. Sponsor: M. Solan, Society of Environmental Toxicology and Chemistry

KEYWORDS: *In Vitro* and Alternatives; Hazard Identification/Reduction; International Harmonization; Skin Sensitization; UVCB

ABSTRACT: Background and Purpose: The skin sensitization adverse outcome pathway (AOP) published by the OECD in 2012 defined the key events (KEs) leading to allergic contact dermatitis. The AOP enabled the development of targeted non-animal methods focused on the first three KEs of the AOP, including the OECD guidelines 442C (KE1), 442D (KE2), and 442E (KE3). While none are standalone replacements, the methods can be combined under defined approaches (DAs) within OECD 497 or used in weight of evidence (WoE)-based evaluation. OECD 497 initially included one assay per guideline in the 2 out of 3 (2o3) DA: Direct Peptide Reactivity (OECD 442C), KeratinoSens (OECD 442D) and the Human cell-line activation test (OECD 442E). These three assays have limited applicability for challenging substances, including Unknown or Variable composition, Complex reaction products, or Biological materials (UVCBs). Inclusion of new assays in OECD 442C, D, and E to address KEs 1-3 prompted a revision of OECD 497 to include more methods. Here we demonstrate how the assays included in the latest revision of OECD 497 enable a 2o3 DA for UVCBs. **Methods:** GARDskin (OECD 442E) is a genomic, machine learning-based assay targeting KE3 (dendritic cell activation) of the AOP. The method utilizes a dendritic-like cell line, SenzaCell®, and provides binary hazard identification by measuring transcriptional responses captured by a 196-gene endpoint-specific biomarker signature that enables predictions via positive (≥0; sensitizer) or negative (<0; non-sensitizer) mean Decision Values (DV). Multiple peer-reviewed studies have demonstrated the method's applicability to challenging test materials like hydrophobic substances (LogP>3.5) and UVCBs attributable to its broad solvent compatibility. EpiSensA (OECD 442D) is an *in vitro* skin sensitization assay using a Reconstructed Human Epidermis (RhE) model targeting KE2 (keratinocyte activation). It quantifies expression of 4 target genes associated with inflammatory and cytoprotective responses via RT-qPCR. A test material is a sensitizer if at least one of the mean fold-induction values are exceeded. Direct test material application to the RhE surface makes the EpiSensA suitable for evaluating challenging materials. **Results:** Three UVCBs were assessed for sensitization potential: a phthalate ester (PE; LogP=8.12), a polyalphaolefin (PAO; LogP=10.64) and an

adipate ester (AE; LogP=10.64). for the GARDskin assay, the test materials were solubilized in ethanol, hexane, and dimethyl sulfoxide, respectively. For EpiSensA, all test materials were found to be soluble in acetone: olive oil (4:1). Hazard predictions for the UVCBs were made following acceptance of the test criteria and viability measurements. None of the test materials reduced viability or exceeded defined target gene thresholds in the EpiSensA assay. In the GARDSkin assay, the mean DVs were -0.272, -1.79, and -1.33 for PE, PAO, and AE, respectively. Taken together under the 2o3 DA, all three test materials are non-sensitizers. **Conclusions:** GARDskin and EpiSensA assays have broad chemistry applicability, making them suitable for challenging substances. We have demonstrated a successful 2o3 DA for non-sensitizers using KE2 and KE3 for three UVCBs. For potency categorization, an Integrated Testing Strategy (ITS) including OECD 442C assay must be used. However, OECD 442C assays remain problematic for many UVCBs substances due to molar ratio requirements of the constituents or because of solubility/stability issues. Still, the combined GARDskin and EpiSensA assays are particularly well suited for UVCB hazard evaluation and may support potency categorization with additional data in a WoE approach.

ABSTRACT NUMBER: 5199 **Poster Board Number:** K763

TITLE: Minimize false positive results in the h-CLAT assay by utilizing flow cytometry data and Isotype response

AUTHORS (FIRST INITIAL, LAST NAME) AND INSTITUTIONS: M. Duplaa[1], P. Jenkinson[1], D. Guyomar[1], J. Kurtz[2], and *M. Diop*[2]. [1]CEHTRA SAS, Cenon, France; and [2]V. MANE Fils, Le Bar-sur-Loup, France.

KEYWORDS: Chemical Hazard Assessment; *In Vitro* and Alternatives; Cytotoxicity; Skin sensitisation

ABSTRACT: Background and Purpose: The h-CLAT assay is one of the battery of three *in chemico/in vitro* assays currently recommended by ECHA to meet the skin sensitization (SS) endpoint in a REACH dossier. The OECD 497 guideline for Defined Approaches (DAs) for SS, combines information from three test methods based on *in chemico* (Key Event 1) and *in vitro* (Key Events 2 and 3) data, with or without *in silico* tools (DEREK or QSAR Toolbox), and applies a fixed interpretation procedure to the results to generate a prediction. Whatever the DA used to conclude on the SS potential of a substance, i.e., “2 out of 3” (2o3) or the Integrated Testing Strategy (ITS), obtaining a false positive or false negative result can create a difficulty to interpret the data set of an ITS. **Methods:** We present h-CLAT data for two substances from different chemical classes both with a purity of 99.6% and with essentially negative SS profiles (DPRA, SENS-IS, DEREK Nexus, OECD TB DASS), except for the h-CLAT assay. One substance was positive in CD54 only (both experiments), whilst the other was positive in CD54 in both experiments, but positive in CD86 only in 1 experiment. However, both substances induced a clear dose-related increase in the fluorescence of the mouse IgG1 isotype control antibodies. Furthermore, the flow cytometry data (FACS plots) showed a marked dose-related increase in the overlap in the signals for live and dead cells, and in addition, a dose-related accumulation in the number of dead cells excluded from the cell count data by the PI gate setting. **Results:** The OECD 442E test guideline does not inform on the exact purpose of the Isotype control, but normally it is to control for random, non-specific antibody binding to the cell membrane. Furthermore, the guideline does not provide information on the meaning of an increase in the isotype response. Other sources indicate that an increase in Isotype antibody binding may be caused by autofluorescence of the substance. However, if the substance is not autofluorescent (as is the case for these substances), then the literature does not provide alternative explanations for a dose-related increase in Isotype antibody fluorescence. In the h-CLAT, the Mean Fluorescence Intensity (MFI) of the

Isotype controls is subtracted from the MFI values of the CD86 and CD54 antibodies, to control for the non-specific binding of the antibodies. However, FACS experts indicate that in cases where the plots of the live and dead cells overlap, then the correction for the Isotype control should be done by ratio, not subtraction. If the data for these two substances are corrected by ratio, then different results are obtained, whilst the positive controls retain their activity. **Conclusions:** We propose that excessive toxicity, not identified using the standard procedures, but identifiable using available data, may be the cause of the increase in isotype binding and consequently for the conflicting SS results for these two substances.

ABSTRACT NUMBER: 5200 **Poster Board Number:** K764

TITLE: Improving the safety profiles of fragrance formulations: modulating the skin sensitization potential to reduce or eliminate the risk of allergic skin reactions

AUTHORS (FIRST INITIAL, LAST NAME) AND INSTITUTIONS: T. Lindberg[1], R. Gradin[1], F. Henderup[1], A. Saint-Paul[2], E. Perrotta[2], and *A. Forreryd*[1]. [1]SenzaGen AB, Lund, Sweden; and [2]Coty Inc., Versoix, Switzerland.

KEYWORDS: Dose-Response; Risk Assessment; GARD

ABSTRACT: Background and Purpose: Fragrances are small, volatile and reactive chemicals. These physicochemical properties are essential for their function but also allow interactions with biological systems that can lead to adverse reactions. Of particular interest from a toxicological perspective is the endpoint of skin sensitization, and the potential of these molecules to give rise to Allergic Contact Dermatitis (ACD). Sensitization is a threshold phenomenon, and although many fragrance molecules are skin sensitizers, they can be formulated at safe concentrations in final products. To reduce sensitization risk, some fragrance developers are proactively exploring strategies to reduce the sensitization potential of fragrance mixtures while preserving olfactory performance. Sensitization testing is preferably conducted using New Approach Methods from the OECD test battery described in Test Guidelines 442 C, D and E. However, these methods are not validated for testing mixtures and do not provide quantitative potency information. GARDskin Dose-Response (DR) (OECD TGP 4.106) is based on the validated protocols of GARDskin (OECD TG 442E) and was developed to address these limitations. The readout of the assay is a predicted human No Expected Sensitization Induction Level (NESIL), or Local Lymph Node Assay (LLNA) EC3 value. The purpose of the current work was to investigate the potential of modulators to reduce the skin sensitization potency of fragrance formulations using GARDskin DR as the analytical tool to verify effects. **Methods:** A preliminary study was conducted to evaluate the impact of different parameters on the effectiveness of the modulator to reduce the sensitization potential of hydroalcoholic fragrance formulations. Formulations (n=2) and modulators (n=3) were evaluated using different concentration ratios. Testing was conducted using GARDskin DR under blinded conditions. Differences in potency, reflected by shifts in NESILs, were used to determine effects of the investigated parameters. Following completion of the preliminary study, further optimization and reproducibility studies were conducted by repeated testing of a single formulation with different batches of modulators (n=6), as well expanding the testing to additional formulations (N=7). Finally, a modified protocol of GARDskin DR was evaluated, where the total number of replicates for each concentration (n=6) in the dose-curve was increased to improve resolution for detecting small differences in potency. **Results:** The preliminary study identified the most effective modulator, established a threshold concentration for optimal performance, and demonstrated that the effect was reproducible across different batches. Among

evaluated formulations, the modulator successfully reduced the skin sensitizing potency of five of the seven formulations, demonstrating broad utility across various fragrance formulations. For a subset of the formulations, the modulator did not only decrease the potency but pushed the NESIL value above the sensitization threshold (NESIL > 25 000, LLNA EC3 > 100%), at which the risk of sensitization is considered negligible. Finally, the modified GARDskin DR protocol was demonstrated to improve the resolution and increase the statistical power to detect small differences in sensitization potency. **Conclusions:** The herein proposed strategy to add modulators to reduce the sensitization potency of fragrance formulations complements conventional quantitative risk assessment by increasing the sensitization threshold, and in some cases shifting the NESIL above the sensitization limit, reducing the sensitization risks and improving the consumer safety, particularly for sensitive populations. The potential of GARDskin DR to provide high resolution quantitative potency data was critical to verify effects of modulators while supporting policies aimed at reducing animal use in safety assessments.

ABSTRACT NUMBER: 5201 **Poster Board Number:** K765

TITLE: Evaluation of Sorafenib-Induced Cardiotoxicity with Donor-Specific iPSC-CMs: the Sex Differences in Transcriptome

AUTHORS (FIRST INITIAL, LAST NAME) AND INSTITUTIONS: *L. Pang*[1], V. Vijay[1], L. Ren[1], V. Srinivasasainagendra[2], H. Tiwari[2], A. Matter[3], K. Papineau[1], L. Schnackenberg[1], and U. Broeckel[3]. [1]US FDA-NCTR, Jefferson, AR; [2]University of Alabama at Birmingham, Birmingham, AL; and [3]Medical College of Wisconsin, Milwaukee, WI.

KEYWORDS: Induced Pluripotent Stem Cells; Toxicogenomics; *In Vitro* and Alternatives; Sex difference

ABSTRACT: Background and Purpose: Sex differences may significantly affect cardio-oncology outcomes, including both cancer drug toxicity and the effectiveness of cardioprotective strategies. Although women generally experience more adverse drug reactions, male patients are found to have a higher risk of cardiotoxicity following anthracycline and immune checkpoint inhibitor treatment. While kinase inhibitors (KIs) are widely used clinically to treat various malignancies, the impact of sex on the incidence and severity of KI cardiotoxicity remains largely unknown. Induced pluripotent stem cell-derived cardiomyocytes (iPSC-CMs) generated from both male and female donors may be a valuable model for investigating inter-individual variability and sex differences in anti-cancer treatment-induced cardiotoxicity. **Methods:** Twenty-four iPSC-CM lines were carefully selected to ensure equal representation of males and females, black and white individuals, and patients with high and low ejection fractions. Twelve KIs with different targets and variable cardiotoxicity incidence were tested on the iPSC-CM panel. Sex-related differential responses between male and female cells were compared for cardiomyocyte cytotoxicity and transcriptomic changes. **Results:** Among the 12 KIs examined, only sorafenib treatment demonstrated statistically significant differential responses between male and female cells. Compared to female cells, male cells showed greater sensitivity to 1× Cmax sorafenib treatment. Ingenuity pathway analysis (IPA) of relative gene expression changes in 1× Cmax sorafenib- versus DMSO-treated samples revealed inhibition of striated muscle contraction and activation of dilated cardiomyopathy signaling pathways in both male and female cells. Notably, while inhibition of phagosome formation and activation of TP53-regulated transcription of cell death genes were more pronounced in female cells, several pathways related to inflammation, calcium signaling, and glucose metabolism were significantly affected only in male cells following sorafenib treatment. **Conclusions:** Toxicity evaluation using iPSC-CM panels generated from both male and female donors can be utilized

to investigate sex-specific characteristics in cardio-oncology and may provide valuable mechanistic insights to guide clinical treatment decisions. **Statements and Declarations:** This abstract reflects the views of the authors and does not necessarily reflect those of the U.S. Food and Drug Administration. Any mention of commercial products is for clarification only and is not intended as approval, endorsement, or recommendation. The authors declare that there is no conflict of interest. **Funding information:** This work was funded by the NIH R01HL140493 and the FDA National Center for Toxicological Research (NCTR).

ABSTRACT NUMBER: 5202 **Poster Board Number:** K766

TITLE: Utilizing Human Intestinal Organoids to Understand Environmental Toxicant Interactions in the Gut

AUTHORS (FIRST INITIAL, LAST NAME) AND INSTITUTIONS: A. Banerjee, C. N. Coffman, and *J. G. In*. University of New Mexico, Albuquerque, NM.

KEYWORDS:

ABSTRACT: Background and Purpose: The human gastrointestinal (GI) tract acts as a critical entry point for ingested environmental toxicants as it is composed of a diverse number of cell types with complex cellular interactions that play a vital role in gut homeostasis. Cancer derived cell lines and animal models are commonly utilized to study toxin interactions, but do not fully encapsulate the complexity of the gut epithelium. While rodent models are essential for examining animal health outcomes, the rodent GI tract is dissimilar to the human, making it difficult to translate results into human health outcomes. Understanding gastrointestinal disease progression in the presence of environmental toxins requires models that can represent the intricate physiology of the GI epithelium. Human Intestinal Organoids (HIOs) are a breakthrough in translational sciences. HIOs are derived from intestinal stem cells (ISCs) from biopsies of any section of the GI tract and can indefinitely proliferate while maintaining the donor's genetics. Colonic HIOs, or colonoids, contain ISCs as well as cycling transit amplifying cells, secretory progenitors, enteroendocrine cells, tuft cells, absorptive progenitors, colonocytes, and mucus-secreting goblet cells. This makes them an ideal model system for understanding how environmental toxicants impact the colonic epithelium. Our goal is to utilize patient-derived HIOs to identify changes in the dynamics of the colonic mucus layer and in goblet cell physiology upon exposure to uranium-bearing dust (UBD,) an environmental toxin. **Methods:** To study UBD exposure to the colonic epithelium, we used two organoid model systems. We grew HIOs in 3D form, allowing insight to the cellular changes and molecular mechanisms in toxin exposure. To mimic luminal toxin exposure in the epithelium and understand how the colonic mucus layer changes, the 3D HIOs were then digested to single cells and were grown into 2D monolayers on transwells, forming the second model system. The monolayers are capable of secreting a thick MUC2+ mucus layer on their apical surface, providing us with understanding of how the layer is impacted by UBD. UBD was collected from the area surrounding the Jackpile Paguate Uranium mine, one of the largest open-pit uranium mines in the United States, located outside of the Pueblo of Laguna. The 3D colonoids were exposed to UBD at 50 µg/ml and the 2D monolayers were exposed at 20 µg/ml, both for 24h. The control systems were exposed to cell culture media and aluminum silicate, the predominant clay component found near the mine. **Results:** UBD exposure in monolayers degraded the mucus layer to a thickness of 5 µm compared to 15 µm in control monolayers. Immunoblotting further confirmed this degradation, yielding 64% for UBD treated colonoids compared to 100% for cell media and 96.6% for aluminum silicate colonoids. To characterize transcriptomic

changes in the 3D models, control and UBD-exposed colonoids (n=3 donors) were processed for droplet-based single cell sequencing. This revealed an expansion in secretory cells with UBD exposure. Specifically, we found upregulation in cells expressing ATOH1, a master transcription factor in intestinal secretory cell differentiation (0.29% control to 3.6% UBD) and MUC2 (8.7% control to 51.7% UBD). Immunostaining of Trefoil factor 3, a goblet cell marker, further confirmed this. Additionally, there was upregulation in the expression of the adherent mucins MUC1 (6.8% control to 31% UBD), MUC13 (6.5% control to 32.2%), and MUC17 (0.2% control to 1.6% UBD). **Conclusions:** Our results indicate that UBD exposure degrades the gastrointestinal mucus layer resulting in goblet cell hyperplasia and upregulation of cells expressing mucins to restore barrier integrity. This work exemplifies the use of organoids as novel models for environmental toxicant exposure in organ systems.

ABSTRACT NUMBER: 5203 **Poster Board Number:** K767
TITLE: Human Embryonic Stem Cell-Derived Dopaminergic Neuron Reporter Line for Neurodevelopmental Toxicology Screening

AUTHORS (FIRST INITIAL, LAST NAME) AND INSTITUTIONS: *G. E. Mallo*[1], *A. Kreutz*[1], G. Hu[2], and *E. J. Tokar*[1]. [1]NIEHS/DTT, Research Triangle Park, NC; and [2]NIEHS, Research Triangle Park, NC.
KEYWORDS: Stem Cells; Neurotoxicity; Metals

ABSTRACT: Background and Purpose: Traditionally, identification of developmental neurotoxicants for risk assessment have utilized *in vivo* methods. However, these methods are expensive and time-consuming, limiting their potential for high-throughput screening. In an effort to assemble *in vitro* new approach methodologies (NAMs) that could serve as an alternative to traditional *in vivo* guideline studies for developmental neurotoxicity, we have developed a model utilizing human embryonic stem cells (hESCs). As hESC differentiation closely mimics embryonic development *in vivo*, this project aims to establish a cellular model to identify and characterize environmental chemicals that may impact the development of dopaminergic (DA) neurons, due to their sensitivity to environmental factors and implication in neurodegenerative diseases, such as Parkinson's Disease. **Methods:** Using CRISPR-mediated genome editing technology, we have created a hESC dual fluorescence reporter line to monitor DA neuron development. The reporter line includes NESTIN-EGFP to detect neural progenitor lineage and tyrosine hydroxylase-mScarlet to detect maturation into DA neurons. We followed the ThermoFisher Dopaminergic Neuron Differentiation Kit protocol, which is divided into three stages: specification, expansion, and maturation. hESCs first undergo specification into midbrain floor plate (FP) cells. FP cells are then expanded to create a cell bank, and lastly, differentiated into DA neurons. We used fluorescence-activated cell sorting and qPCR to monitor the sequential differentiation from hESCs toward the FP lineage and DA neurons. Once differentiation was verified, DA neurons were treated at various concentrations with sodium arsenite (0.1µM, 7.5ppb and 0.01µM, 0.75ppb) or cadmium chloride (1µM, 112ppb and 0.1µM, 11.2ppb) for 10 days and imaged using the Opera Phenix high-content imaging platform. **Results:** NESTIN-EGFP and tyrosine hydroxylase-mScarlet expression reflect successful differentiation into the neuronal lineage as well as maturation into DA neurons, respectively. After 10 days of floor plate specification, 15% of cells were GFP positive. After further expansion at the FP stage, GFP-positive cells increased to 30%. Differentiation was further verified using qPCR. Following 10 days of specification into neural progenitor cells, we confirmed the presence of NESTIN, a neuroepithelial stem cell marker. After 10 days of floor plate cell expansion, we confirmed the presence of markers for midbrain floor plate progenitors and midbrain DA neuron transcription factors, CORIN and FOXA2. After

15 days of maturation into DA neurons, expression of DA neuron markers DAT and VMAT2 were confirmed. Following 10 days of treatment with sodium arsenite and cadmium chloride in the DA neuron maturation stage, preliminary results showed neither metal had cytotoxic effects at either concentration. **Conclusions:** These results suggest that the reporter line will be a useful resource in monitoring DA neuron differentiation efficiency. Using live cell imaging and molecular analyses, the cell line will be further utilized to screen environmental chemicals and toxicants for their impact on the differentiation process. This will allow for careful assessment of specific timepoints in which toxicants may exert their effects. Subsequently, we aim to investigate mechanisms of action for hit compounds. Overall, *in vitro* hESC differentiation into DA neurons provides a useful model to identify and characterize environmental chemicals that impact Parkinson's Disease and other neurological disorders.

ABSTRACT NUMBER: 5204 **Poster Board Number:** K768

TITLE: A cross-species hepatocyte platform to evaluate CAR-driven proliferation and xenobiotic responses

AUTHORS (FIRST INITIAL, LAST NAME) AND INSTITUTIONS: C. M. Götz[1], A. Scheffschick[1], O. S. Talkhan[1], G. Schicht[1], V. P. Brandt[1], M. Vogler[1], M. Goettel[2], A. Doi[3], E. Fabian[4], D. Seehofer[1], R. Landsiedel[4,5], and *G. Damm*[1]. [1]University Hospital of Leipzig, Department of Hepatobiliary and Transplantation Surgery, Leipzig, Germany; [2]BASF SE, Global Toxicology Agricultural Solutions, Limburgerhof, Germany; [3]BASF Agricultural Solutions US LLC, Regulatory Toxicology Crop Protection, Research Triangle Park, NC; [4]BASF SE, Experimental Toxicology and Ecology, Ludwigshafen, Germany; and [5]Freie Universität Berlin, Pharmazie, Pharmakologie und Toxikologie, Berlin, Germany.

KEYWORDS: Hepatocytes; *In Vitro* and Alternatives; Carcinogenesis

ABSTRACT: Background and Purpose: The constitutive androstane receptor (CAR) is a central regulator of hepatic xenobiotic metabolism and a key driver of non-genotoxic, rodent-specific liver tumorigenesis through stimulation of hepatocyte proliferation. Phenobarbital (PB), an indirect CAR activator, promotes liver tumor formation in rodents but not in humans, highlighting profound species differences in CAR signaling. To support chemical safety evaluation, we developed a primary hepatocyte platform that allows parallel assessment of proliferation and xenobiotic metabolism to compare CAR responses across species. **Methods:** Primary mouse hepatocytes (PMH; male and female) and human hepatocytes (PHH; male) were exposed to PB (200 or 1000 µM) or to epidermal and hepatocyte growth factors (EGF/HGF; 50 ng/mL) as proliferative controls, under steatotic and non-steatotic conditions. Cell viability was evaluated by AlamarBlue™ and BCA assays, morphology by microscopy, proliferation by Ki-67 and BrdU staining, and CYP activity and transcript levels by AROD assays and qPCR. Findings were compared with data from male C57BL/6J mice administered 500 ppm PB *in vivo*. **Results:** EGF/HGF robustly stimulated proliferation across all groups, confirming proliferative competence; however, steatosis blunted this response relative to non-steatotic controls. PB induced strong proliferation in PMH: male PMH exhibited a ~5-fold Ki67/BrdU increase. Female PMH demonstrated a ~20-fold peak at 48 h, however not significantly, and levels declined by 72 h. In contrast, PHH did not proliferate in response to PB, showing only baseline levels. CYP activity and RNA expression decreased over time *in vitro*, consistent with dedifferentiation, but PB-induced CYP mRNA remained detectable, with up to ~10-fold induction at 48 h compared with ~50-fold *in vivo*. **Conclusions:** Together, these results recapitulate the well-known species divergence in CAR-dependent hepatocyte proliferation: PMH respond robustly to PB, whereas PHH remain largely refractory. This primary hepatocyte system thus provides a functional tool to probe

CAR-related modes of action and supports risk assessment, while further optimization (e.g., 3D/sandwich formats) may enhance metabolic stability and predictive capacity.

ABSTRACT NUMBER: 5205 **Poster Board Number:** K769
TITLE: Examining the effectiveness of AhR ligand combinations as novel therapeutics in triple-negative breast cancer

AUTHORS (FIRST INITIAL, LAST NAME) AND INSTITUTIONS: D. Elson, J. R. Kreitzer, and *S. Kolluri*. Oregon State University, Corvallis, OR.
KEYWORDS: Receptor; Aryl Hydrocarbon; Apoptosis; Triple-Negative Breast Cancer

ABSTRACT: Background and Purpose: Triple-negative breast cancer (TNBC) represents around 15% of the 2.26 million breast cancers diagnosed annually worldwide and has the worst prognosis. Despite recent therapeutic advances, there remains a lack of targeted therapies for this breast cancer subtype. The Aryl Hydrocarbon Receptor (AhR) is a ligand-activated transcription factor with biological roles in regulating development, xenobiotic metabolism, cell cycle progression, and cell death. Previous work in the Kolluri lab (Elson et al., 2023) has demonstrated that AhR activation by specific ligands, such as 11-Cl-BBQ, can promote tumor suppression and growth inhibition in multiple cancer types. A screening of compounds was performed to identify potential synergies with previously identified AhR ligands. A few promising compounds that enhanced the effects of 11-Cl-BBQ were identified. **Methods:** The compounds of interest were identified in a screening of a drug and natural products library, where TNBC cells were treated with the library compounds individually and in combination with 11-Cl-BBQ. Triple Negative Breast Cancer cells were treated with the library compounds, in combination with previously identified AhR ligands to examine their effectiveness and identify potential synergies. The optimal concentrations for compounds that enhance the effects of ligands were identified via dose-response ranges on TNBC cell lines. To examine the effect of combination treatment on healthy cells, primary breast epithelial cells were treated with the combinations, in parallel with identical treatments on TNBC cells. **Results:** These combination treatments highlighted several promising synergies between compounds as well as several combinations that demonstrated additive effects in TNBC cells. Combination treatments have no detrimental effect on the primary breast epithelial cells, indicating that the effects of combination treatment are targeted and specific to cancerous cells. This lack of impact on healthy cells, combined with the dramatic efficacy against TNBC cells, makes the combination treatment with11-Cl-BBQ an incredibly promising therapeutic avenue for TNBC. **Conclusions:** We identified compounds that in combination with 11-Cl-BBQ, greatly reduce viability in TNBC cell lines. The reduction in cell viability is specific to cancerous cells, showing minimal toxicity to normal healthy breast tissue cells. AhR Ligand combinations show great promise as targeted therapeutics for TNBC and are a prime target for translation efforts.

ABSTRACT NUMBER: 5206 **Poster Board Number:** K770

TITLE: Assessment of the Carcinogenic Potential of Automotive Gasoline in Humans Based on Mechanistic Evidence

AUTHORS (FIRST INITIAL, LAST NAME) AND INSTITUTIONS: *I. A. Lea*, *B. Rivera*, *S. Rogers*, and *S. J. Borghoff*. ToxStrategies LLC, Asheville, NC.

KEYWORDS: Carcinogenesis; Genotoxicity; Automotive gasoline

ABSTRACT: Background and Purpose: Liquid gasoline (CAS 86290-81-5) is produced by the fractional distillation of crude oil and mainly consists of volatile organic compounds; finished automotive gasoline products may also include various additives. The objective of this study was to review mechanistic data on automotive gasoline potentially associated with mutagenic or genotoxic endpoints, as well as indications suggestive of immunosuppressive and/or epigenetic activity pertaining to possible carcinogenic potential in humans. **Methods:** Literature searches were conducted in PubMed and Embase on August 12, 2025 and October 29, 2024. The search strategy consisted of terms associated with automotive gasoline, cancer and mechanistic data in occupationally-exposed human subjects, mammalian *in vivo* models and *in vitro* models. Study quality was determined using Klimisch scores (animal and *in vitro* studies) or using a modification of the National Toxicology Program (NTP)'s Office of Health Assessment and Translation (OHAT) Risk of Bias (RoB) approach (human subjects). **Results:** Based on TiAb review, a total of 2,630 papers were identified as containing a potential exposure to automotive gasoline and data relevant to cancer pathways. From these, 57 papers were confirmed (at full text) as studies of genotoxicity, 22 papers as studies of immunosuppression and 9 as studies of epigenetic alterations in exposed human subjects. All studies were conducted in fuel station attendants assumed to be occupationally exposed to gasoline. Following study quality appraisal, six reliable observational studies showed a significantly elevated frequency of genetic damage in workers compared to controls and two studies showed no elevated frequency of genetic damage in fuel stations workers. Animal model and human cell line studies, with a better characterized exposure, did not produce consistent evidence of genotoxic activity. Insufficient reliable studies existed to conclude whether occupational exposure to gasoline resulted in immunosuppressive or epigenetic changes. **Conclusions:** This analysis provides some evidence of genotoxic activity in fuel station attendants exposed to a poorly characterizedcomplex mixture of chemicals (e.g., including automotive fuel, diesel and gasoline engine exhaust, rubber and metal particles from tire wear, and asphalt particulates from road wear) containing a mixture of known genotoxic substances and recognized human carcinogens. In summary, due to the poor characterization of the chemical mixture to which people were occupationally exposed, there is insufficient evidence to conclude that genotoxic activity observed in occupationally-exposed human subjects should be directly attributed to automotive gasoline alone.

ABSTRACT NUMBER: 5207 **Poster Board Number:** K771

TITLE: The Influence of Marijuana and Tobacco Co-Use Through Marijuana Blunts on Delivery of N'-Nitrosonornicotine and Nicotine

AUTHORS (FIRST INITIAL, LAST NAME) AND INSTITUTIONS: *A. Gupta*[1], T. Klupinski[1], H. Kim[2], and E. Peters[1]. [1]Battelle, Columbus, OH; and [2]The Ohio State University, Columbus, OH.

KEYWORDS: Tobacco Products; Inhalation Toxicology; Respiratory Toxicology; marijuana, cannabis, smoke

ABSTRACT: Background and Purpose: Marijuana blunts, which are prepared by filling tobacco-derived cigar wrappers with marijuana, have become an increasingly popular form of marijuana use. Thus, marijuana-blunt-smoking may hypothetically expose users to tobacco-related toxicants that are absent from other types of marijuana smoke or the constituents of edible marijuana products. The goal of this study was to characterize the mainstream smoke from marijuana blunts in order to quantify the amounts of *N'*-nitrosonornicotine (NNN), which is designated as being carcinogenic to humans (Group 1) by the International Agency for Research on Cancer (IARC), and nicotine, the major addictive constituent of tobacco. **Methods:** Marijuana blunts were prepared by filling emptied cigar wrappers with either 0.8 g of marijuana for a small blunt or 2.0 g of marijuana for a large blunt. The marijuana blunts and unmodified cigars were then machine-smoked separately using each of two different puffing topographies. Total particulate matter (TPM) samples were collected from the resulting mainstream smoke on glass fiber filter pads. The TPM samples were extracted for analysis by liquid chromatography-tandem mass spectrometry and gas chromatography-mass spectrometry to determine the amounts of NNN and nicotine, respectively. In addition, particle sizes of the mainstream smoke were measured in real time in the size range of 5-1000 nm using a differential mobility spectrometer. **Results:** The mean amounts of NNN detected in marijuana blunt smoke ranged from 18.5 to 50.5 ng/rod, showing significant differences associated with both blunt size and puffing topography. The mean amounts of nicotine ranged from 0.07 to 0.21 mg/rod, also showing significant differences associated with both blunt size and puffing topography. The amounts of both chemicals in marijuana blunt smoke were significantly lower than those in cigar smoke, as might be expected. Particle sizes were generally similar for marijuana blunt smoke and cigar smoke, as evident from measured count median diameters of 196-256 nm and 206-226 nm, respectively, suggesting that delivery to the lungs of particle-bound toxicants such as NNN is equally efficient for marijuana blunt smoke and cigar smoke. **Conclusions:** The co-use of marijuana and tobacco in marijuana blunts exposes users to both NNN and nicotine even when all tobacco is removed from inside the cigar wrapper during blunt preparation. Other research has demonstrated that some people who smoke marijuana blunts do not consider themselves to be tobacco users. The results from the present research are valuable in suggesting the potential harms that those marijuana blunt users—and indeed all marijuana blunt users—may face from exposure to the carcinogen NNN and the addictive chemical nicotine.

ABSTRACT NUMBER: 5208 **Poster Board Number:** K772

TITLE: Associations between Secondhand Electronic Cigarette Aerosol Exposure in Vape Shops and Airway Mechanics

AUTHORS (FIRST INITIAL, LAST NAME) AND INSTITUTIONS: *S. L. Langmo*, *H. Chen*, K. Lee, M. Niu, L. Umaguing, and Y. Zhu. University of California, Los Angeles, Los Angeles, CA.

KEYWORDS: Tobacco Products; Lung; Pulmonary or Respiratory System; Secondhand

ABSTRACT: Background and Purpose: Exposure to secondhand cigarette smoke is known to induce acute respiratory effects, including changes in lung function. Electronic cigarettes (e-cigs) have surpassed cigarettes in popularity among youth in the US, with one-third of middle and high school students reporting secondhand exposure as of 2018. Despite the increase in vaping prevalence, the acute respiratory effects of secondhand e-cig exposure remain poorly understood. More than 70% of e-cig aerosol is exhaled by users. This raises concerns regarding exposure among bystanders. Previous work by our laboratory demonstrated that vaping density, quantified by puff count, is a strong indicator of $PM_{2.5}$ concentrations in vape shops, supporting $PM_{2.5}$ mass concentration and vape shops themselves as good exposure metrics and field-based exposure assessment tools. Building on these findings and published laboratory-based exposure studies, we investigated acute changes in respiratory mechanics, a component of lung function, associated with real-world exposure conditions to secondhand e-cig pollutants in active commercial vape shops. **Methods:** Thirty-one healthy non-e-cig users with no diagnosed respiratory disease were recruited to spend six hours in one of two commercial vape shops with previously characterized indoor air quality. Participants experienced real-world secondhand e-cig aerosol exposure, measured by observation notes and real-time air monitoring. Airway mechanics were measured using Impulse Oscillometry, an evaluation of lung function that assesses airway resistance and reactance, before and after the vape shop visit, and at a follow-up assessment the next day. Linear regression models were used to examine the association between $PM_{2.5}$ mass concentration and airway mechanics, adjusting for shop location and sex, and the interaction between mass concentration and shop location. **Results:** Results indicate a dose-response relationship between secondhand e-cig aerosol exposure and acute changes in airway mechanics. Under real-world exposure conditions, each participant experienced a unique exposure, documented in real time through air monitoring and participant observation notes. Consistent with prior work from our laboratory, observed puffs correlated with $PM_{2.5}$ concentrations, indicating vaping behavior as the primary driver of exposure. Multiple linear regression was used to evaluate the association between $PM_{2.5}$ mass concentration and changes in lung function pre- and post-vape shop visit, adjusting for vape shop location and the interaction between mass concentration and location. The results revealed that higher $PM_{2.5}$ mass concentration was associated with increase in total airway resistance (B= 0.021 per ug/m^3, 95% CI: 0.0067 to 0.035, p=0.006), area of reactance (B=0.054 per ug/m^3, 95% CI: 0.016 to 0.092, p=0.0074), and the peripheral airways (B=0.0088 per ug/m^3, 95% CI: 0.00074 to 0.01678, p=0.038). No significant associations were observed in the larger airway measures, supporting the likelihood that the increase in resistance occurs in the peripheral airways. **Conclusions:** These findings demonstrate that acute exposure to secondhand e-cig aerosol in commercial vape shops is associated with exposure-dependent increases in total airway resistance and altered airway mechanics, predominantly in the peripheral airways. Increased airway resistance is observed in multiple respiratory diseases, including asthma, so these results raise concerns regarding potential health implications for bystanders in vaping environments, particularly employees of vape shops. This study underscores the importance of using

real-world, field-based exposure assessment to characterize relevant e-cig aerosol exposures. To our knowledge, this is among the first studies to identify a dose-response relationship between secondhand e-cig aerosol exposure and acute changes in lung function.

ABSTRACT NUMBER: 5209 **Poster Board Number:** K773
TITLE: Nicotine Ameliorates Depressive-like Behaviors by Restoring Hippocampal Serotonergic Neurotransmission via the Gut-Brain Axis in a CUMS Model

AUTHORS (FIRST INITIAL, LAST NAME) AND INSTITUTIONS: W. Hongjuan, G. Xia, L. Shigang, T. Yushan, L. Xiao, C. Lili, S. Zheng, H. Shulei, C. Huan, and H. Hongwei. China National Tobacco Quality Supervision & Test Center, Zhengzhou, China. Sponsor: *X. Cao*
KEYWORDS:

ABSTRACT: Background and Purpose: Depression pathogenesis involves monoamine neurotransmitter imbalance, particularly serotonin (5-HT) disruption. The gut-brain axis, mediated by gut microbiota, is crucial in regulating central nervous homeostasis. Nicotine, a tobacco alkaloid with known antidepressant potential, may exert its effects via this axis, yet its toxicological profile and mechanisms at low, sustained doses remain unclear. **Methods:** This study investigated the effects of chronic low-dose nicotine (0.2 mg/kg/d, subcutaneous sustained-release) on hippocampal 5-HT metabolism and the mediating role of gut microbiota in a CUMS mouse model. CUMS-induced depression-like behaviors were assessed. Neurotransmitter levels (Trp, 5-HTP, 5-HT, 5-HIAA) and gene expression (TPH2, MAOA, Slc6a4) in the hippocampus were analyzed via LC-MS/MS and qPCR. **Results:** CUMS mice exhibited significant behavioral deficits, reduced hippocampal 5-HT/5-HTP, elevated 5-HIAA and 5-HIAA/5-HT ratio, downregulated TPH2/Slc6a4, and upregulated MAOA expression. Nicotine intervention reversed all these alterations, restoring neurochemical and transcriptional balance. **Conclusions:** These findings suggest that low-dose, sustained nicotine may alleviate depression-like phenotypes by modulating gut microbiota to normalize hippocampal serotonergic function via the gut-brain axis, providing a toxicological and mechanistic basis for its potential therapeutic application, contingent upon further safety and dependence evaluations.

ABSTRACT NUMBER: 5210 **Poster Board Number:** K774
TITLE: Chemical characterisation of Tobacco-Free Nicotine pouches reveals marked reductions in toxicant levels when compared to combustible cigarettes

AUTHORS (FIRST INITIAL, LAST NAME) AND INSTITUTIONS: O. Komini[1], B. Edwards[1], O. Dethloff[2], and *M. Stevenson*[1]. [1]Imperial Brands PLC, Bristol, United Kingdom; and [2]Reemtsma Cigarettenfabriken GmbH, Hamburg, Germany.
KEYWORDS: Risk Assessment; Safety Evaluation; Tobacco Free Nicotine Pouches

ABSTRACT: Background and Purpose: Tobacco-free oral nicotine pouches (TFNPs) are a recent innovation which contain pharmaceutical-grade, high-purity nicotine combined with a plant-fibre substrate (e.g., wheat or bamboo). Unlike traditional tobacco products, TFNPs contain no tobacco and involve no combustion. Instead, they deliver nicotine buccally through the gums.TFNPs have gained popularity among adult smokers in North America and Europe. However, publicly available scientific data on their harm reduction potential remain limited. In this study, we present chemical characterisation data for four TFNP variants (Zone® nicotine pouches with different flavours and

nicotine strengths obtained from the UK market) and provide a toxicological risk assessment of any quantifiable constituents. **Methods:** The TFNPs were analysed against the GOTHIATEK® analyte list, which includes a range of toxicants such as Tobacco-Specific Nitrosamines (TSNAs), nitrite, NDMA (N-Nitrosodimethylamine), benzo[a]pyrene, carbonyls, metals, and mycotoxins. From this list, a subset of analytes was compared to levels measured in smoke from the 1R6F reference cigarette, specifically: NNN, NNK, benzo[a]pyrene, acetaldehyde, formaldehyde, crotonaldehyde, cadmium, and arsenic. All analyses were conducted using validated methods in an ISO 17025-accredited laboratory. Reference cigarettes were smoked according to ISO 20778:2018 (55 mL puff volume, 30-second puff interval, 2-second puff duration, bell-shaped puff profile). **Results:** All GOTHIATEK® analytes were below their maximum limits, with only formaldehyde and acetaldehyde detected at quantifiable levels. When compared to cigarette smoke, these analytes were reduced by approximately 99.2-99.9% across all product variants. A toxicological risk assessment of these two constituents indicated no significant concerns, as potential exposures were below regulatory toxicant limits. **Conclusions:** This initial dataset supports the potential role of TFNPs in tobacco harm reduction by demonstrating marked reduction of toxicants relative to cigarettes.

ABSTRACT NUMBER: 5211 **Poster Board Number:** K775

TITLE: Heating-coil and device design parameters as critical determinants of electronic cigarette aerosol toxicity

AUTHORS (FIRST INITIAL, LAST NAME) AND INSTITUTIONS: N. Leigh[1], A. Aherrera[2], Z. T. Bitzer[3], M. C. Brinkman[4], F. Effah[5], *I. Rahman*[5], A. El-Hellani[4], I. Olfert[6], A. M. Rule[7], N. Gray[8], and *T. Muthumulage*[9]. [1]Roswell Park Comprehensive Cancer Center, Buffalo, NY; [2]University of Pennsylvania, Philadelphia, PA; [3]Penn State College of Medicine, Hershey, PA; [4]The Ohio State University, College of Public Health, Columbus, OH; [5]University of Rochester Medical Center, Rochester, NY; [6]West Virginia University School of Medicine, Morgantown, WV; [7]Johns Hopkins Bloomberg School of Public Health, Baltimore, MD; [8]Center for Disease Control and Prevention, Atlanta, GA; and [9]Purdue University School of Health Sciences, West Lafayette, IN.

KEYWORDS: Tobacco Products; Toxicity; Acute; Toxicity; Chronic; Product design, e-cigarettes

ABSTRACT: Background and Purpose: Electronic cigarettes (ECs) have evolved from simple, low-powered tobacco-flavored smoking cessation aids to customizable recreational devices with variable e-liquid composition, nicotine strength, device power, and heating-coil configurations, all of which can alter aerosol composition, delivered dose, and harmful constituents. Heating-coil characteristics (electrical resistance, surface area, and coil alloy type) and wick design (material and geometry) influence operating temperature, aerosol formation, and the generation of chemical and metal species that may exceed acceptable toxicological thresholds. **Methods:** This narrative review evaluated published studies across multiple generations of EC devices to characterize how coil and device design parameters, in combination with e-liquid composition, affect the physicochemical properties and toxicity of EC aerosols. Peer-reviewed studies reporting relationships among coil material, resistance, power, wick configuration, and e-liquid formulation with emissions of carbonyls, reactive oxygen species, and metals, along with associated adverse outcome pathways, were identified and compared. **Results:** Across studies, higher power settings and lower-resistance sub-ohm or degraded/aged coils consistently produced increased carbonyl and reactive oxygen species emissions. Certain alloy components substantially increased aerosol metal concentrations under specific operating conditions,

while wick composition and coil geometry modified local temperature profiles and capillary liquid transport, leading to distinct aerosol physicochemical profiles and toxicant formation. **Conclusions:** In conclusion, heating-coil and device design are critical determinants of EC aerosol toxicity. Integrating e-liquid chemistry, nicotine-flavoring chemical interactions, and coil- and device-level parameters into inhalation toxicology studies, exposure assessment, and the regulatory toxicology of emerging EC products may improve exposure characterization and support risk-informed product evaluation. These findings have important implications for regulatory agencies, toxicologists, and public health stakeholders, as they demonstrate that device hardware, coil materials, and user-modifiable operating conditions are important considerations of EC aerosol toxicity. The findings and conclusions in this report are those of the authors and do not necessarily represent the official position of the National Institutes of Health, U.S. Food and Drug Administration, or Centers for Disease Control and Prevention.

ABSTRACT NUMBER: 5212 **Poster Board Number:** K776

TITLE: Chemical Composition and Inhalation Toxicity of Commercial Essential Oil Aromatherapy Vape Products

AUTHORS (FIRST INITIAL, LAST NAME) AND INSTITUTIONS: J. L. Thies[1], *D. O. Jegede*[2], A. P. Tackett[2], M. C. Brinkman[2], *A. El Hellani*[2], and *M. E. Rebuli*[1]. [1]University of North Carolina, Chapel Hill, NC; and [2]The Ohio State University, Columbus, OH.

KEYWORDS:

ABSTRACT: Background and Purpose: Essential oil aromatherapy vape products (EAVPs) have recently emerged as a new inhalable product and are marketed as natural alternatives to electronic cigarettes. However, the chemical composition and associated respiratory health effects from their use remain uncharacterized. This study integrated targeted chemical characterization with *in vitro* respiratory toxicity assessment to evaluate 10 flavors of nicotine-free EAVPs sold by MONQ that are marketed for use in "evoking feelings" in the user. **Methods:** MONQ flavors (Love, Happy, Sexy, Relieve, Fresh, Focus, Peace, Zen, Ocean, Sleepy) were purchased from an online vendor. Liquid from these varieties was extracted using liquid-liquid extraction and analyzed for 14 targeted compounds (i.e., menthol, eugenol, linalool, linalyl acetate, terpinen-4-ol, trans-caryophyllene, limonene, eucalyptol, caffeine, nicotine, cinnamaldehyde, damascenone, pinene, and pulegone) using gas chromatography-mass spectrometry. Margin of Exposure (MOE) calculations were conducted based on the available No Observed Adverse Effect Levels (NOAELs). For *in vitro* toxicity testing, aerosols were generated using a vaping machine puffing regimen and delivered to human bronchial epithelial cells (16HBEs) at the air-liquid interface using the Vaping Product Exposure System. Cytotoxicity, protein levels for inflammatory cytokines (IL-6, IL-8, IL-1β) and MMP-9, and estrogen receptor gene expression (ESR1, ESR2, GPER30) were assessed after 10- or 30-puff exposures and compared with non-vaped vegetable glycerin controls. **Results:** Liquids had substantial heterogeneity across flavors, with a limited number of compounds dominating composition. For example, Love EAVP was menthol-dominated (1,417 μg/g). In comparison, Sexy contained very high concentrations of eugenol (1,638 μg/g) along with trans-caryophyllene (544 μg/g), and Focus exhibited notable eugenol levels (340 μg/g) and had the greatest chemical diversity. Happy and Sleepy were enriched in linalool (248 and 117 μg/g, respectively), along with linalyl acetate (89 and 29 μg/g, respectively), whereas Fresh showed a simpler profile with lower menthol content (81 μg/g). Caffeine (16 μg/g) was detected only in Love and Focus, and nicotine was not detected in any product. Measured levels were below risk thresholds, however these comparisons are limited because

calculations mostly used NOAELs estimated from ingestion due to lack of relevant inhalation data. Exposure to EAVP aerosols induced significant respiratory outcomes. All tested EAVP aerosols induced cytotoxicity greater than 25% compared to non-vaped VG control at both exposures. Similarly, all tested EAVPs, aside from Sleepy, induced robust protein expression of IL-6 and IL-8. At 10 puffs, Sleepy displayed 0.5x decrease of IL-1β, while Zen exhibited 1.3x and 2x increase of IL-1β at 10 and 30 puffs, respectively. At 10 puffs, all EAVPs displayed significant downregulation of estrogen receptors; ERα (0.0x - 0.3x), ERβ (0.2x - 0.48x), and GPER30 (0.1x - 0.38x). At 30 puffs, Zen showed a 2.7x increase in ERα, Ocean displayed a 2.1x increase in ERβ, while Sleepy decreased 0.3-fold. Lastly, GPER30 increased 2.3-fold following Relieve aerosol exposure, but decreased 0.1-fold with Sleepy. MMP-9 was significantly increased for all EAVP aerosols, but Sleepy, at 10 puff density. Ocean, Sleepy, Peace, and Sexy all displayed increased MMP-9 protein at 30 puffs, suggesting inflammation-associated tissue remodeling and oxidative damage. **Conclusions:** Our mixed-method approach of targeted chemical analysis and respiratory toxicity assay showed that essential oil constituents present in EAVPs were associated with cytotoxicity, inflammation, and endocrine-disrupting effects in respiratory epithelial cells. Furthermore, in some cases, no large differences were identified between the two exposures, suggesting damage from initial exposure primarily drives observed effects. These findings demonstrate that inhalation of EAVP aerosols is not biologically benign and highlight the need for continued evaluation of these products using integrated methods, particularly as this category of inhalable products continues to expand.

ABSTRACT NUMBER: 5213 **Poster Board Number:** K777

TITLE: Quantitative Assessment of Airway Remodeling and Genotoxic Stress in 3D Human Tracheobronchial Epithelium Induced by Nicotine and Nicotinamide Electronic Cigarette Aerosols

AUTHORS (FIRST INITIAL, LAST NAME) AND INSTITUTIONS: A. Choi, *R. Phandthong*, M. Kudsi, B. Ramirez, M. Elias, M. Nashed, T. Martinez, and *P. Talbot*. University of California, Riverside, Riverside, CA.

KEYWORDS: Respiratory Toxicology; Inhalation Toxicology; Tobacco Products; 3D human airway epithelial model; nicotine, nicotinamide

ABSTRACT: Background and Purpose: While electronic cigarette (EC) aerosols contain chemical mixtures capable of producing adverse effects in airway epithelium, quantitative characterization of EC-induced airway pathology remains limited. Squamous metaplasia (SM) occurs in cigarette smokers but has not yet been studied in the context of EC exposure and emerging “nicotine-free” alternatives. Nicotinamide-containing EC formulations, such as Nixotine®, are increasingly marketed as safer substitutes for nicotine; however, their effects on airway epithelial fate and genomic stability are unknown. This study used a three-dimensional (3D) human tracheobronchial epithelial tissue (hTET) model derived from airway basal stem cells to quantitatively assess concentration-dependent airway remodeling, define transitions between secretory and squamous phenotypes, and evaluate DNA damage responses induced by nicotine- and nicotinamide-containing EC aerosols. **Methods:** Human airway basal stem cells from a deceased female donor were expanded and differentiated at the air-liquid interface for 4 weeks to generate mucociliary hTETs. Tissues were exposed daily for 3 weeks to 1 or 5 puffs of aerosols generated using a Cultex® exposure system. Exposure groups included clean air, 50:50 PG/VG (propylene glycol/vegetable glycerin), PG/VG containing 36 mg/mL of Nixotine®, and PG/VG containing 36 mg/mL of nicotine. Airway remodeling and injury were quantified using a multiparametric assay including

immunofluorescence of secretory mucins (MUC5AC and MUC5B), squamous differentiation (involucrin), cilia (acetylated α-tubulin), and DNA damage (γ-H2AX). Quantitative morphometric endpoints included epithelial thickness and nuclear orientation. Measurements were extracted from both histological sections and bird's-eye-view (BEV) whole-mount images using image-analysis methods to objectively assess pathological remodeling and cellular injury. **Results:** Relative to the clean air control, 3 weeks of exposure to 1 puff/day induced a significant increase in the secretory mucins (MUC5AC and MUC5B) across PG/VG, PG/VG + 36 mg/mL nicotine, and PG/VG + 36 mg/mL Nixotine® conditions, consistent with early goblet cell hyperplasia. While exposure to 5 puffs/day of PG/VG-alone increased mucin, the same exposures to PG/VG containing nicotine or Nixotine® caused a significant loss in mucin, elevation in involucrin, depletion of cilia, thinning of the epithelium, and horizontal realignment of the nuclei. These changes were detected using both histological and BEV-based quantitative analyses and were absent in clean air controls. At 5 puffs/day, nicotine- and Nixotine®-containing aerosols produced comparable changes in squamous remodeling. DNA damage, assessed by γ-H2AX immunolabeling, was significantly elevated across most EC exposure conditions, indicating widespread genotoxic stress. In contrast to Nixotine®, γ-H2AX induction was near the control level in the 5 puffs/day PG/VG + nicotine group, suggesting progression to squamous metaplasia. Integrated quantitative analysis showed a concentration-dependent shift from mucin-dominant remodeling at low exposure to a squamous-dominant pathology with associated increase in DNA damage at higher exposure levels. **Conclusions:** EC aerosols induced a concentration-dependent progression of airway epithelial remodeling, characterized by early mucin overproduction, DNA damage, and subsequent loss of secretory cells with induction of squamous metaplasia at higher exposures. Nicotinamide-containing EC aerosols generally produced pathological and genotoxic responses comparable to aerosols containing nicotine. This study challenges the perceived safety of "nicotine-free" EC products and highlights the importance of stem cell-derived 3D airway models coupled with quantitative, multi-endpoint assays for evaluating inhaled toxicants.

ABSTRACT NUMBER: 5214 **Poster Board Number:** K778

TITLE: The Effect of Regulating mtDNA Copy Number on Nicotine-Induced Conditioned Place Preference

AUTHORS (FIRST INITIAL, LAST NAME) AND INSTITUTIONS: W. Hongjuan, Z. Shuhong, L. Shigang, T. Yushan, L. Xiao, C. Lili, S. Zheng, H. Shulei, C. Huan, and H. Hongwei. China National Tobacco Quality Supervision & Test Center, Zhengzhou, China. Sponsor: *X. Cao*

KEYWORDS:

ABSTRACT: Background and Purpose: Mitochondrial DNA (mtDNA) copy number is a crucial indicator of mitochondrial function. Previous studies suggest that decreased leukocyte mtDNA copy number in peripheral blood is a potential biomarker for nicotine addiction, and hippocampal mtDNA copy number is significantly reduced in addiction-related brain regions of nicotine-addicted mice. **Methods:** This study investigated the impact of hippocampal mitochondrial DNA (mtDNA) copy number regulation on nicotine addiction using an animal model. Employing a dorsal/ventral hippocampal subregion-specific strategy, we stereotaxically injected rAAV vectors to overexpress or knockdown TFAM (transcription factor A, mitochondrial) in 6-week-old male C57BL/6J mice, thereby establishing models with upregulated or downregulated hippocampal mtDNA copy number. Three weeks post-viral expression, nicotine addiction-like behavior was assessed via the conditioned place preference (CPP) paradigm (0.5 mg/kg nicotine). **Results:** Results confirmed corresponding changes in TFAM protein and mtDNA copy number in the manipulated models. While wild-type control mice developed significant nicotine-induced

CPP, TFAM-overexpressing mice failed to form such preference, indicating that increased mtDNA copy number prior to conditioning attenuates the rewarding effect of nicotine. Spontaneous locomotor activity decreased only in the TFAM knockdown group. Notably, nicotine exposure universally reduced mtDNA copy number across all groups, with final levels in the TFAM overexpression group remaining below the wild-type baseline despite pre-elevation. **Conclusions:** In conclusion, elevated mtDNA copy number represents an important mechanism inhibiting nicotine-induced CPP, providing novel experimental evidence for the role of mitochondrial genome regulation in nicotine reward.

ABSTRACT NUMBER: 5215 **Poster Board Number:** K779

TITLE: Quantitative Risk Assessment: Use of Cumulative Excess Lifetime Cancer Risk in an Electronic Nicotine Delivery System Premarket Review

AUTHORS (FIRST INITIAL, LAST NAME) AND INSTITUTIONS: *J. M. Guynn*, *C. A. Griggs*, C. J. Bequette, A. E. Postiglione, and *C. K. West*. RAI Services Company, Winston Salem, NC.

KEYWORDS: Risk Assessment

ABSTRACT: Background and Purpose: Electronic Nicotine Delivery System (ENDS) products have attracted substantial scientific interest since their introduction in the U.S. Although long-term epidemiology studies are not yet available, a rapidly growing body of scientific evidence suggests that ENDS products are likely to be far less harmful to individual health than combusted cigarettes. As the regulatory landscape for ENDS evolves, the U.S. Food and Drug Administration (FDA) has recently incorporated cumulative excess lifetime cancer risk (ELCRc) estimates to inform its scientific evaluations. This approach reflects a shift toward quantitative risk assessment (QRA) frameworks in tobacco product regulation, particularly for assessing toxicological risk in Premarket Tobacco Product Applications (PMTAs). ELCRc estimates have been used to compare cancer risks between an ENDS and a reference combusted tobacco product, providing a quantitative basis in support of regulatory conclusions. This analysis aims to evaluate how ELCRc was applied in FDA's review of an ENDS product, highlighting the scientific studies critical for inclusion in the ELCRc calculations, and to assess the implications of this methodology in FDA's determination. **Methods:** In support of the PMTAs, a robust science package was executed, including aerosol analyses for harmful and potentially harmful constituents (HPHCs) and leachables from the container closure system. Aerosol generation for HPHC quantitation was performed using both non-intense and intense puffing regimens consistent with CORESTA Recommended Method No. 81 and CORESTA Technical Guide No. 22, respectively. Aerosol HPHCs were measured and quantitated using validated methods that evaluated puff groups representative of the full life cycle of the ENDS products. A simulated leachables study was conducted to identify potential aerosol leachables. Given aerosol data is most representative of consumer exposure, an aerosol leachables study was conducted to detect and quantitate a selected suite of elemental and organic leachables, based on the results of the simulated leachables study, potentially present in the ENDS aerosols. Additionally, untargeted scans were collected and manually evaluated to determine if organic leachables identified in the simulated leachables study transferred to the aerosol. FDA's Technical Project Lead (TPL) review for the ENDS products was examined for ELCRc estimates based on Tier 1-3 and Tier 1-4 constituent groupings. Tier 1-3 includes known carcinogens evaluated by the International Agency for Research on Cancer or United States Environmental Protection Agency, while Tier 1-4 incorporates additional aerosol and leachable constituents based on weight-of-evidence analysis. Comparative assessments were made against the ELCRc of a reference combusted cigarette (1R6F), and FDA's qualitative risk descriptors were

applied to interpret relative risk levels. **Results:** Aerosol testing demonstrated reductions in HPHCs, with many replicates below the limit of quantification (LOQ). Leachables studies identified seven constituents present in aerosols above 1.5 µg/cartridge. ELCRc values were substantially lower than those of combusted cigarettes. Tier 1-3 estimates were all less than 31 excess cancer cases per 100,000 users, while Tier 1-4 estimates ranged from 110 to 720 excess cancer cases per 100,000 users. **Conclusions:** These estimates represent less than 0.31% to 7.2% of the cited 1R6F benchmark of 10,000 excess cancer cases per 100,000 users. FDA's determination cited these findings as predictive of lower cancer risk for people who exclusively use the new products compared to those who smoke combusted cigarettes.

ABSTRACT NUMBER: 5216 **Poster Board Number:** K780

TITLE: Chronic exposure to e-cigarette aerosols causes metal dyshomeostasis in mouse brain regions associated with Parkinson's disease

AUTHORS (FIRST INITIAL, LAST NAME) AND INSTITUTIONS: L. Petropoulou-Vathi[1], C. Parodi[1], C. Jaafar[1], M. A. Arthur[1], B. Notarainni[1], V. Ilievski[1], A. Silva[1], A. Sanchez[1], I. Attard[2], J. Kohli[3], I. T. Folkerts[1], A. Navas-Acien[1], B. Yan[1], N. J. Kleiman[1], K. Schilling[1], *M. Hilpert*[1], and *D. B. Re*[1]. [1]Columbia University, New York, NY; [2]New York University, New York, NY; and [3]Barnard College, New York, NY.

KEYWORDS: Tobacco Products; Neurotoxicity; Metals; *In Vivo* Models

ABSTRACT: Background and Purpose: The long-term health consequences of e-cigarette use remain poorly understood, with the exception of increased respiratory and cardiovascular disease risk. When heated, e-liquids generate chemically complex aerosols containing reactive aldehydes and neurotoxic metals that are linked to cognitive and motor dysfunction. Metal exposure is among the primary risk factors for Parkinson's disease (PD). In a pilot study, we previously showed that short-term exposure to e-cigarette aerosol induces metal dyshomeostasis in wild-type (WT) female mouse brain regions critically involved in PD pathology: the striatum (STR), ventral midbrain (VMB), and frontal cortex (FC). Here, in a larger study, we investigated whether chronic e-cigarette exposure alters brain metal homeostasis in the same regions in both sexes and assessed gene-environment interactions using LRRK2-R1441C knock-in mice, a genetic model linked to PD. We also investigated the respective and combined effects of exposure to aldehydes, metals, and nicotine by exposing mice not only to e-cigarette aerosols but also to metal-reduced aerosols generated with a collision-type aerosolizer ("Aerosolizer") that lacks a metallic heating coil. **Methods:** WT and LRRK2-R1441C male and female mice were exposed to e-cigarette aerosol for six months using an open-system device (iStick Pico 25) and "Vixen's Kiss" flavor (0% or 6% nicotine; Pale Whale, CA). To generate metal-depleted but aldehyde-rich aerosol, e-liquid was aerosolized by operating the Aerosolizer at 200 °C, which served as a negative control for most metals. Mice (n = 128) were subdivided by genotype and sex into four exposure groups (Air, Aerosolizer, 0% NIC, and 6% NIC; n = 16/group). At study end, FC, STR, and VMB were dissected and concentrations of twelve metals (V, Cr, Mn, Fe, Co, Ni, Cu, Zn, Se, Sr, Tl, and Pb) were quantified in each region by inductively coupled plasma mass spectrometry. One- and two-way ANOVA were used to compare metal levels across exposure conditions, sex, and genotypes. **Results:** Chronic aerosol exposure produced robust, brain region-, genotype- and sex-specific alterations in PD-relevant metals including Mn, Fe, Cu, Zn, and Se. One of the most striking features observed in females—particularly LRRK2-R1441C mice—was a simultaneous significant increase of Mn, Co, Zn, and Se in FC alongside a corresponding decrease in the STR. In contrast, Cu only significantly increased in the FC, and Fe was found to be significantly decreased in both brain regions. Curiously, Cu levels in both FC and STR across

genotypes and sexes in the Aerosolizer-exposed group increased, despite the very small amount of Cu in this aerosol. This observation suggests that some metal increases may not necessarily reflect metal deposition from the aerosol, but rather altered homeostatic control. In contrast, Fe levels decreased in the same Aerosolizer-exposed animals. Remarkably, in the VMB, only metal increases were observed, predominantly in the 0% NIC group, and particularly in LRRK2-R1441C female mice. **Conclusions:** This study demonstrates that chronic exposure to e-cigarette aerosol dysregulates essential PD-relevant metals in the brain in a region-, sex-, genotype-, and nicotine-dependent manner. Overall, the FC exhibited broader changes across sexes and genotypes. In contrast, the STR and the VMB showed a more selective and genotype-dependent response. Importantly, while the presence of nicotine appears to drive the changes in metal levels measured in the FC and STR, it is the absence of nicotine that appears to determine metal deposition in the VMB. Females exhibit greater susceptibility to metal dyshomeostasis across regions, and LRRK2-R1441C mice show increased vulnerability, supporting a gene-metal interaction in this PD model. The inverse relationships observed for Mn, Co, Zn, and Se between FC and STR likely arise from regional differences in metal homeostasis regulation via metal transporters and metal binding proteins, or from metal redistribution between connected brain areas, as reported in previous PD studies. Further investigations are required to define the molecular and cellular mechanisms underlying these effects. Altogether, our data suggests that vaping induces endogenous metal imbalances in the CNS that may contribute to PD risk by creating an environment permissive to neurodegeneration.

ABSTRACT NUMBER: 5217 **Poster Board Number:** K781

TITLE: Integrated Multi-Omics and Network Toxicology in Human Lung Organoids for Evaluating Respiratory Risks of Heated Tobacco Products

AUTHORS (FIRST INITIAL, LAST NAME) AND INSTITUTIONS: Z. Song[1], X. Li[1], Y. Tian[1], Y. Wu[1], Y. Jiang[1], H. Wang[1], S. Han[1], L. Cui[1], H. Chen[1,2], and H. Hou[2]. [1]China National Tobacco Quality Supervision &Test Center, Zhengzhou, China; and [2]Beijing Life Science Academy, Beijing, China. Sponsor: *S. Jia*

KEYWORDS: Cytotoxicity; Risk Assessment; Respiratory Toxicology

ABSTRACT: Background and Purpose: Conventional toxicological models fail to accurately simulate the complex physiology and systemic responses of the human lung. An advanced system integrating human lung organoids with multi-omics analysis and network toxicology provides a highly biomimetic *in vitro* platform amenable to systematic analysis for mechanism-driven toxicity assessment.Applying this integrated strategy, this study conducted a comparative analysis of two typical heated tobacco products. By examining their multidimensional molecular responses and pathway perturbation profiles, it aims to elucidate their comparative toxicity and mechanisms of action, thereby systematically evaluating potential respiratory toxicity risks within this product class. **Methods:** This study utilized lung organoids differentiated from human induced pluripotent stem cells (hiPSCs) as the experimental model. Two representative heated tobacco products (labelled as HTP-1 and HTP-2) were selected for exposure experiments at varying concentrations. After 48 hours of exposure, organoid samples were collected for transcriptomic, proteomic, and metabolomic analyses. Based on the multi-omics data, the Network Perturbation Analysis (NPA) computational model was employed to assess the overall toxicity and toxicity risk distribution of the different products. Gene Set Enrichment Analysis (GSEA) was further applied to investigate the association between exposure and lung disease phenotypes, as well as related pathway alterations. Integrated multi-omics analysis was subsequently conducted to identify the core

biological pathways and key toxicity pathways. **Results:** NPA analysis indicated that at equivalent exposure concentrations, HTP-2 exhibited lower overall toxicity than HTP-1. Both heated tobacco products primarily induced cell stress and inflammatory response, and their toxicity mechanisms were highly similar at high doses. GSEA enrichment analysis based on the MSigDB Human Phenotype Ontology (HPO) revealed increased risks of carcinogenesis/precancerous lesions, inflammation/infection, COPD/pulmonary fibrosis, and abnormal lung function. Concurrently, protective and remodelling pathways, such as those involved in lung development, regeneration, and pulmonary vascular homeostasis, were downregulated, suggesting impaired tissue repair capacity. Compared with HTP-1, HTP-2 was associated with a lower overall risk of inducing these lung disease phenotypes. GSEA using the MSigDB Hallmark gene sets further linked these pulmonary disorders and tissue injury to the activation of injury-related pathways: coagulation cascade, inflammatory signaling, and oxidative stress (associated with inflammation/infection and COPD); TGF-β signaling and hypoxia response (linked to pulmonary fibrosis); and DNA damage response and KRAS signaling (related to carcinogenesis). Integrated multi-omics network analysis demonstrated that both heated tobacco products significantly activated ferroptosis and glutathione (GSH) metabolism pathways, suggesting these may represent the primary toxicity mechanisms involved. **Conclusions:** This study demonstrates that the integration of human lung organoids, multi-omics profiling, and network-based computational toxicology provides a physiologically relevant and mechanistically insightful platform for product safety assessment. The approach enables systematic dissection of molecular pathways and phenotypic risks associated with respiratory exposures. It offers a robust strategy for the comparative and mechanism-driven evaluation of inhaled products.

ABSTRACT NUMBER: 5218 **Poster Board Number:** K782

TITLE: Toxicity Assessment of Menthol- and Tobacco-Flavored E-Cigarettes Using a 3D Airway Organoid Model

AUTHORS (FIRST INITIAL, LAST NAME) AND INSTITUTIONS: X. Li[1,2], Y. Tian[1,2], J. Su[2], Y. Luo[2], L. Hong[2], Q. Sun[2], Y. Jiang[1], and H. Chen[1,2]. [1]China National Tobacco Quality Supervision & Test Center, Zhengzhou, China; and [2]Quality Research and Evaluation Joint Laboratory Innovation Platform of Jinsheng, Zhengzhou, China. Sponsor: *S. Jia*

KEYWORDS: Tobacco Products; Respiratory Toxicology; Risk Assessment

ABSTRACT: Background and Purpose: The increasing global use of e-cigarettes has raised significant public health concerns regarding their potential respiratory toxicity. While flavor additives such as menthol are widely used to enhance product appeal, their specific contributions to pulmonary injury remain poorly understood. **Methods:** A three-dimensional mouse airway organoid (MAO) model was established from adult lung stem cells to closely recapitulate the structural and functional complexity of the native airway epithelium. Using this physiologically relevant platform, we systematically compared the toxicological effects of aerosol extracts from tobacco-flavored and menthol-flavored e-cigarettes. Assessments encompassed organoid viability and growth, oxidative stress (reactive oxygen species levels), DNA damage (γ-H2AX foci formation), epithelial differentiation (via cell-type-specific marker expression), inflammatory cytokine profiling, and transcriptomic sequencing. **Results:** Our results demonstrate that both extracts significantly and concentration-dependently reduced organoid viability and growth, and similarly induced epithelial remodeling reminiscent of chronic airway disease, including goblet cell hyperplasia, ciliated cell loss, and basal cell expansion. However, their underlying

mechanisms were distinct. Menthol-flavored aerosol provoked substantially higher oxidative stress and DNA damage, and induced a broad immunosuppressive response. In contrast, tobacco-flavored aerosol exhibited more potent pro-apoptotic effects and drove a Th2-skewed allergic inflammation. Transcriptomic analysis corroborated these flavor-specific mechanisms, revealing that tobacco flavor primarily activated cellular stress and apoptotic pathways, whereas menthol flavor distinctly perturbed lipid metabolism and metabolic homeostasis. **Conclusions:** Collectively, our study not only delineates distinct mechanistic landscapes by which different e-cigarette flavors induce airway injury, but also underscores the critical role of flavor chemistry in defining specific toxicological outcomes. This work validates the utility of organoid models for flavor-specific risk assessment and provides mechanistic insights to support evidence-based regulation of e-cigarette flavorings.

ABSTRACT NUMBER: 5219 **Poster Board Number:** K783

TITLE: Prenatal exposure to e-cigarette humectants alters placental methylation status correlating with lung dysfunction in a juvenile mouse model of house dust mite-induced asthma

AUTHORS (FIRST INITIAL, LAST NAME) AND INSTITUTIONS: *A. Zaman*[1], T. Cook[1], M. Schexnayder[2], *S. Thota*[1], and *A. Noël*[1]. [1]Louisiana State University School of Veterinary Medicine, Baton Rouge, LA; and [2]IDEXX Laboratories, Inc., Westbrook, ME.

KEYWORDS: Developmental Toxicity; Prenatal; Inhalation Toxicology; Tobacco Products

ABSTRACT: Background and Purpose: In the U.S., maternal vaping prevalence is estimated at 5-15%. While the humectants in e-liquids, propylene glycol (PG) and glycerin (VG), are FDA-classified "Generally Recognized as Safe" only for ingestion, the gestational effects caused by inhaling PG/VG following electronic-cigarettes (e-cigs) use are poorly understood. Thermal degradation of PG/VG produces carbonyls, which can induce airway irritation and impair uteroplacental remodeling. We previously showed in mice that prenatal exposures to e-cig aerosols, containing nicotine and flavor (mint), exacerbated asthmatic responses in offspring, driven by increased *Il10* gene expression. However, the extent to which prenatal exposures to PG/VG, representing over 80% of e-liquid composition, influences asthmatic severity in juvenile offspring remains understudied. Here, we investigated whether prenatal exposure to PG/VG alone alters placental methylation status, and whether these changes are associated with exacerbation of HDM-induced asthmatic responses in juvenile male and female mouse offspring. **Methods:** Female C57BL/6 dams (N=11-13/group) were whole-body exposed to either filtered air or PG/VG e-cig aerosols (0.20 mg/puff; particle size distribution count median diameter: 144.4 nm; GSD: 2.2) produced by a third-generation e-cig device for 1.5 h/day for 14 days before mating plus gestational days 1-20. Tissues were collected in dams and offspring at birth, and at 5-6 weeks of age in offspring following intranasal instillation of either PBS or 50 µg of HDM (N=8-14/group). Lung function testing (*flexiVent*), broncho-alveolar lavage fluid (BALF) cytology, and lung gene expression were assessed. Functional gene networks were identified using DAVID. **Results:** Placentas of PG/VG exposed dams showed significant ($p < 0.05$) global DNA hypomethylation and dysregulation of 21 genes ($|\text{fold-change}| > 1.5$), enriched in networks associated with peptide/steroid hormone regulation, placental remodeling, inflammation, and chromatin modification. At 5-6 weeks of age, lung function testing revealed in PG/VG+HDM exposed females statistically elevated ($p < 0.05$) area under the curve (AUC) for pressure-volume loops when compared to PG/VG+PBS females, indicative of an obstructive asthmatic phenotype. In contrast, male offspring exposed to PG/VG+HDM had reduced AUC for pressure-volume loops in comparison to Air+PBS, and a significant increase in respiratory system elastance, tissue damping, and

tissue elastance at a methacholine dose of 50 mg/mL, compared to PG/VG+PBS males. These distinct pathways of respiratory dysfunction following prenatal PG/VG±HDM exposures suggest sex-based differences. In BALF, male and female offspring exposed to PG/VG+HDM showed a significant increase ($p < 0.05$) in percentage of neutrophils and eosinophils, compared to Air+PBS or to PG/VG+PBS exposed counterparts. Inflammation in females was eosinophilic, typical of Th2 asthma, while inflammation in males was mixed neutrophilic-eosinophilic. PG/VG exacerbated HDM-induced upregulation of *Il10* compared to Air+HDM (fold-change in males: 23.7 v. 7.2; in females: 31.7 v. 29.6, respectively), with PG/VG+PBS exposed females showing a baseline 1.8-fold *Il10* increase. In addition, PG/VG+HDM exposure was associated with dysregulation of 20 key lung genes enriched in networks associated with Th1/Th2 cell differentiation in both sexes; T cell proliferation and lipid metabolism in females; and Th17 cell differentiation in males. Placental repression of *Il2*, which is known to reduce regulatory T cell fetal compartments, plus the upregulation of estradiol-activating *Hsd17b1*, combined with upregulation of *Il10* in offspring lungs, known to regulate the differentiation of CD4+ T cells into Th2 and regulatory T cells (Treg) subsets, may have influenced the observed Th2-dominant response in females and multipolar (Th1/Th2/Th17) profile in males. **Conclusions:** These findings demonstrate that prenatal exposure to PG/VG e-cig aerosols alters the placenta methylation status and transcriptome, in addition to aggravating asthmatic responses in offspring. Funded by the NHLBI under award R01HL176980.

ABSTRACT NUMBER: 5220 **Poster Board Number:** K784

TITLE: *In Vitro* Toxicological Assessment of Modern Oral Nicotine Product Extracts in the Ames, Micronucleus, and Neutral Red Uptake Assays

AUTHORS (FIRST INITIAL, LAST NAME) AND INSTITUTIONS: *B. Keyser*[1], I. Crooks[2], E. Bishop[2], D. Breheny[2], and B. Ganesh[1]. [1]RAI Services Company, Winston-Salem, NC; and [2]BAT Investments Limited, Southampton, United Kingdom.

KEYWORDS: Tobacco Products; Genotoxicity; Regulatory Science/Regulatory Toxicology

ABSTRACT: Background and Purpose: Current next generation tobacco products (NGPs) include Modern Oral (MO) nicotine products contain nicotine, either synthetic or derived from tobacco, and do not contain any tobacco leaf. *In vitro* toxicological assessments of tobacco products are a significant part of the US FDA's premarket tobacco product application (PMTA) process, providing data for a weight of evidence (WoE) approach to determine if the marketing of a new MO tobacco product is appropriate for the protection of the public health (APPH). Data for these products is important due to the limited information for this product class and their accelerating growth in the market. **Methods:** The *in vitro* toxicological assessment of a marketed MO nicotine pouch product, spanning a variety of flavors and nicotine levels, along with a market MO product and a market comparator combustible cigarette (CC) was conducted using a battery of well-established assays. These assays included the Bacterial Reverse Mutation (Ames), *In Vitro* Micronucleus (ivMN), and Neutral Red Uptake (NRU) assays to assess mutagenicity, genotoxicity, and cytotoxicity, respectively. The MO test products and the MO market comparator were tested using complete artificial saliva (CAS) extract sample preparations. Sample extracts were prepared at a concentration of 300 mg product (mixture of pouch content and pouch material) per milliliter CAS. On each experimental day, pad-collected CC total particulate matter (TPM) combined with gas vapor phase (GVP) captured in calcium and magnesium free buffered saline (CMF-PBS) was prepared under ISO 20778 (2018) puffing parameters, extracted in DMSO 24 mg/mL and combined with GVP on a 1:1 basis to achieve a final concentration of 12 mg/mL TPM + GVP. All test

sample preparations were analyzed for nicotine (CAS and TPM+GVP) and carbonyls (TPM+GVP only). The Ames assay utilized the preincubation method in *Salmonella* tester strains TA98, TA100, TA102, TA1535, and TA1537 with and without metabolic activation (±S9). In the ivMN and NRU assays, V79 and Balb/c 3T3 cells, respectively, were exposed to a range of concentrations of either CAS or TPM+GVP preparations. In the ivMN, experiments were conducted under the standard three (3) exposure schedules (short-term with S9, short- and long-term without S9) prior to micronuclei scoring via flow cytometry. For each assay, three independent sample preparations and experimental trials were conducted. The concentration ranges used were dependent on solvent and cytotoxicity limitations for each assay type, as outlined in their respective method guidelines. All assays were conducted under GLP following the corresponding OECD and Health Canada guidelines. **Results:** The CC TPM+GVP (positive control) was found to be mutagenic in strains TA98 (±S9), TA100 (-S9), and TA1537 (+S9). CC TPM was found to be genotoxic, inducing micronuclei in two ivMN exposure schedules, and cytotoxic (IC_{50} = 60 µg/mL TPM+GVP) in the NRU assay. In contrast, MO and the MO comparator did not induce mutagenic activity (Ames), micronuclei (ivMN), or cytotoxicity (NRU). **Conclusions:** Overall, the *in vitro* test battery results presented here add to the WoE that the marketed MO products to have did not exhibit *in vitro* toxicity (mutagenicity, genotoxicity, and cytotoxicity) compared to combustible cigarettes. These results add to the growing body of evidence on MO products and support that use of MO products would reduce consumer exposure to toxic compounds present in CC and provide a potentially lower risk alternative, where combustible cigarettes represent the most harmful tobacco product and next generation tobacco products (e.g., MO) fall along a decreasing risk continuum.

ABSTRACT NUMBER: 5221 **Poster Board Number:** K785

TITLE: Transcriptional Impact of E-Cigarette Aerosol Exposures on Human Airway Epithelium Associated with Major E-Liquid Components

AUTHORS (FIRST INITIAL, LAST NAME) AND INSTITUTIONS: *H. Chen*, A. Harui, G. Del Vecchio, K. Lee, Y. Zhu, and M. Roth. University of California Los Angeles, Los Angeles, CA.

KEYWORDS: Tobacco Products; Gene Expression/Regulation; Inhalation Toxicology

ABSTRACT: Background and Purpose: As the landscape of e-cigarettes (e-cigs) continues to rapidly evolve, identifying key product features that drive lung exposure and toxicity is critical for informing regulation and protecting public health. Currently dominant nicotine salt formulations enable palatable delivery of high-dose nicotine, and most e-cig products also contain flavoring or sensory agents that reduce aerosol harshness and facilitate more intense use. However, the contributions of these constituents to lung exposure and toxicity remain poorly understood. To address this gap, we employed a ventilated artificial lung exposure system to evaluate aerosols generated from different e-liquid formulations and to characterize their transcriptional effects on human airway epithelial cells. **Methods:** A pervious developed ventilated artificial lung system, validated as a physiologically relevant *in vitro* model of human lung exposures, was used to expose primary human bronchial epithelial cells (HBECs) to e-cig aerosols. Fully differentiated HBEC layers cultured at air-liquid interface (ALI) were placed in the lung chamber and ventilated at 10 breaths per min with a tidal volume of 480 mL. ALI cultures were exposed to e-cig aerosols via 13 intermittent vaping sessions per day over two consecutive days to simulate habitual e-cig use. Each vaping session consisted of four consecutive puffs delivered at 1-min intervals (2-s puff duration, 33 mL puff volume). Four experimental groups were included: a ventilated control (no e-cig exposure) and three exposure groups subjected to aerosols generated from different e-

liquids: (i) polyethylene glycol/vegetable glycerol (PG/VG, 30:70), (ii) PG/VG supplemented with 5% (w/w) nicotine benzoate (PG/VG+Nic), and (iii) commercially marketed Virginia Tobacco JUUL pods containing 5% (w/w) nicotine benzoate. These exposure groups were designed to represent major constituents of widely used e-liquid formulations in a progressive manner. Two independent replicate experiments were conducted using ALI cultures derived from the same donor at the same passage number. Following exposure, the HBEC tissue cultures and supernatants were collected and prepared for mRNA-seq and biomarker analysis, respectively. Total sample sizes were n=13 for control and JUUL groups and n=14 for PG/VG and PG/VG+Nic groups. **Results:** Short-term exposure to e-cigarette aerosols over two days did not induce overt cytotoxicity in HBECs, as separately assessed by cell viability, mitochondrial function, or histological evaluation. However, RNA sequencing revealed distinct transcriptional responses across exposure groups. Compared with ventilated controls, exposure to aerosols generated from PG/VG, PG/VG+Nic, and JUUL resulted in 182, 350, and 415 differentially expressed genes, respectively (adjusted $p < 0.05$, $|\log_2 FC| > 0.5$), indicating progressively broader transcriptomic perturbations with the inclusion of nicotine and additional additives. Gene set enrichment analysis showed that all exposures activated pathways related to epithelial stress and tissue remodeling. PG/VG aerosols preferentially altered ciliary motility-related programs, whereas nicotine-containing aerosols promoted aberrant epithelial differentiation. JUUL aerosols elicited the most complex response, marked by enhanced differentiation and immune-related signaling. Ongoing likelihood ratio-based analyses will further resolve exposure-specific gene expression patterns and classify them into biologically informative modules associated with individual e-liquid components. **Conclusions:** By exposing HBECs to e-cig aerosols generated from e-liquids that progressively represent major formulation constituents and resolving gene expression patterns associated with these components, this study reveals subtle but biologically meaningful transcriptional responses in airway epithelium. These findings highlight component-specific effects of e-cig aerosols that may contribute to airway remodeling and disease risk, providing mechanistic insight relevant to regulatory evaluation of e-cig products.

ABSTRACT NUMBER: 5222 **Poster Board Number:** K786
TITLE: Cigarettes, Snus, and Nicotine Pouches: Determining the Risk Reduction Potential

AUTHORS (FIRST INITIAL, LAST NAME) AND INSTITUTIONS: *S. Moses*, A. Dwivedi, A. Naranjo Chacón, E. Arnberg, and J. Lindholm. Swedish Match North Europe AB, Stockholm, Sweden.
KEYWORDS: Tobacco Products; Risk Assessment; nicotine pouch; nicotine

ABSTRACT: Background and Purpose: Oral nicotine pouches (NPs) are designed to deliver nicotine and flavor via oral mucosal absorption and are considered a potentially safer alternative to cigarettes and tobacco-based oral products due to their reduced toxicant profile. This study provides scientific evidence on toxicant levels and toxicological profiles of NPs compared to cigarettes and Swedish snus, highlighting product characteristics and relative risk differences. **Methods:** A diverse range of NPs—including dry and moist formulations with varying flavors, pH, and nicotine content (1.5-16.5 mg/unit), marketed as ZYN™ outside the United States—were analyzed for harmful and potentially harmful constituents (HPHCs) and compared with tobacco-based reference products (Swedish snus/CRP1.1 and reference cigarette 1R6F). The assessment included:
1) Rigorous clearance of ingredients, with hazard characterization and toxicological risk assessment (TRA) to ensure regulatory compliance and consumer safety.

2) Quantification of 38 HPHCs, including the nine priority toxicants recommended for mandated lowering in cigarette smoke by the World Health Organization's (WHO) Study Group on Tobacco Product Regulation (TobReg), in NPs and snus, and compared to published reference cigarette smoke data. 3) *In vitro* toxicological testing of four mint-flavored NPs (1.5, 6, 11, and 16.5 mg nicotine/unit) using artificial saliva extracts, compared to CRP1.1 and reference cigarette 1R6F smoke extracts. The toxicological tests investigated the product's potential to induce mutagenicity (Ames assay), genotoxicity (*in vitro* micronucleus (*iv*MN) assay), and cytotoxicity (neutral red uptake [NRU] assay). **Results:** All NP ingredients met the TRA safety criteria. NP variants exhibited substantially lower HPHC levels than the other tested tobacco products. There were no detectable TSNAs and >99% average reduction of the of the nine TobReg constituents compared to cigarette smoke. Product variations (flavor, moisture, nicotine content) did not significantly affect toxicant levels. In the *in vitro* studies, all NPs and CRP1.1 were non-mutagenic, non-genotoxic, and non-cytotoxic, whereas reference cigarette smoke extracts were mutagenic, genotoxic, and cytotoxic. **Conclusions:** This comprehensive toxicological assessment demonstrates that NPs, regardless of formulation, consistently exhibit significantly reduced toxicant levels and lack *in vitro* toxicity compared to cigarettes. NPs also show an improved HPHC profile relative to snus. These findings support NPs as a substantially lower-risk alternative to cigarettes when used exclusively. *Funding: This research was funded and sponsored by Swedish Match North Europe, an affiliate of Philip Morris International*

ABSTRACT NUMBER: 5223 **Poster Board Number:** K787

TITLE: Comparative *In Vitro* Toxicological Assessment of Electronic Nicotine Delivery Systems (ENDS)

AUTHORS (FIRST INITIAL, LAST NAME) AND INSTITUTIONS: R. McRae[1], *U. Doshi*[1], D. Lakshmanan[2], and P. Kosachevsky[2]. [1]Altria, Richmond, VA; and [2]Labstat International, Kitchener, ON, Canada.

KEYWORDS: Genetic Toxicology; Tobacco Products; Electronic Nicotine Delivery Systems (ENDS)

ABSTRACT: Background and Purpose: Electronic nicotine delivery systems (ENDS) are an expanding category of inhalable, non-combustible tobacco products that may offer a reduced harm alternative compared to traditional combustible tobacco products. The current study evaluated the toxicity profile of 8 prototype and 2 commercially available ENDS products against a combustible test item (1R6F) using established regulatory *in vitro* toxicity assays. **Methods:** Aerosol collected matter (ACM) or total particulate matter (TPM) and gas vapor phase (GVP) test samples were generated from each product using a Borgwaldt RM20D rotary smoke machine. Mainstream aerosol from the ENDS test items was generated according to the ISO 20768 regimen. ACM test samples were collected in DMSO (dimethyl sulfoxide) at concentrations of 200 mg ACM/mL while GVP samples were collected in PBS (Phosphate Buffered Saline) at concentrations of 200 mg ACM equivalent/mL. Mainstream smoke from the 1R6F combustible reference test item was generated according to the Health Canada Intense regimen with TPM test samples collected in DMSO at concentrations up to 40 mg TPM/mL and GVP test samples collected in PBS at concentrations up to 40 mg TPM equivalent/mL. Test samples from the test items were evaluated for their mutagenic potential in the AMES bacterial reverse mutation assay in the presence (+) and absence (-) of metabolic activation (S9). Cytotoxic and genotoxic potential were assessed in CHO cells using the Neutral Red Uptake (NRU) assay and the *in vitro* Micronucleus (ivMN) assay, respectively. The maximum test sample concentration evaluated was either limited by toxicity or by solvent restrictions. For all test items, chemical analyses including the measurement of nicotine, glycerol, propylene glycol, and water were performed on the TPM and ACM test samples while the

content of select carbonyls was determined from GVP test samples. **Results:** For the AMES assay, TPM test samples from the combustible test item, 1R6F, induced mutagenic responses in bacterial strains TA98(+/-S9) and TA1537(+S9) and were concluded as mutagenic, overall. For the NRU assay, TPM test samples and GVP test samples from 1R6F were considered cytotoxic yielding IC_{50} values of 96.0 µg/mL and 207.8 µg/mL, respectively. Similarly, in the ivMN assay, both TPM and GVP test samples from 1R6F induced genotoxic responses in CHO cells under all treatment conditions. In contrast, all ENDS test samples, even when tested at concentrations approximately 10-fold higher compared with the combustible test samples, were negative for mutagenicity, cytotoxicity, and genotoxicity. Furthermore, chemical analyses demonstrated that ACM and GVP test samples from the ENDS test items contained substantially lower levels of harmful and potentially harmful chemicals (HPHCs) compared to the combustible reference test item, perhaps explaining the lack of response induced by the ENDS test items in the *in vitro* assays. **Conclusions:** Collectively, these data indicate that the ENDS products tested in this study present a potentially lower toxicological risk than combustible tobacco products.

ABSTRACT NUMBER: 5224 **Poster Board Number:** M798

TITLE: The Concawe approach to new approach methodologies: technical readiness and strategic adaptation for petroleum substances

AUTHORS (FIRST INITIAL, LAST NAME) AND INSTITUTIONS: D. Holland[1], *I. Chipinda*[2], L. Kamelia[3], *N. Kocabas*[4], and N. Synhaeve[5]. [1]Exxonmobil, Machelen, Belgium; [2]Phillips 66, Houston, TX; [3]Shell Global Solutions International BV, The Hague, Netherlands; [4]TotalEnergies RC, Seneffe, Belgium; and [5]Concawe, Brussels, Belgium.

KEYWORDS: *In Vitro* and Alternatives; Metabolomics

ABSTRACT: Background and Purpose: Applying New Approach Methodologies (NAMs) within Next Generation Risk Assessment (NGRA) remains challenging for UVCB substances (Unknown or Variable composition, Complex reaction products, or Biological materials) due to their compositional variability and dosing complexity. The Concawe NAM strategy therefore focuses on reducing animal testing through enhanced read-across and evidence integration across different data streams while building technical readiness for *in vitro* testing. We hereby present results from three different initiatives towards the implementation of the 3Rs for Hydrocarbon UVCB substances. **Methods:** 1) Enhanced read-across: A series of OECD TG422 studies on 14 Gas Oils substances from three different manufacturing categories was conducted together with comprehensive analytical investigations and metabolomics. 2) Evidence integration: Gas Oil compositional data were analyzed for similarity metrics, and computational clustering was compared with biological outcome. A prototype data integration platform was developed to align compositional, metabolomic, and TG422 outcomes for read-across- evaluation. 3) *in vitro* dosing: A systematic review of *in vitro* dosing methods for difficult-to-test substances and UVCBs was conducted across major scientific databases to assess applicability to petroleum substance (PS) UVCBs and to identify technical gaps. **Results:** The metabolomic analysis of rat blood plasma samples from dietary *in vivo* TG422 studies showed that samples can be grouped based on biological/metabolomic similarity. Effects were ranging from no effects (< 5 %) to strong effects (> 20 %) and some systemic toxicological similarities were found, mainly in male animals. Further computational analysis of compositional and biological effect data and initial clustering analysis found an overlap between compositional and bioactivity clustering. Integration of compositional and metabolomic data revealed clear grouping patterns, with substances of similar PAH content showing the highest similarity

that supports the read-across assessment. The *in vitro* dosing review identified several techniques applicable to complex substances. Methodological adaptations such as non-standard test systems and concentration verification were identified as critical for PS testing. Remaining limitations were mapped to specific assay requirements and recommendations were made for further work to establish *in vitro* testing for PS UVCBs. **Conclusions:** This work exemplifies practical NAM adaptations for UVCB substances, specifically PS. Findings include: (1) demonstrated benefits and boundaries of incorporating metabolomics into OECD TG422 studies for read-across, (2) initial implementation of a data integration framework linking chemistry, biological responses incl. metabolomics and (3) clear technical requirements for improving *in vitro* dosing of complex substances. These results advance the development of scientifically robust and regulatory relevant NAM strategies for UVCBs and support reduced reliance on animal studies in the near to midterm. The strategy and findings can guide similar efforts for other UVCBs and difficult-to-test substances.

ABSTRACT NUMBER: 5225 **Poster Board Number:** M799
TITLE: High-throughput identification of an efficient estradiol-degrading bacterium using an aptamer conformational switching fluorescence biosensor

AUTHORS (FIRST INITIAL, LAST NAME) AND INSTITUTIONS: C. Niu, and C. Ye. Zhengzhou Tobacco Research Institute of CNTC, Zhengzhou, China. Sponsor: *R. Meng*
KEYWORDS: Biotransformation; Endocrine; Estrogens

ABSTRACT: Background and Purpose: Estradiol poses a significant potential risk to human health due to its bioaccumulation and biomagnification within aquatic food chains. Microbial degradation is considered a green and promising strategy for the remediation of estradiol-contaminated water environments. The purpose of this study was to develop an efficient screening approach for estradiol-degrading microorganisms and to identify strains with high degradation capability. **Methods:** A high-affinity estradiol-binding aptamer (CN-Es2), previously identified by our group, was used to construct a fluorescence biosensor based on aptamer conformational switching. Based on this biosensor, a high-throughput microplate-based screening strategy was established for the rapid identification of estradiol-degrading microorganisms. Microbial screening was performed in a mineral medium using estradiol as the sole carbon source, followed by strain isolation and identification. **Results:** Using the proposed biosensor-assisted screening strategy, a strain identified as Nocardioides alkalitolerans was successfully isolated. This strain exhibited strong estradiol-degrading capability, degrading more than 90% of estradiol within 24 h. Compared with conventional plate-based screening methods, the biosensor-assisted approach markedly improved screening efficiency. **Conclusions:** The isolated Nocardioides alkalitolerans strain demonstrates considerable potential for the biodegradation and remediation of estradiol pollution. Moreover, the biosensor-assisted high-throughput screening strategy provides an efficient and reliable tool for the rapid identification of estradiol-degrading microorganisms.

ABSTRACT NUMBER: 5226 **Poster Board Number:** M800

TITLE: Application of Surrogate Matrices in PCR-Based Method Development and Validation

AUTHORS (FIRST INITIAL, LAST NAME) AND INSTITUTIONS: K. C. Reeves[1], M. M. Warr[1], and T. Iles[2]. [1]Labcorp, Greenfield, IN; and [2]Labcorp, Harrogate, United Kingdom. Sponsor: *J. Herman*

KEYWORDS: Alternatives Assessment; Ocular Toxicity; Methods/Mechanism

ABSTRACT: Background and Purpose: Regulatory guidance from the FDA emphasizes the need for scientifically sound, reproducible, and validated analytical methods while supporting ethical practices consistent with the principles of Replacement, Reduction, and Refinement (3Rs). In PCR-based method development and validation, animal-derived biological matrices are frequently used to assess assay performance; however, key biological matrices are often difficult to obtain. The use of comparable surrogate matrices, including non-animal alternatives, represents an effective strategy to reduce animal use while maintaining compliance with FDA expectations for analytical validation. **Methods:** To assess the use of surrogate matrices in qPCR method development, we developed an assay to detect and quantify cytomegalovirus (CMV) promotor sequence from AAV viral vector. We compared the recovery of intact AAV viral particle DNA and extracted AAV DNA in DNA extraction of potential surrogate matrices (plasma, synthetic aqueous humor, and synthetic vitreous humor) to authentic vitreous and aqueous humors. Samples were spiked with either intact AAV virus or extracted viral DNA, and DNA from all matrices was extracted and CMV-expressing DNA was quantified by qPCR. Recovery of the spiked-in viral material was compared across potential surrogate matrices and authentic biological matrices. **Results:** Acceptable recovery was obtained from all surrogate and authentic matrices using both intact AAV virus and extracted viral DNA, with overall higher recovery obtained from intact virus particles. In artificial humor-associated matrices, the average recovery ranged from 64-71% for intact AAV virus and 51-79% for extracted viral DNA. In vitreous humor-associated matrices, the average recovery ranged from 64-73% for intact AAV virus and 46-49% for extracted viral DNA. The amount of test material recovered from surrogate matrices was comparable to that recovered from authentic matrices, with the % difference between authentic and synthetic aqueous and vitreous humor of -12 to -3%. Plasma also resulted in comparable % recovery to authentic aqueous humor, but with higher % difference of 9-39%. **Conclusions:** Surrogate matrices may be used in place of difficult to obtain, biologically important matrices, such as ocular humors, in method validation. The use of surrogate matrices in method validation can replace the use of animals and costly, difficult to obtain matrices, while still allowing full validation of extraction methodology. When appropriately qualified, surrogate matrices enable reliable PCR method development while reducing dependence on animal samples, supporting both regulatory compliance and ethical research practices.

ABSTRACT NUMBER: 5227 **Poster Board Number:** M801
TITLE: Modality specific approaches for hepatotoxicity assessment

AUTHORS (FIRST INITIAL, LAST NAME) AND INSTITUTIONS: V. Mehta[1], S. A. Rajan[2], M. Cirit[2], V. Madgula[1], G. Karnam[1], and J. Jose[1]. [1]Sai Life Sciences ltd, Hyderabad, India; and [2]Javelin Biotech, Woburn, MA. Sponsor: V. Madgula, International Society for the Study of Xenobiotics
KEYWORDS: Alternatives to Animal Testing; Liver; Organ-on-chips, Spheroids, MPS; ASO

ABSTRACT: Background and Purpose: Drug Induced Liver Injury (DILI) remains a leading cause of late-stage drug attrition, as highlighted by a recent survey from the IQ-DILI Consortium. With emerging therapeutic modalities increasingly dominating discovery pipelines, the survey emphasized a lack of modality-specific nonclinical DILI assessment approaches. Here, we present two advanced New Approach Methodologies (NAM) for chronic DILI assessment: (i) a primary human hepatic spheroid model for small molecules and (ii) a 3D multicellular liver-on-chip model for ASOs. **Methods:** The spheroid model was qualified using the IQ-MPS recommended tool compound set under repeated-dose conditions (every 48 h for 7 days). The liver-on-chip tool used PK-driven dosing for up to 2 weeks to assess ASO mediated toxicity. **Results:** The model correctly flagged DILI+ compounds with no false positives. In contrast, ASO (mipomersen) showed IC_{50} values (~100 μM) exceeding therapeutic exposure ranges in the spheroid model indicating limited penetration with 10-fold difference. Evaluation of mipomersen at physiological concentrations in a multicellular liver-on-chip system developed by Javelin demonstrated enhanced target suppression (ApoB) and reduced albumin production than seen in the spheroids aligning with known clinical hepatotoxicity signals. **Conclusions:** Overall, these results highlight Sai's next-generation NAM toolbox for improved hepatotoxicity prediction.

ABSTRACT NUMBER: 5228 **Poster Board Number:** M802
TITLE: Accelerated Toxicity Assessment of Volatiles Using *In Vitro* Modeling

AUTHORS (FIRST INITIAL, LAST NAME) AND INSTITUTIONS: K. Ingram[1,2], M. E. Huddleston[1,2], R. J. Moore[1,2], K. A. Jones[1,2], and *M. W. Grogg*[2]. [1]AV, Inc., Dayton, OH; and [2]Air Force Research Laboratory, Wright Patterson Air Force Base, OH.
KEYWORDS: Inhalation Toxicology; *In Vitro* and Alternatives; Biomarkers; Sulfur dioxide

ABSTRACT: Background and Purpose: Military personnel are exposed to a variety of chemical and physical stressors in the operational environment, and decisions about health risks must be made quickly and, often, with limited data. Traditional *in vivo* toxicity tests using laboratory animals are cost- and time-intensive, limiting the number of existing chemicals with sufficient information to support development of exposure guidelines, nor do they reliably predict human biological responses. The overall objective of this study is to evaluate the utility of a suite of *in vitro* assays to predict the qualitative and quantitative risk of acute lung injury (ALI) in Airmen and identify the most efficient test protocol for future assessments of inhaled hazards. **Methods:** Sulfur dioxide was chosen as a model gas to validate this *in vitro* workflow. Several different alveolar and bronchial cell and tissue models were exposed to five concentrations of sulfur dioxide for four hours to evaluate a dose response. Toxicological analysis of cells and cell culture media included cell barrier integrity, quantification of live, dead and apoptotic response, lactate dehydrogenase release, and glutathione activity. **Results:** Higher concentrations of sulfur dioxide caused the most cytotoxic effects, including increased proportion of dead cells, decrease in cell or tissue barrier, and an increase in lactate dehydrogenase release across the

different non-animal models as predicted. However, the various lung models exhibited differential responses to the varying concentrations of sulfur dioxide. **Conclusions:** Capturing the unique biological signals from both alveolar and bronchial cells enables a faster, more holistic lung assessment than traditional methods, enhancing our ability to protect Warfighter health. This methodology is a sound way to quickly screen volatile chemicals like sulfur dioxide and could be used to examine unknown toxicological effects of other gases. In addition, this system can be expanded to incorporate more complex exposures that could be harmful to Warfighters. Future studies are planned to incorporate ultra-fine particles and heat into the workflow in combination with sulfur dioxide to simulate inhalation of jet fuel. In addition, future studies will also include transcriptomics to offer an even more in-depth investigation into cellular response.

ABSTRACT NUMBER: 5229 **Poster Board Number:** M803

TITLE: The devTOX quickPredict™ assay: A high reproducible *in vitro* NAM for developmental toxicity prediction as demonstrated by an interlaboratory blinded study

AUTHORS (FIRST INITIAL, LAST NAME) AND INSTITUTIONS: D. Kidd[1], D. Bramham[1], I. Komjarova[2], C. Griffiths[2], P. Bushdid[3], *J. Palmer*[4], and E. Donley[4]. [1]Labcorp, Harrogate, United Kingdom; [2]Labcorp, Huntingdon, United Kingdom; [3]Labcorp, Greenfield, IN; and [4]Stemina Biomarker Discovery Inc, Madison, WI.

KEYWORDS: Developmental Toxicity; Prenatal; *In Vitro* and Alternatives; Induced Pluripotent Stem Cells

ABSTRACT: Background and Purpose: There have been increased efforts in the pharmaceutical and chemical industries to incorporate new approach methods (NAMs) (*in vitro*, *ex vivo*, or *in silico*) for developmental toxicity testing earlier in the product development pipeline. Additionally, numerous regulatory agencies have released guidelines that permit the use of NAMs in conjunction with or in place of the traditional *in vivo* embryo-fetal development (EFD) studies. Assessing a NAM's reproducibility is a necessary step to establish confidence in a method and enable its use in a regulatory setting. The devTOX *quick*Predict (devTOX^{qP}) assay has been used by multiple industries for compound prioritization for over a decade and is included as part of the Next Generation Risk Assessment (NGRA) strategies being developed by multiple companies for animal-free assessment of developmental and reproductive toxicity (DART) testing. This assay is an *in vitro* human pluripotent stem (hPS) cell-based assay that predicts the developmental toxicity potential of chemicals with high accuracy based on changes in ornithine and cystine metabolism, represented as the ratio of ornithine to cystine (o/c ratio). **Methods:** The interlaboratory reproducibility of the devTOX^{qP} assay was evaluated in a blinded study conducted by an independent laboratory (Labcorp) that was fully trained by the developer (Stemina Biomarker Discovery Inc). In this study, eight compounds with known developmental toxicity profiles (2 non-developmental toxicants, 6 developmental toxicants) were tested blinded using the devTOX^{qP} standard operating procedures (as supplied by Stemina). The developmental toxicity potential (dTP, o/c ratio) and toxicity potential (TP, cell viability) concentrations were calculated from both laboratories. Assay reproducibility was assessed by comparing the dTP and TP concentrations obtained from Labcorp treatments to those obtained at Stemina. **Results:** Excellent agreement was observed between the o/c ratio and cell viability results obtained at Labcorp and Stemina. The Labcorp data yielded a response in the o/c ratio for the six developmental toxicants tested and no response was observed for the two non-developmental toxicants. These data were fully concordant with the results obtained at Stemina for the same compounds. The difference in the dTP and TP concentrations was less than three-fold between

Labcorp and Stemina, demonstrating excellent assay reproducibility. **Conclusions:** Testing 6 developmental toxicants and 2 non-developmental toxicants (each with known developmental toxicity profiles) in two independent laboratories using a blinded study design has demonstrated that the devTOX quickPredict™ assay is a highly reproducible NAM and can be used with confidence for prediction of developmental toxicities *in vivo*.

ABSTRACT NUMBER: 5230 **Poster Board Number:** M804
TITLE: Evaluating sulfatase activity *in vitro* via physiologically-relevant assay conditions reveal discrete sulfatase enzyme catalytic signatures

AUTHORS (FIRST INITIAL, LAST NAME) AND INSTITUTIONS: T. A. Witkowski, R. R. Chapleau, *R. A. Moyer*, and *P. H. Beske*. Battelle Memorial Institute, West Jefferson, OH.
KEYWORDS: *In Vitro* and Alternatives; Methods/Mechanism; Mode-of-Action; Sulfatase

ABSTRACT: Background and Purpose: The sulfatases are a broad family of highly conserved enzymes that hydrolyze sulfate esters, regulating many biochemical processes from hormonal modulation to macromolecule metabolism. Furthermore, sulfation is one pathway for Phase II metabolism to detoxify xenobiotic or endogenous compounds, a process that can be reversed by sulfatases. Sulfatase deficiencies are rare genetic disorders that impair the breakdown of sulfate-containing molecules, leading to lysosomal storage, cellular dysfunction, and progressive multi-system disease. Standard *in vitro* sulfatase assays use a one-size-fits all approach to measure activity at pH 5, using conditions that are based upon lysosomal sulfatases but fail to capture the full physiological pH range where sulfatases may be active. Given the various physiological environments where sulfatases function, it is critical to use high-throughput *in vitro* assay conditions that also reflect these physiological contexts. This is essential to accurately define sulfatase activity and their role in detoxification, metabolic regulation, and human health. **Methods:** This study optimized physiologically relevant *in vitro* sulfatase assay conditions, using sulfatases isolated from *Helix pomatia* and *Patella vulgata*, to enable assay optimization for toxicology applications. We tested sulfatase activity in sodium acetate buffer at pH 5 to represent lysosomal environments, and in HEPES at pH 7.4 to represent extracellular environments and blood. Conventional endpoint sulfatase assays were performed using p-nitrocatechol sulfate (PNCS) as the substrate in sodium acetate buffer at pH 5. Sulfatase activity was quantified by colorimetric detection at 515 nm following reaction termination with sodium hydroxide, because its chromophore is only detectable at high pHs not conducive to enzyme activity. To enable real-time kinetic analysis, we also developed a p-nitrophenyl sulfate (PNPS) substrate sulfatase assay and evaluated the same buffer conditions. PNPS allows continuous monitoring of sulfatase activity because its chromophore can be detected without extreme pH shifts at 317 nm under acidic conditions or 405 nm near neutral pH. By varying substrate concentrations across these assay conditions, we determined Michaelis-Menten parameters for each sulfatase, providing insight into enzyme performance under physiologically relevant environments. **Results:** Across assay buffer conditions, sulfatase from *Helix pomatia* exhibited a comparable V_{max} and K_m for both PNPS and PNCS. This indicated that the sulfatases in *Helix pomatia* extracts had similar catalytic efficiency, regardless of substrate or pH environment. Sulfatase from *Patella vulgata* showed the highest V_{max} and lowest K_m for PNCS at pH 5, indicating strong catalytic efficiency under lysosomal-like conditions. For PNPS at pH 5, activity decreased with a lower V_{max} and higher K_m, while at pH 7, PNPS yielded the lowest V_{max} and highest K_m, reflecting reduced affinity and turnover in neutral environments. **Conclusions:** By developing assay conditions that incorporate both

endpoint and kinetic formats across physiologically relevant pH environments, we provide a framework to identify the conditions under which sulfatases are most active. Using this approach, we found that *Helix pomatia* sulfatases exhibit broad adaptability with similar V_{max} and K_m across substrates and pH, while *Patella vulgata* sulfatases shows strong preference for PNCS under acidic conditions and markedly reduced activity for PNPS at neutral pH. These optimized assays not only reveal substrate and pH dependencies but also provide *in vitro* systems to rapidly test sulfatase activity across physiological conditions, permitting the characterization for the roles of discrete sulfatase in xenobiotic metabolism, chemical toxicity, and human disease.

ABSTRACT NUMBER: 5231 **Poster Board Number:** M805
TITLE: Ascalable human primary liver modelwith unidirectional flowto study cell-cell interactions

AUTHORS (FIRST INITIAL, LAST NAME) AND INSTITUTIONS: L. d. Haan, V. v. Duinen, I. Schilt, S. d. Ruiter, R. van Vught, L. Cuzi, M. Coenraad, and L. v. Broek. MIMETAS B.V, Oegstgeest, Netherlands. Sponsor: *S. Kundu*
KEYWORDS:

ABSTRACT: Background and Purpose: Mimicking the complex biology and physiology of the liver with *in vitro* models is essential to understand the mechanisms of liver diseases and to develop effective therapies. Most scalable *in vitro* human liver models often compromise biological complexity and lack the necessary cellular interactions required to predict drug responses in complex diseases. Conversely, more complex *in vitro* models frequently involve intricate setups and limited throughput. **Methods:** We developed an *in vitro* primary human liver model that preserves biological relevance by embedding primary human hepatocytes, liver-derived endothelial cells, hepatic stellate cells, and Kupffer cells in a hydrogel within a microfluidic platform. Material from various donors was successfully used to establish the primary liver culture, which was maintained under unidirectional perfusion in the OrganoPlate® Graft UF, featuring 32 parallel, membrane-free chips. This model leverages UniFlow technology to create a fully perfusable microvascular system under unidirectional flow, supporting cell polarization, sustained nutrient exchange, and vascular stability across the culture period. **Results:** Cultures remained stable for at least 14 days, demonstrating sustained production of albumin (>5 µg/mL per day) and active drug-metabolizing enzyme (DME) function at endpoint. Immunofluorescent analysis confirmed the presence of CD16- and CD163-positive Kupffer cells, and stimulation with LPS induced elevated IL-6 secretion, indicating an active inflammatory response. **Conclusions:** This model is scalable and recapitulates the spatial and cellular architecture of the liver lobule, enabling studies in a physiologically relevant hepatic microenvironment. The integration of vascular, immune, and parenchymal compartments supports complex cell-cell interactions and tissue functionality. As such, this platform offers a physiologically relevant tool for disease modeling and drug evaluation.

ABSTRACT NUMBER: 5232 **Poster Board Number:** M806
TITLE: A high-throughput humanblood-brain barrier (BBB)-on-a-chip model forassessment of barrierintegrity,endothelialactivationand inflammation

AUTHORS (FIRST INITIAL, LAST NAME) AND INSTITUTIONS: J. Admiraal, A. Lekshmi Nair, L. Groenendijk, R. Overdevest, T. M. Fowke, R. Annida, O. Mocellin, R. v. Vught, I. Joore, H. E. de Vries, and N. R. Wevers. MIMETAS B.V, Oegstgeest, Netherlands. Sponsor: *S. Kundu*
KEYWORDS:

ABSTRACT: Background and Purpose: The blood-brain barrier (BBB) is a highly selective interface that maintains a homeostatic environment for the central nervous system (CNS). BBB dysfunction, inflammation, and immune cell infiltration are hallmarks of many CNS disorders, including multiple sclerosis and stroke. Currently employed animal and two-dimensional (2D) *in vitro* models do not adequately predict human BBB dysfunction and neuroinflammation. **Methods:** Here, we present a high-throughput BBB-on-a-chip model comprising human brain microvascular endothelial cells (HBMECs) cultured in a microfluidic platform that enables parallel culture of 40 chips. In each chip, a perfused HBMEC vessel was grown against an extracellular matrix gel in a membrane-free configuration. BBBs-on-chips were exposed to test molecules, and their effects were measured using a trans-epithelial electrical resistance (TEER) assay. Time-resolved effects were detected for NMDA, thrombin, and VEGF, demonstrating the utility of this readout for assessing changes in barrier integrity. **Results:** BBBs-on-chips were also exposed to varying concentrations of pro-inflammatory cytokines to mimic inflammation, resulting in impaired barrier function and aberrant cell morphology in a concentration-dependent manner. Moreover, we observed increased expression of cell adhesion molecules and enhanced monocyte adhesion. T cells extravasated from inflamed blood vessels and migrated toward a C-X-C motif chemokine ligand 12 (CXCL12) gradient. T cell adhesion was significantly reduced, and a trend toward decreased migration was observed in the presence of natalizumab, an antibody that blocks very late antigen-4 (VLA-4) and is used in the treatment of multiple sclerosis. **Conclusions:** In conclusion, we report a primary human BBB-on-a-chip model implemented in a high-throughput microfluidic platform that is compatible with standard laboratory equipment and automation. This model can support drug safety evaluations through the assessment of barrier integrity, endothelial activation, and inflammation.

ABSTRACT NUMBER: 5233 **Poster Board Number:** M807
TITLE: Forming a Hypoxic Tumor Microenvironment in Glioblastoma for High Throughput Drug Testing

AUTHORS (FIRST INITIAL, LAST NAME) AND INSTITUTIONS: E. J. Yao, and S. Chen. UC San Diego, San Diego, CA. Sponsor: S. Chen, American Association for the Advancement of Science
KEYWORDS: Biological Modeling; Biomaterial

ABSTRACT: Background and Purpose: Glioblastoma Multiforme (GBM) is the most common malignant brain and central nervous system tumor with grim prognosis and high recurrence rates. Its dynamic ecosystem contains high intratumor and interpatient heterogeneity, consisting of hallmarks such as hypoxia and necrosis that often strengthen the tumor. This heterogeneity complicates toxicological evaluation of chemotherapeutics, as conventional 2D cultures fail to capture spatially driven differences in drug response and cytotoxicity. In the past few decades, GBM organoids have emerged to increase cellular heterogeneity compared to traditional 2D cultures, however, they are often low throughput and

lack reproducibility. Here, we harnessed rapid 3D bioprinting to create biomimetic GBM models that recapitulate the mechanical and structural properties of native tumor microenvironment, creating a physiologically relevant *in vitro* toxicology model for therapeutic screening. By manipulating cell density, we were able to build off this base GBM model and create high cell density (HCD) GBM tissues to introduce a key GBM hallmark - pathological hypoxia - which arises due to lack of oxygen and nutrients. Paired with chemotherapy and radiotherapy testing, our approach offers a reproducible method to model hypoxia-driven GBM progression and lays the groundwork for future therapeutic testing. **Methods:** Human patient derived glioblastoma stem cell CW468 and human GBM immortalized U87 cells were encapsulated within GelMA bioink with LAP photoinitiator to achieve a printable hydrogel formulation. Bioprinting was performed using a digital light processing system to generate 3D constructs with high spatial resolution and high throughput. Base constructs refer to standard cell density tissue models, while high cell density refers to a great number of cells encapsulated. Constructs were cultured under standard conditions. Gene expression was evaluated via qPCR using primers including HIF1α, VEGFA, CXCL12, and other GBM-specific markers within the bioprinted environment. Invasion assays were conducted to quantify the migratory capacity of CW468 cells, using GFP to visually track their movement throughout one week. To assess chemotherapeutic response, bioprinted models were treated with temozolomide (TMZ) and viability was measured using CellTiter-Glo assay, with luminescence quantified via a TECAN plate reader. All experiments were performed in biological triplicates unless otherwise specified. **Results:** Mechanical characterization of our GBM models demonstrated that with our tailored bioink formulation, combined with optimized printing parameters and cell density, yields physiologically relevant stiffness that closely mimics native GBM tissue. Building upon this base model, we developed a HCD model with GSCs that pathologically establishes a hypoxic microenvironment over culture time, as shown by the upregulation of HIF1α expression measured by qPCR. The U87 cell line did not show an upregulation of HIF1α, indicating that either a greater cell density is required to form this hypoxic microenvironment, or U87 cells are more robust in nature. Proceeding with only the GSC line CW468, invasion assays revealed that the HCD group exhibited significantly greater invasiveness, with a 40% invasion area extending beyond the original bioprinted construct, compared to just 3% in the base model. These results suggest that the HCD environment may contribute to a more aggressive tumor phenotype.Drug response studies using the standard-of-care chemotherapeutic agent TMZ showed that both the base and HCD models exhibited increased resistance compared to traditional 2D cultures, indicating that these GBM cells are more resilient in the 3D microenvironment. We are currently expanding our investigation by testing additional GBM-targeted drugs, incorporating radiotherapy to further evaluate therapeutic responses within our models, and adding additional GBM cell types. **Conclusions:** Ultimately, our goal is to establish a platform for personalized treatment testing by integrating patient-derived GBM cells into our 3D bioprinted constructs. This study demonstrates the potential of 3D bioprinting to generate GBM models that replicate both the mechanical and pathological features of native tumors, offering a robust tool for studying tumor progression and therapeutic resistance. This system supports personalized dose-response profiling for evaluating efficacy and toxicity of potential therapies in a clinically relevant context.

ABSTRACT NUMBER: 5234 **Poster Board Number:** M808
TITLE: A 3D-Based Immunofluorescence Platform for Characterizing COPD Pathology and Evaluating Treatments in Whole Airway Tissue Models

AUTHORS (FIRST INITIAL, LAST NAME) AND INSTITUTIONS: X. Huang, C. Ferreira, J. Vernaz, N. Simonnet, *S. Constant*, S. Huang, B. Boda, and G. Arib. Epithelix, Plan les Ouates, Switzerland.
KEYWORDS: Respiratory Toxicology; *In Vitro* and Alternatives; Preclinical Assessments

ABSTRACT: Background and Purpose: Chronic obstructive pulmonary disease (COPD) is a common respiratory disease, fourth leading cause of death worldwide, and characterized by an abnormal chronic inflammatory response of the distal airways, exposed to noxious particles and fumes, such as cigarette smoke and environmental pollutants. Ongoing inflammation results over time in functional alterations of airway epithelia leading to a progressive and irreversible airflow limitation. Goblet cell hyperplasia and MUC5AC mucin overproduction are hallmark features of the lung epithelium of COPD patients. Traditionally, the assessment of MUC5AC protein produced by goblet cells is conducted using an immunohistochemical (IHC) approach. This method involves sectioning tissue into thin slices, followed by selective protein staining and image-based quantification. Although powerful, IHC is tedious, time-consuming, and requires significant expertise. **Methods:** To overcome these challenges and avoid potential sample damage from mechanical steps, we propose a new approach that combines 3D confocal microscopic imaging of immunofluorescent-labeled whole tissue with image analysis based on an in-house algorithm. **Results:** Our results indicate that in IL-13 induced COPD models, which exhibit typical overproduction of MUC5AC by metaplastic goblet cells, Lebrikizumab, an IL-13 receptor antagonist, can block the effects of IL-13. Additionally, tissue models derived from the lower airway (MucilAir™ bronchial and SmallAir™) better replicate the hyperplasia phenotype compared to nasal tissue (MucilAir™ Nasal). **Conclusions:** The described 3D-based immunofluorescence platform could complement or replace the IHC-based approach for characterizing MUC5AC-producing goblet cells.

ABSTRACT NUMBER: 5235 **Poster Board Number:** M809
TITLE: A 3D Bioprinted Human iPSC-Liver Model for Predictive Toxicology: Evaluating Drug-Induced Hepatotoxicity and Nanoparticle Safety under Dynamic Perfusion

AUTHORS (FIRST INITIAL, LAST NAME) AND INSTITUTIONS: T. Lu[1], W. Zhu[2], and S. Chen[1]. [1]UCSD, San Diego, CA; and [2]CELLINK, San Diego, CA. Sponsor: *J. Luyendyk*
KEYWORDS: Biomaterial; Cytotoxicity; *In Vitro* and Alternatives; Bioprinting

ABSTRACT: Background and Purpose: Traditional 2D cell cultures and animal models often fail to accurately predict human drug-induced liver injury (DILI) due to interspecies differences and lack of physiological complexity. This study aimed to develop a highly predictive, human-relevant 3D *in vitro* liver platform using induced pluripotent stem cell (iPSC)-derived hepatocytes and endothelial cells. Our objective was to validate this bioprinted model as a robust tool for evaluating the hepatotoxic potential of both clinical pharmaceuticals and manufactured nanomaterials under physiologically relevant dynamic culture conditions. **Methods:** Multi-cellular liver constructs were bioprinted using iPSC-derived hepatocytes and endothelial cells within a remodelable hydrogel matrix. Integrated microfluidic perfusion maintained long-term metabolic function, assessed by albumin/urea secretion and cytochrome P450 activity. Predictive performance was evaluated by exposing constructs to clinical hepatotoxicants (e.g., acetaminophen, troglitazone) and metal nanoparticles. **Results:** The bioprinted

liver model maintained stable metabolic activity and inducible CYP function for over 21 days under dynamic perfusion. In drug-screening assays, the platform accurately identified clinically relevant hepatotoxic compounds, with IC_{50} and benchmark dose (BMD) values matching reported human maximum plasma concentration (C_{max}) thresholds. Dynamic perfusion significantly increased sensitivity compared to static cultures. Furthermore, the 3D model exhibited a more resilient, human-like defense against CuO nanoparticles—showing lower reactive oxygen species (ROS) generation and higher viability compared to 2D cultures, which tended to overestimate toxicity. **Conclusions:** This study demonstrates that a perfusable, bioprinted iPSC-liver model provides superior predictive accuracy for human hepatotoxicity compared to conventional systems. By recapitulating physiological microenvironments, this platform effectively identifies toxic responses for both drugs and nanomaterials, offering a human-relevant alternative to animal testing.

ABSTRACT NUMBER: 5236 **Poster Board Number:** M810

TITLE: Optimization of Human ESC-Derived Colon Organoids for Detection of Genotoxicity Relevant to Predictive Toxicology

AUTHORS (FIRST INITIAL, LAST NAME) AND INSTITUTIONS: P. Pediaditakis[1,2], *N. Takahashi*[1,3], I. Shats[1], X. Zhang[1], T. V. Ton[1], *E. J. Tokar*[1], and A. R. Pandiri[1]. [1]NIEHS/NIH, RTP, NC; [2]EPL Inc., Rtp, NC; and [3]The Institute of Environmental Toxicology, Ibaraki, Japan.

KEYWORDS: Alternatives to Animal Testing; Gastrointestinal; Cell Culture; organoid

ABSTRACT: Background and Purpose: Incidence of early-onset colorectal cancer (EOCRC) increased markedly in recent decades, with epidemiological evidence implicating environmental, dietary, and lifestyle-related exposures as contributors to disease etiology. EOCRC often lacks clear hereditary drivers, highlighting a need for experimental systems capable of testing suspected etiologic agents and identifying early molecular initiating events in the human colonic epithelium. This underscores a need for human-relevant, scalable *in vitro* models suitable for screening and prioritizing potential exposures related to EOCRC. Primary human colon organoid (CO) models lack standardization, exhibit high donor and batch variability, require costly media, and are limited in scalability, restricting comparative testing across agents. Human embryonic stem cell (ESC)-derived COs generated under defined conditions offer a standardized, cost-effective, and higher-throughput alternative. The objective of this study was to optimize ESC-derived COs and evaluate their utility as a screening platform for detecting genotoxic responses to metabolically activated dietary carcinogens implicated in EOCRC. **Methods:** H9 human ES cells were differentiated into COs over 55 days using defined modulation of Wnt and BMP signaling pathways. Colonic lineage specification was confirmed by RT-qPCR and immunofluorescence for absorptive epithelial (Villin, CA4, KRT20), secretory (MUC2), enteroendocrine (CHGA, NEUROG), and stem/progenitor (SOX9) markers. To assess genotoxicity, organoids were exposed to 2-amino-1-methyl-6-phenylimidazo [5-b]pyridine (PhIP; 0, 10, 20, and 30 µM), a dietary heterocyclic amine that requires metabolic activation. PhIP was preincubated with phenobarbital/β-naphthoflavone-induced rat liver S9 fraction (0.5% v/v) for 20 minutes before treatment with CO. After 4h, the S9/PhIP medium was replaced with normal media containing Celltox Green (CTG). Cytotoxicity was evaluated using live-cell imaging with CTG and ATP-based viability assays. DNA damage was assessed using long-amplicon PCR of the β-globin gene and immunofluorescent detection of γH2AX nuclear localization. **Results:** Differentiated COs exhibited organized colonic crypt-like architecture and robust expression of colonic lineage markers at transcript and protein levels. At day 4 expansion, RT-qPCR demonstrated marked

upregulation of Villin (11-fold), CA4 (1,268-fold), KRT20 (25,189-fold), MUC2 (28,087-fold), CHGA (275-fold), NEUROG (9,538-fold), and SOX9 (80-fold). Immunofluorescence confirmed apical localization of Villin and E-cadherin, sparse CHGA- and GLP-1-positive enteroendocrine L cells, and clustered MUC2-positive goblet cells. ESC-derived COs demonstrated reliable expansion and higher split ratios (1:4) compared with primary colonoids (1:2). Exposure to metabolically activated PhIP resulted in a concentration-dependent decrease in cellular ATP levels to 68%, 53%, and 46% of control at 10, 20, and 30 µM, respectively, indicating cytotoxicity. The S9 fraction alone produced no detectable cytotoxicity. Genotoxic injury showed a 16.5% and 40% reduction in amplifiable β-globin DNA at 20 µM and 30 µM PhIP, respectively. Immunofluorescence demonstrated increased nuclear γH2AX foci in treated organoids. **Conclusions:** The results demonstrate that ESC-derived COs provide a scalable, metabolically competent human epithelial model capable of detecting genotoxic injury relevant to colorectal carcinogenesis. This platform is well suited for systematic screening and prioritization of suspected EOCRC-associated environmental and dietary agents using human-relevant mechanistic endpoints. The observed DNA damage responses align with key events in genotoxic adverse outcome pathways. As a New Approach Methodology, this system supports reproducible cell generation, longer-term exposure paradigms, and integrated molecular readouts to inform hazard identification, exposure prioritization, and next-generation risk assessment, consistent with DTT/NIEHS translational goals.

ABSTRACT NUMBER: 5237 **Poster Board Number:** M811

TITLE: Development of an *in vitro* placental barrier model to assess the teratogenicity potential of chemicals

AUTHORS (FIRST INITIAL, LAST NAME) AND INSTITUTIONS: N. Indolfo[1], A. S. Stival[2], G. C. Bento[1], M. D. Ganzerla[1], G. F. Sousa[1], J. F. Costa[1], and M. C. Valadares[2]. [1]Natura, Cajamar, Brazil; and [2]ToxIn Lab - UFG, Goiânia, Brazil. Sponsor: N. Indolfo, Society of Environmental Toxicology and Chemistry

KEYWORDS: *In Vitro* and Alternatives; Reproductive and Developmental Toxicology

ABSTRACT: Background and Purpose: Teratogenicity is one of the toxicological endpoints assessed during the safety assessment of pharmaceutical, agricultural, cosmetic, and general chemical ingredients. It is included under the reproductive toxicity endpoint, which is further divided into effects on adult fertility and effects on embryonic and fetal development (teratogenicity). Cosmetic ingredients classified as reproductive toxins are prohibited for use in cosmetic products according to European regulations. Currently, several ingredients in the cosmetic industry, particularly fragrance ingredients, are undergoing hazard classification in Europe. The validated methods currently used to assess this hazard rely on animal testing. Therefore, the development of alternative methodologies to assess teratogenicity is of utmost importance, as it remains a toxicological endpoint for which there is no validated *in vitro* test. The existence of an *in vitro* methodology will help us anticipate these potential classifications, assisting in decision-making regarding ingredient bans and product reformulations. To evaluate the teratogenic potential of substances, it is essential to understand their ability to cross the placental barrier and reach the embryo/fetus. Thus, the placenta is an organ of critical importance in the assessment of this toxicological endpoint. **Methods:** This work aimed to develop an *in vitro* placental barrier equivalent using cell lines JEG-3 and HUVEC in an insert. The characterization of this organ equivalent was performed using cell viability assays as MTT and Live/Dead, Transepithelial/Transendothelial Electrical Resistance (TEER) measurement, gene expression, permeability and imaging techniques. **Results:** Characterization data shows a robust barrier equivalent,

with TEER measurement consistent with data from the literature. Furthermore, favorable viability results were obtained, showing that the tissue cells were viable days after the biofabrication of the barrier. Gene expression data show that the equivalent expresses markers associated with tissue, organismal, and embryonic development, functions related to the physiology and biological mechanisms of the placenta. **Conclusions:** Preliminary data indicate the development of a promising placental barrier equivalent for *in vitro* teratogenicity studies. Further characterization techniques need to be applied for complete validation of the model. As a prospective use, this model could be integrated into a microphysiological system alongside other organ equivalents to assess the teratogenic potential of substances of interest.

ABSTRACT NUMBER: 5238 **Poster Board Number:** M812

TITLE: Human Intestinal *In Vitro* Models for the Assessment of Pre-Systemic Metabolism Following Oral Administration

AUTHORS (FIRST INITIAL, LAST NAME) AND INSTITUTIONS: P. Lundquist[1], M. Ceylan[1], R. Hammar[1], A. C. Lopes[1], M. Sellin[1], H. S. Wagner[2], O. Poetz[2,3], and P. Artursson[1]. [1]Uppsala University, Uppsala, Sweden; [2]SIGNATOPE, Reutlingen, Germany; and [3]NMI Natural and Medical Institute at the University of Tuebingen, Reutlingen, Germany. Sponsor: O. Poetz, International Society for the Study of Xenobiotics

KEYWORDS: *In Vitro* and Alternatives; Proteomics; Bioavailability; Gut model

ABSTRACT: Background and Purpose: The EU-funded RISK-HUNT3R project aims to improve the assessment of human exposure to chemicals and pharmaceuticals via the lungs, skin and gastrointestinal tract. A key objective of the project is to develop new approach methods (NAMs) that more accurately replicate human absorption barriers and generate high-quality input data for predictive toxicokinetic models. For the assessment of oral exposure, intestinal permeability through epithelial cells is a crucial factor for systemic availability after ingestion. Although permeability measurements provide valuable information, a realistic assessment of oral absorption also requires the quantification of intestinal first-pass metabolism, i.e. the proportion of a compound that is metabolised by enterocytes in the small intestine. Existing *in vitro* models, particularly Caco-2 cells, are of limited use in this regard due to their insufficient expression of relevant metabolising enzymes. Therefore, we focused on the development of advanced, human-relevant intestinal models that capture both permeability and metabolic capacity. **Methods:** The Caco-2 cell model is often used to evaluate intestinal permeability, but it lacks many of the important drug-metabolising enzymes present in human intestinal epithelium. To overcome this limitation, we have developed primary human jejunum enterocyte models that retain a comprehensive range of intestinal metabolic activity. Primary enterocytes are isolated from human jejunum mucosa obtained from patients who have undergone gastric bypass surgery at Uppsala University Hospital. Cell isolation is performed using a gentle, enzyme-free method to preserve cell integrity and function. In parallel, we developed 3D models of small intestine organoids (enteroids) derived from human jejunum stem cells, which allow for a more differentiated investigation of both permeability and metabolism. All intestinal models were comprehensively characterised at the protein level for cytochrome P450 enzymes, ABC and SLC transporters, and UDP glucuronosyltransferases (UGTs). Protein quantification was performed by immunoaffinity-liquid chromatography coupled to mass spectrometry. In short, the proteins were digested with trypsin and the peptides derived from the proteins of interest were enriched using antibodies that recognise common C-terminal amino acid motifs. The peptides were then quantified by immunoaffinity LC-MS/MS using synthetic isotope-labelled standards. **Results:** The

method of isolating enterocytes consistently yielded cells with a viability of over 90%. While 25-35% of cells exhibited caspase-8 expression, indicative of early apoptosis, proteomic analyses revealed robust expression of key ADME-relevant proteins. These included several cytochrome P450 isoforms and phase II metabolising enzymes. This enabled the direct assessment of the presystemic intestinal metabolism of orally administered compounds. Additionally, human jejunum enteroids were successfully established and cultured in apical-outward and basal-outward configurations. Functional characterisation revealed that the expression levels of many ADME proteins in the enteroids were very similar to those in native intestinal tissue and isolated enterocytes. Overall, the enteroid models exhibited physiologically relevant expression of CYP enzymes, drug transporters, and conjugating enzymes. **Conclusions:** The newly developed intestinal models - primary human enterocytes and 3D enteroids derived from the jejunum - exhibit ADME protein expression profiles that are very similar to those of the human intestinal mucosa *in vivo*. Compared to Caco-2 cell cultures, these models better reflect human mucosal tissue with regard to metabolic and transport processes.The reproducibility of enterocyte isolation and enteroid cultivation, combined with their physiologically relevant enzyme and transporter expression, underscores their great potential as next-generation *in vitro* tools. Taken together, these advances represent a significant step towards a more accurate and human-relevant assessment of oral drug absorption and intestinal metabolism.

ABSTRACT NUMBER: 5239 **Poster Board Number:** M813

TITLE: Advancing Translational Toxicology: Development of a Long-Term *Ex Vivo* Human Skin Perfusion System for Mechanistic and Therapeutic Studies

AUTHORS (FIRST INITIAL, LAST NAME) AND INSTITUTIONS: A. Ejaz. University of Pittsburgh, Pittsburgh, PA. Sponsor: A. Ejaz, American Association for Cancer Research

KEYWORDS: Alternatives to Animal Testing; *In Vitro* and Alternatives; Chemical and Biological Weapons

ABSTRACT: Background and Purpose: The translation of preclinical toxicology findings to human outcomes remains limited by fundamental metabolic, anatomical, and physiological differences between animal models and human tissues. Although organ-on-a-chip platforms have advanced human cell-based modeling, they lack the full architectural, vascular, and microenvironmental complexity required to accurately assess tissue-level toxicologic responses. To address this gap, we developed a novel *ex vivo* perfused human fasciocutaneous flap model using surgical discard tissue, enabling long-term maintenance of native human skin for mechanistic and translational toxicology studies. **Methods:** Human fasciocutaneous tissue was surgically refined and perfused through anatomically relevant angiosomes using a custom-engineered bioreactor system. Perfusion media and flow parameters were optimized to maintain tissue viability and physiological function for up to three weeks. Perfusion integrity was confirmed using thermal imaging and fluorescent tracers. Metabolic health was continuously monitored via glucose consumption and lactate production. Tissue integrity and cellular responses were assessed by histology, TUNEL staining, and gene expression analyses. Vascular functionality was evaluated through physiological responses to vasoactive agents. Chemical (nitrogen mustard) and radiation-induced toxicity were evaluated by histology, protein, gene, and transcriptomics analysis. **Results:** The perfusion system maintained structural, metabolic, and vascular viability over extended culture periods. The platform demonstrated broad applicability for toxicologic investigations, including modeling radiation- and chemical-induced skin injury, assessment of tissue-level injury responses, and evaluation of wound-healing kinetics. Histological evaluation of chemical and radiation

injuries showed signature dynamic changes in human skin related to these injuries, confirmed by protein and gene expression analysis. Bulk transcriptomic analysis showed novel regenerative pathways deregulated by chemical and radiation toxicity. Manipulation of these pathways opens new directions for mechanism-based therapeutics development. **Conclusions:** This *ex vivo* human skin perfusion model provides a physiologically and anatomically relevant platform for translational toxicology research. By enabling direct assessment of human tissue responses to toxic insults under controlled conditions, this system has the potential to improve human risk prediction, accelerate therapeutic development, and reduce reliance on animal models.

ABSTRACT NUMBER: 5240 **Poster Board Number:** M814

TITLE: Next-generation full-thickness human bronchial epithelial model produced using 3D electrospun scaffolds and animal-component-free culture media

AUTHORS (FIRST INITIAL, LAST NAME) AND INSTITUTIONS: J. Chakravarty, E. McFadden, J. Rangel, J. T. Le Do, L. M. Fitzgerald, R. Hodroj, N. F. Long, M. D. Phaneuf, and *P. J. Hayden*. BioSurfaces Inc, Ashland, MA.

KEYWORDS: Alternatives to Animal Testing; Respiratory Toxicology; Bronchial Tissue Model

ABSTRACT: Background and Purpose: *In vitro* full-thickness human bronchial tissue models are important tools for testing environmental pollutants and chemicals, screening of new pharmaceuticals, and human disease modeling research. However, these models commonly utilize animal-derived collagen as a main structural element of the stromal matrix. Animal-derived collagen constructs suffer from stability and contraction issues, resulting in a short lifespan and poor reproducibility. Additionally, culture media utilized to produce these models commonly contain undesirable animal-derived components including fetal bovine serum (FBS) and bovine pituitary extract (BPE). To address these shortcomings, we developed full-thickness human bronchial models without animal-derived collagen using electrospun scaffolds as structural components of the stromal constructs, together with FBS/BPE-free culture media formulations. **Methods:** Electrospun polyester (Bio-Spun™-PET) scaffolds are composed of randomly oriented fibers with nm to low µm diameters, similar in structure to native extracellular matrix. The scaffolds were attached to Transwell® inserts in place of typical 2D microporous membrane supports. The electrospun scaffold inserts can be attached to a variety of insert formats including 6-, 12- and 24-well individual Transwell® inserts, as well as 24-well and 96-well Transwell® high throughput screening (HTS) formats. The thickness of the scaffolds can also be customized. Scaffolds utilized in the current study were 150 µm in thickness. To produce the stromal components, Bio-Spun™ scaffold inserts (BioSurfaces) were seeded with primary human lung fibroblasts (LifeLine Cell Technologies) and cultured under submerged conditions in FBS/BPE-free medium (LifeLine or Lonza) supplemented with ascorbic acid and TGF-β1. FBS in the fibroblast medium was replaced with human platelet lysate or human serum. Primary human bronchial epithelial cells (LifeLine) were then seeded onto the stromal components. The constructs were cultured at the air-liquid interface (ALI) in FBS/BPE-free ALI differentiation medium (PneumaCult™ ALI, STEMCELL Technologies) to produce the fully-developed 3D organotypic full-thickness bronchial tissue models. Histochemical (H&E staining) and immunohistochemical staining of formalin fixed paraffin sections were utilized to evaluate morphological features of the tissue models. Functional tissue barrier was evaluated by measuring transepithelial electrical resistance (TEER). **Results:** H&E-stained paraffin sections revealed robust stromal components populated with viable fibroblasts. The fibroblasts proliferated within the synthetic

scaffolds and synthesized native collagen and extracellular matrix materials that self-assembled *in situ* to produce robust and stable stromal matrices within 4-10 days. Copious amounts of *in situ* produced stromal extracellular matrix material was evident throughout the scaffold. Immunohistochemical staining revealed uniform collagen I deposition throughout the entire electrospun stromal component. H&E, alcian blue and immunostained paraffin sections also showed well-developed pseudostratified epithelium by Day 21 of ALI culture, consisting of basal, club, ciliated (α-tubulin) and goblet cells (mucin). A uniform viable epithelium with 3-4 cell layers and TEER of ~200 Ω x cm^2 was maintained out to at least Day 35 after ALI (longest timepoint evaluated to date), providing an extended window of useful downstream experimentation time. **Conclusions:** Next-generation, *in vitro* full-thickness human bronchial models (Bio-Spun FT-Bronchial Models) were produced using animal collagen-free 3D electrospun scaffolds and FBS/BPE-free culture media formulations. The fully human bronchial models provide long-term stability and do not suffer from contraction and stromal degradation issues. The models display a well-developed pseudostratified epithelium, with *in vivo*-like cellular composition, as well as a barrier similar to *in vivo* bronchial tissue. These next-generation full-thickness human bronchial models offer promise for completely animal-product-free testing of environmental pollutants and chemicals, tobacco products, screening of new pharmaceuticals and more human-relevant disease modeling.

ABSTRACT NUMBER: 5241 **Poster Board Number:** M815
TITLE: Development of a Scalable Liver MPS Platform for Predictive Safety Assessment

AUTHORS (FIRST INITIAL, LAST NAME) AND INSTITUTIONS: G. Kulkarni[1], L. Chen[2], J. Seo[1], R. Grall[3], P. Gilbride[1], Y. Yuan[1], M. Albaum-Getzen[1], J. McCormack[1], X. Qian[1], G. Ouedraogo[3], X. Xie[1], and H. Bai[1]. [1]Xellar Biosystems, Boston, MA; [2]Advanced Research, L'Oréal Research & Innovation China, Shanghai, China; and [3]L'Oréal Research & Innovation France, Aulnay-Sous-Bois, France. Sponsor: G. Ouedraogo, EUROTOX
KEYWORDS: *In Vitro* and Alternatives; Predictive Toxicology; Acetaminophen

ABSTRACT: Background and Purpose: Drug-induced liver injury (DILI) remains a major cause of failures in the drug development process, due to the limitations of traditional animal and in *vitro* models in accurately predicting human toxicity. Recent developments in new approach methodologies (NAMs) such as liver-on-chip models have offered improved physiological relevance. However, their adoption has been limited due to high costs, limited scalability, and low reproducibility. Here, we present a primary human hepatocyte (PHH) derived, scalable liver-on-chip microfluidic platform designed to support safety assessments. **Methods:** PHHs were cultured on Xellar's OC-Plex platform and maintained under optimized microfluidic conditions to support long-term viability and metabolic function. Hepatocyte health and functionality were assessed using albumin, viability, and cytochrome P450 activity and gene expression. Acetaminophen (APAP) was used as a tool compound to establish model sensitivity to hepatotoxicity. To evaluate potential hepatotoxicity, six hepatic functional markers, such as albumin secretion, cell viability using live/dead staining, cytokeratin-18 (CK18) release, urea production, CYP3A4 activity, and mitochondrial membrane potential, were assessed as predictors of hepatocellular dysfunction and injury. As a proof-of-concept for evaluating its predictive performance, the OC-Plex platform was challenged with a panel of 17 well-characterized compounds: 13 were known to cause hepatotoxicity, while 4 were not hepatotoxic. **Results:** Untreated PHHs cultured on the platform maintained high levels of albumin levels, cell viability, and metabolic function over the duration of the

culture. Consistent dose-dependent APAP toxicity across all readouts confirmed the model's ability to capture metabolically mediated hepatotoxicity. The model demonstrated a high predictive performance with the 13-compound panel, achieving 85.7% sensitivity, 100% specificity, and 92.3% overall accuracy. **Conclusions:** These results demonstrate a robust, cost-effective, and scalable liver-on-chip platform that can detect human-relevant hepatotoxicity with high accuracy. With continued development and validation, this approach has the potential to replace animal testing and serve as a New Approach Methodology (NAM) for predictive toxicology and chemical safety assessment.

ABSTRACT NUMBER: 5242 **Poster Board Number:** M816

TITLE: A Tri-Cell Culture Model of Human Intestine Constructed on Electrospun Polyurethane Scaffold Inserts in the MIVO Millifluidic Device: Effect of Static vs. Dynamic Flow Culture Conditions

AUTHORS (FIRST INITIAL, LAST NAME) AND INSTITUTIONS: M. E. Palamà[1], M. Aiello[1], S. Scaglione[1], *P. J. Hayden*[2], and M. D. Phaneuf[2]. [1]React4life, Genoa, Italy; and [2]BioSurfaces Inc, Ashland, MA.

KEYWORDS: *In Vitro* and Alternatives; Gastrointestinal; Alternatives to Animal Testing; Organ-on-a-chip

ABSTRACT: Background and Purpose: Accurate *in vitro* modelling of the human gut is a key need for drug development and disease treatment. However traditional *in vitro* models struggle to accurately replicate the gut's complex mechanisms. The aim of the current work is to develop an *in vitro* model that more accurately reproduces the morphological and functional aspects of the human intestinal epithelium, including incorporation of dynamic *in vivo*-like basolateral perfusion to mimic interstitial fluid flow and peristaltic mechanical forces. **Methods:** A tri-culture model consisting of human dermal fibroblasts (HDF), and a mixture of enterocyte-like Caco-2 cells and goblet cell-like HT29-MTX cells was finely tuned and employed. The cells were co-cultured on flexible scaffolds comprised of electrospun polyurethane nanofibers (Bio-Spun™ PU scaffolds) contained within Transwell-type cell culture inserts. The inserts were cultured on the MIVO millifluidic organ on chip device under both static and dynamic flow medium conditions mimicking the physiological flow, to determine effects on morphological differentiation and barrier development. Inserts containing traditional rigid microporous membranes were utilized as controls to assess the relative effects in comparison to flexible Bio-Spun™ PU scaffolds. To prepare the model, HDF were first seeded onto the Bio-Spun™ PU scaffolds to form a subepithelial extracellular matrix (ECM) foundation. The mixture of epithelial cells was then applied to the inserts and cultured for up to 2 additional weeks. Epithelial barrier function was monitored every 2 days via transepithelial electrical resistance (TEER) measurements. At the conclusion of the culture period, tissue barrier was further evaluated by measuring permeation of FITC-dextran, and tissues were fixed for histological analysis: morphology was assessed by H&E staining of 5 µm paraffin sections and light microscopy. Images and quantitative measurements were obtained on an Olympus IX51microscope equipped with CellSens imaging and analysis software. **Results:** TEER and FITC-dextran permeation results demonstrated development of significant barrier in models produced on either rigid microporous membranes or flexible Bio-Spun™ PU scaffolds. The barrier of the tissues cultured on the rigid membranes was slightly stronger than the barrier on the flexible Bio-Spun™ PU scaffolds. However, in both cases the barrier was significantly improved under dynamic flow conditions ($p < 0.05$), and both tissue models achieved FITC-dextran permeation rates of < 4% under dynamic flow conditions, indicative of healthy differentiated intestinal epithelium. The Bio-Spun™ PU nanofiber scaffolds provided better attachment of the tissues compared to rigid porous membranes, and completely avoided loss of cultures due to contraction and detachment. For both rigid microporous membranes and flexible nanofiber

scaffolds, histological analysis showed that the HDF/ECM layer cultured under dynamic flow conditions appeared thicker and more robust compared to static conditions. The effect of dynamic flow on the epithelial component was particularly noteworthy: dynamic flow induced a more differentiated epithelium with a higher proportion of cells with prominent goblet cell morphology on both rigid membranes and flexible Bio-Spun™ PU scaffolds. However, the rigid membranes produced mostly monolayer epithelia, while the Bio-Spun™ scaffolds produced thicker, multilayered epithelium with histological appearance of Paneth cells as well as goblet cells, indicating that the flexibility of the scaffold is better able to transmit the effects of dynamic flow forces to the tissue construct. **Conclusions:** A novel *in vitro* tri-culture model of human intestinal epithelium was produced on flexible Bio-Spun™ PU scaffolds using the MIVO millifluidic device. The flexible BioSpun™ scaffolds provided improved tissue attachment compared to common rigid microporous membrane substrates. Improved epithelial barrier and intestinal differentiation were also achieved on the flexible nanofiber PU scaffolds under dynamic medium flow conditions. The use of flexible electrospun nanofiber PU scaffold inserts in the MIVO millifluidic device may be applicable to development and improvement of other *in vitro* model systems as well.

ABSTRACT NUMBER: 5243 **Poster Board Number:** M817
TITLE: First Use of *In Vitro* Respiratory Tract Models for a TSCA Test Order: Evaluating Hexafluoropropylene Oxide (HFPO) Effects Across Three Regions of the Respiratory Tract

AUTHORS (FIRST INITIAL, LAST NAME) AND INSTITUTIONS: *E. A. Huber*, R. Chartier, H. Kellner, C. Clayton, D. Kessans, N. Washington, E. Piel, *S. Bell*, and *S. D. McCullough*. RTI International, Durham, NC.
KEYWORDS: *In Vitro* and Alternatives; Respiratory Toxicology; Regulatory Science/Regulatory Toxicology; TSCA; Hexafluoropropylene oxide (HFPO)

ABSTRACT: Background and Purpose: On January 4th, 2023, the United States Environmental Protection Agency (EPA) issued a Test Order for trifluoro(trifluoromethyl)oxirane, also known as hexafluoropropylene oxide (HFPO; CASRN 428-59-1), under Section 4 of the Toxic Substances Control Act (TSCA) (EPA-HQ-OPPT-2021-0910). HFPO is a gas that is included in the EPA's list of Per- and Polyfluoroalkyl Substances (PFAS). HFPO is manufactured and used under well controlled and enclosed conditions at two facilities in the US. HFPO is an intermediate for the manufacture of essential fluorinated monomers and polymers. It is an extremely reactive intermediate, resulting in no residual HFPO in the final products. In addition to negligible potential for worker exposure, there is negligible potential for exposure to the general population outside of the fence line. Among other studies, the Test Order requires the use of human-derived *in vitro* cell-based respiratory tract models for the collection of exposure effects data. Here, we report the results for the first use of *in vitro* respiratory to evaluate inhaled chemical exposures effects required by a TSCA Test Order. **Methods:** This study utilized *in vitro* differentiated primary human cell-based air-liquid interface (ALI) donor-matched co-culture models of the nasal, bronchial, and alveolar regions of the respiratory tract. Acute four-hour exposures were conducted using six HFPO concentrations (100 to 2,500 ppm) derived using extant *in vivo* animal exposure data. The effects of exposures were observed on cytotoxicity, epithelial barrier integrity, and pro-inflammatory cytokine and growth factor release in models representing all three regions, and apical secretion of the mucin MUC5AC in nasal and bronchial co-cultures 24 hours post exposure. Acute exposure outcomes were used to inform a subsequent repeated exposure consisting of 14 daily 4-hour HFPO exposures. Effects of repeated exposures were evaluated using the same endpoints as the acute

exposure arm with the addition of histological analysis of the epithelial layer. **Results:** Acute exposures caused minor, but significant increases in cytotoxicity in the nasal (≥1,250 ppm) and bronchial (≥1,770 ppm) models. Acute alveolar co-culture model exposures resulted in increased secretion of VEGFA, a key event in the adverse outcome pathway for pulmonary edema and a consistent finding animals exposed to higher HFPO concentrations from extant data. The effects of 14-day exposures were evaluated in the nasal and bronchial models using two concentrations (880 and 1,770 ppm) determined based on the acute exposure outcomes. Repeated exposures increased epithelial barrier integrity but not cytotoxicity, in both models. Repeated exposures also resulted in remodeling of the epithelial cell layer as evidenced by changes in goblet and ciliated cell densities that differed between nasal and bronchial co-cultures. **Conclusions:** Collectively, the outcomes observed in the *in vitro* exposures reflect the outcomes of extant *in vivo* studies where applicable comparable data are available. Observations from this study also demonstrate significant inter-individual variability across donors in some endpoints that supports the inclusion of more than a limited number of (e.g., 1-3) donors in future *in vitro* studies. Donor variability may have challenged the observation of statistically significant changes in outcomes in this study; however, it also highlighted the importance of improving our understanding of the role of inter-individual variability in primary cell-derived respiratory models and *in vitro* exposure outcomes. Bridging this knowledge gap will facilitate the successful integration of *in vivo* relevant *in vitro* models into future toxicity testing while also increasing their relevance to *in vivo* human biology and exposure outcomes.

ABSTRACT NUMBER: 5244 **Poster Board Number:** M818

TITLE: Mechanistic Divergence in Inhalation Toxicity of Structurally Analogous Quaternary Ammonium Compounds (BKC and DDAC) at the Air-Liquid Interface

AUTHORS (FIRST INITIAL, LAST NAME) AND INSTITUTIONS: *M. Kim*, J. Bang, S. Lee, H. Kim, J. Kim, H. Ku, and H. Yi. Animal and Plant Quarantine Agency, Gimcheon-si, Gyeongsangbuk-do, Korea, Republic of.

KEYWORDS: *In Vitro* and Alternatives; Respiratory Toxicology

ABSTRACT: Background and Purpose: Benzalkonium chloride (BKC) and didecyldimethylammonium chloride (DDAC) are representative quaternary ammonium compounds (QACs) and cationic surfactants, widely utilized for their potent antimicrobial and disinfectant properties. Their increasing use in aerosolized products has heightened concerns regarding respiratory toxicity. Notably, variations in alkyl chain length and configuration dictate the degree of lipophilicity and membrane permeabilization, potentially leading to distinct toxicological profiles. This study evaluated and compared the underlying mechanisms of cytotoxicity and oxidative stress induced by aerosolized BKC and DDAC using human lung epithelial models (A549 and Calu-3) cultured at the physiologically relevant air-liquid interface (ALI). **Methods:** A549 and Calu-3 cells were cultured at the ALI and exposed to aerosolized BKC and DDAC using the VITROCELL® Cloud system to mimic inhalation exposure. Cytotoxicity was assessed 4 and 24 hours post-exposure via WST-1, CellTiter-Glo (ATP), and LDH assays. Oxidative stress was measured by reactive oxygen species (ROS) generation. Barrier integrity was monitored via transepithelial electrical resistance (TEER) and morphological changes (H&E staining). **Results:** Both QACs induced concentration-dependent reductions in cell viability, with Calu-3 cells exhibiting greater sensitivity than A549 cells. While both compounds displayed similar cytotoxic potency, their underlying toxicological signatures were distinct. BKC exposure led to extensive membrane disruption characterized by significant LDH release. In contrast, DDAC elicited a more robust and pronounced increase in ROS generation compared to BKC, suggesting that DDAC-induced toxicity is primarily driven by heightened oxidative stress rather

than the predominant membrane damage observed with BKC. **Conclusions:** These findings demonstrate that while BKC and DDAC are structural analogs, they elicit mechanistically distinct toxic responses: primarily membrane-lytic for BKC and predominantly oxidative stress-driven for DDAC. This study highlights the importance of mechanistically-informed risk assessment. The comparative analysis under ALI conditions provides critical data for the refinement of compound-specific toxicity profiles and informs the regulatory safety assessment of aerosolized disinfectants

---

ABSTRACT NUMBER: 5245 **Poster Board Number:** M819
TITLE: A human primary-cell colon-on-chip model to investigate intestinal responses to orally administered tamoxifen under dynamic flow

AUTHORS (FIRST INITIAL, LAST NAME) AND INSTITUTIONS: A. Abols. Cellbox Labs, Riga, Latvia. Sponsor: *C. Roper*
KEYWORDS: Cell Culture; *In Vitro* and Alternatives; Methods/Mechanism

ABSTRACT: Background and Purpose: Assessing gastrointestinal toxicity caused by orally administered anticancer drugs remains a key limitation of conventional preclinical testing. Tamoxifen citrate, a commonly prescribed selective estrogen receptor modulator, is associated with alterations in intestinal epithelial function that are not adequately captured by static *in vitro* models. Human-relevant microphysiological systems offer an opportunity to better reproduce intestinal physiology and improve prediction of drug-induced gastrointestinal effects. **Methods:** In this work, we present a primary-cell-based colon-on-chip model developed using human colonic epithelial cells sourced from ALTIS Biosystems and implemented on a microfluidic platform from Cellbox Labs. The system incorporates continuous luminal flow to mimic the dynamic intestinal environment and supports epithelial differentiation and barrier formation. Model characterization was performed using immunofluorescent staining of epithelial and functional markers, including ZO-1, Villin, MUC2, and CHGA, together with assessment of barrier integrity.Tamoxifen citrate was administered via the luminal channel across a range of concentrations to evaluate drug uptake and epithelial toxicity under dynamic conditions. Cellular viability and cytotoxicity were quantified using CCK-8 and LDH assays, respectively, while compound transport and uptake were measured by HPLC. Structural and functional changes in the epithelial layer following exposure were further analyzed through marker expression and morphological assessment. **Results:** The results demonstrate that the colon-on-chip model enables reproducible epithelial maturation, quantitative drug uptake analysis, and detection of dose-dependent toxic effects. Tamoxifen exposure led to reduced epithelial viability, increased cytotoxicity, and pronounced alterations in tissue organization, highlighting the utility of this platform for studying gastrointestinal responses to oral therapeutics. **Conclusions:** Overall, this approach provides a physiologically relevant *in vitro* framework for evaluating intestinal safety liabilities early in drug development.

ABSTRACT NUMBER: 5246 **Poster Board Number:** M820

TITLE: Advancing key event 4 (t-cell activation)-based pbmc methods for non-animal screening of skin and respiratory sensitizers

AUTHORS (FIRST INITIAL, LAST NAME) AND INSTITUTIONS: A. B. Ramos[1], B. Rodrigues[1,2,3], C. V. Colaço[4], A. I. Sebastião[1,2,5], A. Silva[2,5], B. Neves[6], and *M. T. Cruz*[1,2,5]. [1]Faculty of Pharmacy, University of Coimbra, Coimbra, Portugal; [2]Center for Innovative Biomedicine and Biotechnology (CIBB), University of Coimbra, Coimbra, Portugal; [3]CEMMPRE, ARISE, Department of Chemical Engineering, Faculty of Sciences and Technology, University of Coimbra, Coimbra, Portugal; [4]Faculty of Medicine, University of Coimbra, Coimbra, Portugal; [5]Center for Neuroscience and Cell Biology (CNC), University of Coimbra, Coimbra, Portugal; and [6]Department of Medical Sciences and Institute of Biomedicine – iBiMED, University of Aveiro, Aveiro, Portugal.

KEYWORDS: *In Vitro* and Alternatives; Inflammation; Respiratory Sensitization; PBMC

ABSTRACT: Background and Purpose: In the pharmaceutical, chemical, and cosmetic industries, rigorous screening of product components is required to assess their potential risks to human health. Several worldwide policies have boosted New Approach Methodologies (NAM), such as the 7th Amendment to the EU Cosmetic Directive. Significant advances have been made in assessing skin sensitization using NAM aligned with three key events of the Adverse Outcome Pathway (AOP). However, evaluating adaptive immune response in the draining lymph node (fourth key event) remains challenging. Furthermore, the lack of validated methods to identify respiratory sensitizers persists as an unmet regulatory need. **Methods:** To address these urgent needs, a human *in vitro* method was developed using peripheral blood mononuclear cells (PBMCs) isolated from healthy donors. PBMCs were first stimulated directly with selected respiratory and cutaneous sensitizers and then, in a parallel experiment, exposed to lysates derived from keratinocytes previously treated with skin sensitizers. Cellular responses were evaluated by flow cytometry to assess activation and proliferation within the different PBMC subpopulations, and by ELISA to characterize the cytokine secretion profile We aimed to identify immune signatures capable of classifying chemicals as sensitizers and, among sensitizers, discriminating between respiratory and skin types. **Results:** Using this method, skin sensitizers showed a tendency to increase the expression of activation markers, such as CD25, on monocytes and T cells. In addition, CD54 expression was increased on monocytes, while HLA-DR expression was decreased in both antigen-presenting cells (B cells and monocytes). Regarding cytokine production, a predominantly pro-inflammatory profile was observed, exemplified by elevated IL-1β levels (48 hours and 6 days following exposure to skin sensitizers). Interestingly, the IL-12/IL-10 ratio indicated that the cytokine milieu remained pro-inflammatory at 48 hours post-exposure. At the six-day mark, an anti-inflammatory shift was also observed, suggesting regulatory events. It is important to note that incubation with lysates from sensitizer-exposed keratinocytes resulted in a more pronounced response for some events. Respiratory sensitizers did not show significant differences, highlighting the need for further optimization. **Conclusions:** These findings highlight the dynamic nature of immune activation and cytokine responses in PBMCs, particularly during skin sensitization. Overall, this method shows potential to recapitulate key biological responses observed in *in vivo* models under *in vitro* conditions and represents a starting point for its application to a broader range of sensitizers. Further validation is required to strengthen its robustness and support its future use in regulatory and pre-clinical settings.

ABSTRACT NUMBER: 5248 **Poster Board Number:** M822

TITLE: Generative AI-Driven Quantitative Knowledge-Activity Relationships (QKARs) for Advancing Drug Toxicity Prediction

AUTHORS (FIRST INITIAL, LAST NAME) AND INSTITUTIONS: D. Li[1], T. Li[1], Y. Qu[1], A. Chen[1], S. Thakkar[2], and *W. Tong*[1]. [1]US FDA-NCTR, Jefferson, AR; and [2]US FDA-CDER, Silver Spring, MD.

KEYWORDS: Predictive Toxicology; QSAR; Computational Toxicology; Drug safety

ABSTRACT: Background and Purpose: Computational toxicology is essential for assessing drug safety and guiding regulatory decision-making. Traditional models, such as Quantitative Structure-Activity Relationship (QSAR), often predict toxicological responses based solely on molecular structure. However, small structural modifications may result in drastically different toxicity outcomes, limiting these models' applicability. Emerging artificial intelligence (AI) approaches, such as text embeddings and generative AI, enable the integration of broader domain knowledge. This study introduces Quantitative Knowledge-Activity Relationships (QKARs), a novel generative AI-driven framework that leverages chemical, biological, and pharmacological knowledge to enhance drug toxicity prediction. **Methods:** We developed QKAR models for two clinically relevant endpoints: drug-induced liver injury (DILI) and drug-induced cardiotoxicity (DICT). Three knowledge representations with varying levels of knowledge were generated using GPT4o and text-embedding-3 and used as input for model development. Five machine learning (ML) algorithms with different complexity were applied. Model performance was assessed across knowledge representations and algorithms and compared to QSAR models built on identical datasets and methods. Hybrid Q(K+S)AR models combining knowledge-based and structure-based representations were also explored for enhanced prediction accuracy. **Results:** For both toxicity endpoints, QKAR models using the comprehensive knowledge representation consistently performed better than those employing simpler representations. Furthermore, comparative analyses revealed that QKAR models significantly outperformed their QSAR counterparts, achieving 104-747% higher Matthews correlation coefficients (MCCs) for both endpoints. In contrast, there was little association between algorithmic complexity and predictive outcomes, suggesting that the choice of algorithms was not critical. Notably, QKARs demonstrated superior discrimination between drugs with similar structures but distinct toxicity profiles for six out of eight drug pairs. Finally, the integrated Q(K+S)AR framework yielded additional improvement in predictive performance. **Conclusions:** These findings demonstrated that QKARs is a robust, knowledge-driven approach that leverages generative AI for improved drug toxicity prediction. By moving beyond structural constraints of QSARs, QKARs may enable broader and more versatile applications across chemical and biological domains.

ABSTRACT NUMBER: 5249 **Poster Board Number:** M823

TITLE: Enhancing Reproducibility in Molecular Toxicology: A Robust Biostatistical Tool for qPCR Data Analysis with Low Concentration Targets

AUTHORS (FIRST INITIAL, LAST NAME) AND INSTITUTIONS: W. Zhuang. FDA/NCTR, Jefferson, AR. Sponsor: *D. Wang*

KEYWORDS: RT-PCR; Risk Assessment; Bioinformatics; sequencing techniques

ABSTRACT: Background and Purpose: Recent studies by regulators and researchers have highlighted the value of informative data, even when it is uncertain, in patient and disease management. In toxicological risk assessment, modern approaches often rely on gene-expression measurements obtained by qPCR or sequencing-based methods, where low-concentration targets frequently lead to uncertain or incomplete values. These uncertainties pose a reproducibility challenge that can undermine regulatory acceptance and erode the credibility of the scientific evidence regulators rely on. This poster presents a new computational tool specifically designed to analyze qPCR data from low-concentration targets, enabling robust sensitivity analyses and addressing the reproducibility challenge. **Methods:** Our work began by establishing the critical nature of the statistical reproducibility deficit in qPCR data analysis with low abundance. To address this challenge, we developed a robust statistical CTOT (Cycle-To-Threshold) method using a nonparametric time-to-event approach that explicitly accounts for incomplete or censored cycle-to-threshold qPCR data characteristic of low-abundance targets. The CTOT methodology models cycle-to-threshold values as time-to-event outcomes and incorporates flexible semiparametric regression together with robust nonparametric two-group comparison and hypothesis-testing procedures. This framework enables the principled inclusion of observations with uncertainty—such as late or partially observed amplification—rather than excluding them or applying ad hoc substitutions. The methodology was evaluated using extensive simulation studies and real-world qPCR datasets and was implemented in a R Shiny app to facilitate standardized statistical analysis and inference across diverse contexts including toxicological scenarios. **Results:** Analyses of 300,000 simulated qPCR datasets and 17 real-life two-group qPCR comparisons on nephrotoxicity data showed that CTOT outperformed common qPCR statistical methods across a wide range of scenarios by accurately identifying significant gene-expression changes that would otherwise be overlooked. In real-world nephrotoxicity analyses of 17 two-group comparisons of serum microRNAs (miR-128-3p and miR-210-3p) in rats exposed to melamine and cyanuric acid, CTOT confirmed all non-significant similarities between control and exposure groups and detected all but one significant difference when using the more conservative Ct cutoff value of 32. Compared to CTOT's performance, the maximum cycle (MC) method detected 1 fewer significant difference, while the complete-observation (CO) method detected 4 fewer significant differences, demonstrating CTOT's superior sensitivity for identifying true biological effects in toxicological studies. Most recently, we implemented this methodology into the online MCTOT (Multi-Functional Cycle-To-Threshold Statistical Analysis Tool) app to facilitate accessible and reproducible analysis. Applications to diverse toxicological scenarios—including both direct toxicant-response data and matrix-interference conditions such as hemolysis—showed that MCTOT could help confirm or clarify the true signal of toxic and biological effects. The application successfully processed and analyzed datasets with a sample size ranging from 10 to 24 with Ct cutoff values of 32 or 40 cycles, accommodating the typical ranges encountered in toxicological qPCR studies. The MCTOT app is open access and can be used at https://ctot.shinyapps.io/bioinformatics/ to analyze qPCR data with measurements at low concentrations. **Conclusions:** Our work provides a publicly available tool for

analysis and inference of informative but uncertainly determined qPCR data. By facilitating the analytical rigor of qPCR analyses, the MCTOT tool provides a quantitative basis for the reliable application of gene-expression data in risk evaluation and disease management, specifically in cases where target transcripts are naturally low in abundance. MCTOT, as a source-available biostatistical platform, can be integrated seamlessly with other qPCR tools (e.g., shinyCurves) to remove technical and financial barriers to cross-lab collaboration and reproducibility. This validated new tool for qPCR data analysis can be efficiently scaled to analyze low-abundance targets measured with sequencing techniques, leveraging advanced AI and modern toxicological assessment approaches.

ABSTRACT NUMBER: 5250 **Poster Board Number:** M824
TITLE: Mechanistically anchored Cell Painting approach for robust mutagenicity prediction across laboratories and metabolic conditions

AUTHORS (FIRST INITIAL, LAST NAME) AND INSTITUTIONS: T. Watanabe[1], T. Takahashi[1], T. Oshiro[1], S. Hayashi[1], *D. Mucs*[2], *S. Ito*[1], P. Shire[3], D. Ruhlandt[3], S. Schreiter[3], and K. Kottig[3]. [1]Japan Tobacco Inc., Yokohama, Japan; [2]JT International S.A., Geneva, Switzerland; and [3]Evotec SE, Hamburg, Germany.
KEYWORDS:

ABSTRACT: Background and Purpose: New Approach Methodologies (NAMs) are increasingly being promoted for chemical safety assessments, yet ensuring mechanistic relevance, robustness across experimental conditions, and regulatory acceptance remain key challenges. We previously reported a proof-of-concept for integrating Cell Painting (CP) morphological profiles with transcriptomic biomarkers to inform mutagenicity predictions. The objective of the current study was to refine the model and evaluate its transferability across laboratories and metabolic conditions, while maintaining mechanistic interpretability. **Methods:** A dataset of 77 Ames-positive and 35 Ames-negative chemicals was curated from NIHS Japan and EURL ECVAM databases. Mechanistic anchoring was achieved by selecting CP data from concentration ranges where transcriptomic signatures of DNA damage response were activated to inform leveraging of TGx-DDI biomarker concepts. U-2 OS cells were exposed to compounds for 24 hours, followed by washout and an additional 24-hour incubation prior to CP or RNA-seq assays. A Gradient Boost classifier was trained on 100 morphological features selected via Minimum Redundancy Maximum Relevance. The model was then applied to CP data generated independently at another facility under distinct conditions: 96-well plates instead of 384-well, predominantly manual handling rather than automated workflows, varied culture reagent lots (e.g., fetal bovine serum), and U-2 OS cells from different sources. Exposure durations also differed, with several chemicals tested at 4 hours versus the original 24 hours. Thirteen chemicals (9-aminoacridine, Fenbendazole, Eugenol, Saccharin, Sorbitol, AF2, Rotenone, Ethacrynic acid, Mitomycin C, Cyclophosphamide, Berberine Chloride, B[a]P, and 2-AA) were evaluated in the presence and absence of metabolic activation (MA). **Results:** The refined model maintained strong performance (balanced accuracy = 0.86, precision = 0.85, recall = 0.91, F1 score = 0.87) in the initial training set evaluation. When applied to independently generated data, the model achieved high predictive accuracy, despite differences in plate format, automation, cell source, and exposure time. Notably, the model classified pro-mutagens like benzo[a]pyrene and cyclophosphamide as negative without MA and positive with MA, despite being trained only on data without MA. Among the 13 chemicals tested under different metabolic conditions, predictions generally aligned with their known mutagenicity profiles. Investigation of five chemicals predicted as positive but classified as Ames-negative in public databases revealed that all had either positive results using *in vitro* mammalian cell

genotoxicity assays, such as the mouse lymphoma or comet assays, or equivocal results with specific Ames strains. **Conclusions:** The successful validation on external data, despite variations in reagents and protocols, confirms that the model is not overfitted to specific experimental conditions but rather captures genuine biological phenotypes associated with mutagenicity. A key result was the model's ability to predict mutagenicity with MA and without using MA data for training. This suggests that the model prioritizes morphological features representing fundamental cellular genotoxic stress responses shared by both direct-acting mutagens and metabolically activated pro-mutagens. Furthermore, the "false positive" predictions for Ames-negative chemicals were consistent with mammalian genotoxicity data, indicating that the model detects broader genotoxic stress rather than random classification errors, thereby enhancing its biological plausibility. Based on our results, mechanistically anchored CP models can deliver interpretable, transferable predictions across laboratories, plate formats, exposure durations, and metabolic conditions. This approach supports possible integration into Next-Generation Risk Assessment (NGRA) frameworks aligned with principles for Integrated Approaches to Testing and Assessment (IATA) and the 3Rs, offering a scalable and mechanistically relevant strategy for mutagenicity testing.

ABSTRACT NUMBER: 5251 **Poster Board Number:** M825
TITLE: An Integrated Approach to Threshold of Toxicological Concern for Botanical Substances

AUTHORS (FIRST INITIAL, LAST NAME) AND INSTITUTIONS: D. Allen[1], T. Burke[2], M. Cronin[3], A. Cuciureanu[4], *C. Galli*[5], H. Holnagel[6], Q. Jia[7], T. Kawamoto[8], C. Mahony[9], M. Marinovich[5], G. Melzi[5], S. Pfuhler[7], J. Rathman[10], and *C. Yang*[10]. [1]ICCS, New York, NY; [2]Reckitt, Hull, United Kingdom; [3]Liverpool John Moores University, Liverpool, United Kingdom; [4]ICCS, Brussels, Belgium; [5]University of Milan, Milan, Italy; [6]Dow, Horgen, Switzerland; [7]P&G, Cincinnati, OH; [8]Henkel, Tokyo, Japan; [9]P&G, Reading, United Kingdom; and [10]Ohio State University, Columbus, OH.
KEYWORDS: Botanicals; Safety Evaluation; Threshold of Toxicological Concern

ABSTRACT: Background and Purpose: The Threshold of Toxicological Concern (TTC) is a risk assessment approach used in the evaluation of low-level exposure to substances where toxicity data may be limited or unavailable. TTC provides a threshold below which the risk of adverse effects is considered negligible and that may be applied to food, fragrances, and cosmetics. This study extends the TTC approach to botanicals, plant-based Natural Complex Substances (NCS). Our goal is to build a database and establish robust TTC datasets, derive appropriate thresholds for systemic/target organ and reproductive/developmental toxicities, and ultimately establish a decision framework for this integrated approach. **Methods:** A new integrated database was designed and constructed to represent both NCS and associated phytochemicals. The database provides information on no observed adverse effect level (NOAEL) values for repeated dose (RDT), developmental (DvT) and reproductive toxicity (RpT) as well as botanical composition analysis. Botanical TTC datasets were derived from this database applying study inclusion criteria. Distribution of NOAEL values and fifth percentiles were determined for each endpoint separately (RDT, DvT, RpT) and collectively by selecting the lowest NOAEL across endpoints as the Point of Departure (POD). Biological-chemical inclusion criteria were developed by profiling botanical species via phytochemical ToxPrint chemotype features. **Results:** NCS reported from diverse use types were included, such as food-related (dietary supplements, additives, flavourings, functional), herbal remedies, and traditional Asian medicine (TCM). The database currently contains NOAEL values for 600 NCS covering over 700 phytochemicals from 130 species. NCS were identified by taxonomy nomenclature

(e.g., family, genus, species, scientific name, synonym). The physicochemical characteristics of the NCS tested were specified via e.g., solvent, extract form, and % plant-originated material fraction. These data were used to define identifiers for unique test articles. Individual TTC datasets were established by determining the PODs from the lowest qualified NOAELs for RDT (n=253), DvT (n=105), and RpT (n=57). The fifth percentile thresholds were 16.7 mkd for RDT, 20.9 mkd for DvT, and 2.0 mkd for RpT. To develop an integrated approach, the threshold for the overall TTC dataset (n=370) was determined to be 14.5 mkd. The tails of these distributions below the fifth percentile were populated with potent botanicals associated with well-known phytochemicals of concern. For example, *Aristolochia* and *Sanguinaria* species, and *A. rusticana*, containing aristolochic acid, sanguinarine, and allylisothiacynate, respectively, are well-known for genotoxicity, Na/K-ATPase inhibition, and GSH depletion. After mapping the relationships between NCS, phytochemicals, and modes of action leading to toxicity, the botanical-phytochemical space was profiled employing ToxPrint chemotypes to explore botanical-chemical feature space. For example, steroidogenesis inhibitors found in *Tripterygium wilfordii* and *Melaleuca alternifolia* share common chemotypes such as specific chain branching and cyclic/ring features. Profiling modes of action of NCS through their phytoconstituents is important for establishing cohort of concern criteria when applying the botanical TTC decision tree. It also enables the exclusion of genotoxic botanicals/constituents for their known role in cancer development. **Conclusions:** A new database for plant-based NCS and phytochemicals has been constructed to prepare datasets for botanical TTC approaches. The TTC decision for non-genotoxic botanical extracts is based on the threshold determined from the overall fifth percentile. The proposed decision tree includes both workflows for genotoxic/non-genotoxic botanicals by establishing a clear set of inclusion and exclusion criteria. This integrated approach marks a significant step forward in addressing the practical needs associated with the use of botanicals in cosmetics and other applications.

ABSTRACT NUMBER: 5252 **Poster Board Number:** M831

TITLE: Integrating New Approach Methodologies (NAMs) into the Protein Safety Assessment Framework for Genetically Modified Crops

AUTHORS (FIRST INITIAL, LAST NAME) AND INSTITUTIONS: *Y. J. Zhang*[1], *J. LaRocca*[2], C. Mathesius[3], I. Lamb[3], and K. Yau[3]. [1]Corteva AgriScience, Raleigh, NC; [2]Corteva AgriScience, Indianapolis, IN; and [3]Corteva AgriScience, Johnston, IA.

KEYWORDS: *In Vitro* and Alternatives; Risk Assessment; Regulatory Science/Regulatory Toxicology; Protein Safety, Genetically Moified Crops

ABSTRACT: Background and Purpose: Genetically modified (GM) crops are engineered to express newly expressed proteins (NEPs) that confer agronomic traits such as insect resistance and herbicide tolerance. NEP safety evaluation follows a weight-of-evidence framework that integrates history of safe use (HoSU), bioinformatic screening, *in vitro* protein characterization, stability testing, and dietary exposure assessment. In some jurisdictions, animal studies continue to be requested in the absence of identified risks, highlighting the need for modernized, science-based approaches tailored to protein safety assessment. Emerging new approach methodologies (NAMs) offer opportunities to modernize NEP risk assessment by improving mechanistic understanding, reducing unnecessary animal testing, and strengthening the scientific basis for regulatory decisions. **Methods:** We conducted a structured review of current available NAMs and evaluated their biological relevance, maturity, and alignment with protein safety assessment framework. Opportunities for NAMs integration into the existing WoE

framework were mapped across hazard identification, exposure assessment, and toxicity assessment. **Results:** A hypothesis-driven, tiered safety assessment framework highlights several points where NAMs could meaningfully enhance protein safety assessment. In the first tier, which includes HoSU, bioinformatic screening, and mechanism-of-action investigation, tools such as structural modeling, *in silico* binding simulations, development of curated toxin and safe protein databases, and AI-enabled structure and function prediction can improve early hazard identification. Tier II focuses on exposure assessment and depends on characterizing protein expression levels in GM crops and evaluating the stability of NEPs during food processing and gastrointestinal digestion. This tier can be enhanced through refined SGF/SIF digestion protocols and kinetic modeling approaches that more closely reflect physiological conditions. Higher tier toxicity assessment is only needed when Tier I and Tier II findings are inconclusive or indicate a plausible risk. In this tier, human-relevant *in vitro* systems, including intestinal epithelial cell (IEC) assays, stem cell-derived intestinal organoids, and multi-cell co-culture model, could support evaluation of epithelial barrier integrity, cytotoxicity, and cellular stress responses. Aligning outputs from these NAM platforms within a hypothesis-driven, tiered framework enables targeted, mechanistic evidence generation and reduces reliance on rodent studies while improving human relevance. Although promising, most NAMs require additional method development, model refinement, and assay validation before they are ready for regulatory use in protein safety assessment. **Conclusions:** Integrating NAMs into protein safety assessment for GM crops provides science-based, fit-for-purpose approaches that reinforce the existing WoE paradigm with greater mechanistic insight and human relevance while minimizing animal use. Continued collaboration among academia, the private sector, and regulatory authorities will be essential to advance methodological readiness, promote transparency, and enable broader acceptance of NAMs within regulatory decision making.

ABSTRACT NUMBER: 5253 **Poster Board Number:** M832
TITLE: Neonicotinoid Insecticides in Breastmilk: Occurrence, Exposure, and Risk Assessment

AUTHORS (FIRST INITIAL, LAST NAME) AND INSTITUTIONS: *M. M. Adetoba*, W. Xi, A. Kahler, *H. Lehmler*, and D. Thompson. University of Iowa, Iowa City, IA.
KEYWORDS: Exposure, Environmental; Infant; Neonicotinoids

ABSTRACT: Background and Purpose: Neonicotinoid insecticides (NEOs) are neurotoxic substances that individuals may encounter through environmental exposure and dietary intake. The systemic characteristics of NEOs, combined with their persistent effects, have led to their detection across diverse biological samples. However, biomonitoring data on U.S. breast milk are limited. This study aims to assess lactational exposure to NEOs, as infants are particularly vulnerable to environmental pollutants through breast milk. **Methods:** Breastmilk samples (n = 42) were obtained from biobanks across nine states (Midwest = 6, West = 3) in the US in 2013 and analyzed for ten NEOs and eleven metabolites using LC-MS/MS. Nonparametric tests (Kruskal-Wallis) were used to evaluate differences in the regional distribution of exposure between the Midwest and the West and the demographic (age and parity) impact. Estimated daily intake (EDI) was calculated from measured concentrations and a standardized milk consumption volume of 0.75 L/day with an average infant body weight of 7.2 kg. Risk indices (RI) were derived by normalizing the EDI to the chronic reference dose of 57 µg/kg/day for imidacloprid. **Results:** The analysis indicated that at least one neonicotinoid or its metabolite was present in 55% of the tested samples. Concentrations of the parent compounds were generally below detection limits, with imidacloprid being the most frequently detected neonicotinoid, identified in 40.5% of the samples.

The median total concentration of neonicotinoids was 12.3 ng/L, with an interquartile range (IQR) of 0 to 27.0 ng/L. In the Midwest, imidacloprid was the only neonicotinoid detected among the states (n = 4), with the highest mean concentration recorded in Illinois at 57.2 ng/L. However, no statistically significant differences were observed across the states (P = 0.31). In the Western states, both imidacloprid and thiamethoxam were detected across all three states, with the highest mean concentration of imidacloprid found in Washington at 62.1 ng/L. No statistically significant differences were noted for the two compounds (p = 0.09 and p = 0.07, respectively). The mean estimated daily intakes (EDIs) for individual neonicotinoids were 3.43 ng/kg/day, ranging from 0.03 to 0.85 ng/kg/day. The total mean neonicotinoid EDI in the Midwest was 2.17 ng/kg/day, while the West reported a higher EDI of 5.67 ng/kg/day. Specifically, imidacloprid had an EDI of 0.67 ng/kg/day, and thiamethoxam had an EDI of 0.37 ng/kg/day. No statistically significant differences were found across the states and regions ($p > 0.05$). Risk indices (RIs) for the individual compounds varied between 5.4×10^{-7} and 1.5×10^{-5}. The total RI values for the Midwest and the West were 3.8×10^{-5} and 9.9×10^{-5}, respectively, which were several orders of magnitude below the threshold of one. This indicates a low risk under current exposure assumptions. Additionally, no statistically significant differences were observed based on region, age, or parity ($p > 0.05$). **Conclusions:** The detection of neonicotinoid insecticides and their metabolites in U.S. breast milk signifies that infants are exposed to these substances at low yet measurable levels. The findings indicate multi-compound exposure during critical developmental phases, underscoring the need for biomonitoring to evaluate potential mixture effects and subclinical impacts, even though the estimated exposures and risk indices remain several orders of magnitude below chronic toxicity benchmarks

---

ABSTRACT NUMBER: 5254 **Poster Board Number:** M833

TITLE: Efsa's new methodology for historical control data in regulatory toxicology: framework and ongoing implementation activities

AUTHORS (FIRST INITIAL, LAST NAME) AND INSTITUTIONS: A. Chiusolo[1], L. Martino[1], T. Coja[2], P. Craig[3], B. Desprez[4], I. Dewhurst[1], E. McVey[5], A. Lanzoni[1], A. Suontausta[1], and *M. Wilks*[6]. [1]European Food Safety Authority (EFSA), Parma, Italy; [2]Austrian Agency for Health and Food Safety (AGES), Wien, Austria; [3]University of Durham, Durham, United Kingdom; [4]French Agency for Food, Environmental and Occupational Health and Safety (ANSES), Paris, France; [5]National Institute for Public Health and the Environment (RIVM), Bilthoven, Netherlands; and [6]Swiss Centre for Applied Human Toxicology, Basel, Switzerland.

KEYWORDS: Regulatory Science/Regulatory Toxicology; Historical Control Data, harmonization

ABSTRACT: Background and Purpose: Historical Control Data (HCD) are legally required for pesticide active substances in the EU and consist of data from studies performed under similar conditions as the index study. Their compilation, evaluation and use have been heterogeneous, with limited statistical assessment and inconsistent reporting, leading to variability in regulatory interpretations. In 2025, the EFSA Panel on Plant Protection Products and their Residues (PPR) introduced a stepwise, quantitative, and reproducible framework for HCD planning, evaluation, and integration in the analysis of the index studies, supported by harmonized templates. A recently established implementation strategy includes stakeholder engagement, training design, and development of decision-support tools to enable regulatory uptake. **Methods:** The EFSA framework proceeds through three clusters: (1) Planning by developing an a priori protocol for collation, evaluation, and potential integration of HCD; (2) Evaluation

by assessing biological/statistical adequacy, selecting datasets, and modelling within and between study variability; (3) Use by statistical comparison with concurrent control, and integration into index study analyses. Implementation activities initiated in late 2025 include: a recorded webinar (October 2025) detailing the methodology; design of physical training sessions for Member States competent authorities in the first half of 2026; preparation of e learning modules; submission of a Continuing Education Course (CEC) proposal on HCD to EUROTOX 2026; and scoping of a statistical decision support tool aligned with the framework. Continuous feedback mechanisms (surveys/interviews) are planned to inform refinements. **Results:** Early outputs include delivery of the webinar, finalization of the training concept and case-study package, and availability of harmonized templates for data collation and reporting across mammalian and ecotoxicology endpoints. These actions translate the EFSA methodology into practical steps for implementation and are expected to improve consistency, transparency, and regulatory acceptability of HCD. Next steps for 2026 include development of the statistical tool, coordinated support for applicants and assessors (e.g., help desk concept), and consideration of alignment opportunities with OECD guidance and emerging initiatives (e.g., Virtual Control Groups). **Conclusions:** The EFSA framework offers a structured approach to standardize HCD practices and improve transparency in regulatory toxicology. The recently launched implementation strategy, combining stakeholder engagement, training programs, and development of decision-support tools, marks a key step toward practical adoption and strengthens the scientific basis for regulatory decision-making. Upcoming activities in 2026 will focus on deploying these tools, expanding training delivery, and aligning with international initiatives to ensure consistency and long-term applicability.

ABSTRACT NUMBER: 5255 **Poster Board Number:** M834

TITLE: Estimation of Human Equivalent Doses for Flavoring Compounds in ENDs Aerosols from *In Vivo* and *In Vitro* Points of Departure

AUTHORS (FIRST INITIAL, LAST NAME) AND INSTITUTIONS: *J. Zhang*[1], *T. Antonijevic*[2], *M. Moreau*[2], D. McHugh[3], D. Sciuscio[3], *U. Doshi*[1], K. Luettich[3], and M. Gutierrez[1]. [1]Altria Client Services LLC, Richmond, VA; [2]ScitoVation, LLC, Durham, NC; and [3]Philip Morris International R&D, Philip Morris Products S.A., Neuchatel, Switzerland.

KEYWORDS: Dosimetry; Physiologically Based Pharmacokinetics; *In Vitro* and Alternatives; Flavoring compounds; Flavoring compounds

ABSTRACT: Background and Purpose: Electronic nicotine delivery systems (ENDs) products are not risk-free; however, evidence suggests reduced harm relative to combustible cigarettes. Thus, it is critical to assess individual constituents in ENDs aerosols as part of the product health risk assessment. Traditional risk assessment usually utilizes a point of departure (POD) derived from *in vivo* testing. The use of new approach methodologies (NAMs), such as *in vitro* and *in silico* methods, may offer novel approaches for chemical risk assessment, especially for chemicals with limited *in vivo* toxicity data. In this case study, we determined PODs based on an *in vivo* chronic inhalation study in the A/J mouse model in conjunction with the *in vitro* ToxTracker assay (Toxys, Leiden, NL) for 32 selected flavoring compounds present in the assessed ENDs aerosols. Subsequently, we calculated corresponding human equivalent doses (HED) using a physiologically based pharmacokinetic (PBPK) model that was specifically developed for ENDs aerosols (presented separately: Antonijevic et al. SOT 2026). **Methods:** PODs obtained from the *in vivo* study represent the estimated tissue concentrations in the upper respiratory tract (URT) and in the alveolar region (estimated using the mouse PBPK model), which were derived from the lowest-

observed-adverse-effect concentration (LOAEC), simulating a 6-hours/day, 5-days/week exposure schedule as reported. The PODs obtained from the ToxTracker assay included nominal IC_{50} values for cytotoxicity (the nominal top dose was utilized when a cytotoxicity IC_{50} was not determined), nominal doses at which reporter-gene values were above the 2-fold threshold for each ToxTracker endpoint, as well as the estimated intracellular concentration derived using the Armitage *in vitro* mass balance distribution model. These PODs were then used to estimate HED using the human PBPK model with puff topography and use scenario parameters consisting of the puff duration (2 seconds), puff volume (50 mL), inter-puff interval (30 seconds), and puff number (15 per session), for one use session hourly, over 16 hours, to mimic the daily use profile of ENDs products. **Results:** For the *in vivo* mouse PODs, preliminary results indicated that the URT exhibited tissue concentrations two to five orders of magnitude higher than the alveolar region in mice, suggesting that the distribution was compound-specific. When converted to the HED using the human model (HED_{in_vivo}), the calculated HEDs specific to the URT were 1 - 300-fold greater than those specific to the alveolar region. For the *in vitro* PODs, when the *in vitro* mass balance distribution was considered, the estimated cell levels of the flavoring compounds were up to ~ 200 times higher than the nominal medium concentration, with the exception of isobutyraldehyde, whose intracellular concentration was about 69% of the nominal medium concentration. The *in vitro* PODs were overall much higher than the *in vivo* PODs, with up to ten orders of magnitude and up to four orders of magnitude higher for alveolar and URT regions, respectively. Consequently, the resulting HED_{in_vitro} were consistently higher than the HED_{in_vivo}. **Conclusions:** This study explored multiple options for selecting PODs for estimating HEDs and demonstrated the potential utility of NAMs in risk assessment. Although the HED_{in_vivo} derived from alveolar tissue concentrations is more conservative than that derived from the URT region, the alveolar region warrants closer evaluation for future consideration and assessment as part of a risk assessment, given the close anatomical correlation with humans. Furthermore, additional investigation and verification with refined models, such as benchmark dose modeling, are necessary to support the use of *in vitro* data in risk assessment, and variability of puff topography and use scenario should also be considered to ensure that the risk assessment is protective of users. The use of *in vitro*-derived data alone is less conservative, and, therefore, appropriate validation and verification of the *in vitro* method is recommended for quantitative risk assessment purposes.

ABSTRACT NUMBER: 5256 **Poster Board Number:** M835

TITLE: Exploring Community Scale and Regional Scale Air Quality Variability in BTEX Exposures and Human Health Risks

AUTHORS (FIRST INITIAL, LAST NAME) AND INSTITUTIONS: *A. M. Bamber, MS, DABT*[1], *M. Lumpkin, PhD, DABT*[2], *D. Foster, PhD*[1], C. Flanigan, MPH[1], and *C. A. Barlow, PhD*[1]. [1]Aetia Scientific Collaborative, Boulder, CO; and [2]Exponent, Denver, CO.

KEYWORDS: Risk Assessment; Regulatory Science/Regulatory Toxicology; Volatile Organic Compound(s)

ABSTRACT: Background and Purpose: Volatile organic compounds (VOCs), including benzene, toluene, ethylbenzene and xylenes (BTEX) are recognized as priority air toxics and established risk drivers of potential public health risk in communities located near industrial or vehicular sources. Understanding whether community scale air monitoring data comport with regional air quality trends is critical for risk assessment, regulatory decision-making, and community health protection. This study evaluates ambient BTEX concentrations measured at monitoring sites surrounding a major petroleum refinery in

Commerce City North Denver (CCND), Colorado, and compares these community-scale measurements to regional air quality data. **Methods:** Annual and quarterly BTEX concentration datasets from federal- and state-operated ambient air monitoring as well as independent community air quality sampling conducted in CCND between 2021 and 2024 were visually analyzed using Microsoft Power BI to characterize spatial variability and temporal trends in BTEX concentrations. The representativeness of regional-scale air quality monitoring data was assessed in comparison to community-scale measurements. **Results:** All reported community BTEX concentrations were below established chronic health-based reference values. From 2021 through 2024, time-weighted average benzene concentrations were 0.25 ppb across all community monitoring locations, with the highest average of 0.41 ppb (n=239; 1-hour and 7-day sampling duration), well below the conservative chronic reference level of 3 ppb (ATSDR chronic MRL). Regional air monitoring for benzene began in 2024 at the Commerce City location, and average 24-hour benzene concentrations were 0.27 ppb (1.6 ppbc), with a maximum arithmetic mean of 1.1 ppb (6.6 ppbc; n= 60). Community-scale BTEX concentration results were generally consistent with available regional monitoring data, showing good alignment across spatial scales while still capturing localized variability. **Conclusions:** These findings highlight the value of site-specific monitoring for confirming that regional air quality data accurately reflect local conditions and potential public health risks. The results can guide targeted community exposure assessments and support regulatory strategies for monitoring and mitigating potential air toxics exposures.

ABSTRACT NUMBER: 5257 **Poster Board Number:** M836

TITLE: A Framework for Identifying Occupational Exposure and Toxicology Data Gaps Across the Rare Earth Element Life Cycle: Application to Cerium

AUTHORS (FIRST INITIAL, LAST NAME) AND INSTITUTIONS: *S. Brown*[1], C. Boles[2], *S. Dotson*[3], T. Kondash[4], W. DuBose[4], and J. Sahmel[4]. [1]Insight Exposure & Risk Sciences Group, San Mateo, CA; [2]Insight Exposure & Risk Sciences Group, Raleigh, NC; [3]Insight Exposure & Risk Sciences Group, Cincinnati, OH; and [4]Insight Exposure & Risk Sciences Group, Boulder, CO.

KEYWORDS: Risk Assessment; Exposure Assessment; Rare Earth Elements; Rare Earth Elements

ABSTRACT: Background and Purpose: Global production and processing of rare earth elements (REEs) have expanded rapidly over the past two decades, with recent U.S. initiatives accelerating domestic mining, processing, and manufacturing. This growth is expected to increase worker exposure across the REE life cycle, including mining, processing and production of REE-containing products, end-product use, and recycling. However, occupational exposure, human health, and toxicological data for REEs remain limited, and are rarely differentiated by REE chemical or physical form or life cycle stage, despite their influence on exposure potential and toxicological relevance. To address these gaps, we developed the REE Occupational Exposure and Toxicology Gap Framework (REETox-Gap), a process- and form-based approach to evaluate data adequacy and prioritize research needs across REE life cycle stages. This framework emphasizes early identification of opportunities to reduce occupational hazards and exposures associated with REE production and use. **Methods:** Occupational health considerations across the REE life cycle were evaluated using cerium (Ce) forms (e.g., $CeCl_3$ and CeO_2) as a representative case, due to Ce's relatively high production volume among REEs. The Ce life cycle was defined following Du and Graedel (2011), and included (1) mining, (2) separation, (3) fabrication, (4) manufacturing, (5) end-product use, and (6) waste management/recycling. A literature review was conducted, and included peer-reviewed publications, government and regulatory reports, and technical assessments identified

through PubMed, Google Scholar, OSHA, NIOSH, EPA, and MSHA. This preliminary application focused on occupational exposures and health hazards associated with Ce forms at each life cycle stage. **Results:** The REETox-Gap is an eight-step, process- and form-based framework that systematically maps REE life cycle stages, identifies predominant chemical and physical forms, evaluates task- and process- specific exposure potential, assesses toxicological and epidemiological evidence within relevant exposure contexts, assigns data sufficiency tiers, and prioritizes data needs to inform occupational risk assessment and risk management. Data sufficiency tiers were qualitatively defined as *adequate* (sufficient data); *partial* (limited data); or *inadequate* (insufficient data) to characterize potential occupational exposure and/or health effects at each life cycle stage. Our preliminary application of the REETox-Gap framework to Ce indicated that data adequacy varied across the life cycle stages: occupational exposure and human health data were *inadequate* for (1) mining, (2) separation, (3) fabrication, and (6) recycling, and were *partial* for (4) manufacturing, and (5) downstream occupational end-use, with no occupational cohort or case-control studies identified in the peer-reviewed literature. Consequently, worker exposure concentrations and associated health effects for Ce remain poorly characterized across life cycle stages. Limited human evidence suggests that prolonged occupational exposure to certain forms of Ce fumes or dusts may be associated with respiratory effects, including pneumoconiosis. Experimental studies indicate that different Ce compounds may affect multiple organ systems depending on Ce form and exposure route, via mechanisms involving oxidative stress, apoptotic activation, and cytokine-mediated inflammation. EPA IRIS has derived a RfC of 0.9 μg/m³ based on an unpublished subchronic inhalation study of cerium oxide in rats. **Conclusions:** Application of the REETox-Gap framework illustrates the utility of a process- and form-based approach for identifying occupational exposure and health hazard data gaps and prioritizing research needs in exposure-relevant occupational contexts across the REE life cycle. Using Ce as an example, the framework revealed substantial data deficiencies across mining, separation, and fabrication, which are life cycle stages with high potential for worker exposure, while data for manufacturing and downstream occupational activities were limited. REETox-Gap provides a structured basis for coordinating data generation among researchers, industry, and regulators, and supports integration of future exposure and toxicologic information to enable evidence-based identification of research priorities and early opportunities to reduce occupational hazards and exposures associated with REE production and use.

ABSTRACT NUMBER: 5258 **Poster Board Number:** M837

TITLE: Standardized Default Central Tendency Exposure Factors for use in Superfund Human Health Risk Assessments

AUTHORS (FIRST INITIAL, LAST NAME) AND INSTITUTIONS: M. Burgess[1], L. Raterink[1], J. Rothrock[2], *M. Follansbee*[2], *K. Salinas*[2], R. Shaw[2], and B. Lebeck[2]. [1]EPA Office of Superfund and Emergency Management, Washington, DC; and [2]SRC, Inc., Syracuse, NY.

KEYWORDS: Risk Assessment; Exposure Assessment

ABSTRACT: Background and Purpose: The EPA uses human health risk assessment (HHRA) to characterize the nature and magnitude of risks resulting from human exposure to chemical contaminants or mixtures. One of the policy goals of the Superfund program is to protect a “high-end,” but not worst-case, exposure experienced by human receptors: the reasonable maximum exposure (RME). The RME is to include all exposures and is an estimate of a conservative exposure case (i.e., well above the average case) that is still within the range of possible exposures that are reasonably expected

to occur. The RME risk is generally the principal basis when setting preliminary remediation goals at Superfund sites. Presenting a range of exposure estimates for a given exposure scenario (e.g., central tendency, high end, and sensitive subgroups such as children) can more fully describe and bound risk estimates. EPA's 1995 *Risk Characterization Policy* notes that the description of risk should indicate what is being assessed and should include high end and central tendency estimates of the exposure distribution. The central tendency exposure (CTE) is an estimate of the average exposures to a receptor. In 2014, the former EPA Office of Solid Waste and Emergency Response (OSWER) published recommended default RME factors in an effort to reduce variability and uncertainty in the exposure assumptions used by regional EPA Superfund staff in HHRAs (the "2014 OSWER Directive"). Herein, we present a set of preliminary standardized CTE factors for potential future use in HHRA to help ensure a consistent approach to presenting and considering central tendency exposure estimates, particularly when site-specific data are not available. **Methods:** The CTEs were derived from the EPA *Exposure Factors Handbook*, an externally peer-reviewed document that provides a summary of current information and data on exposure factors; the 2014 OSWER Directive; and EPA's *Risk Assessment Guidance for Superfund (RAGS) Part E*. Conventions followed to derive CTE factors included selecting mean values instead of median values when both were available, rounding numbers at the end of the calculation rather than at intermediary steps in the calculation, and standardizing the number of significant digits (e.g., reporting calculated skin surface area to 2 significant digits and calculated soil ingestion rates to 1 significant digit). **Results:** Preliminary results for standardized default CTE parameters are presented for each of the exposure parameters listed in the 2014 OSWER Directive: ingestion and dermal contact rates; exposure frequency, exposure duration, and exposure time variables; averaging time and lifetime. For context, these CTE parameters were compared to values in the 2014 OSWER Directive and values published in EPA's 1993 *Superfund's Standard Default Exposure Factors for the Central Tendency and Reasonable Maximum Exposure*. **Conclusions:** As noted in EPA's *Risk Assessment Guidance for Superfund, Part A*, the advantage of presenting both CTE and RME exposure factors is that the resulting range of exposures provides some measure of the variability and uncertainty surrounding the risk estimates. Future consideration of these CTE factors by EPA's Office of Land and Emergency Management (OLEM) will help ensure a standardized and consistent approach to using exposure factors, particularly in cases where site-specific data are unavailable. Standard and consistent use of the CTE across various Superfund sites will ultimately enhance the effectiveness of environmental response actions.

ABSTRACT NUMBER: 5259 **Poster Board Number:** M838

TITLE: Risk Assessment of Wood Preservatives in South Korea Using the Biocide Risk Assessment Management System

AUTHORS (FIRST INITIAL, LAST NAME) AND INSTITUTIONS: *I. Shim*, J. Lee, H. Lim, and K. Park. National Institute of Chemical Safety, Incheon, Korea, Republic of.

KEYWORDS: Risk Assessment; Exposure Assessment

ABSTRACT: Background and Purpose: Accurate exposure and risk assessments are essential to ensure the safe use of biocidal products. Consumers, particularly the general public, represent a primary vulnerable group with potential exposure to active substances in these products. In South Korea, the Consumer Chemical Products and Biocides Safety Control Actaims to protect human health and the environment while enhancing public safety by establishing specific procedures for the risk assessment of

biocidal products. The National Institute of Chemical Safety (NICS) provides guidance on human health risk assessment for manufacturers and importers of biocides, including hazard identification, exposure assessment, and risk characterization. In the case of wood preservatives, consumers may be exposed to substances such as 3-iodo-2-propynyl butylcarbamate (IPBC) or permethrin through various exposure routes, including dermal absorption and inhalation. Therefore, assessing potential risks through systematic exposure and risk assessment processes is critical. **Methods:** calculated based on their respective points of departure. Exposure factors, scenarios, and routes relevant to public exposure to wood preservatives were identified. Exposure amounts for different scenarios involving commercially distributed wood preservatives in South Korea were estimated using these exposure factors. Risks associated with the biocidal products were evaluated by calculating hazard quotients (HQs). In addition, exposure estimates were compared using the NICS Biocide Risk Assessment Management System (BRAMS) and the ConsExpo tool developed by the National Institute for Public Health and the Environment (RIVM). **Results:** For wood preservatives, estimated dermal exposure levels calculated using BRAMS and ConsExpo were approximately 3.46×10^{3} to 4.52×10^{3} and 1.27×10^{5} to 1.39×10^{7} times higher, respectively, than estimated inhalation exposure levels. These results indicate that dermal exposure is the dominant exposure route for consumers using wood preservatives. The HQs calculated using BRAMS and ConsExpo ranged from 2.53×10^{-3} to 9.29×10^{-3} and from 1.26×10^{-3} to 4.63×10^{-3}, respectively. Comparison of HQ values showed that those derived using BRAMS were approximately twice as high as those obtained using ConsExpo. **Conclusions:** Overall, risk assessments conducted using both BRAMS and ConsExpo indicated that the evaluated wood preservatives are safe for general consumers. BRAMS produced more conservative risk estimates than ConsExpo, although this difference may vary depending on the type of biocidal product and the active substances involved. Further systematic studies are needed, particularly for biocidal products containing multiple active substances and for newly introduced product types that have not yet been fully evaluated.

ABSTRACT NUMBER: 5260 **Poster Board Number:** M839
TITLE: Risk Assessment of Dermal Exposure to PFOA from Firefighter Turnout Gear Textiles

AUTHORS (FIRST INITIAL, LAST NAME) AND INSTITUTIONS: *M. C. Domanico*, *A. A. Han*, L. E. McFadden, *M. T. Donnell*, R. Avanasi, and *A. K. Madl*. Valeo Sciences, Ladera Ranch, CA.
KEYWORDS: Risk Assessment; Textiles; Perfluorooctanoic acid (PFOA)

ABSTRACT: Background and Purpose: Elevated blood levels of per- and polyfluoroalkyl substances (PFAS), including the abundant congener perfluorooctanoic acid (PFOA), have been observed in firefighters when compared to the general population. Firefighting turnout gear textiles have been suggested as a potential source of occupational PFOA exposure for firefighters. Thermal liner textiles comprise the inner-most layer of turnout gear. The National Institute of Standards and Technology (NIST) characterized various turnout gear textiles for PFAS in unstressed and stressed conditions (abrasion, exposure to high temperature, and laundering). However, there is a gap in understanding potential health risks associated with dermal PFOA exposures among firefighters from stressed or damaged turnout gear textiles. The aim of this analysis was to estimate dermal PFOA exposures and potential health risks resulting from occupational wear of firefighting turnout gear. **Methods:** Chemical characterization data for solvent-extracted PFOA in firefighting turnout gear was obtained from the NIST dataset for 5 thermal liners under unstressed and stressed conditions, including abrasion, high temperature, and laundering. Dermal PFOA exposures were estimated based on PFOA-specific dermal

absorption factors and a range of conservative firefighter occupational use conditions (e.g., varying shift durations and assumed gear wear time per day) over a 30-year career span. Available chronic non-cancer and cancer health guidance values (HGVs) for PFOA were identified and reviewed. Because no dermal HGVs for PFOA are currently available, dermal HGVs were derived from oral HGVs through route-to-route extrapolation and accounting for differences in relative bioavailability. Potential chronic non-cancer and cancer health risks were assessed by comparing estimated PFOA exposures from wearing firefighting turnout gear to the derived dermal HGVs and represented as hazard quotients (HQs) and cancer risk (CR), respectively. **Results:** All exposure scenarios evaluated for wearing firefighting turnout gear with PFOA-containing thermal liner textiles under unstressed and stressed conditions resulted in HQs far less than 1, ranging from 0.0001 to 0.01 for chronic non-cancer risk. CR estimates ranged from 1 in 2.5 billion to 1 in 24 million. Separate analyses were conducted for different firefighter demographics (age and sex). While some textile treatment conditions influenced the extent of PFOA exposures (with abraded liner textiles as the highest, and laundered and unstressed liner textiles as the lowest), there were no increased risks for non-cancer and cancer health effects across different age groups and sexes. Interestingly, there was no single textile across the 5 evaluated liners that consistently had the highest estimated PFOA exposure and risk under the various unstressed and stressed conditions. **Conclusions:** This preliminary health risk assessment indicates that PFOA in firefighter turnout gear thermal liner textiles do not pose a health risk of non-cancer and cancer health effects to firefighters. This assessment demonstrated that even under varying textile stress conditions, age or sex of the firefighter, and conservative estimates for wearing turnout gear, there was no increased risk of non-cancer or cancer health effects. In the process of conducting this risk assessment, future needed areas of research were revealed including additional empirical data on 1) dermal PFAS absorption or bioavailability, 2) testing across a broader range of PFAS congeners, textile products, and textile use scenarios, and 3) standardized methods for quantifying PFAS release from textiles under realistic dermal exposure conditions. In conclusion, while the NIST testing measured PFOA in the thermal liners of firefighter turnout gear, this potential PFOA exposure to a firefighter does not present an increased risk of non-cancer or cancer health effects.

ABSTRACT NUMBER: 5261 **Poster Board Number:** M840

TITLE: A Chemical Category Approach to Identify Potential Human Health Hazards of Aryl Phosphate Flame Retardants

AUTHORS (FIRST INITIAL, LAST NAME) AND INSTITUTIONS: *J. Rhoades*[1], *J. Melia*[1], *H. Carlson-Lynch*[1], M. Kawa[1], L. Morlacci[1], A. Fistrovich[1], *S. Stevens*[1], D. Herber[1], M. Riccardi[1], S. Rosenberg[1], Y. Sobhi[1], *E. Golden*[1], *C. Heit*[2], *F. Belmonte*[1], *C. McGuire*[1], N. Craig[1], *A. Healey*[3], M. Doldron[1], and B. Salinas[1]. [1]SRC, Inc., North Syracuse, NY; [2]SRC, Inc.; currently CalEPA OEHHA, North Syracuse, NY; and [3]SRC, Inc.; currently Pfizer, North Syracuse, NY.

KEYWORDS: Aryl phosphate flame retardants

ABSTRACT: Background and Purpose: Organophosphorus compounds have been used to replace polybrominated diphenyl ethers as flame retardants in consumer products and building materials. Exposure to these compounds is widespread; however, toxicological data are limited. A chemical category approach was used to identify hazards for aryl phosphate flame retardants (APFRs), which are a structural subclass of non-halogenated organophosphorus flame retardants. **Methods:** Short-term *in vivo* toxicity studies that included liver transcriptomic analysis were available for 6 APFRs (triphenyl

phosphate, tricresyl phosphate, tert-butylphenyl diphenyl phosphate, isopropylated phenyl phosphates, 2-ethylhexyl diphenyl phosphate, isodecyl diphenyl phosphate). To expand the list of chemicals in the category, analogue searches were conducted using the OECD QSAR Toolbox and the EPA Comptox Chemicals Dashboard. Systematic review methods were used for literature searching, screening, data extraction and study quality evaluation of health effects data in experimental animals. A chemical category definition for APFRs was established by evaluating similarity across several contexts including structural characteristics, physicochemical properties, toxicokinetics, health effects, bioactivity, and mechanisms associated with potential modes of action [MOA]. **Results:** Analogue search and refinement methods resulted in a list of 35 APFRs with potential health effects data. Structural similarity was noted for all category members, characterized by the presence of diaryl or triaryl phosphate esters, with or without alkyl substituents (carbon chain lengths C1-C12). Physiochemical properties were also similar across the category members. Toxicokinetic data were limited; however, metabolism data for 7 APFRs demonstrated hydrolysis and oxidation reactions catalyzed by cytochrome P450 (CYP). Each hydrolysis reaction released a hydroxylated phenyl metabolite, and oxidation reactions resulted in phenol ring hydroxylation or hydroxylation of alkyl substituents. Animal studies using repeat-dose, reproductive, or developmental protocols were available for 9 APFRs (105 studies). The most common sensitive health outcomes (i.e., those with the lowest LOAELs) included hepatic, endocrine/metabolic, neurological, reproductive, and developmental effects. Study quality evaluation of 47 peer-reviewed studies revealed that most studies were well conducted with an overall confidence rating of Medium or High. Bioactivity and mechanistic data identified candidate molecular initiating events related to some toxicological effects observed in animals. Candidate mechanisms that were common to many of the APFRs included interaction with nuclear receptors (PXR, AhR, ER, AR) and perturbation of genes involved in lipid metabolism, steroidogenesis, and neuronal morphology and function. **Conclusions:** Human biomarker data for APFRs indicate that exposure to these compounds is widespread; however, data describing the potential human health effects for these compounds are limited and many APFRs have not been tested. A chemical category for APFRs was defined based on similarity in structural characteristics, physicochemical properties, metabolism, health effects in animal studies, and bioactivity and mechanistic/MOA data. Similarity across multiple contexts increases confidence in the predictions for data poor chemicals. Potential human health hazards identified for APFRs included liver toxicity, adrenal effects, neurotoxicity, male and female reproductive toxicity, and developmental and neurodevelopmental effects. Similar health effects can be predicted for category members lacking experimental data or the information could be used to develop a targeted testing strategy.

ABSTRACT NUMBER: 5262 **Poster Board Number:** M841

TITLE: Exposure and Health Risk Characterization of Lithium in Municipal Drinking Water: Evidence from Afyonkarahisar, Türkiye

AUTHORS (FIRST INITIAL, LAST NAME) AND INSTITUTIONS: S. Cetinkaya. University of Health Sciences, Ankara, Turkey. Sponsor: S. Cetinkaya, EUROTOX

KEYWORDS: Risk Assessment; Lithium, Drinking water exposure, Non-carcinogenic

ABSTRACT: Background and Purpose: Lithium (Li) has recently gained attention as an emerging contaminant in drinking water, with routine monitoring initiated in several countries, including the United States, due to concerns regarding potential neurodevelopmental and endocrine effects. Despite this growing interest, information on Li occurrence and its associated health risks in drinking water remains limited in Türkiye. The present study aimed to investigate Li concentrations in municipal tap water and to characterize potential non-carcinogenic and carcinogenic health risks in comparison with selected regulated toxic metals (Cr, Ni, Cd, Pb). **Methods:** Drinking water samples were collected from all districts of Afyonkarahisar, Türkiye, to ensure comprehensive spatial coverage. Concentrations of Li, Cr, Ni, Cd, and Pb were determined using inductively coupled plasma-mass spectrometry (ICP-MS). A health risk assessment was conducted for children following U.S. EPA guidelines. Chronic daily intake (CDI), hazard quotient (HQ), hazard index (HI), and incremental lifetime cancer risk (ILCR) were calculated to evaluate both non-carcinogenic and carcinogenic risks associated with long-term exposure through drinking water ingestion. **Results:** Lithium was detected in all sampled districts, with concentrations ranging from 0.96 to 110.59 µg/L (mean: 17.73 µg/L), and was identified as the dominant contributor to overall child-specific non-carcinogenic risk. Chromium and nickel concentrations ranged from 1.01-28.77 µg/L (mean: 4.45 µg/L) and 0.42-15.85 µg/L (mean: 2.45 µg/L), respectively. Cadmium and lead concentrations were below detection limits in all samples. Non-carcinogenic risk assessment indicated that Li posed the highest potential health concern, with maximum HQ values exceeding unity (HQ_{max} = 3.69) in several districts, whereas HQ values for Cr and Ni remained below the acceptable threshold. Carcinogenic risk estimates for Cr were within or marginally above the acceptable range, with ILCR values reaching up to 1.4×10^{-4}. **Conclusions:** The findings demonstrate that lithium represents a dominant contributor to non-carcinogenic health risk in municipal drinking water from Afyonkarahisar. These results emphasize the need to consider lithium in routine drinking water monitoring programs alongside regulated metals. Overall, the study underscores the toxicological relevance of lithium exposure through drinking water and supports growing international concern regarding its potential public health implications.

ABSTRACT NUMBER: 5263 **Poster Board Number:** M842

TITLE: Evaluation of QSPR Models for Key Toxicokinetic Parameters in Screening Level Risk Assessment

AUTHORS (FIRST INITIAL, LAST NAME) AND INSTITUTIONS: *M. Scherer*[1,2], and *C. Ring*[1]. [1]United States Environmental Protection Agency, Research Triangle Park, NC; and [2]Oak Ridge Institute for Science and Education, Oak Ridge, TN.

KEYWORDS: Computational Toxicology; Risk Assessment; QSPR

ABSTRACT: Background and Purpose: *In vitro*-to-*in vivo* extrapolation (IVIVE) requires chemical-specific toxicokinetic (TK) parameters to translate effective concentrations generated using *in vitro* new approach methodologies (NAMs) to human exposure estimates. These frameworks rely on certain TK parameters as critical inputs however, experimental determination is often not feasible due to time and cost constraints. Quantitative structure-property relationship (QSPR) models address this issue by estimating TK parameters including fraction unbound in plasma (fup), intrinsic hepatic clearance (Clint), and Caco-2 permeability via chemical structure. **Methods:** Experimental fup, Clint, and Caco-2 values were measured via *in vitro* assay for 170 chemicals and the raw mass spectrometer peak area data were processed via the "invitroTKstats" R package to generate quantitative TK parameter values. Two Random Forest QSPR models were used to estimate TK values for the same group of 170 chemicals; Dawson et al. (2021) for fup and Clint values and Honda et al. (2024) for Caco-2 permeability values. *In vitro* AC50 values were downloaded from ToxCast and converted to Administered Equivalent Doses (AEDs) and the corresponding point of departure (POD) was selected using the R package “httk” using the experimental and QSPR modeled TK parameters. *In vivo* points of departure (POD_{trad}) were downloaded from ToxValDB and filtered based on Pradeep et al. (2020) to ensure studies had adequate data for modeling and reported effect levels in mg/kg/day units. The *in vitro* and QSPR modeled PODs ($POD_{in\ vitro}$ and POD_{QSPR}, respectively) were compared to the POD_{trad} to determine the accuracy and influence of the modeled TK values. **Results:** Results of this analysis show that the model predictions skewed towards high permeability, thereby overpredicting intestinal absorption and resulting in $POD_{QSPR} < POD_{in\ vivo}$. The model heavily overpredicted chemicals to have higher intestinal clearance and underpredicted the fraction unbound in plasma, both of which led to $POD_{QSPR} > POD_{in\ vivo}$. **Conclusions:** The overprediction for the Clint and underprediction for the fup modeled values and resulting POD_{QSPR} may lead to larger human equivalent concentrations, thus underestimating the actual exposure risk. The *in vivo* ToxCast Caco-2 values were lower than their predicted counterparts, resulting in a protective POD_{QSPR}. Comparing the modeled PODs with traditional, *in vivo* PODs is a crucial next step towards elucidating the applicability of these QSPR models and highlighting the areas in which refinement is needed to improve predictive accuracy in chemical risk assessment scenarios. *This abstract does not reflect U.S. EPA policy.*

ABSTRACT NUMBER: 5264 **Poster Board Number:** M843

TITLE: Comparative Analysis of Endpoint-Specific Parameters of Posterior Distributions in Bayesian Benchmark Dose Analyses

AUTHORS (FIRST INITIAL, LAST NAME) AND INSTITUTIONS: *A. Hirose*, S. Nakae, T. Hayashi, A. Tanabe, and A. Fukushima. Chemicals Evaluation and Research Institute, Japan, Tokyo, Japan.

KEYWORDS: Risk Assessment; Regulatory Science/Regulatory Toxicology; Benchmark dose

ABSTRACT: Background and Purpose: Benchmark dose (BMD) modeling has become the prevailing approach for dose-response assessment in toxicology. It has replaced the NOAEL/LOAEL paradigm by leveraging the full shape of the dose-response curve and providing transparent, quantitative criteria for points of departure. In our earlier analysis of approximately 500 continuous datasets, the calculated BMDL values showed high concordance overall, though the degree of agreement varied by toxicity endpoint between BBMD and ToxicR. Since Bayesian posterior parameter distributions are generally sensitive to prior distributions, especially when dataset size is small and most tools rely on uninformative or general-purpose priors, it is important to consider the development of endpoint-specific priors. To support the proper use of Bayesian BMD methods, we are researching the development of endpoint-specific priors. **Methods:** To develop endpoint-specific parameter priors, we examined the posterior distributions generated under each tool's default settings. The aim of this study was to characterize these posterior distributions for each endpoint and compare patterns across tools. ToxicR and BMDBMR use the same model-averaging framework, whereas BBMD uses different statistical models. To enable consistent comparisons across tools, we focused on the Exponential-5 model, implemented in both ToxicR and BBMD. This model estimates five parameters ("a"-"d" and "sigma") related to response level, curve shape, and variance. We analyzed 12 endpoints (RBC, HGB, HCT, reticulocyte count, methemoglobin, ALP, ALT, ChE, BUN, creatinine, liver weight, and kidney weight). For each tool, we extracted the posterior distribution of each parameter in each dataset using the default prior. **Results:** A generally consistent pattern emerged for parameters a through d across all evaluated organs and endpoints, although the patterns differed partially between ToxicR and BBMD for some endpoints. Parameter a, which represents the baseline or background response level, showed strong agreement between BBMD and ToxicR. Regardless of the endpoint, the two tools produced nearly identical baseline estimates. In contrast, parameter b, which controls the slope or scale of the dose-related increase, exhibited a systematic divergence. BBMD consistently produced larger values than ToxicR. This suggests that BBMD generally shows the low-dose region of the dose-response curve to be steeper. This could lead to different interpretations depending on the tool used, especially for low-dose behavior. Parameter c, which determines the horizontal positioning or transition point of the curve, also showed consistent directional differences. ToxicR frequently produced smaller c estimates than BBMD, and values for some datasets were negative. This suggests a leftward shift in the dose-response curve under ToxicR, indicating that the apparent onset occurs earlier under ToxicR than under BBMD. Parameter d, which governs the curve's curvature or shape, tended to be larger in BBMD across most endpoints. This suggests that BBMD often yields more pronounced curvature or sharper shaping than ToxicR. There are notable differences in the patterns of several endpoints between the two tools, particularly with regard to the shape of the curves and the sharpness of the responses. Therefore, to investigate the characteristics of the posterior distribution specific to each endpoint, a more detailed sensitivity analysis should be performed for each endpoint, or comparisons should be conducted using multiple tools. **Conclusions:** This cross-tool evaluation indicates that posterior distributions may be

important information for developing endpoint-specific priors in future research. The strong and reproducible agreement for baseline parameter a supports the use of informative baseline priors. However, systematic, tool-dependent differences were observed for parameters b, c, and d. As differences in b, c, and d may reflect distinctions in functional form or shape constraints between tools, more endpoint-specific dose-response shapes should be characterized. When transferring priors across model classes, matching model structures or inflating prior variance may help accommodate these discrepancies. Further pooling of posterior results and evaluation of priors for additional models will be necessary.

ABSTRACT NUMBER: 5265 **Poster Board Number:** M844

TITLE: Estimation of background daily intake of phthalates in the United States population based on NHANES urinary biomarker data

AUTHORS (FIRST INITIAL, LAST NAME) AND INSTITUTIONS: C. Busch[1], D. Campbell[1], C. Bocklage[1], S. Zentner[2], and *E. M. Beckett*[1]. [1]Benchmark Risk Group, Chicago, IL; and [2]Benchmark Risk Group, Grand Rapids, MI.

KEYWORDS: Phthalates; Exposure Assessment; Biomonitoring

ABSTRACT: Background and Purpose: Phthalates are a group of chemical plasticizers commonly found in a wide variety of consumer products, including hair care products, cosmetics, and medications. Phthalates can also readily leach out of plastic products, such as medical tubing, food packaging, and certain textiles, and has also been shown to be present in dust, further contributing to its ubiquitous nature. Phthalates are classified as endocrine disrupting chemicals (EDCs), having been shown to interfere with endocrine signaling pathways, which has led to links with various adverse health outcomes, including reproductive cancers. Despite the prevalence of these chemicals in consumer products, population-level exposure to these compounds has not been fully characterized in the literature. Urinary phthalate metabolites have been measured across multiple cycles of the National Health and Nutrition Examination Survey (NHANES), including mono(carboxyoctyl) phthalate (COP), mono-2-ethyl-5-carboxypentyl phthalate (ECP), mono-n-butyl phthalate (MBP), mono-(3-carboxypropyl) phthalate (MC1), mono-ethyl phthalate (MEP), mono-(2-ethyl-5-hydroxyhexyl) phthalate (MHH), cyclohexane 1,2-dicarboxylic acid monohydroxy isononyl ester (MHNC), mono-(2-ethyl)-hexyl phthalate (MHP), mono-isobutyl phthalate (MIB), mono-(2-ethyl-5-oxohexyl) phthalate (MOH), mono-benzyl phthalate (MZP), and mono-oxo-isononyl phthalate (MONP). **Methods:** The range of median daily intake (DI) of phthalates in the general public was estimated based on available urinary phthalate metabolite concentrations collected from the NHANES databases between 1999 and 2018. Analytes with over 40% of the sample concentrations reported as below the limit of detection (LOD) were excluded from analysis (n = 5). Associated demographic data regarding age, gender, income, and race were identified for each participant from each of the relevant cycles. DI was estimated from creatinine-adjusted, urinary phthalate metabolite concentration via reverse dosimetric extrapolation using validated fractional urinary excretion (F_{ue}) values for each phthalate metabolite; if a validated F_{ue} value was not identified for a given phthalate metabolite, that metabolite was excluded from the analysis. **Results:** The final analysis was performed on 12 phthalate metabolites (COP, ECP, MBP, MC1, MEP, MHH, MHNC, MHP, MIB, MOH, MZP, MONP) after exclusion due to either a lack of a validated F_{ue} value (n = 10) or a large proportion of the concentration values being below the LOD (n = 5). The analysis ultimately included samples from >21,000 participants. The overall ranges for median daily intake measurements (mg/kg/day) for the

corresponding parent compounds were 0.00042 - 0.0016 for benzyl-butyl phthalate (BzBP); 0.0033 - 0.011 for di-n-butyl phthalate (DBP); 0.0026 - 0.012 for di(2-ethylhexyl) phthalate (DEHP); 0.0040 - 0.017 for di-ethyl phthalate (DEP); 0.00054 - 0.00059 for 1,2-Cyclohexane dicarboxylic acid, diisononyl ester (DINCH); 0.0026 - 0.015 for di-isononyl phthalate (DNP); and 0.00097 - 0.0014 for di-isobutyl phthalate (DiBP). **Conclusions:** Based on the results presented herein, there is ubiquitous exposure to phthalates among the United States population associated with daily life. These data provide important context to ongoing research into the health outcomes associated with phthalates, as well as any human health risk assessments of products containing phthalates.

ABSTRACT NUMBER: 5266 **Poster Board Number:** M845

TITLE: Characterizing Community Exposure to Tetrachloroethylene (PCE) Near Contaminated Sites Using Exhaled Breath Analysis

AUTHORS (FIRST INITIAL, LAST NAME) AND INSTITUTIONS: M. Alajlouni[1], S. Amin[1], S. Saad[1], A. Gronkiewicz[1], B. Latham[2], S. Littell[2], P. Balakumar[3], M. Oladosu[3], E. Pinsker[3], M. Turyk[3], and S. Liu[1]. [1]Purdue University, West Lafayette, IN; [2]Martinsville Environmental Community Action Project, Martinsville, IN; and [3]University of Illinois Chicago, Chicago, IL. Sponsor: *M. Azaizeh*

KEYWORDS: Volatile Organic Compound(s); Exposure Assessment; Environmental Toxicology; Epidemiology and Public Health; Tetrachloroethylene (PCE)

ABSTRACT: Background and Purpose: Tetrachloroethylene (PCE) is one of the most prevalent environmental contaminants and a probable human carcinogen and neurotoxicant, with health effects mainly observed among occupational groups with high exposure levels. It can contaminate groundwater, soil, and indoor air and cause exposure in community settings. Despite widespread PCE contamination, biomonitoring data on personal exposure is sparse, especially among individuals living near contamination sites, as exposure assessment often only relies on environmental monitoring and environmental measurements. Martinsville, Indiana, is a midwestern working-class community that overlies four known PCE groundwater and soil contamination sites. A cross-sectional study was conducted to characterize PCE exposure among individuals living in the community. Six field sampling campaigns were conducted in 2024-2025, with the last one completed in November 2025. This poster reports the initial exposure analysis investigating the determinants and variations of PCE personal exposure via exhaled breath analysis. **Methods:** Exhaled breath samples were collected and analyzed within hours of sample collection, using a proton transfer reaction mass spectrometry equipped in a mobile laboratory. Exhaled breath samples were collected in spring, summer, and fall seasons, including repeated measurements from a subset of participants, with some households contributing more than one individual to the study. Questionnaires collected information on covariates. Data analysis took a domain-based approach. Univariate descriptives and bivariate analyses were conducted within separate domains: demographics (age, gender, education, income), house characteristics (plume status, building/basement type, AC use, ventilation, water source, etc.), smoking (cigarette, tobacco, e-cigarette, home smokers), and occupation (employment, VOC/metal jobs and exposure, respirator use). Average PCE concentrations were calculated for participants with multiple measurements. Significant covariates will be forwarded to multivariable and mixed-effect modeling. **Results:** Four hundred and ninety (490) exhaled breath samples were collected from 297 participants (mean age 41.6 years, SD 13.4; range 18 - 70; 68.1% female; 33.6% ≤high school education; 29.7% ≤$50k income; 40% current/former smokers). The participants were from 228 unique household addresses. PCE

concentrations among all the samples ranged from 0.02 to 15.16 ppb (mean 0.53 ppb, SD 1.25); personal averages of PCE in exhaled breath samples had a geometric mean of 0.34 ppb (SD 0.76, skew 7.75), indicating right-skewed environmental exposure. Descriptive analysis of mean PCE exhaled breath concentration in participants revealed 64% of samples were collected in the fall season, 94.5% AC use, 13.0% dirt basements, 36.1% attached garages, 91.4% municipal water, 48% use bottled water, 41.1% paint/fuel storage, 12.0% current cigarette smokers, 97.6% no VOC-exposure related occupations, and 66.4% full-time employment. Bivariate analyses (log-PCE as outcome variable) identified dirt basements (p=0.012) and AC use (p=0.048) as significant house characteristics, while plume/buffer residents (n=50) tended to have higher PCE concentrations than residents outside of the plume (p=0.364). Additional bivariate analyses showed seasonal variation (means: spring, 0.53 ppb; summer, 0.29 ppb; fall, 0.32 ppb; p=0.110). Average PCE concentration did not differ significantly across other variables in the demographic, smoking, and occupation domains. **Conclusions:** Preliminary analysis suggested that house characteristics, e.g., air conditioning use and basement type, were significantly associated with PCE concentrations in exhaled breath. These results suggest that residential property characteristics may influence personal PCE exposure more than spatial proximity to contamination sites alone, but conclusions await further analysis to adjust for household clustering and repeated measurements.

ABSTRACT NUMBER: 5267 **Poster Board Number:** M846

TITLE: A Critical Review of Scientific Data Pertaining to Dermal Exposures to Per- and Polyfluoroalkyl Substances (PFAS)

AUTHORS (FIRST INITIAL, LAST NAME) AND INSTITUTIONS: *J. Heywood*[1], *S. Dotson*[2], J. Lotter[3], S. Tack[1], S. Gaffney[4], and J. Sahmel[1]. [1]Insight Exposure and Risk Sciences Group, Boulder, CO; [2]Insight Exposure and Risk Sciences Group, Cincinnati, CO; [3]Insight Exposure and Risk Sciences Group, Chicago, IL; and [4]Insight Exposure and Risk Sciences Group, San Francisco, CA.

KEYWORDS: Skin; dermal exposures; PFAS

ABSTRACT: Background and Purpose: Per- and polyfluoroalkyl substances (PFAS) are synthetic highly fluorinated organic compounds used in a wide range of industrial, commercial, and consumer products, including cookware, food packaging, medical devices, textiles, firefighting foam, and cosmetics and personal care products (PCPs). While oral ingestion is generally considered the dominant exposure route for most PFAS, dermal contact may represent a relevant pathway in certain occupational, environmental, and consumer-use scenarios. For the two most widely used and studied PFAS compounds, perfluorooctanoic acid (PFOA) and perfluorooctane sulfonic acid (PFOS), epidemiology studies suggest potential associations with health outcomes including reproductive, developmental, immune, and endocrine effects, among others. Human PFAS exposure can occur through multiple pathways and routes. Despite increasing attention to PFAS hazards, few studies have systematically characterized PFAS dermal exposure and uptake potential. Our analysis included a targeted literature review of studies evaluating PFAS dermal exposure potential, with emphasis on (1) transfer and loading to the skin surface, (2) empirical dermal exposure assessment factors, and (3) estimates of external and internal dermal doses. **Methods:** We performed a critical, targeted review of the literature on dermal exposure to PFAS using PubMed and citation tracking to identify studies relevant to human dermal exposure to PFAS. These included studies that measured PFAS concentrations on the human skin surface, studies that evaluated the PFAS content of products with frequent or extended dermal contact, studies which presented human exposure estimates based on biological sampling, and *in vitro* studies

that allowed for assessment of exposure potential. In total, our initial search returned 174 studies following removal of duplicates. Of these, 125 were screened and excluded at the title level. An additional 12 were excluded following full text review, leaving a final set of 37 core studies across four categories, including PFAS exposure potential related to dust, cosmetics and PCPs, clothing, and other scenarios. **Results:** A relatively small number of relevant publications were identified in this review, with 37 studies identified as the core sources for our analysis. Across most evaluated scenarios and compounds, estimated dermal PFAS intakes were generally <1 ng/kg-bw/day and represented a small fraction of total PFAS exposure relative to ingestion or inhalation. Higher dermal exposure estimates were reported for select cosmetics, PCPs, and textiles; however, such estimates were sensitive to assumptions regarding product use, skin loading, and absorption fractions. Empirical data on dermal flux, permeability, and compound-specific absorption were sparse and highly variable across PFAS, reflecting substantial heterogeneity in physicochemical properties and experimental methods. For many less common PFAS, physicochemical parameters have not been experimentally defined. Given the prevalence of PFAS in items of daily commerce, it can be difficult to isolate the contribution of any one product or work activity to a total, time-weighted PFAS dose. In the future, given the variability in the physicochemical properties of PFAS substances, it is likely to be helpful in many instances to evaluate human PFAS exposures, dermal or otherwise, in aggregate using methods such as biological monitoring, in the absence of well-defined detection methods or source/product profiles for specific, less widely used compounds. **Conclusions:** Available evidence suggests that dermal exposure to PFAS is typically a minor contributor to total PFAS dose for most human exposure scenarios. Stronger conclusions may be possible following further research, including future analyses of physiochemistry across the range of PFAS compounds. Quantitative characterization of dermal transfer, loading, and absorption remains limited for the vast majority of PFAS. Future research would benefit from improved physicochemical characterization, standardized dermal exposure assessment methods, and toxicological studies conducted at dermal doses relevant to estimated human exposures.